

Dynamic Modeling and Econometrics in  
Economics and Finance 29

Giuseppe Orlando  
Alexander N. Pisarchik  
Ruedi Stoop *Editors*

# Nonlinearities in Economics

An Interdisciplinary Approach  
to Economic Dynamics, Growth and  
Cycles

 Springer

# **Dynamic Modeling and Econometrics in Economics and Finance**

Volume 29

## **Series Editors**

Stefan Mittnik, Department of Statistics, Ludwig Maximilian University of Munich,  
München, Germany

Willi Semmler, New School for Social Research, New York, NY, USA and Bielefeld  
University, Germany

In recent years there has been a rapidly growing interest in the study of dynamic nonlinear phenomena in economic and financial theory, while at the same time econometricians and statisticians have been developing methods for modeling such phenomena. Despite the common focus of theorists and econometricians, both lines of research have had their own publication outlets. The new book series is designed to further the understanding of dynamic phenomena in economics and finance by bridging the gap between dynamic theory and empirics and to provide cross-fertilization between the two strands. The series will place particular focus on monographs, surveys, edited volumes, conference proceedings and handbooks on:

- Nonlinear dynamic phenomena in economics and finance, including equilibrium, disequilibrium, optimizing and adaptive evolutionary points of view; nonlinear and complex dynamics in microeconomics, finance, macroeconomics and applied fields of economics.
- Econometric and statistical methods for analysis of nonlinear processes in economics and finance, including computational methods, numerical tools and software to study nonlinear dependence, asymmetries, persistence of fluctuations, multiple equilibria, chaotic and bifurcation phenomena.
- Applications linking theory and empirical analysis in areas such as macrodynamics, microdynamics, asset pricing, financial analysis and portfolio analysis, international economics, resource dynamics and environment, industrial organization and dynamics of technical change, labor economics, demographics, population dynamics, and game theory.

The target audience of this series includes researchers at universities and research and policy institutions, students at graduate institutions, and practitioners in economics, finance and international economics in private or government institutions.

More information about this series at <http://www.springer.com/series/5859>

Giuseppe Orlando • Alexander N. Pisarchik •  
Ruedi Stoop  
Editors

# Nonlinearities in Economics


An Interdisciplinary Approach to Economic  
Dynamics, Growth and Cycles

 Springer



*Editors*

Giuseppe Orlando   
Department of Economics & Finance  
University of Bari Aldo Moro  
Bari, Italy

Alexander N. Pisarchik   
Technical University of Madrid  
Center for Biomedical Technology, Campus  
Montegancedo  
Pozuelo de Alarcón, Madrid, Spain

Ruedi Stoop   
Institute of Neuroinformatics  
Swiss Federal Institute of Technology  
Zürich, Switzerland

ISSN 1566-0419                      ISSN 2363-8370 (electronic)  
Dynamic Modeling and Econometrics in Economics and Finance  
ISBN 978-3-030-70981-5              ISBN 978-3-030-70982-2 (eBook)  
<https://doi.org/10.1007/978-3-030-70982-2>

© The Editor(s) (if applicable) and The Author(s), under exclusive license to Springer Nature Switzerland AG 2021

This work is subject to copyright. All rights are solely and exclusively licensed by the Publisher, whether the whole or part of the material is concerned, specifically the rights of translation, reprinting, reuse of illustrations, recitation, broadcasting, reproduction on microfilms or in any other physical way, and transmission or information storage and retrieval, electronic adaptation, computer software, or by similar or dissimilar methodology now known or hereafter developed.

The use of general descriptive names, registered names, trademarks, service marks, etc. in this publication does not imply, even in the absence of a specific statement, that such names are exempt from the relevant protective laws and regulations and therefore free for general use.

The publisher, the authors, and the editors are safe to assume that the advice and information in this book are believed to be true and accurate at the date of publication. Neither the publisher nor the authors or the editors give a warranty, expressed or implied, with respect to the material contained herein or for any errors or omissions that may have been made. The publisher remains neutral with regard to jurisdictional claims in published maps and institutional affiliations.

This Springer imprint is published by the registered company Springer Nature Switzerland AG.  
The registered company address is: Gewerbestrasse 11, 6330 Cham, Switzerland

# Reviews

Finally, a volume is coming out in our Springer Series *Dynamic Modeling and Econometrics in Economics and Finance* that will be of great service to the community of nonlinear modelers in economics—with very comprehensive surveys on history, theory, and econometrics of complex systems.

Arnhold Professor of International Cooperation and Development at The New School for Social Research

New York, NY, USA  
May 2021

Willi Semmler

Handling nonlinear dynamic phenomena has always been a difficult challenge in economics. The contributions in this volume present new perspectives and views—also from disciplines outside of economics—helping to tackle these challenges. The volume thus provides valuable impulses for advancing economic theory as well as empirical research.

Chair of Financial Econometrics - LMU Munich

Munich, Germany  
May 2021

Stefan Mittnik

This highly-valuable book is a great entry-point for understanding the economy as a self-organizing non-linear dynamical system. This book not only introduces the reader to advanced techniques but also applies them to modern economic growth and business cycle models.

Princeton, New Jersey, USA  
May 2021

Markus Brunnermeier

# Preface

Dear Reader,

Rather unanticipated, this book became a demonstration of how fruitful scientific meetings can be if held among open-minded participants. During a recent Non-linear Dynamics of Electronic Systems (NDES) conference, an inquisitive-minded economist from Bari (Giuseppe Orlando, G.O.) sparked the idea that economics should be treated along the guidelines that we use for the analysis of systems composed of strongly nonlinear subsystems, such as magnets, neurons, and more. Pretty much all of the people agreed that it was a pity that a book leading students of economics or similarly interested readers into such a direction seemed to be missing. Usually, things end after having arrived at such an agreement, in particular if you are not an economist. However, never-tired, incredibly patient, and gentle insistence by G.O. pushed a bunch of us into preparing for such a journey with him. This book is the result of the journey, where we have been strongly supported by former teachers and academic friends of G.O. Together, we hope that the collected volume will prove helpful in leading a young generation of scholars to new pathways of understanding economics. Specifically, the text aims at providing a bridge between nonlinear dynamics (with chaotic behaviour lurking in the background) towards opening new horizons of insight into economics, by the tools and concepts provided. Therefore, the book starts with a mathematical introduction into nonlinear dynamics, followed by a layout of signal analysis tools and their application to some well-known abstract models of economics generating chaotic response, before we present new insights into how we see economic dynamics. Finally, we present economics models that emerge in this perspective and demonstrate that real-world data supports their validity and usefulness. Since students are the strongest motivation and a main privilege of our profession, I take this opportunity to dedicate my part in this book to my late student and friend Clemens Wagner. Had not his heart suddenly stopped beating before we started writing this book, my contribution would have been with him. I would also like to strongly thank Celso Grebogi for his never-fading generous and unselfish support for everything that advances Nonlinear Science.

Without him, many exciting developments and events (not least the mentioned NDES conferences) would not have been achieved.

We hope that you will find the text inspiring and useful. Let even the parts that you might like less sharpen your view and become beneficial to you in this way as well.

Bari, Italy  
Pozuelo de Alarcón, Madrid, Spain  
Zürich, Switzerland  
May 2021

Giuseppe Orlando  
Alexander N. Pisarchik  
Ruedi Stoop

# Acknowledgments

This book was a long trip with great companions that strengthened both academic and human ties between authors and co-editors. To some extent, this was at the expense of our families, and of friends not engaged in this endeavour.

Giuseppe Orlando, in particular, would like to ask the indulgence of his children Niccolò Libero and Gaia Carmela Francesca who have many good reasons to complain about their father during this period. He would also like to express his sincere gratitude and appreciation to Carlo Lucheroni at the University of Camerino for numerous helpful comments, to Nicola Basile at the University of Bari for valuable suggestions provided, to Luigi Fortuna and his colleagues at the University of Catania for having organized the NDES2019—Nonlinear Dynamics of Electronic Systems Conference and to Edward Bace at the Middlesex University for his help in polishing some of the chapters. Sincere special thanks go to Michele Mininni at the University of Bari who has been a firm point of reference from G.O.'s early study days on. Last but not least, he expresses his profound obligation to his parents, as without support and love by the parents, not much can be accomplished during one's lifetime.

# Contents

<b>1</b>	<b>Introduction</b> .....	1
	Giuseppe Orlando, Alexander N. Pisarchik, and Ruedi Stoop	
<b>Part I Mathematical Background</b>		
<b>2</b>	<b>Dynamical Systems</b> .....	13
	Giuseppe Orlando and Giovanni Tagliatalata	
<b>3</b>	<b>An Example of Nonlinear Dynamical System: The Logistic Map</b> .....	39
	Giuseppe Orlando and Giovanni Tagliatalata	
<b>4</b>	<b>Bifurcations</b> .....	51
	Giuseppe Orlando, Ruedi Stoop, and Giovanni Tagliatalata	
<b>5</b>	<b>From Local Bifurcations to Global Dynamics: Hopf Systems from the Applied Perspective</b> .....	73
	Hiroyuki Yoshida	
<b>6</b>	<b>Chaos</b> .....	87
	Giuseppe Orlando, Ruedi Stoop, and Giovanni Tagliatalata	
<b>7</b>	<b>Embedding Dimension and Mutual Information</b> .....	105
	Giuseppe Orlando, Ruedi Stoop, and Giovanni Tagliatalata	
<b>Part II Signal Analysis and Modelling Tools for Economic Systems</b>		
<b>8</b>	<b>Signal Processing</b> .....	111
	Ruedi Stoop	
<b>9</b>	<b>Applied Spectral Analysis</b> .....	123
	Fabio Della Rossa, Julio Guerrero, Giuseppe Orlando, and Giovanni Tagliatalata	

<b>10</b>	<b>Recurrence Quantification Analysis: Theory and Applications</b> .....	141
	Giuseppe Orlando, Giovanna Zimatore, and Alessandro Giuliani	
<b>Part III Emergence of Cycles and Growth in Economics</b>		
<b>11</b>	<b>On Business Cycles and Growth</b> .....	153
	Giuseppe Orlando and Mario Sportelli	
<b>12</b>	<b>Trade-Cycle Oscillations: The Kaldor Model and the Keynesian Hansen–Samuelson Principle of Acceleration and Multiplier</b> .....	169
	Giuseppe Orlando	
<b>13</b>	<b>The Harrod Model</b> .....	177
	Giuseppe Orlando, Mario Sportelli, and Fabio Della Rossa	
<b>14</b>	<b>Growth and Cycles as a Struggle: Lotka–Volterra, Goodwin and Phillips</b> .....	191
	Giuseppe Orlando and Mario Sportelli	
<b>15</b>	<b>Stable Periodic Economic Cycles from Controlling</b> .....	209
	Ruedi Stoop	
<b>Part IV New Horizons for Understanding Economics</b>		
<b>16</b>	<b>Kaldor–Kalecki New Model on Business Cycles</b> .....	247
	Giuseppe Orlando	
<b>17</b>	<b>Recurrence Quantification Analysis of Business Cycles</b> .....	269
	Giuseppe Orlando and Giovanna Zimatore	
<b>18</b>	<b>An Empirical Test of Harrod’s Model</b> .....	283
	Giuseppe Orlando and Fabio Della Rossa	
<b>19</b>	<b>Testing a Goodwin’s Model with Capacity Utilization to the US Economy</b> .....	295
	Ricardo Azevedo Araujo and Helmar Nunes Moreira	
<b>20</b>	<b>Financial Stress, Regime Switching and Macrodynamics</b> .....	315
	Pu Chen and Willi Semmler	
	<b>Appendix A</b> .....	337
	<b>Back Cover</b> .....	361

# Contributors

**Ricardo Azevedo Araujo** University of Brasilia, Department of Economics, Brasília (DF), Brazil

**Pu Chen** Melbourne Institute of Technology, Melbourne, Australia

**Alessandro Giuliani** Environment and Health, Istituto Superiore di Sanità (ISS), Rome, Italy

**Julio Guerrero** University of Jaén, Department of Mathematics, Jaén, Spain

**Helmar Nunes Moreira** University of Brasilia, Department of Mathematics, Brasília, Brazil

**Giuseppe Orlando** University of Bari, Department of Economics and Finance, Bari, Italy

University of Camerino, School of Sciences and Technology, Camerino, Italy

**Alexander N. Pisarchik** Technical University of Madrid, Center for Biomedical Technology, Campus Montegancedo, Pozuelo de Alarcón, Madrid, Spain

**Fabio della Rossa** University of Naples “Federico II”, Department of Electrical Engineering and Information Technology, Naples, Italy

Department of Electronics Information and Bioengineering, Politecnico di Milano, Milan, Italy

**Willi Semmler** New School for Social Research, Department of Economics, New York, USA

University of Bielefeld, Department of Economics, Universitätsstraße 25, Bielefeld, Germany

**Mario Sportelli** University of Bari, Department of Mathematics, Bari, Italy

**Ruedi (Rudolf) Stoop** ETHZ and University of Zurich, Institute of Neuroinformatics, Zürich, Switzerland

Emeritus and Regent’s Professor, University of Xi’an, Xi’an, P.R. China



**Giovanni Tagliatela** Department of Economics and Finance, Bari, Italy

**Hiroyuki Yoshida** College of Economics, Nihon University, Tokyo, Japan

**Giovanna Zimatore** eCampus University, Department of Theoretical and Applied Sciences, Rome, Italy

# Chapter 1

## Introduction



Giuseppe Orlando, Alexander N. Pisarchik, and Ruedi Stoop

*Philosophy is written in this grand book, the universe, which stands continually open to our gaze. But the book cannot be understood unless one first learns to comprehend the language and read the letters in which it is composed. It is written in the language of mathematics, and its characters are triangles, circles, and other geometric figures without which it is humanly impossible to understand a single word of it; without these, one wanders about in a dark labyrinth.*  
Galileo Galilei  
*The Assayer*

### 1.1 Nonlinearity and Unpredictability in Economics

Until the twentieth century, many mathematical economists, such as Francis Edgeworth, William Jevons, Alfred Marshall, Leon Walras, and Vilfredo Pareto, developed economic models based on principles of Newtonian mechanics by focusing exclusively on static states or equilibrium points. Later, their ideas culminated

---

G. Orlando (✉)

University of Bari, Department of Economics and Finance, Bari, Italy

University of Camerino, School of Sciences and Technology, Camerino, Italy

e-mail: [giuseppe.orlando@uniba.it](mailto:giuseppe.orlando@uniba.it); [giuseppe.orlando@unicam.it](mailto:giuseppe.orlando@unicam.it)

A. N. Pisarchik

Technical University of Madrid, Center for Biomedical Technology, Campus Montegancedo, Pozuelo de Alarcón, Madrid, Spain

e-mail: [alexander.pisarchik@ctb.upm.es](mailto:alexander.pisarchik@ctb.upm.es)

R. Stoop

ETHZ and University of Zurich, Institute of Neuroinformatics, Zurich, Switzerland

Technical University of Xi'an, Xi'an, Shaanxi, China

e-mail: [ruedi@ini.phys.ethz.ch](mailto:ruedi@ini.phys.ethz.ch); [smith@smith.edu](mailto:smith@smith.edu)

© The Author(s), under exclusive license to Springer Nature Switzerland AG 2021

G. Orlando et al. (eds.), *Non-Linearities in Economics*, Dynamic Modeling and Econometrics in Economics and Finance 29,

[https://doi.org/10.1007/978-3-030-70982-2\\_1](https://doi.org/10.1007/978-3-030-70982-2_1)

in a general equilibrium theory (see, for example, Debreu [6], Arrow and Hann [1], etc.). Only at the beginning of the twentieth century, to describe market dynamics in economic models of business cycles, economists did start using difference and differential equations. Ragnar Frisch [10], for example, suggested to study the evolution of economics in time from a dynamical systems viewpoint. The future state of such a system depends only on its past and present. Such a slush in economic theory is largely due to outstanding discoveries of mathematicians in the field of nonlinear dynamics made at the end of the nineteenth century. The most prominent achievements were the development of stability theory by Aleksandr Lyapunov and the solution of three-body problem by Henri Poincaré [32].

Three centuries later, Birkhoff showed that Poincaré's geometric intuition can be cast within a mathematically precise description. This could have been the early official birthday of chaos theory, if aspects of irregular, unpredictable dynamics were recognised as relevant for real-world experimental systems as well. If appropriately perceived, Van der Pol, who presented almost simultaneously with Birkhoff his electronic heart pacemaker circuit (showing, in addition to period "heartbeats" also chaotic behaviour), would have provided this experimental connection.

Originally, the term "chaos" was generally used for dynamical processes that lacked aspects of order that would render their dynamics easily seizable in the sense of predictability. As a consequence, the main understanding was, for a long time, that we would never be able to arrive at a thorough understanding of such phenomena. A chaotic system has specific properties that differ from a stochastic or noisy system. First of all, a chaotic motion is deterministic (in the sense that every event is physically determined by an unbroken chain of earlier events) and crucially depends on initial conditions.

The reason why this more precise notion of chaos took so long to penetrate into the standard science was twofold. First, apart from the mentioned more global approaches, the preferred mathematical analysis methods were linearisation around fixed points of the motion, from which the asymptotic dynamics were extracted. This local approach, however, is sufficient only for linear systems. Nonlinearity provides fixed-objects that are not present in linear systems, such as limit cycles, that are not captured by linearization methods.

Edward Norton Lorenz was among the first to discover in the 1960s a so-called strange attractor in a three-dimensional continuous-time dynamical system, when carrying out numerical experiments on convection flows [15]. Indeed, the advent of direct numerical simulations of differential equations on computers made it finally possible to access and to explore the chaos phenomenology, to anyone for whom computational power was available. Initially, Lorenz was able to publish his work in marginal journals only. Until well into the late 1970s, several physics scholars in the western world, in particular, Mitchell Feigenbaum [2, 7] established the breakthrough of the new view on dynamics. He drew the attention of the scientific society to the ubiquitousness of this phenomenon, and offered new pathways of how to characterise and to predict such phenomena. It would, however, be unfair to withhold the great contributions to this area by scientists of the former Soviet Union, such as Andrey Kolmogorov, Vladimir Arnold, Aleksandr Andronov, Oleksandr

Sharkovsky, and others. In fact, Feigenbaum’s findings aroused interest and finally got accepted only after a presentation of Feigenbaum given to Soviet scientists. Through the research conducted by many scholars not following the scientific mainstream, and their collaborative efforts, it was finally shown that, seen on a higher level, chaotic dynamics is not only ordered [9] and therefore intelligible but also that it is deterministic and controllable [30, 33, 34].

It took some time to work out the fundamentals of chaotic dynamics and then, the analysis proceeded towards the description and the exploitation of chaos for applications. A field that seems particularly attractive and suitable for this is economics that, from its statistical description, can be expected to be organised along the fundamental principles of symmetry breaking and self-organisation as well, and manifests a behaviour that could, with an appropriate permitting analysis, be associated with chaotic processes. Economic dynamics is obviously nonlinear. In particular, it is characterised by cyclical fluctuations called “business cycles”. Burns and Mitchell [4] define business cycles as a type of fluctuation which “consists of expansions occurring at about the same time in many economic activities, followed by similarly general recessions, contractions, and revivals which merge into the expansion phase of the next cycle” (where a recession is a negative variation of the economy for two consecutive quarters cf. Fig. 1.1).

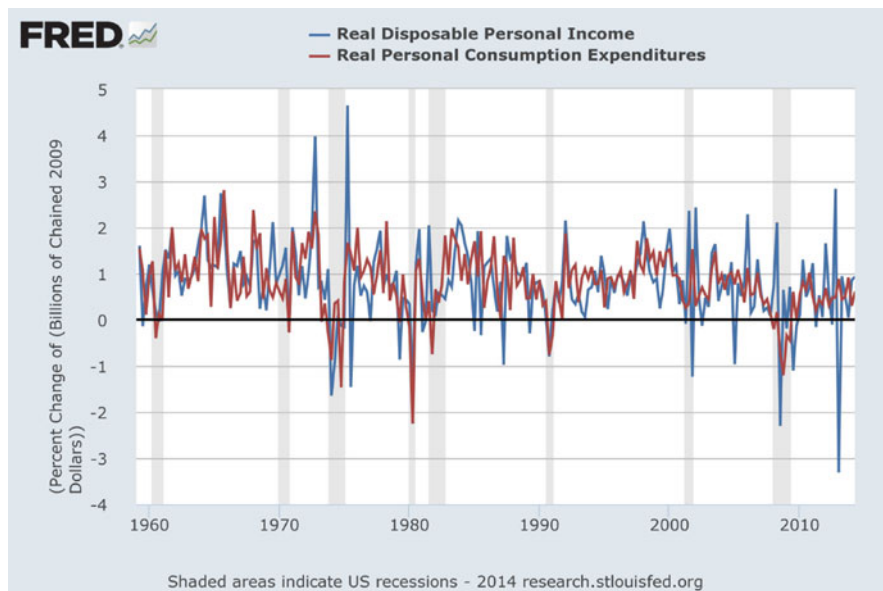


**Fig. 1.1** Changes in US real disposable personal income (i.e., the personal income net of income taxes) (blue—DSPIC96) and Real personal consumption expenditures (red—PCECC96) 1959 (Q1)—2014 (Q2). Source: Federal Reserve Economic Data (FRED), St. Louis Fed. Greyed vertical areas correspond to periods of economic recessions (i.e., economic contraction) as reckoned by FRED (Table A.1)

The emergence of these very robust cycles is one strong motivation for our proposed change of paradigm. In contrast to the stochastic models focusing exclusively on external and random shocks (like the so-called real business cycle (RBC)), we propose to—alternatively or synergetically—consider structural system characteristics that are endogenous (in contrast to the exogenous influences considered in the traditional approaches). In that regard, by comparing an Ornstein–Uhlenbeck stochastic process [22, 23] with a Kaldor–Kalecki [17, 18] deterministic chaotic model, Orlando et al. [28] exhibited that nonlinearity in the latter model permits to represent reality at least as well as the stochastic model. Furthermore, the Kaldor–Kalecki model was able to reproduce an extreme event (black swan [28, 35]). A further confirmation can be found in Orlando et al. [29], where it was shown that real and simulated business cycle dynamics have similar characteristics, thus validating the chaotic model as a suitable tool to simulate reality. Notwithstanding economic dynamics is not purely deterministic, a strong stochastic component always exists and should be included in economic models. Therefore, statistical analysis of economic data is important to reveal the presence of determinism in the behaviour and to forecast future evolution. However, the effect of random fluctuations is unpredictable although probabilistic analysis in financial modelling can provide us with some information about possible scenarios. For example, increasing noise could indicate an impending financial crisis, because the dynamical systems are known [8, 14] to amplify random fluctuations when approaching a critical point. Another promising application of nonlinear analysis methods to economy would be the possibility to predict sudden jumps or drops in stock prices that occur for no apparent reason. By considering these jumps as extreme events, the same approach as for forecasting sudden weather changes [3], giant laser pulses [31], or forthcoming epileptic seizures [11] could be used. Such a research (not included in this book) is still under development.

## 1.2 Scheme of This Book

The whole endeavour taken by this work embraces (i) finding suitable models of business cycles, (ii) searching for indicators for structural changes in economic signals, and (iii) comparing time series generated by the studied models versus real-world time series [27–29]. Our book consists of four parts. Focusing on a particularly attractive class of economic nonlinear models related to growth and business cycles, we explore chaotic behaviour of these models by means of numerical analysis, recurrence quantification, and statistical techniques, and demonstrate that the results are consistent with those obtained by applying the same techniques to time series of real-world macroeconomic data. This implies that with the help of these methods we are able to (i) identify common features between data and model whenever they exist, (ii) to discover features that guide economic dynamics, and (iii) to extract indicators of structural changes in the signal (e.g., precursors of crashes and more general catastrophes). We emphasise the

importance of nonlinear analysis and outline methodological prospects of dynamical approaches which can help to solve fundamental economic problems such as “Is the economy growing?”, “How efficiently are the resources being utilised?”, “Is economy stochastic or deterministic?”, and “Is it possible to predict changes in economy?” These problems cannot be solved by traditional methods of stochastic and linear analyses.

Part I is formal-methodological, providing the mathematical background for the remainder. In the aforementioned part we introduce the reader to the complex system theory and provide the theoretical basis for the rest of the book. This part is divided into Chaps. 2–7. Chapter 2 starts with basic definitions widely accepted in Nonlinear Dynamics, such as types of dynamical systems and attractors, and we derive Schwarz and Sarkovsky theorems that are fundamental theorems in chaos theory.

Then, using the generic example of the Logistic map, in Chap. 3 we demonstrate how the route to chaos proceeds if nonlinearity is increased via a cascade of period-doubling bifurcations when a control parameter is increased. Finally, we describe the main properties of chaos, using measures like information on the corresponding attractors. In Chap. 4 we provide the definition of homoclinic and heteroclinic orbits and we provide a summary on local bifurcations for both the continuous case and the discrete-time case. In Chap. 5, we pay a special tribute to the Hopf bifurcation from the applicative point of view. In fact, the Hopf theorem was one of the most powerful tools to prove the existence of closed orbits for systems of ordinary differential equations. Using two popular dynamical system models, i.e., the Lorenz and Rössler ones, we describe different types of bifurcations and chaotic attractors. Then, we discuss Shilnikov’s chaos through homoclinic orbits and emphasise the importance of the concept of delay-differential equations in economics. Special attention is given to delay-differential equations due to the fact that changes in economy are not immediate. Finally, brief comments on some applications of economic models are added at the end of each section. Chapter 6 first explains the concept of an embedding dimension. Then we discuss the deeper meaning of the term “chaos” and highlight its relation to the sensitive dependence on initial condition, stretching and folding of the phase-space. Statistical measurement characterising these features such as the Lyapunov exponents and measures of attractors are introduced. Finally, the last Chap. 7 is dedicated to the embedding dimension and the mutual information which are relevant for dealing with measured time series and experimental data.

Part II is divided into Chaps. 8–10. Chapter 8 presents a specific view of signal processing. After providing some basic definitions of signal processing, we explain the topic in more detail by a selection of relevant algorithms and approaches. In a nutshell, the idea is that signal processing is a process of computation, that computation describes the process of information destruction, and that the efficacy of this process can be measured. Chapter 9 explains what a signal in economy looks like and what physical properties it has, such as frequency, spectral energy, phase, power, etc. Furthermore, some examples are provided on how to analyse a signal. Chapter 10 is devoted to the so-called recurrence quantification analysis (RQA). We describe mathematical basis and requirements for the recurrent plot analysis. We

explain how this method can be applied to detect spatio-temporal recurrent patterns underlying different dynamical regimes in economic time series. Such analysis allows us to reveal the nature of business cycles and corresponding macroeconomic variables, i.e., whether their character is deterministic or stochastic. Furthermore we show how RQA provides an indicator of structural changes in chaotic time series [25, 26].

As a book on economic dynamics, Part III focuses more on economics itself, providing more specifically economics-related background and literature. While in economics the phenomenon of chaos may be expected to contribute many fascinating aspects, to go beyond purely intellectual constructions with limited real-world explanatory strength, we provide the reader the background information regarding theories on growth and business cycles. In particular, Chap. 11 focuses on the ties between real-world economics and nonlinear dynamics. Chapter 12 provides a sketch of the Keynesian multiplier and of the multiplier-accelerator model by Hansen and Samuelson, and of the Kaldor model. Chapter 13 explains Domar's and the Harrod's model separately. In contrast to standard economic literature that glues those models together, in our view Harrod instability (tested in Chap. 18) has nothing to do with the mathematical notion of the instability characterising the Domar model. Chapter 14 is about the interpretation of cycles as a struggle between capitalists and workers. This is introduced by the Phillips curve (which statistically relates unemployment with the rate of change of nominal wages), followed by the Lotka–Volterra model which is the basic framework of the Goodwin model. The latter reinterprets, in economic terms, the dynamics of prey-predator of biological systems. Chapter 15 explains how control over a system that becomes unstable or highly noisy can be achieved. The objective is to calm down and optimise the system's behaviour. We show that such measures lead to stable cycles in any generic nonlinear system and that hard-limiter control follows a nongeneric dynamical system behaviour with a bifurcation cascade to chaos that is fundamentally distinct from the Feigenbaum case.

Part IV consists of Chaps. 16–20 that are devoted to new perspectives in understanding economics. A reality check on the theories discussed in earlier parts by the means described in Parts I–III is provided. Chapter 16 introduces the experimental Part of the book, following Goodwin's opinion that nonlinearities are the origin of oscillations in economics [12]. We use this approach to study cycles with Kaldor's framework, as is detailed in Chap. 12. The model presented is an alternative to the usual models available in literature [17, 18]. Additional features, such as a full set of parameters and the ability to embed randomness, open the way to a mixture of stochastic and deterministic chaos. Chapter 17 describes an indicator that exhibits structural changes in a signal/time series related to chaos [25]. To achieve that, RQA and statistical techniques are applied, to both real time series and model-generated time series [26]. Our aim is to (i) find common properties if and where they do exist, (ii) discover some hidden features of economic dynamics and (iii) highlight some

indicators of structural changes in the signal (i.e., in our case to look for precursors of a crash). In Chap. 18 we focus on the Harrod's model detailed in Chap. 13. We present a specification of Harrod's model where chaos is a consequence of the gaps between actual, warranted and natural rates of growth. For this model, we prove that real-world economic dynamics can be replicated by a suitable calibration of the parameters of the model. Moreover, we prove that opening the economy to foreign trade can lead to reducing cyclical instability, thus confirming Harrod's conjecture [19]. Chapter 19 presents an extension of the Goodwin growth-cycle model that considers the rate of capacity utilisation as a new variable in an adapted Lotka–Volterra system of differential equations, where capacity utilisation is proportional to the difference between the output expansion function and capital accumulation. With this approach, connections between demand, labour market, and capital accumulation are established in a model that generates a cyclical pattern amongst the employment rate, the profit share, and capacity utilisation. The model is then tested against the US economy, using quarterly data from 1970 to 2019 and the Vector Auto-Regression (VAR). The latter is a stochastic process model widely used in econometrics to capture the linear interdependencies between time series. The conclusion is that positive profit share innovation affects positively both the employment rate and the rate of capacity utilisation, suggesting a profit-led pattern supporting the theoretical model presented (especially to the profit-squeeze mechanism).

Lastly, Chap. 20 summarises advances in nonlinear model predictive control (NMPC) through multi-regime cointegrated VAR (MRCIVAR). The study exhibits the impact of financial stress shocks and monetary policy at macroeconomic level in different countries. The chapter illustrates the vector error correction model (VECM), that is commonly used to model macroeconomic time series, because VECM is able to connect the economic theory around equilibrium and the dynamic process towards the equilibrium into a set of empirically testable relations. The said feature has been exploited to study business cycles during different phases by many (e.g., see Mittnik and Semmler [16], Chen et al. [5] and Hamilton [13]). MRCIVAR is used to examine the impact of real activities on the financial stress. The outcome is that financial shocks have asymmetric effects on the short term interest rate, depending on the regime the economy is in. More precisely, in the rate-cut regime a financial stress shock will decrease the short term rate while, in the non-rate-cut regime, the shock will increase the short term rate (even though in some cases the effects are not statistically significant).

We hope that, with this book we provide some food for thought to a wide audience and stimulate curiosity in approaching economics unconventionally by hybridisation with physics, engineering, and economics. We have left out our research on financial mathematics [20, 21, 23, 24] intentionally, as this matter runs parallel to the presented material as long as market stability, solvency, and resilience of financial institutions are concerned.



## References

1. Arrow, K.J., Hahn, F.: General Competitive Analysis. Holden-Day (1971)
2. Briggs, K.: A precise calculation of the Feigenbaum constants. *Math. Comput.* **57**, 435–439 (1991). <https://doi.org/10.1090/S0025-5718-1991-1079009-6>
3. Broska, L.H., Poganietz, W.R., Vögele, S.: Extreme events defined—a conceptual discussion applying a complex systems approach. *Futures* **115**, 102490 (2020)
4. Burns, A.F., Mitchell, W.C.: Measuring Business Cycles. National Bureau of Economic Research, Cambridge (1946)
5. Chen, P., Semmler, W.: Financial stress, regime switching and spillover effects: evidence from a multi-regime global VAR model. *J. Econ. Dyn. Control* **91**, 318–348 (2018)
6. Debreu, G.: Theory of Value: An Axiomatic Analysis of Economic Equilibrium, vol. 17. Yale University Press, Yale (1959)
7. Feigenbaum, M.J.: Quantitative universality for a class of nonlinear transformations. *J. Stat. Phys.* **19**(1), 25–52 (1978). <https://doi.org/10.1007/BF01020332>
8. Feudel, U., Pisarchik, A.N., Showalter, K.: Multistability and tipping: from mathematics and physics to climate and brain—minireview and preface to the focus issue. *Chaos* **28**, 033501 (2018)
9. Frenkel, D.: Ordered chaos. *Nat. Phys.* **4**, 345 (2008)
10. Frisch, R.: Propagation Problems and Impulse Problems in Dynamic Economics, vol. 3. G. Allen & Unwin, Crows Nest (1933)
11. Frolov, N.S., Grubov, V.V., Maksimenko, V.A., Lüttjohann, A., Makarov, V.V., Pavlov, A.N., Sitnikova, E., Pisarchik, A.N., Kurths, J., Hramov, A.E.: Statistical properties and predictability of extreme epileptic events. *Sci. Rep.* **9**(1), 1–8 (2019)
12. Goodwin, R.M.: The nonlinear accelerator and the persistence of business cycle. *Econometrica* **19**(1), 1–17 (1951)
13. Hamilton, J.D.: Time Series Analysis. Princeton University Press, Princeton (2020)
14. Kravtsov, Y.A., Surovyatkina, E.: Nonlinear saturation of prebifurcation noise amplification. *Phys. Lett. A* **319**(3–4), 348–351 (2003)
15. Lorenz, E.N.: Deterministic nonperiodic flow. *J. Atmos. Sci.* **20**, 130–141 (1963)
16. Mittnik, S., Semmler, W.: Regime dependence of the fiscal multiplier. *J. Econ. Behav. Organ.* **83**, 502–522 (2013)
17. Orlando, G.: A discrete mathematical model for chaotic dynamics in economics: Kaldor’s model on business cycle. *Math. Comput. Simul.* **125**, 83–98 (2016). <https://doi.org/10.1016/j.matcom.2016.01.001>
18. Orlando, G.: Chaotic business cycles within a Kaldor–Kalecki Framework. In: *Nonlinear Dynamical Systems with Self-Excited and Hidden Attractors* (2018). [https://doi.org/10.1007/978-3-319-71243-7\\_6](https://doi.org/10.1007/978-3-319-71243-7_6)
19. Orlando, G., Della Rossa, F.: An empirical test on Harrod’s open economy dynamics. *Mathematics* **7**(6), 524 (2019). <https://doi.org/10.3390/math7060524>
20. Orlando, G., Mininni, R.M., Bufalo, M.: A New Approach to CIR Short-Term Rates Modelling, pp. 35–43. Springer, Berlin (2018). [https://doi.org/10.1007/978-3-319-95285-7\\_2](https://doi.org/10.1007/978-3-319-95285-7_2)
21. Orlando, G., Mininni, R.M., Bufalo, M.: A new approach to forecast market interest rates through the CIR model. *Studies in Economics and Finance* (2019). <https://doi.org/10.1108/SEF-03-2019-0116>
22. Orlando, G., Mininni, R.M., Bufalo, M.: Forecasting interest rates through Vasicek and CIR models: a partitioning approach. *J. Forecasting* **39**, 569–579 (2020). <https://doi.org/abs/10.1002/for.2642>
23. Orlando, G., Mininni, R.M., Bufalo, M.: Interest rates calibration with a CIR model. *J. Risk Financ.* (2019). <https://doi.org/10.1108/JRF-05-2019-0080>
24. Orlando, G., Tagliatalata, G.: A review on implied volatility calculation. *J. Comput. Appl. Math.* **320**, 202–220 (2017). <https://doi.org/10.1016/j.cam.2017.02.002>

25. Orlando, G., Zimatore, G.: RQA correlations on real business cycles time series. In: Indian Academy of Sciences Conference Series—Proceedings of the Conference on Perspectives in Nonlinear Dynamics—2016, vol. 1, pp. 35–41. Springer, Berlin (2017). <https://doi.org/10.29195/iascs.01.01.0009>
26. Orlando, G., Zimatore, G.: Recurrence quantification analysis of business cycles. *Chaos Solitons Fractals* **110**, 82–94 (2018). <https://doi.org/10.1016/j.chaos.2018.02.032>
27. Orlando, G., Zimatore, G.: RQA correlations on business cycles: a comparison between real and simulated data. *Adv. Nonlinear Dyn. Electron. Syst.* **17**, 62–68 (2019). [https://doi.org/10.1142/9789811201523\\_0012](https://doi.org/10.1142/9789811201523_0012)
28. Orlando, G., Zimatore, G.: Business cycle modeling between financial crises and black swans: Ornstein–Uhlenbeck stochastic process vs Kaldor deterministic chaotic model. *Chaos* **30**(8), 083129 (2020)
29. Orlando, G., Zimatore, G.: Recurrence quantification analysis on a Kaldorian business cycle model. *Nonlinear Dyn.* (2020). <https://doi.org/10.1007/s11071-020-05511-y>
30. Ott, E., Grebogi, C., Yorke, J.A.: Controlling chaos. *Phys. Rev. Lett.* **64**(11), 1196 (1990)
31. Pisarchik, A.N., Jaimes-Reátegui, R., Sevilla-Escoboza, R., Huerta-Cuellar, G., Taki, M.: Rogue waves in a multistable system. *Phys. Rev. Lett.* **107**(27), 274101 (2011)
32. Poincaré, H.: *New Methods of Celestial Mechanics*, vol. 13. Springer, Berlin (1992)
33. Romeiras, F.J., Grebogi, C., Ott, E., Dayawansa, W.: Controlling chaotic dynamical systems. *Phys. D: Nonlinear Phenom.* **58**(1–4), 165–192 (1992)
34. Schuster, H.: *Handbook of Chaos Control*. Wiley, London (1999)
35. Taleb, N.N.: *The Black Swan: The Impact of the Highly Improbable*, vol. 2. Random House (2007)

**Part I**  
**Mathematical Background**

# Chapter 2

## Dynamical Systems



Giuseppe Orlando and Giovanni Tagliatela

### 2.1 Dynamical Systems and Their Classification

The concept of dynamical system that we will use here is taken from R.E. Kalman [1] who introduced it in the 1960s while studying the problem of linear filtering and prediction.

Roughly speaking, a system consists of a set of the so-called states (generally vectors of real numbers), where the adjective *dynamics* emphasizes the fact that these states vary in time according to a suitable dynamical law. This concept of dynamical system is cast in the following definition.

**Definition 2.1 (Dynamical System)** A *dynamical system* is an entity defined by the following axioms:

1. There exist an ordered set  $T$  of times, a set  $X$  of states and a function  $\phi$  from  $T \times T \times X$  to  $X$ .  $\phi$  is called a *state transition function*.
2. For all  $t, \tau \in T$  and for all  $x \in X$  one has that  $\phi(t, \tau, x)$  represents the state at time  $t$  of a system whose initial state at time  $\tau$  is  $x$ .
3. The function  $\phi$  satisfies the following properties:

Consistency:  $\phi(\tau, \tau, x) = x$  for all  $\tau \in T$ , and for all  $x \in X$ .

---

G. Orlando (✉)

University of Bari, Department of Economics and Finance, Bari, Italy

University of Camerino, School of Sciences and Technology, Camerino, Italy

e-mail: [giuseppe.orlando@uniba.it](mailto:giuseppe.orlando@uniba.it); [giuseppe.orlando@unicam.it](mailto:giuseppe.orlando@unicam.it)

G. Tagliatela

University of Bari, Department of Economics and Finance, Bari, Italy

e-mail: [giovanni.tagliatela@uniba.it](mailto:giovanni.tagliatela@uniba.it)

Composition:  $\phi(t_3, t_1, x) = \phi(t_3, t_2, \phi(t_2, t_1, x))$ , for all  $x \in X$  and for all  $t_1, t_2, t_3 \in T$  with  $t_1 < t_2 < t_3$ .

In the following we always consider  $X = \mathbb{R}^n$ .

**Definition 2.2 (Reversibility)** If the state transition function  $\phi$  defined for any  $(t, \tau)$  in  $T \times T$ , once assigned the initial time  $\tau$  and the initial state  $x$ , the state of the system is uniquely determined for the future (i.e. for all  $t > \tau$ ), as well as for the past (i.e. for  $t < \tau$ ), the system is said to be *reversible*.

If the state transition function  $\phi$  is defined only for  $t \geq \tau$ , then the system is said to be *irreversible*.

**Definition 2.3 (Event, Orbit and Flow)** For all  $t \in T, x \in X$ , the pair  $(t, x)$  is called an *event*. Moreover, for  $\tau$  and  $x$  fixed, the function  $t \in T \mapsto \phi(t, \tau, x) \in X$  is called a *movement* of the system. The set of all movements is called a *flow*. The image of the movement, i.e. the set

$$\left\{ \phi(t, \tau, x) \mid t \in T \right\},$$

is called an *orbit* (or a *trajectory*) of the system, i.e. the orbit passing through the state  $x$  at time  $\tau$ .

It is not always possible to find a closed formula for the orbits of dynamical systems, but it is possible to study the behaviour of the orbits for long time nonetheless.

**Definition 2.4 (Fixed or Equilibrium Point)** A state  $x^* \in X$  is called a *fixed point* (or an *equilibrium point*) of the dynamics, if there exist  $t_1, t_2 \in T$ , with  $t_2 > t_1$ , such that

$$\phi(t, t_1, x^*) = x^*, \quad \text{for all } t \in T \cap [t_1, t_2].$$

$x^*$  is said to be a *fixed point in an infinite time* if there exists  $t_1 > T$  such that

$$\phi(t, t_1, x^*) = x^* \quad \text{for all } t \in T \cap [t_1, +\infty[.$$

**Definition 2.5 (Eventually Fixed Orbit)** An orbit is said to be *eventually fixed* if it contains a fixed point.

**Definition 2.6 (Eventually Fixed Point)** A point is called *eventually fixed* if its orbit is eventually fixed.

**Definition 2.7 (Stability)** The fixed point  $x^*$  is *stable* if for every  $\varepsilon > 0$  there exist  $\delta > 0$  and  $t_0 \in T$  such that for all  $x \in X$  with  $|x - x^*| \leq \delta$ ,

$$|\phi(t, \tau, x) - x^*| \leq \varepsilon \quad \text{holds for any } t > t_0.$$

The fixed point  $x^*$  is *asymptotically stable* if it is stable and there exists a  $\delta > 0$  such that for all  $x \in X$  with  $|x - x^*| \leq \delta$  it holds that

$$\lim_{t \rightarrow \infty} |\phi(t, \tau, x) - x^*| = 0 \quad \text{holds.}$$

The fixed point  $x^*$  is *globally asymptotically stable* if it is stable and

$$\lim_{t \rightarrow \infty} |\phi(t, \tau, x) - x^*| = 0, \quad \text{for any } \tau \in T \text{ and } x \in X.$$

**Definition 2.8 (Autonomous System)** The system is called *autonomous* if

$$\phi(t, \tau, x) = \tilde{\phi}(t - \tau, x) \tag{2.1}$$

for some suitable function  $\tilde{\phi}$ .

That is, an autonomous system does not explicitly depend on the independent variable. If the variable is time ( $t$ ), the system is called *time-invariant*. For example, the classical harmonic oscillator yields to an autonomous system. A nonautonomous system of  $n$  ordinary first order differential equations can be changed into an autonomous system, by enlarging its dimension using a trivial component, often of the form  $x_{n+1} = t$ .

**Definition 2.9 (Discrete and Continuous System)** The system is called *discrete*, if the time set  $T$  is a subset of the set of the integers  $\mathbb{Z} = \{\dots, -3, -2, -1, 0, 1, 2, 3, \dots\}$ .

The system is called *continuous* if  $T$  is an interval of real numbers.

In Sect. 2.2.1 we consider continuous-time dynamical systems, and in Sect. 2.5 we consider discrete-time dynamical systems.

## 2.2 Continuous-Time Dynamical

### 2.2.1 Continuous-Time Dynamical Systems from Ordinary Differential Equations

Let  $I = [a, b] \subset \mathbb{R}$  and let  $f: I \times \mathbb{R} \rightarrow \mathbb{R}$ .

We recall the following version of the Cauchy–Lipschitz Theorem (see Bonsante and Da Prato[3]).

**Theorem 2.1 (Cauchy–Lipschitz)** Assume that there exists  $L > 0$  such that

$$|f(t, x_1) - f(t, x_2)| \leq L|x_1 - x_2|, \tag{2.2}$$

for any  $t \in I$  and  $x_1, x_2 \in \mathbb{R}$ . Then for any  $\tau \in I$ ,  $\xi \in \mathbb{R}$  the Cauchy problem

$$\begin{cases} \dot{x}(t) = f(t, x(t)) & , t \in I, \\ x(\tau) = \xi \end{cases} \quad (2.3)$$

has a unique solution in  $[a, b]$ .

From Theorem 2.1 it follows that the ordinary differential equation

$$\dot{x} = f(t, x) \quad (2.4)$$

defines a continuous reversible dynamic system. In fact the time set is  $T = I$ , the state set is  $X = \mathbb{R}$  and the state transition function  $\phi$  is the function from  $I \times I \times \mathbb{R}$  to  $\mathbb{R}$  such that for all  $t, \tau \in I$ ,  $\xi \in \mathbb{R}$  one has that

$$\phi(t, \tau, \xi) = x(t),$$

where  $x(t)$  is the unique solution of the Cauchy problem (2.3). In this case the movements are the solutions to Eq. (2.4) and, for any solution  $x$ , the corresponding orbit is on the interval  $\{x(t) \mid t \in I\}$ .

The system is autonomous if, and only if, the function  $f$  does not depend explicitly on  $t$ , that is we have

$$\dot{x}(t) = f(x(t))$$

(i.e. in the case of a differential equation of the form  $\dot{x} = f(x)$ , with  $f: \mathbb{R} \rightarrow \mathbb{R}$  derivable function with continuous and bounded derivative), since in this case one has

$$\phi(t, \tau, x) = \phi(t - \tau, 0, x) \quad \text{for all } t, \tau, x \in \mathbb{R}. \quad (2.5)$$

An equilibrium point is a solution of the differential equation  $\dot{x} = f(x)$ , which is constant on the interval  $J = [t_1, t_2] \subset I$ . Hence, the equilibrium points of the system are the solutions  $x^* \in \mathbb{R}$  of the equation  $f(x) = 0$ .

## 2.2.2 Continuous-Time Dynamical Systems from Systems of Ordinary Differential Equations

The discussion contained in the previous Sect. 2.2.1 for a single equation can be extended to systems of ordinary differential equations.

In fact, if  $\mathbf{x} = (x_1, x_2, \dots, x_n) \in \mathbb{R}^n$ , let  $\mathbf{f} = \mathbf{f}(t, \mathbf{x})$  be a vector function from  $I \times \mathbb{R}^n$  to  $\mathbb{R}^n$ , and let  $f_1, f_2, \dots, f_n$  be the components of  $\mathbf{f}$ .

Assume that  $f_1, f_2, \dots, f_n$  are continuous functions in  $I \times \mathbb{R}^n$ , that the partial derivatives of  $f_1, f_2, \dots, f_n$  with respect to all variables  $x_1, x_2, \dots, x_n$  exist and are continuous in  $I \times \mathbb{R}^n$ , and that these partial derivatives are bounded in  $[a, b] \times \mathbb{R}^n$  for all  $[a, b] \subset I$ .

Then, for all  $t_0 \in I$  and  $\mathbf{x}_0 \in \mathbb{R}^n$  the Cauchy problem

$$\begin{cases} \dot{\mathbf{x}}(t) = \mathbf{f}(t, \mathbf{x}(t)), & t \in I, \\ \mathbf{x}(t_0) = \mathbf{x}_0 \end{cases} \quad (2.6)$$

has one and only one solution on the interval  $I$ .

Therefore, the system of ordinary differential equations

$$\dot{\mathbf{x}}(t) = \mathbf{f}(t, \mathbf{x}(t))$$

defines a *reversible* continuous dynamical system.

The time set is  $T = I$ , the state set is  $X = \mathbb{R}^n$  and the state transition function is the mapping  $\phi$  from  $I \times I \times \mathbb{R}^n$  to  $\mathbb{R}^n$  such that for all  $t, \tau \in I, \mathbf{x} \in \mathbb{R}^n$  one has that  $\phi(t, \tau, \mathbf{x})$  is the value in  $t$  of the unique solution of the Cauchy problem (2.6).

In this case, the movements are solutions of the system (2.6) and, for any solution  $\mathbf{x}(t)$  of such a system of differential equations, the corresponding orbit is a curve in  $\mathbb{R}^n$  of the parametric equation  $\mathbf{x} = \mathbf{x}(t), t \in I$ .

As before, the system is autonomous if  $\mathbf{f}$  is independent of  $t$ , i.e. in the case of a system of differential equations of the form  $\dot{\mathbf{x}} = \mathbf{f}(\mathbf{x})$ . In this case, an equilibrium point is a solution of the system of differential equations  $\dot{\mathbf{x}} = \mathbf{f}(\mathbf{x})$  that is constant on an interval  $J \subset I$ . Thus, the equilibrium points of the system are the solutions  $\mathbf{x}^* \in \mathbb{R}^n$  of the system of equations  $\mathbf{f}(\mathbf{x}^*) = \mathbf{0}$ .

*Remark 2.1* A nonautonomous system of  $n$  ordinary first order differential equations can be changed into an autonomous system, by enlarging its dimension using a trivial component, often of the form  $x_{n+1} = t$ .

*Remark 2.2* The notion of dynamical system, as outlined in Definition 2.1, describes the case in which the evolution of the system depends only on internal causes.

However, there are situations where the evolution of the system can be modified through the action of external forces, i.e. by means of a time-dependent input vector function  $\mathbf{u}$ . In this case Definition 2.1 can be generalized in the sense that a dynamic system is characterized by a time set  $T$ , a state set  $X$ , an input set  $U$  with a set  $\Omega$  of admissible input functions from  $T$  to  $U$  and a state transition function  $\phi$  from  $T \times T \times X \times \Omega$  to  $X$  such that for all  $t, \tau \in T, \mathbf{x} \in X, \mathbf{u} \in \Omega, \phi(t, \tau, \mathbf{x}, \mathbf{u})$  represents the state of the system at time  $t$ , if the state is  $\mathbf{x}$  at time  $\tau$  with an input function  $\mathbf{u}$  acting on the system.



Obviously, the state of the system at time  $t$  will only depend on the initial time  $\tau$ , the initial state  $\mathbf{x}$  and the restriction of the input function  $\mathbf{u}$  to the interval of extremes  $t$  and  $\tau$ . Hence, we have to assume that the state transition function  $\phi$  satisfies the following properties.

Consistency:  $\phi(\tau, \tau, \mathbf{x}, \mathbf{u}) = \mathbf{x}(\tau) \quad \forall (\tau, \mathbf{x}, \mathbf{u}(\cdot)) \in T \times X \times \Omega$ .

Composition:  $\phi(t_3, t_1, \mathbf{x}, \mathbf{u}) = \phi(t_3, t_2, \phi(t_2, t_1, \mathbf{x}, \mathbf{u}), \mathbf{u})$  for each  $(\mathbf{x}, \mathbf{u}) \in X \times \Omega$ , and for each  $t_1 < t_2 < t_3$ .

Causality: If  $\mathbf{u}, \mathbf{v} \in \Omega$  and  $\mathbf{u}|_{[\tau, t]} = \mathbf{v}|_{[\tau, t]}$ , then  $\phi(t, \tau, \mathbf{x}, \mathbf{u}) = \phi(t, \tau, \mathbf{x}, \mathbf{v})$ .

This framework can be used for theoretical approaches in continuous-time systems.

### 2.3 Stability of Continuous-Time Systems

We recall some known facts about the *exponential* of square matrix.

**Definition 2.10 (Exponential of Square Matrix)** Given a square matrix  $A$ , the *exponential* of  $A$  is defined by

$$\exp(A) = \sum_{j=0}^{+\infty} \frac{1}{j!} A^j = I + A + \frac{1}{2} A^2 + \frac{1}{6} A^3 + \cdots + \frac{1}{j!} A^j + \cdots$$

The basic properties of the exponential are listed below:

- If  $0$  is the null matrix, then  $\exp(0) = I$ .
- If  $A$  and  $B$  commute, that is  $AB = BA$ , then  $\exp(A) \exp(B) = \exp(A + B)$ .  
In particular  $\exp(\alpha A) \exp(\beta A) = \exp((\alpha + \beta)A)$ , for any  $\alpha, \beta \in \mathbb{R}$ .
- For any square matrix  $A$ ,  $\exp(A)$  is invertible; moreover

$$[\exp(A)]^{-1} = \exp(-A).$$

- $\exp(A^T) = \exp(A)^T$ .
- $\det(\exp(A)) = e^{\text{tr}(A)}$ , where  $\text{tr}(A)$  denotes the trace of  $A$ .
- If  $B = PAP^{-1}$ , where  $P$  is an invertible matrix, then

$$\exp(B) = P \exp(A) P^{-1}.$$

- If  $A$  is diagonal

$$A = \begin{pmatrix} \lambda_1 & 0 & \dots & 0 \\ 0 & \lambda_2 & & \\ \vdots & & \ddots & \vdots \\ 0 & \dots & & 0 & \lambda_n \end{pmatrix},$$

then

$$\exp(A) = \begin{pmatrix} e^{\lambda_1} & 0 & \dots & 0 \\ 0 & e^{\lambda_2} & & 0 \\ \vdots & & \ddots & \vdots \\ 0 & \dots & & 0 & e^{\lambda_n} \end{pmatrix}.$$

When we deal with a linear system of differential equations expressed in matrix form as

$$\dot{\mathbf{x}} = A\mathbf{x},$$

$A$  being a fixed matrix, the solution for the initial point  $\mathbf{x}_0$  at  $t = 0$  is given by

$$\mathbf{x}(t) = \exp(tA) \mathbf{x}_0.$$

Indeed, as

$$\mathbf{x}(t) = \sum_{j=0}^{+\infty} \frac{t^j}{j!} A^j \mathbf{x}_0$$

we have

$$\begin{aligned} \dot{\mathbf{x}}(t) &= \sum_{j=1}^{+\infty} \frac{t^{j-1}}{(j-1)!} A^j \mathbf{x}_0 = \sum_{j=0}^{+\infty} \frac{t^j}{j!} A^{j+1} \mathbf{x}_0 \\ &= A \sum_{j=0}^{+\infty} \frac{t^j}{j!} A^j \mathbf{x}_0 = A \mathbf{x}(t). \end{aligned}$$

We can obtain the behaviour of the solution  $\mathbf{x}(t)$  by studying the eigenvalues of the matrix  $A$ . Indeed, assume for example that  $A$  is diagonalizable and all the eigenvalues  $\lambda_j$ ,  $j = 1, \dots, n$ , have negative real part. We then have

$$\mathbf{x}(t) = \exp(tA) \mathbf{x}_0 = P \begin{pmatrix} e^{\lambda_1 t} & 0 & \dots & 0 \\ 0 & e^{\lambda_2 t} & & 0 \\ \vdots & & \ddots & \vdots \\ 0 & \dots & & 0 & e^{\lambda_n t} \end{pmatrix} P^{-1} \mathbf{x}_0,$$

for some invertible matrix  $P$ . As  $e^{\lambda_n t} \rightarrow 0$  for  $t \rightarrow +\infty$ , we see that the solution  $\mathbf{x}(t) = \mathbf{0}$  is stable.

The Hartman–Grobman Theorem 2.2 given below will elucidate the behaviour around the fixed points of nonlinear systems by a linearization in a neighbourhood

of the equilibrium. To this end, we need to introduce the following definitions (Zimmerman [11]).

**Definition 2.11 (Homeomorphism)** A function  $h: X \rightarrow Y$  is a *homeomorphism* between  $X$  and  $Y$  if it is continuous and bijective (one-to-one and onto function) with a continuous inverse denoted by  $h^{-1}$ .

*Remark 2.3* A homeomorphism means that  $X$  and  $Y$  have similar structure and that  $h$  (resp.,  $h^{-1}$ ) may stretch and bend the space but does not tear it.

**Definition 2.12 (Diffeomorphism)** A function  $f: U \subseteq \mathbb{R}^n \rightarrow V \subseteq \mathbb{R}^n$  is called *diffeomorphism of class  $C^k$*  if it is surjective (onto) and injective (one-to-one), and if the components of  $f$  and its inverse have continuous partial derivatives up to the  $k$ -th order with respect to all variables.

**Definition 2.13 (Embedding)** An *embedding* is a homeomorphism onto its image.

**Definition 2.14 (Topological Conjugacy)** Given two maps,  $f: X \rightarrow X$  and  $g: Y \rightarrow Y$ , the map  $h: X \rightarrow Y$  is a *topological semi-conjugacy* if it is continuous, surjective and  $h \circ f = g \circ h$ , with  $\circ$  function composition.

In addition, if  $h$  is a homeomorphism between  $X$  and  $Y$ , then we say that  $h$  is a *topological conjugacy* and that  $X$  and  $Y$  are homomorphic.

**Definition 2.15 (Hyperbolic Fixed Point)** In the case of continuous-time dynamical system,

$$\dot{\mathbf{x}} = \mathbf{f}(\mathbf{x}),$$

a *hyperbolic fixed point* is a fixed point  $\mathbf{x}^*$  for which all the eigenvalues of the Jacobian matrix

$$D\mathbf{f} = \begin{pmatrix} \partial_{x_1} f_1 & \partial_{x_1} f_2 & \dots & \partial_{x_1} f_n \\ \partial_{x_2} f_1 & \partial_{x_2} f_2 & \dots & \partial_{x_2} f_n \\ \vdots & & & \\ \partial_{x_n} f_1 & \partial_{x_n} f_2 & \dots & \partial_{x_n} f_n \end{pmatrix}$$

calculated in  $\mathbf{x}^*$  have a non-zero real part.

**Theorem 2.2 (Hartman–Grobman)** Let  $\mathbf{f}$  be  $C^1$  on some  $E \subset \mathbb{R}^n$  and let  $\mathbf{x}^*$  be a hyperbolic fixed point that without loss of generality we can assume  $\mathbf{x}^* = \mathbf{0}$ . Consider the nonlinear system  $\dot{\mathbf{x}} = \mathbf{f}(\mathbf{x})$  with flow  $\phi(t, 0, \mathbf{x})$  and the linear system  $\dot{\mathbf{x}} = \mathbf{A}\mathbf{x}$ , where  $\mathbf{A}$  is the Jacobian  $D\mathbf{f}(\mathbf{0})$ . Let  $I_0 \subset \mathbb{R}$ ,  $X \subset \mathbb{R}^n$  and  $Y \subset \mathbb{R}^n$  such that  $X$ ,  $Y$  and  $I_0$  each contain the origin. Then, there exists a homeomorphism  $H: X \rightarrow Y$  such that for all initial points  $\mathbf{x}_0 \in X$  and all  $t \in I_0$

$$H(\phi(t, 0, \mathbf{x}_0)) = e^{t\mathbf{A}}H(\mathbf{x}_0)$$

holds. Thus, the flow of the nonlinear system is homeomorphic to  $e^{tA}$  (i.e. to the flow of the linearized system).

A sufficient condition for an equilibrium  $\mathbf{x}_a$  to be stable is given by the following theorem.

**Theorem 2.3 (Lyapunov [8])** *Let  $\Omega$  be an open subset of  $\mathbb{R}^n$ , and  $\mathbf{f} : \Omega \rightarrow \mathbb{R}^n$  be a  $C^1$  function. Let  $\mathbf{x}_a \in \Omega$  be a zero of  $\mathbf{f}$ .*

*Consider the dynamical system*

$$\dot{\mathbf{x}}(t) = \mathbf{f}(\mathbf{x}(t)), \quad \mathbf{x} \in \mathbb{R}^n.$$

*The equilibrium  $\mathbf{x}(t) = \mathbf{x}_a$  is stable if all the eigenvalues of the Jacobian matrix of  $\mathbf{f}$  at  $\mathbf{x}_a$  have a negative real part.*

We end this section recalling a useful tool to prove the stability of equilibria.

**Definition 2.16 (Lyapunov Function)** Let  $\mathbf{f} : \mathbb{R}^n \rightarrow \mathbb{R}^n$ , with  $\mathbf{f}(\mathbf{x}_0) = \mathbf{0}$ , and consider the autonomous dynamical system

$$\dot{\mathbf{x}}(t) = \mathbf{f}(\mathbf{x}(t)),$$

so that  $\mathbf{x}(t) \equiv \mathbf{x}_0$  is an equilibrium point.

A *weak Lyapunov function* (resp., a *strong Lyapunov function*) with respect to  $\mathbf{x}_0$  is a scalar  $C^1$  function  $L$  defined in a neighbourhood  $\mathcal{U}$  of  $\mathbf{x}_0$  such that:

- $L(\mathbf{x}_0) = 0$  and  $L(\mathbf{x}) > 0$  for all  $\mathbf{x} \in \mathcal{U} \setminus \{\mathbf{x}_0\}$ ;
- $\nabla V(\mathbf{x}) \cdot \mathbf{f}(\mathbf{x}) > 0$  (resp.,  $\nabla V(\mathbf{x}) \cdot \mathbf{f}(\mathbf{x}) \geq 0$ ) for all  $\mathbf{x} \in \mathcal{U} \setminus \{\mathbf{x}_0\}$ .

**Theorem 2.4** *If there exists a weak Lyapunov function (resp., a strong Lyapunov function) with respect to the point  $\mathbf{x}_0$ , then  $\mathbf{x}_0$  is Lyapunov stable. (resp., asymptotically stable).*

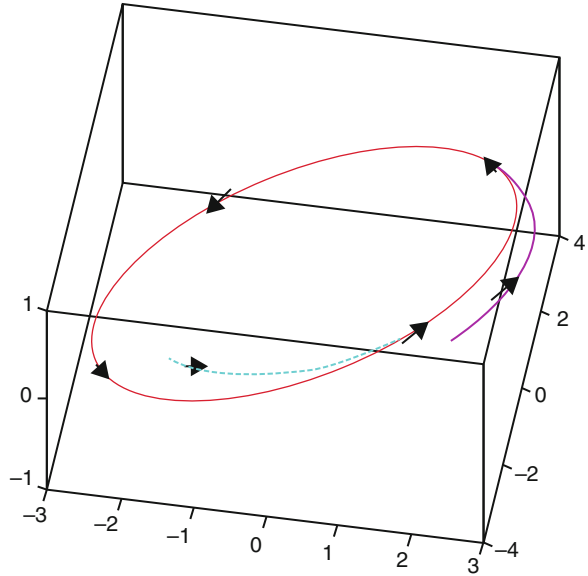
## 2.4 Limit Cycles and Periodicity of Continuous-Time Systems

In this section we consider a continuous-time dynamical system described by the state transition function  $\phi(t, \tau, x)$ . If differently specified, the following definitions and results are taken from R. Devaney [5], H. W. Lorenz [7] and S. Sternberg [10]

**Definition 2.17 (Limit Cycle)** A limit cycle (see Fig. 2.1) is a closed orbit  $\Gamma$  for which there exists a tubular neighbourhood  $U(\Gamma)$  [9] such that for all  $x \in U(\Gamma)$  one has

$$\lim_{t \rightarrow +\infty} d(\phi(t, \tau, x), \Gamma) = 0, \tag{2.7}$$

**Fig. 2.1** A limit cycle in the three-dimensional phase space



where we have

$$d(y, \Gamma) = \inf_{z \in \Gamma} |y - z|. \quad (2.8)$$

In order to establish the existence of limit cycles, in the two-dimensional case, we can refer to the following theorem by Poincaré and Bendixson.

**Theorem 2.5 (Poincaré–Bendixson [7])** *Let  $D$  be a non-empty, compact (i.e. closed and bounded) set of the plane not containing fixed points of a  $C^1$  vector field  $f$  from  $D$  to  $\mathbb{R}^2$  and let  $\gamma \subset D$  be an orbit of the system  $\dot{x} = f(x)$ . Then, either  $\gamma$  is a closed orbit or  $\gamma$  asymptotically approaches a closed orbit (i.e. there exists a limit cycle in  $D$ ).*

The limitations of Theorem 2.5 are related to finding a suitable set  $D$  and to the fact that it is valid only in two dimensions. For example, we suppose that there exists a compact set  $D \subset \mathbb{R}^3$  with the vector field pointing inwards to  $D$  (see Fig. 2.2b) and that there is a unique unstable equilibrium. Nevertheless, it is possible that no closed orbit exists because a trajectory can arbitrarily wander in  $\mathbb{R}^3$  without neither intersecting itself nor approaching a limit set (see Fig. 2.3).

It is a simple consequence of the theorem of Poincaré and Bendixson together with the uniqueness of the solutions of such systems that while two-dimensional systems can produce limit cycles, for obtaining chaos, dimension three is required.

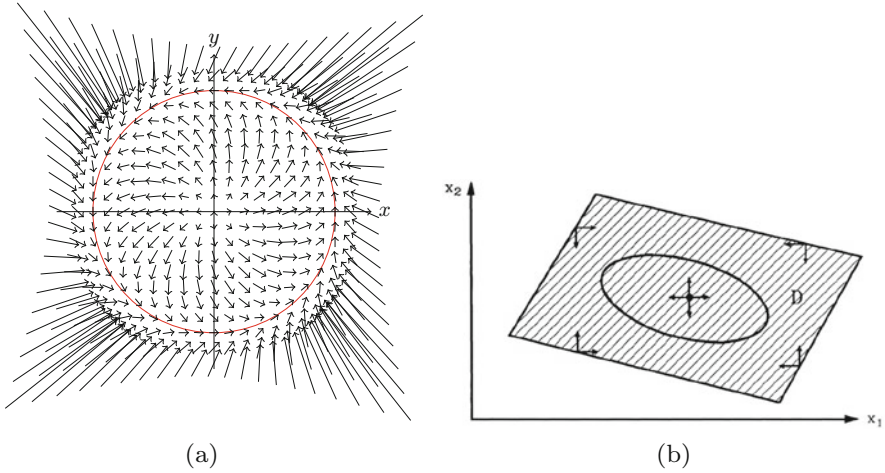


**Fig. 2.2** Convergence to the limit cycle. On the boundary of  $D$ , the vector field points inwards the set. Therefore, once a trajectory enters in  $D$ , it will stay on it forever. **(a)** A system with a stable limit cycle in a vector field. **(b)** Limit cycle in a compact set  $D$  [7]

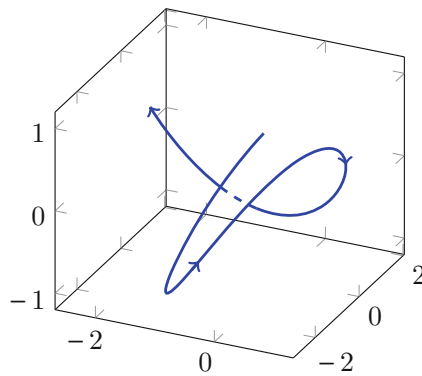


**Fig. 2.3** In  $\mathbb{R}^3$  Poincaré–Bendixson is invalid

The following result, in contrast to Theorem 2.5, provides a criterion to establish the non-existence of closed orbits of a dynamical system in  $\mathbb{R}^2$ :

**Theorem 2.6 (Bendixson Negative Criterion [2])** *Let*

$$B_R = \{(x, y) \in \mathbb{R}^2 \mid x^2 + y^2 < R\},$$

*with  $R > 0$ , and let  $f, g \in C^1(B_R)$  be such that*

$$\partial_x f(x, y) + \partial_y g(x, y)$$

*has constant sign and vanishes only at a finite number of points.*

Then there exists no closed orbits in  $B_R$  of the autonomous system

$$\begin{cases} x' = f(x, y) \\ y' = g(x, y). \end{cases}$$

Theorem 2.6 holds true in a more general setting: we can replace  $B_R$  by a generic *simply connected* subset of  $\mathbb{R}^2$ , and assume that  $\partial_x f(x, y) + \partial_y g(x, y)$  has constant sign except a set with zero measure.

In the one-dimensional systems, there are no periodic solutions. To put it another way, trajectories increase or decrease monotonically, or remain constant. What is more, the Poincaré–Bendixson theorem provides an important result in the two-dimensional systems. It states that if a trajectory is confined to a closed and bounded region that contains no equilibrium points, then the trajectory must eventually approach a closed orbit. This result implies that chaotic attractors cannot happen in nonlinear planar dynamical systems.

## 2.5 Discrete-Time Dynamical Systems

**Definition 2.18 (Map)** Let  $X$  be a subset of  $\mathbb{R}^d$ ,  $d \geq 1$ , and let  $f: X \rightarrow X$  be any function. The recursive formula

$$x_{n+1} = f(x_n) \tag{2.9}$$

defines a discrete dynamical system referred to as a *d-dimensional map*.

If we denote by the symbol  $f^{\circ n}$  the *n-th iterate* of  $f$ , i.e. for  $n = 0$   $f^{\circ 0}$  is the identity on  $X$  and for  $n \geq 1$  the composition of  $f$  with itself  $n$  times, that is

$$f^{\circ n}(x) = \begin{cases} x & \text{if } n = 0, \\ f(x) & \text{if } n = 1, \\ (f \circ f^{\circ(n-1)})(x) = f(f^{\circ(n-1)}(x)) & \text{if } n > 1, \end{cases} \tag{2.10}$$

then the state transition function  $\phi$  is defined by

$$\phi(t, \tau, x) = f^{\circ(t-\tau)}(x) \quad \text{for all } t, \tau \in \mathbb{N}, \text{ and } t \geq \tau, \tag{2.11}$$

since it is evident that  $\phi$  satisfies the consistency and composition properties.

In this case, a movement is a sequence  $\{x_n\}_{n \in \mathbb{N}}$  such that  $x_{n+1} = f(x_n)$  for all  $n$ , whereas an *orbit* is a set of the form  $\{x_0, x_1, x_2, \dots, x_n, \dots\}$  with  $x_{n+1} = f(x_n)$  for all  $n \in \mathbb{N}$ .

In the following we focus on 1-dimensional dynamical systems.

*Example 2.1* If  $d = 1$ , and  $f(x) = x^2$ , the orbit of  $f$  with initial point  $x_0 = 2$  is the set  $\{2, 4, 16, 256, \dots\} = \{2^{2^n}\}_{n \in \mathbb{N}}$ .

*Remark 2.4* Note that the dynamical system defined by Eq. (2.9) is autonomous (cfr. Eq. (2.1)). Moreover it is reversible if and only if the function  $f$  is bijective.

Indeed, if  $f^{-1}$  is the inverse of  $f$ , we can extend the definition of  $f^{on}$  also to negative  $n$  by

$$f^{\circ(-n)} = (f^{-1})^{\circ n}, \quad \text{for } n \in \mathbb{N};$$

hence, (2.11) holds true also for  $t < \tau$ .

*Example 2.2* If  $f(x) = x^2$ , as  $f$  is not injective, the associated dynamical system is not reversible: by knowing  $x_1 = 1$ , one cannot deduce if the initial point is  $x_0 = 1$  or  $x_0 = -1$ .

**Definition 2.19 (Fixed or Equilibrium Point for a Discrete-Time System)** A *fixed point* (or a *equilibrium point*)  $x^*$  is a point of  $X$  such that  $f(x^*) = x^*$ . In this discrete-time case, the orbit departing from  $x^*$  is the singleton  $\{x^*\}$ .

*Example 2.3* Let  $f(x) = x^2$ .

The points 0 and 1 are the only fixed points for  $f$ . The point  $x = -1$  is not fixed, but it is an eventually fixed point for  $f$  because  $f(-1) = 1 \neq -1$ .

**Definition 2.20 (Periodic orbit, cycle)** The orbit of initial point  $x_0$  is said to be *periodic*, or a *cycle*, if there exists  $p \in \mathbb{N}$  such that  $f^{\circ p}(x_0) = x_0$ . In this case,  $x_0$  is a *periodic* (or a *cyclic*) point.

The smallest number  $p$  such that  $f^{\circ p}(x_0) = x_0$  is called the *period* of  $x_0$  (or of its orbit). To emphasize the period  $p$ , we say that  $x_0$  (or its orbit) is a *p-periodic point* (or a *p-periodic orbit*).

*Remark 2.5* A periodic orbit means that after a finite number of iterations we return to the initial point and therefore the orbit has a finite number of elements.

*Remark 2.6 (Period of an Orbit)* A point  $x_0$  is periodic of period  $p$  if and only if  $x_0$  is a fixed point of  $f^{\circ p}$ . In particular, a fixed point  $x_0$  for  $f$  is fixed for all iterates of  $f$ .

Often, fixed points are also called period-1 fixed points.

*Example 2.4* If  $f(x) = -x$ , then  $x_0 = 0$  is the only fixed point of  $f$  and all other points have period 2, the orbits being the sets of the form  $\{x, -x\}$ .



**Definition 2.21 (Eventually Periodic Orbit)** An orbit is said to be *eventually periodic* if it contains a periodic point. Analogously, a point is called *eventually periodic* if its orbit is eventually periodic.

*Example 2.5* Consider the function  $f(x) = 1 - x^4$ . The point  $x_0 = -1$  is an eventually periodic point because  $f(-1) = 0$  and 0 is contained in the cycle  $(0, 1)$ .

*Remark 2.7 (Recursive Methods for Finding Fixed Points)* Recursive expressions of the form of Eq. (2.9) are often used in numerical computations for solving equations. An example is given by the so-called Babylonian algorithm to approximate the square root of a number  $a > 0$

$$x_{n+1} = \frac{1}{2} \left( x_n + \frac{a}{x_n} \right). \quad (2.12)$$

A more general algorithm is the Newton method of approximating zero of a differentiable function  $g$  as

$$x_{n+1} = x_n - \frac{g(x_n)}{g'(x_n)}. \quad (2.13)$$

For example, if  $g(x) = x^2 - a$ ,  $g'(x) = 2x$ , then the Newton algorithm in Eq. (2.13) reduces to Eq. (2.12).

### 2.5.1 Cobweb Diagram

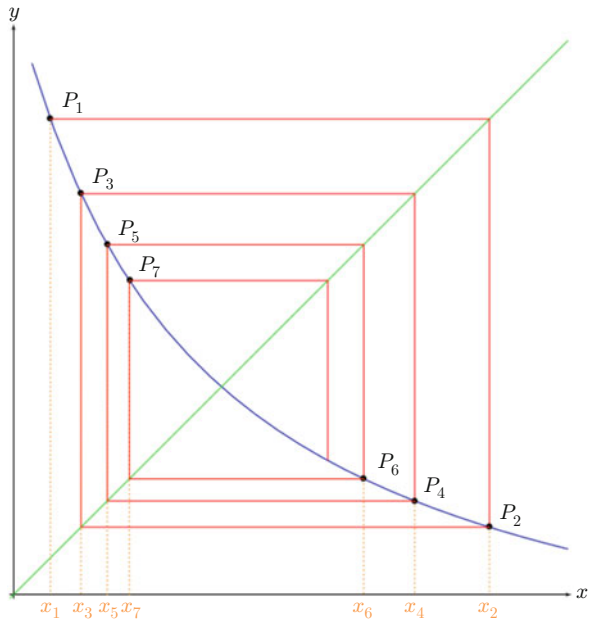
For a one-dimensional map  $f$ , the *cobweb diagram* (or *Verhulst diagram*) is a method to graphically describe the orbit of an initial point  $x_0$ .

After drawing the graph of  $f(x)$  and the bisector  $r$  of first and third quadrants, draw the point  $P_0 \equiv (x_0, f(x_0))$ .

Let  $x_1 = f(x_0)$ , draw the horizontal line from  $P_0$  to the point on  $r$  with coordinates  $(x_1, x_1)$  and draw the vertical line from this point to the graph of  $f$  with coordinates  $P_1 \equiv (x_1, f(x_1))$ .

For higher iterates we repeat the procedure. From  $x_2 = f(x_1)$ , we draw the horizontal line from  $P_1$  to the point on  $r$  with coordinates  $(x_2, x_2)$  and the vertical line from this point to the graph  $f$  with coordinates  $P_2 \equiv (x_2, f(x_2))$  (Fig. 2.4).

**Fig. 2.4** The cobweb diagram



## 2.6 Attractors and Repellers

In this section, we provide some definitions concerning the behaviour of dynamical systems that, unless differently specified, follow the conventions in R. Devaney [5], H. W. Lorenz [7] and S. Sternberg [10].

Throughout the section  $f : \mathbb{R} \rightarrow \mathbb{R}$  is a twice continuously differentiable function, and  $f^{on}$  denotes its  $n$ -th iterate (cf. (2.10)).

**Definition 2.22 (Critical Point)** We say that  $x_c \in \mathbb{R}$  is a *critical point* of  $f$  if  $f'(x_c) = 0$ .

The critical point  $x_c$  is *degenerate* if  $f''(x_c) = 0$  and *non-degenerate* if  $f''(x_c) \neq 0$ .

*Remark 2.8* Degenerate critical points may be maxima, minima or inflection points; non-degenerate critical points, instead, must be either maxima or minima.

*Example 2.6* Consider the functions  $f_n(x) = x^n, n \in \mathbb{N}$ .

If  $n \geq 2$ , then  $f_n$  has a critical point in  $c = 0$ . In particular, if  $n = 2$  the critical point is non-degenerate, whereas if  $n > 2$  the critical point is degenerate.

If  $n$  is even, the critical point is a minimum, whereas if  $n$  is odd the critical point is an inflection point.

*Remark 2.9 (Classification of Critical Points [4])* A critical point can be stable if the orbit of the system is inside a bounded neighbourhood to the point for all times  $n$

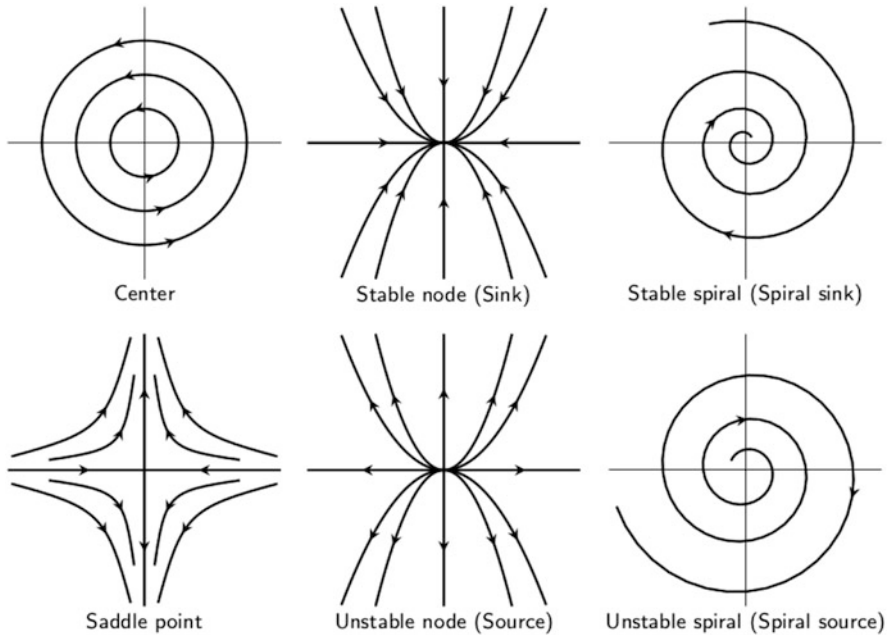


**Fig. 2.5** Different examples of critical points. From top left clockwise: a centre denoting a stable but not asymptotically stable point, an asymptotically stable node and an asymptotically stable spiral both denoted as a *sink*. Then an unstable spiral and an unstable node, i.e. *source*. Last figure shows a saddle node where some orbits converge and some others diverge

after some  $n^*$ . A point is asymptotically stable if it is stable and the orbit approaches the critical point as  $n \rightarrow \infty$ . If a critical point is not stable, then it is unstable (see Fig. 2.5). In some instances these critical points could have mixed characteristics (see Fig. 2.6).

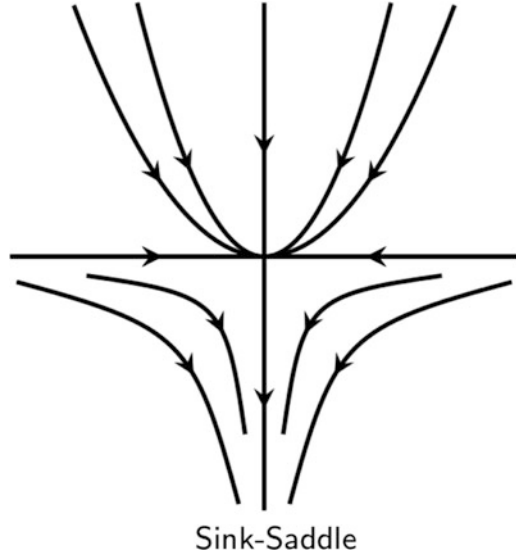
**Definition 2.23 (Limit Set)** Given  $x \in X$ , the *limit set* of  $x$  is the set  $A$  of points  $\omega \in X$  for which there is an increasing sequence of natural numbers  $\{n_j\}_{j \in \mathbb{N}}$  such that

$$\lim_{j \rightarrow +\infty} f^{n_j}(x) = \omega.$$

**Definition 2.24 (Attractor)** A compact (i.e. a closed and bounded) set  $A \subset X$  is an *attractor* if there is an open set  $U$  containing  $A$  such that  $A$  is a limit set of all points in  $U$ .

**Definition 2.25 (Basin of Attraction)** The set of all  $x$  having  $A$  as limit set is called the *basin of attraction* of  $A$ .

**Fig. 2.6** A critical point combining a sink (I and II quadrants) and saddle (III and IV quadrants)



*Remark 2.10* In particular, a singleton  $\{x_a\}$  is an attractor if there exists  $\delta > 0$  such that for all  $x \in ]x_a - \delta, x_a + \delta[$  the sequence  $(f^{on}(x))_{n \in \mathbb{N}}$  has a subsequence converging to  $x_a$ .

**Theorem 2.7** Let  $x_a$  be a fixed point of  $f$  with  $|f'(x_a)| < 1$ . Then  $a$  is asymptotically stable and the set  $\{x_a\}$  is an attractor.

More precisely there exists  $\delta > 0$  such that for all  $x \in ]x_a - \delta, x_a + \delta[$  the sequence  $(f^{on}(x))_n$  tends to  $x_a$ .

**Proof** Let  $K \in \mathbb{R}$  be such that  $|f'(x_a)| < K < 1$ , as

$$\lim_{x \rightarrow x_a} \frac{|f(x) - x_a|}{|x - x_a|} = \lim_{x \rightarrow x_a} \left| \frac{f(x) - f(a)}{x - x_a} \right| = |f'(x_a)| < K$$

and since there exists  $\delta > 0$  such that for all  $x \in ]x_a - \delta, x_a + \delta[$ , one has

$$\left| \frac{f(x) - f(a)}{x - x_a} \right| < K .$$

Hence

$$|f(x) - x_a| < K|x - x_a| < K\delta . \tag{2.14}$$

As  $K < 1$  we deduce that if  $x_0 \in ]x_a - \delta, x_a + \delta[$ , then  $x_1 = f(x_0) \in ]x_a - \delta, x_a + \delta[$ .

Applying (2.14) to  $x = x_n$ , we have

$$|x_{n+1} - x_a| < K|x_n - x_a|,$$

as  $x_{n+1} = f(x_n)$ . Thus it follows by induction that for all  $x_0 \in ]x_a - \delta, x_a + \delta[$  and for all  $n \in \mathbb{N}$  one has that

$$|x_n - x_a| < K^n|x_0 - x_a| < K^n\delta.$$

Hence, for all  $x_0 \in ]x_a - \delta, x_a + \delta[$  the distance of  $f^{on}(x_0)$  from  $a$  decreases at a geometric rate  $K < 1$  and therefore tends to 0, as desired.

*Remark 2.11* If one has  $f'(0) = 0$ , then the preceding argument shows that the distance of  $f^{on}(x)$  from  $a$  decreases at a geometric rate  $K$  for all  $K \in ]0, 1[$ .

The above remark justifies the following definition.

**Definition 2.26 (Superattractor)** A fixed point  $x^*$  such that  $f'(x^*) = 0$  is called a *superattractor* or *superstable*.

*Remark 2.12* If  $|f'(x_a)| > 1$ , then, for a fixed  $K \in \mathbb{R}$  such that  $1 < K < |f'(x_a)|$ , there exists  $\delta > 0$  such that for all  $x \in ]x_a - \delta, x_a + \delta[$  one has  $|f(x) - x_a| > K|x - x_a|$ ; hence the distance of  $f^{on}(x)$  from  $a$  increases at a geometric rate  $K > 1$ , and therefore there exists  $n \in \mathbb{N}$  such that  $|f^{on}(x) - x_a| > \delta$ .

This motivates the following definition.

**Definition 2.27 (Repeller)** A fixed point  $x^*$  with  $|f'(x^*)| > 1$  is called *unstable* or a *repeller*.

*Example 2.7* Let us consider a function  $g$  twice continuously differentiable and the Newton method of Eq. (2.13). In this case

$$f(x) = x - \frac{g(x)}{g'(x)}, \quad (2.15)$$

and hence

$$f'(x) = 1 - \frac{g'(x)}{g'(x)} + \frac{g(x)g''(x)}{g'(x)^2} = \frac{g(x)g''(x)}{g'(x)^2}. \quad (2.16)$$

If the point  $x_a$  is a non-degenerate zero of  $g$ , then  $x_a$  is a superattractive fixed point.

*Remark 2.13* As already mentioned above, a periodic point  $x_p$  of a period  $n$  is a fixed point of  $f^{on}$  ( $n$ -fold composition of  $f$ ).

Moreover, if  $x_p$  is periodic, the points

$$x_p, f(x_p), f^{\circ 2}(x_p), \dots, f^{on-1}(x_p) \quad (2.17)$$

are also periodic, and by the chain rule, the derivative of  $f^{on}$  in those points is the same and equal to

$$(f^{on})'(x_p) = f'(x_p) f'(f(x_p)) \cdots f'(f^{on-1}(x_p)). \tag{2.18}$$

**Definition 2.28 (Hyperbolic Bifurcation Point)** Let  $x_p$  be a periodic point of prime period  $n$  (see Remark 2.6), and the point  $x_p$  is called *hyperbolic* if

$$|(f^{on})'(x_p)| \neq 1. \tag{2.19}$$

The number  $(f^{on})'(x_p)$  is called a *hyperbolic point multiplier*.

**Definition 2.29 (Bifurcation Point)** A non-hyperbolic fixed point is called a *bifurcation point*.

**Definition 2.30 (Attractive Periodic Orbit)** If  $x_p$  is an attractive (resp., a repeller) fixed point for  $f^{on}$ , then so are all others, and it is called an *attractive periodic orbit*.

**Definition 2.31 (Superattractive Periodic Orbit)** A periodic point is superattractive for  $f^{on}$  if and only if  $f'(s) = 0$  at least for one of the points  $x_p, f(x_p), f^{\circ 2}(x_p), \dots, f^{on-1}(x_p)$ .

*Example 2.8* As was mentioned above, an attractor as well as a repeller can be a fixed or a periodic point. For example, the function  $f(x) = -x^3$  has two cyclic points  $-1$  and  $+1$  of period 2 and a fixed one  $x_0 = 0$  (see Fig. 2.7a).

It can easily be verified that  $x_0$  is an attractor for the basin  $(-1, +1)$  and that the cyclic orbit  $-1, +1$  is a repeller. To show that it is sufficient to study the function

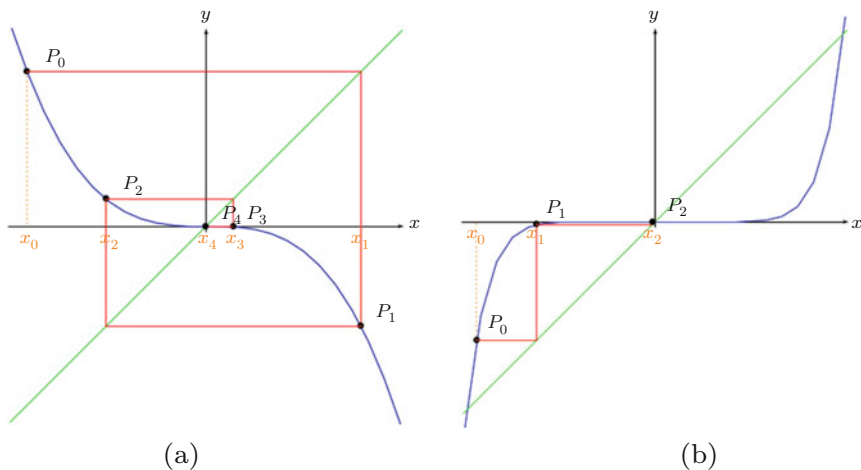


**Fig. 2.7** Convergence to the attractor. Panel (a) represents  $f(x) = -x^3$  that is a mirror image of  $f(x) = x^3$  and panel (b) corresponds to the graph of  $f^{\circ 2}(x) = x^9$

$f^{\circ 2}(x)$  for which  $-1$  and  $+1$  are fixed repeller points, and since neither is fixed for  $f$ , then they will be cyclic repellers (see Fig. 2.7b).

We end this section with the  $n$ -dimensional version of Theorem 2.7.

**Theorem 2.8** *Consider the discrete-time dynamical system*

$$\mathbf{x}_{n+1} = \mathbf{f}(\mathbf{x}_n),$$

where  $\mathbf{f}: \mathbb{R}^n \rightarrow \mathbb{R}^n$  is a smooth map. Let  $\mathbf{x}_a$  be a fixed point of  $\mathbf{f}$ , that is

$$\mathbf{f}(\mathbf{x}_a) = \mathbf{x}_a,$$

and assume that the eigenvalues of the Jacobian matrix of  $\mathbf{f}$

$$D\mathbf{f} = \begin{pmatrix} \partial_{x_1} f_1 & \partial_{x_1} f_2 & \dots & \partial_{x_1} f_n \\ \partial_{x_2} f_1 & \partial_{x_2} f_2 & \dots & \partial_{x_2} f_n \\ \vdots & & & \\ \partial_{x_n} f_1 & \partial_{x_n} f_2 & \dots & \partial_{x_n} f_n \end{pmatrix}$$

calculated at  $\mathbf{x}_a$  lie inside the unit circle  $\{z \in \mathbf{C} \mid \|z\| < 1\}$ .

Then  $\mathbf{x}_a$  is an attractor.

## 2.7 Existence of Periodic Behaviour

In this section we present some definitions that will be used in Sect. 3.1.

### 2.7.1 Schwarz Derivative

**Definition 2.32 (Schwarz Derivative)** Let  $f$  be a one-dimensional map defined in the real field, three times derivable. The Schwarz derivative of  $f$  is defined by

$$f^S(x) = \frac{d}{dx} \left( \frac{f''(x)}{f'(x)} \right) - \frac{1}{2} \left( \frac{f''(x)}{f'(x)} \right)^2, \quad (2.20)$$

or, equivalently, by

$$f^S(x) = \frac{f'''(x)}{f'(x)} - \frac{3}{2} \left( \frac{f''(x)}{f'(x)} \right)^2. \quad (2.21)$$

The relevant property of the Schwarz derivative is to preserve the sign with the composition, in the sense that if  $f^S(x) > 0$ , then it is also  $(f^{\circ n})^S(x) > 0 \quad \forall n \in \mathbb{N}$ . To prove this statement we first prove a ‘‘chain rule’’ formula for the Schwarz derivative.

**Lemma 2.1** *Let  $f, g$  be three times derivable, and then*

$$(f \circ g)^S(x) = f^S(g(x))(g'(x))^2 + g^S(x). \quad (2.22)$$

**Proof** According to the (ordinary) chain rule, we have

$$(f \circ g)'(x) = f'(g(x))g'(x)$$

$$(f \circ g)''(x) = f''(g(x))(g'(x))^2 + f'(g(x))g''(x)$$

$$(f \circ g)'''(x) = f'''(g(x))(g'(x))^3 + 3f''(g(x))g'(x)g''(x) + f'(g(x))g'''(x).$$

Hence,

$$\begin{aligned} (f \circ g)^S(x) &= \frac{f'''(g(x))(g'(x))^3 + 3f''(g(x))g'(x)g''(x) + f'(g(x))g'''(x)}{f'(g(x))g'(x)} \\ &\quad - \frac{3}{2} \left( \frac{f''(g(x))(g'(x))^2 + f'(g(x))g''(x)}{f'(g(x))} \right)^2 \\ &= \left[ \frac{f'''(g(x))}{f'(g(x))} - \frac{3}{2} \left( \frac{f''(g(x))}{f'(g(x))} \right)^2 \right] (g'(x))^2 \\ &\quad + \frac{g'''(x)}{g'(x)} - \frac{3}{2} \left( \frac{g''(x)}{g'(x)} \right)^2 \\ &= f^S(g(x))(g'(x))^2 + g^S(x). \end{aligned}$$

By (2.22), if  $f^S < 0$  and  $g^S < 0$ , then  $(f \circ g)^S < 0$ . In particular, if  $f^S$  is negative, then  $(f^{\circ n})^S$  is also negative for all  $n > 1$ . This yields the following theorem (for illustration see Ref. [5]).

**Theorem 2.9 (Schwarz Theorem)** *If  $f^S < 0$  and if  $f$  has  $n$  critical points, then  $f$  has at most  $n + 2$  attracting periodic orbits.*

From (2.21) we see that if  $Q$  is a polynomial of degree at most 2, then  $Q^S < 0$ . For higher degree polynomials, we have the following proposition.

**Proposition 2.1** *Let  $Q(x)$  be a polynomial whose first derivative  $Q'(x)$  has real roots. Then  $Q^S(x) < 0$ .*



**Proof** Suppose that

$$Q'(x) = \prod_{i=1}^n (x - a_i) \quad \text{with } a_i \text{ real.} \quad (2.23)$$

Then

$$Q''(x) = \sum_{j=1}^n \frac{\prod_{i=1}^n (x - a_i)}{x - a_j} = \sum_{j=1}^n \frac{Q'(x)}{x - a_j}. \quad (2.24)$$

Therefore, by (2.20),

$$\begin{aligned} Q^S(x) &= \frac{d}{dx} \left( \sum_{j=1}^n \frac{1}{x - a_j} \right) - \frac{1}{2} \left( \sum_{j=1}^n \frac{1}{x - a_j} \right)^2 \\ &= - \sum_{j=1}^n \frac{1}{(x - a_j)^2} - \frac{1}{2} \left( \sum_{j=1}^n \frac{1}{x - a_j} \right)^2 < 0. \end{aligned}$$

## 2.7.2 Singer's Theorem

As mentioned before, the Schwarz derivative preserves the sign under composition that is useful in the following theorem.

**Theorem 2.10 (Singer [7])** *Let  $f$  be a map from a closed interval  $I \subseteq [0, b]$  onto itself; then the dynamical system  $x_{n+1} = f(x_n)$  has at most one periodic orbit in the interval  $I$  if the following conditions are met:*

1.  $f$  is a function  $\mathcal{C}^3$ ;
2. There exists a critical point  $x_c \in I$  such that

$$\begin{cases} f'(x) > 0, & \text{for } x < x_c, \\ f'(x) = 0, & \text{for } x = x_c, \\ f'(x) < 0, & \text{for } x > x_c. \end{cases}$$

3. The origin is a repeller for  $f$ , that is

$$f(0) = 0, \quad \text{and} \quad |f'(0)| > 1;$$

4. The Schwarz derivative is

$$f^S(x) \leq 0 \quad \text{for all } x \in I \setminus \{x_c\}.$$

### 2.7.3 Sharkovsky's Theorem

Let us introduce the following ordering on natural numbers.

**Definition 2.33 (Sharkovsky Ordering [10])**

$$\begin{aligned}
 3 \triangleright 5 \triangleright 7 \triangleright \dots \quad 2 \cdot 3 \triangleright 2 \cdot 5 \triangleright 2 \cdot 7 \triangleright \dots \quad 2^2 \cdot 3 \triangleright 2^2 \cdot 5 \triangleright 2^2 \cdot 7 \triangleright \dots \\
 \dots \quad 2^n \cdot 3 \triangleright 2^n \cdot 5 \triangleright 2^n \cdot 7 \triangleright \dots \quad \triangleright 2^n \triangleright 2^{n-1} \triangleright \dots \quad \triangleright 2^3 \triangleright 2^2 \triangleright 2 \triangleright 1
 \end{aligned}
 \tag{2.25}$$

That is, first all odd integers except one are listed, and then they are followed by 2 times that odd number,  $2^2$  times the odd,  $2^3$  times the odd, etc. This exhausts all the natural numbers with the exception of the powers of two that are listed last, in a decreasing order.

**Theorem 2.11 (Sharkovsky)** *Let  $I$  be an interval of  $\mathbb{R}$  and let  $f: I \rightarrow I$  be a continuous function with a periodic point of prime period  $k$ . If  $k \triangleright l$  in the Sharkovsky ordering of Def. 2.33, then  $f$  also has a periodic point of period  $l$ .*

For a proof see Devaney [5, p. 63] or [6].

We limit ourselves to showing the last part of the theorem, which is as follows.

**Proposition 2.2** *Let  $f$  be a continuous function with a periodic point of prime period  $2^n$ , for some  $n \geq 1$ . Then  $f$  also has a periodic point of period  $2^{n-1}$ .*

**Proof** We consider at first the case  $n = 1$ ; thus, we have to prove that if  $f$  has a 2-periodic point, then  $f$  has a fixed point.

Let  $a$  be a 2-periodic point of  $f$ , and consider  $b = f(a)$ . If  $a = b$ , then  $a$  is a fixed point of  $f$  and we have finished. If  $a \neq b$ , define

$$g(x) = f(x) - x.$$

We have

$$\begin{aligned}
 g(a) &= f(a) - a = b - a, \\
 g(b) &= f(b) - b = f(f(a)) - b = a - b.
 \end{aligned}$$

As  $g(a)$  and  $g(b)$  have opposite signs, then there exists at least one value  $c$  between  $a$  and  $b$  for which  $g(c) = 0$ , that is  $c$  is a fixed point of  $f$ .

Now we consider the case of a generic  $n$ . Let  $\varphi(x) = f^{\circ 2^{n-1}}(x)$ , and as  $\varphi^{\circ 2}(x) = f^{\circ 2^n}(x)$ , the  $2^n$  periodic point of  $f$  is a 2-periodic point of  $\varphi$ . Hence  $\varphi$  has a fixed point, that is  $f$  has a  $2^{n-1}$  periodic point.

As in the Sharkovsky ordering, the largest number is 3, and we obtain the following result.

**Corollary 2.1 (Period Three Implies All Periods)** *If  $f$  has a periodic orbit of period three, then it has periodic orbits of all periods.*

As the set of the smallest numbers in the Sharkovsky ordering is the set of the powers of 2, the following corollary holds:

**Corollary 2.2** *If  $f$  has a periodic point of prime period  $k$ , with  $k$  not a power of two, then  $f$  has infinitely many periodic points. Conversely, if  $f$  has only finitely many periodic points, then they all necessarily have periods that are powers of two.*

For multidimensional maps or for discontinuous maps, Sharkovsky's Theorem is no longer valid, as shown by the following two examples.

*Example 2.9* Consider the 2-dimensional map

$$\begin{cases} x_{n+1} = -\frac{1}{2}x_n - \frac{\sqrt{3}}{2}y_n, \\ y_{n+1} = \frac{\sqrt{3}}{2}x_n - \frac{1}{2}y_n, \end{cases}$$

which corresponds to a rotation of  $120^\circ$  about the origin.

Clearly the origin is a fixed point, whereas any other point has period 3: there are no orbits with period different from 3.

*Example 2.10* Consider the function  $f: [0, 1[ \rightarrow [0, 1[$

$$f(x) = \begin{cases} x + \frac{1}{3} & \text{if } x \in \left[0, \frac{2}{3}\right[ , \\ x - \frac{2}{3} & \text{if } x \in \left[\frac{2}{3}, 1\right[ . \end{cases}$$

It is easy to check that  $f^{\circ 3}(x) = x$ ; hence, any point has period 3 and there are no orbits with period different from 3.

## References

1. Antoulas, A.: *Mathematical System Theory—The Influence of R. E. Kalman*. Springer, Berlin (1991). <https://doi.org/10.1007/978-3-662-08546-2>
2. Bendixson, I.: Sur les courbes définies par des équations différentielles. *Acta Math.* **24**, 1–88 (1901). <https://doi.org/10.1007/BF02403068>
3. Bonsante, F., Da Prato, G.: *Matematica I* (2008). <http://dida.sns.it/dida2/cl/07-08/folde0/pdf0>
4. Dercole, F., Rinaldi, S.: Dynamical systems and their bifurcations. In: *Advanced Methods of Biomedical Signal Processing* pp. 291–325 (2011)
5. Devaney, R.: *An Introduction to Chaotic Dynamical Systems*, 2nd edn (Addison-Wesley Studies in Nonlinearity). Westview Press, Boulder (1989)

6. Keith, B. Boris, H.: The Sharkovsky theorem: A natural direct proof. *Am. Math. Mon.* **118**, 229–244 (2011)
7. Lorenz, H.W.: *Nonlinear Dynamical Economics and Chaotic Motion*, 2nd edn. edn. Springer, Berlin (1993)
8. Lyapunov, A.: *General Problem of Stability of Motion*. Mathematics Society of Kharkov, Kharkov (1892)
9. Mukherjee, A.: Tubular Neighbourhoods, pp. 199–223. Springer, Cham (2015). [https://doi.org/10.1007/978-3-319-19045-7\\_7](https://doi.org/10.1007/978-3-319-19045-7_7)
10. Sternberg, S.: *Dynamical Systems*. Dover Publications, Mineola, New York (2010)
11. Zimmerman, S.: An undergraduate's guide to the Hartman-Grobman and Poincare-Bendixon theorems (2008). [www.math.hmc.edu/levy/181\\_web/Zimmerman\\_web.pdf](http://www.math.hmc.edu/levy/181_web/Zimmerman_web.pdf)

# Chapter 3

## An Example of Nonlinear Dynamical System: The Logistic Map



Giuseppe Orlando and Giovanni Tagliatalata

### 3.1 The Logistic Map

The behaviour of linear systems is fully described by the eigenvalues of the system at the origin (or any transited point) of the phase space coordinate system. In this way, only escape to infinity (unstable systems), collapse towards the origin (stable systems) or centre motions (marginally stable systems) can be described. While such descriptions can serve as a first approximation, real systems to reveal their true nature generally request a nonlinear description. Fortunately, a simple system offers a basic, but rather complete understanding of how nonlinearity affects the dynamical behaviour of a system.

The *Logistic Map* (also referred to as the *Verhulst dynamics* or the *quadratic parabola map*):

$$f_{\mu}(x) = \mu x(1 - x), \quad x \in [0, 1], \quad \mu \in [0, 4],$$

is a simple example of a nonlinear system with a single parameter ( $\mu$ ) expressing the strength of the nonlinearity (see Fig. 3.1) permitting to follow its dynamics which is critically dependent on  $\mu$ .

---

G. Orlando (✉)

University of Bari, Department of Economics and Finance, Bari, Italy

University of Camerino, School of Sciences and Technology, Camerino, Italy

e-mail: [giuseppe.orlando@uniba.it](mailto:giuseppe.orlando@uniba.it); [giuseppe.orlando@unicam.it](mailto:giuseppe.orlando@unicam.it)

G. Tagliatalata

University of Bari, Department of Economics and Finance, Bari, Italy

e-mail: [giovanni.tagliatalata@uniba.it](mailto:giovanni.tagliatalata@uniba.it)

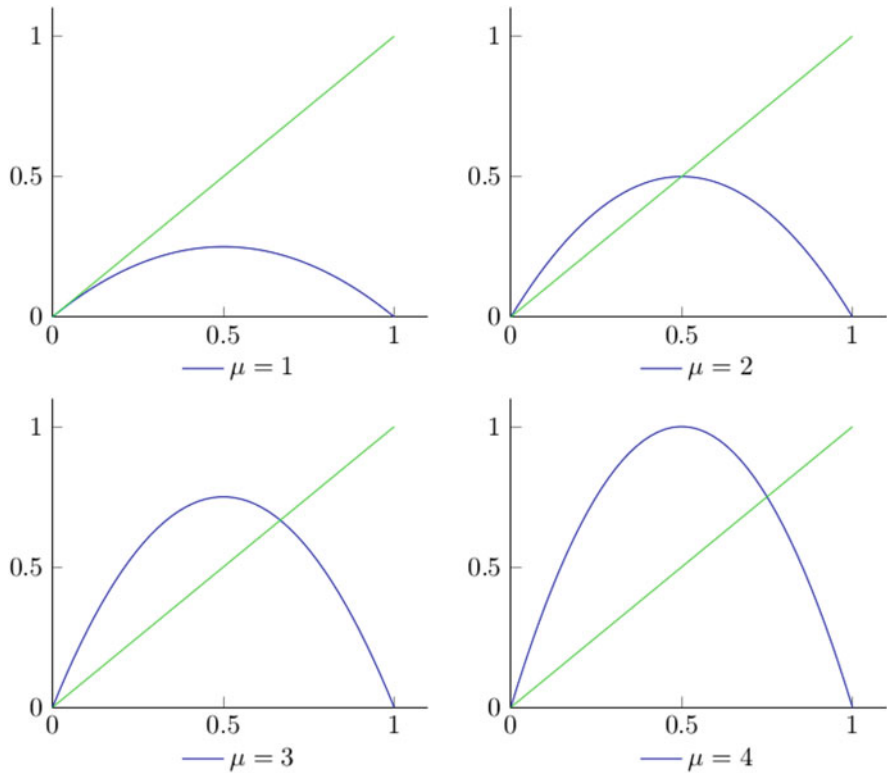


**Fig. 3.1** Logistic map for different values of the parameter  $\mu$

On a heuristic level, it is apparent that the one-dimensionality of this system is enough to represent the bending and stretching of the expanding manifolds (see Chap. 6), which is a characteristic of the behaviour of higher dimensional dissipative nonlinear systems. However, a deeper analysis offers more insight. Nonlinear behaviour is in leading order expressed by the quadratic term of the Taylor expansion of the map describing the system dynamics. Normally, the coefficient of this term will not be zero (the ‘generic’ case). This is why we focus on the second-order map dynamics. For the more ‘rare’ cases where the behaviour is dominated by a higher—e.g., third—order term, parallel effects to what is exhibited by the Logistic Map are observed (e.g., changed ‘Feigenbaum’ constants); a similar statement can be made for area-preserving maps. Even non-polynomial maps show related features but follow laws that deviate more strongly from the generic case (see control of systems in Chap. 15). The one-dimensional nature of this system also allows us to use some of the strong results obtained in the last chapter for such cases. Moreover, we will apply the same approach for the analysis of the economic models in Part III of this book.

There are equations that defy any analytical solution is the content of a famous theorem the first incomplete proof of which was provided by P. Ruffini. The full proof was then completed independently by N.H. Abel and E. Galois (a more recent variant of the proof was given by Y.A. Sinai).

**Theorem 3.1 (Abel–Ruffini Impossibility Theorem [3])** *There is no solution in radicals for a general polynomial equation of degree five or higher with arbitrary coefficients.*

Theorem 3.1 exhibits why computers and graphical methods are essential tools for the analysis of the dynamics generated by the Logistic Map. In fact, we have to use graphical and numerical methods to overcome the problem.

### 3.1.1 Fixed Points

The fixed points of the Logistic Map  $f_\mu$  for  $\mu \in [1, 4]$  are

$$x_1^* = 0 \quad \text{and} \quad x_2^* = 1 - \frac{1}{\mu}.$$

The first derivatives  $f'_\mu(x) = \mu(1 - 2x)$  calculated in these points are

$$f'_\mu(x_1^*) = \mu \quad \text{and} \quad f'_\mu(x_2^*) = 2 - \mu.$$

The number and nature of the fixed points in the interval  $[0, 1]$  change with the parameter  $\mu$  as follows:

1. If  $0 < \mu < 1$ , there is only one fixed point  $x = 0$ , since the other fixed point  $x_2^* = 1 - 1/\mu$  is negative.

Note that point  $x_1^* = 0$  is attractive (but not super-attractive) since  $f'_\mu(0) = \mu \in (0, 1)$ . Moreover, for all  $x \in (0, 1]$ , one has  $0 < f_\mu(x) < x \leq 1$ , and therefore the sequence  $(f_\mu^{on}(x))_n$  is decreasing and converges to 0. Thus, the basin of attraction of 0 is  $[0, 1]$ .

2. If  $\mu = 1$ ,  $f_1(x) = x(1 - x)$ , then 0 is the unique fixed point of  $f_\mu(x)$  and, with the same arguments as before, one proves that 0 is an attractor and that the basin of attraction of 0 is  $[0, 1]$ .

If  $\mu > 1$ , then the fixed point  $x_1^* = 0$  is repelling, and the second fixed point  $x_2^* = 1 - 1/\mu$  lies in  $]0, 1[$ . Moreover,  $1 < \mu < 3$  implies  $|f'_\mu(x_2^*)| = |2 - \mu| < 1$ ; therefore, the point  $x_2^*$  is an attractor, and its basin depends on the parameter  $\mu$  as detailed below.

3. If  $1 < \mu < 2$ , then the fixed point  $x_2^*$  is in  $(0, 1/2)$ , and the first derivative  $f'_\mu(x_2^*) = 2 - \mu$  is in  $(0, 1)$ .

Now, we prove that the basin of attraction is  $(0, 1]$ .

Note that  $f_\mu$  is strictly increasing and strictly concave in the interval  $[0, 1/2]$ ; hence, one has that

$$\begin{aligned} - x \in [0, x_2^*[ &\implies 0 \leq f_\mu(x) < f_\mu(x_2^*) = x_2^* \quad \text{and} \quad f_\mu(x) > x, \\ - x \in ]x_2^*, 1/2] &\implies \\ x_2^* = f_\mu(x_2^*) &< f_\mu(x) \leq f_\mu(1/2) = \mu/4 \leq 1/2 \quad \text{and} \quad 0 < f_\mu(x) < x. \end{aligned}$$

From this, it follows by induction that for all  $n \in \mathbb{N}$ , one has that

$$\begin{aligned} 0 \leq f_\mu^{on}(x) < x_2^* &\quad \text{and} \quad f_\mu^{o(n+1)}(x) > f_\mu^{on}(x), & \text{for all } x \in [0, x_2^*[, \\ x_2^* < f_\mu^{on}(x) \leq 1/2 &\quad \text{and} \quad f_\mu^{o(n+1)}(x) < f_\mu^{on}(x), & \text{for all } x \in ]x_2^*, 1/2]. \end{aligned}$$

Hence, the sequence  $(f_\mu^{on}(x))_n$  is increasing and converging to  $x_2^*$  for all  $x \in ]0, x_2^*[$  and decreasing and converging to  $x_2^*$  for all  $x \in ]x_2^*, 1/2]$ .

Finally, for all  $x \in ]1/2, 1]$ , one has that  $0 \leq f_\mu(x) < f_\mu(1/2) = \mu/4 < 1/2$ , and therefore the sequence  $(f_\mu^{on}(x))_{n \geq 1}$  is increasing or decreasing according to whether  $f_\mu(x) < x_2^*$  or  $f_\mu(x) > x_2^*$ ; in both cases, such a sequence converges to  $x_2^*$ .

4. If  $\mu = 2$ , then we can apply the same reasoning of the case  $\mu < 2$  to prove that the basin of attraction of  $x_2^*$  is  $(0, 1]$ .

Moreover, since

$$x_2^* = 1 - \frac{1}{\mu} = \frac{1}{2} \quad \text{and} \quad f_2'\left(\frac{1}{2}\right) = 0, \quad (3.1)$$

the fixed point  $x_2^*$  is super-attractive, and the sequence  $(f_2^{on}(x))_n$  converges to  $x_2^*$  very fast (faster than geometrically).

5. If  $2 < \mu < 3$ , then  $x_2^* = 1 - (1/\mu) > 1/2$  and

$$f_\mu'(x_2^*) = 2 - \mu \in (-1, 0). \quad (3.2)$$

Therefore, the fixed point  $x_2^*$  is an attractor, but the iterates oscillate around it.

6. If  $\mu = 3$ , then  $x_2^* = 1 - \frac{1}{\mu} = \frac{2}{3}$  and  $f_\mu'(x_2^*) = 2 - \mu = -1$ . It can be proved that the fixed point  $x_2^*$  is still an attractor.

If  $\mu \in ]3, 4[$ , then  $f_\mu'(x_2^*) < -1$ , hence the fixed point  $x_2^*$  is a repeller (see Definition 2.27).

We consider then the second iterate  $f_\mu^{o2}(x)$  (see Fig. 3.2) and its fixed points, i.e., the periodic points of period 2.

Since

$$\begin{aligned} f_\mu^{o2}(x) - x &= \mu f_\mu(x)(1 - f_\mu(x)) - x & (3.3) \\ &= \mu[\mu x(1 - x)][1 - \mu x(1 - x)] - x \\ &= x(\mu - \mu x - 1)(\mu^2 x^2 - \mu^2 x - \mu x + \mu + 1) \\ &= [f_\mu(x) - x](\mu^2 x^2 - \mu^2 x - \mu x + \mu + 1), \end{aligned}$$



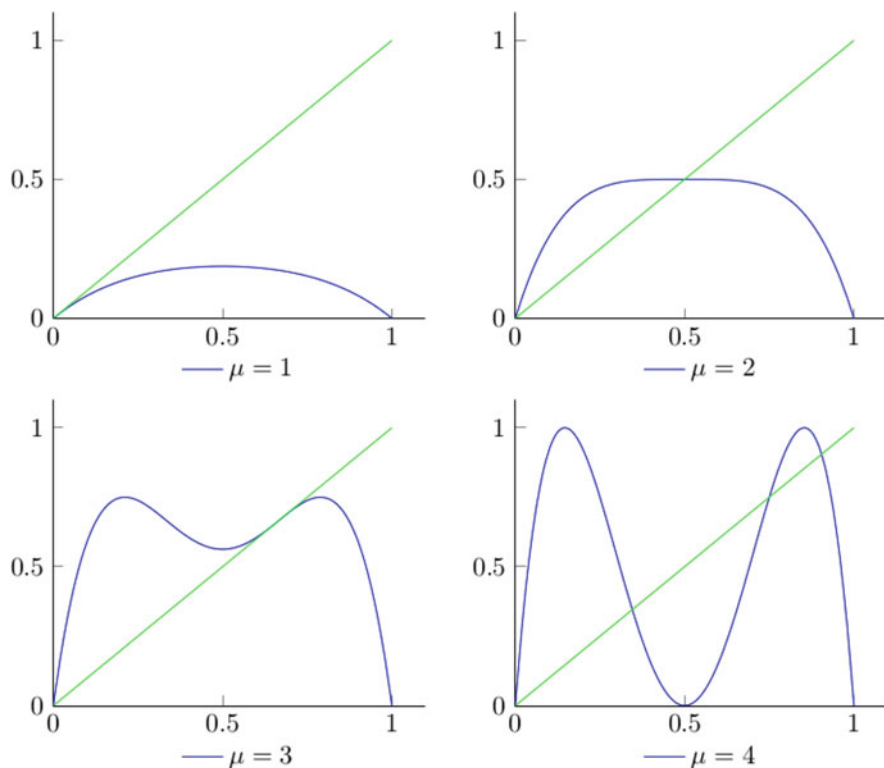


**Fig. 3.2** Second iteration for the logistic map

a fixed point of  $f_\mu^2(x)$  is either a fixed point of  $f_\mu(x)$  or a zero of the quadratic polynomial

$$\mu^2 x^2 - \mu(\mu + 1)x + \mu + 1. \quad (3.4)$$

The discriminant of the polynomial (3.4)

$$\mu^2(\mu + 1)^2 - 4\mu^2(\mu + 1) = \mu^2(\mu + 1)(\mu - 3) \quad (3.5)$$

is positive since  $\mu > 3$ . Hence, the above polynomial (3.4) has two real roots:

$$p_{2\pm} = \frac{1}{2} + \frac{1}{2\mu} \pm \frac{1}{2\mu} \sqrt{(\mu + 1)(\mu - 3)} \in (0, 1). \quad (3.6)$$

To check whether  $p_{2\pm}$  are attractors or repellers, we need to compute the derivative of  $f_\mu^2(x)$  in these points. This can be done in two different but equivalent ways.

*First method.* Computing the derivative of  $f_\mu^{\circ 2}(x)$ , one has

$$(f_\mu^{\circ 2})'(x) = \mu^2(1 - 2x)(2\mu^2x - 2\mu x + 1). \quad (3.7)$$

Then, replacing  $x = p_{2\pm}$ , after some calculation, one gets

$$(f_\mu^{\circ 2})'(p_{2\pm}) = -\mu^2 + 2\mu + 4. \quad (3.8)$$

*Second method.* Using the chain rule, one obtains

$$(f_\mu^{\circ 2})'(x) = [f_\mu(f_\mu(x))]' = f_\mu'(f_\mu(x)) f_\mu'(x). \quad (3.9)$$

Since  $f_\mu(p_{2+}) = p_{2-}$  and  $f_\mu(p_{2-}) = p_{2+}$ , from the above identity, one gets

$$\begin{aligned} (f_\mu^{\circ 2})'(p_{2\pm}) &= f_\mu'(p_{2+}) f_\mu'(p_{2-}) \\ &= \mu^2(1 - 2p_{2+})(1 - 2p_{2-}) \\ &= \mu^2(1 - 2(p_{2+} + p_{2-}) + 4p_{2+}p_{2-}). \end{aligned} \quad (3.10)$$

From Eq. (3.4), we obtain

$$p_{2+} + p_{2-} = (\mu + 1)/\mu \quad \text{and} \quad p_{2+} \cdot p_{2-} = (\mu + 1)/\mu^2. \quad (3.11)$$

Thus, we get

$$(f_\mu^{\circ 2})'(p_{2\pm}) = -\mu^2 + 2\mu + 4. \quad (3.12)$$

Therefore,  $(f_\mu^{\circ 2})'(p_{2\pm})$ , as a function of  $\mu$ , decreases in the interval  $[3, 4]$  and equals 1 for  $\mu = 3$  and  $-1$  for  $\mu = \mu_1 := 1 + \sqrt{6} = 3.449499\dots$

7. If  $3 < \mu < \mu_1$ , as we have already shown, the two fixed points are repelling for  $f_\mu$ , while the two periodic points of period 2 are attracting for  $f_\mu^{\circ 2}$ .

For  $\mu > \mu_1$ , the periodic points of period 2 become unstable (repelling), and four periodic points of period 4 appear. These points are stable (attracting) for  $\mu < \mu_2 = 3.54409\dots$  and unstable for  $\mu > \mu_2$ .

Iterating this procedure, one can construct a sequence  $(\mu_n)_n$  such that for  $\mu > \mu_n$  a cycle of order  $2^n$  appears.

8. For  $\mu = 1 + 2\sqrt{2}$ , chaos begins: an orbit of period 3 appears. We have (see Fig. 3.3)

$$\begin{aligned} f_\mu^{\circ 3}(x) &= \mu^3(1 - x)x(\mu x^2 - \mu x + 1) \times \\ &\quad \times (\mu^3 x^4 - 2\mu^3 x^3 + \mu^3 x^2 + \mu^2 x^2 - \mu^2 x + 1) \end{aligned}$$

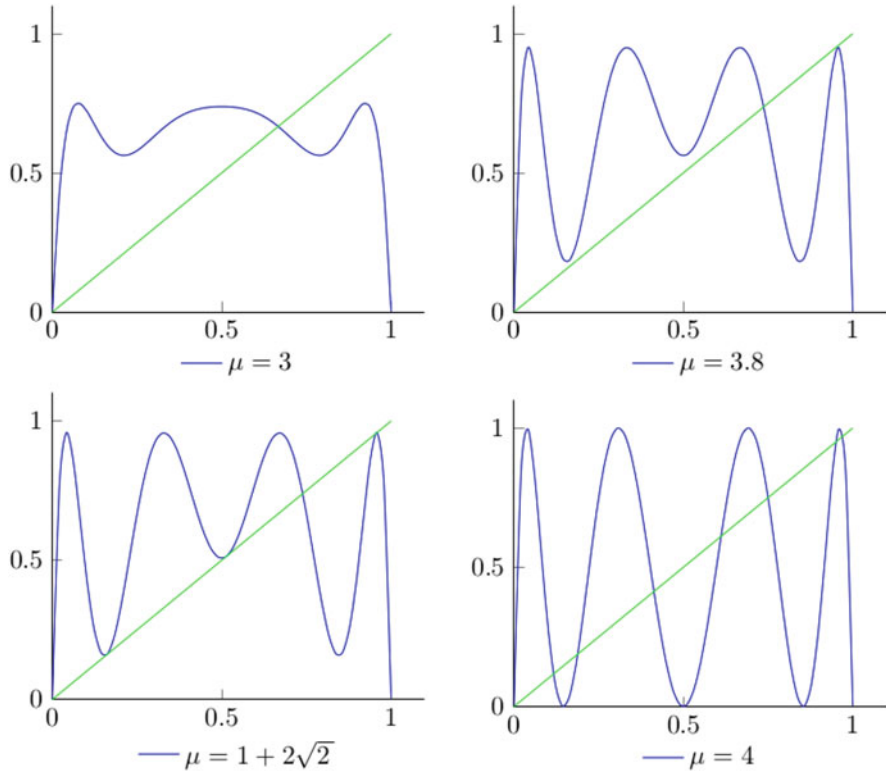


**Fig. 3.3** Third iteration for the logistic map

and

$$f_{1+2\sqrt{2}}^{\circ 3}(x) - x = [f_{1+2\sqrt{2}}(x) - x][p(x)]^2,$$

where

$$p(x) = (25 + 22\sqrt{2})x^3 - (42 + 35\sqrt{2})x^2 + (21 + 14\sqrt{2})x - 3 - \sqrt{2}$$

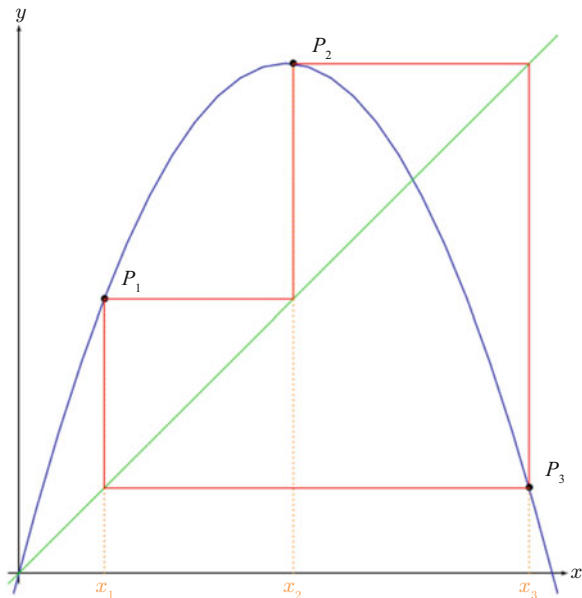
has three real roots different from the fixed points 0 and  $\frac{2}{7}(4 - \sqrt{2})$  of  $f_{1+2\sqrt{2}}$ :

$$x_1 = 0.15993\dots, \quad x_2 = 0.51436\dots, \quad x_3 = 0.95632\dots \quad (3.13)$$

These three numbers form a cycle of period 3 for  $f_\mu$ , see Fig. 3.4.

By Sarkovsky's Theorem 2.7.3, there exist orbits of any period.

**Fig. 3.4** Graph of  $f_{1+2\sqrt{2}}$  and the 3-cycle in (3.13)



9. Regarding the limit case  $\mu = 4$ , by direct calculation, one has

$$f_{\mu}^{\circ 3}(x) - x = (f_{\mu}(x) - x)(64x^3 - 112x^2 + 56x - 7)(64x^3 - 96x^2 + 36x - 3). \tag{3.14}$$

The two polynomials of degree 3 have three real roots in  $(0, 1)$ , namely, the numerical values

$$x_1 = 0.18825\dots, \quad x_2 = 0.61126\dots, \quad x_3 = 0.95048\dots \tag{3.15}$$

for the first polynomial and

$$x_4 = 0.11697\dots, \quad x_5 = 0.41317\dots, \quad x_6 = 0.96984\dots \tag{3.16}$$

for the second polynomial. These are two cycles of period 3.

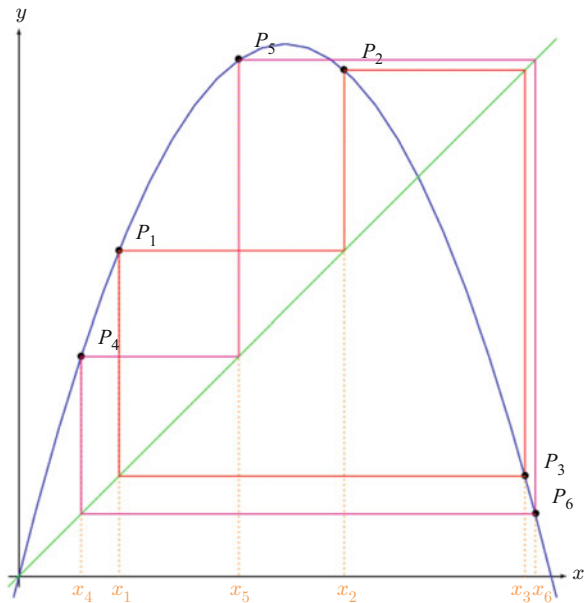
The two triplets form a 2-cycle of period 3 for  $f_4$ , see Fig. 3.5.

### 3.1.2 Feigenbaum's Universal Constants

M.J. Feigenbaum showed [1] that the sequence  $(\mu_n)_n$  of period-doubling bifurcation values follows the rule

$$\lim_{n \rightarrow \infty} \frac{\mu_n - \mu_{n-1}}{\mu_{n+1} - \mu_n} = \delta_F \approx 4.6692\dots, \tag{3.17}$$

**Fig. 3.5** Graph of  $f_4$  and the two 3-cycles in (3.15) and (3.16)



where  $\delta_F$  is a constant that is universal (i.e., universally valid) for any one-dimensional maps with a quadratic maximum or for any differential equation for which the second-order term of its Taylor expansion does not vanish. This condition is satisfied by any generic nonlinear differentiable system, e.g., by  $f(x) = ax \exp(-x)$  or  $f(x) = a \sin(\pi x)$ , neuron equations [4], each equations with a feedback loop [2] and more. Differential equation systems such as those obtained from the latter can be converted to maps via Poincaré sections; it can therefore not come as a surprise that they also follow Feigenbaum’s paradigm. Systems that may look very similar to the quadratic parabola may also produce periodic doubling but fail to follow Feigenbaum’s paradigm to different extent. For the much smaller class of systems of quartic maxima, e.g., a statement very similar to Feigenbaum’s holds, only with different (larger) constants. Notice that these systems are extreme in the class of ‘natural systems from a measure-theoretical point of view’. In addition, their bifurcation scenario, due to the larger size of the constants, is far more difficult to observe.

The *tent maps*, or the *flat-topped maps* that will be used later to explain one potential cause for the emergence of stable economic cycles, differ more strongly from Feigenbaum’s paradigm.

As a consequence of Eq. (3.17), if two successive bifurcation values are known, the next bifurcation can be predicted, and the end point of the geometric series of bifurcations (after which we naturally expect chaotic behaviour) can be estimated.

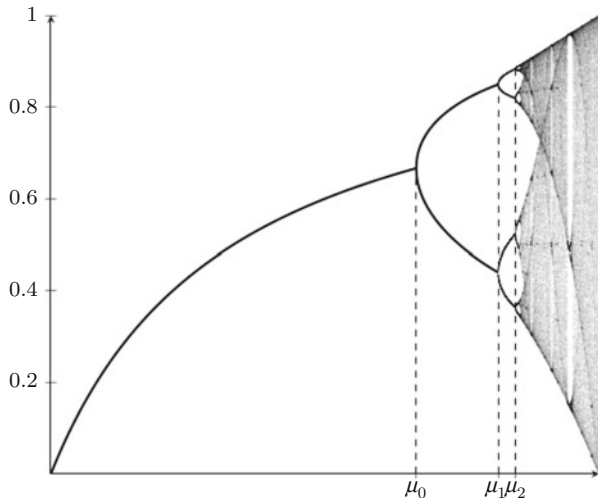


**Fig. 3.6** Period doubling for the logistic map

For the quadratic parabola, the limit point of the period-doubling sequence is  $\mu_c \approx 3.5699\dots$  (see Fig. 3.6).

### 3.1.3 Schwarz Derivative

Since

$$f'_\mu(x) = \mu - 2\mu x, \quad f''_\mu(x) = -2\mu, \quad f'''_\mu(x) = 0, \tag{3.18}$$

for the Schwarz derivative 2.32 of the Logistic Map, one has

$$f^S(x) = -\frac{6}{(1 - 2x)^2} < 0 \quad \text{for any } x \neq \frac{1}{2}. \tag{3.19}$$

Thus, according to Schwarz’s theorem (see Theorem 2.9 in Chapter 2), there exist at most three attracting periodic orbits.

### 3.1.4 Singer’s Theorem Applied to the Logistic Map

In this paragraph, we show that for the function  $f_\mu(x) = \mu x(1 - x)$  with  $\mu > 1$ , it is easy to check that the four conditions of Singer’s Theorem 2.10 are all satisfied. Indeed,

1.  $f_\mu$  is infinitely differentiable.
2. The derivative is  $f'_\mu(x) = \mu(1 - 2x)$ , and therefore for  $x_c = 1/2$ , one has

$$\begin{cases} f'(x) > 0, & \text{for } x < \frac{1}{2}, \\ f'\left(\frac{1}{2}\right) = 0, \\ f'(x) < 0, & \text{for } x > \frac{1}{2}. \end{cases}$$

3. The origin is a repeller for  $f_\mu$  since  $f_\mu(0) = 0$  and  $f'_\mu(0) = \mu > 1$ .
4.  $f^S(x)_\mu = -\frac{6}{(1-2x)^2} < 0 \quad \forall x \in I \setminus \{c\}$  (see Sect. 3.1.3).

### 3.1.5 Closed Formulas

In general, it is not possible to find a closed formula

$$x_n = F(n, x_0).$$

However, if  $\mu = 2$ , we have

$$x_n = \frac{1}{2} \left[ 1 - \exp[2^n \log(1 - 2x_0)] \right], \quad (3.20)$$

whereas if  $\mu = 4$ ,

$$x_n = \frac{1}{2} \left[ 1 - \cos[2^n \arccos(1 - 2x_0)] \right]. \quad (3.21)$$

Both (3.20) and (3.21) are proved by induction. We begin with (3.20). For  $n = 0$ , (3.20) is clearly true. Assuming it for some  $n$ , we have

$$\begin{aligned} 2x_n(1-x_n) &= \left[ 1 - \exp[2^n \log(1 - 2x_0)] \right] \times \\ &\quad \times \left[ 1 - \frac{1}{2} \left[ 1 - \exp[2^n \log(1 - 2x_0)] \right] \right] \\ &= \frac{1}{2} \left[ 1 - \exp[2^n \log(1 - 2x_0)] \right] \left[ 1 + \exp[2^n \log(1 - 2x_0)] \right] \\ &= \frac{1}{2} \left[ 1 - \exp[2^{n+1} \log(1 - 2x_0)] \right] = x_{n+1}. \end{aligned}$$

Now, we prove (3.21). For  $n = 0$ , (3.21) is clearly true. Assuming it for some  $n$ , we have

$$\begin{aligned} 4x_n(1-x_n) &= 2\left[1 - \cos\left[2^n \arccos(1-2x_0)\right]\right] \times \\ &\quad \times \left[1 - \frac{1}{2}\left[1 - \cos\left[2^n \arccos(1-2x_0)\right]\right]\right] \\ &= \left[1 - \cos\left[2^n \arccos(1-2x_0)\right]\right] \left[1 + \cos\left[2^n \arccos(1-2x_0)\right]\right] \\ &= \left[1 - \cos^2\left[2^n \arccos(1-2x_0)\right]\right]. \end{aligned}$$

Recalling the formula  $\cos(2\alpha) = 2\cos^2(\alpha) - 1$ , we get

$$\begin{aligned} 4x_n(1-x_n) &= \left[1 - \frac{1}{2}\left[1 + \cos\left[2^{n+1} \arccos(1-2x_0)\right]\right]\right] \\ &= \frac{1}{2}\left[1 - \cos\left[2^{n+1} \arccos(1-2x_0)\right]\right] \\ &= x_{n+1}. \end{aligned}$$

## References

1. Feigenbaum, M.J.: Quantitative universality for a class of nonlinear transformations. *J. Stat. Phys.* **19**(1), 25–52 (1978). <https://doi.org/10.1007/BF01020332>
2. Gomez, F., Stoop, R.L., Stoop, R.: Universal dynamical properties preclude standard clustering in a large class of biochemical data. *Bioinformatics* **30**(17), 2486–2493 (2014)
3. Rosen, M.I.: Niels Hendrik Abel and equations of the fifth degree. *Am. Math. Mon.* **102**(6), 495–505 (1995)
4. Stoop, R., Buchli, J., Keller, G., Steeb, W.H.: Stochastic resonance in pattern recognition by a holographic neuron model. *Phys. Rev. E* **67**(6), 061918 (2003)



# Chapter 4

## Bifurcations



Giuseppe Orlando, Ruedi Stoop, and Giovanni Tagliatalata

### 4.1 Bifurcations in the Parameter Space

An impression of how bifurcations are usually distributed in parameter space is provided in Fig. 4.1 using several examples, where at every border of a periodicity change we have a bifurcation. Figure 4.1a (cf. [7]) shows the periodicities obtained for the two-dimensional generalization of the parabola,  $f(x, y) = (-ax^2 + y + 1, bx)$  over the  $(a, b)$ -parameter space. In particular, we can see not fully resolved Feigenbaum bifurcations, escape to infinity, and an extended sea of chaotic behaviour (white). Figure 4.1b (cf. [7]) shows the periodicities (coded in a colour bar, where deep blue contains the chaotic sea) of the nonlinear so-called Nishio–Inaba electronic circuit. The hardware can be described by an ODE; each pixel corresponds to a particular circuit realization (cf. [7]). Figure 4.1c shows the properties of the Goldbeter two-step chemical reaction process describable via an ODE. In the background, we indicate the stability properties (Lyapunov exponents, where black colour indicates stable behaviour) and corresponding periodicities in

---

G. Orlando (✉)

University of Bari, Department of Economics and Finance, Bari, Italy

University of Camerino, School of Sciences and Technology, Camerino, Italy

e-mail: [giuseppe.orlando@uniba.it](mailto:giuseppe.orlando@uniba.it); [giuseppe.orlando@unicam.it](mailto:giuseppe.orlando@unicam.it)

R. Stoop

Institute of Neuroinformatics, ETHZ/University of Zürich, Zürich, Switzerland

e-mail: [ruedi@ini.phys.ethz.ch](mailto:ruedi@ini.phys.ethz.ch)

G. Tagliatalata

University of Bari, Department of Economics and Finance, Bari, Italy

e-mail: [giovanni.tagliatalata@uniba.it](mailto:giovanni.tagliatalata@uniba.it)

© The Author(s), under exclusive license to Springer Nature Switzerland AG 2021

G. Orlando et al. (eds.), *Non-Linearities in Economics*, Dynamic Modeling

and Econometrics in Economics and Finance 29,

[https://doi.org/10.1007/978-3-030-70982-2\\_4](https://doi.org/10.1007/978-3-030-70982-2_4)

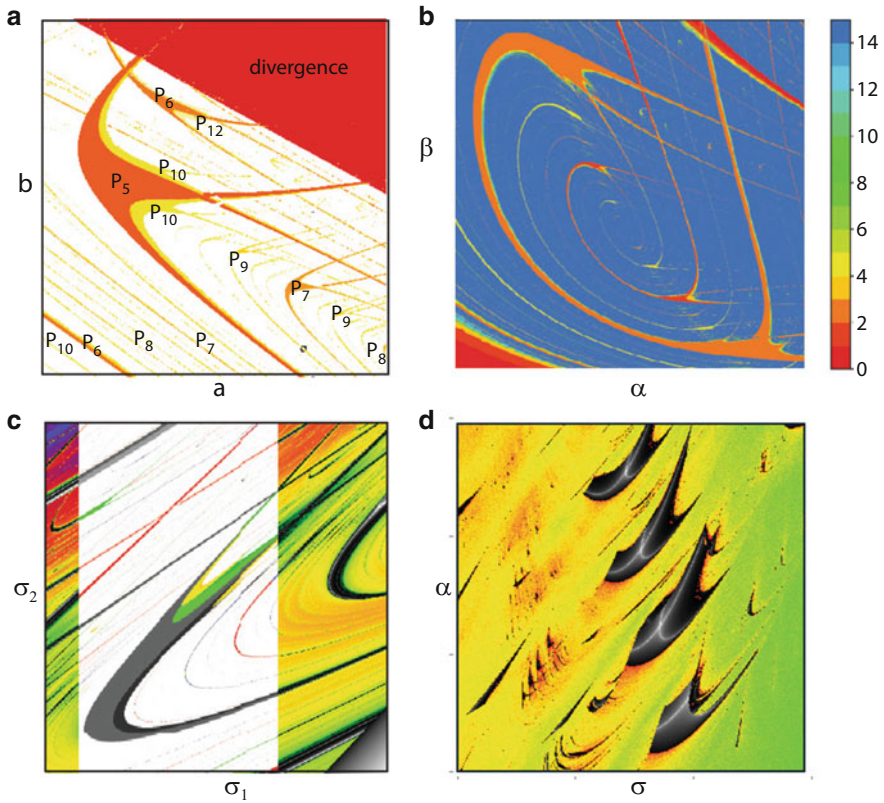


**Fig. 4.1** Abundance of bifurcations demonstrated by periodicity and stability over ranges of the nonlinearity parameters. Bifurcations emerge where periodicity changes or where stability becomes marginal. (a) Periodicities generated by a two-dimensional map generalizing the quadratic parabola. Across the shrimp-like structures, Feigenbaum cascades are obtained (only partially resolved). (b) Results from simulations of the Nishio–Inaba nonlinear circuit. (c) Goldbeter’s two-step chemical reaction, showing stability of generated solutions overlaid with periodicity as the inset. (d) Stability of solutions generated by Rulkov’s neuron model. For more details, see text

the foreground inset, where the white colour again embraces the sea of chaotic behaviour (cf. [1]). Figure 4.1d shows the dynamical properties of a Rulkov neuron. Colours embrace the sea of chaotic behaviour; black indicates stable behaviour and the white lines the loci of superstable behaviour.

## 4.2 Homoclinic and Heteroclinic Orbits

**Definition 4.1 (Heteroclinic)** Let us consider a continuous dynamical system described by the ordinary differential equation (ODE)

$$\dot{x} = f(x),$$

with equilibria in  $x = x_0$  and  $x = x_1$ . A solution  $x(t)$  is a *heteroclinic* orbit from  $x_0$  to  $x_1$  if

$$x(t) \rightarrow x_0 \quad \text{as } t \rightarrow -\infty$$

and

$$x(t) \rightarrow x_1 \quad \text{as } t \rightarrow +\infty.$$

**Definition 4.2 (Homoclinic—Continuous Case)** Let us consider a continuous dynamical system described by the ordinary differential equation (ODE)

$$\dot{x} = f(x)$$

with an equilibrium in  $x = x_0$ . A solution  $x(t)$  is a *homoclinic orbit* if

$$x(t) \rightarrow x_0 \quad \text{as } t \rightarrow \pm\infty.$$

**Definition 4.3 (Homoclinic—Discrete Case)** In the discrete case, for the map  $f: \mathbb{R} \rightarrow \mathbb{R}$ , if there exists a fixed point or a periodic point  $x^*$  for which

$$\lim_{n \rightarrow \pm\infty} f^{(n)}(x) = x^*,$$

then  $x^*$  is a *homoclinic point*.

## 4.3 Local and Global Bifurcations

Consider the family of dynamical systems

$$\dot{x}(t) = f(x(t); \mu), \quad x \in \mathbb{R}^n, \quad (4.1)$$

depending on a real parameter  $\mu \in \mathbb{R}$ .

**Definition 4.4 (Structural Stability)** The dynamical system (4.1) is *structurally stable* for  $\mu = \mu_0$  if there exists  $\varepsilon > 0$  such that for all  $\mu_1$  with  $|\mu_1 - \mu_0| < \varepsilon$ , there

exists a topological conjugacy (as defined in Definition 2.14) between the dynamical system (4.1) with  $\mu = \mu_0$  and  $\mu = \mu_1$ .

Recalling that a topological conjugacy is a continuous bijective map, Definition 4.4 requires to map each orbit of the vector field generated with  $\mu = \mu_0$  to an orbit of the vector field generated by the system with  $\mu = \mu_1$  close to  $\mu_0$ . In other words, it is possible to continuously morph the trajectories of the system by small variations of the parameter  $\mu$ . When the system is structurally stable, the orbit of the system does not change dramatically with the parameter.

**Definition 4.5 (Bifurcation)** If the dynamical system (4.1) is not structurally stable for  $\mu = \mu_0$ , we say that it has a bifurcation at  $\mu = \mu_0$ , and we call  $\mu_0$  a *bifurcation point*.

A bifurcation occurs whenever a change in one of the parameters induces a qualitative change of the orbits of the system. Thus, the set of bifurcation points divides the parameter space into different regions that are characterized by the same qualitative behaviour.

Assume that for some  $\mu_0 \in \mathbb{R}$ ,  $\mathbf{x}_0$  is an equilibrium point of (4.5), so that

$$\mathbf{f}(\mathbf{x}_0; \mu_0) = 0. \quad (4.2)$$

**Lemma 4.1** *A critical value  $\mu_0$  of the parameters is a bifurcation point if the number of fixed points changes in any neighbourhood of  $\mu_0$ .*

**Proof** If the number of fixed points changes, then the trajectories associated with the appearing or disappearing fixed points can no longer be mapped. Therefore, a topological conjugacy between the vector field obtained for the system at  $\mu = \mu_0$  and that at the neighboring parameter  $\mu$  can no longer exist.  $\square$

We now recall the Dini classical implicit function theorem.

**Theorem 4.1** *Let  $\mathcal{U}$  be a neighbourhood of  $(\mathbf{x}_0; \mu_0) \in \mathbb{R}^n \times \mathbb{R}$ , and let  $\mathbf{f}: \mathcal{U} \rightarrow \mathbb{R}^n$  be a  $\mathcal{C}^1$  function. Assume (4.2), and assume that the Jacobian of  $\mathbf{f}$  with respect to the  $\mathbf{x}$  variables, that is,*

$$\mathbf{J}(\mathbf{x}; \mu) = \begin{pmatrix} \partial_{x_1} f_1(\mathbf{x}; \mu) & \partial_{x_2} f_1(\mathbf{x}; \mu) & \cdots & \partial_{x_n} f_1(\mathbf{x}; \mu) \\ \partial_{x_1} f_2(\mathbf{x}; \mu) & \partial_{x_2} f_2(\mathbf{x}; \mu) & \cdots & \partial_{x_n} f_2(\mathbf{x}; \mu) \\ \vdots & \vdots & \ddots & \vdots \\ \partial_{x_1} f_n(\mathbf{x}; \mu) & \partial_{x_2} f_n(\mathbf{x}; \mu) & \cdots & \partial_{x_n} f_n(\mathbf{x}; \mu) \end{pmatrix} \quad (4.3)$$

*is invertible in  $(\mathbf{x}_0; \mu_0)$ .*

*Then, there exist  $\delta, \varepsilon > 0$  and a  $\mathcal{C}^1$  function  $\gamma: (\mu_0 - \varepsilon, \mu_0 + \varepsilon) \rightarrow \mathbb{R}^n$  such that  $\mathbf{x}_\mu = \gamma(\mu)$  is the unique solution of*

$$\mathbf{f}(\mathbf{x}_\mu; \mu) = \mathbf{0},$$

*with  $\|\mathbf{x} - \mathbf{x}_0\| < \delta$  and  $|\mu - \mu_0| < \varepsilon$ .*

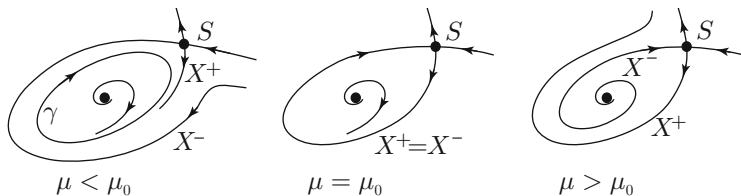


**Fig. 4.2** Three state portraits of a two-dimensional dynamical system (4.1) that has a homoclinic bifurcation at  $\mu = \mu_0$ . At the bifurcation, the stable manifold  $X^-$  of the saddle  $S$  collides with its unstable manifold  $X^+$  generating the homoclinic loop. Note that, in this bifurcation, a limit cycle  $\gamma$  disappears

From the above theorem, we deduce that if  $\det Jf(x_0; \mu_0) \neq 0$ , then  $x_\mu = \gamma(\mu)$  is the unique equilibrium solution for  $\mu$  sufficiently close to  $\mu_0$ . Thus, in the bifurcations that can be identified with Lemma 4.1, we can conclude that at the critical value  $\mu_0$ , there exists  $\varepsilon > 0$  such that in the interval  $[\mu_0, \mu_0 + \varepsilon[$  (resp., in the interval  $] \mu_0 - \varepsilon, \mu_0 ]$ ), there exist (at least) two functions  $\gamma_1$  and  $\gamma_2$  of class  $\mathcal{C}^1$  such that  $\gamma_1(\mu)$  and  $\gamma_2(\mu)$  are fixed points for each  $\mu \in [\mu_0, \mu_0 + \varepsilon[$  (resp., for each  $\mu \in ] \mu_0 - \varepsilon, \mu_0 ]$ ), and  $\gamma_1(\mu_0) = \gamma_2(\mu_0) = x_0$ .  $\gamma_1(\mu)$  and  $\gamma_2(\mu)$  are called *the branches of the fixed point*.

Notice that, in this case, by the implicit function theorem, it is necessary that

$$f(x_0; \mu_0) = 0 \quad \text{and} \quad \det Jf(x_0; \mu_0) = 0. \tag{4.4}$$

This is why in Definition 2.29 of Chap. 2, for a non-hyperbolic fixed point the term “bifurcation point” was justified.

Bifurcations that involve the degeneracies of some eigenvalue of the Jacobian evaluated at an equilibrium point (or of some of the multipliers of the system limit cycles—see Definition 2.28) are called *local bifurcations*. By contrast, *global bifurcations* cannot be revealed by eigenvalue degeneracies and usually involve the collision of stable and unstable manifolds of one or more saddles. For example, if the system (4.1) has a homoclinic orbit only for  $\mu \leq \mu_0$ , then  $\mu_0$  is a global bifurcation point (see Fig. 4.2).

In this chapter, we will concentrate on local bifurcations and their implications on the state space changes. The most famous global bifurcation (Shilnikov bifurcation) will be presented in the next chapter.

### 4.4 Local Bifurcations in the Continuous Case

From the above discussion it follows that a local bifurcation can be seen as the collision of different limit sets (see Definition 2.23).

The graphical representation of fixed points (and of limit cycles) for the systems in terms of changes in the parameters is called *bifurcation diagram*. This diagram is useful to describe and detect local bifurcation points. For example, Fig. 3.6 in Chap. 3 represents a bifurcation diagram for the logistic map depicting the bifurcations for that system.

Note that if  $f(x; \mu)$  has a bifurcation point in  $(x_0; \mu_0)$ , the function

$$\tilde{f}(x; \mu) = f(x + x_0; \mu + \mu_0)$$

has a bifurcation point in  $(\mathbf{0}; 0)$ , and thus we can assume, with no loss of generality, that  $(x_0; \mu_0) = (\mathbf{0}; 0)$ .

In the following, we discuss the most common types of bifurcation: saddle-node, transcritical, pitchfork and Hopf. The first three can occur in any space dimension, whereas the Hopf bifurcation can appear only if  $n \geq 2$ .

#### 4.4.1 Bifurcations with Colliding Equilibria

For the sake of simplicity, we treat the first three types of bifurcation in dimension one, i.e.,

$$\dot{x}(t) = f(x(t); \mu) \quad x \in \mathbb{R}. \quad (4.5)$$

According to the above considerations, we assume that  $f$  is a regular function defined in a neighbourhood of the origin in  $\mathbb{R}$  and

$$f(0; 0) = 0 \quad \text{and} \quad \partial_x f(0; 0) = 0. \quad (4.6)$$

##### 4.4.1.1 Saddle-Node Bifurcations

**Definition 4.6** We say that  $\mu_0$  is a *saddle-node bifurcation* (or a *fold bifurcation*) if there exists no equilibrium for  $\mu < \mu_0$  and there exist two branches of equilibria for  $\mu > \mu_0$ , or if there exist two branches of equilibria for  $\mu < \mu_0$  and no equilibrium for  $\mu > \mu_0$ .

A sufficient condition for having a saddle-node bifurcation at  $\mu_0 = 0$  is the following.

**Theorem 4.2 (Saddle-Node Bifurcation)** *Assume that  $f$  is a  $C^2$  function verifying (4.6) and*

$$\partial_{xx}^2 f(0; 0) \neq 0 \quad \text{and} \quad \partial_\mu f(0; 0) \neq 0. \quad (4.7)$$

*Then,  $(0; 0)$  is a saddle-node bifurcation.*

More precisely, there exists  $\varepsilon > 0$  such that

if  $\partial_{xx}^2 f(0; 0) \partial_\mu f(0; 0) > 0$ , there are two fixed points for  $\mu \in ]-\varepsilon, 0[$  and no fixed points for  $\mu \in ]0, \varepsilon[$ ;

if  $\partial_{xx}^2 f(0; 0) \partial_\mu f(0; 0) < 0$ , there are no fixed point for  $\mu \in ]-\varepsilon, 0[$  and two fixed points for  $\mu \in ]0, \varepsilon[$ .

Condition (4.7) is called the *transversality condition for the saddle-node bifurcation*.

*Example 4.1* Consider the dynamic system (4.5) with

$$f(x; \mu) = \mu - x^2.$$

$x_0 = 0$  is a fixed point for  $\mu_0 = 0$ , and, since  $\partial_x f(x; \mu) = -2x$ , condition (4.6) holds true. We have

$$\partial_{xx}^2 f(x; \mu) = -2, \quad \partial_\mu f(x; \mu) = 1,$$

and hence

$$\partial_{xx}^2 f(0; 0) \partial_\mu f(0; 0) = -2 < 0.$$

According to Theorem 4.2,  $\mu_0 = 0$  is a bifurcation point such that for  $\mu < 0$  there are no fixed points, while for  $\mu > 0$  there are two fixed points. Indeed, the fixed points are given by the equation  $\mu - x^2 = 0$ , which has no solution for  $\mu < 0$ , and two solutions  $x = \pm\sqrt{\mu}$  for  $\mu > 0$ .

We can solve explicitly the equation

$$\dot{x}(t) = \mu - x^2(t). \tag{4.8}$$

If  $\mu < 0$ , we have no stationary solution and

$$x(t) = -\sqrt{-\mu} \tan(\sqrt{-\mu}(t + C)), \quad \text{with } C \in \mathbb{R}.$$

If  $\mu = 0$ , we have  $x(t) = 0$  or

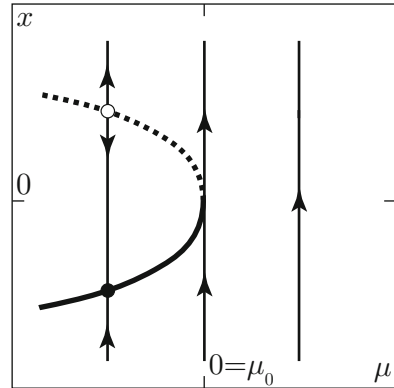
$$x(t) = \frac{1}{t + C}, \quad \text{with } C \in \mathbb{R}.$$

If  $\mu > 0$ , we have  $x(t) = \pm\sqrt{\mu}$  or

$$x(t) = \sqrt{\mu} \tanh(\sqrt{\mu}(t + C)), \quad \text{with } C \in \mathbb{R}.$$

As  $x(t) \rightarrow \sqrt{\mu}$  for  $t \rightarrow +\infty$ , we see that  $x(t) = \sqrt{\mu}$  is a stable solution. As  $x(t) \rightarrow -\sqrt{\mu}$  for  $t \rightarrow -\infty$ , we see that  $x(t) = -\sqrt{\mu}$  is an unstable solution.

**Fig. 4.3** Bifurcation diagram for  $\dot{x} = f(x; \mu) = \mu - x^2$ . The state space of the system is represented on the vertical straight lines, with the arrows indicating the system dynamics. Lines of stable equilibria are solid, lines of unstable equilibria are dotted



In Fig. 4.3, we can see the bifurcation graph of Eq. (4.8). Notice that we adopt the convention to mark the stable equilibria by a solid line and unstable equilibria with a dotted line.

#### 4.4.1.2 Transcritical Bifurcations

Roughly speaking, a bifurcation point  $\mu_0$  is a fold bifurcation if there is an equilibrium for  $\mu = \mu_0$  (i.e., Eq. (4.6) holds) and there are no equilibria for  $\mu < \mu_0$  or for  $\mu > \mu_0$ . At this point, we consider the case in which the two branches of equilibria exist in a neighbourhood of  $\mu_0$ , but they change their nature after passing through  $\mu_0$ .

**Definition 4.7 (Transcritical Bifurcation)** A bifurcation point  $\mu_0$  is called *transcritical* if there exist  $\varepsilon > 0$  and two  $C^1$  branches of equilibria  $\gamma_1$  and  $\gamma_2$ , defined in  $]\mu_0 - \varepsilon, \mu_0 + \varepsilon[$ , such that

1.  $\gamma_1(\mu_0) = \gamma_2(\mu_0)$ ,
2.  $\gamma_1'(\mu_0) \neq \gamma_2'(\mu_0)$  and
3.  $\gamma_1$  is stable for  $\mu \in ]\mu_0 - \varepsilon, 0[$  and unstable for  $\mu \in ]0, \mu_0 + \varepsilon[$ , whereas  $\gamma_2$  is unstable for  $\mu \in ]\mu_0 - \varepsilon, 0[$  and stable for  $\mu \in ]0, \mu_0 + \varepsilon[$ .

A sufficient condition in order to have a transcritical bifurcation for  $\mu_0 = 0$  is the following.

**Theorem 4.3 (Transcritical Bifurcation)** Assume that  $f$  is a  $C^2$  function verifying (4.6),

$$f(0; \mu) = 0 \quad \text{for all } \mu \text{ in a neighbourhood of } 0, \quad (4.9)$$



and

$$\partial_{xx}^2 f(0; 0) \neq 0 \quad \text{and} \quad \partial_{x\mu}^2 f(0; 0) \neq 0. \quad (4.10)$$

Then,  $(0; 0)$  is a transcritical bifurcation.

Condition (4.10) is called the *transversality condition for transcritical bifurcations*.

*Example 4.2* Consider the dynamical system (4.5) with  $f(x; \mu) = \mu x - x^2$ .

$x_0 = 0$  is a fixed point for  $\mu_0 = 0$ , and, since  $\partial_x f(x; \mu) = \mu - 2x$ , condition (4.6) holds true.

Condition (4.9) is satisfied. Moreover, as

$$\partial_{xx}^2 f(x; \mu) = -2, \quad \partial_{x\mu}^2 f(x; \mu) = 1,$$

we have

$$\partial_{xx}^2 f(0; 0) \partial_{\mu} f(0; 0) = -2 < 0,$$

and thus condition (4.10) holds true. By Theorem 4.3,  $\mu_0 = 0$  is a transcritical bifurcation.

Indeed, the fixed points are given by the equation  $\mu x - x^2 = 0$ , which has two solutions for any  $\mu \in \mathbb{R}$ :  $x_1(\mu) = 0$  and  $x_2(\mu) = \mu$ .

As  $\partial_x f(0; \mu) = \mu$ ,  $x_1$  is stable for  $\mu < 0$  and unstable for  $\mu > 0$ , while as  $\partial_x f(\mu; \mu) = -\mu$ ,  $x_2$  is unstable for  $\mu < 0$  and stable for  $\mu > 0$  (see Fig. 4.4).

In contrast, the generic solution of the equation

$$\dot{x}(t) = \mu x - x^2(t) \quad (4.11)$$

is

$$x(t) = \frac{\mu}{1 + c e^{-\mu t}}$$

with  $c \in \mathbb{R}$ , and, therefore,

if  $\mu < 0$ , then

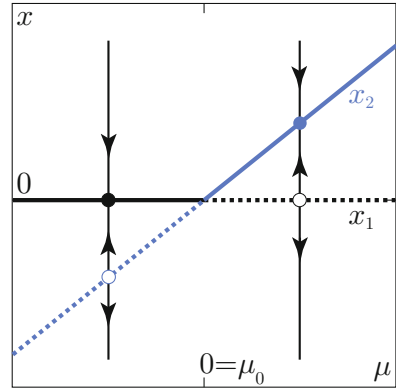
$$x(t) \rightarrow \mu \text{ for } t \rightarrow +\infty \quad \text{and} \quad x(t) \rightarrow 0 \text{ for } t \rightarrow -\infty;$$

if  $\mu > 0$ , then

$$x(t) \rightarrow 0 \text{ for } t \rightarrow +\infty. \quad \text{and} \quad x(t) \rightarrow \mu \text{ for } t \rightarrow -\infty;$$

for a graphical depiction see Fig. 4.4.

**Fig. 4.4** Phase diagram for  $\dot{x} = \mu x - x^2$ . The state space of the system is represented on the vertical straight lines, with the arrows indicating the system dynamics. Lines of stable equilibria are solid, lines of unstable equilibria are dotted



### 4.4.1.3 Pitchfork Bifurcations

**Definition 4.8 (Pitchfork Bifurcations)** A bifurcation point  $\mu_0$  is called a *pitchfork* bifurcation point if

1. There exists a branch of equilibria  $\gamma_0(\mu)$  the stability of which changes for  $\mu = \mu_0$  (i.e.,  $\gamma_0(\mu)$  is stable for  $\mu < \mu_0$  and unstable for  $\mu > \mu_0$ , or vice versa);
2. For  $\mu < \mu_0$  (resp., for  $\mu > \mu_0$ ),  $\gamma_0(\mu)$  is the unique equilibrium, whereas for  $\mu > \mu_0$  (resp., for  $\mu < \mu_0$ ), there exist two branches of equilibria  $\gamma_1(\mu)$  and  $\gamma_2(\mu)$ , such that
  - (a)  $\gamma_1(\mu_0) = \gamma_2(\mu_0) = \gamma_0(\mu_0)$ ,
  - (b)  $\gamma_1(\mu_0) < \gamma_0(\mu_0) < \gamma_2(\mu_0)$ , for  $\mu > \mu_0$  (resp., for  $\mu < \mu_0$ ) and
  - (c) the stability of  $\gamma_1(\mu)$  and  $\gamma_2(\mu)$  is the opposite of that of  $\gamma_0(\mu)$ .

The pitchfork bifurcation is *supercritical* if  $\gamma_1(\mu)$  and  $\gamma_2(\mu)$  are stable and *subcritical* if  $\gamma_1(\mu)$  and  $\gamma_2(\mu)$  are unstable. Instead of *pitchfork bifurcation* also the term *trident bifurcation* is sometimes used.

We restrict our study to the case in which  $f$  is *odd with respect to  $x$* , that is,

$$f(-x; \mu) = -f(x; \mu), \quad \text{for any } x, \mu \in \mathbb{R}^2. \quad (4.12)$$

Note that if  $f$  is odd with respect to  $x$ , then  $f(0; \mu) = 0$  for all  $\mu$ , and differentiating twice (4.12) with respect to  $x$ , we see that also  $\partial_{xx}^2 f$  is odd with respect to  $x$ , and hence  $\partial_{xx}^2 f(0; \mu) = 0$  for all  $\mu$ . Thus, the first condition in (4.10) cannot be satisfied.

A sufficient condition in order to have a pitchfork bifurcation for  $\mu_0 = 0$  is the following.

**Theorem 4.4 (Pitchfork Bifurcation)** Assume that  $f$  is a  $C^3$  function, odd with respect to  $x$ , verifying (4.6) and

$$\partial_{xxx}^3 f(0; 0) \neq 0 \quad \text{and} \quad \partial_{x\mu}^2 f(0; 0) \neq 0. \quad (4.13)$$

Then,  $(0; 0)$  is a pitchfork bifurcation.

More precisely,

if  $\partial_{xxx}^3 f(0; 0) \partial_{x\mu}^2 f(0; 0) < 0$ , the bifurcation is supercritical;

if  $\partial_{xxx}^3 f(0; 0) \partial_{x\mu}^2 f(0; 0) > 0$ , the bifurcation is subcritical.

Condition (4.13) is called the transversality condition for pitchfork bifurcations.

*Example 4.3* Consider the dynamic system (4.5) with

$$f(x; \mu) = \mu x - x^3. \quad (4.14)$$

$x_0 = 0$  is a fixed point for  $\mu_0 = 0$ , and, since  $\partial_x f(x; \mu) = \mu - 3x^2$ , condition (4.6) holds true.

$f$  is odd with respect to  $x$ , moreover, as

$$\partial_{xxx}^3 f(x; \mu) = -6, \quad \partial_{x\mu}^2 f(x; \mu) = 1,$$

we have

$$\partial_{xxx}^3 f(0; 0) \partial_{x\mu}^2 f(0; 0) = -6 < 0,$$

and thus condition (4.13) holds true, and by Theorem 4.4,  $\mu_0 = 0$  is a pitchfork supercritical bifurcation point. Indeed, the fixed points are given by the equation  $\mu x - x^3 = 0$ , which has a unique solution  $x_0(\mu) = 0$  for  $\mu \leq 0$ , and three solutions,  $x_0(\mu) = 0$ ,  $x_1 = \sqrt{\mu}$  and  $x_2 = -\sqrt{\mu}$  for  $\mu > 0$ . As  $\partial_x f(0; \mu) = \mu$ ,  $x_0$  is stable for  $\mu < 0$  and unstable for  $\mu > 0$ , while as  $\partial_x f(\pm \sqrt{\mu}; \mu) = -2\mu$ , both  $x_1$  and  $x_2$  are stable for  $\mu > 0$ .

We can solve explicitly the equation  $\dot{x} = \mu x - x^3$ :

If  $\mu < 0$ , we have  $x(t) = 0$  or

$$x_{\pm}(t) = \pm \sqrt{\frac{-\mu}{e^{-2\mu(t+C)} - 1}}, \quad \text{with } C \in \mathbb{R}.$$

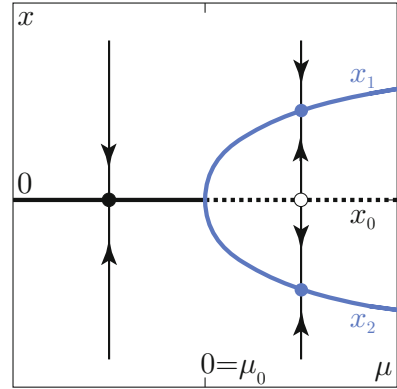
As  $x_{\pm}(t) \rightarrow 0$  for  $t \rightarrow +\infty$ , we see that  $x(t) = 0$  is a stable solution.

If  $\mu = 0$ , we have  $x(t) = 0$  or

$$x_{\pm}(t) = \pm \frac{1}{\sqrt{2(t+C)}}, \quad \text{with } C \in \mathbb{R}.$$

As  $x_{\pm}(t) \rightarrow 0$  for  $t \rightarrow +\infty$ , we see that  $x(t) = 0$  is a stable solution.

**Fig. 4.5** Phase diagram for  $\dot{x} = \mu x - x^3$ . The state space of the system is represented on the vertical straight lines, with the arrows indicating the system dynamics. Lines of stable equilibria are solid, lines of unstable equilibria are dotted



If  $\mu > 0$ , we have

$$x_{\pm}(t) = \pm \sqrt{\frac{\mu}{e^{-2\mu(t+C)} + 1}}, \quad \text{with } C \in \mathbb{R}.$$

As  $x_{\pm}(t) \rightarrow 0$  for  $t \rightarrow -\infty$ , we see that  $x(t) = 0$  is an unstable solution; as  $x_{\pm}(t) \rightarrow \pm\sqrt{\mu}$  for  $t \rightarrow +\infty$ , we see that  $x(t) = \pm\sqrt{\mu}$  are stable solutions.

Figure 4.5 shows the bifurcation in the state space and the parameter space.

### 4.4.2 Hopf Bifurcation

Hopf bifurcations can only occur in dimensions  $n > 1$ . The peculiarity of this bifurcation is that at the bifurcation point, a fixed point changes into a closed orbit behavior. The bifurcation is named after E. Hopf, who, parallel with A.A. Andronov in the Soviet Union, discussed this bifurcation in 1942 [3]. For a historical account, see Sect. 11.4.1.

**Definition 4.9 (Hopf Bifurcation)** We say that the Hopf bifurcation is *supercritical* (Fig. 4.7) if the cycles are attractive, and *subcritical* (Fig. 4.6) if they are repulsive (Fig. 4.7).

Let us assume that the continuous dynamical system (4.1) has a single fixed point  $x_0$  for  $\mu = \mu_0$ , and assume that the Jacobian of  $f$  (cf. Eq. (4.3)) is invertible at  $(x; \mu_0)$ .

Thus, by the implicit function theorem (Dini’s implicit functions theorem), there exist  $\varepsilon > 0$  and a regular function  $x^*: ]\mu_0 - \varepsilon, \mu_0 + \varepsilon[$  such that for each  $\mu \in ]\mu_0 - \varepsilon, \mu_0 + \varepsilon[$ , there is a corresponding single fixed point  $x^*(\mu)$ .

The following theorem ensures the existence of closed orbit in a neighbourhood of  $(x_0; \mu_0)$  (for more details, see [2]).

**Fig. 4.6** Subcritical Hopf bifurcation

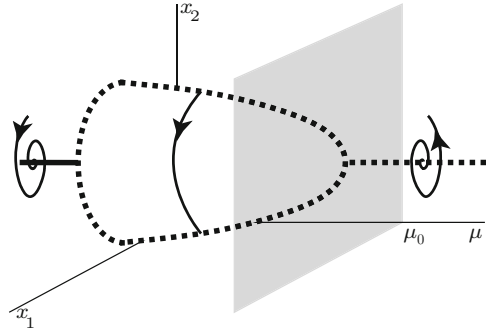
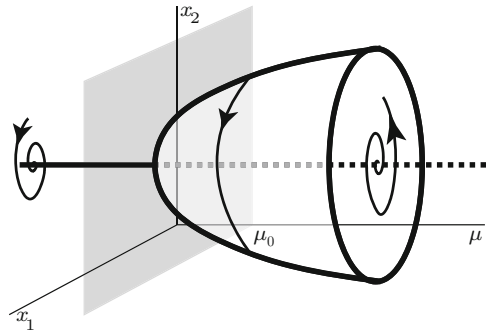


**Fig. 4.7** Supercritical Hopf bifurcation



**Theorem 4.5 (Hopf Bifurcation)** Consider the continuous dynamic system (4.1), with  $f$  and  $\mathbf{x}_0$  as above.

Let  $\lambda_1(\mu), \dots, \lambda_n(\mu)$  be the eigenvalues of  $J(\mathbf{x}_0; \mu)$ , and assume that

1.  $J(\mathbf{x}_0; \mu_0)$  has a pair of complex-conjugated eigenvalues with zero real part, while the other eigenvalues have negative real part:

$$\begin{aligned} \operatorname{Re}\lambda_1(\mu_0) = \operatorname{Re}\lambda_2(\mu_0) = 0, \quad \operatorname{Im}\lambda_1(\mu_0) = -\operatorname{Im}\lambda_2(\mu_0) = \omega_0 > 0, \\ \operatorname{Re}\lambda_j(\mu_0) < 0, \quad \text{for } j = 3, \dots, n; \end{aligned}$$

2. the eigenvalue  $\lambda_1(\mu)$  is differentiable and results

$$\left. \frac{d}{d\mu}(\operatorname{Re}\lambda_1(\mu)) \right|_{\mu=\mu_0} > 0.$$

Then, a periodic solution will bifurcate from  $\mathbf{x}_0$ , with an amplitude growing as  $\sqrt{|\mu - \mu_0|}$  and a period approaching  $\frac{2\pi}{\omega_0}$ , for  $\mu \rightarrow \mu_0$ .

*Remark 4.1* The case  $\left. \frac{d}{d\mu}(\operatorname{Re}\lambda_1(\mu)) \right|_{\mu=\mu_0} < 0$  can be treated replacing  $\mu$  with  $-\mu$ .

The Hopf bifurcation is subcritical or supercritical according to the sign of  $l_1(0)$ , the first Lyapunov coefficient of the dynamical system near the equilibrium.

To compute  $l_1(0)$ , consider the Taylor expansion of  $\mathbf{x} \mapsto \mathbf{f}(\mathbf{x}, 0)$  at  $x = 0$ :

$$\mathbf{f}(\mathbf{x}, 0) = J\mathbf{x} + \frac{1}{2}B(\mathbf{x}, \mathbf{x}) + \frac{1}{6}C(\mathbf{x}, \mathbf{x}, \mathbf{x}) + O(\|\mathbf{x}\|^4),$$

where  $J$  is the Jacobian of  $f$ , whereas  $B(\mathbf{x}, \mathbf{y})$  and  $C(\mathbf{x}, \mathbf{y}, \mathbf{z})$  are the multilinear functions with components

$$B_j(\mathbf{x}, \mathbf{y}) = \sum_{k,l=1}^n \partial_{\xi_k \xi_l}^2 f_j(\xi, 0) \Big|_{\xi=0} x_k y_l,$$

$$C_j(\mathbf{x}, \mathbf{y}, \mathbf{z}) = \sum_{k,l,m=1}^n \partial_{\xi_k \xi_l \xi_m}^3 f_j(\xi, 0) \Big|_{\xi=0} x_k y_l z_m,$$

for  $j = 1, 2, \dots, n$ . Let  $\mathbf{v} \in \mathbb{C}^n$  be an eigenvector of  $J$ , corresponding to the purely imaginary eigenvalue  $i\omega_0$ :

$$J\mathbf{v} = i\omega_0\mathbf{v},$$

and let  $\mathbf{w} \in \mathbb{C}^n$  be the adjoint unitary eigenvector:

$$J^T\mathbf{w} = -i\omega_0\mathbf{w}, \quad \text{and} \quad \langle \mathbf{v}, \mathbf{w} \rangle = 1.$$

Here,  $\langle \mathbf{v}, \mathbf{w} \rangle = \bar{\mathbf{v}}^T \mathbf{w}$  is the inner product in  $\mathbb{C}^n$ . Then (cf. [4]),

$$l_1(0) = \frac{1}{2\omega_0} \operatorname{Re} \left[ \langle \mathbf{w}, C(\mathbf{v}, \mathbf{v}, \bar{\mathbf{v}}) \rangle - 2 \langle \mathbf{w}, B(\mathbf{v}, J^{-1}B(\mathbf{v}, \bar{\mathbf{v}})) \rangle \right. \\ \left. + \langle \mathbf{w}, B(\bar{\mathbf{v}}, (2i\omega_0 I_n - J)^{-1}B(\mathbf{v}, \mathbf{v})) \rangle \right], \quad (4.15)$$

where  $I_n$  is the unit  $n \times n$  matrix.

Recalling that a fixed point is stable if  $\operatorname{Re}(\lambda) < 0$ , we can deduce that with a passage from  $\mu < \mu_0$  to  $\mu > \mu_0$ , the asymptotic stable fixed point degenerates into a closed orbit, leaving this process as an unstable fixed point.

Now, we consider the case of the two-dimensional system:

$$\begin{cases} \dot{x}(t) = f(x(t), y(t); \mu), \\ \dot{y}(t) = g(x(t), y(t); \mu). \end{cases} \quad (4.16)$$

Assume that  $(x_0, y_0)$  is an equilibrium for  $\mu_0$ , and the Jacobian of the system is of the form

$$J(x_0, y_0; \mu_0) = \begin{pmatrix} 0 & -\omega_0 \\ \omega_0 & 0 \end{pmatrix}, \quad \omega_0 > 0.$$

Let

$$\delta := \frac{d}{d\mu} \operatorname{Im} \lambda(\mu_0),$$

and it is clear that if  $\delta > 0$  (resp., if  $\delta < 0$ ), the equilibrium point  $(x(\mu), y(\mu))$  is stable (resp., unstable) for  $\mu < \mu_0$  and unstable (resp., stable) for  $\mu > \mu_0$ .

Setting  $\mathbf{v} = \mathbf{w} = \frac{1}{\sqrt{2}} \begin{pmatrix} 1 \\ -i \end{pmatrix}$ , Eq. (4.15) leads to

$$\begin{aligned} l_1(0) &:= \frac{1}{16} (\partial_{xxx}^3 f + \partial_{xyy}^3 f + \partial_{xxy}^3 g + \partial_{yyy}^3 g) \\ &+ \frac{1}{16\omega_0} (\partial_{xy}^2 f (\partial_{xx}^2 f + \partial_{yy}^2 f) - \partial_{xy}^2 g (\partial_{xx}^2 g + \partial_{yy}^2 g) \\ &- \partial_{xx}^2 f \partial_{xx}^2 g + \partial_{yy}^2 f \partial_{yy}^2 g). \end{aligned} \quad (4.17)$$

**Theorem 4.6 (Hopf Bifurcation for  $n = 2$ )** *If  $\delta l_1(0) > 0$  (resp., if  $\delta l_1(0) < 0$ ), there exists a unique curve of periodic solution for  $\mu < \mu_0$  (resp., for  $\mu > \mu_0$ ).*

*The amplitude of such curves grows as  $\sqrt{|\mu - \mu_0|}$ , whereas the period approaches  $\frac{2\pi}{\omega_0}$ .*

*Example 4.4* Consider the system (4.16) with

$$\begin{aligned} f(x, y; \mu) &= \mu x - y - x(x^2 + y^2), \\ g(x, y; \mu) &= x + \mu y - y(x^2 + y^2). \end{aligned} \quad (4.18)$$

We first note that  $(0, 0)$  is the unique equilibrium for any  $\mu \in \mathbb{R}$ . Next, the Jacobian of (4.18) for  $x = 0$  and  $y = 0$  is

$$f(0, 0; \mu) = \begin{pmatrix} \mu - 1 \\ 1 \quad \mu \end{pmatrix},$$

which has a pair of complex eigenvalues  $\mu \pm i$ . If  $\mu < 0$ , the origin is an attractor, while if  $\mu > 0$ , it is a repeller. We have  $\delta = 1$ , whereas, as

$$\begin{aligned} \partial_{xx}^2 f(x, y; \mu) &= -6x, & \partial_{xy}^2 f(x, y; \mu) &= -2y, & \partial_{yy}^2 f(x, y; \mu) &= -2x, \\ \partial_{xx}^2 g(x, y; \mu) &= -2y, & \partial_{xy}^2 g(x, y; \mu) &= -2x, & \partial_{yy}^2 g(x, y; \mu) &= -6y, \\ \partial_{xxx}^3 f(x, y; \mu) &= -6, & \partial_{xxy}^3 f(x, y; \mu) &= -2, \\ \partial_{xxy}^3 g(x, y; \mu) &= -2, & \partial_{yyy}^3 g(x, y; \mu) &= -6, \end{aligned}$$

from (4.17), we have  $b = -1$ . According to Theorem 4.6, we have a supercritical Hopf bifurcation: the cycles that appear for  $\mu > 0$  are attractors.

On the other side, we can directly solve the system

$$\begin{cases} \dot{x}(t) = \mu x(t) - y(t) - x(t)(x^2(t) + y^2(t)), \\ \dot{y}(t) = x(t) + \mu y(t) - y(t)(x^2(t) + y^2(t)). \end{cases} \quad (4.19)$$

Introducing polar coordinates

$$\begin{cases} x(t) = \rho(t) \cos(\theta(t)), \\ y(t) = \rho(t) \sin(\theta(t)), \end{cases}$$

system (4.19) gives

$$\begin{cases} \dot{\rho} \cos(\theta) - \rho \sin(\theta) \dot{\theta} = \mu \rho \cos(\theta) - \rho \sin(\theta) - \rho^3 \cos(\theta), \\ \dot{\rho} \sin(\theta) + \rho \cos(\theta) \dot{\theta} = \rho \cos(\theta) + \mu \rho \sin(\theta) - \rho^3 \sin(\theta), \end{cases}$$

and hence

$$\begin{cases} \dot{\rho} = \mu \rho - \rho^3, \\ \dot{\theta} = 1. \end{cases} \quad (4.20)$$

We can solve explicitly the system (4.20):

If  $\mu < 0$ , we have

$$\begin{cases} \rho(t) = \sqrt{\frac{\mu}{1 - \exp(-2\mu(t + C_1))}}, \\ \theta(t) = t + C_2, \end{cases} \quad , \text{ with } C_1, C_2 \in \mathbb{R}.$$

We see that  $\rho(t) \rightarrow 0$  for  $t \rightarrow +\infty$ , and hence  $(0, 0)$  is the unique attractor.

If  $\mu = 0$ , we have

$$\begin{cases} \rho(t) = \frac{1}{\sqrt{2(t + C_1)}}, \\ \theta(t) = t + C_2, \end{cases} \quad , \text{ with } C_1, C_2 \in \mathbb{R}.$$

We see that  $\rho(t) \rightarrow 0$  for  $t \rightarrow +\infty$ , and hence  $(0, 0)$  is the unique attractor.

If  $\mu > 0$ , we have



$$\begin{cases} \rho(t) = \sqrt{\frac{\mu}{1 - \exp(-2\mu(t + C_1))}}, \\ \theta(t) = t + C_2, \end{cases}, \text{ with } C_1, C_2 \in \mathbb{R},$$

if  $\rho(0) > \sqrt{\mu}$ , and

$$\begin{cases} \rho(t) = \sqrt{\frac{\mu}{1 + \exp(-2\mu(t + C_1))}}, \\ \theta(t) = t + C_2, \end{cases}, \text{ with } C_1, C_2 \in \mathbb{R},$$

if  $\rho(0) < \sqrt{\mu}$ .

We see that in both cases  $\rho(t) \rightarrow \sqrt{\mu}$  for  $t \rightarrow +\infty$ , and hence the cycle  $x^2 + y^2 = \sqrt{\mu}$  is an attractor.

We also note that if  $\rho(0) < \sqrt{\mu}$  (the orbit starts inside the limit cycle), then  $\rho(t) \rightarrow 0$  for  $t \rightarrow -\infty$ , and hence  $(0, 0)$  is a repeller.

### 4.4.3 Degenerate Hopf Bifurcation in the van der Pol Equation

**Definition 4.10 (van der Pol Equation)** The second-order ordinary differential equation

$$\ddot{x}(t) - \mu(1 - x^2(t))\dot{x}(t) + x(t) = 0 \quad (4.21)$$

is called the *van der Pol equation*. Here,  $\mu$  is a scalar parameter indicating the nonlinearity and the strength of the damping.

Let  $y(t) := \dot{x}(t)$ , and Eq. (4.21) is then equivalent to the system

$$\begin{cases} \dot{x}(t) = y(t), \\ \dot{y}(t) = -x(t) + \mu(1 - x^2(t))y(t). \end{cases} \quad (4.22)$$

First of all, if  $\mu = 0$ , Eq. (4.22) reduces to the linear system

$$\begin{cases} \dot{x}(t) = y(t), \\ \dot{y}(t) = -x(t), \end{cases}$$

which can be solved directly:

$$\begin{cases} x(t) = C_1 \sin(t) + C_2 \cos(t), \\ y(t) = C_1 \cos(t) - C_2 \sin(t), \end{cases} \quad C_1, C_2 \in \mathbb{R}.$$

Thus, in this case, the system has infinitely many periodic orbits.

If  $\mu \neq 0$ , the system is nonlinear; however,  $(x(t), y(t)) = (0, 0)$  is a solution of Eq. (4.22). The Jacobian in  $(0, 0)$  of the function

$$\begin{pmatrix} x \\ y \end{pmatrix} \mapsto \begin{pmatrix} y \\ -x + \mu(1-x)y \end{pmatrix}$$

is

$$\begin{pmatrix} 0 & 1 \\ -1 & \mu \end{pmatrix},$$

the eigenvalues of which are  $\lambda_{\pm} = \frac{1}{2}(\mu \pm \sqrt{\mu^2 - 1})$ . It is easy to see that the real part of the eigenvalues has the same sign as  $\mu$ ; thus,  $(0, 0)$  is stable for  $\mu > 0$  and unstable for  $\mu < 0$ . The imaginary part of the eigenvalues is non-zero if  $|\mu| < 1$ . The existence of a limit cycle can be proved in a more general setting.

**Definition 4.11 (Liénard Equation)** Let  $f$  and  $g$  be  $\mathcal{C}^1$  functions defined in a neighbourhood of 0, and assume that  $f$  is even and  $g$  is odd. The second-order ordinary differential equation

$$\ddot{x} + f(x)\dot{x} + g(x) = 0 \tag{4.23}$$

is called *Liénard equation* [5].

*Remark 4.2* As  $g$  is odd,  $g(0) = 0$ , and therefore  $x(t) \equiv 0$  is a solution of (4.23).

Let  $y(t) := \dot{x}(t)$ , and Eq. (4.23) is then equivalent to the system

$$\begin{cases} \dot{x}(t) = y(t), \\ \dot{y}(t) = -g(x(t)) - f(x(t))y(t). \end{cases} \tag{4.24}$$

**Theorem 4.7 (Liénard Stability Cycle [6])** A Liénard system (4.24) has a unique and stable limit cycle around the origin if it satisfies the following properties:

1.  $g(x) > 0$  for all  $x > 0$ ;
2.  $\lim_{x \rightarrow \infty} F(x) := \lim_{x \rightarrow \infty} \int_0^x f(\xi)d\xi = \infty$ ;

3.  $F(x)$  has one positive root in  $x^*$ , with

$$\begin{cases} F(x) < 0 & \text{for } 0 < x < x^*, \\ F(x) > 0 & \text{non-decreasing for } x > x^*. \end{cases} \quad (4.25)$$

The van der Pol equation satisfies the hypothesis of Theorem 4.7 if  $\mu > 0$ . Indeed,

$$F(x) := \int_0^x -\mu(1-s^2)ds = \mu\left(\frac{x^3}{3} - x\right).$$

If  $\mu > 0$ , then  $F$  is negative for  $x \in ]0, \sqrt{3}[$  and positive for  $x > \sqrt{3}$ ; moreover,  $F$  is increasing and goes to  $+\infty$  as  $x \rightarrow +\infty$ .

By Theorem 4.7, we deduce the existence of a unique stable limit cycle for  $\mu > 0$ . To prove the existence of a unique unstable limit cycle for  $\mu < 0$ , we change  $t$  to  $-t$  and apply again Theorem 4.7.

Although the equilibrium  $(0, 0)$  changes its nature and a limit cycle exists, we do not have a proper Hopf bifurcation, as the limit cycles do not approach the equilibrium as  $\mu \rightarrow 0$ .

Indeed, by Bendixon's negative criterion (see Theorem 2.6, Chap. 2), with  $f(x, y) = y$  and  $g(x, y) = -x + \mu(1 - x^2)y$ , we have

$$\partial_x f(x, y) + \partial_y g(x, y) = \mu(1 - x^2),$$

hence, there exist no closed orbits in  $B_R$ , with  $R < 1$ .

## 4.5 Local Bifurcations for Discrete-Time Systems

Consider the discrete dynamical system

$$x_{n+1} = f(x_n; \mu), \quad (4.26)$$

and assume that  $x_0$  is a fixed point for  $\mu = \mu_0$ , that is,

$$x_0 = f(x_0; \mu_0). \quad (4.27)$$

Also in the discrete case, bifurcations divide into equilibria-colliding, and equilibrium-degenerating bifurcations.

If  $\partial_x f(x_0; \mu_0) \neq 1$ , thanks to the implicit function theorem applied to the function

$$F(x; \mu) = f(x; \mu) - x,$$

we see that for  $\mu$  sufficiently near to  $\mu_0$  there exists a unique fixed point  $x_\mu$ . Thus, in the discrete case, we can therefore see the same bifurcations in which equilibria collide we have seen for continuous systems, which are saddle-node, transcritical and pitchfork. In this case, however, the degeneracy condition (4.6) (taking without loss of generality  $(\mathbf{x}_0; \mu_0) = (\mathbf{0}; 0)$ ) becomes

$$f(0; 0) = 0 \quad \text{and} \quad \partial_x f(0; 0) = 1. \quad (4.28)$$

The Hopf bifurcation Theorem 4.5 changes in the discrete-time case into:

**Theorem 4.8 (Neimark–Sacker Bifurcation)** *Consider the discrete dynamic system (4.26), with  $f$  and  $\mathbf{x}_0$  as above.*

*Let  $\lambda_1(\mu), \dots, \lambda_n(\mu)$  be the eigenvalues of  $J(\mathbf{x}_0; \mu)$ , and assume that*

1.  *$J(\mathbf{x}_0; \mu_0)$  has a pair of complex-conjugated eigenvalues with absolute value equal to 1, while the other eigenvalues have absolute values smaller than 1:*

$$|\lambda_1(\mu_0)| = |\lambda_2(\mu_0)| = 1,$$

$$0 < \omega_0 = \arg(\lambda_1(\mu_0)) = -\arg(\lambda_2(\mu_0)) < \pi,$$

$$|\lambda_j(\mu_0)| < 1, \quad \text{for } j = 3, \dots, n;$$

2.  *$e^{ik\omega_0} \neq 1$ , for  $k = 1, 2, 3, 4$ ;*
3. *the eigenvalue  $\lambda_1(\mu)$  is differentiable and we have*

$$\left. \frac{d}{d\mu} (|\lambda_1(\mu)|) \right|_{\mu=\mu_0} > 0.$$

*Then, the fixed point  $\mathbf{x}_0$  is surrounded by a bifurcating unique closed invariant curve. The amplitude of such invariant curve grows as  $\sqrt{|\mu - \mu_0|}$ .*

Also the Hopf (or Neimark–Sacker) bifurcation can be supercritical or subcritical (or better, *soft* or *sharp*), according to the negative or positive sign of the first Lyapunov coefficient  $l_1(0)$  that assumes the expression

$$\begin{aligned} l_1(0) = & \frac{1}{2} \operatorname{Re} \left[ \langle \mathbf{w}, C(\mathbf{v}, \mathbf{v}, \bar{\mathbf{v}}) \rangle - 2 \langle \mathbf{w}, B(\mathbf{v}, (I_n - J)^{-1} B(\mathbf{v}, \bar{\mathbf{v}})) \rangle \right. \\ & \left. + \langle \mathbf{w}, B(\bar{\mathbf{v}}, (e^{2i\omega_0} I_n - J)^{-1} B(\mathbf{v}, \mathbf{v})) \rangle \right]. \end{aligned} \quad (4.29)$$

Another bifurcation that can occur in a discrete-time system is the so-called flip, *period-doubling*, that we have already met in the previous chapter. A flip bifurcation occurs if, after passing through a critical value  $\mu_0$ , the fixed point changes its stability and a period-2 orbit appears. A flip bifurcation is, essentially, a pitchfork bifurcation of  $f^{\circ 2}$ , the second iterate of  $f$ .

A sufficient condition in order to have a flip bifurcation is the following.

**Theorem 4.9 (Flip Bifurcation)** *Let  $f: \mathbb{R} \times \mathbb{R} \rightarrow \mathbb{R}$ , and let  $x_0$  be a fixed point of  $f$  for  $\mu = \mu_0$ . Assume that*

$$\begin{aligned} \partial_x f(x_0; \mu_0) &= -1, \\ \partial_{xx}^2 f(x_0; \mu_0) - 2\partial_{x\mu}^2 f(x_0; \mu_0) &\neq 0, \\ l_1(0) = -2\partial_{xxx}^3 f(x_0; \mu_0) - 3(\partial_{xx}^2 f(x_0; \mu_0))^2 &\neq 0; \end{aligned}$$

*then,  $(x_0; \mu_0)$  is a flip bifurcation point, and the last two conditions 1 and 2 are called transversal conditions of the flip.*

Also, the flip bifurcation can be supercritical or subcritical. In the first case, the generated period-doubled periodic orbit involved in the bifurcation is stable, otherwise it is unstable. The stability of the period-doubled periodic orbit depends on the sign of the Lyapunov coefficient  $l_1(0)$  (negative/positive sign and supercritical/subcritical bifurcation).

*Example 4.5* Consider the logistic map (cf. Chap. 3),

$$x_{n+1} = \mu x_n(1 - x_n),$$

i.e., (4.26) with  $f(x; \mu) = \mu x(1 - x)$ .

If  $\mu_0 = 3$ , the unique fixed point in  $]0, 1[$  is  $x_0 = \frac{2}{3}$ , and since  $\partial_\mu f(x; \mu) = \mu(1 - 2x)$ , we have  $\partial_\mu f\left(\frac{2}{3}, 3\right) = -1$ .

As

$$\partial_{xx}^2 f(x; \mu) = -2\mu, \quad \partial_{x\mu}^2 f(x; \mu) = 1, \quad \partial_{xxx}^3 f(x; \mu) = 0,$$

we have

$$l_1(0) = -12\mu^2.$$

The hypotheses of Theorem 4.9 are satisfied, and hence we have a supercritical flip bifurcation at  $\mu_0 = 3$ .

## References

1. Gomez, F., Stoop, R.L., Stoop, R.: Universal dynamical properties preclude standard clustering in a large class of biochemical data. *Bioinformatics* **30**(17), 2486–2493 (2014)
2. Guckenheimer, J., Holmes, P.J.: Nonlinear oscillations, dynamical systems, and bifurcations of vector fields. In: *Applied Mathematical Sciences*, vol. 42. Springer, New York (2013). <https://doi.org/10.1007/978-1-4612-1140-2>
3. Hopf, E.: Bifurcation of a periodic solution from a stationary solution of a system of differential equations. *Berlin Math. Phys. Klasse* **94**, 3–32 (1942)
4. Kuznetsov, Y.: Elements of Applied Bifurcation Theory. In: *Elements of Applied Bifurcation Theory*, vol. 112. Springer, New York (2004). <https://doi.org/10.1007/978-1-4757-3978-7>
5. Liénard, A.: Étude des oscillations entretenues. *Revue Générale de l'Électricité* **23**, 901–912 (1928)
6. Perko, L.: *Differential Equations and Dynamical Systems*, vol. 7. Springer, Berlin (2013)
7. Stoop, R., Kanders, K., Lorimer, T., Held, J., Albert, C.: Big data naturally rescaled. *Chaos Solitons Fractals* **90**, 81–90 (2016)

# Chapter 5

## From Local Bifurcations to Global Dynamics: Hopf Systems from the Applied Perspective



Hiroyuki Yoshida

### 5.1 Hopf Bifurcation Theorem

The Hopf bifurcation theorem is one of the most famous tools to prove the existence of closed orbits for systems of ordinary differential equations. Consider the following continuous-time system:

$$\dot{x} = f(x, \mu), \quad x \in \mathbb{R}^n, \quad \mu \in \mathbb{R}. \tag{5.1}$$

Assume that the system (5.1) has a fixed point  $x^*$  at a parameter value  $\mu = \mu_H$ ;

$$f(x^*, \mu_H) = 0. \tag{5.2}$$

Furthermore, we assume that the Jacobian matrix evaluated at the fixed point  $x^*$ ,

$$J = \begin{bmatrix} \frac{\partial f_1(x^*; \mu)}{\partial x_1} & \frac{\partial f_1(x^*; \mu)}{\partial x_2} & \dots & \frac{\partial f_1(x^*; \mu)}{\partial x_n} \\ \frac{\partial f_2(x^*; \mu)}{\partial x_1} & \frac{\partial f_2(x^*; \mu)}{\partial x_2} & \dots & \frac{\partial f_2(x^*; \mu)}{\partial x_n} \\ \vdots & \vdots & \ddots & \vdots \\ \frac{\partial f_n(x^*; \mu)}{\partial x_1} & \frac{\partial f_n(x^*; \mu)}{\partial x_2} & \dots & \frac{\partial f_n(x^*; \mu)}{\partial x_n} \end{bmatrix}, \tag{5.3}$$

has a simple pair of pure imaginary eigenvalues and no other eigenvalues with zero real part when  $\mu = \mu_H$ . By the implicit function theorem, this assumption implies that there is a fixed point  $x^*(\mu)$  near  $x^*(\mu_H)$  which varies smoothly with  $\mu$ .

---

H. Yoshida (✉)  
 College of Economics, Nihon University, Chiyoda City, Japan  
 e-mail: [yoshida.hiroyuki@nihon-u.ac.jp](mailto:yoshida.hiroyuki@nihon-u.ac.jp)

Since the Jacobian matrix depends on  $\mu$ , each eigenvalue of the Jacobian matrix is a function of  $\mu$  as well. In particular, let us express a simple pair of pure imaginary eigenvalues as a function of  $\mu$ :

$$\lambda(\mu), \bar{\lambda}(\mu) = \rho(\mu) \pm \omega(\mu)i, \rho(\mu_H) = 0, \omega(\mu_H) \neq 0, \quad (5.4)$$

where  $\text{Re } \lambda = \rho$  and  $\text{Im } \lambda = \omega$ . In the following, the existence part of the Hopf bifurcation is provided.

**Theorem 5.1 (Hopf Bifurcation<sup>1</sup>)** *Consider the system of ordinary differential equations on an open set  $U \subseteq \mathbb{R}^n$ ,*

$$\dot{x} = f(x, \mu), \quad (5.5)$$

where  $x \in U$  and  $\mu$  is a real parameter varying in some open interval  $I \subseteq \mathbb{R}$ . Suppose that for each  $\mu$  in  $I$  there exists an equilibrium point  $x^* = x^*(\mu)$  of (5.5). Assume that the Jacobian matrix of  $f$  with respect to  $x$ , evaluated at  $x^*(\mu)$ , has a pair of complex conjugate eigenvalues,  $\lambda(\mu)$  and  $\bar{\lambda}(\mu)$ , which satisfy the following (transversality conditions of the Hopf bifurcation):

$$(H1) \quad \text{Re } \lambda(\mu_H) = 0, \quad \text{Im } \lambda(\mu_H) \neq 0,$$

$$(H2) \quad \left. \frac{d \text{Re } \lambda(\mu)}{d\mu} \right|_{\mu=\mu_H} \neq 0,$$

while  $\text{Re } \gamma(\mu_H) \neq 0$  for any other eigenvalues  $\gamma$ . Then, (5.5) has a family of non-constant, periodic solutions.

The important point to note is that there are two types of Hopf bifurcations: a supercritical Hopf bifurcation and a subcritical Hopf bifurcation. In the supercritical case, we observe a stable limit cycle around the unstable equilibrium point as  $\mu$  passes through the bifurcation value  $\mu = \mu_H$ . From the economic point of view, this case is desirable in the sense that the stable limit cycle can be considered as the representation of the actual economic fluctuations in the theory of the business cycle. This situation is shown in Fig. 5.1a, where we can detect an unstable equilibrium point  $E$  and a stable limit cycle. On the other hand, in the subcritical case, we notice an unstable limit cycle around a stable equilibrium point as  $\mu$  passes through the bifurcation value  $\mu = \mu_H$ . In this case, we cannot observe the same persistent and bounded cycles as in the supercritical Hopf bifurcation. However, this case is also important and interesting from an economic point of view. It is well known that Leijonhufvud [11] suggested the concept of ‘‘corridor stability,’’ which states that sufficiently large shocks advance the working of centrifugal forces in the economy, while small shocks have no persistent effects on the economy. His concept of

---

<sup>1</sup>This version is adopted from Hassard et al. [9] and Invernizzi and Medio [10].



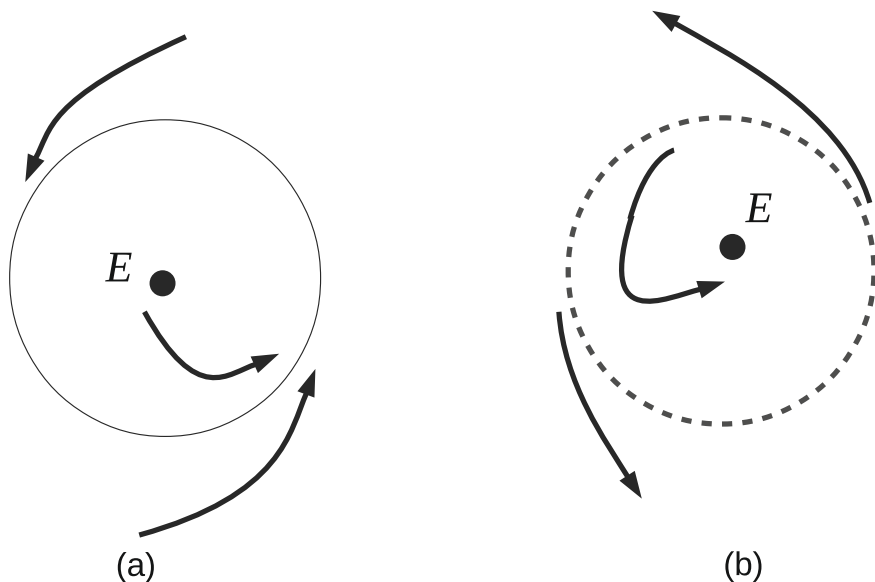


**Fig. 5.1** Two types of Hopf bifurcations. Panel (a) on the left displays a supercritical bifurcation; panel (b) on the right displays a subcritical bifurcation

corridor stability corresponds to the subcritical Hopf bifurcation. This circumstance is depicted in Fig. 5.1b, where we can find a stable equilibrium point  $E$  and an unstable limit cycle.

Let us now turn to another important point regarding the Hopf bifurcations. As stated above, the Hopf bifurcation theorem is explained in terms of the properties of eigenvalues. For theoretical investigations, it is useful to rewrite the conditions of eigenvalues by using the coefficients of characteristic equations. From now on, we shall deal with two-, three-, and four-dimensional systems in order.

**Two-dimensional System** In the case of a two-dimensional system, the Jacobian matrix is a  $2 \times 2$  matrix.

**Theorem 5.2** *The second-order polynomial equation*

$$P(\lambda) = \lambda^2 + b_1\lambda + b_2 = 0 \quad (5.6)$$

*has a pair of pure imaginary roots if and only if*

$$b_1 = 0, \quad b_2 > 0. \quad (5.7)$$

*Remark* In this case, we can easily verify that  $\lambda_{1,2} = \pm\sqrt{b_2}i$ .

**Three-dimensional System** When we consider the case of a three-dimensional system, the Jacobian matrix is a  $3 \times 3$  matrix.

**Theorem 5.3** *The third-order polynomial equation*

$$P(\lambda) = \lambda^3 + b_1\lambda^2 + b_2\lambda + b_3 = 0 \quad (5.8)$$

*has a pair of pure imaginary roots and one non-zero real root if and only if*

$$b_2 > 0, \quad b_1b_2 - b_3 = 0. \quad (5.9)$$

*Remark* See Asada and Semmler [2] for a complete discussion.

**Four-dimensional System** In the case of a four-dimensional system, we have the Jacobian matrix with a dimension of  $4 \times 4$ .

**Theorem 5.4** *The fourth-order polynomial equation*

$$P(\lambda) = \lambda^4 + b_1\lambda^3 + b_2\lambda^2 + b_3\lambda + b_4 = 0 \quad (5.10)$$

*has a pair of pure imaginary roots and two roots with non-zero real parts if and only if either of the following set of conditions (A) or (B) is satisfied:*

$$(A) \quad b_1b_3 > 0, \quad b_4 \neq 0, \quad \Delta_3 = b_1b_2b_3 - b_3^2 - b_1^2b_4 = 0. \quad (5.11)$$

$$(B) \quad b_1 = 0, \quad b_3 = 0, \quad b_4 < 0. \quad (5.12)$$

*Remark* See Asada and Yoshida [3] for a complete discussion.

Furthermore, we shall draw our attention to the result of Liu [12]. He developed an elegant criterion for a class of Hopf bifurcations by restricting his analysis to “simple” Hopf bifurcations, where all the eigenvalues except a pair of purely imaginary ones have negative real parts. For this reason, he could obtain a useful criterion from the Routh–Hurwitz condition, which gives the necessary and sufficient condition for all the eigenvalues of an  $n$ th-order characteristic equation to have negative real parts. In this case, we consider the following theorem:

**Theorem 5.5** *The characteristic equation*

$$P(\lambda) = \lambda^n + b_1\lambda^{n-1} + b_2\lambda^{n-2} + \cdots + b_{n-1}\lambda + b_n = 0 \quad (5.13)$$

*has a pair of pure imaginary roots and  $(n - 2)$  roots with negative real parts if and only if*

$$\Delta_1 = b_1 > 0, \quad \Delta_2 = \begin{vmatrix} b_1 & b_3 \\ 1 & b_2 \end{vmatrix} > 0, \quad \Delta_3 = \begin{vmatrix} b_1 & b_3 & b_5 \\ 1 & b_2 & b_4 \\ 0 & b_1 & b_3 \end{vmatrix} > 0, \dots,$$

$$\Delta_{n-1} = \begin{vmatrix} b_1 & b_3 & b_5 & b_7 & \cdots & 0 & 0 \\ 1 & b_2 & b_4 & b_6 & \cdots & 0 & 0 \\ 0 & b_1 & b_3 & b_5 & \cdots & 0 & 0 \\ 0 & 1 & b_2 & b_4 & \cdots & 0 & 0 \\ \vdots & \vdots & \vdots & \vdots & \ddots & \vdots & \vdots \\ 0 & 0 & 0 & 0 & \cdots & b_n & 0 \\ 0 & 0 & 0 & 0 & \cdots & b_{n-1} & 0 \\ 0 & 0 & 0 & 0 & \cdots & b_{n-2} & b_n \\ 0 & 0 & 0 & 0 & \cdots & b_{n-3} & b_{n-1} \end{vmatrix} = 0, \quad b_n > 0. \quad (5.14)$$

Let us note, finally, that the condition (H2) of the Hopf bifurcation theorem is also an important factor when we apply this theorem to nonlinear systems of differential equations. This condition states that the real part of a pair of complex eigenvalues is not stationary with respect to the parameter value  $\mu$  at  $\mu = \mu_H$ . Fortunately, this condition is equivalent to

$$\left. \frac{\Delta_{n-1}(\mu)}{d\mu} \right|_{\mu=\mu_H} \neq 0. \quad (5.15)$$

Notice that  $\Delta_{n-1}$  is a function of  $\mu$  since every  $b_i$  is a function of  $\mu$ . For a complete proof of this statement, see Liu [12].

## 5.2 Two Specific Examples: Lorenz and Rössler Systems

Lorenz was a pioneer in deterministic chaos. In his paper, Lorenz [13] discovered that nonperiodic solutions could emerge in a nonlinear system of ordinary differential equations. In particular, he realized that small changes in initial conditions cause large changes in long-term outcome in his model, showing the SDIC we introduced in Definition 6.4 necessary to have a strange attractor.

The Lorenz system is a system of three differential equations as follows:

$$\dot{x} = -\sigma x + \sigma y, \quad (5.16a)$$

$$\dot{y} = rx - y - xz, \quad (5.16b)$$

$$\dot{z} = xy - \beta z, \quad (5.16c)$$

where  $\sigma$ ,  $r$ , and  $\beta$  are parameters. This system is algebraically simple: the right-hand side of these equations has two nonlinear terms ( $xz$  and  $xy$ ). However, contrary to common sense at that time, the system produces a complex and strange behaviour as shown in Fig. 5.2. In this case, we set the parameter values as

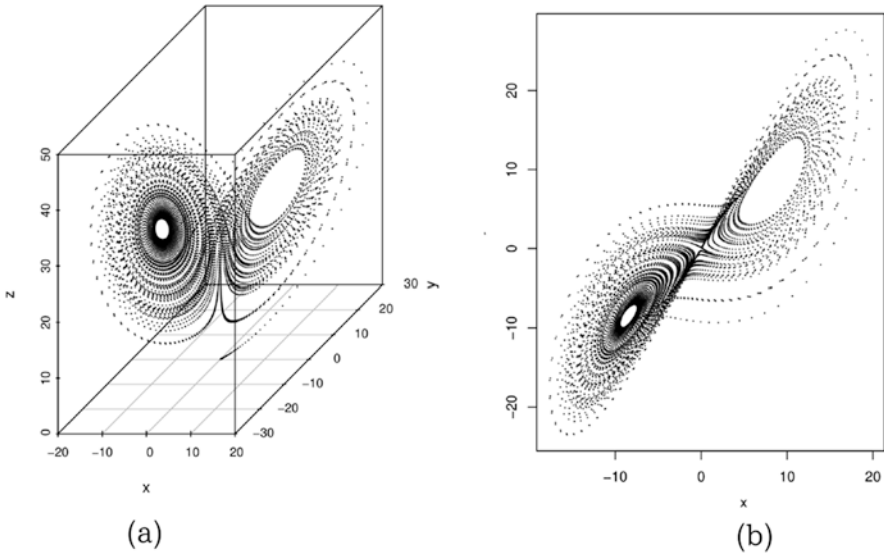


**Fig. 5.2** Lorenz attractor. (a) Three-dimensional phase space. (b) Projection on the  $x$ - $y$  plane

$(\sigma, r, \beta) = (10, 28, 3/8)$ . In addition, it should be noted that we can observe various types of dynamic behaviours, depending on the parameter values. For other values, the system yields stable equilibrium points, stable limit cycles, period-doubling bifurcations, and so on.<sup>2</sup>

The Rössler system is also a well-known system that produces chaotic motions in continuous time. Rössler [17] investigated the following system:

$$\dot{x} = -y - z, \quad (5.17a)$$

$$\dot{y} = x + ay, \quad (5.17b)$$

$$\dot{z} = b + z(x - c), \quad (5.17c)$$

where  $a$ ,  $b$ , and  $c$  are parameters. Note that, in comparison with the Lorenz system, the Rössler system has a simplified structure in that it takes a single quadratic nonlinearity ( $xz$ ) on the right-hand side of (5.17). When  $(a, b, c) = (0.1, 0.3, 12)$ , we can obtain the typical Rössler attractor, which is shown in Fig. 5.3. Depending on the parameter values, the system yields a stable equilibrium point or a stable limit cycle. Moreover, we can see period-doubling bifurcations when a specific parameter is varied.

<sup>2</sup>For a thorough analysis of the Lorenz system, see Sparrow [21].

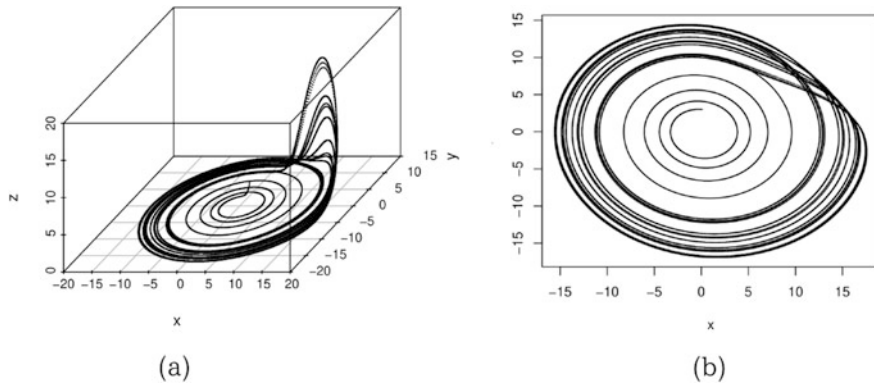


**Fig. 5.3** Rössler attractor. **(a)** Three-dimensional phase space. **(b)** Projection on the  $x$ - $y$  plane

Immediate applications of the Lorenz and Rössler systems are rare in economic dynamics. An interesting and valuable exception is Goodwin [8]. He developed his own insight into modern capitalist economies by combining the ideas of Keynes, Marx, and Schumpeter and proposed several models in his book. For example, he examined the following system:

$$\dot{v} = -0.5u + 0.15v - 0.3z, \quad (5.18a)$$

$$\dot{u} = 0.5v, \quad (5.18b)$$

$$\dot{z} = 0.01 + 85z(v - 0.05). \quad (5.18c)$$

Figure 5.4 shows the emergence of a chaotic attractor in the Goodwin model. We can say with fairly certainty that this system is a modified Rössler model. This is because the Goodwin model has the same quadratic term ( $zv$ ) in the right-hand side of (5.18c) as in the Rössler system. Owing to this similarity, the chaotic attractor in the Goodwin system is very similar to the Rössler attractor.

### 5.3 Shilnikov's Theorem

Numerous efforts have been made to investigate the chaotic behaviour of nonlinear dynamical systems of ordinary differential equations from the analytical point of view. The most famous transition from order to chaos is the Feigenbaum cascade, or period doubling cascade, that we have analysed in Chap. 2. Among them, it is worthwhile to take a brief look at the Shilnikov theorem.

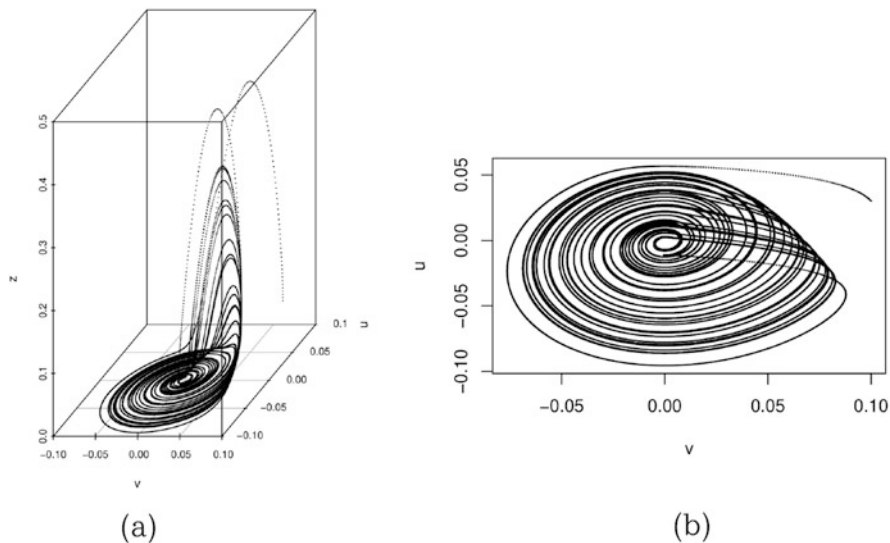


**Fig. 5.4** Chaos in the Goodwin model. **(a)** Three-dimensional phase space. **(b)** Projection on the  $v$ - $u$  plane

**Theorem 5.6 (The Shilnikov Theorem<sup>3</sup>)** Consider the system

$$\dot{x} = \rho x - \omega y + P(x, y, z), \quad (5.19a)$$

$$\dot{y} = \omega x + \rho y + Q(x, y, z), \quad (5.19b)$$

$$\dot{z} = \lambda z + R(x, y, z), \quad (5.19c)$$

where  $P$ ,  $Q$ , and  $R$  vanish together with their first derivatives at the equilibrium point  $E = (x_*, y_*, z_*)$ . Let us assume that one of the orbits, denoted by  $\Gamma_0$ , is asymptotic to  $E$  as  $t \rightarrow \pm\infty$ , being bounded away from any other singularity ( $\Gamma_0$  is then a homoclinic connection). Then, if

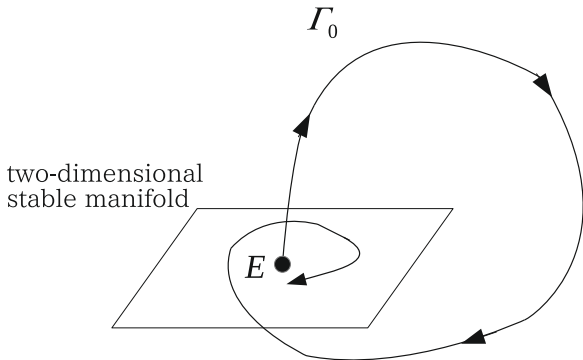
$$|\lambda| > |\rho| > 0, \quad \lambda\rho < 0, \quad (5.20)$$

every neighbourhood of the orbit  $\Gamma_0$  contains a countable set of unstable periodic solutions of saddle type.

From (5.20), there are two essential conditions for the application of the Shilnikov theorem. For the time being, we consider the case of  $\lambda > 0$ . First,

<sup>3</sup>The original theorem was given by Shilnikov [19]. This version is adopted from Arneodo et al. [1] and Silva [20].

**Fig. 5.5** Homoclinic orbit in the Shilnikov scenario



the system has a saddle-node equilibrium point, which means the existence of a one-dimensional unstable manifold and a two-dimensional stable manifold. This condition is easily examined from the local point of view. Second, the system has a homoclinic orbit, which connects an equilibrium point  $E$  to itself;  $\lim_{t \rightarrow \pm\infty} \Gamma(t) = E$  and  $\Gamma(0) \neq E$ . This condition prescribes a global nature of the system. The combination of these two conditions implies topological conjugacy in a neighbourhood of the homoclinic orbit with the horseshoe dynamics that we introduced in Sect. 6.2.1.

A graphical presentation of the Shilnikov conditions is shown in Fig. 5.5. After moving away from the equilibrium point  $E$  along the one-dimensional unstable manifold, the trajectory  $\Gamma_0$  returns to the identical equilibrium point on the two-dimensional stable manifold.<sup>4</sup>

As a numerical example of the occurrence of chaos in the Shilnikov scenario, consider the following system of three differential equations:

$$\dot{x} = y, \tag{5.21a}$$

$$\dot{y} = -x + yz, \tag{5.21b}$$

$$\dot{z} = -z + xy + 0.39, \tag{5.21c}$$

which was reported in Sprott [23]. This system has a saddle-node equilibrium at point  $(0, 0, 0.39)$ , with eigenvalues  $\lambda_1 = -1$  and  $\lambda_{2,3} = 0.195 \pm 0.980803i$ . This implies that the system satisfies the local conditions of the Shilnikov theorem:  $|\lambda| > |\rho| > 0$  and  $\lambda\rho < 0$ . As it is difficult to detect the existence of a homoclinic orbit from an analytical point of view, we show the numerical simulations of the initial value problem given by system (5.21). By setting the initial conditions as

---

<sup>4</sup>If  $\lambda < 0$ , we have to consider the equilibrium point with a one-dimensional stable manifold and a two-dimensional unstable manifold. In this case, the direction of arrows on the homoclinic orbit  $\Gamma_0$  is opposite to that in Fig. 5.5.

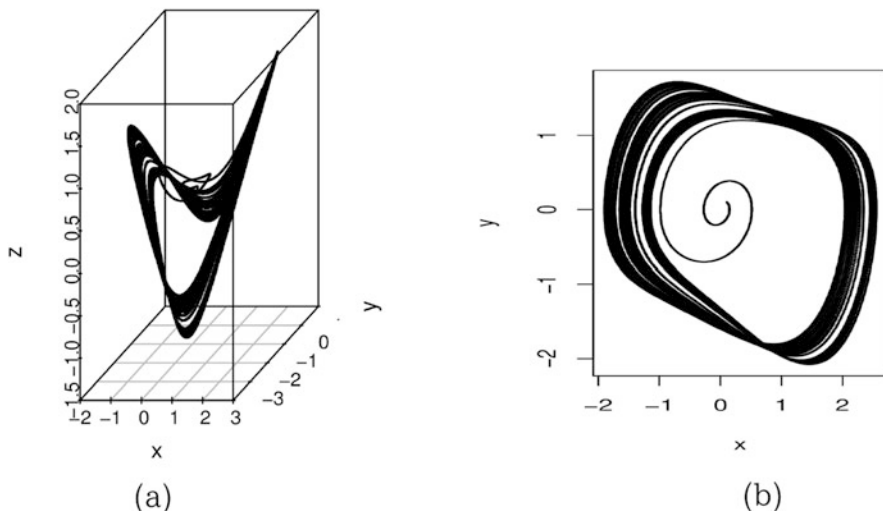


**Fig. 5.6** The chaotic attractor of system (5.21). (a) Three-dimensional phase space. (b) Projection on the  $x$ - $y$  plane

$(x(0), y(0), z(0)) = (0.1, 0.1, 0.3)$ , we can verify that the system displays a chaotic motion as shown in Fig. 5.6.

Macroeconomic applications of the Shilnikov theorem can be found in several works. Lorenz [14] investigated two macroeconomic models. One is a business cycle model with inventories; another is a linear multiplier-accelerator model with nonlinear government activity. Sportelli [22] developed a Harrodian-type macrodynamic model by considering the interactions among the actual rate of growth, the warranted rate of growth, and the fraction of income saved. Tsuzuki et al. [24] proposed an investment model and, finally, Bella et al. [4] examined the dynamics of an endogenous growth model with human capital accumulation in the dynamic optimization framework.

## 5.4 Delay-Differential Equations

This section considers two nonlinear systems of delay-differential equations investigated using numerical simulations: the Mackey–Glass system [16] and the Shibata–Saito system [18]. While the former investigated a physiological problem, the latter examined the population dynamics of two competing species with a time-delayed saturation.

It is well known that deterministic chaos occurs in the continuous-time framework only when the dimension of the dynamical system is equal to or more than



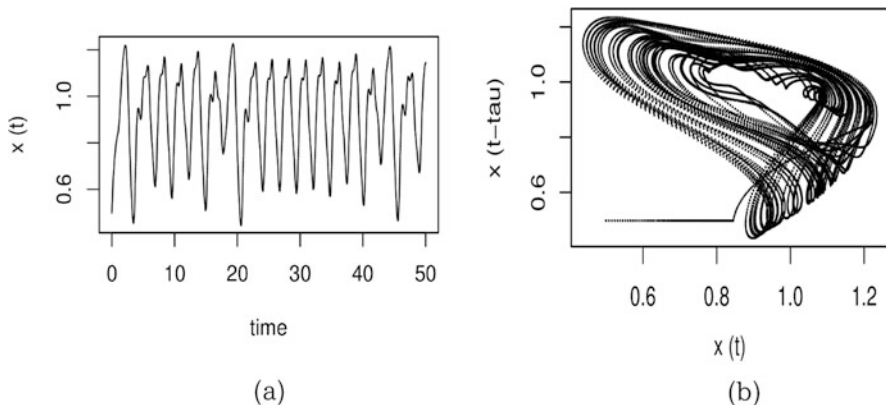


**Fig. 5.7** Chaotic motion of the Mackey–Glass system. **(a)** Time series. **(b)** Phase plot

three. That is, we cannot observe chaotic motions in one- and two-dimensional systems of autonomous ordinary differential equations (cf. Sect. 2.4).

If once we turn our attention towards delay-differential equations, the situation is completely different. We can observe chaotic fluctuations in the delay-differential equation with one variable. In fact, Mackey and Glass [16] provided an interesting model by using the following system:

$$\dot{x}(t) = \frac{ax(t - \tau)}{1 + x^n(t - \tau)} - \gamma x(t), \tag{5.22}$$

where  $a > 0$ ,  $\tau > 0$ , and  $\gamma > 0$ . Figure 5.7 shows chaotic motion of (5.22) with  $a = 3.6$ ,  $\tau = 1$ ,  $n = 10$ , and  $\gamma = 2$ .

The main reason for the emergence of chaotic fluctuations is that the Mackey–Glass system has an infinite dimension. Its solution space has an infinite dimension, with a continuous function on the closed interval  $[-\tau, 0]$  as the initial condition. Roughly speaking, we need an infinite number of initial conditions to solve the initial value problem of (5.22).

We shall now consider the following system of integro-differential equations:

$$\dot{x}(t) = \frac{ay_m(t)}{1 + [y_m(t)]^n} - \gamma x(t), \tag{5.23}$$

where

$$y_m(t) = \int_{-\infty}^t \omega(s)x(s)ds, \tag{5.24}$$

$$\omega(s) = \left(\frac{m}{\tau}\right)^m \frac{(t-s)^{m-1}}{(m-1)!} e^{-(m/\tau)(t-s)}, \tau > 0. \tag{5.25}$$

Note that  $m$  is a positive integer. Since  $\int_{-\infty}^t \omega(s) ds = 1$ , we can see that the function  $\omega(s)$  is a weighting function, which is identical with a density function with the mean,  $\tau$ , and the variance,  $\tau^2/m$ .

If  $m = 1$ , it is the exponential distribution. For  $m \geq 2$ , the functional shape of  $\omega(s)$  has a one-humped curve with a maximum value at  $s = t - (m - 1)\tau/m$  when  $t$  is fixed. Moreover, we can obtain  $y_m(t) = x(t - \tau)$  if  $m \rightarrow \infty$ . This is because the function  $\omega(s)$  becomes the Dirac delta function that appears as a sharp peak at  $t = \tau$  when  $m \rightarrow \infty$ . Thus, we reasonably conclude that system (5.23) is equivalent to the Mackey–Glass system (5.22) when  $m \rightarrow \infty$ .

We shall now look at another subject related to the Mackey–Glass system. Here, we seek to transform the Mackey–Glass system into the tractable system by using MacDonald’s linear chain trick.<sup>5</sup> Let us define new variables:

$$y_j(t) = \int_{-\infty}^t \left(\frac{m}{\tau}\right)^j \frac{(t-s)^{j-1}}{(j-1)!} e^{-(m/\tau)(t-s)} x(s) ds, \quad j = 1, 2, \dots, m. \quad (5.26)$$

By differentiating (5.26) with respect to  $t$  and using (5.23), we obtain the following system of ordinary differential equations:

$$\dot{x}(t) = \frac{ay_m(t)}{1 + [y_m(t)]^n} - \gamma x(t), \quad (5.27a)$$

$$\dot{y}_1(t) = (m/\tau)[x(t) - y_1(t)], \quad (5.27b)$$

$$\dot{y}_j(t) = (m/\tau)[y_{j-1}(t) - y_j(t)], \quad j = 2, 3, \dots, m. \quad (5.27c)$$

Consequently, this result means that we can transform the Mackey–Glass system into the system of  $(m + 1)$ -dimensional ordinary differential equations. In the course of the above argument, we arrive at the conclusion that the Mackey–Glass system corresponds to the system of infinite-dimensional ordinary differential equations by means of MacDonald’s chain trick. This property is fundamental for the generation of complex dynamics.

By using computational approaches, Farmer [7] extensively examined the properties of the chaotic attractors observed in the Mackey–Glass system. Specifically, he studied the time series, power spectra, the dimension of chaotic attractors, the spectrum of Lyapunov exponents, and so forth. In his paper, he kept the parameters  $a$ ,  $n$ , and  $\gamma$  fixed at  $a = 0.2$ ,  $n = 10$ , and  $\gamma = 0.1$ . On the other hand, the delay time  $\tau$  is a variable parameter. For example, when  $\tau = 17$ , he found that the largest Lyapunov exponent of the chaotic attractor is 0.007 and the fractal dimension is 2.13.<sup>6</sup>

<sup>5</sup>On this point, see MacDonald [15].

<sup>6</sup>For a mathematical explanation of the Lyapunov exponents and fractal dimension, see Sects. 6.2 and 6.3, respectively.

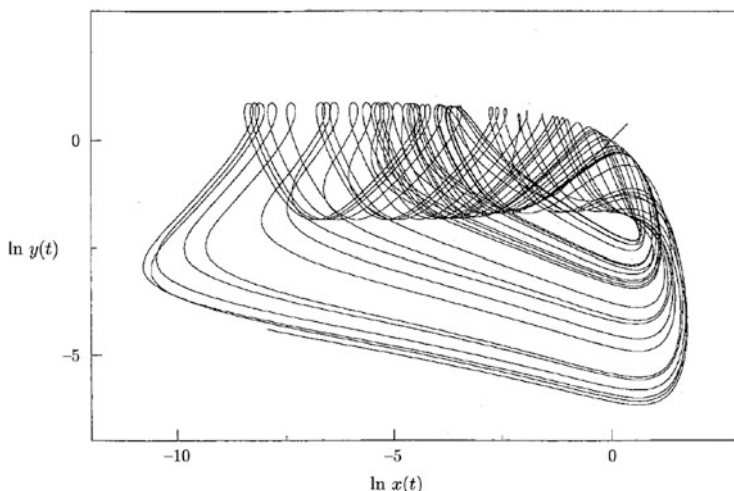


**Fig. 5.8** Chaotic attractor of the Shibata–Saitô system

Finally, we turn to the Shibata and Saitô system, and we consider the dynamics of the system of delay-differential equations with two variables. Shibata and Saitô [18] investigated the following system:

$$\dot{x}(t) = [\varepsilon_1 - a_{11}x(t - \alpha_1) - a_{12}y(t)]x(t), \quad (5.28a)$$

$$\dot{y}(t) = [\varepsilon_2 - a_{21}x(t) - a_{22}y(t - \alpha_2)]y(t). \quad (5.28b)$$

By setting  $a_{11} = a_{22} = 2$ ,  $a_{12} = a_{21} = 1$ ,  $\varepsilon_1 = \varepsilon_2 = 2$ ,  $\tau_1 = 1.5$ , and  $\tau_2 = 0.9$  for the parameters, we obtain Fig. 5.8, which shows the emergence of a chaotic attractor.

The analysis of time lags is fundamental for economics. In particular, the existence of time lags involved in the policy process has a large effect on macroeconomic stability, from both the practical and theoretical points of view. Many economists found the occurrence of complex business cycles by means of numerical simulations. For more information, see Fanti and Manfredi [6], Yoshida and Asada [25], and De Cesare and Sportelli [5].

**Acknowledgment** The author would like to thank a reviewer and Professor Giuseppe Orlando for their useful suggestions and helpful comments on earlier versions. All remaining errors are my own.

## References

1. Arneodo, A., Coulet, P., Tresser, C.: Oscillators with chaotic behavior: an illustration of a theorem by Shil'nikov. *J. Stat. Phys.* **27**(1), 171–182 (1982)
2. Asada, T., Semmler, W.: Growth and finance: an intertemporal model. *J. Macroecon.* **17**(4), 623–649 (1995)
3. Asada, T., Yoshida, H.: Coefficient criterion for four-dimensional Hopf bifurcations: a complete mathematical characterization and applications to economic dynamics. *Chaos Solitons Fractals* **18**(3), 525–536 (2003)
4. Bella, G., Mattana, P., Venturi, B.: Shilnikov chaos in the Lucas model of endogenous growth. *J. Econ. Theory* **172**, 451–477 (2017)
5. De Cesare, L., Sportelli, M.: Fiscal policy lags and income adjustment processes. *Chaos Solitons Fractals* **45**(4), 433–438 (2012)
6. Fanti, L., Manfredi, P.: Chaotic business cycles and fiscal policy: an IS-LM model with distributed tax collection lags. *Chaos Solitons Fractals* **32**(2), 736–744 (2007)
7. Farmer, D.: Chaotic attractors of an infinite-dimensional dynamical system. *Phys. D* **4**, 366–93 (1982)
8. Goodwin, R.M.: *Chaotic Economic Dynamics*. Oxford University Press, Oxford (1990)
9. Hassard, B.D., Kazarinoff, N.D., Wan, Y.H.: *Theory and Applications of Hopf Bifurcation*, vol. 41. CUP Archive (1981)
10. Invernizzi, S., Medio, A.: On lags and chaos in economic dynamic models. *J. Math. Econ.* **20**(6), 521–550 (1991)
11. Leijonhufvud, A.: Effective demand failures. *Swedish J. Econ.* **75**(1), 27–48 (1973)
12. Liu, W.M.: Criterion of Hopf bifurcations without using eigenvalues. *J. Math. Anal. Appl.* **182**(1), 250–256 (1994)
13. Lorenz, E.N.: Deterministic nonperiodic flow. *J. Atmos. Sci.* **20**, 130–141 (1963)
14. Lorenz, H.W.: Complex dynamics in low-dimensional continuous-time business cycle models: The Shil'nikov case. *Syst. Dyn. Rev.* **8**(3), 233–250 (1992)
15. MacDonald, N.: *Time Lags in Biological Models*, vol. 27. Springer, Berlin (2013)
16. Mackey, M.C., Glass, L.: Oscillation and chaos in physiological control systems. *Science* **197**(4300), 287–289 (1977)
17. Rössler, O.E.: An equation for continuous chaos. *Phys. Lett. A* **57**(5), 397–398 (1976)
18. Shibata, A., Saito, N.: Time delays and chaos in two competing species. *Math. Biosci.* **51**(3–4), 199–211 (1980)
19. Shilnikov, L.P.: A case of the existence of a denumerable set of periodic motions. In: *Doklady Akademii Nauk*, vol. 160, pp. 558–561. Russian Academy of Sciences, Moscow (1965)
20. Silva, C.P.: Shil'nikov's theorem, a tutorial. *IEEE Trans. Circuits Syst. I: Fundam. Theory Appl.* **40**(10), 675–682 (1993)
21. Sparrow, C.: *The Lorenz Equations Bifurcations, Chaos, and Strange Attractors*. Springer, Berlin (1982)
22. Sportelli, M.C.: Dynamic complexity in a Keynesian growth-cycle model involving Harrod's instability. *J. Econ.* **71**(2), 167–198 (2000)
23. Sprott, J.: Strange attractors with various equilibrium types. *Eur. Phys. J. Special Topics* **224**(8), 1409–1419 (2015)
24. Tsuzuki, E.: Coefficient criterion for Shil'nikov chaos: application to a simple investment model. In: Hsu, J.C. (ed.) *Business Cycles in Economics: Types, Challenges and Impacts on Monetary Policies*, chap. 5, pp. 69–86. Nova Science Publishers, Hauppauge (2014)
25. Yoshida, H., Asada, T.: Dynamic analysis of policy lag in a Keynes–Goodwin model: stability, instability, cycles and chaos. *J. Econ. Behav. Organ.* **62**(3), 441–469 (2007)

# Chapter 6

## Chaos



Giuseppe Orlando, Ruedi Stoop, and Giovanni Tagliatalata

### 6.1 Chaos

As mentioned, the Logistic map exhibits an irregular behaviour that, according to the following definitions, we call *chaotic*.

**Definition 6.1 (Closure)** Let  $S$  be a subset of  $\mathbb{R}^{\ell}$ . The *closure* of  $S$ , denoted by  $\overline{S}$ , is the set of points  $\mathbf{x}$  such that every open ball centred at  $\mathbf{x}$  contains a point of  $S$ .

**Definition 6.2 (Dense Set)** Let  $D \subset S$  be;  $D$  is *dense* in  $S$  if  $\overline{D} = S$ .

*Example 6.1* The set of rational numbers  $\mathbb{Q}$  is dense in  $\mathbb{R}$ .

**Definition 6.3 (Topological Transitivity)** The map  $f: S \rightarrow S$  is said to be *topologically transitive* if for any pair of open sets  $U, V \subset S$ , there exists  $n \in \mathbb{N}$  such that  $f^{\circ n}(U) \cap V \neq \emptyset$ .

*Remark 6.1* The idea is that a topologically transitive map has points that move under iteration from one arbitrarily small neighbourhood to any other. This means

---

G. Orlando (✉)

University of Bari, Department of Economics and Finance, Bari, Italy

University of Camerino, School of Sciences and Technology, Camerino, Italy

e-mail: [giuseppe.orlando@uniba.it](mailto:giuseppe.orlando@uniba.it); [giuseppe.orlando@unicam.it](mailto:giuseppe.orlando@unicam.it)

R. Stoop

Institute of Neuroinformatics, ETHZ/University of Zürich, Zurich, Switzerland

e-mail: [ruedi@ini.phys.ethz.ch](mailto:ruedi@ini.phys.ethz.ch)

G. Tagliatalata

University of Bari, Department of Economics and Finance, Bari, Italy

e-mail: [giovanni.tagliatalata.it@uniba.it](mailto:giovanni.tagliatalata.it@uniba.it)

© The Author(s), under exclusive license to Springer Nature Switzerland AG 2021

G. Orlando et al. (eds.), *Non-Linearities in Economics*, Dynamic Modeling

and Econometrics in Economics and Finance 29,

[https://doi.org/10.1007/978-3-030-70982-2\\_6](https://doi.org/10.1007/978-3-030-70982-2_6)

that the dynamical system cannot be decomposed into two disjoint open sets that are invariant under the map.

**Definition 6.4 (Sensitive Dependence on Initial Conditions (SDIC))**  $f: S \rightarrow S$  has *sensitive dependence on initial conditions* if there exists  $\delta > 0$  such that, for any  $x \in S$  and any neighbourhood  $N$  of  $x$ , there exists  $y \in N$  and  $n \geq 0$  such that

$$|f^{cn}(x) - f^{cn}(y)| > \delta.$$

*Remark 6.2* Sensitive dependence on initial conditions for a map means that if there exist points arbitrarily close to  $x$ , at least one of those will eventually move away from  $x$  by at least  $\delta$  under iteration of  $f$ . Such a behaviour may magnify small errors caused by round-off errors in computations.

*Example 6.2* The Logistic map possesses sensitive dependence on initial conditions for  $\mu > 2 + \frac{1+\sqrt{5}}{2}$ .

A popular definition of chaos is as follows.

**Definition 6.5 (Chaos)** The map  $f: S \rightarrow S$  is said to be *chaotic* on  $S$  if

1.  $f$  is topologically transitive,
2. the set of the periodic points is dense in  $S$ , and
3.  $f$  has sensitive dependence on initial conditions.

*Remark 6.3* Banks et al. [3] have shown that the first two conditions are sufficient for defining chaos when  $S$  is not a finite set.

**Theorem 6.1 (Banks et al. [3])** *If the map  $f: S \rightarrow S$  is topologically transitive and is dense in  $S$ , then  $f$  has sensitive dependence on initial conditions.*

*Li–Yorke showed that if a system has a period 3 orbit, it has chaotic behavior.*

## 6.2 Measuring Sensitive Dependence on Initial Conditions

Now, let us consider the mapping  $f: \mathbb{R}^\ell \rightarrow \mathbb{R}^\ell$ , the recursive expression

$$\mathbf{x}_{n+1} = f(\mathbf{x}_n), \tag{6.1}$$

and two initial points  $\mathbf{x}_0 - \mathbf{y}_0$  close to each other such that

$$\mathbf{x}_0 - \mathbf{y}_0 = \Delta_0. \tag{6.2}$$

We denote iterations from the first one to the  $n$ th one as

$$\begin{aligned} \mathbf{x}_1 - \mathbf{y}_1 &= f^{\circ 1}(\mathbf{x}_0) - f^{\circ 1}(\mathbf{y}_0), \\ \vdots & \\ \mathbf{x}_n - \mathbf{y}_n &= f^{\circ n}(\mathbf{x}_0) - f^{\circ n}(\mathbf{y}_0), \end{aligned} \quad (6.3)$$

their linear approximations as

$$\begin{aligned} \mathbf{x}_1 - \mathbf{y}_1 &\approx \frac{df^{\circ 1}(\mathbf{x}_0)}{dx} \Delta_0, \\ \vdots & \\ \mathbf{x}_n - \mathbf{y}_n &\approx \frac{df^{\circ n}(\mathbf{x}_0)}{dx} \Delta_0, \end{aligned} \quad (6.4)$$

and by  $J^1, \dots, J^n$  the corresponding  $n$  Jacobian matrices evaluated in  $\mathbf{x}_0$ , i.e.,  $J^k = \frac{df^{\circ k}(\mathbf{x}_0)}{dx}$ ,  $k = 1, \dots, n$ .

Assume that  $J^n$  has  $n$  real eigenvalues  $\Lambda_1^n, \Lambda_2^n, \dots, \Lambda_\ell^n$ , ordered in such a way that  $\Lambda_1^n \geq \Lambda_2^n \geq \dots \geq \Lambda_\ell^n$ .

**Definition 6.6 (Lyapunov Exponents)** The real numbers  $\lambda_1, \lambda_2, \dots, \lambda_\ell$  defined by

$$\lambda_i = \lim_{n \rightarrow \infty} \frac{1}{n} \log_2(\Lambda_i^n) \quad (6.5)$$

are called *Lyapunov exponents*. Alternatively, often natural logarithms are used in this definition.

*Remark 6.4* Notice that if we consider the trajectories departing from  $x_0$  and  $y_0$ , then we have

$$\mathbf{y}_n - \mathbf{x}_n = f^{\circ n}(\mathbf{y}_0) - f^{\circ n}(\mathbf{x}_0) \simeq A^n(\mathbf{y}_0 - \mathbf{x}_0). \quad (6.6)$$

Therefore, the leading Lyapunov exponent is the rate at which nearby trajectories diverge (see, for example, [21] and [5]). This indicates how fast predictability of the system is lost. For this reason, the Lyapunov exponents are often used as a measure of chaos.

**Definition 6.7 (Lyapunov Spectrum)** The set of all Lyapunov exponents is called the *Lyapunov spectrum*, and the sign of each exponent determines whether stretching or folding dominates, in the direction associated with the exponent.

*Example 6.3* Let us consider the Logistic map with parameter  $\mu = 2.5$ . For a one dimensional map  $f$ , the eigenvalue of the jacobian  $J^1$  in  $x_0$  is given by  $f'(x_0)$ ,

**Table 6.1** Finite time Lyapunov exponent approximation  $\lambda(n)$  of the Logistic map evaluated over  $n$  iterations. For  $n \rightarrow \infty$ , the Lyapunov exponent is positive and close to 1. Source H. W. Lorenz [14]

$t$	$x_t$	$f'(x_t)$	$\prod_{t=1}^n f'(x_t)$	$\lambda(n)$
1	0.600	0.799	0.799	-0.321
2	0.960	3.680	2.944	0.778
3	0.153	2.771	8.158	1.009
4	0.520	0.160	1.307	0.096
$\vdots$	$\vdots$	$\vdots$	$\vdots$	$\vdots$
21	0.262	1.899	$0.178 \times 10^7$	0.989
22	0.774	2.195	$0.392 \times 10^7$	0.995
$\vdots$	$\vdots$	$\vdots$	$\vdots$	$\vdots$
99	0.221	2.225	$0.598 \times 10^7$	0.999

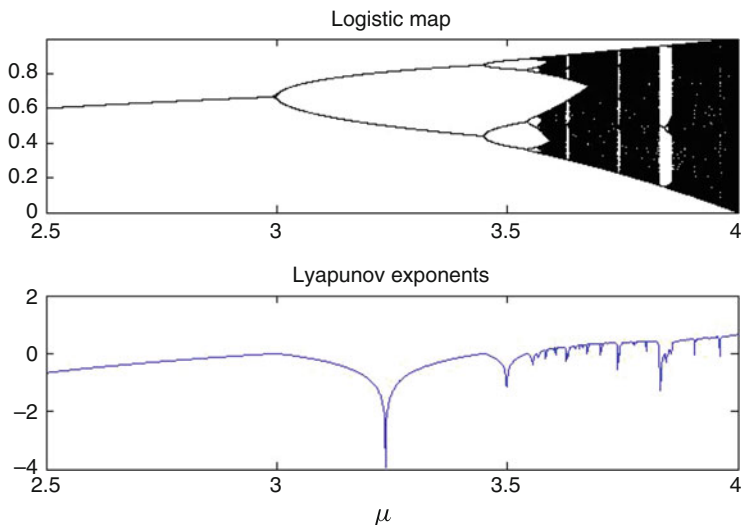


**Fig. 6.1** (Upper panel) Bifurcation diagram and (lower panel) corresponding Lyapunov exponent of the Logistic map versus  $\mu$

and the eigenvalue of  $J^n$  is the product of the derivatives along the orbit:  $\Lambda^n = f'(x_0) \cdots f'(x_{n-1})$ . If we choose  $x_0 = \frac{3}{5}$ , we have  $f'(x_0) = \frac{1}{2}$ . As  $x_0$  is a fixed point, we have  $\Lambda^n = 0.5^n$ . The Lyapunov exponent is  $\lambda = \log_2(0.5^n)/n = \frac{n}{n} \log_2 \frac{1}{2} = -\log_2(2) = -1$ , which means that the orbit rapidly converges to the fixed point.

In Table 6.1 are listed some Lyapunov exponents of the Logistic map, while in Fig. 6.1 we plot the bifurcation diagram of the Logistic map and the Lyapunov exponent versus parameter  $\mu$ .

Other, earlier, measures of the complexity of behaviour related to the Lyapunov exponents are different notions of topological entropy.



### 6.2.1 Stretching and Folding

Let us start with an example of a function called the Horseshoe map that works by stretching and folding the space. For brevity, we will rely only on the graphic illustration, without going into details. Figure 6.2 provides a visual example on how the Horseshoe map transforms the square of vertices, A, B, C, and D into a rectangle and then folds it. On this horseshoe shape, the Horseshoe map carries out a stretching and folding again. The grey area represents how much of the starting set is preserved under the iterations

As just seen, there are (functional) transformations that stretch, bend, and contract space. The strange attractors are precisely the result of such continuous spatial deformations, and Lyapunov exponents are useful in measuring them. Obviously, when we talk about attractors we are referring to dynamic dissipative systems, therefore if, for example, our starting point is in a circle of radius  $r_0$ , the immediately following phase will be projected into an object of different shape and orientation (see Fig. 6.3).

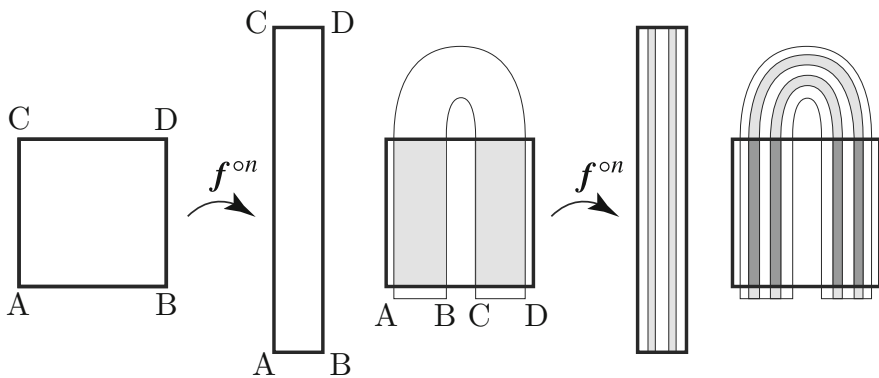


Fig. 6.2 The horseshoe map transforming the space

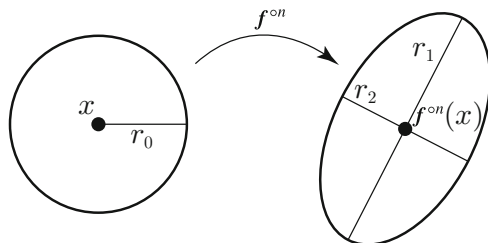


Fig. 6.3 Stretching and contracting the space along two dimensions

Assuming that this object is an ellipse with axis  $r_1$  and  $r_2$ , we denote  $r_1 = \mu_1 r_0$  and  $r_2 = \mu_2 r_0$ , that is,

$$\mu_i = \frac{r_i}{r_0}, \quad i = 1, 2.$$

If the transformation is linear, after  $n$  steps, we will have an ellipse with axis  $r_{1,n}$  and  $r_{2,n}$ , so that  $r_{i,n} = \mu_i^n r_0$  or equivalently, or

$$\log_2 \mu_i = \frac{1}{n} \log_2 \frac{r_{i,n}}{r_0};$$

In general, if the limit

$$\log_2 \mu_i = \lim_{n \rightarrow \infty} \frac{1}{n} \log_2 \frac{r_{i,n}}{r_0}$$

exists and is finite,  $\log_2 \mu_i$  equals the Lyapunov exponent and  $\mu_i$  is called the Lyapunov number.

*Remark 6.5* Exponents with a negative sign indicate a contraction of the starting space, while those with a positive sign indicate a stretch. As the direction of stretching and contraction changes from time to time, this implies a continuous bending.

*Remark 6.6* The stretch reflects the divergence of two orbits originally close to each other and therefore the sensitive dependence on initial conditions (SDIC). Therefore, Lyapunov's exponents indicate how quickly the points move away from each other.

At this point, we can give a simplified definition of a chaotic system as follows:

**Definition 6.8 (Chaotic System - Lyapunov Exponents)** A dissipative dynamic system is chaotic if its largest Lyapunov exponent is positive.

### 6.3 Measures on Attractors

For one-dimensional maps, chaos can occur on a set of an entire trivial support. Examples are the fully developed (i.e., their peak is at height 1) tent maps: they are chaotic on the whole unit interval, but the distribution of the support of the motion is flat (and thus differentiable). In higher dimensions, it makes, however, generally sense to characterize chaotic attractors (i) according to their geometric properties, (ii) regarding their information properties (i.e., the frequencies with which trajectories visit various parts of the attractor), and (iii) with respect to the dynamics occurring on the attractors.

### 6.3.1 Geometry of Attractors

Let us denote by  $B_r(u)$  the open ball centred in  $u$  with radius  $r$ :

$$B_r(u) = \left\{ x \in \mathbb{R}^\ell \mid |x - u| < r \right\}. \tag{6.7}$$

**Definition 6.9 (Box-Counting Dimension)** Given  $A \subset \mathbb{R}^\ell$ , consider the minimum number  $N(\varepsilon)$  of balls of radius  $\varepsilon > 0$  needed to cover  $A$ , and denote it by  $N(\varepsilon)$ . Then, the *box-counting dimension* is defined by

$$D_{BC}(A) = \limsup_{\varepsilon \rightarrow 0} \frac{\log N(\varepsilon)}{\log(1/\varepsilon)}. \tag{6.8}$$

*Example 6.4* Let  $I$  be an interval of  $\mathbb{R}$ , then  $D_{BC}(I) = 1$ .

Let  $S$  be a square in  $\mathbb{R}^2$ , then  $D_{BC}(S) = 2$ .

*Example 6.5 (Sierpinski Triangle)* Given an equilateral triangle of side length  $l$ , divide it into four equilateral triangles of side length  $l/2$ , and erase the central part. Divide each of the three remaining triangles into four equilateral triangles of side length  $l/4$  and erase the central parts. Repeating indefinitely this process, the limit set is a fractal called *Sierpinski triangle* (see Fig. 6.4). It is easily seen that the box-counting dimension of the Sierpinski triangle is  $\frac{\log 3}{\log 2}$ .

As an alternative, non-uniform open balls of radius less than  $< \varepsilon$  can be used to cover the attractor instead of using balls of the same radius.

**Definition 6.10 (Lyapunov Dimension)** Given an ordered set of Lyapunov exponents such that  $\lambda_1 \geq \lambda_2 \geq \dots \geq \lambda_d$  the *Lyapunov dimension* is

$$D_L = k + \frac{\lambda_1 + \lambda_2 + \dots + \lambda_d}{|\lambda_{k+1}|}, \tag{6.9}$$

where  $k$  is the maximum value of  $i$  such that  $\xi_i = \lambda_1 + \lambda_2 + \dots + \lambda_i > 0$ .



Fig. 6.4 The Sierpinski triangle

*Remark 6.7 (Kaplan–Yorke Conjecture)* The Kaplan–Yorke conjecture states that  $D_1 = D_L$  for “typical systems,” where  $D_1$  is the ‘information dimension’ [16].

**Definition 6.11 (Hausdorff Measure)** Let us consider a compact set  $X \subset \mathbb{R}^\ell$ ; for each real number  $d \geq 0$ , we define the  $d$ -dimensional *Hausdorff measure* of  $X$  as

$$\mathcal{H}^d(X) = \lim_{\varepsilon \rightarrow 0} \inf_{(u_i), (r_i)} \sum_{i=1}^{\infty} r_i^d, \quad (6.10)$$

where the infimum is taken on the set of the sequences  $(u_i)$  of points of  $X$  and positive numbers  $(r_i)$  such that

$$X \subset \bigcup_{i=1}^{\infty} B_{r_i}(u_i) \text{ and } r_i < \varepsilon \text{ for all } i. \quad (6.11)$$

**Definition 6.12 (Hausdorff Dimension)** The *Hausdorff dimension* of a compact set  $X$  is defined by

$$\begin{aligned} D_H(X) &= \inf \left\{ d \geq 0 \mid \mathcal{H}^d(X) = 0 \right\} \\ &= \sup \left\{ d \geq 0 \mid \mathcal{H}^d(X) = +\infty \right\}, \end{aligned}$$

where we use the convention  $\inf \emptyset = +\infty$ .

*Remark 6.8* The Hausdorff dimension of many sets is listed in [1]. For example, the set of periodic points of the Logistic map with  $\mu = \mu_c$  (see Sect. 3.1.2) has a Hausdorff dimension of 0.538.

There exist a number of distinct and only vaguely related concepts of dimension in mathematics and physics. Whereas for mathematics, the linear algebra notion of dimension as the maximal number of linear independent vectors (a positive integer value) is prevalent, in physics it is the number of degrees of freedom of a motion. It was the discovery of the mathematicians Hausdorff and Cantor that in this case a probabilistic notion of dimension is preferable and that such a dimension can be fractal, i.e., can be non-integer.

**Definition 6.13 (Fractal Dimension)** An object is said to have a *fractal dimension* if its (generally: Hausdorff) dimension is non-integer.

**Definition 6.14 (Strange Attractor)** In loose terms, *Strange attractors* are attractors specific to chaotic systems that possess the following properties:

- They attract trajectories (at least those which start from points close to them).
- They are of a SDIC type, i.e., if one takes a pair of initial points close to each other, and if the trajectories they originate are attracted by the strange attractor, they will diverge more and more with time.
- They have a fractal dimension.

### 6.3.2 Measures of Information

The box-counting dimension of Definition 6.9 can be difficult to compute. An easier way of computing fractal dimensions is the correlation dimension approach outlined in the following.

#### 6.3.2.1 Correlation

**Definition 6.15 (Heaviside Function)** The *Heaviside* or *step function* is defined as follows:

$$\mathcal{H}(y) = \begin{cases} 1 & \text{if } y > 0, \\ 0 & \text{otherwise.} \end{cases}$$

**Definition 6.16 (Correlation Integral [14])** The *correlation integral* is a spatial correlation measure aiming to measure the degree of “kinship” between two different points on the (strange) attractor. This integral is defined for  $m$  sub-series of the orbit  $\gamma$  as

$$C(r) = \lim_{N \rightarrow \infty} \frac{1}{N^2} \sum_{i,j=m}^N \mathcal{H}(r - \|[m]\mathbf{x}_i - [m]\mathbf{x}_j\|), \quad i \neq j, r \geq 0 \quad (6.12)$$

with  $[m]\mathbf{x}_i = (x_i, x_{i-1}, \dots, x_{i-m+1})$ .

An estimator of the correlation integral is the correlation sum.

**Definition 6.17 (Correlation Function [2])** Let  $\gamma = \{x_1, x_2, \dots\}$  be an orbit of the map  $f$  on  $\mathbb{R}^n$ . Given  $r > 0$ , we define the *correlation function*  $C_\gamma(r)$  as

$$C_\gamma(r) = \lim_{N \rightarrow +\infty} \frac{1}{N^2} \sum_{i,j=1}^N \mathcal{H}(r - |x_i - x_j|).$$



The *Kolmogorov–Sinai entropy* is then defined as

$$KS = - \lim_{\varepsilon \rightarrow 0} \lim_{T \rightarrow \infty} \lim_{\delta \rightarrow 0} \frac{1}{T \delta} \sum_c \rho_{c_1, c_2, \dots, c_n} \log \rho_{c_1, c_2, \dots, c_n}. \quad (6.14)$$

**Definition 6.20 (An Approximation of the Kolmogorov–Sinai Entropy)** Since Eq. (6.14) is difficult to compute, Grassberger and Procaccia [8] suggested to approximate it through the correlation integral. In particular, they denoted with  $C^m(\varepsilon)$  the correlation integral of a time series with embedding dimension  $m$  (i.e. a measure indicating the smallest dimension required to embed an object, see Chapter 7). Thus, the approximation of the Kolmogorov–Sinai entropy is

$$KS_2 = \lim_{m \rightarrow \infty} \lim_{\varepsilon \rightarrow 0} \frac{1}{\delta} \log \frac{C^m(\varepsilon)}{C^{m+1}(\varepsilon)}. \quad (6.15)$$

*Remark 6.11* It was shown by Grassberger and Procaccia [8] that  $KS_2$  provides a good estimate of the Kolmogorov–Sinai entropy, where  $KS_2 \leq KS$ .

*Remark 6.12* According to Pesin’s theorem [18], the sum of all positive Lyapunov exponents gives an estimate of the Kolmogorov–Sinai entropy. So, if  $KS > 0$ , then the highest Lyapunov exponent is positive and the system is chaotic [14].

### 6.3.3 Thermodynamic Formalism: The Ring That Ties (Almost) All

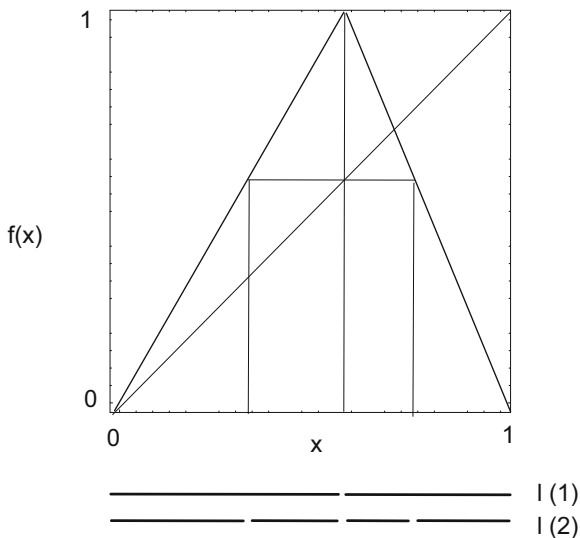
The reader might now wonder in what sense the different concepts of entropy would—if correctly evaluated—yield the same results. This is not the case. The analysis [4, 17, 27] shows that all of them can be embraced by a two-parameter family of sampling procedures described by a generalized partition function. For the one-dimensional case (the generalization to higher dimension is straightforward), the generalized partition function has the form

$$GZ(q, \beta, n) = \sum_{j \in (1, \dots, M)^n} p_j^q l_j^\beta,$$

where  $p_j$  is the probability of falling into the  $j$ th region of the partition, given the partition level  $n$ , and  $l_j$  describes the size of this region (for an illustration focusing on the size or length scales, see Fig. 6.6).

In the symbolic dynamics sense, symbol  $j$  indicates the history of each contribution to the sum. The sum has the form of a Boltzmann sum, if we introduce local scalings as  $l_j = e^{-n\varepsilon_j}$  and  $p_j = l_j^{\alpha_j}$ . To this Boltzmann sum, we associate the

**Fig. 6.6** First two levels of the dynamic length scale partition used for the dynamical spectrum  $S(\varepsilon)$



generalized free energy

$$GF(q, \beta) = \lim_{n \rightarrow \infty} \frac{1}{n} \log GZ(q, \beta, n).$$

To the generalized free energy, we associate a generalized entropy  $GS(\langle \alpha \rangle, \langle \varepsilon \rangle)$  via the usual Legendre transformation, leading to  $\langle \varepsilon \rangle = -\frac{\partial}{\partial \beta} GF(q, \beta)$  and  $\langle \alpha \rangle = -\frac{\partial}{\partial q} \frac{GF(q, \beta)}{\langle \varepsilon \rangle}$ .

The generalized entropy function  $GS$ , presented in Fig. 6.7 for a ternary Cantor set which measure, is, however, often degenerate. For fully unfolding this function, we need three scales; if only two scales are present, the function collapses into a sheet (over a generally non-straight line support in the  $(\alpha, \varepsilon)$ -plane). In the “ideal” case, the entropy function is a convex hypersheet (of dimension 2 in the described  $(\alpha, \beta)$ -case). The ideal case allows us to explain how various better known entropy functions—like the dimension spectrum  $f(\alpha)$  [10] or the dynamical scaling functions  $\phi(\lambda)$ [17] or  $g(\Lambda)$  [15] and related characterizations [6, 11, 20, 29]—emerge from the generalized entropy function by conditioning, e.g., by setting  $q = 0$ , which yields the “dynamical spectrum” of “local” Lyapunov exponents  $S(\varepsilon)$ , by looking for the zero of the free energy  $F(q, \beta)$ , which yields the spectrum of local dimensions  $f(\alpha)$ , or by setting  $\beta = 0$ , which leads to the less prominent spectrum  $S(\alpha)$ . Similarly, we arrive at the simpler case with only one variable if probabilities scale as the lengths do.

To simplify the discussion, we concentrate on the characterizations by  $S(\varepsilon)$  and  $f(\alpha)$  that exemplify the forms that specialized entropy functions generally assume. In Fig. 6.8, we show the dynamical spectrum  $S(\varepsilon)$  of two realizations of the tent map (full lines). These spectra are easy to understand as follows. The leftmost



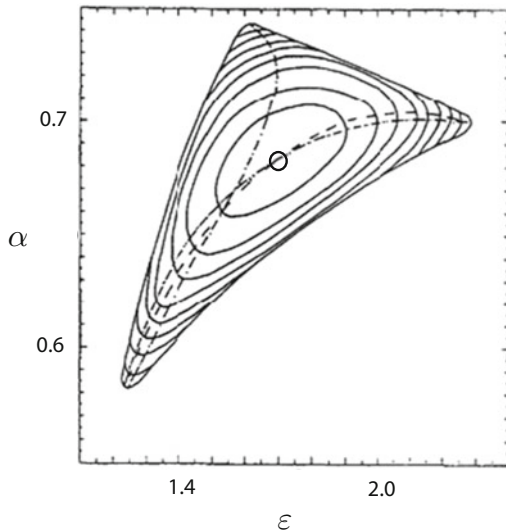


**Fig. 6.7** Generalized entropy function for a generalized partition function of a non-uniform three-scale Cantor set with measure (contour lines of distance 0.1, numerical approximation). By conditioning, partial entropy functions emerge from it, e.g.,  $S(\alpha)$  from setting  $\beta = 0$  (not shown), the dynamical spectrum of “local” Lyapunov exponents  $S(\varepsilon)$  (short dash-dotted), or  $g(\lambda)$  (dashes), and the dimension spectrum  $f(\alpha)$  (long dash-dotted). The maximum at  $\log(3)$  of the function is the topological entropy (location indicated by a circle); the maxima on the borders are at  $\log(2)$ . Corners (ideally, points) at zero entropy indicate the pure states corresponding to strings of only one symbol

value (equal to zero) of a convex entropy function is obtained from sampling only the most probable single event and the rightmost from the least probable single event. Natural sampling of the process corresponds to the (normally single) point of the entropy graph that touches the diagonal, cf. Fig. 6.8. In the case of the characterization by local dimensions, this corresponds to the natural sampling of the probability, yielding as the average the information dimension. In the case of the dynamical description, the Lyapunov exponent of the process is obtained. A finite-time prediction of this value will persist when the sampling time (or the partition depth) goes to infinity. The maximal entropy in the dynamical description is obtained from  $\beta = 0$  and corresponds to the topological entropy (in the case of dimensions, to the Hausdorff dimension). It can be seen that in this case, all partition elements are treated with weight equal to one, irrespective of their natural probability.

For fully developed asymmetric tent maps, we always obtain convex “dynamical” entropy functions  $S(\varepsilon)$  (cf. Fig. 6.8). The associated invariant density is always flat; therefore, the dimension spectrum  $f(\alpha)$  is trivial ( $f(\alpha) = 1$  for  $\alpha = 1$  and zero otherwise). The fully developed ( $a = 4$ ) parabola shows a “true” violation of convexity, which is interpreted as a phase transition as follows.  $S(\varepsilon)$

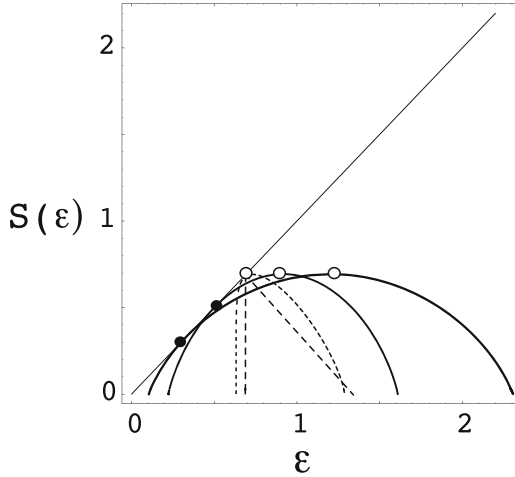


**Fig. 6.8** Entropy functions ( $\varepsilon$ ) of different systems. In the case of the tent map, the entropy depends on the map's skewness, which is shown by two examples (full lines). As a comparison,  $S(\varepsilon)$  of the quadratic parabola at  $a = 4$ , computed for a finite level of the partition depth  $n$  (shorter dashes) and asymptotically (longer dashes), is shown. In all functions, open circles mark the topological entropy, and full circles mark the Lyapunov exponent (for the parabola, the topological entropy and the Lyapunov exponent coincide)

converges asymptotically in  $n$  to a graph of triangular form with corner points,  $(\log(2), 0)$ ,  $(\log(2), \log(2))$ , and  $(\log(2), \log(2))$ , cf. Fig. 6.8. The dimension spectrum  $f(\alpha)$  assumes again the triangular shape (of expression  $f(\alpha) = 2\alpha - 1$ ). Technically, this violation of convexity is generated from the non-hyperbolicity of the map (in contrast, tent maps are hyperbolic). Non-hyperbolicity is generally a substantial nuisance due to their bad convergence properties, but in natural systems such a complication is generically unavoidable. The developed framework also explains under what conditions phase transitions can be observed in some more specialized entropy functions and when they are not observable [22, 23, 28]. These examples illustrate the wide range of observed results that emerge from different statistical descriptions of complex behaviour. Last but not least, if we have a system with global escape (e.g., from a repeller), the entropy function moves away from the diagonal, where the distance to the diagonal provides a measure for the escape rate.

The aforementioned multivariate account can also be applied for the description of a whole range of seemingly unrelated additional effects, where, e.g., a jump measure captures in an elegant way the diffusive behaviour on a grid or lattice of cells (cf. [24–26]).

For stochastic systems, Jayawardena et al. [12] introduced a measure that is more robust to noise than the  $KS$  correlation entropy.

**Definition 6.21 (Modified Correlation Entropy (MCE)—Jayawardena et al. [12])** Given the correlation sum computed for two values of the embedding dimension, e.g.,  $m$  and  $m + 2$ , the modified correlation entropy is

$$KS_3 = \lim_{m \rightarrow \infty} \lim_{\varepsilon \rightarrow 0} \frac{1}{2\delta} \log \frac{C^m(\varepsilon)}{C^{m+2}(\varepsilon)} + \frac{1}{2\delta} \log \frac{m - \frac{d \log C^m(\varepsilon)}{d \log \varepsilon}}{m - D_C}. \quad (6.16)$$

In the following algorithm, the information dimension of the Hénon attractor is approximated.

After relaxation on the attractor,  $NT = 10,000$  attractor points are sampled. Around  $NP = 20$  points on the attractor, the number of data points that fall into neighbourhoods of logarithmically chosen radii is counted and averaged. Then, the slope of a log–log plot of the “mass” as a function of the shell radius yields an approximation of the fractal information dimension.

In contrast, covering the attractor with equally sized boxes that contain at least one point approximates the topological (Hausdorff) dimension via the slope of a log–log plot of the numbers of boxes versus size. In this way, the two most significant fractal dimensions of the fractal dimension spectrum  $f(\alpha)$  can be obtained.

```
(*Generation of 10000 data points of the Henon attractor,
after 40000 attractor relaxation steps*)

hen[{x_,y_}]:={-1.4 x^2+y+1,0.3 x};
Nest[hen,{0.1,0.1},20000];
BB=NestList[hen,Nest[hen,{0.1,0.1},40000],60000];

(*Computational speed-up by converting real into integer data*)

aa=Table[Round[1000*BB[[j]][[1]]+1000},{j,1,60000}];

(*Set-up: Data structure, distance function,
NP local neighbourhoods to consider*)

b[i_,n_]:=Table[aa[[i+j]},{j,0,n-1}];
Dis[i_,j_]:=Max[Abs[b[i,3]-b[j,3]]];
Pu=Table[Random[Integer,{1,1000}},{i,1,20}];
NT=10000;NP=20;

(*Counting neighbours within logarithmically placed
neighbourhood shells*)

Anzneig[jj_,r_]
:= Module[{i,i=0;
Do[{If[Dis[jj,k]<r,i+=1,]},{k,1,NT}];
v=(i-1)/NT;Return[v];

aaa=Table[{nn*Log[2]},{p=0;
Do[{Anzneig[Evaluate[Pu[[ii]]],2^(nn)],p+=v},{ii,1,NP}];
```

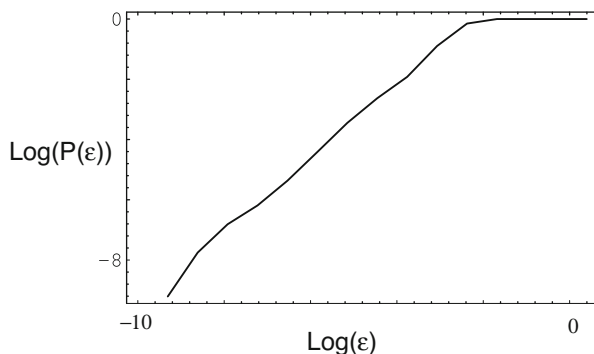


**Fig. 6.9** Log–log curves for Hénon’s dissipative attractor using an embedding dimension of 3. The slope approximates the fractal information dimension of the attractor quite well ( $d_f \approx 1.26$ )

```
(*Interpolation of relevant data, where the slope
   is the fractal dimension.
   The non-saturating interval is chosen to be 1-15*)
```

```
Log [N [p/NP] ] }, {nn, 1, 15} ] ;
```

```
bbb=Partition [Flatten [aaa] , 2] ;
```

```
ListPlot [bbb, Frame->True] ;
```

```
Fit [bbc, {1, x}, x] ;
```

Using an embedding dimension of 3, the slope of the fit to the log–log curve yields an approximation of the fractal information dimension of the attractor of  $d_I \approx 1.26$  (see Fig. 6.9).

## References

1. List of fractals by Hausdorff dimension—Wikipedia (2019). [https://en.wikipedia.org/wiki/List\\_of\\_fractals\\_by\\_Hausdorff\\_dimension](https://en.wikipedia.org/wiki/List_of_fractals_by_Hausdorff_dimension). Accessed 31 Jul 2019
2. Alligood, K., Sauer, T., Yorke, J.: Chaos: An Introduction to Dynamical Systems. Textbooks in Mathematical Sciences. Springer, New York (2000)
3. Banks, J., Brooks, J., Cairns, G., Davis, G., Stacey, P.: On Devaney’s Definition of Chaos. *Amer. Math. Monthly* **99**, 332–334 (1992). <https://doi.org/10.2307/2324899>
4. Beck, C., Schögl, F.: Thermodynamics of Chaotic Systems: An Introduction. Cambridge Nonlinear Science Series. Cambridge University Press, Cambridge (1993). <https://doi.org/10.1017/CBO9780511524585>
5. Cvitanović, P., Artuso, R., Mainieri, R., Tanner, G., Vattay, G.: Lyapunov exponents. In: Chaos: Classical and Quantum, chap. 6. Niels Bohr Institute, Copenhagen (2012). <http://ChaosBook.org/version14ChaosBook.org/version14>
6. Eckmann, J.P., Procaccia, I.: Fluctuations of dynamical scaling indices in nonlinear systems. *Phys. Rev. A* **34**, 659–661 (1986). <https://doi.org/10.1103/PhysRevA.34.659>

7. Grassberger, P., Procaccia, I.: Characterization of strange attractors. *Phys. Rev. Lett.* **50**, 346–349 (1983)
8. Grassberger, P., Procaccia, I.: Estimation of the Kolmogorov entropy from a chaotic signal. *Phys. Rev. A* **28**, 2591–2593 (1983). <https://doi.org/10.1103/PhysRevA.28.2591>
9. Grassberger, P., Procaccia, I.: Measuring the strangeness of strange attractors. *Phys. D* **9**, 189–208 (1983)
10. Halsey, T.C., Jensen, M.H., Kadanoff, L.P., Procaccia, I., Shraiman, B.I.: Fractal measures and their singularities: the characterization of strange sets. *Phys. Rev. A* **33**, 1141–1151 (1986). <https://doi.org/10.1103/PhysRevA.33.1141>
11. Horita, T., Hata, H., Mori, H., Morita, T., Tomita, K.: Singular local structures of chaotic attractors due to collisions with unstable periodic orbits in two-dimensional maps. *Progr. Theor. Phys.* **80**(6), 923–928 (1988). <https://doi.org/10.1143/PTP.80.923>
12. Jayawardena, A., Xu, P., Li, W.K.: Modified correlation entropy estimation for a noisy chaotic time series. *Chaos* **20**(2), 023104 (2010)
13. Li, T.Y., Yorke, J.A.: Period three implies chaos. *Am. Math. Mon.* **82**(10), 985–992 (1975)
14. Lorenz, H.W.: *Nonlinear Dynamical Economics and Chaotic Motion*, 2nd edn. edn. Springer, Berlin (1993)
15. Oono, Y., Takahashi, Y.: Chaos, external noise and fredholm theory. *Progr. Theor. Phys.* **63**(5), 1804–1807 (1980). <https://doi.org/10.1143/PTP.63.1804>
16. Ott, E.: Attractor dimensions. *Scholarpedia* **3**(3), 2110 (2008). <https://doi.org/10.4249/scholarpedia.2110>. Revision #91015
17. Peinke, J., Parisi, J., Rössler, O.E., Stoop, R.: *Encounter with Chaos: Self-Organized Hierarchical Complexity in Semiconductor Experiments*. Springer, Berlin (2012)
18. Pesin, Y.B.: Characteristic Lyapunov exponents and smooth ergodic theory. *Russ. Math. Surv.* **32**, 55–114 (1977). <https://doi.org/10.1070/RM1977v032n04ABEH001639>
19. Robinson, J.C.: *Infinite-Dimensional Dynamical Systems: An Introduction to Dissipative Parabolic PDEs and the Theory of Global Attractors*. Cambridge University Press, Cambridge (2001)
20. Sano, M., Sato, S., Sawada, Y.: Global spectral characterization of chaotic dynamics. *Progr. Theor. Phys.* **76**(4), 945–948 (1986). <https://doi.org/10.1143/PTP.76.945>
21. Sivakumar, B., Berndtsson, R.: *Advances in Data-Based Approaches for Hydrologic Modeling and Forecasting*, chap. 9, pp. 411–461. World Scientific, Singapore (2010)
22. Stoop, R.: Dependence of phase transitions on small changes. *Phys. Rev. E* **47**, 3927–3931 (1993). <https://doi.org/10.1103/PhysRevE.47.3927>
23. Stoop, R.: On hyperbolic elements hiding phase transitions. *Phys. Lett. A* **173**(4), 369–372 (1993). [https://doi.org/10.1016/0375-9601\(93\)90252-U](https://doi.org/10.1016/0375-9601(93)90252-U)
24. Stoop, R.: Bivariate thermodynamic formalism and anomalous diffusion. *Phys. Rev. E Stat. Phys. Plasmas Fluids Relat. Interdiscip. Topics* **49**(6), 4913–4918 (1994). <https://doi.org/10.1103/physreve.49.4913>
25. Stoop, R.: The diffusion-related entropy function: the enhanced case. *Europhys. Lett.* **29**(6), 433–438 (1995). <https://doi.org/10.1209/0295-5075/29/6/001>
26. Stoop, R.: Thermodynamic approach to deterministic diffusion of mixed enhanced-dispersive type. *Phys. Rev. E* **52**, 2216–2219 (1995). <https://doi.org/10.1103/PhysRevE.52.2216>
27. Stoop, R., Gomez, F.: Auditory power-law activation avalanches exhibit a fundamental computational ground state. *Phys. Rev. Lett.* **117**, 038102 (2016). <https://doi.org/10.1103/PhysRevLett.117.038102>
28. Stoop, R., Peinke, J., Parisi, J., Röhrich, B., Huebener, R.: A p-Ge semiconductor experiment showing chaos and hyperchaos. *Phys. D: Nonlinear Phenom.* **35**(3), 425–435 (1989)
29. Szépfalussy, P., Tél, T.: New approach to the problem of chaotic repellers. *Phys. Rev. A* **34**, 2520–2523 (1986). <https://doi.org/10.1103/PhysRevA.34.2520>

# Chapter 7

## Embedding Dimension and Mutual Information



Giuseppe Orlando, Ruedi Stoop, and Giovanni Tagliatalata

The concept of dynamical system that we will use here is taken from R.E. Kalman [1], who introduced it in the 1960s while studying the problem of linear filtering and predictions.

### 7.1 Embedding Dimension

Let us consider the map

$$x_{k+1}^i = f_i(\mathbf{x}_k), \quad \mathbf{x} \in \mathbb{R}^n, \quad i = 1, \dots, n, \quad (7.1)$$

but suppose that the variable  $x^i$  is not directly observable.

---

G. Orlando (✉)

University of Bari, Department of Economics and Finance, Bari, Italy

University of Camerino, School of Sciences and Technology, Camerino, Italy

e-mail: [giuseppe.orlando@uniba.it](mailto:giuseppe.orlando@uniba.it); [giuseppe.orlando@unicam.it](mailto:giuseppe.orlando@unicam.it)

R. Stoop

Institute of Neuroinformatics, ETHZ/University of Zürich, Zurich, Switzerland

e-mail: [ruedi@ini.phys.ethz.ch](mailto:ruedi@ini.phys.ethz.ch)

G. Tagliatalata

University of Bari, Department of Economics and Finance, Bari, Italy

e-mail: [giovanni.tagliatalata@uniba.it](mailto:giovanni.tagliatalata@uniba.it)

© The Author(s), under exclusive license to Springer Nature Switzerland AG 2021

G. Orlando et al. (eds.), *Non-Linearities in Economics*, Dynamic Modeling

and Econometrics in Economics and Finance 29,

[https://doi.org/10.1007/978-3-030-70982-2\\_7](https://doi.org/10.1007/978-3-030-70982-2_7)

**Definition 7.1 (Time Series)** For the observable variable

$$\bar{x}_k^i = h(x_k), \quad (7.2)$$

we denote with  $\{\bar{x}_k^i\}_{k=1}^T$  the *time series* of observations.

The embedding dimension is a statistical measure that indicates the smallest dimension required to embed an object, for instance a chaotic attractor [4], and it is defined as follows.

**Definition 7.2 (Embedding Dimension)** Let us consider the last  $m$  element of observations as arranged in the vector  ${}_{[m]}\bar{\mathbf{x}}_T^i = \{\bar{x}_T^i, \bar{x}_{T-1}^i, \dots, \bar{x}_{T-m+1}^i\}$  in the observed time series, and let us repeat the grouping for each  $\bar{x}_k^i$  in the descending order of time  $t = T, \dots, 1$  by dropping the remaining  $m - 1$  elements.

If  $m$  denotes the *embedding dimension*, this results in the  $m$ -dimensional vectors

$$\begin{aligned} {}_{[m]}\bar{\mathbf{x}}_T^i &= \{\bar{x}_T^i, \bar{x}_{T-1}^i, \dots, \bar{x}_{T-m+1}^i\}, \\ {}_{[m]}\bar{\mathbf{x}}_{T-1}^i &= \{\bar{x}_{T-1}^i, \bar{x}_{T-2}^i, \dots, \bar{x}_{T-m}^i\}, \\ &\vdots \\ {}_{[m]}\bar{\mathbf{x}}_m^i &= \{\bar{x}_m^i, \bar{x}_{m-1}^i, \dots, \bar{x}_1^i\}. \end{aligned}$$

*Remark 7.1* The vector  ${}_{[m]}\bar{\mathbf{x}}_T^i$  is also called *m-history* and describes a point in an  $m$ -dimensional space, where the coordinates are the delayed observed values  $\{\bar{x}_T^i, \bar{x}_{T-1}^i, \dots, \bar{x}_{T-m+1}^i\}$ . The sequence  $\{{}_{[m]}\bar{\mathbf{x}}_k^i\}_{k=m}^T$  of points forms a geometric object in this space.

*Remark 7.2* F. Takens [6] showed that if

1. The variables  $x^i$  of the true dynamical system are located on an attractor (i.e. there are no transients),
2. The original dynamical system and the observation function  $h(x)$  are smooth, and
3.  $m > 2n - 1$ ,

then the sequence  $\{\bar{x}_t^i\}_{t=m}^T$  is topologically equivalent to the object generated by the true dynamical system described by Eq. (7.1).

### 7.1.1 Time Lag

Instead of considering the  $m$ th element of observations as arranged in the vector

$${}_{[m]}\bar{\mathbf{x}}_T^i = \{\bar{x}_T^i, \bar{x}_{T-1}^i, \dots, \bar{x}_{T-m+1}^i\},$$

one may take the vector

$${}_{[m]}\bar{\mathbf{x}}_{T-\tau}^i = \{\bar{x}_T^i, \bar{x}_{T-(1+\tau)}^i, \dots, \bar{x}_{T-(m-1+\tau)}^i\}$$

by sampling the time as follows:  $t = T, T - (1 - \tau), \dots, \tau$ . This vector is called *delayed* or *time lagged*, and the delay  $\tau$  corresponds to the spacing between the observations.

While the embedding procedure is a very elegant tool for obtaining information about a system from a single scalar time series, the procedure of choosing the optimal embedding dimension is a nontrivial one. In rough terms, the embedding dimension must be chosen from a self-consistent region of the embedding dimensions, meaning that for every embedding the characteristics of the embedding are consistent with those of the whole time series. This requirement poses severe constraints on the length of the time series that may often not be long enough for a solid application of the procedure, see Eckmann and Ruelle [3].

## 7.2 Mutual Information

The delay  $\tau$  is to be determined in a way that the values  ${}_{[m]}\bar{\mathbf{x}}_T^i$  and  ${}_{[m]}\bar{\mathbf{x}}_{T-\tau}^i$  are “sufficiently independent to be useful as coordinates in a time-delay vector but not so independent as to have no connection with each other at all” [5]. To this end, it might be useful recurring to the mutual information defined as follows.

**Definition 7.3 (Mutual Information [2])** Let us consider two jointly discrete random variables  $X$  and  $Y$ , and the *mutual information* as the double sum

$$I(X; Y) = \sum_{y \in \mathcal{Y}} \sum_{x \in \mathcal{X}} p_{(X,Y)}(x, y) \log \left( \frac{p_{(X,Y)}(x, y)}{p_X(x) p_Y(y)} \right),$$

where  $p_{(X,Y)}$  and  $p_X, p_Y$  denote, respectively, the joint distribution and the marginal probability mass functions of  $X$  and  $Y$ , respectively.

The first minimum of average mutual information marks the delay time that adds maximal information to the knowledge we have. Accordingly, this value is often used as the delay time for phase space reconstruction by embedding. Alternatively, the method of false nearest neighbors is often used.

## References

1. Antoulas, A.: Mathematical System Theory—The Influence of R. E. Kalman. Springer, Berlin (1991). <https://doi.org/10.1007/978-3-662-08546-2>
2. Cover, T., Thomas, J.: Elements of Information Theory. Wiley, London (1991)



3. Eckmann, J.P., Ruelle, D.: Ergodic theory of chaos and strange attractors. *Rev. Mod. Phys.* **57**, 617–656 (1985). <https://doi.org/10.1103/RevModPhys.57.617>
4. Letellier, C.: Fortran code for estimating the minimum embedding dimension (2013). <http://www.atomosyd.net/spip.php?article128>
5. Ruskeepaa, H.: Chaotic data: Delay time and embedding dimension. Wolfram Demonstrations Project (2017)
6. Takens, F.: Dynamical systems and turbulence. In: *Lecture Notes in Mathematics*, vol. 898, chap. Detecting Strange Attractors in Turbulence, pp. 366–381. Springer, Berlin (1981)

**Part II**  
**Signal Analysis and Modelling Tools**  
**for Economic Systems**

# Chapter 8

## Signal Processing



Ruedi Stoop

### 8.1 Signal Processing as a Process of Computation

Put into a nutshell, I promote below the view that signal processing is a process of computation, that computation describes the process of information destruction, and that the efficacy of this process can be measured.

#### 8.1.1 *Signal Observation and Perception*

Signal processing means, in the most general form of the term, the observation of real-world or artificial (e.g., computer-generated) signals. Innate in this process is the choice of an observable, generally by the human senses. This process already singles out a particular aspect of the observed process. As an example, let us look at the stars at night. What we see from the stars is a very limited light spectrum (from 380 to 740 nanometres) accessible to our eyes [25]. For assessing other frequencies of the radiation, we need dedicated and often sophisticated additional tools that each of them singles out again a particular frequency range of its own, some of them reaching even beyond of what we could ever hope to sense within our limited lifespan in a more direct approach. Having said that, it is immediately clear that the process of observation is accompanied by a strong destruction of the original information sent out by the stars: in the observational process, we dismiss—or destroy—all the information that we do not consider worthwhile in a given context.

---

R. Stoop (✉)

Institute of Neuroinformatics, ETHZ/University of Zürich, Zurich, Switzerland  
e-mail: [ruedi@ini.phys.ethz.ch](mailto:ruedi@ini.phys.ethz.ch)

As it is intrinsically impossible for us to observe all aspects of an object and process its full generality, we bundle what our senses think as the ‘relevant’ aspects to a feature vector, a vector containing as its entries the properties of interest to us of the object. Time changes these vectors where, primarily, the components that change most are important to us: they define the dynamics of the objects. This procedure of observation is clearly not objective, as it leads to the creation of larger classes of objects by a process that is generally termed ‘clustering’. This process, which is closely related to human perception, subdivides the space of objects into sets composed of more ‘similar’ objects. To each of such sets, a tag, or symbol, can be associated. That this is not a trivial task can be inferred from human perception that in a large number of experiments misleads a human spectator into an illusion.

There are a large number of clustering algorithms, but all work with a notion of a ‘distance’. The distance between objects then allows us to classify. Here, we already encounter the first undesired bias in the clustering process. While this can be solved in an optimized manner depending on the field (often by rescaling the different information to same weight [16]), there are a number of elements of bias [4, 14, 15] that, unfortunately, got historically into various approaches without noticing their danger. For example, the very prominent K-MEANS clustering fails if the clusters have non-Gaussian spatial distributions [4, 14]. Clusters are, however, generally not just noisy clouds, and clusters generated by nonlinear processes have, generically, a nontrivial ‘shrimp’-like structure [4].

More surprisingly, even the agglomerative Wards-type clustering approaches fail in this case for a similar reason [4]. See Ref.[15] for an approach that takes a full account of the bias introduced by a clustering approach.

### ***8.1.2 Computation Performed on a Signal***

Let us now point out in a first example how in a similar way classical computation eliminates information. Consider, e.g., the OR gate (or any universal gate, if you prefer, from which you will get a similar insight). The input to this gate plays the role of information arriving that can be characterized as a (./.) two pair, or vector of dimension 2, of bits. The computation performed by the gate produces as the result a vector of only dimension 1. If this result is ‘1’, it is not known any more whether channel A was ‘1’ or channel B, or both. The fundament of such a process of computation is irreversibility.

The classical universal gates, the computational elements from which all classical computational devices can be composed, reiterate how computation destroys information. A classical  $n$ -ary universal gate is NOR or NAND. Take the latter gate that has an output that is normally at logic level ‘1’ and only goes to ‘0’ iff ALL of its inputs are at logic level ‘1’. For output ‘1’, it is, therefore, no longer clear, what the input configuration was. This is exactly where the input information is destroyed; the destruction is unavoidable because the input was  $n > 1$  bits and the output consists of one bit only. Since the heat generated by erasing (‘grounding’) one bit of

information, is in the Landauer–von Neumann limit is around  $10^{-21}$  J, for a modern computer with a lot of computer power this sums up to a considerable amount of heat that is difficult to get rid of, which is a main limitation against achieving higher computational power.

The elimination of this problem was one major idea behind the quantum computer, as in quantum computation, up to the final read-out, and all operations are reversible. While this approach solves one problem, it, unfortunately, creates another one. Quantum gates (such as the Toffoli or the Fredkin universal quantum gates [5]) have, to preserve reversibility, as many lines-out as there are lines-in. For exactly that reason, many steps of computation lead to an explosion of the associated memory requirement.

Biological computation works along similar lines. Neural networks, a particularly important instance of natural computation, are capable of forming universal gates by means of a suitable combination of excitatory and inhibitory neurons. The heat production of the brain is huge (about 2% of the body weight, 15% of the cardiac output, 20% of the total oxygen consumption, and 25% of the total body glucose utilization), as is the energy consumption of the brain (about 0.4 J per minute vs. even 6 J per minute during crossword puzzle solving), cf. [6, 19]).

The additional aspect that comes into play in biological computation is dynamics that works along similar lines of information elimination. The Bernoulli-shift map  $y = 2x \bmod 1$  on the  $[0,1]$  unit interval, can serve as a simple example of how dynamics kills, with each iteration, the presently highest digit of the initial condition. In the computer, after a number of iterations equal to the length of the binary representation of numbers, the process thus arrives at 0, independent of the initial condition, despite the fact that this map is a famous prototype of a hyperbolic chaotic dynamical system.

### 8.1.3 Dynamics Between Symbols

Dynamics leads from one set (with tags often called ‘states’) into another, by which we obtain from the dynamics as a mapping among a set of symbols or states. One major aspect of interest is the probability with which we jump from one symbol to another. If this process does not depend on more than the immediate present, this is called a Markov process. Should the process depend on a longer history of symbols, we have memory and the process is called of higher Markov order

$$Pr(C_t|C_{t-1}, C_{t-2}, \dots) = Pr(C_t|C_{t-1}, \dots, C_{t-l}). \quad (8.1)$$

Fortunately, higher order Markov processes can always be converted into Markov processes of first order (i.e. of a one-step memory). For a general modern survey, see, e.g., [26].

In dynamics, a generating partition is an example of a mapping among such symbols. A first-order Markov process can always be written as a quadratic non-negative matrix of dimension equal to the number of symbols. For such a situation, the celebrated Frobenius–Perron theory [1, 17] provides the mathematical basis for solution existence if the matrices are irreducible.

Sometimes, we deal with situations where we want to know in what state a system is by indirect observation. For such cases, the concept of hidden Markov processes has been developed. Nowadays, tailored implemented algorithms are available that answer the main questions that are natural to be asked in such a context [26].

### 8.1.4 Complexity of the Prediction of Dynamics

In many cases, models made for understanding and predicting dynamics. In dynamics, the complexity of a process embraces the difficulty of predicting its future values. How much complexity resides in a dynamical model is therefore embodied in the entropy function of the process. In this sense, the more and the more abundant states are offered by the dynamics, the more complex a process is. Note that such a characterization does not just apply to dynamics in its purest form. Even if we look at a figure or a picture, we are engaged in a dynamical process, by trying to infer to totality of the object from partial, initial perceptions that we consequently refine and verify or dismiss. Expressed in terms of entropy, the observability of an invariant measure  $\varepsilon$  during  $n$  steps of the evolution decays as  $O(\varepsilon) \sim e^{-n(S(\varepsilon)-\varepsilon)}$ . For each measure of  $\varepsilon$ , the relative distance  $S(\varepsilon - \varepsilon)$  to the diagonal  $S(\varepsilon) = \varepsilon$  is therefore a measure for its difficulty of prediction. Averaging over the different invariant measures provides therefore a good indicator of the complexity of correctly predicting a process. A deeper analysis demonstrates that for the multiplicative measure  $\varepsilon$ , the suitably scaled entropy integral

$$\int S(\varepsilon)/\varepsilon d\varepsilon$$

is a consistent measure for the difficulty of prediction.

The most general form of the latter measure is

$$C_s(\beta, \alpha) = \varepsilon_0^{2\beta} \varepsilon_1 / (\varepsilon_1 - \kappa) \int (S(\varepsilon)/\varepsilon)^\alpha d\varepsilon,$$

where  $\kappa$  is the escape rate,  $\varepsilon_1$  is the natural measure entropy, and  $\varepsilon_0$  is the topological length scale.

By this formula, all invariant measures, respectively, the strength of the escape from them, are taken into account, where the contribution of observable invariant measure is maximal, and  $S(\varepsilon)/\varepsilon$  is the dimension of the set with index  $\varepsilon$ . For all

systems, this definition of complexity yields positive and finite values. Moreover, and of equal importance, for purely random systems the value is 0 and maximal for intermittent systems. This conforms to Langton's notion of 'life at the edge of chaos' [12], and it corresponds extremely well with human perception of complexity. For more details and examples, see the original publication [24].

### **8.1.5 Measuring Computation**

Computation described as information destruction simplifies the object under investigation, which leads, after each computation, to a reduced complexity of the object. The idea now is that each dynamical process can be seen as a mapping, each mapping can be characterized by a complexity, and the effect contributed by a process (natural or artificial) can be cast in how much the complexity of the object is reduced. Taking as an input a signal of arbitrary complexity and defining computation as the reduction of complexity performed, the inverse  $1/(C_s(1, 0) + 1)$  (where addition of 1 prohibits the occurrence of a pole for zero complexities) is a convenient measure to express the computation performed by a process of signal processing. The value of the measure is between 0 (very little computation performed by, e.g., fully intermittent systems) and 1 (full computation, e.g., if the result is a fixed number). Interestingly, under this view hyperbolic and non-hyperbolic systems do not differ in any fundamental manner. For more details and examples, see the original publication [23].

## **8.2 Signal Processing by Neural Networks**

Neural networks can be seen as a variant of clustering based on a weighted graph, where weights are determined via an optimization process set up to deliver for a set of input patterns desired, often labelled, responses (similar to the action performed by a teacher). In this process, a much too large network of potential relations is optimized to give a desired result, often an association between input and class to which an example belongs to. Also in this case a massive destruction of information occurs. In a high-dimensional space of potential relations between input and output, the weights delivering the desired results are implemented in a subspace of normally considerably lower dimension (of a truncation of small weights to zero is applied). After optimizing the weights, the weighted graph classifies by means of generalization, similar to what would be obtained if after clustering, for new data the nearest data set is determined and its label is selected as the result. However, the emerging graph is, by no means, unique. In fact, from the graph itself, the logical structure implemented by the network cannot be inferred. As a solution, neural network learning can be combined with evolutionary optimization, where the

sparseness of the solution is taken into the goal function (i.e., is part of the decision to what extent the implementation matches the human-sensed results).

The main distinction to clustering is—as a downside—that, generally, the number of classes needs to be given (in supervised learning). In more modern variants of self-organised clustering this emerges from the process itself. On the plus side, generally, several layers are given in the network which permit to implement theoretical, abstract, concepts like ‘lines’ and similar, if convolutions between the layers are used.

The strong relationship between clustering and neural networks is emphasized by self-organized clustering based on firing models of neurons, where the synaptic connection between them starts from an all-to-all structure and random interaction, where the strengths of neural connection reflect the distance in object space. During the temporal evolution, the connection strengths are updated according to Hebb’s principle [7]: ‘..who fires together, wires together’. At the end of the process, near-to-zero weight connections distinguish between different clusters.

In the recurrent neural networks paradigm, a complex input (often of temporal characteristics) is transferred into a simplified firing pattern in the chaotic sea of neurons to which a simple read-out layer process is applied to read out the desired result.

Self-organized learning can be implemented to, e.g., learn an optimized behavioural task. These approaches have in common that they generally provide one out of many possible solutions. If an optimized short algorithm has to be found, this goal has to be implemented into the goal function (i.e., be added to the goal of performing in a correct manner). An elegant implementation proceeds via genetic programming.

The construction element of an artificial neuronal network is a mathematical abstraction of the behaviour of a biological computational unit. Historically, to implement basic logical operations, first, an element with two real-valued input values was considered (for complex variants, see, e.g., [20]), supported by a base input (often called ‘bias’) that acts as a means to shift the operation point of activation. Multiplicative weights along the inputs permit to adjust and optimize the unit for a desired operation (this process of this adjustment is called ‘learning’), and the activation function determines how much output is generated in response to the weighted input. The smoothness of the sigmoidal function also simplifies the implementation of the learning process by a gradient descent optimization but imports a kind of ‘fuzzyness’ (residing in the steepness of the sigmoidal function) requiring to rectificate the output to digit values such as 0 and 1.

As an illustration, we present a Mathematica programme, in which  $a$  defines the steepness of the sigmoidal function and  $eta$  defines the speed of adjustment during the gradient descent optimization of the weights  $w$  (to be chosen to harmonize with the size of  $a$  (cf. weight update rule). The task to implement the AND gate that after a large number of learning steps is approximated quite well, as is shown by the output.

```
a = 1; f[x_] := 1/(1 + Exp[-a x]);
w = Table[Random[], {i, 1, 4}];
```



```

eta = 0.5;
ioPaar = {{{0, 0, 1}, 0}, {{0, 1, 1}, 0}, {{1, 0, 1}, 0},
          {{1, 1, 1}, 1}};
Errorliste = Table[{in, t} = ioPaar[[Random[Integer, {1, 4}]]]];
  y = w.in;
  e = t - f[y];
  w += eta in f'[y] e;
  {e, w}, {i, 1, 150000}];

Do[Print[f[w.ioPaar[[i, 1]]]], {i, 1, 4}]
1.55237*10^-9
0.00109336
0.00108848
0.9987

```

The behaviour can be optimized by gradually increasing the steepness  $a$  of the output function towards implementing the desired step function. This has, however, to be done with care, otherwise the learning adjustment  $w+ =$  will not work well. Alternatively, this can be achieved by a rectification of the output. These difficulties demonstrate that artificial neurons are, basically analogue and not digital.

Applications of neural networks to pattern recognition applications use as many inputs as there are pixels in the pattern. In this case, noninteger neuronal outputs are fed into the next layer's neurons, adding to the 'dummy' unitary input from the bias of the neuron itself.

### 8.3 Noise-Cleaning of Signals

Noise is generally unavoidable in real-world applications, but what is noise, and what is 'natural' variation between objects satisfying the same class labelling is generally hard to fathom. For dynamical processes, things are simpler, due to the intrinsic manifold structure of dynamics (expanding manifolds along which the experimental data are organized). In the vector space, states are characterized by a distance. The choice of a distance measure is not objective, which can result in a bias. The dynamics of chaotic systems is organized along expanding manifolds [3]. One way of performing noise-cleaning is therefore to project noise-prone data onto these manifolds [9]. This is usually done using a local main axis decomposition of the data. After keeping only the main directions after setting the coefficients pertaining to less significant direction, the data points are projected onto the manifold.

If more than this is known about the data structure, for example, in the case of noise-prone speech data, the input signal can be noise-cleaned by using a more tailored basis for the data decomposition, e.g., wavelet decomposition or even better, matching pursuit decomposition [10]. Interestingly, the human senses use strongly nonlinear effects for noise-cleaning and signal separation [2].

Finally, if almost no assumption can be made regarding the structure of the underlying system (e.g., if the system is too high-dimensional for allowing a detailed representation via expanding manifolds), clustering methods can provide the guidelines for the underlying dynamical (attractor) structure. This is of importance in particular if a Markov modelling approach of the data is desired. The technical means of the reduction to states is clustering, that is deeply based on the notion of a distance between objects. By clustering, a potential infinity of real-world letters is reduced to an alphabet. In this example, a real-world letter is commonly a vector with entries that correspond to the grey level of a dot in the picture of the handwritten letter the result is the place in the alphabet (a third information destruction). How clustering is done and which input-conversion procedures are applied is again a matter of choice and yet another source of bias.

To provide an explicit example, K-means divisive and agglomerative (Wardstype) clustering start from the idea that the points of a cluster should follow a Gaussian distribution. The pure presence of nonlinearities in the system, however, introduces structures and features of the clusters that—as has been already exposed—are universal but not Gaussian [21]. Typically, they are of swallow-tail or shrimp-like form, geometric forms that the mentioned clustering approaches cannot favourably deal with. To fight the emerging problems with standard clustering approaches, for different clustering approaches (from two main classes: agglomerative and divisive approaches), a whole set of distance measures has been introduced, which, since missing the origin of the problem (universal non-Gaussian geometric cluster forms) are of rather limited help. The fact that and why they fail why they fail has remained hidden for a surprisingly long time.

## 8.4 Symbolic, Probabilistic, and Metric Characterizations

Using clustering, we may reduce real-world or model-based dynamics to a mapping between symbols tagging the clusters (so-called symbolic dynamics). Alternatively, symbols are often introduced by using a generating partition, i.e., a partition into sub-domains that is refined by the dynamics in the most simple manner, by mapping boundaries of the partition on boundaries. For the parabola, this is possible only for selected values of the parameter  $a$ ; an example is the fully developed parabola of  $a = 4$ , where a generating partition is introduced by dividing the unit interval into two parts using the highest point on the parabola as the dividing boundary point. There is a huge bibliography on symbolic dynamics and the characteristics one can extract from symbols alone (thus omitting metric aspects). Classics are Refs. [11, 13].

Along with a symbolic dynamics, particular features of the process can be associated. The most prominent features are probability, stability, or diffusion properties, leading to different variants of the characterization by invariants of the system. If the focus is on probability, we deal with several ways of sampling fractal dimensions and associated entropies. If the focus is on dynamical stability, we deal

with Lyapunov exponents and the Kolmogorov–Sinai entropy. If the focus is on diffusion measures, we are able to distinguish among distinct diffusional behaviour, such as normal, subdiffusive or accelerated diffusion. While all characterizations are extractable without difficulties for given dynamical equations, in particular, the extraction of the set of relevant Lyapunov exponents from time series is involved and requires special care, cf. [22]. For additional details and references, see the chapter ‘Thermodynamic formalism’.

## 8.5 Fourier and Power Spectrum Analysis

The number of extent orbits can, in particular, be used as an indicator for whether we deal with a regular or a chaotic system. Fourier and power spectra exhibit isolated frequency peaks for periodic motion but continuum-like frequency distributions for chaotic motion. Note that, similar to a characterization of a system by means of closed orbits, also combinations of frequencies are reported. For example, if we have two frequencies  $f_1, f_2$  in the system, also their combination  $f_3 = f_1 + f_2$  will be found, etc.

As described in Chap. 9, the basic functions for Fourier-based signal analysis are the FFT (Fast Fourier Transform), the Power Spectrum, and the Cross Power Spectrum CPS. Using these function blocks, additional functions such as frequency response, impulse response, coherence, amplitude spectrum, and phase spectrum can be derived. FFT and the Power Spectrum can be used for measuring the frequency content of stationary or transient signals. FFT measures the average frequency content of a signal over the entire time that the signal was acquired. Therefore, FFT should preferably be applied to stationary signals or if only the average energy at each frequency line is requested. For time-variable frequency information, joint time-frequency functions (e.g., Gabor Spectrogram, see Chap. 9) should be used.

Whereas the FFT returns the frequency component amplitudes of the signal, the two-sided power spectrum returns an array of values that are proportional to the amplitude squared of each frequency component of the time-domain signal, containing in this way symmetrically negative and positive frequencies. If  $A_k$  is the peak amplitude of the sinusoidal component at frequency  $k$ , the height of the spectrum at index  $k$  is  $\frac{A_k^2}{A_0}$ , where  $A_0$  is the amplitude of the DC component in the signal. In real-world frequency analysis, we are mostly interested in the positive part of the frequency spectrum. The transformation from a two-sided into a one-sided spectrum yields non-DC values at a height of  $\frac{A_k^2}{2}$ , which is equivalent to the root mean square (rms) amplitude of the sinusoidal component at frequency  $k$ . According to the Nyquist criterion, the sampling frequency  $F_s$  applied to the signal must be at least twice the maximum frequency component in the signal. If this criterion is violated, a phenomenon known as ‘aliasing’ occurs, and the analysis reports an additional ‘fake’ frequency  $F_s - f_0$ , where  $f_0$  denotes a component at

frequency  $\frac{f_0}{2} < f_0 < F_s$  (similarly, fake frequencies can generate further fake frequencies).

To characterize the relationship between two time-domain signals  $A$  and  $B$ , we can calculate a  $CPS(AB) = S(AB) = \frac{FFT(B)FFT^*(A)}{N^2}$ , where the star denotes complex conjugation, and  $N$  is the length of the two-sided power spectrum, mostly equal to the acquired number of points of the time-domain signal (for computational reasons, mostly chosen as a power of 2). The CPS, frequency response, impulse response, coherence, amplitude spectrum, and phase spectrum of a system can be computed (for details, see the classical Refs. [8, 18]).

## References

1. Frobenius, F.G.: Über matrizen aus nicht negativen elementen (1912)
2. Gomez, F., Saase, V., Buchheim, N., Stoop, R.: How the ear tunes in to sounds: a physics approach. *Phys. Rev. Appl.* **1**(1), 014003 (2014)
3. Gomez, F., Stoop, R.: Quantitative assessment of the log-log-step method for pattern detection in noise-prone environments. *PLOS One* **6**(12), e28107 (2011)
4. Gomez, F., Stoop, R.L., Stoop, R.: Universal dynamical properties preclude standard clustering in a large class of biochemical data. *Bioinformatics* **30**(17), 2486–2493 (2014)
5. Hardy, Y., Steeb, W.H.: *Classical and Quantum Computing: With C++ and Java Simulations*. Birkhäuser, Basel (2012)
6. Hart, L.A.: *How the Brain Works: A New Understanding of Human Learning, Emotion, and Thinking*. Basic Books, New York (1975)
7. Hebb, D.O.: *The organization of behavior: a neuropsychological theory*. Wiley; Chapman & Hall (1949)
8. Horowitz, P., Hill, W.: *The Art of Electronics*. Cambridge University Press, Cambridge (1989)
9. Kern, A., Steeb, W.H., Stoop, R.: Local correlation's potential for noise reduction and symbolic partitions. *Z. Naturforsch. A* **54**(6–7), 404–410 (1999)
10. Kern, A., Stoop, R.: Principles and typical computational limitations of sparse speaker separation based on deterministic speech features. *Neural Comput.* **23**(9), 2358–2389 (2011)
11. Kitchens, B.P.: *Symbolic Dynamics: One-Sided, Two-Sided and Countable State Markov Shifts*. Springer, Berlin (2012)
12. Langton, C.: Computation at the edge of chaos: phase transitions and emergent computation. *Phys. D* **42**(1–3), 12–37 (1990)
13. Lind, D., Marcus, B., Douglas, L., Brian, M., et al.: *An Introduction To Symbolic Dynamics and Coding*. Cambridge University Press, Cambridge (1995)
14. Lorimer, T., Held, J., Stoop, R.: Clustering: how much bias do we need? *Philos. Trans. R. Soc. A: Math. Phys. Eng. Sci.* **375**(2096), 20160293 (2017)
15. Lorimer, T., Kanders, K., Stoop, R.: Natural data structure extracted from neighborhood-similarity graphs. *Chaos Solitons Fractals* **119**, 326–331 (2019)
16. Ott, T., Kern, A., Schuffenhauer, A., Popov, M., Acklin, P., Jacoby, E., Stoop, R.: Sequential superparamagnetic clustering for unbiased classification of high-dimensional chemical data. *J. Chem. Inf. Comput. Sci.* **44**(4), 1358–1364 (2004)
17. Perron, O.: Zur Theorie der Matrizen. *Math. Ann.* **64**(2), 248–263 (1907)
18. Randall, R., Tech, B.: *Frequency Analysis*. Brüel and Kjær, Nærum (1979)
19. Rigden, J.S.: *Macmillan. Encyclopedia of Physics*, p. 353. Simon & Schuster, New York (1996)
20. Stoop, R., Buchli, J., Keller, G., Steeb, W.H.: Stochastic resonance in pattern recognition by a holographic neuron model. *Phys. Rev. E* **67**(6), 061918 (2003)

21. Stoop, R., Kanders, K., Lorimer, T., Held, J., Albert, C.: Big data naturally rescaled. *Chaos Solitons Fractals* **90**, 81–90 (2016)
22. Stoop, R., Meier, P.: Evaluation of Lyapunov exponents and scaling functions from time series. *J. Opt. Soc. Am. B* **5**(5), 1037–1045 (1988)
23. Stoop, R., Stoop, N.: Natural computation measured as a reduction of complexity. *Chaos* **14**(3), 675–679 (2004)
24. Stoop, R., Stoop, N., Bunimovich, L.: Complexity of dynamics as variability of predictability. *J. Stat. Phys.* **114**(3-4), 1127–1137 (2004)
25. Von Helmholtz, H.: *Handbuch der Physiologischen Optik*, vol. 9. Voss (1867)
26. Zucchini, W., MacDonald, I.L., Langrock, R.: *Hidden Markov Models for Time Series: An Introduction Using R*. CRC Press, Boca Raton (2017)

# Chapter 9

## Applied Spectral Analysis



Fabio Della Rossa, Julio Guerrero, Giuseppe Orlando,  
and Giovanni Tagliatalata

### 9.1 Frequency, Spectral Analysis, Phase and Phasor

A signal is a representation of a physical phenomenon that evolves in time. There are two methods to describe the signal: time analysis and frequency analysis. The Fourier transform (FT) is the basic tool to pass from time to frequency analysis.

**Definition 9.1 (Frequency)** The *frequency*  $\nu$  is the number of occurrences of a repeating event or oscillation per unit of time. Therefore if an event is periodic of period  $T$ , then

$$\nu = \frac{1}{T}.$$

---

F. D. Rossa

University of Naples “Federico II”, Department of Electrical Engineering and Information Technology, Naples, Italy

Department of Electronics, Information and Bioengineering, Milan, Italy  
e-mail: [fabio.dellarossa@unina.it](mailto:fabio.dellarossa@unina.it); [fabio.dellarossa@polimi.it](mailto:fabio.dellarossa@polimi.it)

J. Guerrero

University of Jaén, Department of Mathematics, Jaén, Spain  
e-mail: [julio.guerrero@ujaen.es](mailto:julio.guerrero@ujaen.es)

G. Orlando (✉)

University of Bari, Department of Economics and Finance, Bari, Italy

University of Camerino, School of Sciences and Technology, Camerino, Italy  
e-mail: [giuseppe.orlando@uniba.it](mailto:giuseppe.orlando@uniba.it); [giuseppe.orlando@unicam.it](mailto:giuseppe.orlando@unicam.it)

G. Tagliatalata

University of Bari, Department of Economics and Finance, Bari, Italy  
e-mail: [giovanni.tagliatalata@uniba.it](mailto:giovanni.tagliatalata@uniba.it)

Frequency is measured in Hertz (Hz) (i.e. in cycles per second, cps). Alternatively  $\omega = 2\pi\nu$  denotes the angular frequency, which measures the number of radians swept per unit of time in a circular motion.

A signal can contain many frequencies, i.e. it can be the sum of various components with different periods.

**Definition 9.2 (Spectrum)** The frequency content of a signal, i.e. the frequencies of the different components of the signal, is denoted as the *spectrum* of the signal.

The term *spectrum* (and its plural *spectra*), which etymologically refers to “images” or “apparitions” of persons not present physically (like ghosts), was introduced by Sir Isaac Newton to refer to the range of colours observed when light is dispersed through a prism. This term was rapidly adopted by the scientific community to refer to the fundamental components of any wave (like sound waves, seismic waves, electric signals, etc.).

**Definition 9.3 (Spectral Analysis)** The analysis of a signal in terms of a spectrum of frequencies or related quantities such as energies, eigenvalues, etc. is called *spectral analysis*.

**Definition 9.4 (Phase)** Let  $x(t)$  be a time series or a periodic signal and  $T$  be its period,

$$x(t + T) = x(t) \quad \forall t.$$

Then the phase of  $x(t)$  with respect to the initial time  $t_0$  is

$$\varphi(t) = 2\pi \left[ \left[ \frac{t - t_0}{T} \right] \right],$$

where  $[\cdot]$  denotes the fractional part of a real number. Clearly, if  $t_0$  is shifted by  $T$ ,  $\varphi(t)$  does not change. Therefore, the phase depends on  $t_0 \bmod T$ .

A sinusoid can be represented mathematically by the Euler’s formula, i.e. as the sum of two complex-valued functions:

$$A \cdot \cos(\omega t + \theta) = A \cdot \frac{e^{i(\omega t + \theta)} + e^{-i(\omega t + \theta)}}{2},$$

where  $i$  is the imaginary unit,  $A$  the *amplitude* (i.e. the maximum absolute height of the curve),  $\omega$  the *angular frequency* (i.e. how rapidly the function oscillates) and  $\theta$  the *phase* (i.e. the starting point for the cosine wave). The frequency of the wave measured in Hertz is  $\omega/2\pi$ .

A sinusoid can also be written as

$$A \cdot \cos(\omega t + \theta) = \operatorname{Re}\{A \cdot e^{i(\omega t + \theta)}\},$$

where  $\text{Re}\{\cdot\}$  is the real part. In fact

$$\begin{aligned}\text{Re}\{A \cdot e^{i(\omega t + \theta)}\} &= \text{Re}\{A \cdot \cos(\omega t + \theta) + iA \cdot \sin(\omega t + \theta)\} \\ &= A \cdot \cos(\omega t + \theta).\end{aligned}$$

**Definition 9.5 (Phasor)** Given a sinusoidal signal represented in the time-domain form as

$$v(t) = A \cdot \cos(\omega t + \theta),$$

the *phasor* is the corresponding representation in the frequency-domain form

$$V(i\omega) = A \cdot e^{i\theta} = A\angle\theta.$$

Therefore a phasor is a “complex number, expressed in polar form, consisting of a magnitude equal to the peak amplitude of the sinusoidal signal and a phase angle equal to the phase shift of the sinusoidal signal referenced to a cosine signal” [20].

### 9.1.1 Fourier Series and Transform

**Definition 9.6 (Fourier Series)** Let us consider a complex-valued function  $S(x)$  periodic with period  $T$ , which is integrable on any interval of length  $T$ . A *Fourier series* for  $S(x)$  is

$$S_N(x) = \sum_{n=-N}^N c_n \cdot e^{i\frac{2\pi nx}{T}},$$

where the coefficients  $c_n$  are given by

$$c_n = \frac{1}{T} \int_T S(x) e^{-i\frac{2\pi nx}{T}} dx.$$

If  $S(x)$  is real, then  $\bar{c}_n = c_{-n}$ .

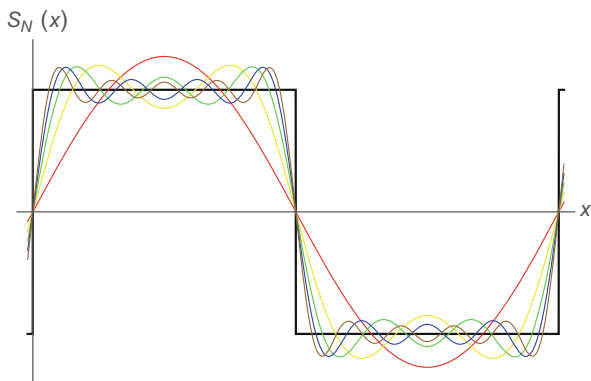
Under suitable condition, is

$$S(x) = \lim_{N \rightarrow \infty} S_N(x).$$

Fourier series allows to represent periodic signals in terms of sums of simple sinusoidal functions (complex exponentials or sine and cosine functions), usually denoted as *harmonics*. The weight of each harmonic  $e^{i\frac{2\pi nx}{T}}$  is given by the Fourier



**Fig. 9.1** Gibbs phenomenon for a square wave (in black) for  $N = 1, 3, 5, 7$  and 9



coefficient  $c_n$ , providing a representation of the periodic signal  $S(x)$  in terms of the coefficients  $\{c_n\}_{n \in \mathbb{Z}}$ .

Care should be taken when approximating a periodic signal  $S(x)$  by its truncated Fourier series  $S_N(x)$ , specially in the case where  $S(x)$  is not continuous at some point  $x_0$ , since in this case  $\lim_{N \rightarrow \infty} S_N(x) = \tilde{S}(x)$  with

$$\tilde{S}(x_0) = \frac{1}{2} \left( \lim_{x \rightarrow x_0^+} S(x) + \lim_{x \rightarrow x_0^-} S(x) \right).$$

In addition,  $S_N(x)$  presents oscillations around  $x_0$  that do not decrease in magnitude when  $N$  grows, known as Gibbs phenomenon (see Fig. 9.1).

**Definition 9.7 (Fourier transform (FT))** The *Fourier transform* of a Lebesgue integrable function  $f: \mathbb{R} \rightarrow \mathbb{C}$  is

$$\hat{f}(\xi) = \int_{-\infty}^{\infty} f(x) e^{-2\pi i x \xi} dx,$$

for any real number  $\xi$ .

*Remark 9.1 (Fourier Transform)* The Fourier transform is a representation of the function in terms of frequency instead of time; thus, it is a frequency-domain representation. It is invertible in the sense that  $\hat{f}(\xi)$  can be taken back to  $f(x)$ . Therefore, linear operations that could be performed in the time domain have counterparts that can often be performed more easily in the frequency domain. Frequency analysis also simplifies the understanding and interpretation of the effects of various time-domain operations, both linear and non-linear. For instance, only non-linear or time-variant operations can create new frequencies in the frequency spectrum.

*Remark 9.2 (Fourier Transform)* The Fourier transform derives from the study of Fourier series in which complicated but periodic functions are reduced to the sum

of simple waves represented by sines and cosines. The Fourier transform extends the Fourier series such that the period of the represented function goes to infinity. Thus, “the Fourier transform converts an infinitely long time-domain signal into a continuous spectrum of an infinite number of sinusoidal curves” [10].

*Remark 9.3 (Fourier Transform)* The Fourier transform, applied to a given complex function defined over the real line, returns a frequency spectrum containing all information of the original signal. For this reason the original function can be completely reconstructed through the inverse Fourier transform. However, in order to do so, the preservation of both the amplitude and phase of each frequency component is required.

**Definition 9.8 (Discrete Fourier Transform (DFT))** Let us consider the complex numbers  $x_0, \dots, x_{N-1}$ . The *discrete Fourier transform (DFT)* is defined as

$$X_k = \sum_{n=0}^{N-1} x_n e^{-i2\pi kn/N} \quad k = 0, \dots, N-1, \quad (9.1)$$

with  $e^{i2\pi/N}$  a primitive  $N^{\text{th}}$  root of 1.

*Remark 9.4 (Fast Fourier Transform (FFT))* Given the Fourier series defined in Definition 9.6 and the discretization in Definition 9.8, the problem of calculating (9.1) requires  $O(N^2)$  operations (where operation means complex multiplication followed by complex addition). The reason is that there are  $N$  calculations  $X_k$ , and each calculation requires a sum of  $N$  terms. Cooley and Tukey [3] proposed an efficient method called *fast Fourier transform (FFT)* to compute the discrete Fourier transform, requiring only  $O(2N \log_2 N)$  operations.

### 9.1.2 Spectral Density, Power Spectrum and Periodogram

**Definition 9.9 (Energy Spectral Density)** The *energy spectral density* of a continuous-time signal  $x(t)$  describes how the energy of a signal or a time series is distributed with frequency, and it is denoted as  $\mathcal{E}_x$  (unit<sup>2</sup> · second<sup>2</sup>)

$$\mathcal{E}_x(f) = |\hat{x}(f)|^2$$

where

$$\hat{x}(f) = \int_{-\infty}^{\infty} e^{-2\pi ift} x(t) dt$$

is the Fourier transform of the signal and  $f$  is the frequency. The total energy of the signal is

$$\mathcal{E} = \int_{-\infty}^{\infty} |x(t)|^2 dt = \int_{-\infty}^{\infty} |\hat{x}(f)|^2 df.$$

If the signal is discrete, the total energy is defined as

$$\mathcal{E} = \sum_{n=-\infty}^{\infty} |x(n)|^2.$$

**Definition 9.10 (Average Power)** Given a signal  $x(t)$ , the average power  $P$  over all time is

$$P = \lim_{T \rightarrow \infty} \frac{1}{T} \int_0^T |x(t)|^2 dt.$$

*Remark 9.5* A stationary process may have a finite power but an infinite energy. This happens because energy is the integral of power, and the stationary signal continues over an infinite time. For this reason in such cases we cannot use the energy spectral density in Definition 9.9, but we need to introduce the concept of power spectral density.

**Definition 9.11 (Amplitude Spectral Density)** In analyzing the frequency content of the signal  $x(t)$ , one might like to compute the Fourier transform. However, for many signals of interest the Fourier transform does not formally exist. In such a case one can use a truncated Fourier transform where the signal is integrated only over a finite interval  $[0, T]$  called as *amplitude spectral density*

$$\hat{x}_T(\omega) = \frac{1}{\sqrt{T}} \int_0^T x(t) e^{-i\omega t} dt.$$

**Definition 9.12 (Power Spectral Density [19])** The *power spectral density* is

$$S_{xx}(\omega) = \lim_{T \rightarrow \infty} |\hat{x}_T(\omega)|^2.$$

*Remark 9.6 (Spectral Density)* The *spectral density* describes how the energy of a continuous-time signal is distributed with frequency. The union of the various spectral densities is called *power spectrum* of the signal.

The spectral density is usually estimated using Fourier transform methods (such as the Welch method). Let us consider a sampling  $x_n$ ,  $n = 1, \dots, \lfloor T/\Delta \rfloor$  of the signal  $x(t)$  in the time window  $[0, T]$ , with sampling period  $\Delta$ . Obviously, from this sampling we can evaluate only the spectral densities that are in  $[2\pi/T, 2\pi/\Delta]$ , since smaller frequencies generate waveforms with period longer than the time

window we are considering, while higher frequencies cannot be captured by the used sampling time.

**Definition 9.13 (DFT Periodogram)** For the regularly sampled signal  $x_n, n = 1, \dots, N$  with sampling time  $\Delta$  of the signal  $x(t)$  ( $x(n\Delta) = x_n$ ), the *periodogram*  $P$  is the function

$$P\left(\frac{k}{N\Delta}\right) = |X_k| = \left| \sum_{j=0}^{N-1} e^{-ik\frac{2\pi j}{N}} x_{j+1} \right|.$$

The periodogram can be used to estimate the spectral density of the signal<sup>1</sup> and is a first approximation of the signal power spectrum. For longer signals, it is possible to refine the power spectrum by averaging (even online) the different periodograms one obtains in each time window of length  $T$ . In other words, to estimate the power spectrum of a signal we need first to understand which windows of frequencies we are interested in. This define our sampling time and the length  $T$  of the time window. Then, in each time window  $[kT, (k + 1)T]$ , compute the periodogram from the sampled signal and obtain the power spectrum of the signal by averaging the obtained periodograms.

*Remark 9.7* The power spectrum of a signal is a fundamental instrument to identify the regularity of the signal. In fact, it answers the question “How much of the signal is at a certain frequency?” Signals generated by a system that exhibits a limit cycle will peak at the frequency related to the period of the limit cycle. Signals generated by a system that behave quasi-periodically give peaks at each of the different frequencies. Signals generated by a chaotic system give broad band components to the spectrum. Indeed this later can be used as a criterion for identifying that the system dynamics is chaotic.

The “most” chaotic signal is the one that exhibits a flat power spectrum, i.e. that has the same power at any frequency. This signal is called *white noise* and is defined as follows.

**Definition 9.14 (White Noise)** We say that the time series  $\epsilon_t$  is a *white noise process* if

$$\begin{aligned} E(\epsilon_t) &= 0 & \forall t \\ \text{Var}(\epsilon_t) &= \sigma^2 & \forall t \\ \text{Covar}(\epsilon_t, \epsilon_s) &= 0 & \forall s \neq t. \end{aligned} \tag{9.2}$$

---

<sup>1</sup>Other more sophisticated and more efficient methods can be used to estimate the power spectrum in case of non-equally sampled signals [4, 23].

If the random variable  $\epsilon_t$  is normally distributed for all  $t$ , the white noise process is called *Gaussian white noise process*.

*Remark 9.8* The covariances in the third line of Eq. (9.2) are called *autocovariances* of the time series  $\epsilon_t$ .

### 9.1.3 Time–Frequency Representations of Signals: Gabor and Wavelet Transform

The Fourier transform of a non-periodic signal provides an accurate representation of the different frequencies (harmonics) of the signal, but with no information about the time at which each frequency is present. To avoid this problem other more sophisticated transforms are necessary.

**Definition 9.15 (Gabor Transform)** The Gabor transform of a signal  $x(t)$  is given by Gabor [7] and Feichtinger and Strohmer [6]

$$G(x)(\tau, \omega) = \int_{-\infty}^{\infty} x(t) e^{-\pi(t-\tau)^2} e^{-i\omega t} dt.$$

Note that the Gabor transform of  $x(t)$  is the Fourier transform of  $x(t) \cdot e^{-\pi(t-\tau)^2}$ , and therefore Gabor transform inherits all nice properties from Fourier transform. In fact it behaves even better since, due to the Gaussian, ill behaved signals  $x(t)$  that do not have a Fourier transform can have a Gabor transform. The Gaussian factor  $e^{-\pi(t-\tau)^2}$  can be seen as a window  $e^{-\pi t^2}$  that it is shifted in the time domain to perform a *local* Fourier transform of the signal  $x(t)$  at different times.

Depending on the application, better results can be obtained by substituting the Gaussian by a different window function (suitably normalized)  $w(t)$  with compact support or with fast decay at infinity, in formula

$$G(x)(\tau, \omega) = \int_{-\infty}^{\infty} x(t) w(t - \tau) e^{-i\omega t} dt.$$

This more general type of transform is also denoted as Gabor transform, *short time Fourier transform* or *windowed Fourier transform*.

**Definition 9.16 (Inverse Gabor Transform)** The inverse Gabor transform is given by

$$x(t) = \int_{-\infty}^{\infty} \int_{-\infty}^{\infty} G(x)(\tau, \omega) w(t - \tau) e^{i\omega t} d\omega d\tau.$$

Gabor analysis is similar to Fourier analysis, but each harmonic is multiplied by a window function displaced in time. Thus Gabor analysis is a time–frequency representation of a signal. A 3D plot representation (or a contour plot) of  $|G(x)(\tau, \omega)|$  is known as *spectrogram*. The redundancy introduced in this two-dimensional representation of a one-dimensional signal  $x(t)$  traduces into a more accurate time representation of the different frequency components of the signal.

However, it is not possible to achieve an infinite precision for the localization in the time–frequency plane. In fact, the localization properties of the Gabor transform are restricted by the *uncertainty principle* (yes!, the same Heisenberg uncertainty principle of quantum mechanics, since the mathematics underlying these two fields are the same). This principle states that if the length of the time window grows, we obtain an accurate localization of frequencies but a poor description in time. On the contrary, if the length of the time window is decreased, we obtain better resolution in time, but poorer resolution in frequency.

Depending on the signal, one should select one of the two possibilities, or search for a compromise between both, and this is obtained for the original Gabor transform with a Gaussian window function, providing in addition the maximum theoretical localization in the time–frequency plane (for window functions of the same length). In practice other window functions  $w(t)$  can be used, like the rectangular Hann/Hanning or Ham/Hamming windows [5, 15], to reduce computational cost or to enhance other properties of the Gabor transform. See Fig. 9.2 for a representation of the *uncertainty principle*.

We can increase the degree of localization (although at different rates for different frequencies) using a so-called time-scale representation instead of the time–frequency representation. This can be achieved with the following transform.

**Definition 9.17 (Wavelet Transform)** The wavelet transform of a signal  $x(t)$  is given by Holschneider [8] and Mallat [11]

$$W(x)(a, \tau) = \frac{1}{\sqrt{a}} \int_{-\infty}^{\infty} x(t) \bar{\gamma} \left( \frac{t - \tau}{a} \right) dt, \quad \tau \in \mathbb{R}, a > 0,$$

where  $\bar{\gamma}(t)$  denotes the complex conjugate of  $\gamma(t)$ , which is a (generally complex) window function satisfying the admissibility condition:

$$0 < \int_{-\infty}^{\infty} \frac{|\hat{\gamma}(\omega)|^2}{|\omega|} d\omega < \infty.$$

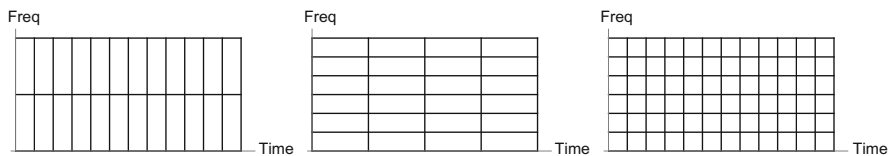


**Fig. 9.2** Uncertainty principle in the time–frequency plane for a short time window (left), a wide time window (centre) and Gabor’s Gaussian window

The admissibility condition implies, in particular, that  $\hat{\gamma}(0) = 0$ , i.e.  $\gamma(t)$  has zero mean and must have oscillations, that is the reason for the name *wavelet* (or *ondelette* in French, since it is a wave with a short duration). The function  $\gamma(t)$  is usually denoted as the *mother wavelet*, and the functions

$$\gamma_{a,\tau}(t) = \frac{1}{\sqrt{a}}\gamma\left(\frac{t-\tau}{a}\right)$$

are called *daughter wavelets*, representing scaled and displaced versions of the mother wavelet. The factor  $1/\sqrt{a}$  is to preserve the total energy.

**Definition 9.18 (Inverse Wavelet Transform)** The inverse wavelet transform is given by

$$x(t) = \int_0^\infty \frac{da}{a^2} \int_{-\infty}^\infty d\tau W(x)(a, \tau)\gamma_{a,\tau}(t).$$

In Fig. 9.3 we plot the Haar wavelet [18], a real wavelet that is one period of a square wave, and its daughter wavelets for  $a = 2$  and  $a = 1/2$ .

For large values of  $a$ ,  $W(x)(a, \tau)$  will provide information on the long range behaviour of the signal  $x(t)$  (where lower frequencies are important, and the effect of higher frequencies cancels out due to the oscillatory character of the wavelets). On the contrary, for small  $a$ ,  $W(x)(a, \tau)$  scrutinizes the short range

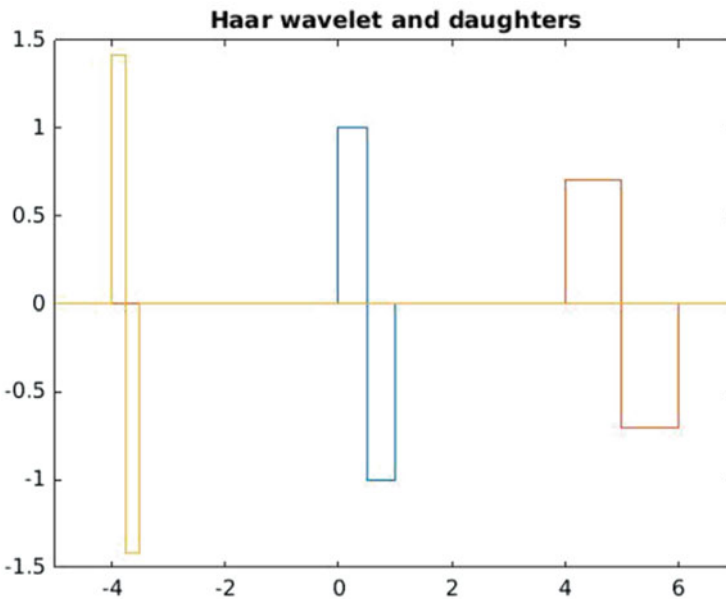


**Fig. 9.3** Haar wavelet (centre) and its daughter wavelets for  $a = 2$  (right) and  $a = 1/2$  (left)

behaviour of  $x(t)$  (where higher frequencies contribute and the lower frequencies cancel out). This indicates that although scales and frequencies are not the same, there is a reciprocal relation between them. In practise, the scales are represented logarithmically (in base 2), in the form  $a = 2^{1/\lambda}$ , in such a way that frequency  $\propto \lambda$ . Thus, although scale and frequency are not the same, it is possible to associate an approximate frequency, known as *pseudo-frequency*, to each scale (although this depends on the particular mother wavelet and the sampling time used).

Also, it is clear that for large values of  $a$  (lower frequencies) there is a poor resolution in time (since the daughter wavelet has a long duration), whereas for small values of  $a$  (higher frequencies) there is a good temporal resolution (since the daughter wavelet has a short duration). Therefore, the resolution of the wavelet transform is not uniform in the time-scale plane. Wavelets are commonly used in the analysis of signals with frequency varying in time (chirps [13, 21]), signals with discontinuities (like edges in images), fractals, etc., where the multiresolution properties of the wavelets provide more information than just the Fourier and Gabor analysis.

A 3D plot (or contour plot) of  $|W(x)(a, \tau)|$  is denoted as *scalogram*, since the wavelet transform provides a scale-time representation of the signal.

In summary, Gabor and wavelet transforms, in contrast to the Fourier transform, provide information about a signal simultaneously in both time and frequency domains. They are widely applied tools in several fields where signal processing is required.

## 9.2 Applications

### 9.2.1 Power Spectrum of the Logistic Map

As in H.W. Lorenz [9] let us assume that a time series  $x_j, j = 1, \dots, n$  of a single variable has been observed at equidistant points in time. The Fourier transform of the series  $x_j$  is defined as

$$\bar{x}_k = \frac{1}{\sqrt{n}} \sum_{j=1}^n x_j \exp(-2\pi i j k / n), \quad k = 1, \dots, n.$$

It can be shown that the *autocorrelation function*, defined by

$$\psi_m = \frac{1}{n} \sum_{j=1}^n x_j x_{j+m},$$



can be written in terms of the Fourier transform:

$$\psi_m = \frac{1}{n} \sum_{k=1}^n |\bar{x}_k|^2 \cos\left(\frac{2\pi mk}{n}\right). \quad (9.3)$$

Inverting Eq. (9.3), we get

$$|\bar{x}_k|^2 = \frac{1}{n} \sum_{m=1}^n \psi_m \cos\left(\frac{2\pi mk}{n}\right).$$

The graph obtained by plotting  $|\bar{x}_k|^2$  as a function of the frequency  $2\pi k/n$  is the *power spectrum*.

*Remark 9.9 (Power Spectrum Interpretation)* A power spectrum displaying several distinguishable peaks is a sign of *quasiperiodic* behaviour. Dominating “peaks represent the basic frequencies of the motion, while minor peaks can be explained as linear combinations of the basic frequencies. If the underlying system is discrete, a single peak corresponds to a period-2 cycle, the emergence of two additional peaks to the left and to the right sides of the first peak, respectively, correspond to a period-4 cycle, 7 peaks correspond to a period-8 cycle, etc.” [9].

If peaks emerge in a continuum the time series is either random or chaotic. In Fig. 9.4 it is shown the power spectrum of the logistic map for two different values of the bifurcation parameter  $\mu$ .

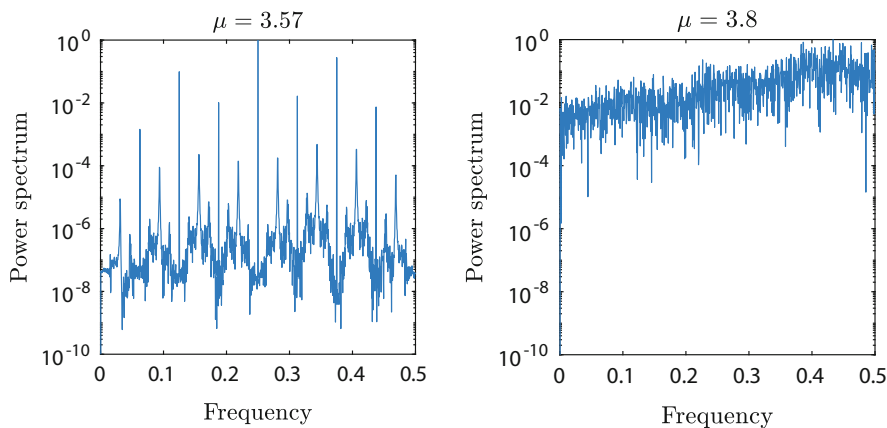


**Fig. 9.4** Power spectrum of the logistic map obtained from a simulation starting at  $x_0 = 0.5$  of 2000 samples. Figure on the left is obtained for  $\mu = 3.57$ , when the unique stable orbit having period 557120 ( $2^6 \cdot 5 \cdot 1741$ ) is present. The power spectrum (obtained for a time series that is shorter than the attractor period) displays regular peaks. Figure on the right shows the power spectrum in the chaotic region where it is not possible to isolate dominating frequencies

### 9.2.2 State Space and Power Spectrum of a Periodic, Quasiperiodic and Chaotic Signals

In order to show how the power spectrum changes with the signal, let us consider the well-studied prototype of a generic two-dimensional map: the Hénon’s two-dimensional dissipative map [1] defined by

$$\begin{cases} x_{n+1} = 1 + \beta x_n - \alpha y_n^2 \\ y_{n+1} = x_n \end{cases} \tag{9.4}$$

The system in Eq. (9.4) is periodic, quasiperiodic or chaotic depending on the parameters  $\alpha$  and  $\beta$ . For example, Fig. 9.5 shows for a periodic signal a discrete peak at the harmonic; Fig. 9.6 shows for a quasiperiodic signal discrete peaks at the harmonics and subharmonics; Fig. 9.7 shows for a chaotic signal a broadband component in its power spectrum. The latter decomposes the signal such that ones can detect whether the source is random/chaotic and its dominating frequencies.

### 9.2.3 Fourier Methods for Finding Frequency Components of a Given Signal

Matlab provides convenient libraries for spectral analysis. In this section we use Fourier transforms to find the frequency components of a signal buried in noise as retrieved in [12].

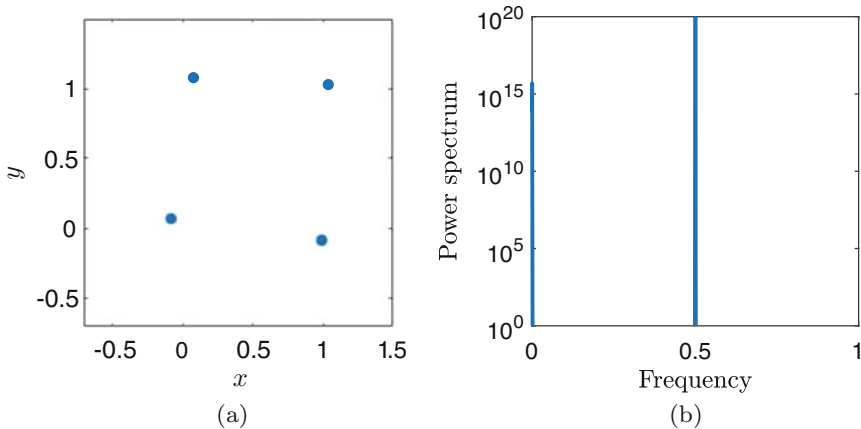


**Fig. 9.5** (a) State space and (b) power spectrum for Eq. (9.4) with parameters  $\alpha = 1$  and  $\beta = 0.05$  (periodic signal)

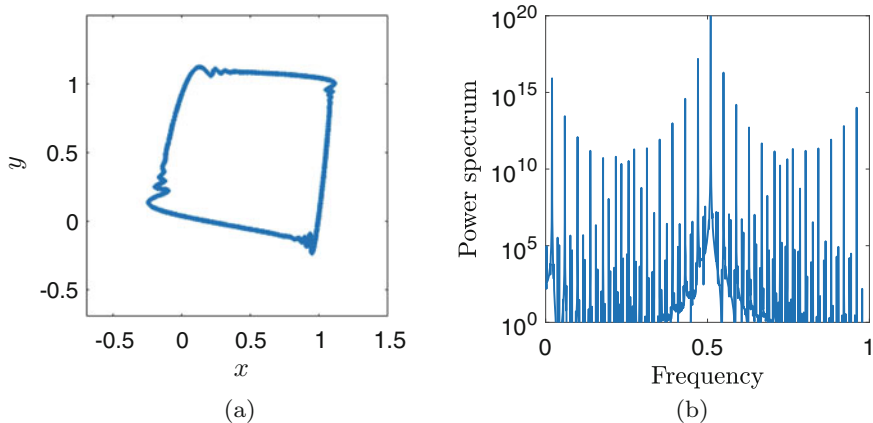


**Fig. 9.6** (a) State space and (b) power spectrum for Eq. (9.4) with parameters  $\alpha = 1$  and  $\beta = 0.12$  (quasiperiodic signal)

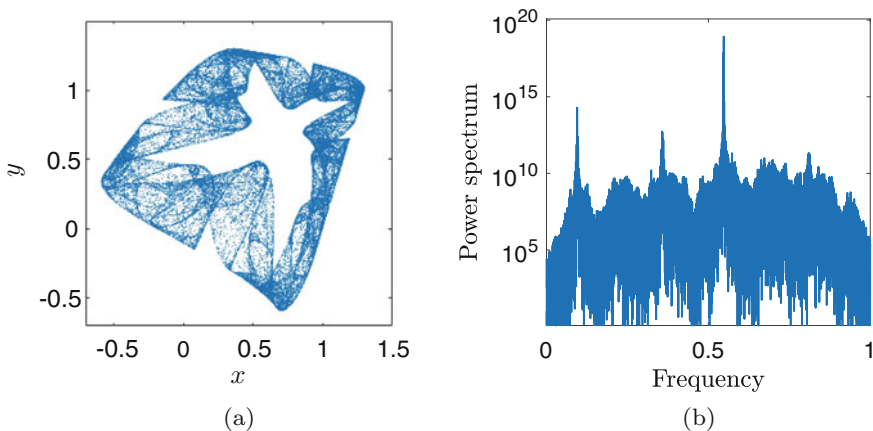


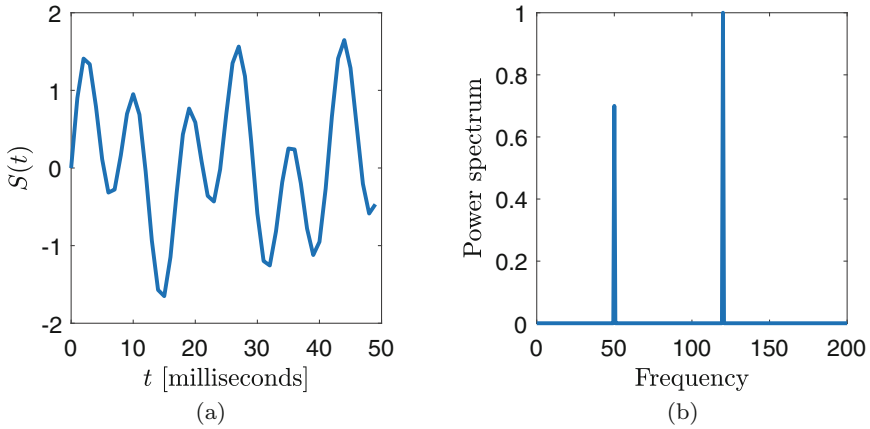
**Fig. 9.7** (a) State space and (b) power spectrum for Eq. (9.4) with parameters  $\alpha = 1$  and  $\beta = 0.3$  (chaotic signal)

Let us consider a signal containing a 50 Hz sinusoid of amplitude 0.7 and 120 Hz sinusoid of amplitude 1:

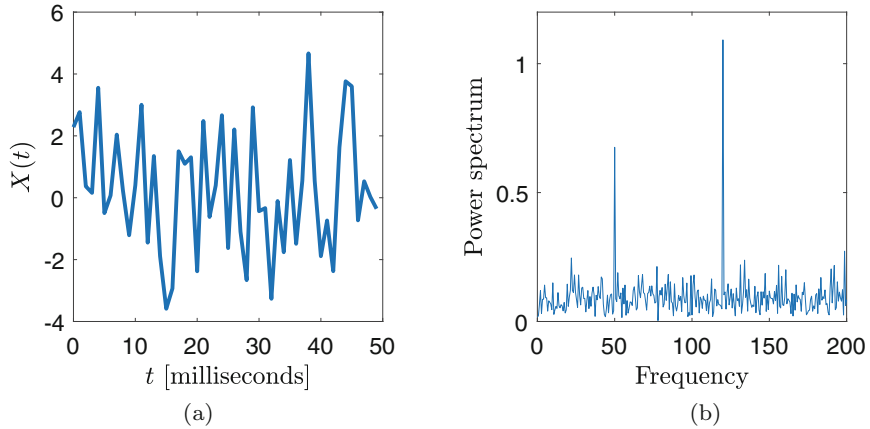
$$S = 0.7 \sin(2\pi 50t) + \sin(2\pi 120t), \quad (9.5)$$

and let us corrupt the signal with zero-mean white noise as defined in Definition 9.14 with a variance of 4:

$$X = S + 2\epsilon_t. \quad (9.6)$$



**Fig. 9.8** Power spectrum for Eq. (9.4). Data sampled at 1 Hz. (periodic signal). (a) Signal in Eq. (9.5) in the time domain. (b) Phase spectrum for Eq. (9.5)



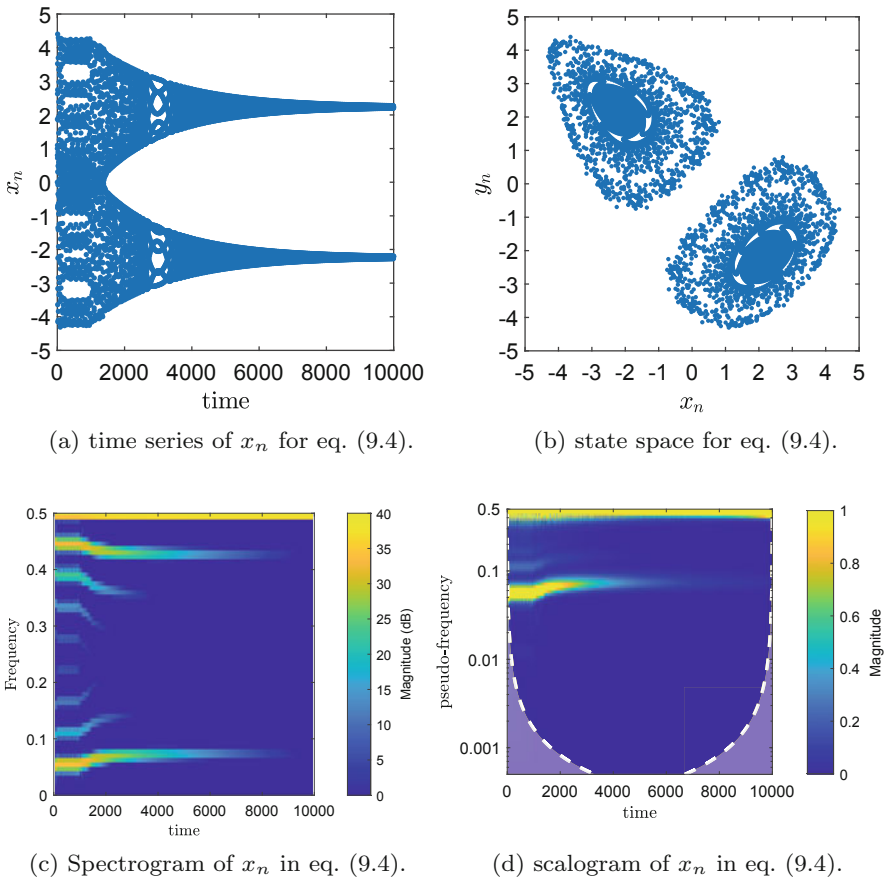
**Fig. 9.9** Power spectrum for Eq. (9.6). Data sampled at 1 Hz. (periodic signal mixed with noise). (a) Signal in Eq. (9.6) in the time domain. (b) Power spectrum for Eq. (9.6)

Figure 9.8 shows the signal in the time domain as well as its power spectrum with just two spikes at 50 and 120 Hz, i.e. the dominating frequencies. Figure 9.9 shows the signal in the time domain as well as its power spectrum with a broadband component in its power spectrum. However, the two spikes at 50 and 120 Hz are clearly distinguishable along with other frequencies due to noise. For applications to economics see Chap. 16 and [16, 17].

### 9.2.4 Gabor and Wavelet Analysis of Hénon's Map

Let us consider Hénon's map (9.4) with  $\alpha = 0.2$  and  $\beta = 0.9991$ , with state space shown in Fig. 9.10b. Applying the Gabor transform to the time series  $x_n$ , we obtain the spectrogram shown in Fig. 9.10c, where a few main frequencies can be observed, but with values that change with time. In particular, it is possible to see that at the beginning of the simulation more frequencies are present, which disappear while the system achieves convergence onto the map attractor, that is a period-2 cycle. The same can also be observed in the scalogram, when the wavelet transform is applied, in Fig. 9.10d, where the fact that different scales are used for different frequencies allowed us to better highlight this phenomenon at smaller frequencies.

See [22] for applications of Gabor analysis in economics, and see [2, 14] for applications of wavelets in economics.



**Fig. 9.10** (a) Time series, (b) state space, (c) spectrogram and (d) scalogram for Eq.(9.4) with parameters  $\alpha = 0.2$  and  $\beta = 0.9991$

## References

1. Benedicks, M., Carleson, L.: The dynamics of the Hénon map. *Ann. Math.* **133**(1), 73–169 (1991)
2. Caus, V.A., Badulescu, D., Gherman, M.C., et al.: Using wavelets in economics. An application on the analysis of wage-price relation. *Oradea J. Bus. Econ.* **2**(1), 32–42 (2017)
3. Cooley, J.W., Tukey, J.W.: An algorithm for the machine calculation of complex Fourier series. *Math. Comput.* **19**(90), 297–301 (1965)
4. Cross, M.: Introduction to Chaos (2000). [http://www.cmp.caltech.edu/~mcc/Chaos\\_Course/](http://www.cmp.caltech.edu/~mcc/Chaos_Course/). Accessed 19 Jul 2019
5. Essenwanger, O.M.: Elements of Statistical Analysis. Elsevier, Amsterdam (1986)
6. Feichtinger, H.G., Strohmer, T.: Gabor Analysis and Algorithms: Theory and Applications. Springer, Berlin (2012)
7. Gabor, D.: Theory of communication. Part 1: the analysis of information. *J. Inst. Electrical Eng. III: Radio Commun. Eng.* **93**(26), 429–441 (1946)
8. Holschneider, M.: Wavelets: An Analysis Tool. Oxford Science Publications, Oxford (1995)
9. Lorenz, H.W.: Nonlinear Dynamical Economics and Chaotic Motion, 2nd edn. edn. Springer, Berlin (1993)
10. Lynch, S.: Dynamical Systems with Applications Using MATLAB. Springer, Berlin (2014)
11. Mallat, S.: A Wavelet Tour of Signal Processing. Academic Press, London (1999)
12. MathWorks: Fast Fourier transform (2020). <https://www.mathworks.com/help/matlab/ref/fft.html>. Accessed 12 Aug 2020
13. MathWorks: Generate Chirp Signal (2020). <https://www.mathworks.com/help/thingspeak/remove-dc-component-and-display-results.html>. Accessed 20 Sep. 2020
14. de Melo, F., Maslennikov, V.V., Popova, E.V., Bezrukova, T.L., Kyksova, I.V.: Quantitative analysis in economics based on wavelet transform: a new approach. *Asian Soc. Sci.* **11**(20), 66 (2015)
15. Oppenheim, A.V.: Discrete-Time Signal Processing. Pearson, London (1999)
16. Orlando, G.: A discrete mathematical model for chaotic dynamics in economics: Kaldor’s model on business cycle. *Math. Comput. Simul.* **125**, 83–98 (2016). <https://doi.org/10.1016/j.matcom.2016.01.001>
17. Orlando, G.: Chaotic business cycles within a Kaldor–Kalecki Framework. In: Nonlinear Dynamical Systems with Self-Excited and Hidden Attractors (2018). [https://doi.org/10.1007/978-3-319-71243-7\\_6](https://doi.org/10.1007/978-3-319-71243-7_6)
18. Percival, D.B., Walden, A.T.: Wavelet Methods for Time Series Analysis, vol. 4. Cambridge University Press, Cambridge (2000)
19. Reike, F., Warland, D., De Ruyter van Steveninck, R., Bialek, W.: Spikes: Exploring the Neural Code. MIT Press, Cambridge (1997)
20. Rizzoni, G.: Fundamentals of Electrical Engineering. McGraw-Hill, New York (2009)
21. Smith, S.: Digital Signal Processing: A Practical Guide for Engineers and Scientists. Elsevier, Amsterdam (2013)
22. Turhan-Sayan, G., Sayan, S.: Use of time-frequency representations in the analysis of stock market data. In: Computational Methods in Decision-Making, Economics and Finance, pp. 429–453. Springer, Berlin (2002)
23. Welch, P.: The use of fast Fourier transform for the estimation of power spectra: a method based on time averaging over short, modified periodograms. *IEEE Trans. Audio Electroacoust.* **15**(2), 70–73 (1967)

# Chapter 10

## Recurrence Quantification Analysis: Theory and Applications



Giuseppe Orlando, Giovanna Zimatore, and Alessandro Giuliani

### 10.1 Motivation

The need to quantify relevant features of time series is present in any discipline. Economics is not an exception as in other fields of investigation dealing with complex systems, has a twofold consideration of the ontological nature of time-dependent signals. On one side they are considered as the expression of a ‘hidden’ dynamical system obeying some (largely unknown) constitutive laws which the investigator tries to observe from time series features (this is the approach technologists call ‘reverse engineering’); on the other side, a time series is nothing else than a trajectory of a system observed within a temporal frame in which the system itself reacts to contingent events happening in time. The difference between the two aspects is as different as a physical essay on thermal conduction (the problem at the basis of Fourier spectral analysis) and the Robinson Crusoe novel where the plot evolves based on the interaction between the character and the external events. In complex systems we have both physical laws (often ‘hidden’) that drive the system to change and random noise (exogenous or endogenous) that interacts with the

---

G. Orlando (✉)

University of Bari, Department of Economics and Finance, Bari, Italy

University of Camerino, School of Sciences and Technology, Camerino, Italy

e-mail: [giuseppe.orlando@uniba.it](mailto:giuseppe.orlando@uniba.it); [giuseppe.orlando@unicam.it](mailto:giuseppe.orlando@unicam.it)

G. Zimatore

eCampus University, Department of Theoretical and Applied Sciences, Novedrate, Italy

e-mail: [giovanna.zimatore@unicampus.it](mailto:giovanna.zimatore@unicampus.it)

A. Giuliani

Environment and Health, Istituto Superiore di Sanità (ISS), Rome, Italy

e-mail: [alessandro.giuliani@iss.it](mailto:alessandro.giuliani@iss.it)

© The Author(s), under exclusive license to Springer Nature Switzerland AG 2021

G. Orlando et al. (eds.), *Non-Linearities in Economics*, Dynamic Modeling

and Econometrics in Economics and Finance 29,

[https://doi.org/10.1007/978-3-030-70982-2\\_10](https://doi.org/10.1007/978-3-030-70982-2_10)

system. The tricky point is that when dealing with complex systems we need to adopt both aspects: the heartbeat of a person (the series of the time intervals between subsequent beats) is dependent on both physical features of the spreading of electric signals across the myocardium and the environmental contingencies occurring in time (e.g. wake/sleep, emotions, metabolic changes, etc.). Strictly speaking, to consider a series as a proper ‘time-dependent’ signal needs both constitutive (e.g. physical laws) and contingent (environmental perturbations) drivers. As a matter of fact, in an ideal pendulum trajectory there is no real time course: the oscillatory behaviour is invariant in time and the system repeats at regular intervals exactly the same path; this is why it can be described by a circle in a phase space, i.e. by a figure with no beginning and no end that can be traversed an infinite number of times. On the other hand, the relative motions of an ensemble of particles at equilibrium have no time-dependent properties and can be described by a static probability distribution of space occupation. In economics this fact is immediate to grasp: an economic system governed by some constitutive ‘rules’ is continuously challenged by environmental solicitations coming from largely unpredictable contingencies happening in time that influence its trajectory. This state of affairs heavily impinges on the data analysis tools more apt to describe such a blend of constitutive and context dependent features.

The ‘perfect’ tool must have the three following basic features:

1. It must be free from any stationarity assumption (the sensitivity to detect tipping-points is of utmost importance).
2. It must be able to deal with both quantitative and symbolic variables.
3. It must be able to deal with very short series.

The above requirements contribute to a fourth ‘corollary’: the mathematics must be as simple as possible.

The recurrence plot approach fulfils the above three requirements, and the mathematics at the basis of the method is the simplest one: nothing more than Pythagoras’ theorem in many dimensions. Basically, we deal with a distance matrix between subsequent epochs in a time series and mark as a ‘recurrence’ any pair of epochs whose distance is below a given threshold (radius). The number of such recurrences and their disposition in time generate a set of quantitative descriptors able to fully characterize the studied system. These properties made recurrence plots (RP) and their quantitative extension (recurrence quantification analysis [RQA]) the method of choice in fields as diverse as biomolecular sequence analysis (where time is substituted by the linear order of monomers along polymer chains), engineering, physiology, psychology, text analysis and clearly economics.

In Sect. 10.4 it can be observed how this approach is useful in detecting spatio-temporal recurrent patterns of dynamical regimes of economic time series. Some indications on the nature of business cycles (i.e. deterministic or stochastic) as well as on the nature of macroeconomic variables and the economy are reported.



## 10.2 Recurrence Plot: Introduction

To introduce RQA it is mandatory to understand what exactly a recurrence plot is and how it was built. The phase space is the space that permits geometrical description of the dynamical evolution of complex nonlinear systems. The dimension of the phase space is the number of variables necessary to describe the state of the system in an instant. An equivalent phase space can be built by time delay embedding procedure from a time series data.

Let  $x_i$  be the orbit of a dynamical system, and let us consider the so-called *delayed vectors* denoted as

$$\mathbf{x}_i = (x_i, x_{i+1}, \dots, x_{i+(m-1)}), \quad (10.1)$$

where  $m$  is the embedding dimension (see 7.2).

Fixed a  $\epsilon > 0$ , for all coordinates  $(i, j)$ , we can define the function

$$R_{i,j}(\epsilon) = \mathcal{H}(\epsilon - \|\mathbf{x}_i - \mathbf{x}_j\|) \quad i, j = 1, \dots, N. \quad (10.2)$$

**Definition 10.1 (Recurrence Plot [1])** A *recurrence plot* (RP) is a matrix of dots in a  $N \times N$  square, where the coordinates  $(i, j)$  are displayed if  $R_{i,j}(\epsilon) = 1$ , i.e. the distance between  $\mathbf{x}_i$  and  $\mathbf{x}_j$  is less than  $\epsilon$ .

Therefore, the RP of  $\mathbf{x}_i \approx \mathbf{x}_j$  shows, for a given  $t$ , the indices of times at which a phase-space trajectory visits the same area in the phase space. The diagonal is called line of identity (LOI), while vertical segments represent phase-space trajectories that remain in the same phase-space region for some time, whereas diagonal lines represent trajectories that run parallel for some time. Thus, the RP enables us to investigate the  $m$ -dimensional phase-space trajectory through a two-dimensional representation of its recurrences. Large scale structures in RP can be classified as homogeneous, periodic, drift and disrupted (*see* Fig. 10.1). Small scale structures (isolated dots, diagonal lines and vertical/horizontal lines and rectangular regions) are the basis of a quantitative analysis of the RPs.

## 10.3 Recurrence Quantification Analysis

Recurrence quantification analysis (RQA) describes quantitatively the recurrence plot. ‘Recurrence’ is defined as the ability of a dynamic system to return to the proximity of the initial point in phase space, and, consequently, RQA was developed by C. Webber and J. Zbilut [12] to understand the behaviour of the phase-space trajectory of dynamical systems. RQA can be defined as a graphical, statistical and analytical tool for the study of nonlinear dynamical systems, and it is successfully used in a multitude of different disciplines from physiology [15, 16] to earth science [17] and economics [9, 10].

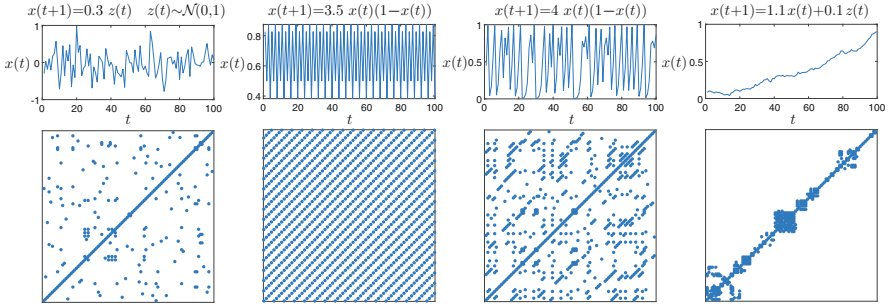


**Fig. 10.1** Recurrence plots coupled with their time series for different systems. Top panels: Signals. Bottom panels: RP. From left to right we consider a white noise, the logistic map with periodic ( $\mu = 3.5$ ) and chaotic ( $\mu = 4$ ) behaviour, and an auto-regressive process

### 10.3.1 RQA Measures

In the RQA, the following measures can be defined.

- S.1 Recurrence (REC), i.e. the density of recurrence points in a recurrence plot (RP). This measure counts those pairs of points whose spacing is below a predefined cut-off distance. Its value is a function of the periodicity of the systems: the more periodic the signal dynamics, the higher the REC.
- S.2 Determinism (DET) measures the number of diagonals and indicates the duration of stable interactions that is graphically represented by the recurrence points in the RP, whose forming lines are parallel to the line of identity (LOI). However, it must be noted that high values of DET ‘might be an indication of determinism in the studied system, but it is just a necessary condition, not a sufficient one’ (Marwan [2]).
- S.3 Maximal deterministic line (MAXLINE) measures the length of the said line found in the computation of DET. According to Eckmann et al. [1], line lengths on RP are directly related to the inverse of the largest positive Lyapunov exponent, and therefore small MAXLINE values are ‘indicative of randomlike behaviour’. ‘In a purely periodic signal, lines tend to be very long, so MAXLINE is large’ [4]. Last but not least, there is a positive probability that white noise processes can have a high MAXLINE, although this is unlikely.
- S.4 Entropy (ENT) is the Shannon entropy measured in bits because of the base-2 logarithm, which are the bins over the diagonals. ‘ENT quantifies the distribution of the diagonal line lengths. The larger the variation in the lengths of the diagonals, the more complex the deterministic structure of the RP’ [4].
- S.5 Trend (TREND) is the regression between the density of recurrence points parallel to the LOI and its distance to the LOI. As TREND measures how quickly a recurrence point departs from the main diagonal, it aims to detect nonstationarity.

S.6 Laminarity (LAM), analogous to DET, measures the number of recurrence points that form vertical lines and indicates the amount of laminar phases (intermittency) in the system.

S.7 Trapping time (TT) measures the average length of the vertical lines, therefore showing how long the system remains in a specific state.

*Remark 10.1* With regard to the RP, points on the LOI are excluded from the measures S.1, S.2 and S.3 because they are trivially recurrent. REC, DET, ENT, MAXLINE and TREND are sensitive to parallel trajectories along different segments of the time series. LAM and TT are able to find chaos–chaos transitions. The ratio of determinism is represented by the lengths of diagonal lines.

### 10.3.2 RQA Epoch by Epoch Correlation Index

We start from the definition of a rolling window because, as mentioned in Webber [3], ‘one of the most useful applications of recurrence quantifications is to examine long time series of data using a small moving window traversing the data. For example, in retrospective studies it is possible to study subtle shifts in dynamical properties just before a large event occurs’.

Slight changes and transition in the dynamics of complex systems can be studied when RQA measures are calculated separately on rolling and overlapping segments. Dynamical transitions like periodic-chaos or chaos–chaos transitions can be observed with this approach.

**Definition 10.2 (Rolling Window)** Let us set  $\mathcal{I} = \{1, \dots, n\} \subseteq \mathbb{N}$  and, for each  $(k, i) \in \mathbb{N}^* \times \mathbb{N}^*$  with  $k < n$  and  $i \leq n - k + 1$ .

A discrete time *rolling or sliding window* is

$$\mathcal{I}_{k,i} = \{i, \dots, i + k - 1\} \subset \mathbb{N}, \quad (10.3)$$

where  $k$  and  $i$  are, respectively, the size and the window’s index.

*Remark 10.2* It can be noted that the number of windows of size  $k$ , as defined in Eq. (10.3), is  $q = n - k + 1 (\geq 2)$ .

**Definition 10.3 (Recurrence Quantification Epoch [13])** When a time series is divided into a series of *windows* or *epochs* of smaller length, the resulting RQA on those multiple sub-series is called *recurrence quantification epoch (RQE)*.

*Remark 10.3* When performing the RQE, it can happen that some windows may overlap. For example, Webber [11] partitioned a time series of 227,957 points in shorter windows (or epochs), each 1.024 seconds long, and ‘adjacent windows were offset by 256 points (75% overlap), fixing the time resolution to 256 ms’.

**Definition 10.4 (Sampling)** For each  $(k, i, l) \in \mathbb{N}^* \times \mathbb{N}^* \times \mathbb{N}^*$  we denote  $S_{k,i}^l$  the  $l$ -th RQA measure of the epoch as

$$S_{k,i} = \{S_t \mid t \in \mathcal{I}_{k,i}\}. \quad (10.4)$$

**Definition 10.5 (RQE Correlation Index)** For each  $l \neq m$ , we denote  $\rho^{l,m}$  the Spearman's correlation coefficient between  $S_{k,i}^l$  and  $S_{k,i}^m$ .

Therefore, there are  $p = \binom{L}{2}$  pairs of correlations  $\rho^{l,m}$  and  $q \times p$  pair of epoch correlations  $\rho_{k,i}^{l,m}$  so that the product

$$P(RQE)_{k,i} = \prod_{\substack{l,m=1 \\ l \neq m}}^L (1 + \rho_{k,i}^{l,m}) \quad (10.5)$$

can be defined as the *RQE correlation index* for the rolling window  $\mathcal{I}_{k,i}$ , and it varies between 0 and  $2^p$ .

**Definition 10.6 (RQE Absolute Correlation Index)** The product

$$P_{abs}(RQE)_{k,i} = \prod_{\substack{l,m=1 \\ l \neq m}}^L (1 + |\rho_{k,i}^{l,m}|) \quad (10.6)$$

can be defined as the *RQE absolute correlation index* for the rolling window  $\mathcal{I}_{k,i}$ , and it varies between 1 and  $2^p$ .

## 10.4 RQA Applications

RQA is meant to be an efficient and relatively simple tool in nonlinear analysis because it allows the identification of the hidden structure of the time series as well as sudden phase changes. For the first purpose, we run PCA over RQA measures Sect. 10.4.1; for the second, we propose a correlation index based on RQA with the final aim to obtain an indicator for early detection of recessions Sect. 10.4.2.

### 10.4.1 Principal Component Analysis (PCA) on RQA

The recurrence quantification analysis (RQA) introduces few parameters as synthetic descriptors of the global complexity of the signal, while it is possible to exalt the minor components present in it by filtering out the redundant information through principal component analysis (PCA). The descriptors obtained by the RQA

could be re-dimensioned through applying the principal component analysis (PCA) technique. PCA is a common statistical technique that provides the possibility to (1) reduce the dimension of a data set without consistent loss of information and (2) to separate the different and independent features of the data. The PCA procedure describes the original data set with a lower number of parameters called main components (PC1, PC2).

For example, the combined use of the RQA and PCA is a useful method in clinical applications [14, 15]. In economics the PCA has been applied to recurrence measures estimated from business cycle data [8]. Thanks to that, it was possible to observe that RQA could distinguish differences between income, capital, investment and consumption (see Chap. 17).

### 10.4.2 RQE Correlation Index on a Sample Signal

As suggested in Orlando et al. [7], in order to test whether the aforementioned correlation index can help to understand changes in a time series, we start by considering a known signal. Let us simulate a random signal distributed as  $\varepsilon \sim \mathcal{N}(\mu, \sigma^2)$ , and let us change its mean and variance as in Table 10.1 and shown in Fig. 10.2.

Now let us apply the RQA to both the original and transformed signals by using the parameters in Table 10.2. The resulting correlations for the original signal and the final signal are displayed in Figs. 10.3 and 10.4, respectively. It is worth noting that the RQE absolute correlation (10.6) is able to detect 9 of the 10 intervals appearing in Table 10.1 (one being clouded by the windowing filtering).

In Orlando et al. [9], the index was tested on the income time series as generated from a Kaldor–Kalecki model [5, 6] with similar results.

**Table 10.1** Perturbed random signal according to a given  $\mu$  and  $\sigma^2$ . For example, for the first interval, 100 points have been randomly generated from a  $\mathcal{N}(0, 1)$  distribution. For the second interval, 40 points have been randomly generated from a  $\mathcal{N}(1, 1)$  distribution, and so on

N.	Interval	$\mu$	$\sigma^2$
1	0	100	0
2	101	140	1
3	141	200	1
4	201	280	4
5	281	300	4
6	301	400	-5
7	401	420	2
8	421	500	2
8	501	560	0
9	561	600	0
10	601	700	1

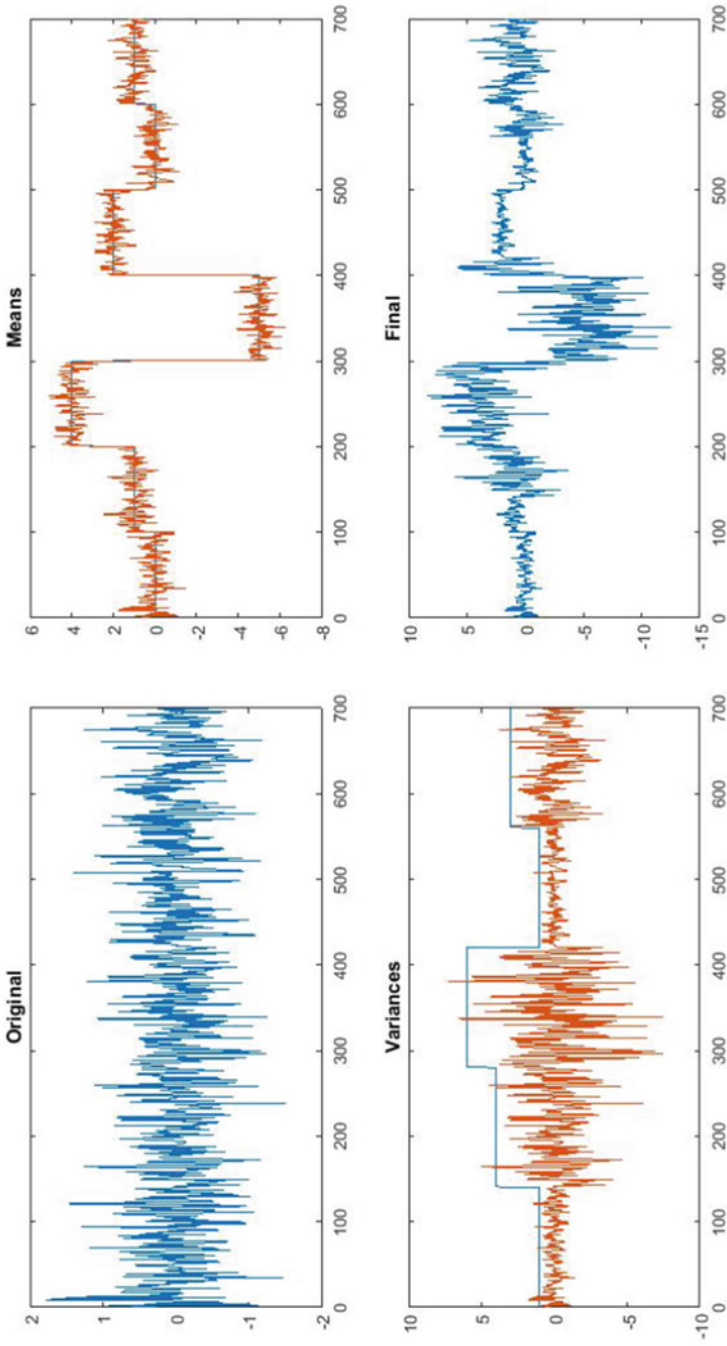


**Fig. 10.2** Clockwise from the top left corner: original sample signal  $\mathcal{N}(0, 1)$ , sample signal with changes in variance and resulting final signal with changed mean and variance

**Table 10.2** RQA parameters of the perturbed signal

Embedding	10
Radius	80
Line	5
Shift	1
Epoch	50
Distance	Meandist, Euclidean
Number of epochs	642

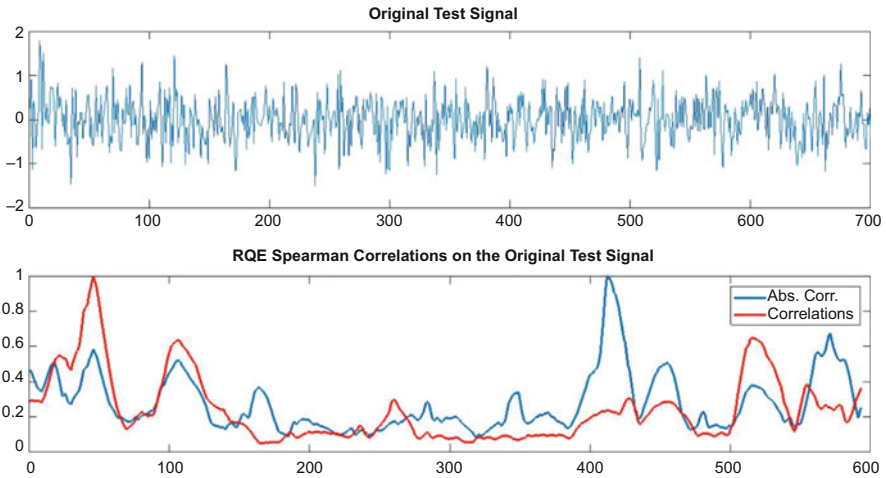


**Fig. 10.3** Original test signal (above) versus Spearman correlations (below). RQE absolute correlation (in blue) is displayed next to correlation (red). Difference in the x-axis numbering between the picture above and below is due to the windowing mechanism

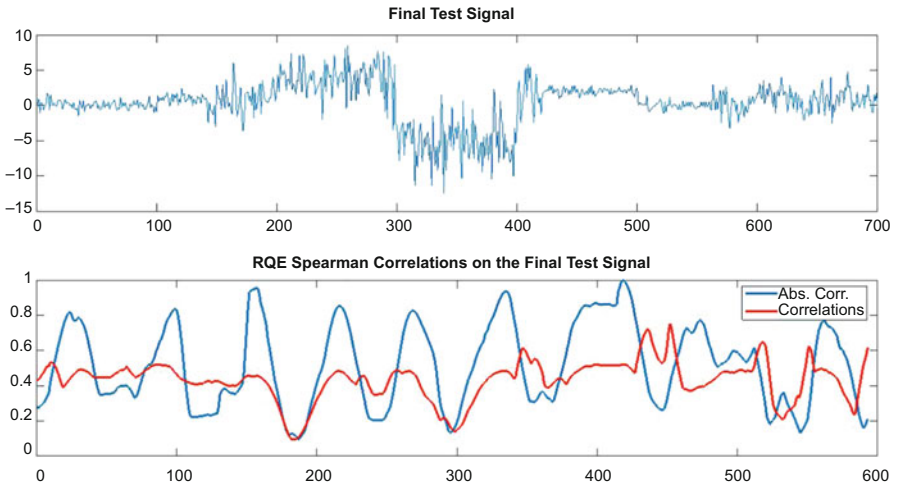


**Fig. 10.4** Altered test signal (above) versus Spearman correlations (below). RQE absolute correlation (in blue) is displayed next to correlation (red). See how the RQE correlation calculated as in Eq. 10.6 is closer than the other, and it is able to detect more fine changes in the times series. The difference in the x-axis between the picture above and below is due to the windowing mechanism

## References

1. Eckmann, J.P., Kamphorst, S.O., Ruelle, D.: Recurrence plots of dynamical systems. *Europhys. Lett.* **4**(9), 973 (1987)
2. Marwan, N.: How to avoid potential pitfalls in recurrence plot based data analysis. *Int. J. Bifurcation Chaos* **21**(4), 1003–1017 (2011)
3. Marwan, N., Webber, C.L. (eds.): *Recurrence Quantification Analysis: Theory and Best Practices*. Springer, Berlin (2015)
4. Matcharashvili, T., Chelidze, T., Janiashvili, M.: Identification of complex processes based on analysis of phase space structures. In: *Imaging for Detection and Identification*, pp. 207–242. Springer, Berlin (2007)
5. Orlando, G.: A discrete mathematical model for chaotic dynamics in economics: Kaldor's model on business cycle. *Math. Comput. Simul.* **125**, 83–98 (2016). <https://doi.org/10.1016/j.matcom.2016.01.001>
6. Orlando, G.: Chaotic business cycles within a Kaldor–Kalecki Framework. In: *Nonlinear Dynamical Systems with Self-Excited and Hidden Attractors* (2018). [https://doi.org/10.1007/978-3-319-71243-7\\_6](https://doi.org/10.1007/978-3-319-71243-7_6)
7. Orlando, G., Zimatore, G.: RQA correlations on real business cycles time series. In: *Indian Academy of Sciences Conference Series—Proceedings of the Conference on Perspectives in Nonlinear I*, 34–41 (2016). Springer, Berlin (2017). <https://doi.org/10.29195/iascs.01.01.0009>
8. Orlando, G., Zimatore, G.: Recurrence quantification analysis of business cycles. *Chaos Solitons Fractals* **110**, 82–94 (2018). <https://doi.org/10.1016/j.chaos.2018.02.032>
9. Orlando, G., Zimatore, G.: RQA correlations on business cycles: a comparison between real and simulated data. *Adv. Nonlinear Dyn. Electron. Syst.* **17**, 62–68 (2019). [https://doi.org/10.1142/9789811201523\\_0012](https://doi.org/10.1142/9789811201523_0012)
10. Orlando, G., Zimatore, G.: Recurrence quantification analysis on a Kaldorian business cycle model. *Nonlinear Dyn.* (2020). <https://doi.org/10.1007/s11071-020-05511-y>
11. Webber, C., Schmidt, M., Walsh, J.: Influence of isometric loading on biceps EMG dynamics as assessed by linear and nonlinear tools. *J. Appl. Physiol.* **78**(3), 814–822 (1995)
12. Webber, C.L. Jr., Zbilut, J.P.: Dynamical assessment of physiological systems and states using recurrence plot strategies. *J. Appl. Physiol.* **76**(2), 965–973 (1994)
13. Zbilut, J.P.: Use of recurrence quantification analysis in economic time series. In: *Economics: Complex Windows*, pp. 91–104. Springer, Berlin (2005)
14. Zimatore, G., Cavagnaro, M., Skarzynski, P.H., Fetoni, A.R., Hatzopoulos, S.: Detection of age-related hearing losses (ARHL) via transient-evoked otoacoustic emissions. *Clin. Interventions Aging* **15**, 927 (2020)
15. Zimatore, G., Fetoni, A.R., Paludetti, G., Cavagnaro, M., Podda, M.V., Troiani, D.: Post-processing analysis of transient-evoked otoacoustic emissions to detect 4 KHz-notch hearing impairment—a pilot study. *Med. Sci. Monit.* **17**(6), MT41 (2011)
16. Zimatore, G., Gallotta, M.C., Innocenti, L., Bonavolontà, V., Ciasca, G., De Spirito, M., Guidetti, L., Baldari, C.: Recurrence quantification analysis of heart rate variability during continuous incremental exercise test in obese subjects. *Chaos* **30**(3), 033135 (2020). <https://doi.org/10.1063/1.5140455>
17. Zimatore, G., Garilli, G., Poscolieri, M., Rafanelli, C., Terenzio Gizzi, F., Lazzari, M.: The remarkable coherence between two Italian far away recording stations points to a role of acoustic emissions from crustal rocks for earthquake analysis. *Chaos* **27**(4), 043101 (2017)



**Part III**  
**Emergence of Cycles and Growth**  
**in Economics**

# Chapter 11

## On Business Cycles and Growth



Giuseppe Orlando and Mario Sportelli

### 11.1 Nonlinearities in Economics

The dynamic analysis of non-linear phenomena in economics dates back to 1887 with the first cobweb model (see Fig. 11.1), in which demand and supply would adjust to the market equilibrium with some time lag. Regularly, recurring cycles were spotted in the market prices by Benner [7], who found that producers base their current output on the price they observe in the market during the previous year. This behaviour can be found, for example, in agriculture because of the lag between planting and harvesting (for the history of the model and the related theorem see Ezekiel [22]).

One of the main problems of the cobweb dynamics consisted in the complexity of the analysis that it involved, if we remove the naive hypothesis that producers do not change their expectation on the price, despite it being always incorrect *ex post*. In the macroeconomic field, the Keynes general theory [40] did not venture into a dynamic analysis but was limited to explain why the system headed towards a static equilibrium point. Only some of those who inherited Keynesian legacy, such as Harrod in modelling economic growth, tried to embed the Keynesian analysis into a dynamic perspective so that equilibrium or imbalance situations were generated endogenously (for more details see Part IV).

---

G. Orlando (✉)

University of Bari, Department of Economics and Finance, Bari, Italy

University of Camerino, School of Sciences and Technology, Camerino, Italy

e-mail: [giuseppe.orlando@uniba.it](mailto:giuseppe.orlando@uniba.it); [giuseppe.orlando@unicam.it](mailto:giuseppe.orlando@unicam.it)

M. Sportelli

University of Bari, Department Mathematics, Bari, Italy

e-mail: [mario.sportelli@uniba.it](mailto:mario.sportelli@uniba.it)

© The Author(s), under exclusive license to Springer Nature Switzerland AG 2021

G. Orlando et al. (eds.), *Non-Linearities in Economics*, Dynamic Modeling

and Econometrics in Economics and Finance 29,

[https://doi.org/10.1007/978-3-030-70982-2\\_11](https://doi.org/10.1007/978-3-030-70982-2_11)

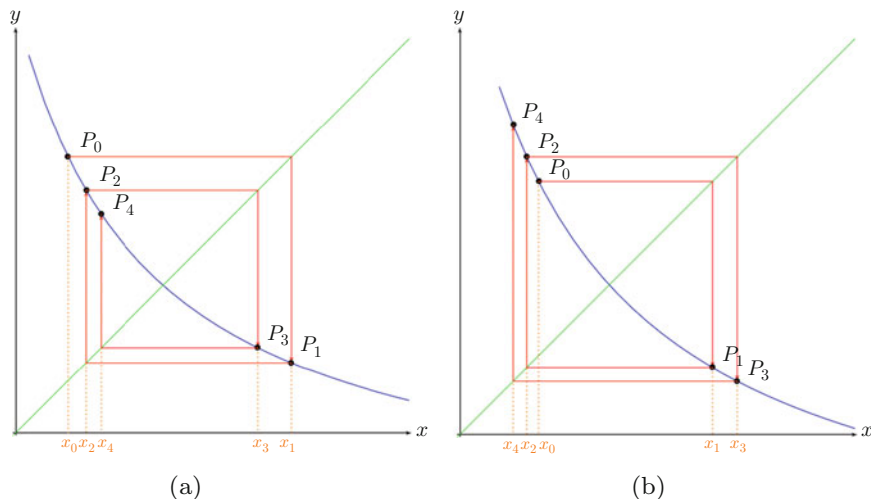


**Fig. 11.1** Fluctuation of prices and quantities in the cobweb model. **(a)** Convergent case. **(b)** Divergent case.

## 11.2 Business Cycles

### 11.2.1 Background and Definition

The pioneering work by Burns and Mitchell [13] gives what is considered the classic definition of business cycles

Business cycles are a type of fluctuation found in the aggregate economic activity of nations that organize their work mainly in business enterprises: a cycle consists of expansions occurring at about the same time in many economic activities, followed by similarly general recessions, contractions, and revivals which merge into the expansion phase of the next cycle.

This definition is useful here for:

1. The creation of composite leading, coincident, and lagging indexes based on the consistent pattern of comovement among various variables over the business cycle (see, e.g., Shishkin [81]);
2. The identification within the business cycles of separate phases or regimes.

The National Bureau of Economic Research (NBER)[56] defines a recession as “a significant decline in economic activity spread across the economy, lasting more than a few months, normally visible in real GDP, real income, employment, industrial production, and wholesale-retail sales. A recession begins just after the economy reaches a peak of activity and ends as the economy reaches its trough. Between trough and peak, the economy is in an expansion. Expansion is the normal state of the economy; most recessions are brief and they have been rare in recent decades”.

With regard to the cycle, Schumpeter [77] mentioned four stages connecting production, stock exchange, public confidence, demand, interest rates, and prices:

1. Expansion (increase in production and prices, while interest rates are relatively low);
2. Crisis (stock exchanges crash and multiple bankruptcies of firms occur);
3. Recession (drops in both prices and production and rise of interest rates);
4. Recovery (stock prices recover because of the fall in prices and incomes).

In addition, Schumpeter suggested that each business cycle has its own typology according to the periodicity, so that a number of cycles were named after their discoverers (see Table 11.1, for a review refer to Korotayev and Sergey [41]).

Figure 11.2 depicts the four stages of a business cycle: (1) expansion, (2) boom period in which aggregate demand rises much more than aggregate output and this overheats the economy bringing it close to its production ceiling, (3) recession, and (4) recovery when the economy restarts to grow after a *trough*. The vertical distance between the peak and the trough is called *specific cycle amplitude*.

**Table 11.1** Business cycles taxonomy sorted by length. From left to right: type of business cycle, name of the scholar who identified it, year in which the cycle was identified, time span of the cycle

Name	Scholar	First studied	Length of cycle
Inventory cycle	Kitchin	1923	From 3 to 5 years
Fixed investment cycle	Juglar	1862	From 7 to 11 years
Demographic cycle	Kuznets	1930	From 15 to 25 years
Technological cycle	Kondratiev	1935	From 45 to 60 years

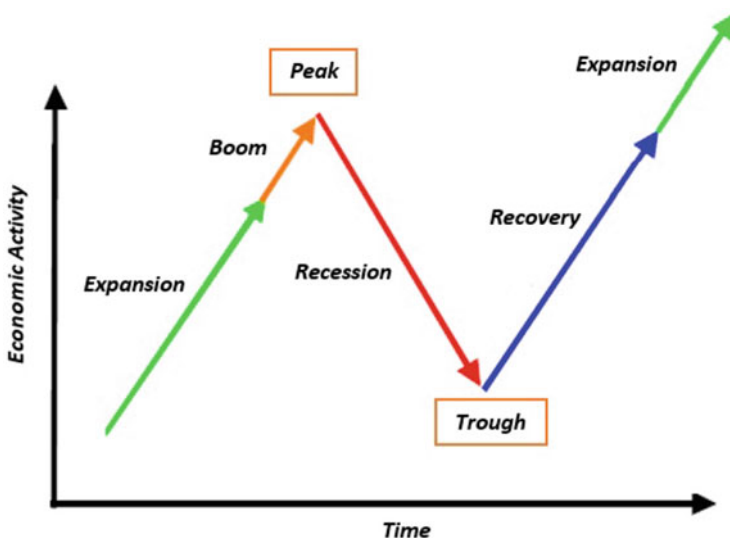


**Fig. 11.2** Business cycle phases where recession (trough) follows expansion (peak)

### 11.2.2 *Literature on the Causes of Business Cycles*

Theories on business cycles (for a review see Semmler [78], Hillinger [37], Zarnowitz [93], Mullineux [55] and Cooley [17]) study volatility of economies and may differ from each other depending on:

1. Their ability to explain cycles without having to rely on outside forces/shocks. They are called *endogenous*. By contrast, *exogenous* business cycle theories require the intervention of the above-mentioned forces/shocks;
2. The assumption of a general equilibrium framework (neoclassical theories) or the assumption of market imperfections and/or disequilibrium (Keynesian theories);
3. The possibility of attributing cycles to real shocks or monetary shocks, or excess/lack of investment or consumption;
4. The derivation of business cycles starting from the interaction of individuals (micro-funded theories) or by considering the aggregate variables as a whole (macro-funded theories).

Until the Keynesian revolution, classical and neoclassical explanations were the mainstream of economic cycles; but after that revolution neoclassical macroeconomics was largely spurned. Starting from the 1980s, there has been a resurgence of neoclassical approaches. The real business cycle (RBC) theory is the most important of them (see the seminal paper of Kydland and Prescott [43]). The main assumption of the neoclassical approach is that individuals and firms always respond optimally. Hence, public intervention, at the best, has no effect on the economy, whereas most of the time it has a negative effect. Even slumps represent, given the situation, the optimal solution. The idea behind this approach is that governments should focus on a long-term growth instead of focussing on stabilization. RBC differs in this way from Keynesian economics and monetarism. These two other approaches relate recessions to some failure of the market. On the contrary, RBC explains business cycle fluctuations with real shocks such as innovations. The success of RBC relies on the fact that it can mimic many measurable business cycle properties. This notwithstanding, RBC models still have some issues notably in interpreting the Solow “residuals”, i.e. the part of growth that is not explained by capital accumulation and labour force expansion. Arguably Solow defined the aforementioned residuals as “a measure of our ignorance”, whereas RBC describes them as a part of the growth that is explained by technical progress.

Hence, the identification of the root caused by economic fluctuations varies between schools of thoughts. The Keynesian/post-Keynesian view is that cycles are caused by the inherent instability of aggregate demand; therefore, unless governed, economy can reach levels below or above full employment. This interpretation created a lively debate among econometricians who had to model and measure economies. For example, Tinbergen [87], [88], and Frisch [26] asserted that the economy is intrinsically stable and the cycles are an effect of exogenous shocks. In particular, Tinbergen, following Slutsky [82], modelled the “economy as a system of stochastically disturbed difference equations, the parameters of which could be

estimated from actual time series” [51]. Similarly, according to Frisch, the cycles result from delays in new capital, spurred by the increased consumer demand. This would cause recurrent, but temporary oscillations in output absorbed in two or three cycles.

Moreover, Schumpeter identified in innovation and creative destruction the factors that deviate the economy from Walrasian equilibrium: “capitalism is by nature a form or method of economic change and not only never is but never can be stationary” [76]. In this context, “imperfections” must be intended as those perturbations of the Walrasian equilibrium that lead to booms because of high profits made by frontrunners. This ends when more and more entrepreneurs copy the strategy of the pioneer firms, and, therefore, greater competition depresses business margins up to forcing foreclosures. At this point, a depression starts and the market is cleansed of unprofitable firms. This equilibrium is maintained until technological or other innovations lay the basis for another expansion.

In addition, Phelps [70] and Lucas [50] explain business cycles on the grounds of incomplete information, given that “key economic decisions on pricing, investment or production are often made on the basis of incomplete knowledge of constantly changing aggregate economic conditions. As a result, decisions tend to respond slowly to changes in economic fundamentals, and small or temporary economic shocks may have large and long-lasting effects on macroeconomic aggregates” [36]. The so-called Austrian School [23, 89] claims that a sustained period of low interest rates leads to an excessive creation of credit and then to an unstable imbalance between savings and investments. From this point of view, a recession (or “credit crunch”) is caused by the need of re-establishing the equilibrium. In other words, monetary shocks influence “relative prices, such as the term structure of interest rates, systematically altering profit rates across economic sectors. Resource use responds to those changes, generating a cyclical pattern of real income. The divergence of the interest rate structure, from the previous and unchanged time preferences, means that the expansion is unsustainable and must end in recession” [1].

The RBC theory [17, 43], which was the mainstream view until the financial crisis of 2008, assumes that markets are perfect. This implies that the business cycle, in itself, is the efficient response to exogenous changes in the real economy. Other theories such as the so-called debt deflation [8, 24, 53], which gained momentum after 2008, contend that over-indebtedness may lead to liquidations, fall of bank assets, credit crunch, and finally to a recession.

Given the different interpretations of business cycles, implications in terms of control of undesired consequences, such as unemployment, inflation, etc. differ too. From a control theory [92] point of view, the economy may be seen as a dynamical system in which the state is limitedly known and the observations contain noise, or which is chaotic by nature [10, 59, 65, 86, 91]. Therefore, it is applicable to the research on controlling stochastic dynamical systems, e.g., Kushner [42], Guo and Wang [33], Fleming and Rishel [25], as well as controlling chaotic dynamical systems, e.g., Romeiras et al. [71], Grebogi and Laib [32], Calvo and Cartwright [14], Pettini [69]. More recently, noise coupled with incomplete information has

been approached in terms of static (Bashkirtseva et al. [6], Bashkirtseva [5]) or dynamic (Bashkirtseva [4]) feedback regulators. Last but not least Orlando et al. [66] compared an Ornstein–Uhlenbeck [61, 62] stochastic process versus a Kaldor–Kalecki [59, 60] deterministic chaotic model and found that not only the latter is able to represent reality as well as the first, but it could reproduce an extreme event (black swans). In fact, in a previous paper, Orlando et al. [67] have shown that real and simulated business cycle dynamics have similar characteristics, which means that the aforementioned deterministic chaotic model could be a suitable tool to simulate reality.

However, the way in which this can be empirically applied in terms of economic policy has not been resolved yet.

### 11.3 Growth

As mentioned by Salvadori [74], “economic growth was central in classical political economy from Adam Smith to David Ricardo, and then in its ‘critique’ by Karl Marx, but moved to the periphery during the so-called ‘marginal revolution’. John von Neumann’s growth model and Roy Harrod’s attempt to generalise Keynesian principle of effective demand to the long-run re-ignited interest in growth theory. Following the publication of papers by Robert Solow and Nicholas Kaldor in the mid-1950s, growth theory became one of the central topics of the economics profession until well into the early 1970s. After a decade of dormancy, since the mid-1980s, economic growth has once again become a central topic in economic theorising. The recent theory is called ‘new growth theory’, since according to it the growth rate is determined from within the model and is not given as an exogenous variable” [74].

While Kaldor’s theory influenced the academic debate on business cycles, Harrod inspired Solow who, with his seminal paper “A Contribution to the Theory of Economic Growth” (1956) [84], set the basis of modern growth theory. However, recent research based on a thorough reading of Harrod’s theory [9, 34], challenges Solow’s interpretation “which ultimately dominated the profession’s view of Harrod” [34]. The idea that the Harrod model “implied a tendency toward progressive collapse of the economy” and that he invoked a fixed-coefficients production function, has “little to do with the problem of long-run growth as Solow understood it, but instead addressed medium-run fluctuations and the ‘inherent instability’ of economies” [34].

There are several reasons why in this book we are dealing with the Harrod’s model. First of all, Harrod, through Solow’s interpretation, contributed to the foundation of modern growth theory. Secondly, the Harrod model provides a dynamic framework and some guidelines for policy-makers in terms of supply-side policies. In fact, they should consider the combination of investment, technological change, population growth, unemployment, and aggregate demand. Another reason is that, in his framework, the warranted rate of growth is not a single moving equilibrium, but

a “highly unstable” one. This is called *Harrod’s knife-edge instability* or *instability principle*.

Similarly, but coming from a different angle (i.e., static analysis and microeconomic foundations of macroeconomic dynamics), Leijonhufvud defines the notion of a corridor of stability as a time-path in which economic activities “are reasonably well coordinated” [45]. Moreover, “the system is likely to behave differently for large than for moderate displacements from the ‘full coordination’ time-path. Within some range from the path (referred to as ‘the corridor’ for brevity), the system’s homeostatic mechanisms work well, and deviation-counteracting tendencies increase in strength. Outside that range these tendencies become weaker as the system becomes increasingly subject to ‘effective demand failures’. If the system is displaced sufficiently ‘far out’, the forces tending to bring it back may, on balance, be so weak and sluggish that for all practical purposes the Keynesian ‘unemployment equilibrium’ model is as sensible a representation of its state as economic statics will allow. Inside the corridor, multiplier-repercussions are weak and dominated by neoclassical market adjustments; outside the corridor, they should be strong enough for effects of shocks to the prevailing state to be endogenously amplified. Up to a point, multiplier-coefficients are expected to increase with distance from the ideal path. Within the corridor, the presumption is in favor of ‘monetarist’ policy prescriptions, outside of it in favour of ‘fiscalist’. Finally, although within the corridor market forces will be acting in the direction of clearing markets, institutional obstacles of the type familiar from the conventional Keynesian literature may, of course, intervene to make them ineffective at some point. Thus, a combination of monopolistic wage-setting in unionized occupations and legal minimum-wage restrictions could obviously cut the automatic adjustment process short before ‘equilibrium employment’ is reached” [45].

Both views, macroeconomic and dynamic (by Harrod) and static and micro-founded (by Leijonhufvud) converge the idea of “existence of thresholds at the start of the mechanisms that are at work” [44]. Therefore, the idea of dynamically unstable multiple equilibria or the alternative Harrod’s suggestion of a Leijonhufvud’s “corridor stability” in our opinion is worth being explored. This is especially because, whereas in the 1970s and the 1980s unemployment and stagflation discarded those theories, in the twentieth century “in the leading Western economies there have been prolonged periods when more saving would have been beneficial, and others with every appearance of inadequate effective demand” [21]. As the Harrod’s model is one of the few able to predict that, “it still deserves serious attention” [21].

## 11.4 Dynamical Systems and Economic Theory

In the last 30 years, attempts to explain and model business cycles and growth have led to adopt in economics some mathematical tools borrowed from dynamical systems theory. The widespread use of non-linear equations in economic models



now appears to have established a symbiosis between the theory of dynamical systems and the theory of economic dynamics.

### ***11.4.1 Historical Foundations of Dynamical System and Chaos Theory from the Economic Perspective***

Many historians of mathematics acknowledge that the basic elements of the dynamical system theory are due to Henry Poincaré.<sup>1</sup> These elements are strictly connected with the foundations of the current notion of dynamical chaos. In the scientific lifework of Poincaré there are three main elements concerning the modern chaos theory: (1) the qualitative theory of differential equations; (2) the study of global stability of sets of trajectories; (3) the notion of bifurcation and the study of families of dynamical systems depending on a parameter [3]. Poincaré introduced the phase portrait (i.e., the set of solution curves traced in the phase space), which is employed to study the behaviour of a system when the underlying differential equations are not solvable. This allowed him to classify and define the singular points in the plane as centres, saddle points, nodes, and foci. Poincaré also developed methods to reduce the study of a continuous-time system to the study of an associated discrete-time system. This technique is the celebrated “first return map” (also known as Poincaré map), which is nowadays considered as one of the most important methods used to reduce the dimension of a system, thus facilitating the study of high-dimension systems. The notion of stability connected with the Poincaré map was taken and refined by Lyapunov [52] and by Andronov’s Gorki school during the twentieth century [20]. Between 1892 and 1899, in his studies of stability, Poincaré discussed a type of orbits he called homoclinic, which are trajectories lying in the intersection of the stable manifold and the unstable manifold of an equilibrium. At that time, however, the scientific community (including Poincaré himself) disregarded any further research on the topic. This happened because research in dynamical systems was mostly devoted to problems involving either stable fixed points or periodic orbits. Poincaré’s studies of homoclinic structures were recovered and further developed firstly by Birkoff [11] and his school, and then, in the 1960s, by Smale [83] and Shilnikov [80].<sup>2</sup> Since then, homoclinic orbits become essential to the study of chaos. In the context of global stability of systems describing rotating fluid masses and planetary motion, Poincaré focused on families of dynamical systems depending on a parameter, in turn depending on external characteristics. In those cases, an exogenous variation of a parameter might drastically change the qualitative characteristics of the system. The qualitative change of a system’s behaviour refers

---

<sup>1</sup>For a detailed survey on Poincaré contributions on dynamical system theory, see Bottazzini [12] and Dahan Dalmedico (1992).

<sup>2</sup>For historical details on the development of the theory concerning the homoclinic orbits, see Shilnikov [79].

to the notion of bifurcation developed by the German mathematician Eberhard Hopf in his work originally published in 1942 and then translated into English in 1976. Hopf suggested the notion of bifurcation that a dynamic system may generate if a parameter changes because of external characteristics of the model. When a bifurcation is detected, the qualitative dynamics of the system may drastically change. The notion of bifurcation spread in the 1970s thanks to the contribution of Ruelle and Takens [73] on hydrodynamics. These authors showed that, as already indicated by Hopf, a sequence of Hopf's bifurcations leads the system from a stationary to a periodic solution. In addition, they showed that, if the frequency of oscillations changes because of changes in a critical parameter, the motion of the system becomes "very complicated, irregular and chaotic" [73, p. 168]. Chaos theory, as currently understood, grew in the 1970s from an interdisciplinary domain involving the qualitative theory of differential equations, fluid mechanics, and parts of engineering and population dynamics. Although Poincaré contributed to the growth of the dynamical system theory, the concept of chaos (as we know it) cannot be described as a linear development of a nucleus of ideas raised and matured among mathematicians alone. Such a development went through important steps in the first half of the twentieth century ([3]). In the mid-1920s, Balthazar van der Pol, a Dutch electrical engineer working for the Philips Research Laboratories, pointed out an example of non-linear dissipative<sup>3</sup> equation without forcing that exhibits sustained oscillations:

$$\ddot{x} + \epsilon(x^2 - 1)\dot{x} + x = 0, \quad \epsilon > 0,$$

known as the van der Pol equation. This second order differential equation describes the amplitude of an oscillating current driven by a triode. In 1926, van der Pol investigated the qualitative behaviour of this equation for values of the parameter  $\epsilon$  larger than 1, thus opening new insights towards the development of the theory of relaxation oscillations. Since then, various generalizations were explored, including the Liénard (1928) equation

$$\ddot{x} + f(x)\dot{x} + g(x) = p(t),$$

which had its first application in economic dynamics by Goodwin [29].

In the 1930s and 1940s, studies on the theory of relaxation oscillations by the physicist Aleksandr A. Andronov allowed the identification of a large class of non-linear structurally stable systems. These studies gave rise to a celebrated treatise written by Andronov himself, together with his colleagues Aleksandr A. Vitt and

---

<sup>3</sup>A dynamical system, either in continuous or in discrete time, can be classified as conservative or dissipative system. The former is a system where the main physical properties remain constant over time. The latter is a system characterized by the contraction of phase space volumes over time. Details on this classification are in Wiggins [90].

Semen E. Kaikin. The treatise was originally published in Russian in 1937<sup>4</sup> and translated from Russian to English in 1949 by Solomon Lefschetz under the title of “Theory of oscillations”. Between the postwar period and the 1960s, the translation to English of other works originally written in Russian allowed a wide diffusion of the non-linear dynamical system theory within the field of pure and applied mathematics.

The work on fluid turbulence of Edward Lorenz [46], in which he studied a relevant application of non-linear dynamical system theory to meteorology (see Sect. 5.2), opened a window on the understanding of the concept of “turbulence”. Such concept was developed and refined by Ruelle and Takens [73], where they also introduced the notion of strange attractor. As shown in Ruelle and Takens [73], in the presence of a strange attractor, a deterministic dynamical system exhibits behaviour like that of a random process.

Finally, Steve Smale, an American mathematician at the University of California (Berkeley), introduced topological tools and methods in the dynamical system theory, thus offering an important contribution in its development. Smale [83] extended the properties of structurally stable systems studied by Andronov to  $n$ -dimensional systems and showed that a two-dimensional system cannot involve a strange attractor, but only a finite collection of fixed points or limit cycles. In contrast, there are higher order dimensional systems ( $n > 2$ ) that he called *hyperbolic*, which exhibit very complicated dynamics, because they may involve an infinite set of periodic trajectories. Universally known as Smale’s *horseshoes*, this finding is one of the most relevant examples of chaos [3].

## 11.5 Mathematical Approaches to Business Cycles

After the Keynesian revolution, Michal Kalecki, Nicolas Kaldor, and Roy Harrod perceived that Clark’s [16] acceleration principle together with the Keynes multiplier were suitable ingredients for the emergence of the cycle. Thus, a mathematical approach to business cycles progressively replaced old theories. However, very soon these models became inadequate to describe the persistence of the cycle, because they made use of linear difference or differential equations that were only able to display damped or undamped oscillations. Consequently, they failed in their main original purpose, which was the description of persistently oscillating behaviours.

As stated in Perona [68], both Kalecki (1935, 1937) and Kaldor (1940) perceived the necessity of employing non-linear functions to account for sustained fluctuations, but did not express their arguments in mathematical terms. In fact, Kalecki was not able to formalize appropriately his intuition regarding the assumption of a finite lag between investment decisions and effective production of capital goods.

---

<sup>4</sup>As a victim of Stalinist purges in 1937, A. Vitt had his name removed from the original Russian edition.

Kaldor, instead, introduced the S-shaped saving and investment curves to explain the cycle, but his analysis was limited to a graphic exposition of the argument. In one of the early issues of *Econometrica* [18], the French mathematician Philip Le Corbeiller produced a brief note suggesting the use of non-linear dynamics to explain the existence of the cycles. Le Corbeiller mentioned the seminal work by van der Pol and encouraged economists to develop applications of this work in economics. However, neither Frisch nor Tinbergen and Schumpeter, i.e., the founders of the Econometric Society and the related journal, attached any importance to the arguments of Le Corbeiller. Probably, this happened because Frisch had the conviction that the economic models, as the economic systems, had to be stable, while cycles were kept alive by exogenous shocks, as emphasized by Slutsky [82]. On this idea, Frisch based his hard critique to the Kalecki models. Such a belief was shared by others economists like Tinbergen, so that the exogenous shock approach to the cycle was accepted as the standard econometric methodology.

Only in the early 1940s, Richard Goodwin, who met Le Corbeiller at Harvard, perceived the great relevance and the potential applications of non-linear dynamics to economics. Initially helped by Le Corbeiller [85], Goodwin devoted his studies (and his life) to restating the economic theory in non-linear terms. In 1948, Goodwin presented his first non-linear model on the cycle at the meeting of the Econometric Society. The paper was published in 1951 on *Econometrica* with the title “The Non-linear Accelerator and the Persistence of the Cycle” [29]. Today, economists consider this paper as the first attempt to formalize in non-linear terms the Harrod (1936) trade cycle theory [35]. Goodwin (1951) showed that the interaction between accelerator and multiplier leads to the formalization of a Liénard type equation. Since the Liénard equation is able to generate stable limit cycles, the persistence of oscillations seemed to be a good description of economic fluctuations. Nonetheless, the Liénard equation received relatively little attention in economic dynamics. This is probably because it is not always possible to reduce a given dynamical system to second order non-linear differential equations like the one suggested by Liénard. Remarkable exceptions are the models by Ichimura [38], Schinasi [75], Glombowski and Krüger [28], and Lorenz [47]. Although the non-linear accelerator model by Goodwin did not receive great attention among the theorists of the cycle, it had the merit of directing the interest of the economists towards the mathematical theory of dynamical systems. Therefore, it represents the real watershed between old and new dynamic theory in economics.

Some pioneering works including the Lyapunov second method on stability and some fundamental theorems of dynamical systems were published at the end of the 1950s and during the 1960s and the 1970s. Among others, we refer to the works by Arrow et al. [2] and Negishi [57] on the stability of a Walrasian general equilibrium model; the work by Rose [72] applied to the context of a Keynesian framework, and the work by Chang and Smyth [15], which re-examined the Kaldor [39] business cycle model, where the Poincaré–Bendixson theorem is applied to prove the existence of limit cycles.

Other fundamental aspects of the dynamical system theory that have been influencing research in economics are the structural stability and the Hopf bifurcation

theorem. The structural stability is a desirable feature of models aimed at explaining real phenomena, as it prevents the limit cycle from vanishing in the face of small perturbations. The Hopf bifurcation theorem and its extensions became a useful tool to detect the structural stability, so that many models using that theorem have been designed in the 1980s and the 1990s. Specifically, the works by Ichimura (1955) and Lorenz [47, 48] provided a different formalization of a Keynesian macro-dynamic model; Schinasi [75] considered a dynamic IS-LM model, while Glombowski and Krüger [28, 28] aimed to reinterpret Harrod's instability principle. Lorenz [49] and Gandolfo [27] provide good surveys of these models. The Goodwin [30] heterodox predator–prey model is another relevant contribution developed in those years. It had the purpose of describing how the Marxian class struggle was a cause of persistent oscillations in the growth rate of the economic system.

### ***11.5.1 Detecting Nonlinearities in Data***

To make the matter even more complicated, economic time series are short because of low sampling frequency. For example, data such as the aggregate capital stock is available only on annual basis, “some prewar U.S. output and price series are only available for benchmark years which may be a decade apart” [19]. For this reason, it is a common practice interpolating data to increase data frequency. However, as explained by Dezhbakhsh and Levy [19], conventional methods are not able to detect stationary processes because “segmented linear interpolation of a stationary process leads to varying moments that may be viewed as an indication of non-stationarity in a conventional sense”. Therefore, the suggestion is to analyse those “series in the context of periodic time-series models rather than by conventional methods” [19].

To date there are different approaches to finding the periodicity of a signal: time–frequency representation and wavelet transformation, spectral representation, Fourier analysis, etc. Among suitable alternatives we mention RQA as it proved the ability in detecting non-linear behaviour or chaos in several fields. This is because RQA is based upon a change in the correlation structure of the observed phenomenon that is known to precede the actual event in many different systems ranging from physiology and genetics to economics. Moreover RQA is able to find evidence of deterministic structures in data (see Moloney et al. [54]).

Gorban et al. [31] studied the behaviour of systems approaching a critical transition through many experiments and observations of groups of humans, mice, trees, grassy plants, and financial time series. They observed that even before obvious symptoms of crisis appear, correlation increases and, at the same time, variance (and volatility) increases too. More specifically, with regard to finance, their case study of the thirty largest companies from the UK stock market within the period 2006–2008 supports the hypothesis of increasing correlations during a crisis and, therefore, that correlation (or equivalently determinism) increases when the market goes down (respectively, decreases when it recovers). Along this line,

Orlando and Zimatore [63] defined the so-called RQE correlation index and they have shown, on a test signal, that it is able to detect regimes' changes. Moreover, by computing the RQE correlation index on USA GDP data [58], they have found that it may help in anticipating recessions [64].

## References

1. Abdulai, A.S.B.: Predicting Intraday Financial Market Dynamics Using Takens' Vectors; Incorporating Causality Testing and Machine Learning Techniques (2015)
2. Arrow, K.J., Block, H.D., Hurwicz, L.: On the stability of the competitive equilibrium, II. *Econometrica* **27**, 82–109 (1959)
3. Aubin, D., Dalmedico, A.D.: Writing the history of dynamical systems and chaos: longue durée and revolution, disciplines and cultures. *Hist. Math.* **29**(3), 273–339 (2002)
4. Bashkirtseva, I.: Controlling stochastic sensitivity by the dynamic regulators. In: AIP Conference Proceedings, vol. 1895. AIP Publishing (2017)
5. Bashkirtseva, I.: Method of stochastic sensitivity synthesis in a stabilisation problem for nonlinear discrete systems with incomplete information. *Int. J. Control* **90**(8), 1652–1663 (2017)
6. Bashkirtseva, I., Ryashko, L., Chen, G.: Controlling the equilibria of nonlinear stochastic systems based on noisy data. *J. Franklin Inst.* **354**(3), 1658–1672 (2017)
7. Benner, S.: Benner's Prophecies of Future Ups and Downs in Prices: What Years to Make Money on Pig-iron, Hogs, Corn and Provisions. Robert Clarke Company (1876)
8. Bernanke, B.S.: The macroeconomics of the Great Depression: a comparative approach. Tech. rep., National Bureau of Economic Research (1994)
9. Besomi, D.: The Making of Harrod's Dynamics. Springer, Berlin (1999)
10. Besomi, D., et al.: Introduction to 'an essay in dynamic theory': 1938 draft by Roy F. Harrod. *Hist. Polit. Econ.* **28**, 245–252 (1996)
11. Birkhoff, G.D.: Sur quelques courbes fermées remarquables. *Bulletin de la Société mathématique de France* **60**: 1-26. Repr. *Collected papers* **2**, 418–443 (1932)
12. Bottazzini, U.: Henri Poincaré, philosophe et mathématicien. *Pour Sci.* (2000)
13. Burns, A.F., Mitchell, W.C.: *Measuring Business Cycles*. National Bureau of Economic Research, Cambridge (1946)
14. Calvo, O., Cartwright, J.H.E.: Fuzzy control of chaos. *Int. J. Bifurcation Chaos* **8**, 1743–1747 (1998)
15. Chang, W.W., Smyth, D.J.: The existence and persistence of cycles in a non-linear model: Kaldor's 1940 model re-examined. *Rev. Econ. Stud.* **38**(1), 37–44 (1971)
16. Clark, J.M.: Business acceleration and the law of demand: a technical factor in economic cycles. *J. Polit. Econ.* **25**(3), 217–235 (1917)
17. Cooley, T.F. (ed.): *Frontiers of Business Cycle Research*. Princeton University Press, Princeton (1995)
18. Corbeiller, P.L.: Les systèmes autoentretenus et les oscillations de relaxation. *Econometrica* **1**, 328–332. (1933)
19. Dezhbakhsh, H., Levy, D.: Periodic properties of interpolated time series. *Econ. Lett.* **44**(3), 221–228 (1994)
20. Diner, S.: Les voies du chaos déterministe dans l'école russe. In: *Chaos et Déterminisme* pp. 331–368 (1992)
21. Eltis, W.: Harrod–Domar Growth Model, pp. 1–5. Palgrave Macmillan, London (2016). [https://doi.org/10.1057/978-1-349-95121-5\\_1267-1](https://doi.org/10.1057/978-1-349-95121-5_1267-1)
22. Ezekiel, M.: The Cobweb theorem. *Q. J. Econ.* **52**(2), 255–280 (1938). <https://doi.org/10.2307/1881734>

23. FA, H.: *Monetary Theory and the Trade Cycle*. Jonathan Cape, London (1933)
24. Fisher, I.: The debt-deflation theory of great depressions. *Econometrica* **1**, 337–357 (1933)
25. Fleming, W.H., Rishel, R.W.: *Deterministic and Stochastic Optimal Control*, vol. 1. Springer, Berlin (2012)
26. Frisch, R.: *Propagation Problems and Impulse Problems in Dynamic Economics*, vol. 3. G. Allen & Unwin, Crows Nest (1933)
27. Gandolfo, G.: *Economic Dynamics*. Springer, Berlin (2009)
28. Glombowski, J., Krüger, M.: On instability principles in the context of growth cycle theory. *Econ. Notes* **11**, 130–147 (1982)
29. Goodwin, R.M.: The nonlinear accelerator and the persistence of business cycle. *Econometrica* **19**(1), 1–17 (1951)
30. Goodwin, R.M.: *Socialism, Capitalism & Economic Growth*. Cambridge University Press, Cambridge (1967)
31. Gorban, A.N., Smirnova, E.V., Tyukina, T.A.: Correlations, risk and crisis: from physiology to finance. *Phys. A: Stat. Mech. Appl.* **389**(16), 3193–3217 (2010)
32. Grebogi, C., Laib, Y.C.: Controlling chaotic dynamical systems. *Syst. Control Lett.* **31**(5), 307–312 (1997)
33. Guo, L., Wang, H.: *Stochastic distribution control system design: a convex optimization approach*. Springer, Berlin (2010)
34. Halmayer, V., Hoover, K.D.: Solow's Harrod: transforming macroeconomic dynamics into a model of long-run growth. *Eur. J. Hist. Econ. Thought* **23**(4), 561–596 (2016). <https://doi.org/10.1080/09672567.2014.1001763>
35. Harrod, R.F.: *Trade Cycle. An Essay*. Oxford University Press, London (1936)
36. Hellwig, C.: *Monetary Business Cycle Models: Imperfect Information*. New Palgrave Dictionary of Economics (2006)
37. Hillinger, C., Sebold-Bender, M.: *Cyclical Growth in Market and Planned Economies*. Oxford University Press, Oxford (1992)
38. Ichimura, S.: Toward a general nonlinear macrodynamic theory of economic fluctuations. In: *Post-Keynesian Economics*, pp. 192–226 (1955)
39. Kaldor, N.: A Model of the Trade Cycle. *Econ. J.* **50**, 78–92 (1940)
40. Keynes, J.M.: *The General Theory of Employment, Interest and Money*. Macmillan Cambridge University Press (1936)
41. Korotayev, A.V., Sergey, T.V.: A spectral analysis of world GDP dynamics: Kondratieff waves, Kuznets swings, Juglar and Kitchin cycles in global economic development, and the 2008–2009 economic crisis. *Struct. Dyn.* **4**(1) (2010)
42. Kushner, H.J.: *Stochastic stability and control, mathematics in science and engineering* (1967)
43. Kydland, F.E., Prescott, E.C.: Time to build and aggregate fluctuations. *Econometrica* **50**(6), 1345–1370 (1982)
44. Le Page, J.: Growth-employment relationship and Leijonhufvud's corridor. *Recherches Economiques de Louvain* **80**(2), 111–124 (2014)
45. Leijonhufvud, A.: Effective demand failures. *Swedish J. Econ.* **75**(1), 27–48 (1973)
46. Lorenz, E.N.: Deterministic nonperiodic flow. *J. Atmos. Sci.* **20**, 130–141 (1963)
47. Lorenz, H.W.: Goodwin's nonlinear accelerator and chaotic motion. *J. Econ.* **47**, 413–418 (1987)
48. Lorenz, H.W.: International trade and the possible occurrence of chaos. *Econ. Lett.* **23**(2), 135–138 (1987)
49. Lorenz, H.W.: *Nonlinear Dynamical Economics and Chaotic Motion*, 2nd edn. Springer, Berlin (1993)
50. Lucas, R.E.: Expectations and the neutrality of money. *J. Econ. Theory* **4**(2), 103–124 (1972)
51. Lucas, R.E.: Methods and problems in business cycle theory. *J. Money Credit Banking* **12**(4), 696–715 (1980)
52. Lyapunov, A.: *Probleme général de la stabilité du mouvement*. *Annals of Mathematical Studies*, Princeton University Press, Princeton (1947)



53. Minsky, H.P.: The Financial Instability Hypothesis. The Jerome Levy Economic Institute, vol. 74 (1992)
54. Moloney, K., Raghavendra, S.: A linear and nonlinear review of the arbitrage-free parity theory for the CDS and bond markets. In: Topics in Numerical Methods for Finance, pp. 177–200. Springer, Berlin (2012)
55. Mullineux, A.W.: The Business Cycle after Keynes. Wheatsheaf Books, Brighton (1984)
56. NBER: National Bureau of Economic Research, The NBER's recession dating procedure business cycle dating committee (2008)
57. Negishi, T.: The stability of a competitive economy: A survey article. *Econometrica* **30**, 635–669 (1962)
58. OECD: Quarterly GDP (indicator) (2016). <https://doi.org/10.1787/b86d1fc8-en>
59. Orlando, G.: A discrete mathematical model for chaotic dynamics in economics: Kaldor's model on business cycle. *Math. Comput. Simul.* **125**, 83–98 (2016). <https://doi.org/10.1016/j.matcom.2016.01.001>
60. Orlando, G.: Chaotic business cycles within a Kaldor–Kalecki Framework. In: Nonlinear Dynamical Systems with Self-Excited and Hidden Attractors (2018). [https://doi.org/10.1007/978-3-319-71243-7\\_6](https://doi.org/10.1007/978-3-319-71243-7_6)
61. Orlando, G., Mininni, R.M., Bufalo, M.: Forecasting interest rates through Vasicek and CIR models: a partitioning approach. *J. Forecasting* **39**, 569–579 (2020). <https://doi.org/abs/10.1002/for.2642>
62. Orlando, G., Mininni, R.M., Bufalo, M.: Interest rates calibration with a CIR model. *J. Risk Financ.* (2019). <https://doi.org/10.1108/JRF-05-2019-0080>
63. Orlando, G., Zimatore, G.: RQA correlations on real business cycles time series. In: Indian Academy of Sciences Conference Series—Proceedings of the Conference on Perspectives in Nonlinear Dynamics—2016, vol. 1, pp. 35–41. Springer, Berlin (2017). <https://doi.org/10.29195/iases.01.01.0009>
64. Orlando, G., Zimatore, G.: Recurrence quantification analysis of business cycles. *Chaos Solitons Fractals* **110**, 82–94 (2018). <https://doi.org/10.1016/j.chaos.2018.02.032>
65. Orlando, G., Zimatore, G.: RQA correlations on business cycles: a comparison between real and simulated data. *Adv. Nonlinear Dyn. Electron. Syst.* **17**, 62–68 (2019). [https://doi.org/10.1142/9789811201523\\_0012](https://doi.org/10.1142/9789811201523_0012)
66. Orlando, G., Zimatore, G.: Business cycle modeling between financial crises and black swans: Ornstein–Uhlenbeck stochastic process vs Kaldor deterministic chaotic model. *Chaos* **30**(8), 083129 (2020)
67. Orlando, G., Zimatore, G.: Recurrence quantification analysis on a Kaldorian business cycle model. *Nonlinear Dyn.* (2020). <https://doi.org/10.1007/s11071-020-05511-y>
68. Perona, E.: Birth and early history of nonlinear dynamics in economics. *Rev. Econ. Estad.* **43**(2), 29–60 (2005)
69. Pettini, M.: Controlling chaos through parametric excitations. In: Dynamics and Stochastic Processes Theory and Applications. Lecture Notes in Physics, vol. 355, pp. 242–250. Springer, Berlin (2005)
70. Phelps, E.: The new microeconomics in inflation and employment theory. *Am. Econ. Rev.* **59**(2), 147–60 (1969)
71. Romeiras, F.J., Grebogi, C., Ott, E., Dayawansa, W.: Controlling chaotic dynamical systems. *Phys. D: Nonlinear Phenom.* **58**(1–4), 165–192 (1992)
72. Rose, H.: On the non-linear theory of the employment cycle. *Rev. Econ. Stud.* **34**, 153–173 (1967)
73. Ruelle, D., Takens, F.: On the nature of turbulence. *Les rencontres Physiciens-mathématiciens de Strasbourg-RCP25* **12**, 1–44 (1971)
74. Salvadori, N.: The Theory of Economic Growth: A “classical” Perspective. Edward Elgar (2003)
75. Schinasi, G.J.: A nonlinear dynamic model of short run fluctuations. *Rev. Econ. Stud.* **48**(4), 649–656 (1981)



76. Schumpeter, J.A.: *Socialism, Capitalism and Democracy*. Harper and Brothers, Manhattan (1942)
77. Schumpeter, J.A.: *History of Economic Analysis*. George Allen & Unwin, London (1954)
78. Semmler, W.: On nonlinear theories of economic cycles and the persistence of business cycles. *Math. Soc. Sci.* **12**(1), 47–76 (1986)
79. Shilnikov, L.: *Homoclinic orbits: Since Poincaré till today* (2005)
80. Shilnikov, L.P.: On a Poincaré–Birkhoff problem. *Mat. Sb.* **116**(3), 378–397 (1967)
81. Shishkin, J.: Signals of Recession and Recovery. NBER Occasional Paper n.77 (1961)
82. Slutsky, E.: The summation of random causes as the source of cyclic processes, *Problems of Economic Condition*, vol. 3, No. 1, The Conjecture Institute, Moscow (1927); *Econometrica* **5**(2), 105–146 (1937) (published in English)
83. Smale, S.: chap. Diffeomorphisms with Many Periodic Points. *Differential and Combinatorial Topology*. Princeton University Press, Princeton (2015)
84. Solow, R.M.: A contribution to the theory of economic growth. *Q. J. Econ.* **70**(1), 65–94 (1956)
85. Sordi, S.: ‘floors’ and/or ‘ceilings’ and the persistence of business cycles. In: *Business Cycle Dynamics*, pp. 277–298. Springer, Berlin (2006)
86. Sportelli, M., Celi, G.: A mathematical approach to Harrod’s open economy dynamics. *Metroeconomica* **62**(3), 459–493 (2011)
87. Tinbergen, J.: *Business Cycles in the United States of America: 1919–1932*. League of Nations (1939)
88. Tinbergen, J.: *Business cycles in the United Kingdom, 1870–1914*. North-Holland, Amsterdam (1951)
89. Von Mises, L.: *On the Manipulation of Money and Credit: Three Treatises on Trade-Cycle Theory*. Liberty Fund (2012)
90. Wiggins, S.: *Introduction to Applied Nonlinear Dynamical Systems and Chaos*, 2nd edn. Springer, Berlin (2003)
91. Yoshida, H.: Harrod’s ‘knife-edge’ reconsidered: An application of the Hopf bifurcation theorem and numerical simulations. *J. Macroecon.* **21**(3), 537–562 (1999)
92. Zabczyk, J.: *Mathematical Control Theory: An Introduction*. Modern Birkhauser Classics. Springer, Berlin (1992). <https://books.google.it/books?id=oe20ngEACAAJ>
93. Zarnowitz, V.: Business cycles: theory, history, indicators, and forecasting. In: *National Bureau of Economic Research Studies in Business Cycles*, vol. 27. The University of Chicago Press, Chicago and London (1992)

# Chapter 12

## Trade-Cycle Oscillations: The Kaldor Model and the Keynesian Hansen–Samuelson Principle of Acceleration and Multiplier



Giuseppe Orlando

### 12.1 Keynesian Multiplier and Hansen–Samuelson Model

Keynesian macroeconomics is a theory for sustained unemployment focusing on the dependence of consumption and savings on income. This was opposed to classic theory for which the rate of interest ensures the equilibrium between investments and savings. In Keynes' view, interest rates are “inert downwards, due to speculation resulting in infinitely elastic liquidity preference, i.e., demand for cash reserves” [17]. In addition, “investments would be inelastic with respect to interest rates even if the latter had been less inert” [17].

According to Keynes, income  $Y$  depends on a parameter  $m$  (called Keynes multiplier) times investment  $I$ . This multiplier is derived from the marginal propensity to consume  $\zeta$ . The dynamic relationship between  $Y$  and  $I$  is

$$Y_t = mI_t = \frac{1}{(1 - \zeta)} I_t. \quad (12.1)$$

An explanation of business cycles is the positive (resp., negative) acceleration due to the effect of income variation on capital accumulation. This model is based on the Keynesian approach, and it was first described by P. Samuelson, who credited H. Hansen for the inspiration [19]. Keynesian theory was static, but Samuelson, building on it, kept the multiplier and ignored the monetary phenomena altogether.

---

G. Orlando (✉)

University of Bari, Department of Economics and Finance, Bari, Italy

University of Camerino, School of Sciences and Technology, Camerino, Italy

e-mail: [giuseppe.orlando@uniba.it](mailto:giuseppe.orlando@uniba.it); [giuseppe.orlando@unicam.it](mailto:giuseppe.orlando@unicam.it)

Then, in Samuelson's view, an investment is determined by the so-called multiplier–accelerator principle. The resulting model (also known as Hansen–Samuelson model) is

$$Y_t = 1 + \zeta(1 + \beta)Y_{t-1} - \zeta\beta Y_{t-2} \quad (12.2)$$

with  $\beta$  representing the sensitivity of investments to changes of consumption  $C$

$$I_t = \beta[C_t - C_{t-1}]. \quad (12.3)$$

The second-order linear difference equation (12.2) displays different solutions depending on the roots of the equation and on the relationship between the parameters [14]. Here, we limit to mention that the equilibrium solution for which  $Y_t = Y_{t-1} = Y_{t-2}$  is a product of an exponential growth factor and a simple harmonic oscillation [17]. Moreover, the frequency of oscillation is an irrational multiple of  $2\pi$ , the motion is quasi-periodic and the resulting time series never repeats. While Samuelson made the theory dynamic through a combination of multiplier and accelerator, its oscillations “can be explosive or damped (disregarding a structurally unstable boundary case)” to the point of being “unrealistically huge”[17].

In order to have bounded and yet sustained oscillations, there was already available a solution suggested by Frisch [3] on Rayleigh's damping system [20] in which oscillations were sustained by exogenous shocks. A second solution was suggested by Hicks [5] through a floor and ceiling system limiting the motion of an otherwise explosive linear model. The mechanism was based on the assumptions that firms follow the linear principle of acceleration. When income falls abruptly, investments may decrease to the point that worn-out capital is not replaced at all leading to capital's destruction. On the other hand, when the income rises fast, some required inputs such as capital, labour, raw materials, etc. become scarce, thus limiting investments.

## 12.2 The Kaldor Model

### 12.2.1 History of the Kaldor Model on Business Cycles

Among economic models, one of the most fruitful applications in the field of chaotic phenomena is the one worked out by Kaldor in 1940 for the business cycle [9]. The author's intention, contrary to the traditional Keynesian multiplier–accelerator concept, was to explain from a macroeconomic viewpoint the fundamental reasons for cyclical phenomena. However, Kaldor did not formalize mathematically his model but gave a qualitative description that prompted out authors to firstly specify the equations and, secondly, to find out under which conditions abnormal behaviour

could be produced or under which conditions bifurcations or even chaos could be generated.

In his work, Morishima [13] along with Yasui [21] and Ichimura [7, 8] was the first in formalizing mathematically Kaldor's ideas and investigating the existence, stability and uniqueness of limit cycles in a nonlinear trade-cycle model. Hicks [6] and Goodwin [4] further studied the model in the form of a system of second-order nonlinear differential equations. In particular, Goodwin [4] built his model on the imbalance between the actual and the desired capital stock and found that without technological progress the equilibrium is unstable and that the economy can oscillate inside a limit cycle. With technological progress, instead, there is no equilibrium and recessions are shorter than expansions (which is in line with the stylized facts on business cycles). Later, Kalecki [10] suggested dividing the investment process into three steps, the first being the decision, the second the time needed for the production and the last the delivery of capital goods. In such a way, the dynamics of capital stock in the economy is described by a nonlinear difference–differential equation that exhibits a complex behaviour (including chaos), and, as a result, oscillations of capital induce fluctuations of other economic variables. After that, Rose [18] introduced the Poincaré–Bendixson theory for a two-dimensional autonomous system, and then Chiarella [2] modified the Goodwin model by introducing a model of monetary dynamics with an adaptive expectation of inflation. In this model, the velocity of money circulation is a nonlinear function of expected inflation.

Thirty years after the original formulation, Chang and Smith [1] reanalysed the model, and they proved that

- The necessary and sufficient conditions enunciated by Kaldor in order to determine that a cycle was established were neither necessary nor sufficient. Instead, these conditions stressed that the onset of the cycle and its amplitude were subordinated to the values of the following parameters:
  - the velocity of adjustment  $\alpha$ ,
  - the initial perturbations,
  - the position of functions  $I$  and  $S$  with respect to each other (see Figs. 12.3 and 12.4).
- Some additional hypotheses to those adopted by Kaldor are necessary for a cycle to arise. The above-mentioned hypotheses are conditions for the existence of a stable equilibrium point (an attractor) for each trajectory.
- Based on the hypothesis explained by them, they were able to determine the onset of a limit cycle by applying the Poincaré–Bendixson theorem.

Next, Krawiec et al. [11] and [12] introduced a time delay in their specification of the Kaldor–Kalecki model. Their model admits a limit cycle. Moreover, the persistence of cycles in the linear approximation depends crucially on the delay parameter and, additionally, on both the speed of adjustment and the initial disturbances. They also noticed that preserving the condition of an S-shaped investment function is not necessary for creating a limit cycle if the mechanism of time delay is introduced into the model. Finally, Orlando [15] and [16] formalized a model in which the

investment and consumption are represented by a hyperbolic tangent instead of the usual periodic arctangent. Moreover, he proved that his model displays a chaotic behaviour.

### 12.3 Formal Description of the Kaldor Model

As mentioned, “old school” economists such as Keynes, Harrod and Kaldor often did not formalize mathematically their models but limited themselves to a description (sometimes even verbal only) of what they meant. Ensuing literature have “interpreted” their theories with greater or lesser adherence to the original author. In this section, let us formalize the Kaldor model as follows. There are two classes of individuals: workers and capitalists. Total income ( $Y$ ) (which corresponds to total production) is shared between them in terms of profits ( $P$ ) and wages ( $W$ )

$$Y = P + W,$$

and the share of income for each class is

$$1 = P/Y + W/Y.$$

A standard assumption adopted by Kaldor is that the propensity to save is higher for capitalists  $S^p > S^w$ . The dynamics of economy is

$$\begin{aligned} \dot{Y}_t &= \alpha(I_t - S_t) \\ \dot{K}_t &= I_t - \delta K_t, \end{aligned} \tag{12.4}$$

where  $Y_t$ ,  $I_t$ ,  $S_t$  and  $K_t$  define, respectively, income, investment, saving and capital at time  $t$ . In Eq.(12.4),  $\alpha$  is the rate by which the output responds to excess investment  $I - S$ , and  $\delta$  represents the depreciation rate of capital  $K$ .

In addition, let us assume with Kaldor that

$$\begin{aligned} I_Y &> 0, \quad I_K < 0, \\ S_Y &> 0, \quad S_K > 0. \end{aligned} \tag{12.5}$$

In order to explain the dynamics of  $I$  and  $S$ , Kaldor suggested that  $I = I(Y, K)$  and  $S = S(Y, K)$  are nonlinear functions of income and capital. This is because, in the usual set-up, linear functions display either a stable equilibrium (see Fig. 12.1) or an unstable one (see Fig. 12.2).

The stable equilibrium is the only level of income level at which savings and investments are equal. When  $S$  and  $I$  are linear, there is a single equilibrium, and it is either stable or unstable. In the first case, the model displays more stability than

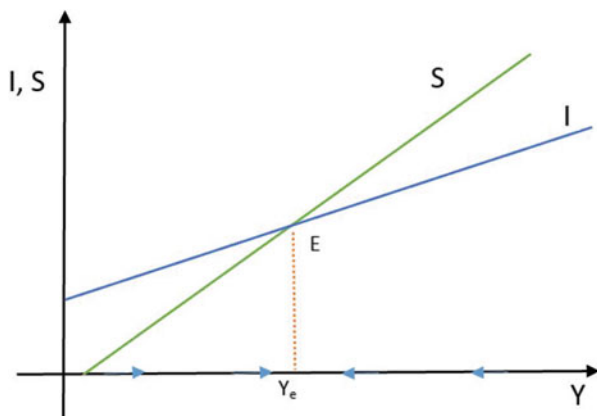


**Fig. 12.1** Investment (blue curve) and saving (green curve) versus income ( $x$ -axis). The equilibrium exists for the level of income corresponding to  $I = S$ . When the income is on the right of  $Y_E$ , high savings are not followed by investments, and, then, the total output will reduce. On the right of  $Y_E$ , instead, investments are higher than savings and the economy grows

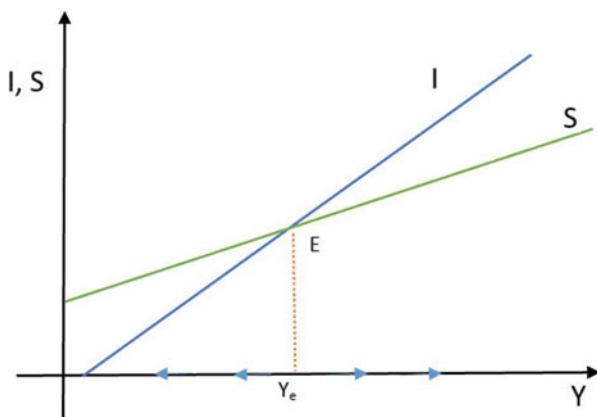


**Fig. 12.2** Investment (blue curve) and saving (green curve) versus income ( $x$ -axis). The equilibrium exists for the level of income corresponding to  $I = S$ . When the income is on the right of  $Y_E$ , high investments push the economy further. On the right of  $Y_E$ , instead, savings are higher than investments, and the economy slows down progressively

appears to be present in the real world, and in the second case, the equilibrium is precarious, and the outcome is either infinite or zero income.

Kaldor’s intuition was to devise a framework in which nonlinear functions moved dynamically. Figure 12.3 shows how the curves  $I(Y)$  and  $S(Y)$  cross each other in three points  $A$ ,  $B$  and  $C$ . Those points correspond to three different equilibrium levels as defined by the equality  $I = S$ .

If production is low at  $Y_A$ , i.e., the level of income corresponding to the equilibrium  $A$ , there will be an excess of capacity. This will absorb an increase

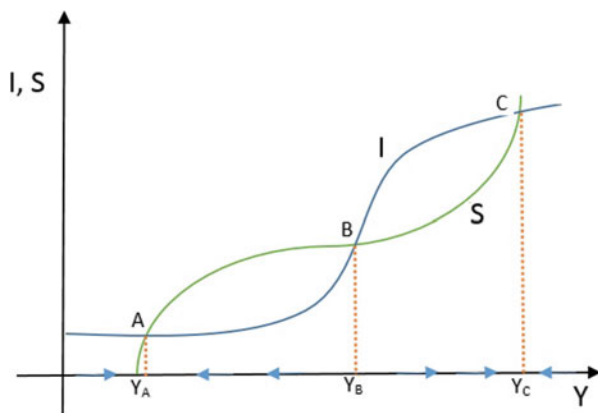


**Fig. 12.3** Investment (blue curve) and saving (green curve) versus income ( $x$ -axis). The equilibrium exists for the level of income corresponding to  $I = S$ . For example, if the income is between  $Y_B$  and  $Y_C$ , the imbalance between investment and saving pushes the economy towards a higher level of income until  $I = S$  in  $C$

in aggregate demand, and, as a consequence, there will be no or little investment. In the case of running high economy, e.g.,  $Y = Y_C$ , the capacity is saturated, and hence the cost of an additional unit of capital increases. On the other hand, the yield of investments decreases as more rewarding initiatives have already been funded. This explains the nonlinearity of investments.

Savings rates are assumed to be high for both low and high levels of output. The reason is that for  $Y = Y_A$ , the income is almost completely consumed, and families have presumably depleted their finances. For this reason, an increase of income would be likely to be directed to restore some savings. For  $Y = Y_C$ , the consumption is already high because an additional income will be saved.

Given the shapes of  $I$  and  $S$ , the income corresponding to the equilibrium is  $Y_A$ ,  $Y_B$  or  $Y_C$ . While  $Y_A$  and  $Y_C$  are stable,  $Y_B$  is not (on the left, savings exceed investments, and on the right, vice versa).

For Kaldor, the business cycle is caused by capital accumulation. For example, let us assume that  $Y = Y_C$  and that  $I$  depends on  $K$  in such a way that  $\frac{dI}{dK} < 0$ . In this case, the stock of capital increases, and then the marginal productivity of capital declines and so does the investments curve  $I$ .

When the production is high, this brings down prices, which implies that more income can be saved. This yields  $\frac{dS}{dK} > 0$ , i.e., the savings curve shifts upwards.

This process has the effect of moving  $Y_C$  down and  $Y_B$  up (see Fig. 12.4), and it will continue until the two points will meet, and the  $S$  and  $I$  curves will be tangent at that point. To the left, the ensuing point of equilibrium is for  $Y = Y_A$ , which represents a crash for the economy.

The equilibrium point  $Y_B = Y_C$  is stable because, on the right, when  $S > I$ , the economy slows down, and on the left, when  $S < I$ , the economy grows.

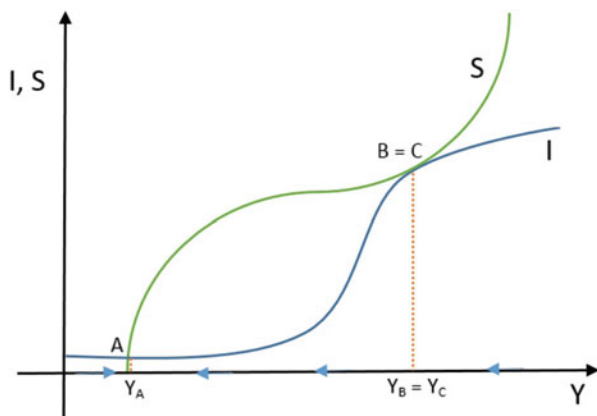


**Fig. 12.4** Representation of investment  $I$  and saving  $S$  dynamic analysis. Because of declining productivity, the investment shifts downwards and the ensuing price's reduction moves saving upwards

Key features of this cyclical process are self-generation and dynamical adjustments of the macroeconomic variables that come into play. When the income is relatively high, other forces keep it in check by producing a downward movement, and vice versa. These forces are namely the shift of investment and saving function and the accumulation and decumulation of capital. Those events occur over the cycle and are embedded in the dynamics.

One additional feature of Kaldor's model concerns the implications in terms of fiscal policy. Income distribution between capitalists and workers determines the amount of investment and saving because the propensity to save of the two classes is different. In other words, a fine tuning of the distribution of income may bring the economy to the equilibrium. This sets the distance between the Kaldor and the Harrod models. While for the first the system is dynamically self-adjusting and distribution mechanism may help in achieving a higher equilibrium, for the second a change of  $I$  in relation to  $S$  kicks off a cumulative process of decline (or growth) in both: income and production without any counterbalance.

The last noteworthy feature of Kaldor's model is the role played by inflation. When  $I > S$ , higher utilization of factors, rising investment and growth of demand under full employment will cause, eventually, higher prices than wages, thus changing the share of income in favour of capitalists. As the propensity to save is higher for those individuals, total savings will increase more than investments, and the equality of  $S$  and  $I$  will be restored. On the other hand, when investment and demand decline, prices relative to wages will tend to decline. The share of workers' income will increase and savings will decline. The new equilibrium where  $S = I$  will be restored for a lower level of income. This mechanism is also called the "Kaldor Effect."



## References

1. Chang, W.W., Smith, D.J.: The existence and persistence of cycles in a non-linear model: Kaldor's 1940 model re-examined. *Rev. Econ. Stud.* **38** 37–44 (1971)
2. Chiarella, C.: *The Elements of a Nonlinear Theory of Economic Dynamic*. Springer, Berlin (1990)
3. Frisch, R.: *Propagation Problems and Impulse Problems in Dynamic Economics*, vol. 3. G. Allen & Unwin, Crows Nest (1933)
4. Goodwin, R.M.: The nonlinear accelerator and the persistence of business cycle. *Econometrica* **19**(1), 1–17 (1951)
5. Hicks, J.R.: *A Contribution to the Theory of the Trade Cycle*, vol. 126. Clarendon Press, Oxford (1950)
6. Hicks, J.R.: *A Contribution to the Theory of the Trade Cycle*. Clarendon Press, Oxford (1950)
7. Ichimura, S.: Notes on non-linear business cycle theories. *Osaka Economic Papers* (1955)
8. Ichimura, S.: Toward a General Nonlinear Macrodynamical Theory of Economic Fluctuations. In: Kurihara, K.K. (ed.) *Post-Keynesian Economics*, chap. 8, pp. 192–226. George Allen & Unwin, London (1955)
9. Kaldor, N.: A model of trade cycle. *Econ. J.* **50**(197), 78–92 (1940)
10. Kalecki, M.: *Studies in the Theory of Business Cycles, 1933–1939*. A.M. Kelley, New York (1966)
11. Krawiec, A., Szydłowski, M.: The Kaldor–Kalecki business cycle model. *Ann. Oper. Res.* Springer, Berlin 89–100 (1999)
12. Krawiec, A., Szydłowski, M.: On nonlinear mechanics of business cycle model. *Regul. Chaotic Dyn.* **6**(1), 101–118 (2001)
13. Morishima, M.: A contribution to the nonlinear theory of the trade cycle. *Z. National.* **18**(4), 166–170 (1959)
14. Mullineux, A.W.: *The Business Cycle after Keynes*. Wheatsheaf Books, Brighton (1984)
15. Orlando, G.: A discrete mathematical model for chaotic dynamics in economics: Kaldor's model on business cycle. *Math. Comput. Simul.* **125**, 83–98 (2016). <https://doi.org/10.1016/j.matcom.2016.01.001>
16. Orlando, G.: Chaotic business cycles within a Kaldor–Kalecki Framework. In: *Nonlinear Dynamical Systems with Self-Excited and Hidden Attractors* (2018). [https://doi.org/10.1007/978-3-319-71243-7\\_6](https://doi.org/10.1007/978-3-319-71243-7_6)
17. Puu, T.: Short history of the multiplier-accelerator model. In: *Business Cycle Dynamics*, pp. 79–112. Springer, Berlin (2006)
18. Rose, H.: On the non-linear theory of the employment cycle. *Rev. Econ. Stud.* **34**, 153–173 (1967)
19. Samuelson, P.A.: Interactions between the multiplier analysis and the principle of acceleration. *Rev. Econ. Stat.* **21**(2), 75–78 (1939)
20. Strutt, J.W., Rayleigh, B.: *The Theory of Sound*. Dover, New York (1945)
21. Yasui, E.: Non-linear self-excited oscillations and business cycles. *Cowles Commission Discussion Paper* (2063), 1–20 (1953)

# Chapter 13

## The Harrod Model



Giuseppe Orlando, Mario Sportelli, and Fabio Della Rossa

### 13.1 Introduction

The theoretical foundation of the Keynesian growth theory is the so-called Harrod–Domar model. This is the consolidated opinion we find in the economic literature. Nevertheless, after a careful reading of both the original writings of Harrod and Domar, that “model” stands out as a commingling of two models, which had different aims and different hypotheses. As pointed out by Pugno [15, p. 152], the Harrod model is really a result of many works written over the period of the author’s whole intellectual life. The first draft dates back to 1938,<sup>1</sup> where, as Harrod always confirmed until his last book published in 1973, the central and crucial aim was to account for the unstable growth path characterizing capitalistic economies.

---

Part of this chapter has appeared in [13].

<sup>1</sup>Besomi [3] has edited this draft.

---

G. Orlando (✉)

University of Bari, Department of Economics and Finance, Bari, Italy

University of Camerino, School of Sciences and Technology, Camerino, Italy

e-mail: [giuseppe.orlando@uniba.it](mailto:giuseppe.orlando@uniba.it); [giuseppe.orlando@unicam.it](mailto:giuseppe.orlando@unicam.it)

M. Sportelli

University of Bari, Department Mathematics, Bari, Italy

e-mail: [mario.sportelli@uniba.it](mailto:mario.sportelli@uniba.it)

F. Della Rossa

University of Naples “Federico II”, Department of Electrical Engineering and Information Technology, Naples, Italy

Department of Electronics, Information and Bioengineering, Milan, Italy

e-mail: [fabio.dellarossa@unina.it](mailto:fabio.dellarossa@unina.it); [fabio.dellarossa@polimi.it](mailto:fabio.dellarossa@polimi.it)

© The Author(s), under exclusive license to Springer Nature Switzerland AG 2021

G. Orlando et al. (eds.), *Non-Linearities in Economics*, Dynamic Modeling and Econometrics in Economics and Finance 29,

[https://doi.org/10.1007/978-3-030-70982-2\\_13](https://doi.org/10.1007/978-3-030-70982-2_13)

In spite of this, as clearly shown by Besomi [2], Harrod's readers interpreted, almost unanimously,<sup>2</sup> his contributions as a theory of economic growth [2]. In particular, soon after the publication of Domar's paper in 1946, the similarities between their formulas (firstly noticed by Schelling, pp. 864-866 [17]) became a sufficient condition to unite the two approaches. Therefore, by the early 1960s, it was a common practice to speak of the "Harrod–Domar model."

### 13.2 Domar's Approach to Economic Dynamics

As Domar himself wrote in the introduction of his 1946 paper [7], his aim was to investigate "the relation between capital accumulation and employment." Defined the productive capacity as the total output produced when all productive factors (labor included) are fully employed, Domar looks for the conditions a growing economy must satisfy to preserve the full employment over time. He pointed out that the growth problem was entirely absent from the Keynesian system, because it was not concerned with changes in the productive capacity. The Keynesian approach dealt with the investment expenditure as an instrument for generating income and disregarded the extremely essential fact that investment also increased the productive capacity [6, pp. 72-73]. The twofold impact of investment in the economic system allowed Domar to identify the tools to derive the conditions under which the economy could grow in a full employment equilibrium. First, the net investment  $I$  increases the productive capacity  $P$ , and second, the change of  $I$  increases the income  $Y$  by means of the Keynesian multiplier.

Domar carried out his analysis on a very abstract and simplified level, so that he defines the potential social average investment productivity as<sup>3</sup>  $\sigma = \frac{\dot{P}}{I}$ , i.e.,

$$\dot{P} = \sigma I. \quad (13.1)$$

Since, by virtue of the Keynesian multiplier,

$$\dot{Y} = \frac{1}{\alpha} \dot{I} \quad (13.2)$$

---

<sup>2</sup>There are few exceptions. Among others, Boianovsky [4], suggested that the Harrod and Domar growth models faced problems of economic instability, not long-term growth.

<sup>3</sup>From now on, a dot over the variable will indicate the operator  $d/dt$  and continuous time assumption.

( $\alpha$  being the marginal propensity to save). The necessary equilibrium condition between productive capacity and aggregate demand leads to

$$\frac{1}{\alpha} \dot{I} = \sigma I \quad (13.3)$$

because  $P = Y \Leftrightarrow \dot{P} = \dot{Y}$ . Assumed that  $\sigma$  and  $\alpha$  are constants, it follows that

$$I(t) = I_0 e^{\alpha\sigma t}. \quad (13.4)$$

Therefore, as long as  $\alpha\sigma$  remains constant, “the maintenance of full employment requires investment to grow at a constant rate” [6, p. 75]. As, by assumption, the equilibrium between productive capacity and income has existed since the time  $t = 0$ , the integration between zero and  $t$  of Eq. (13.2) yields

$$Y(t) = \frac{1}{\alpha} (I_0 e^{\alpha\sigma t} + B) \quad (13.5)$$

because  $\frac{1}{\alpha} I_0 = Y_0$  and  $B = 0$ . The conditions for a steady growth are thus demonstrated.

In the second part of his paper, Domar emphasized the possible disequilibria of the economic system. Probably, this is to account for the dynamic instability of his simple mathematical model. We think that instability was the main element that led to combine Domar’s approach with Harrod’s dynamic theory. However, as we shall see in the next section, the Harrod instability has nothing to do with the mathematical notion of instability characterizing the Domar model.

### 13.3 Harrod’s Approach to Economic Dynamics

Preliminarily, we have to point out that Harrod never formalized his ideas in terms of difference or differential equations. Nevertheless, Harrod (1959, p. 451) [10] acknowledges that there is a similarity between Domar’s work and his own contribution to the theory of a growing economy. This similarity only concerns a potential increase of output (productive capacity) per unit of new investment designed by Domar as  $\sigma$ . Harrod wrote (1959, p. 452) that he considered “how many units of new investment are required . . . to produce an extra unit of output.” In other words, Domar’s  $\sigma$  is equivalent to his capital coefficient  $C_r$ , because  $C_r$  is “valued on the basis that the new investment is no more nor less than that required to produce additional output.”<sup>4</sup> As  $C_r$  deals with a steady rate of growth of income

---

<sup>4</sup>Let us mention that  $C_r$  was denoted by Harrod as  $C$  in his 1939 paper. Specifically, the equivalence is such that  $\sigma = 1/C_r$ .

denoted by Harrod  $G_w = s/C$ , where  $s$  is Domar's  $\alpha$ , the formal identity of the two equilibrium conditions seems to be evident.

Now, we have to point out that this identical result exclusively concerns the equilibrium condition, while it does not entail the equality  $\alpha\sigma = \frac{\dot{I}}{I} = G_w = \frac{\dot{Y}}{Y}$ , which follows from Domar's assumptions. In fact, Harrod (1959, pp. 452-453) clearly wrote, "I make no such assumption . . . . In my equilibrium equation there is no reference, explicit or implicit, to  $\dot{I}$  or  $I$ ." To understand Harrod's viewpoint, we have to recall the process leading to his "fundamental equation" (Harrod, 1939, p. 17).

As said by Harrod, capital goods include both equipment and stock-in-trade, the actual saving in a period is always equal to the increment of the capital stock,

$$S = I = C\dot{Y}, \quad (13.6)$$

where  $S$  is the aggregate saving and  $C$  "the increase in the volume of goods of all kinds ( $I$ ) outstanding at the end over that outstanding at the beginning of the period divided by the increment of production in that same period" (Harrod, 1948, p. 78). Dividing both sides of Eq. (13.6) by  $Y$ , we have

$$\frac{S}{Y} = C \frac{\dot{Y}}{Y} \Rightarrow \frac{S/Y}{C} = \frac{\dot{Y}}{Y} = G, \quad (13.7)$$

i.e., the actual (effective) rate of growth of income. According to the Keynes proposition, saving is necessarily (ex post) equal to investment, but this does not mean that saving will be "equal to ex ante investment . . . , since unwanted accretion or depletions of stocks may occur, or equipment may be found to have been produced in excess of, or short of, requirements" (Harrod, 1939, p. 19). To express the equilibrium of a steady advance, Harrod deduced his fundamental equation

$$G_w = \frac{\widehat{S}/Y}{C_r}, \quad (13.8)$$

where  $G_w$  is the warranted rate of growth (i.e., the rate of growth of production equating ex ante saving and investment),  $C_r$  is the desired capital coefficient (in Harrod's sense), and the expected fraction of income saved  $\widehat{S}/Y$ .<sup>5</sup>

Let us note that both Eqs. (13.7) and (13.8) refer to the average propensity to save that Harrod denotes by  $s$ . This implies that it is not entirely true that Domar's  $\alpha$  is Harrod's  $s$ , unless  $s$  is explicitly assumed to be constant. If this is not the case, the marginal propensity to save may differ from the average. To see the consequence on the steady growth, we can derive the Domar equation from the equilibrium  $S(Y) = I$ . In fact, differentiation of both sides with respect to time yields  $S'\dot{Y} = \dot{I}$ .

<sup>5</sup>Harrod refers to the expected saving in his 1973 book. The symbol  $\widehat{S}$  is introduced by us.

As from Eq. (13.6),  $\dot{Y} = I/C$ , by substitution we get  $\frac{S'}{C} = \frac{\dot{I}}{I}$ , i.e., Eq. (13.2), and from Eq. (13.7), we have  $\frac{S/Y}{C} = \frac{\dot{Y}}{Y}$ . Therefore, if  $S/Y \neq S'$ , then  $\dot{Y}/Y \neq \dot{I}/I$ . To confirm this result, we can define a link between the two rates of growth. Dividing  $\dot{Y}/Y$  by  $\dot{I}/I$ , we get  $\dot{Y}/Y = (1/E_s)\dot{I}/I$ , where  $E_s = S'/(S/Y)$  is the elasticity of saving with respect to income. This coefficient is typically greater than one, so that  $\frac{\dot{Y}}{Y} < \frac{\dot{I}}{I}$ . This happens because, being residual between earnings and consumptions, the aggregate saving has the tendency to vary quicker than income, either in the case the business activity is rising or declining (see [5, 14]). Although the variability of the average propensity to save questions the possibility of a steady growth, we cannot say that this result reflects Harrod's thought. In fact, Harrod prevalently finds his reasoning on the disequilibrium between ex ante and ex post investments. The disequilibrium is the main ingredient of his "instability principle." To understand this principle better, it may be useful to list some specific Harrod's assumptions often neglected by the growth theorists:

- (1) It is crucial to avoid the mistake of considering  $C$  (or  $C_r$ ) as the traditional capital/output ratio or as the technical accelerator coefficient. Harrod (1948, p. 84) explicitly points out that " $C_r$  may not be equal to the capital coefficient in the economy as a whole." Specifically,  $C$  is the ratio of additional goods "of all kinds" (i.e., new equipment and additional stocks) to the production increase carried out at a given period. The mean of  $C_r$  is similar, but unlike  $C$ ,  $C_r$  is the ratio of desired additional goods to the expected production increase based on entrepreneurs' previous expectations. Neither  $C$  nor  $C_r$  may be assumed as constant over time.
- (2) The quantity  $C$  defined by Harrod is measurable and consistent with a stylized fact described by Kaldor [12]: in the long run, the capital/output ratio  $K/Y$  has the tendency to remain constant. Incidentally, let us notice that empirical data suggested by Romer [16] confirm this statement. If we admit that tendency to remain constant means that the capital/output ratio may change inside a bounded interval, so that its average is constant over time, the consistency between  $C$  and  $k = K/Y$  can be easily proved. The differentiation of  $k$  with respect to time yields (after some rearrangement)

$$\dot{k} = \frac{\dot{Y}}{Y} \left( \frac{I}{\dot{Y}} - \frac{K}{Y} \right) = G(C - k). \quad (13.9)$$

From the analytical point of view, this result does not require any particular comment. Given  $G \neq 0$ , the sign of  $\dot{k}$  still depends on the difference  $(C - k)$  that may change over time.

- (3) Equation (13.9) allows us to realize that there is a difference between Harrod's own time scale and the usual notion of long run. Harrod always refers to the "long period" pertaining to the typical industrial trade cycle. The long period is

much less than the long run, and, according to the particular phase of the cycle, meaningful differences between  $C$  and  $k$  are possible. This is because sudden increases or cuts in inventories with respect to a slower change in the productive capacity affect these differences.

Equipped with these assumptions, we can now explain the instability principle. Looking at Eq. (13.9) and following Harrod (1948, p. 81), we can say that it expresses “the conditions in which producers will be content with what they are doing.” This equilibrium condition must be compared with what actually happens to be confirmed. Therefore, Harrod considered Eq. (13.7) and wrote, “the greater  $G$  is, the lower  $C$  will be.” Consequently, if  $G$  has a value above  $G_w$ , “ $C$  will have a value below  $C_r$ .” This implies that “there will be insufficient goods in the pipe-line and/or insufficient equipment.” Therefore, orders will be increased and the production rises. In other words, if the actual growth is above the line of growth consistent with a steady advance, the actual growth rate will further increase. This leads to a new  $C$  that will be further below  $C_r$ . If  $G < G_w$ , the reasoning needs to be reversed. Harrod (1948, p. 86) affirms that this is “an extraordinarily simple and notable demonstration of the instability of an advancing system. Around the line of advance, . . . , centrifugal forces are at work, causing the system to depart further and further from the required line of advance.”

As Harrod did not attempt to build the instability principle in mathematical terms, we think this is the reason why a contradiction emerges in his reasoning, because  $C_r$  seems to be constant. This implies that the gap between  $C$  and  $C_r$  will be always increasing. Really,  $C$  and  $C_r$  are interconnected variables, and the difference between them cannot become explosive.

### 13.4 A Mathematical Foundation of Harrod’s Instability

To give a mathematical foundation to Harrod’s instability, a slight shifting from his definition of the warranted rate of growth is necessary. Since in Harrod’s  $G_w$  there are several ambiguities (see Besomi (1998, pp. 51-53)) [2], we assign to  $G_w$  a practical meaning. In other terms, we interpret this rate of growth as the expected rate of growth founded on the firms’ business forecasts. Following Sportelli [20], we set  $G_w = \frac{\dot{Y}_e}{Y}$ , where  $\dot{Y}_e$  is an expected change of income. Furthermore, according to Harrod’s definition of  $C_r$ , we assume that in every period the firms decide the investment looking at an expected change of demand:

$$I_j = C_r \dot{Y}_e. \quad (13.10)$$

If ex post it turns that the effective change of demand  $\dot{Y}$  is greater than  $\dot{Y}_e$ , then the effective investment will be less than ex ante  $I_j$ , because stocks are below the desired level. This implies that the actual desired coefficient  $C_r$  has become greater

than the actual  $C$ . It follows that, if capacity utilization is near full levels, each firm will decide investments, either to restore stocks levels or to increase (if profitable) its actual productive capacity, to make it consistent with the level of production.

This leads to an increase in  $I$  (at least in inventories only), which will work in its turn for a new  $\dot{Y}$  according to the monotonic multiplier effect. In the course of the period, a new  $C$  will be progressively attained, and, at the same time, as firms are careful to acquire any new information generated by the system to forecast future demand, a new  $Y_e$  will arise. The comparison of this new  $Y_e$  with the perceived current level of demand allows firms to define the actual  $\dot{Y}_e$ . In a period of rising business activity, this value is positive, so that a further amount of investment will be justified. This leads to a new value of  $C_r$ , which will differ from its past value. By virtue of their definition, both  $C$  and  $C_r$  change along the given period. Therefore, if we assume a sequence of periods with  $\dot{Y} > \dot{Y}_e$ , then  $I_j$  will be pushed forward to  $I$ , while  $C_r$  will be pushed ahead of  $C$ . This conclusion allows us to infer that there is a path dependence of  $C_r$  on the difference  $\dot{Y} - \dot{Y}_e$ . The greater this difference is, the more violent the thrust forward of  $C_r$  will be.

It is clear that  $\dot{Y} < \dot{Y}_e$  leads to contrary conclusions. In any case, over a given period, the difference between  $C_r$  and  $C$  never becomes explosive, because the justified investment evolves according to the following derivative:

$$\dot{I}_j = \dot{C}_r \dot{Y}_e + C_r \ddot{Y}_e, \quad (13.11)$$

where the first term on the right-hand side can be interpreted as stock investments filling existing storehouse gap and the latter term as additional goods aimed at restoring actual stock levels to sustain the new  $\dot{Y}_e$  and, eventually, the new equipment required by the change  $\ddot{Y}_e$ . Along the cycle, the sign of  $\ddot{Y}_e$  may be reversed. Sooner or later, this happens, and so the sign of  $\dot{I}_j$  will change. Consequently, the growth of  $C_r$  will slow down initially, and its value will decrease as soon effective investments  $I$  exceed  $I_j$ . Hence, changes in the value of  $C$  (which follows  $C_r$ ) will be bounded over time.

We think that the  $C_r$  path dependence on the difference  $\dot{Y} - \dot{Y}_e$  is the basic component of Harrod's instability principle. Looking at the wide variety of literature inspired by Harrod's dynamic theory, we found only one approach able to give a mathematical foundation to the instability. This is the work by Alexander [1], which received an explicit approval by Harrod (1951, p. 263). The Harrod model described later encloses Alexander's intuitions and takes into account the dynamic link between  $C$  and  $C_r$ . Furthermore, it stresses the interaction between Harrod's three rates of growth (i.e., the actual, warranted, and natural). Discrepancies between these three growth rates are cause and consequence of economic cycles. All this is in accordance with many of Harrod's theses.



## 13.5 Cycles

As already mentioned, Kaldor and Harrod laid down the basis for the modern theory on growth and cycles. In particular, Kaldor suggested that growth depends on income distribution and that the shifts between wages and profits determine the savings ratio. Therefore, an equilibrium is achieved when  $G_n$  (the rate of growth required for a full employment) equates  $G_w$  (the warranted rate of growth).

Keynes argued that in the short run, through the multiplier, more demand (e.g., investments, public spending, and exports) translates into an increase in output. Harrod shares the same opinion regarding the short term, but agrees with Domar about the twofold impact of investment in the economic system. In fact, “he notes that investment not only induces production through the multiplier, but also simultaneously expands capacity. On this basis he shows that investment is sustainable only if it is self-consistent, and for this to hold it must follow a particular growth path which he calls the warranted path” [18]. In other terms, in Harrod’s view, it is the discrepancy between the natural rate of growth ( $G_n$ ), the warranted rate of growth ( $G_w$ ), and the actual one ( $G$ ) that generates instability. This instability could be lessened when the economy is open to foreign trades.

### 13.5.1 Harrod’s Knife-Edge

According to Harrod, “for a country in which  $G_w$  is tending to exceed  $G_n$ , there is by consequence a chronic tendency to depression (because  $G$  cannot exceed  $G_n$ ), a positive value of the balance of trade expressed as a fraction of income (i.e., the net export rate) may be beneficial” [9]. Therefore, Harrod “predicts that incompatibilities between long-term saving and investment opportunity are all but certain to cause prolonged unemployment (which will be structural where  $G_n$  exceeds  $G_w$  and demand deficient where  $G_w$  exceeds  $G_n$ ) with persistent inflation in addition wherever long-term saving is inadequate for the natural rate of growth” [8]. In terms of public policy, “the difficulties may be too great to be dealt with by a mere anti-cycle policy” [11], and hence the government should increase public investment when  $G_w > G_n$  or, conversely, seek to generate more long-term savings when  $G_w < G_n$  (see Figs. 13.1 and 13.2).

### 13.5.2 Discussion

The model we are testing (Sportelli et al. [19]) claims that Harrod’s speculation holds true only for a specific set of parameters and with positive net exports coupled with competitiveness in foreign markets. In those specific conditions, regular cycles in the long period can be achieved. In the following, we list some variables/equations

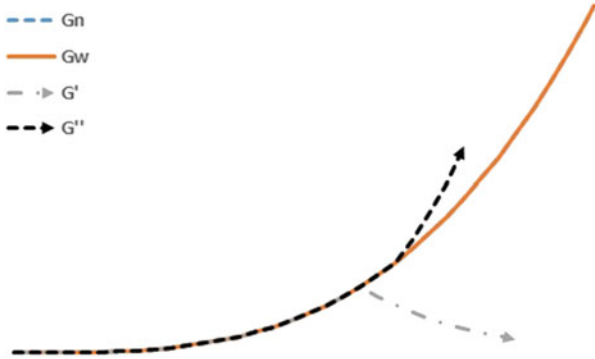


**Fig. 13.1** The Harrod knife-edge denoting an unstable equilibrium. When  $G = G_n = G_w$ , there is sustainable full employment. A departure from this condition may lead to recession ( $G'$ ) or booming periods ( $G''$ )

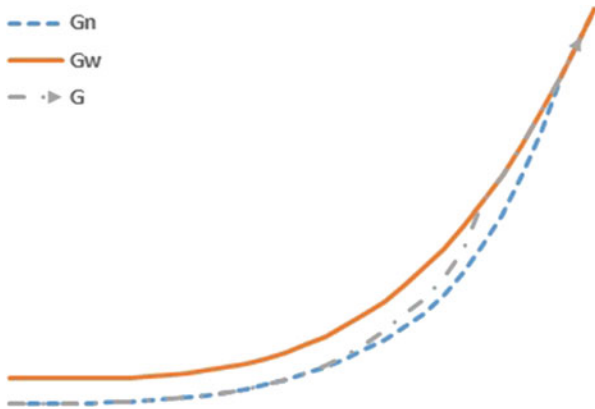


**Fig. 13.2** Supply-side policy to raise the natural growth path. When  $G = G_w > G_n$ , there is a permanent unemployment equilibrium. Policy-makers may employ supply-side policies in order to increase both the actual growth  $G$  and the natural growth  $G_n$

that will be used in the ensuing part where some assumptions will be made and new variables will be identified (Table 13.1).

As in [19], we assume that

- (A) The desired capital is an increasing function  $\Phi$  of the difference between the current and the expected changes of demand, i.e.,

$$C_r = \Phi \left( \frac{\dot{Y} - \dot{Y}_e}{Y} \right) = \Phi (G - G_w) \tag{13.12}$$

such that  $\Phi' > 0$  and  $\Phi(0) = C^* > 1$ , because  $\dot{Y} = \dot{Y}_e$  implies  $I = I_j$ .

**Table 13.1** List of variables in the Harrod model

Variable	Description
$I_j$	Ex-ante investment including both equipment and desired inventory stocks
$I$	Ex-post investment including both equipment and effective inventory stocks
$S$	Ex-post saving
$E$	Exports
$M$	Imports
$X = E - M$	Balance of trade
$Y$	Effective demand
$S/Y = \Sigma$	Share of income saved
$x = X/Y$	Ratio of balance of trade to income (or simply the net export rate)
$I/Y = \Sigma - x$	Share of income invested
$G = \dot{Y}/Y$	Actual rate of growth of domestic income
$Y_e$	Expected demand
$C_r = I_j/\dot{Y}_e$	Desired capital coefficient <sup>note:DesCap</sup>
$C = I_j/\dot{Y}$	Actual capital coefficient <sup>note:AcCap</sup>
$G_w = \dot{Y}_e/Y$	Warranted expected rate of growth of aggregate demand
$G_n$	Technical progress (rate of growth)
$G_f$	Rate of growth of foreign demand
$\phi$	Sensitivity of the difference between actual and warranted relative changes of demand

“The requirement for new capital divided by the increment of output to sustain which the new capital is required” [9]

“The increase in the volume of goods of all kinds outstanding at the end over that outstanding at the beginning of the period divided by the increment of production in the same period” [9]

So that, ex-post, at the equilibrium,  $C_r = C^*$ ,  $I_j = I$ ,  $\Phi(0) = C^* > 1$ , and  $G = G_w$  (or equivalently,  $\dot{Y} = \dot{Y}_e$ ). Denoted  $\phi > 1$  as a reaction parameter representing how sensitive are firms to discrepancies between actual and warranted relative changes of demand, the linearization of (13.12) in  $G - G_w$  can be expressed as

$$C_r = \Phi (G - G_w) = [C^* + \phi(G - G_w)]. \quad (13.13)$$

(B) According to Alexander [1], changes in the growth rate of income depend on the difference between ex-ante and ex-post investments, that is,

$$U = I_j - I = C_r \dot{Y}_e - I, \quad (13.14)$$

so that dividing by  $Y$  and considering that  $I/Y = (S - X)/Y = \Sigma - x$ , the relative gap  $u = U/Y$  can be written as

$$\begin{aligned} u = U/Y &= I_j/Y - I/Y = C_r G_w - (\Sigma - x) \\ &= \Phi (G - G_w) G_w - \Sigma + x. \end{aligned} \quad (13.15)$$

Therefore,  $\dot{G}$  can be expressed as a function  $F$  of  $u$  with  $F$  increasing (resp., decreasing) with  $u$ , and if we assume  $F$  to be linear, we obtain

$$\begin{aligned}\dot{G} &= F(u) = F(\Phi(G - G_w)G_w + \Sigma - x) \\ &= \alpha \{ [C^* + \varphi(G - G_w)]G_w - \Sigma + x \}\end{aligned}\quad (13.16)$$

with  $0 < \alpha < 1$ , because investment changes in the productive capacity make investment sticky.

- (C) The saving rate varies over time depending on unforeseen differences between technical progress and the rate of growth and on income fluctuations:

$$\dot{\Sigma} = \varepsilon(G_n - G_w) + \delta\dot{G}_w, \quad (13.17)$$

where  $\varepsilon$  and  $\delta$  are sensitivity parameters, and the variable  $\dot{G}_w$  describes the economic cycle.

- (D) We set the following Eq. (13.18), where changes in the ratio of the trade balance depend on  $G_f$ ,  $G_n$ , and  $G$  as follows:

$$\frac{\dot{x}}{x} = \Psi(G_f, G_n, G) \quad \text{with} \quad \frac{\partial \Psi}{\partial G_f} > 0, \quad \frac{\partial \Psi}{\partial G_n} > 0 \quad \text{and} \quad \frac{\partial \Psi}{\partial G} < 0. \quad (13.18)$$

We assume that Eq. (13.18) can be rewritten as

$$\frac{\dot{x}}{x} = \Psi(G_f, G_n, G) = (\zeta G_f + \sigma G_n - \mu G - m) \quad (13.19)$$

with  $\zeta, \sigma, \mu > 0$  denoting the sensitivities of the balance of trade to foreign rate of growth, technical progress, and domestic growth rate respectively. We set  $m > 0$  because  $Y(G_f, 0, 0) < 0$ , i.e., a constant domestic production without technical progress has a negative effect on the balance of trade or, equivalently,  $\zeta G_f - m < 0$ .

- (E) The expected rate of change of aggregate demand is defined as an adaptive expectation, i.e.,

$$\dot{G}_w = \gamma(G - G_w), \quad (13.20)$$

where  $\gamma \geq 1$  denotes how quick the expected rate of growth adjusts to the actual growth.

- (F) The dynamics of technological progress is described by a continuous, increasing nonlinear function of share of income saved and devoted to investments:

$$G_n = G_n(\Sigma) = \beta(\xi - \Sigma)\Sigma, \quad \text{with} \quad \beta > 1 \quad \text{and} \quad 0 < \xi < 1. \quad (13.21)$$

Therefore, Harrod's dynamics [19] can be written as

$$\begin{aligned}\dot{G} &= \alpha \{ [C^* + \varphi(G - G_w)] G_w - \Sigma + x \} \\ \dot{\Sigma} &= \varepsilon (G_n - G_w) + \delta \dot{G}_w \\ \dot{x} &= (\zeta G_f + \sigma G_n - \mu G - m) x.\end{aligned}\tag{13.22}$$

By replacing on it Eqs. (13.20) and (13.21), we obtain the following specification we want to test:

$$\begin{aligned}\dot{G} &= \alpha \{ [C^* + \varphi(G - G_w)] G_w - \Sigma + x \} \\ \dot{G}_w &= \gamma (G - G_w) \\ \dot{\Sigma} &= \varepsilon [\beta (\xi - \Sigma) \Sigma - G_w] + \delta \gamma (G - G_w) \\ \dot{x} &= [\zeta G_f + \sigma \beta (\xi - \Sigma) \Sigma - \mu G - m] x,\end{aligned}\tag{13.23}$$

where  $\alpha$ ,  $\gamma$ ,  $\varepsilon$ ,  $\beta$ ,  $\delta$ ,  $\zeta$ ,  $\sigma$ , and  $\mu$  are the parameters that will be calibrated in Chap. 18.

## References

- Alexander, S.S.: Mr. Harrod's dynamic model. *Econ. J.* **60**(240), 724–739 (1950)
- Besomi, D.: Failing to Win Consent: Harrod's Dynamics in the Eyes of His Readers, pp. 38–88. Palgrave Macmillan UK, London (1998)
- Besomi, D., et al.: Introduction to 'an essay in dynamic theory': 1938 draft by Roy F. Harrod. *Hist. Polit. Econ.* **28**, 245–252 (1996)
- Boianovsky, M.: Beyond capital fundamentalism: Harrod, domar and the history of development economics. *Camb. J. Econ.* **42**(2), 477–504 (2018)
- Deaton, A.: Financial policies and saving. In: Klaus Schmidt-Hebbel, J.S., Luis Servén (eds.) *The Economics of Saving and Growth*, chap. 4. Cambridge University Press, Cambridge (1999)
- Domar, E.: *Essays in the Theory of Economic Growth*. Cambridge University Press, New York (1957)
- Domar, E.D.: Capital expansion, rate of growth, and employment. *Econometrica* **14**, 137–147 (1946)
- Eltis, W.: Harrod–Domar Growth Model, pp. 1–5. Palgrave Macmillan, London (2016). [https://doi.org/10.1057/978-1-349-95121-5\\_1267-1](https://doi.org/10.1057/978-1-349-95121-5_1267-1)
- Harrod, R.F.: *Towards a Dynamic Economics: Some Recent Developments of Economic Theory and Their Application to Policy*. MacMillan and Company, London (1948)
- Harrod, R.F.: Domar and dynamic economics. *Eco. J.* **69**(275), 451–464 (1959)
- Harrod, R.F.S.: *Economic Essays*, 2nd edn. Macmillan, London (1972)
- Kaldor, N.: Capital accumulation and economic growth. In: *The Theory of Capital*, pp. 177–222. Springer, Berlin (1961)
- Orlando, G., Della Rossa, F.: An empirical test on Harrod's open economy dynamics. *Mathematics* **7**(6), 524 (2019). <https://doi.org/10.3390/math7060524>
- Piscitelli, L., Sportelli, M.: A simple growth-cycle model displaying sil'nikov chaos. *Econ. Complexity Non-linear Dyn. Multi-Agents Econom. Learn.* **14**, 3–30 (2004)

15. Pugno, M.: Harrod's economic dynamics as a persistent and regime-changing adjustment process. In: *Economic Dynamics, Trade and Growth*, pp. 152–178. Springer, Berlin (1998)
16. Romer, P.: *Capital Accumulation and Long-Term Growth. Modern Business Cycles Theory*. Blackwell, Oxford (1989)
17. Schelling, T.C.: Capital growth and equilibrium. *Am. Econ. Rev.* **37**(5), 864–876 (1947)
18. Shaikh, A.: Economic policy in a growth context: a classical synthesis of Keynes and Harrod. *Metroeconomica* **60**(3), 455–494 (2009). <https://doi.org/10.1111/j.1467-999X.2008.00347.x>
19. Sportelli, M., Celi, G.: A mathematical approach to Harrod's open economy dynamics. *Metroeconomica* **62**(3), 459–493 (2011)
20. Sportelli, M.C.: Dynamic complexity in a Keynesian growth-cycle model involving Harrod's instability. *J. Econ.* **71**(2), 167–198 (2000)

# Chapter 14

## Growth and Cycles as a Struggle: Lotka–Volterra, Goodwin and Phillips



Giuseppe Orlando and Mario Sportelli

### 14.1 Introduction

In the early 1960s, the Phillips work generated many empirical studies of the relationship between the inflation rate and unemployment. In that work, other explanatory variables, not only unemployment, were used to model either wages or price dynamics. However, many papers published in those years did not pay much attention to the evidence suggesting that the Phillips curve was not stable over time.

The breakdown of the empirical Phillips relationship began in the late 1960s with the theoretical works by Phelps [25] and Friedman [14]. According to these authors, workers are rational and take into account the expected price increases. For this reason, Friedman argued that the expectation-augmented Phillips curve would shift in such a way that, in the long run, a higher rate of inflation would not result in any change in unemployment. The price stability is consistent only with a rate of unemployment named by Friedman “natural rate of unemployment.” This rate is determined by the real factors, which affect the amount of frictional and structural unemployment in the economy. On the Keynesian side, inflationary expectations either adjust to past wages and prices or, according to the “new-Keynesian” models of price stickiness, motivate forward-looking inflation expectations [6, 12, 40]. In a series of tests, Rudd and Whelan challenged the validity of those models: e. g. the

---

G. Orlando (✉)

University of Bari, Department of Economics and Finance, Bari, Italy

University of Camerino, School of Sciences and Technology, Camerino, Italy

e-mail: [giuseppe.orlando@uniba.it](mailto:giuseppe.orlando@uniba.it); [giuseppe.orlando@unicam.it](mailto:giuseppe.orlando@unicam.it)

M. Sportelli

University of Bari, Department Mathematics, Bari, Italy

e-mail: [mario.sportelli@uniba.it](mailto:mario.sportelli@uniba.it)

© The Author(s), under exclusive license to Springer Nature Switzerland AG 2021

G. Orlando et al. (eds.), *Non-Linearities in Economics*, Dynamic Modeling

and Econometrics in Economics and Finance 29,

[https://doi.org/10.1007/978-3-030-70982-2\\_14](https://doi.org/10.1007/978-3-030-70982-2_14)

ability of the labor share in a neo-Keynesian version of the Phillips curve to model inflation [31]; the specification of delayed and future inflation (“hybrid” inflation) [29]; the explanatory power of rational sticky price expectations models [30].

The link between the growth, cycles and the Phillips curve was introduced by Goodwin [15] who transformed the conventional labour share model (for a review, see Foley et al. [13]) into a dynamic struggle between capitalists and workers. In fact, while the share between labour and capital could be assumed constant in the long run, it fluctuates in actual economics. The Goodwin model has become a powerful framework able to accommodate extensions in many directions, from the inclusion among the endogenous variables of technical changes [34, 39] to the coupling of Goodwin’s model with the financial instability hypothesis (FIH) by Minsky [16, 23, 36] and from an open economy where the long-term output growth rate is constrained by the balance of payments [9] to the incorporation of elements by Kalecki (investment function independent of savings and mark-up pricing in oligopolistic goods markets) and Marx (the reserve army) [33].

## 14.2 The Phillips Curve

The Phillips curve is a statistical relationship between unemployment and the rate of change of the money wage rate studied by Alban W. Phillips, a New Zealand economist, at the London School of Economics. Published in *Economica* in 1958 [26], the study showed that there was a nonlinear inverse relationship between the annual average percentage rate of unemployment and the annual rate of change of money wage rate:

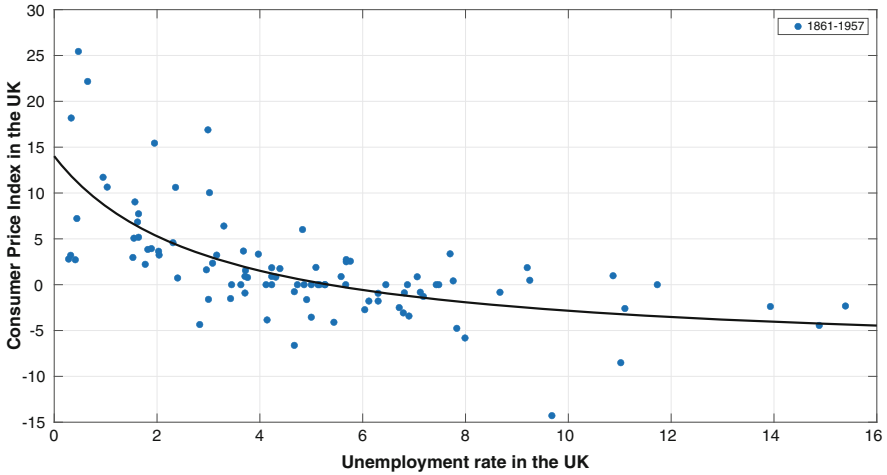
$$\frac{\dot{w}}{w} = f(U) \quad \text{s.t.} \quad f' < 0, \quad (14.1)$$

where  $\dot{w}/w$  is the rate of change of the money wage rate and  $U$  the unemployment. The curve is similar to a hyperbola with horizontal asymptote in the fourth quadrant.

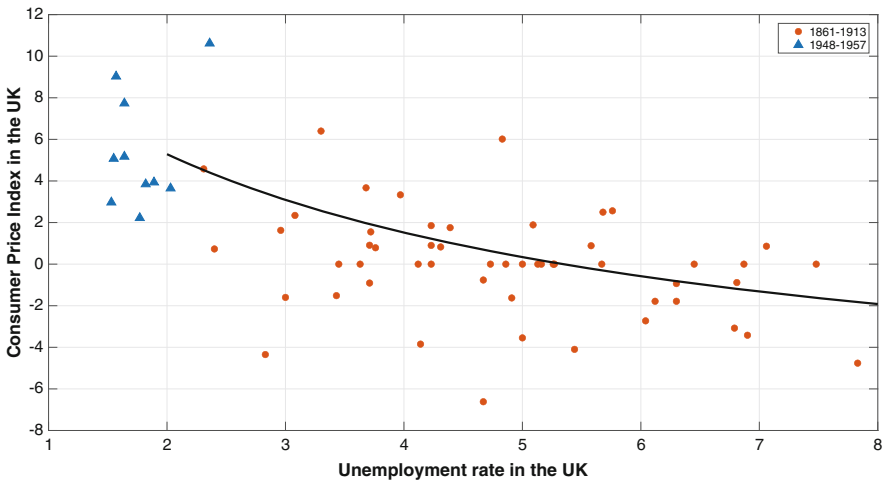
The data used by Phillips were those of UK in 1861–1957. He displayed this relationship by fitting a curve to this data. Since the observations for 1948–1957 lay quite close to the curve fitted for the years 1861–1913, the relationship was thought to be stable and persistent over a long period of time. This was the reason why, in the following years, the Phillips curve played a central role in economic policy decisions to support employment. The use of the curve as an instrument of policy was made possible because, as suggested by Lipsey [19], the curve could be moved from a relationship between  $\dot{w}/w$  and unemployment to one between the rate of change of the price level and unemployment. This is possible both when the markets are assumed perfectly competitive or monopolistic. In the Keynesian framework, the Phillips curve meant that inflation would erode real wages and, thus, boost labour demand.

Figure 14.1 shows the relation between unemployment rate [2] and inflation [1] in the United Kingdom for the whole period studied by Phillips while Fig. 14.2 displays the said relation for the years 1861–1913 and 1948–1947 separately.





**Fig. 14.1** Relation between unemployment rate [2] and inflation [1] in the United Kingdom, 1861-1957.



**Fig. 14.2** Relation between unemployment rate [2] and inflation [1] in the United Kingdom, 1861–1913 (orange dots) and 1948–1947 (blue diamonds).

However, while there might be a relationship between employment and inflation in the short run, Phelps [25] and Friedman [14] argued that such relationship is hard to find in the long run. In particular, Friedman, by giving credit to Samuelson and Solow [32], explained that in the long run, workers and employers negotiate wages by taking into account inflation, so that pay rises increase at rates near anticipated inflation. Given a natural level of employment determined by the characteristics of the economy, an increase of inflation determines a temporary increase of employment. Agents’ expectations play a role in restoring unemployment back to its previous level (how quickly it depends on the context). This process could lead

to stagflation characterized by high inflation and unemployment as experienced in developed economies in 1970s. To prevent stagflation, Friedman suggested that central banks should not set unemployment targets below the natural rate.

A more radical critique to the foundations of Keynesian was made by the rational expectations school led by Robert Lucas and Thomas Sargent which challenged the idea that monetary policy could systematically affect output even in the short run. To those critics, new Keynesian models incorporate rational expectations and assume some price rigidity, i.e., sticky prices. In that context, markets do not clear instantaneously: aggregate output may be below the potential level, and an increase in liquidity can produce a short-run increase in consumption thus boosting output without inflationary consequences. Among others, we mention the paper by Chen et al. [8] in which it is possible to find a baseline disequilibrium AS-AD model empirically calibrated on quarterly time series data of the US economy 1965.1-2001.1. The model exhibits a Phillips curve, a dynamic IS curve and a Taylor interest rate rule. The outcome is “that monetary policy should allow for sufficient steady state inflation in order to avoid stability problems in areas of the phase space where wages are not flexible in a downward direction” [8].

### 14.2.1 Perfectly Competitive Markets

We assume that, in the economy as a whole, labour is the only variable productive factor in the short run. Given the production function  $y = F(L)$  with  $L$  as input, the profit maximization problem of the firm is

$$\max_L \Pi = \max_L (pF(L) - wL), \quad (14.2)$$

where  $\Pi$  is the profit,  $p$  the market price of output  $y$  and  $wL$  the labour cost. The first-order condition  $pF' = w$  requires that the value of the marginal productivity of labour  $F'$  must be equal to his price  $w/p$ . As the marginal productivity is decreasing  $F'' < 0$ , the second-order conditions are satisfied. By setting  $F' = l_m$ , the logarithmic differentiation of the first-order condition with respect to time yields

$$\frac{\dot{p}}{p} = \frac{\dot{w}}{w} - \frac{\dot{l}_m}{l_m}. \quad (14.3)$$

Therefore, by substitution of the Phillips curve, Eq. (14.1), we get

$$\frac{\dot{p}}{p} = f(U) - \frac{\dot{l}_m}{l_m}. \quad (14.4)$$

This means that, in competitive markets, if wages change according to the long-run changes of the marginal productivity of labour, then the average labour cost of produced goods remains unchanged and there will be no price increase in the system.

### 14.2.2 Monopolistic Markets

In this case, the assumption is that firms define the price by means of markup over the average cost of labour

$$p = m \frac{wL}{y} = m \frac{w}{l_a}, \quad (14.5)$$

where  $m$  is the unit markup and  $l_a = y/L$  the average productivity of labour. After the logarithmic differentiation of Eq. (14.5) with respect to time, we still get

$$\frac{\dot{p}}{p} = \frac{\dot{w}}{w} - \frac{\dot{l}_a}{l_a} = f(U) - \frac{\dot{l}_a}{l_a}, \quad (14.6)$$

if the markup is assumed constant. Like the case of competitive markets, the productivity of labour (either marginal or average) plays a role in the price dynamics. Nevertheless, when the markets are not competitive, the market power of the firms cannot be neglected.

### 14.2.3 Calvo Model and New Keynesian Economics

As mentioned in the introduction, new Keynesian economics relies on the reinterpretation of the Phillips curve in terms of forward looking expectations and is based on sticky prices. Among the most influential contributors, we recall Fischer [12], Taylor [40] and Calvo [6].

Because of its simplicity, we use Calvo framework that deals with natural expectations and sticky prices of the new Keynesian economics.

We adopt following notation:

- $z_t$  is the log price at time  $t$ ,
- $\mu$  is the markup over the marginal cost  $mc_t$ ,
- $p_{t+k}^*$  is the log of the optimal price that the firm would set in period  $t+k$  in absence of price rigidity,
- $(1-\theta)^{t+k}$  is the probability for a firm to set its price  $p_{t+k}^*$  in period  $t+k$ ,
- $E_t(z_t - p_{t+k}^*)$  is the expected loss at time  $t$  for a firm that is not able to set the price at  $p_{t+k}^*$ ,
- $0 \leq \beta \leq 1$  is a discount rate,
- $\pi_t = p_t - p_{t-1}$  is the inflation rate.

The loss function for a firm is

$$L(z_t) = \sum_{k=0}^{\infty} (\theta\beta)^k [E_t(z_t - p_{t+k})]^2, \quad (14.7)$$

which implies that all future losses are considered, each one weighted by the discount rate  $\beta$  and the probability  $\theta$ .

Equation (14.7) is minimized by differentiating with respect to the price  $z_t$ :

$$L'(z_t) = 2 \sum_{k=0}^{\infty} (\theta\beta)^k E_t (z_t - p_{t+k}^*) = 0, \quad (14.8)$$

so that

$$\sum_{k=0}^{\infty} (\theta\beta)^k z_t = \sum_{k=0}^{\infty} (\theta\beta)^k E_t (p_{t+k}^*). \quad (14.9)$$

The left-hand side of Eq. (14.9) is

$$\sum_{k=0}^{\infty} (\theta\beta)^k z_t = \frac{z_t}{1 - \theta\beta}, \quad (14.10)$$

and thus

$$\frac{z_t}{1 - \theta\beta} = \sum_{k=0}^{\infty} (\theta\beta)^k E_t (p_{t+k}^*), \quad (14.11)$$

so that

$$z_t = (1 - \theta\beta) \sum_{k=0}^{\infty} (\theta\beta)^k E_t (p_{t+k}^*). \quad (14.12)$$

Note that the second order condition for the minimum is

$$L''(z_t) = 2 \sum_{k=0}^{\infty} (\theta\beta)^k = \frac{2}{(1 - \theta\beta)} > 0 \quad (14.13)$$

which is satisfied because  $\theta$  and  $\beta \in (0, 1)$ . Thus, Eq. (14.12) states that the optimal solution for the firm, in presence of sticky prices, is a weighted average of expected future prices.

Given that firms should set the price as a markup over marginal cost, we may assume that

$$p_{t+k}^* = \mu + mc_{t+k}, \quad (14.14)$$

so the reset price in Eq. (14.12) can be rewritten as

$$z_t = (1 - \theta\beta) \sum_{k=0}^{\infty} (\theta\beta)^k E_t(\mu + mc_{t+k}). \quad (14.15)$$

In general, a first-order stochastic difference equation of type

$$y_t = aE_t(y_{t+1}) + bx_t \quad (14.16)$$

has the following solution:

$$y_t = b \sum_{k=0}^{\infty} a^k E_t(x_{t+k}). \quad (14.17)$$

Eq. 14.15 says that  $z_t$  is the solution of

$$z_t = \theta\beta E_t(z_{t+1}) + (1 - \theta\beta)(\mu + mc_t), \quad (14.18)$$

where  $y_t = z_t$ ,  $x_t = \mu + mc_t$ ,  $a = \theta\beta$  and  $b = 1 - \theta\beta$ .

At the aggregate level, prices are a weighted average of previous prices and current reset prices

$$p_t = \theta p_{t-1} + (1 - \theta)z_t, \quad (14.19)$$

which rearranged is

$$z_t = \frac{1}{1 - \theta}(p_t - \theta p_{t-1}), \quad (14.20)$$

or equivalently

$$\begin{aligned} z_t &= \frac{1}{1 - \theta} \left( (1 - \theta)p_t + \theta p_t - \theta p_{t-1} \right) \\ &= p_t + \frac{\theta}{1 - \theta} (p_t - p_{t-1}) = p_t + \frac{\theta}{1 - \theta} \pi_t \\ z_t &= \frac{1}{1 - \theta} \left( p_t - p_{t-1} + (1 - \theta)p_{t-1} \right) \\ &= \frac{1}{1 - \theta} (p_t - p_{t-1}) + p_{t-1} = \frac{1}{1 - \theta} \pi_t + p_{t-1}. \end{aligned} \quad (14.21)$$

$$\begin{aligned}
p_t + \frac{\theta}{1-\theta}\pi_t &= \theta\beta E_t\left(\frac{1}{1-\theta}\pi_{t+1} + p_t\right) + (1-\theta\beta)(\mu + mc_t) \\
p_t + \frac{\theta}{1-\theta}\pi_t &= \frac{\theta\beta}{1-\theta}E_t(\pi_{t+1}) + \theta\beta p_t + (1-\theta\beta)(\mu + mc_t) \\
\frac{\theta}{1-\theta}\pi_t &= \frac{\theta\beta}{1-\theta}E_t(\pi_{t+1}) + (1-\theta\beta)(\mu + mc_t - p_t).
\end{aligned}$$

So that, by rearranging, we arrive at the *New-Keynesian Phillips curve*

$$\pi_t = \beta E_t(\pi_{t+1}) + \frac{(1-\theta)(1-\beta\theta)}{\theta}(\mu + mc_t - p_t). \quad (14.22)$$

Equation (14.22) states that current prices depend on next period expected inflation rate  $E_t(\pi_{t+1})$  and real marginal costs  $mc_t - p_t$ . As the latter is not observed nor recorded in national accounts, this relationship is hard to test empirically.

### 14.3 Lotka–Volterra Model

The Lotka–Volterra ‘predator–prey’ model describes the interaction between two species: the predator and the prey. This model was initially proposed by Alfred J. Lotka [20], who borrowed from Verhulst the logistic map [43]. Independently, Vito Volterra developed the same equations to explain the dynamics of the fish catches in the Adriatic Sea [44] (cf. for further details Kinoshita [17]).

The assumptions of the model are as follows:

- (a) Preys have access to unlimited food.
- (b) Preys are the unique source of food for predators which, in turn, have limitless appetite.
- (c) The rate of change of both populations is proportional to the size.
- (d) Genetic adaptation and environment changes are not considered.

And the model equations read

$$\begin{aligned}
\frac{dx}{dt} &= \alpha x - \beta xy, \\
\frac{dy}{dt} &= \delta xy - \gamma y,
\end{aligned} \quad (14.23)$$

where

- $x$  is the number of preys,
- $y$  is the number of predators,
- $\alpha$  is the natural growth rate of preys in the absence of predation,
- $\beta$  is the death rate of preys due to predation,

- $\delta x y$  is the natural growth rate of predators or efficiency rate of turning preys into predators,
- $\gamma$  is the natural death rate of predators in the absence of preys.

By dividing the second equation by the first in (14.24), we get

$$\frac{dy}{dx} = -\frac{y}{x} \frac{\delta x - \gamma}{\beta y - \alpha} \quad (14.24)$$

from which integration yields

$$\frac{\beta y - \alpha}{y} dy + \frac{\delta x - \gamma}{x} dx = 0,$$

i.e.,

$$\delta x - \gamma \ln x + \beta y - \alpha \ln y = A,$$

where  $A$  is constant.

## 14.4 The Goodwin Model

Richard M. Goodwin, was one of the first economists to develop a nonlinear model of the business cycle and one of the first pioneers of chaotic dynamics in economics. In his model on the growth cycle [15], Goodwin finds his assumptions on the Harrod intuition that a capitalist economy grows until it arrives near full employment, after which it collapses. To formalize this intuition, that is, the coexistence of growth and cycle in the same model, Goodwin suggests an economic adaptation of the Lotka–Volterra predator–prey system. In contrast to the mainstream approach [7, 11, 35] in which cycles were caused by exogenous shocks, this model had the advantage to explain endogenously output fluctuations together with the ones of employment and wages.

In the framework, we are discussing that the economy produces a single good, workers consume all their wage and capitalists save and invest all their profits. Economic growth rate is positively related to both saving rate and capital share. In fact, as workers do not save, a decrease in the profit share reduces investments and, as a consequence, future output. Thus, during a recession, the lower labour demand brings salaries down and restores the profit share of capitalists (who will again start investing more).

In the Goodwin model and its extensions, when the economy expands, higher labour demand generates wage inflation, so that real wages increase more than labour productivity. This in turn implies that the wage share increases as production increases. So when the economy is expanding, the rigidity of the labor market can increase wages more than productivity, thus reducing investment and growth.

### 14.4.1 Assumptions of Goodwin's Model

The key assumptions of Goodwin, as described in his original work, are

- (a) steady technical progress (disembodied),
- (b) steady growth in the labour force,
- (c) only two factors of production, labour and “capital” (plant and equipment), both homogeneous and non-specific,
- (d) all quantities real and net,
- (e) all wages consumed, all profits saved and invested,
- (f) a constant capital-output ratio,
- (g) a real wage rate that rises in the neighbourhood of full employment.

Caveats in this list are in assumption (e), which could be changed into constant proportional savings without altering the logic of the model, and in assumption (f), which could be softened at the cost of overcomplicating the system. Assumptions (f) and (g) are empirical and disputable.

In the following, we list the symbols that are used in Sect. 14.4.2 and are consistent with Goodwin's original paper:

- (i)  $q$  output,
- (ii)  $k$  capital,
- (iii)  $w$  wage,
- (iv)  $a = a_0 e^{\alpha t}$  labour productivity, where  $\alpha$  is the growth parameter,
- (v)  $s = q/k = 1/\sigma$  capital productivity,
- (vi)  $k/q = \sigma$  capital-output ratio,
- (vii)  $u = w/a$  workers' share of product,
- (viii)  $(1 - w/a)$  capitalists' share of product,
- (ix)  $(1 - w/a)q = \dot{k}$  surplus = profit = savings = investments,
- (x)  $\dot{k}/k = \dot{q}/q = (1 - w/a)/\sigma$  profit rate,
- (xi)  $n = n_0 e^{\beta t}$  labour supply, where  $\beta$  is the growth parameter,
- (xii)  $l = q/a$  employment,
- (xiii)  $v = l/n$  employment rate.

### 14.4.2 Dynamics of Goodwin's Model

The logarithmic differentiation of the employment rate and of the workers' share of product yields, respectively:

$$\begin{aligned} \frac{\dot{v}}{v} &= \frac{\dot{l}}{l} - \frac{\dot{n}}{n} = \frac{\dot{q}}{q} - \alpha - \beta \\ \frac{\dot{u}}{u} &= \frac{\dot{w}}{w} - \alpha, \end{aligned} \tag{14.25}$$



where  $\frac{\dot{w}}{w} = \rho v - \gamma$  is the linearized Phillips curve.

By virtue of notation  $(x)$  the system in Eq. (14.25) becomes

$$\begin{aligned}\dot{v} &= \left[ \frac{1-u}{\sigma} - (\alpha + \beta) \right] v \\ \dot{u} &= [-(\gamma + \alpha) + \rho v] u.\end{aligned}\tag{14.26}$$

At the equilibrium, it must be  $\dot{v} = \dot{u} = 0$ , so the solutions are:  $v = u = 0$  and  $(v^*, u^*)$ , such that

$$\begin{aligned}v^* &= \frac{\gamma + \alpha}{\rho}, \\ u^* &= [1 - (\beta + \alpha)\sigma].\end{aligned}$$

To have economic meaning, Goodwin imposes that  $u^* > 0$ , i.e.  $\frac{1}{\sigma} > (\alpha + \beta)$ .

By means of the linear approximation method near the two equilibria, we get the following Jacobian matrices, respectively:

$$J(0, 0) = \begin{bmatrix} \frac{1}{\sigma} - (\alpha + \beta) & 0 \\ 0 & -(\gamma + \alpha) \end{bmatrix} \quad \text{and} \quad J(v^*, u^*) = \begin{bmatrix} 0 & -\frac{1}{\sigma}v^* \\ \rho u^* & 0 \end{bmatrix}.$$

As  $J_0 = J(0, 0)$  is a diagonal matrix, the eigenvalues are real and of opposite sign, the origin is a saddle point. At the equilibrium point  $(v^*, u^*)$ , the eigenvalues are purely imaginary. Therefore, the fixed point is neutrally stable (or equivalently structurally unstable), and the trajectories are closed orbits. The specific closed orbit where the system will be located depends on the initial condition. We are bound to remind the reader that the system (14.26) is a rare example of integrable system of nonlinear differential equations. The procedure is as follows.

Similarly to the Lotka–Volterra model, let us rewrite the system (14.26) as

$$\begin{aligned}\frac{dv}{dt} &= [s - (\alpha + \beta) - u s] v, \\ \frac{du}{dt} &= [-(\gamma + \alpha) + \rho v] u,\end{aligned}\tag{14.27}$$

and divide the second equation by the first, so that

$$\frac{du}{dv} = \frac{\rho v - \gamma - \alpha}{s - (\alpha + \beta) - u s} \frac{u}{v}$$

or equivalently

$$[s - (\alpha + \beta) - u s] v du + [(\gamma + \alpha) - \rho v] u dv = 0.$$

As the variables are separable, through the division by  $uv$ , we get

$$\left[ \frac{s - (\alpha + \beta)}{u} - s \right] du + \left[ \frac{(\gamma + \alpha)}{v} - \rho \right] dv = 0$$

and integrating

$$\int \left[ \frac{s - (\alpha + \beta)}{u} - s \right] du + \int \left[ \frac{(\gamma + \alpha)}{v} - \rho \right] dv = 0$$

$$\text{i.e. } [s - (\alpha + \beta)] \log u - s u + (\gamma + \alpha) \log v - \rho v = A.$$

It follows that

$$u^{s-(\alpha+\beta)} e^{-s u} v^{\gamma+\alpha} e^{-\rho v} = e^A. \quad (14.28)$$

By setting

$$U = u^{s-(\alpha+\beta)} e^{-s u}, \quad V = v^{-(\gamma+\alpha)} e^{\rho v} \text{ and } B = e^A, \quad (14.29)$$

(14.28) can be rewritten as

$$U(u) = B V(v). \quad (14.30)$$

This equality allows us to obtain the integral curves in the plane  $(v, u)$ . In fact, to each value of the arbitrary constant  $B$ , there is a corresponding integral curve. To draw the integral curves, we have to investigate the shape of the curves  $U$  and  $V$ .

Hence, the curve

- $U$  has a maximum in  $u^*$  because

$$\left. \frac{dU}{du} \right|_{u=u^*} = u^{*,s-(\alpha+\beta)} e^{-s u^*} \left[ \frac{s - (\alpha + \beta)}{u^*} - s \right] = 0$$

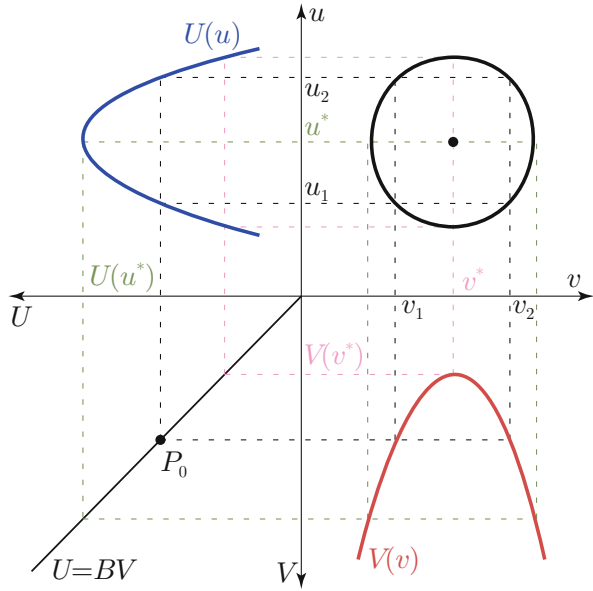
and

$$\left. \frac{d^2 U}{du^2} \right|_{u=u^*} = -U \left[ \frac{s - (\alpha + \beta)}{u^{*,2}} \right] < 0.$$

- $V$  has a minimum in  $v^*$  because

$$\frac{dV}{dv} = v^{-(\gamma+\alpha)} e^{\rho v} \left[ \frac{-(\alpha + \gamma)}{v} + \rho \right] = 0$$

**Fig. 14.3** Graphical proof that system (14.27) displays infinite closed orbits



and

$$\left. \frac{d^2 V}{dv^2} \right|_{v=v^*} = V \left[ \frac{\alpha + \gamma}{v^{*,2}} \right] > 0.$$

Now, we are in position to display the integral curves in Fig. 14.3. In the second and fourth quadrants, we qualitatively report the curves  $U(u)$  (blue) and  $V(v)$  (red) as well as their optima  $u^*$  and  $v^*$ .

Let us now consider a point  $P_0$  satisfying (14.30). This corresponds to choosing a point on the straight line  $U = BV$  in the third quadrant.  $P_0$  can be projected in the second quadrant through the inverse of  $U(u)$  so that points  $u_1$  and  $u_2$  correspond to  $U^{-1}(P_0)$ . Similarly, the inverse mapping  $V^{-1}(P_0)$  identifies points  $v_1$  and  $v_2$  in the fourth quadrant. The projections of the four points in the first quadrant (i.e., the  $(u, v)$  plane) identify the coordinates  $(u_1, v_1)$ ,  $(u_1, v_2)$ ,  $(u_2, v_1)$  and  $(u_2, v_2)$  that satisfy (14.30). Thus, by iterating the process, we can state that the system has a periodic closed orbit corresponding, graphically, to the curve drawn in the  $(u, v)$  plane (first quadrant). Note that, as the choice of the parameter  $B$  is arbitrary, the system has infinitely many periodic closed orbits, around the equilibrium point  $(u^*, v^*)$ .

## 14.5 Kolmogorov Prey–Predator Model

Although the Goodwin model is able to describe persistent oscillations of an economic system, it cannot display structural stability.<sup>1</sup> Many attempts to add this feature were made in the 1970s and the 1980s (e.g., Desai [10] and van der Ploeg [27, 28]). However, despite the use of additional hypotheses, the Goodwin non-trivial equilibrium point remained a centre; if not, it became a stable node or a focus. This type of result is a direct consequence of the structural instability: any small perturbation (as an effect of additional hypotheses) leads to the loss of the cycle. Kolmogorov [18] was the first to raise the problem of structural instability, suggesting a more general version of the predator–prey system as follows:

$$\begin{aligned}\frac{\dot{N}_1}{N_1} &= K_1(N_1, N_2) \\ \frac{\dot{N}_2}{N_2} &= K_2(N_1, N_2),\end{aligned}\tag{14.31}$$

where  $K_1(0, 0) = 0$ ,  $K_2(0, 0) = 0$ ,  $K_1$  and  $K_2$  are continuous functions with continuous first derivatives for all  $N_1$  (the preys) and  $N_2$  (the predators). By imposing some appropriate conditions on  $K_1$  and  $K_2$  the integral curves of system 14.31 are the coordinates displayed in Fig. 14.4.

The isoclines  $K_1 = 0$  and  $K_2 = 0$  divide the first quadrant into four parts (see Fig. 14.4) and the singular points are the origin  $(0, 0)$ ,  $Z = (N_1^*, N_2^*)$  obtained by the intersection of the isoclines  $K_1 = K_2 = 0$  and  $B$  corresponding to  $N_2 = 0$  and  $K_1 = 0$ . Kolmogorov provided the functions  $K_1$  and  $K_2$  with well-founded assumptions in biological theory, and showed that system (14.31) may generate limit cycles when the equilibrium point  $(N_1^*, N_2^*)$  is unstable. As Kolmogorov [18] affirmed, “no integral curve starting in the domain  $N_1 > 0$ ,  $N_2 > 0$  can move asymptotically toward the coordinate axes. In other words, if initially both  $N_1 > 0$  and  $N_2 > 0$ , neither species can completely disappear”. In the classical model, either there is a globally stable equilibrium or there is a globally stable cycle. Other modifications, such as intraspecific competition among prey and predators (e.g., see [24]), confirm the results obtained by Kolmogorov and show that the transition from the globally stable equilibrium to the stable cycle is obtained through non-catastrophic Hopf bifurcations. Contrarily, Tyutyunov et al. [41], by adopting the Patlak–Keller–Segel taxis model for the predator and “assuming that movement velocities of predators are proportional to the gradients of specific cues emitted by prey,” showed that the stationary regime of the model becomes unstable with respect to small perturbations.

---

<sup>1</sup>For a detailed treatment of the subject, see Veneziani et al. [42].

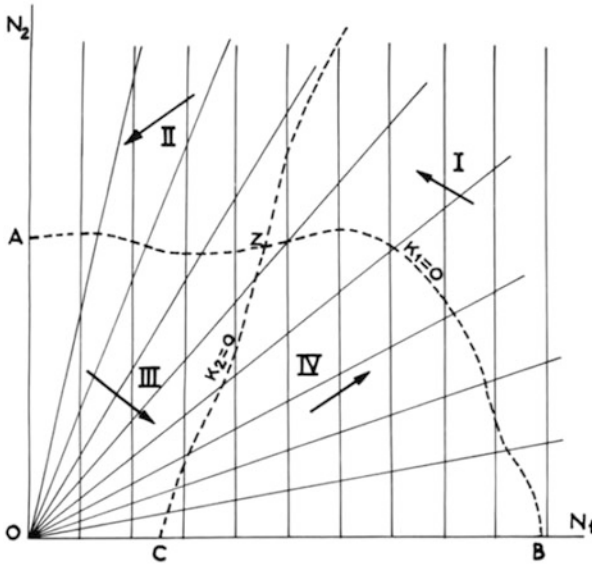


**Fig. 14.4** First quadrant describing the dynamics of prey-predators: in part I (above  $K_1 = 0$  and to the right of  $K_2 = 0$ ) preys decrease and predators increase, in part II (above  $K_1 = 0$  and to the left of  $K_2 = 0$ ) both preys and predators decrease, in part III (below  $K_1 = 0$  and to the left of  $K_2 = 0$ ) preys increase and predators decrease, in part IV (below  $K_1 = 0$  and to the right of  $K_2 = 0$ ) both preys and predators increase. Source [18].

In summary, from a practical standpoint, Kolmogorov’s approach has the merit of emphasizing the analytical properties that a predator–prey system must satisfy, in order to ensure structural stability. Since then, this approach has become a basic landmark for specific predator–prey models in biology and economics. In such models, the existence of stable limit cycles is proved either by the Poincaré–Bendixon theorem or by the Hopf bifurcation theorem.

Among others, see the models by May [21] and Tanner [38] in mathematical biology and Medio [22] and Sportelli [37] for applications to economics. Last but not least, according to the Goodwin model, the wage share should lag behind the employment rate. Moreover, this is not always true in reality, see Fig. 14.5, where wage share ratio (blue line) [3, 5] is not close at all to employment (red line) [4].

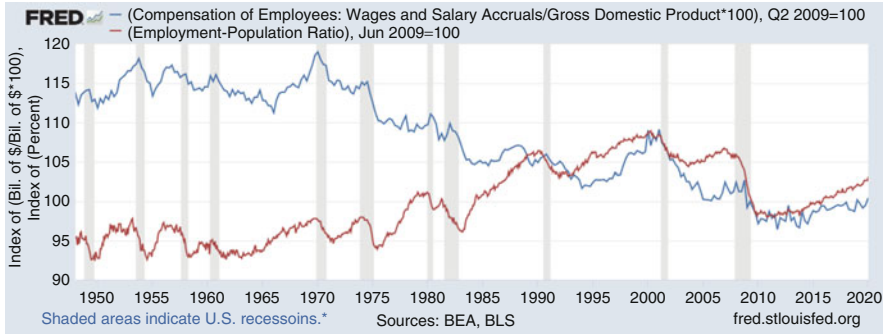


**Fig. 14.5** Blue: compensation of employees: wages and salary accruals/USA GDP \*100), quarterly, seasonally adjusted annual rate. Red: employment-population ratio (percentage), monthly, seasonally adjusted

## References

1. Bank of England: Consumer Price Index in the United Kingdom [CPIUKA], Percent Change, Annual, Not Seasonally Adjusted (2021). <https://fred.stlouisfed.org/series/CPIUKA#0>. Retrieved from FRED, Federal Reserve Bank of St. Louis; November 10, 2021
2. Bank of England: Unemployment Rate in the United Kingdom [UNRTUKA], Percent, Annual, Not Seasonally Adjusted (2021). <https://fred.stlouisfed.org/series/UNRTUKA>. Retrieved from FRED, Federal Reserve Bank of St. Louis; November 10, 2021
3. BEA: Compensation of Employees: Wages and Salary Accruals WASCUR—US. Bureau of Economic Analysis (2020). <https://fred.stlouisfed.org/series/WASCUR>. Retrieved from FRED, Federal Reserve Bank of St. Louis; June 10, 2016
4. BEA: Employment-Population Ratio [EMRATIO]—US. Bureau of Economic Analysis (2020). <https://fred.stlouisfed.org/series/EMRATIO>. Retrieved from FRED, Federal Reserve Bank of St. Louis; June 10, 2016
5. BEA: Gross Domestic Product [GDP]—US. Bureau of Economic Analysis (2020). <https://fred.stlouisfed.org/series/GDP>. Retrieved from FRED, Federal Reserve Bank of St. Louis; June 10, 2016
6. Calvo, G.A.: Staggered prices in a utility-maximizing framework. *J. Monet. Econ.* **12**(3), 383–398 (1983)
7. Chatterjee, S., et al.: From cycles to shocks: Progress in business cycle theory. *Bus. Rev.* **3**, 27–37 (2000)
8. Chen, P., Chiarella, C., Flaschel, P., Semmler, W.: Keynesian macrodynamics and the phillips curve: An estimated model for the US economy. *Contrib. Econ. Anal.* **277**, 229–284 (2006)
9. Dávila-Fernández, M.J., Libânio, G.A.: Goodwin cycles and the BoPC growth paradigm: A macrodynamic model of growth and fluctuations. *Economia* **17**(3), 324–339 (2016)
10. Desai, M.: Growth cycles and inflation in a model of the class struggle. *J. Econ. Theory* **6**(6), 527–545 (1973)
11. Drautzburg, T. et al.: Why are recessions so hard to predict? Random shocks and business cycles. *Econ. Insights* **4**(1), 1–8 (2019)
12. Fischer, S.: Long-term contracts, rational expectations, and the optimal money supply rule. *J. Polit. Econ.* **85**(1), 191–205 (1977)
13. Foley, D.K., Michl, T.R., Tavani, D.: *Growth and Distribution*. Harvard University Press, Harvard (2019)
14. Friedman, M.: The role of monetary policy. *Am. Econ. Rev.* **58**, 102–110 (1968)

15. Goodwin, R.M.: A growth cycle. In: Feinstein, C.H. and Dobb, M. (eds.) *Socialism, capitalism & economic growth*. Cambridge University Press (1967)
16. Grasselli, M.R., Lima, B.C.: An analysis of the Keen model for credit expansion, asset price bubbles and financial fragility. *Math. Financ. Econ.* **6**(3), 191–210 (2012)
17. Kinoshita, S.: 1—Introduction to nonequilibrium phenomena. In: Kinoshita, S. (ed.) *Pattern Formations and Oscillatory Phenomena*, pp. 1 – 59. Elsevier, Boston (2013). <https://doi.org/10.1016/B978-0-12-397014-5.00001-8>
18. Kolmogorov, A.N.: On Volterra’s Theory of the Struggle for Existence, pp. 287–292. Springer, Berlin (2013)
19. Lipsey, R.G.: The relation between unemployment and the rate of change of money wage rates in the United Kingdom, 1862–1957: a further analysis. *Economica* **27**, 1–31 (1960)
20. Lotka, A.: *Elements of Physical Biology*. Williams and Wilkins, Baltimore (1925)
21. May, R.M.: Simple mathematical models with very complicated dynamics. *Nature* **261**(5560), 459–467 (1976)
22. Medio, A.: A classical model of business cycles. In: Nell, E.J. (ed.) *Growth, Profits and Property: Essays in the Revival of Political Economy*, pp. 173–186. Cambridge (1980)
23. Minsky, H.P., Kaufman, H.: *Stabilizing an Unstable Economy*, vol. 1. McGraw-Hill, New York (2008)
24. Muratori, S., Rinaldi, S.: Limit cycles and Hopf bifurcations in a Kolmogorov type system. *Mod. Identif. Control* **10**(2), 91 (1989)
25. Phelps, E.S.: Phillips curves, expectations of inflation and optimal unemployment over time. *Economica* **34**, 254–281 (1967)
26. Phillips, A.W.: The relation between unemployment and the rate of change of money wage rates in the United Kingdom, 1861–1957. *Economica* **25**(100), 283–299 (1958)
27. van der Ploeg, F.: Economic growth and conflict over the distribution of income. *J. Econ. Dyn. Control* **6**, 253–279 (1983)
28. van der Ploeg, F.: Predator-prey and neo-classical models of cyclical growth. *J. Econ. Z. Nazionale* **43**, 235 (1983)
29. Rudd, J., Whelan, K.: New tests of the New-Keynesian Phillips Curve. *J. Monet. Econ.* **52**(6), 1167–1181 (2005)
30. Rudd, J., Whelan, K.: Can rational expectations sticky-price models explain inflation dynamics? *Am. Econ. Rev.* **96**(1), 303–320 (2006)
31. Rudd, J.B., Whelan, K.: Does labor’s share drive inflation? *J. Money Credit Banking* **37**(2), 297–312 (2005)
32. Samuelson, P.A., Solow, R.M.: Analytical aspects of anti-inflation policy. *Am. Econ. Rev.* **50**(2), 177–194 (1960)
33. Sasaki, H.: Cyclical growth in a Goodwin–Kalecki–Marx model. *J. Econ.* **108**(2), 145–171 (2013)
34. Shah, A., Desai, M.: Growth cycles with induced technical change. *Econ. J.* **91**(364), 1006–1010 (1981)
35. Slutsky, E.: The summation of random causes as the source of cyclic processes. *Econometrica* **5**, 105–146 (1937)
36. Sordi, S., Vercelli, A.: Unemployment, income distribution and debt-financed investment in a growth cycle model. *J. Econ. Dyn. Control* **48**, 325–348 (2014)
37. Sportelli, M.C.: A Kolmogoroff generalized predator-prey model of Goodwin’s growth cycle. *J. Econ.* **61**(1), 35–64 (1995)
38. Tanner, J.T.: The stability and the intrinsic growth rates of prey and predator populations. *Ecology* **56**(4), 855–867 (1975)
39. Tavani, D., Zamparelli, L.: Growth, income distribution, and the ‘entrepreneurial state’. *J. Evol. Econ.* **30**(1), 117–141 (2020)
40. Taylor, J.B.: Staggered wage setting in a macro model. *Am. Econ. Rev.* **69**(2), 108–113 (1979)

41. Tyutyunov, Y.V., Titova, L.I., Senina, I.N.: Prey-taxis destabilizes homogeneous stationary state in spatial gause–kolmogorov-type model for predator–prey system. *Ecol. Complexity* **31**, 170–180 (2017)
42. Veneziani, R., Mohun, S.: Structural stability and Goodwin’s growth cycle. *Struct. Change Econ. Dyn.* **17**(4), 437–451 (2006)
43. Verhulst, P.F.: Notice sur la loi que la population suit dans son accroissement. *Correspondence Math. Phys.* **10**, 113–126 (1838)
44. Volterra, V.: Variations and fluctuations of population size in coexisting animal species. In: *Applicable Mathematics of Nonphysical Phenomena I*. Elis Hortwood, New York (1982)



# Chapter 15

## Stable Periodic Economic Cycles from Controlling



Ruedi Stoop

### 15.1 Introduction into Control Fundamentals

The emergence of periodic economic cycles in western economies is a ubiquitous undesired, puzzling and still poorly understood, observation. Even against the large noise component in the data, a relatively simple spectral analysis suggests the presence of different periodic components. Among the most remarkable cycles in the annual GDP growth rates, the Kitchin [19], the Juglar [16], and, less prominent, the Kuznets [22] cycles stand out. As economic booms and bouts affect modern societies with a strong and direct impact on individual biographies, there have been considerable efforts to prevent them or at least to smoothen their effects. Until the 1970s, as the legacy of Keynes [18], cycles were regarded as primarily due to variations in demand (company investments and household consumptions). Unfortunately, this theory offered very little explanation for the observed wavelength of the periodicities. Despite, under its influence, economic analysis focused on monetary and fiscal measures to offset demand shocks. During the 1970s, it became obvious that stabilisation policies based on this theory failed. Shocks on the supply side, in the form of rising oil prices and declining productivity growth, emerged to be equally crucial for the generation of cycles. In 1982, Kydland and Prescott [23] finally offered new approaches to the control of macroeconomic developments. One of their conclusions was that the control should be kept constant throughout a cycle, in order to minimise negative effects.

The remarkable stability of the observed oscillatory behaviour shown in resisting not only against all occurred technological transformations but even against all the attempts to eliminate them, points to a simple, fundamental origin of the

---

R. Stoop (✉)

Institute of Neuroinformatics, ETHZ/University of Zürich, Zürich, Switzerland  
e-mail: [ruedi@ini.phys.ethz.ch](mailto:ruedi@ini.phys.ethz.ch)

phenomenon. It also nourishes the hope that if the origin of the phenomenon could be understood, this insight might be used to engineer towards a softer course of the oscillations. An extreme form of this approach was already taken in the former socialist countries by following the Marxist [26] interpretation of economy, leading to the centrally planned economies. To deal with this problem in democratic societies, it is, however, necessary to be able to communicate a sufficiently simple optimality policy. For this, an understanding of the fundamental nature of the phenomenon and of the response that can be expected from control attempts is necessary. For this, simple models may provide important guidelines [24].

Stability of the oscillations with cycles of nearly doubled wavelength from Kitchin, to Juglar, to Kuznets (roughly 4, 8, and 16 years, the last obviously to be taken with a grain of salt) suggests that the prediction problem of economics might closely be related to chaotic processes. Although the question to which extent real economies can be classified as chaotic can readily be disputed, low-dimensional chaotic models might yield insight into the mechanisms that rule economics and how economics respond to control policies. In particular, for chaotic processes, strategies of control and for prediction have been developed that offer to be adapted for economics. Note that already in early implementations of optimal control programs, it was found that control mechanisms themselves may induce chaotic behaviour [6, 7, 28] and render optimal control impossible. As a general mechanism inherent in many of these examples, chaos is induced by a preference function that depends on past experience. This delay mechanism naturally makes a dynamical system infinite-dimensional, which has the tendency of resulting in a chaotic behaviour. Despite these insights, the quest for a fundamental simple dynamical model for economic cycles is still open.

A connected and very natural goal in economics is the desire to control economic behaviour, in particular when economics develop wave-like fluctuation tendencies. We shall suppose in the following that we are given a ‘temporally stable’ system—meaning by this that we have a behaviour following fixed equations of dynamics, at least over a considered time span, be them periodic or chaotic. That equations may change, expressed in a dependence of system parameters, may be reasonable to assume, but only beyond a relatively long time span compared to the time horizon needed to establish and to maintain control. Getting control over a dynamical systems into a desired system behaviour can be achieved by the so-called control algorithms.

## 15.2 Problem Setting

In chaotic systems, all trajectories are unstable. The aim of chaos control is to stabilise chosen natural trajectories, using additional control structures, in order to render them robust against external perturbations from a large interval of perturbation strength. In the *Handbook of Chaos Control*, Schuster 1999, the interested reader

will find the following passage from the excellent introductory article by Lai and Grebogi:

Besides the occurrence of chaos in a large variety of natural processes, chaos may also occur because one may wish to design a physical, biological or chemical experiment, or to project an industrial plant, to behave in a chaotic manner.

In many-particle systems, often the collective behavior is more ordered than the individual behavior (e.g., in biology (neurons, flocks of animals), economics, etc.), so that hidden control mechanisms seem to be at work. From a similar perspective, if a system request is to be able to respond with selectable periodic behavior, it may be simpler to build first a chaotic system and then to exploit control mechanisms to produce the desired response. To identify the control mechanisms and, in particular, to stabilise the desired simpler behaviours, is the task of chaos control. To realise the full power of this concept, one has to remark that chaos control is also applicable to systems that are not inherently chaotic. The only difference here is that if control is abandoned, the trajectories will settle on the stable solution instead of a chaotic solution in the former case. In what follows, we will provide such examples.

A remarkable illustration of this concept is *gait-control*, i.e., the control of the motion pattern displayed by living systems. It is well-known that animals (amphibia, horses, even humans) change their gait depending on the environmental conditions. Depending on the weight a human is carrying and on the roughness or steepness of the environment, humans dance, march, set on foot after another, etc. It is similarly imaginable that horses have an essentially chaotic gait generator that is controlled by environment, by body weight (changing with age), and by the rider on the horseback, to change from trot, gallop, backward motion, etc. A similar simple control can be expected to be at work in macroeconomics, which is the major theme in this chapter. In principle, on a more general level, chaos control is the resurrection of the old classical problem of the control of a dynamical system seen under a novel angle. In the following, we provide a short overview of chaos control, before we focus on one particular control mechanism where we explore its relevance in the context of economics.

We may distinguish five groups of control mechanisms.

- (1) OGY-parametric control
- (2) Local stabilisation control
- (3) Delay-coordinate control
- (4) Feedback control
- (5) Limiter control

Below we will present but an introductory outline of these methods mostly using 1-d iterated map applications; for a broader and deeper view on this subject we may, e.g., recommend Ref. [35] to the reader. Throughout Sect. 15.2, we will use the letter  $a$  to denote the monitored system parameter [43].

### 1. Parametric Control

This most popular control method was put forward by E. Ott, C. Grebogi and J.E Yorke around 1990 (the ‘OGY’- method [30]). Let us expose the working principle first in dimension one, using the quadratic parabola  $f : x_{n+1} = a_0 x_n (x_n - 1)$  as the example, and let us consider, to start with, an unstable periodic orbit  $\{x(1), x(2), \dots, x(n)\}$  of period  $n$ . Because of the orbits’ instability, after  $i$  iterations, the real orbit  $x_i$  will not coincide with the ‘ideal’ point  $x(i)$ . We thus have

$$\begin{aligned} x_{i+1} - x(i+1) &\approx \frac{\partial f}{\partial x} \Big|_{x=x(i), a=a_0} (x_i - x(i)) + \frac{\partial f}{\partial a} \Big|_{x=x(i), a=a_0} \Delta a_i \\ &= a_0(1 - 2x(i))(x_i - x(i)) + x(i)(1 - x(i))\Delta a_i. \end{aligned}$$

If we want  $x_{i+1}$  to stay ultimately close in a neighbourhood of  $x(i+1)$ , we should have  $|x(i+1) - x_{i+1}| \approx 0$ . From this it follows that we need to choose

$$\Delta a_i = a_0 \frac{(2x(i) - 1)(x_i - x(i))}{x(i)(1 - x(i))}.$$

In higher dimensions, we have

$$\mathbf{x}_{i+1} = \mathbf{F}(\mathbf{x}_i, a),$$

where  $a$  again denotes an external parameter. Similarly to above we will have

$$\begin{aligned} \mathbf{x}_{i+1} - \mathbf{x}(i+1)(a_0) &\approx \mathbf{D}_x \mathbf{F}(\mathbf{x}, a) \Big|_{\mathbf{x}(i)(a_0), a_0} (\mathbf{x}_i - \mathbf{x}(i)(a_0)) \\ &\quad + \mathbf{D}_a \mathbf{F}(\mathbf{x}, a) \Big|_{\mathbf{x}(i)(a_0), a_0} (a - a_0). \end{aligned}$$

From the first contribution we obtain a  $n \times n$ -matrix applied to a vector of dimension  $n$ , and from the second contribution we get a vector of length  $n$ . Using the ansatz

$$a - a_0 \approx -\mathbf{K}^T (\mathbf{x}_i - \mathbf{x}(i)(a_0)),$$

to render the behaviour at  $\mathbf{x}(i)(a)$  stable, the  $1 \times n$  Matrix  $\mathbf{K}^T$  needs to be modified accordingly. This goal is achieved if

$$\begin{aligned} &(\mathbf{x}_{i+1} - \mathbf{x}(i)(a_0)) \\ &= (\mathbf{D}_x \mathbf{F}(\mathbf{x}, a) \Big|_{\mathbf{x}(i)(a_0), a_0} - \mathbf{D}_a \mathbf{F}(\mathbf{x}, a) \Big|_{\mathbf{x}(i)(a_0), a_0} \mathbf{K}^T) (\mathbf{x}_i - \mathbf{x}(i)(a_0)) \\ &=: \mathbf{J} (\mathbf{x}_i - \mathbf{x}(i)(a_0)) (\mathbf{x}_i - \mathbf{x}(i)(a_0)) \end{aligned}$$

is asymptotically stable, which is the case if all eigenvalues of the  $n \times n$  matrix  $\mathbf{J}$  are of absolute size smaller than unity.

For the two-dimensional dissipative Hénon map written in the form  $\mathbf{F} : \{x, y\} \rightarrow \{a + by - x^2, x\}$  we obtain for the period-1 orbit  $\{x_1, y_1\}$   $\mathbf{D}_x \mathbf{F} = \begin{pmatrix} -2x_1 & b \\ 1 & 0 \end{pmatrix}$ , with eigenvalues  $\mu_{s/u} = -x_1 \pm (b + x_1^2)^{1/2}$  and eigenvectors  $\{\mu_{s/u}, 1\}$  and  $\mathbf{D}_a \mathbf{F} = (1, 0)$ . Hence, the control matrix obtains the form  $\mathbf{K} = \begin{pmatrix} -2x_1 - k_1 & b - k_2 \\ 1 & 0 \end{pmatrix}$ .

The determination of the control matrix  $\mathbf{K}$  so that all eigenvalues are of absolute size smaller than unity is a well-known procedure in control theory (called ‘pole placement’). The OGY-method chooses to set the unstable eigenvalues of the matrix  $\mathbf{K}^T$  to zero while letting the stable eigenvalues unchanged. The consequence of this is that after control has been switched on, the trajectories approach the fixed point of the periodic orbit along its stable manifold (in principle, also other, less natural, choices are possible).

More generally, let for parametric control  $a_0$  be the parameter value at which an orbit should be stabilised. Then we may write

$$\begin{aligned} \mathbf{x}_{i+1} - \mathbf{x}(i+1)(a_0) &\approx \mathbf{DF}(\mathbf{x}(i)(a), a)(\mathbf{x}_i - \mathbf{x}(i)(a_0)) \\ &\approx \mathbf{D}_x \mathbf{F}(\mathbf{x}(i))|_{\mathbf{x}(i)=\mathbf{x}(i)(a_0)}(\mathbf{x}_i - \mathbf{x}(i)(a_0)) \\ &\quad + \mathbf{D}_a \mathbf{D}_{\mathbf{x}(i)} \mathbf{F}(\mathbf{x}(i)(a), a)|_{a=a_0} \Delta a_i. \end{aligned}$$

From this we get

$$\mathbf{x}_{i+1} - \mathbf{x}(i+1)(a_0) \approx \mathbf{g} \Delta a_i + \mathbf{DF}(\mathbf{x}(i)(a_0))(\mathbf{x}_i - \mathbf{x}(i)(a_0) - \mathbf{g} \Delta a_i),$$

where  $\mathbf{g} = \frac{\partial \mathbf{x}(i)(a)}{\partial a}|_{a=a_0} \approx \frac{\mathbf{x}(i)(a) - \mathbf{x}(i)(a_0)}{\Delta a_i}$ . Let  $\{\mathbf{f}_i\}$ ,  $i = 1, \dots, n$  denote the contravariant vector basis to the eigenvectors  $\{\mathbf{e}_1, \dots, \mathbf{e}_n\}$  ( $\mathbf{f}_j \mathbf{e}_i = \delta_{ji}$ ). Then we have

$$\mathbf{D}_x \mathbf{F}(\mathbf{x}(i)(a_0)) = \mu_u \mathbf{e}_u \mathbf{f}_u + \mu_s \mathbf{e}_s \mathbf{f}_s,$$

where  $\mu_{u,s}$  describes the unstable/stable eigenvalues. From this we get

$$\mathbf{f}_u(\mathbf{x}_{i+1} - \mathbf{x}(i)(a_0)) = 0,$$

which implies

$$\mathbf{f}_u(\mathbf{g} \Delta a_i + \mathbf{DF}(\mathbf{x}(i)(a_0))(\mathbf{x}_i - \mathbf{x}(i)(a_0) - \mathbf{g} \Delta a_i)) = 0.$$

As a consequence, we obtain

$$\mathbf{g} \Delta a_i \approx \mathbf{DF}(\mathbf{x}(i)(a_0))(\mathbf{x}_i - \mathbf{x}(i)(a_0)) - \mathbf{g} \Delta a_i,$$

which implies that, at time  $i$ , we need to choose the parametric control

$$\Delta a_i \approx \frac{\mathbf{D}_x \mathbf{F}(\mathbf{x}(i)(a_0))(\mathbf{x}_i - \mathbf{x}(i)(a_0))}{\mathbf{g}(\mathbf{Id} - \mathbf{D}_x \mathbf{F}(\mathbf{x}(i)(a_0)))},$$

or, expressed in terms of stable/unstable manifolds, we need to take

$$\Delta a_i \approx \frac{\mathbf{f}_u \mu_u (\mathbf{x}_i - \mathbf{x}(i)(a_0))}{\mathbf{g}(1 - \mu_u) \mathbf{f}_u}. \quad (15.1)$$

From a general point of view, this control only makes sense if the actual orbits are already in the neighbourhood of the orbit that we want to control, which may, in particular initially, take a substantial consumption of time. To speed the process up, targeting algorithms have been designed.

### Control Time

The time needed to control on a chosen orbit (called ‘control time’) is of particular interest in applications. For the chosen control strategy, in dimension  $d = 1$ , the ansatz

$$\langle \tau \rangle \sim \delta^{-\gamma}$$

defines the corresponding scaling exponent  $\gamma > 0$ . From

$$P(\varepsilon, x(i)) = \int_{x(i)-\varepsilon}^{x(i)+\varepsilon} \rho(x(i)) dx \approx 2\varepsilon \rho(x(i)),$$

we get

$$\langle \tau \rangle = \frac{1}{\rho(\varepsilon)} \sim \varepsilon^{-1} = \delta^1,$$

from which one concludes that  $\gamma = 1$ .

In higher dimensions, matters become substantially more complicated. For a class of  $2d$ -maps, the exponent becomes [33]

$$\gamma = 1 + \frac{\ln |\mu_u|}{2 \ln(1/|\mu_s|)}.$$

Control of the dissipative Hénon map, using easy to read elementary Mathematica code, is achieved as follows:

```
(* Set the parameters *)
a=2.1;b=-0.3;
(* Defines the Henon map *)
Henon[{x_,y_}]:={a-x^2+b y,x};
```

```

(* Defines the Jacobian for the Henon map *)
Jacobi[{x_,y_}]={D[Henon[{x,y}][[1]],x],D[Henon[{x,y}][[1]],y]},
  {D[Henon[{x,y}][[2]],x],D[Henon[{x,y}][[2]],y]}};
(* Set the initial point {0.2,1.4} and iterates the Henon map 10001 times *)
p=Nest[Henon,{0.2,1.4},10001];
(* Calculates the eigenvectors of the Jacobian for each iteration *)
v=Eigenvectors[Jacobi[p]];
(* Iterates the Henon map 5 times and stores the results in Henonp *)
perio=5;Henonp[{x_,y_}]:=Nest[Henon,{x,y},perio];
(* Defines the controlled Henon map *)
Hencon[pp_]:=
(* Computes the module for the variables *)
Module[{xn, xn1, h, c, v, u, eiv, hh},
(* Computes the module for the variables *)
  eiv = Eigenvalues[Jacobi[pp]]; h = Max[Abs[eiv]]; hh = 0;
(* If the first max eigenvalue is positive set hh=1 otherwise set hh=-1 *)
  If[h == eiv[[1]], hh = 1,]; If[h == -eiv[[1]], hh = -1,];
(* If the second max eigenvalue is positive set hh=1 otherwise set hh=-1 *)
  If[h == eiv[[2]], hh = 1,]; If[h == -eiv[[2]], hh = -1,];
  Print["h=", h, " _eiv=", eiv, " _hh=", hh];
(* Iterates the Henon map 5 times and stores the results in Henonp *)
  xn1= Henonp[pp];
(* Computes the control as described in Eq. (15.1) *)
  c = ((xn1 - pp)/h)*hh;
% (* v = Eigenvectors[Jacobi[pp]][[2]];*)
  xn = pp - c ;
  Print["x=", pp, " _xn=", xn, " _h=", h, " _c=", c];
  Return[xn]]

```

## 2. Local Stabilisation Control

We return to the one-dimensional case. Let  $\varepsilon$  be the error made after running through a ‘quasiperiod’ (an imprecise orbit) of length  $n$ . This error will, after additional  $t = n$  time steps, grow to

$$\varepsilon' = \varepsilon \prod_{i=1}^n |f'(x_i)|.$$

This implies that the value of  $x_i$  should be corrected by

$$c = \frac{c'}{\prod_{i=1}^n |f'(x_i)|}$$

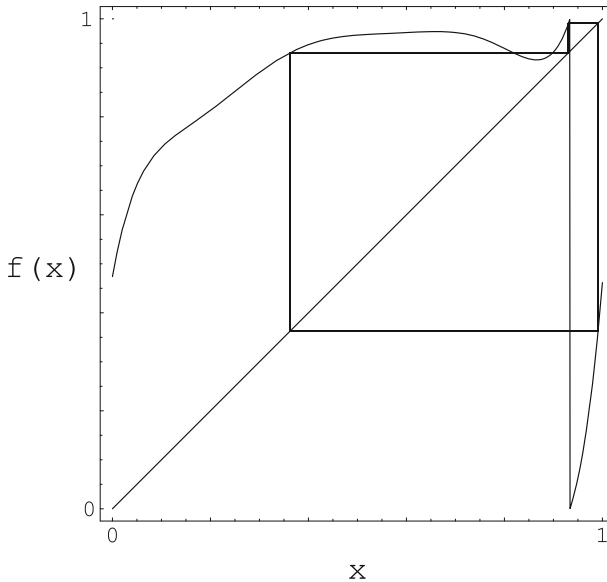


**Fig. 15.1** Stabilised period 3 in the chaotic regime of the inhibitory interaction to pyramidal neurons. The numerical function was extracted from experimentally measured phase response curves (cf. [41])

to stabilise the original orbit (see Fig. 15.1 for an illustration). For higher-dimensional systems, the same procedure can be followed, where the correction has to be applied in the direction of the unstable manifold.

This method can be seen as a variant of the parametric control using a particularly simple control parameter. Control is achieved by means of a change of the slope in the orbit point by the increase of the  $y$ -coordinate by a value of  $c$ :

Control of neural interaction map  $f(x)$  in the stable period 2 regime on a period 3 (see Fig. 15.2):

```
f[x_] := Mod[x + o - (0.986115480593817 - 4.68999548957753*x +
49.50892515516324*x^2 - 247.7425851646342*x^3 +
668.4931471006396*x^4 - 979.050342184131*x^5 +
735.4280170792417*x^6 - 221.9348783929893*x^7), 1];
g[x_] := x + o - (0.986115480593817 - 4.68999548957753*x +
49.50892515516324*x^2 - 247.7425851646342*x^3 +
668.4931471006396*x^4 - 979.050342184131*x^5 +
735.4280170792417*x^6 - 221.9348783929893*x^7);
perio = 3;
fcon[x_] := Module[{xn, xn1},
b = Evaluate[g'[NestList[f, x, perio]]]; h = 1;
Do[h *= b[[i]], {i, 1, perio}]; xn1 = Nest[f, x, perio];
c = (xn1 - x)/h; xn = x - c;
Return[xn]]
```



**Fig. 15.2** Stabilised period 3 for the inhibitory chaotic neural interaction function

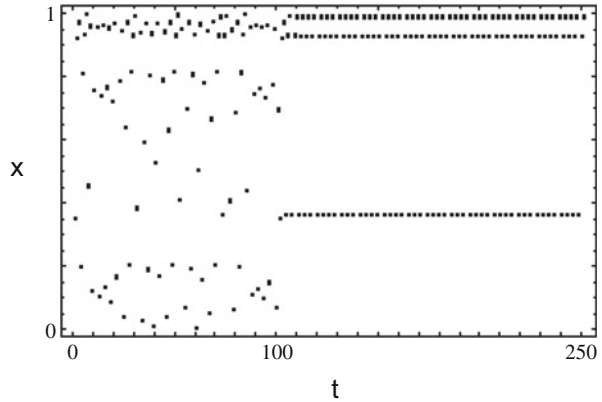
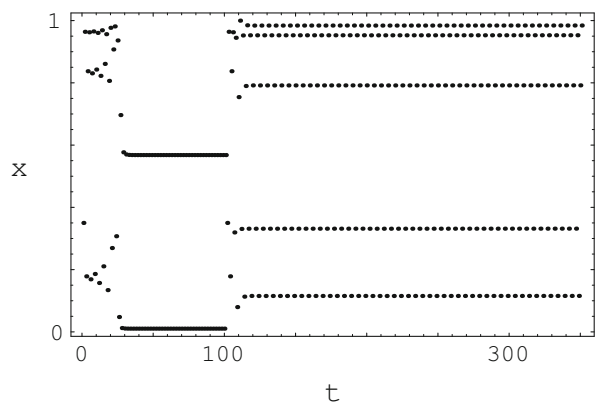


**Fig. 15.3** Stabilised period 5 in the stable regime of the neuron interaction map where the natural motion would be a stable period 2



In Fig. 15.3 we demonstrate that control on an unstable periodic orbit can be achieved not only in the domain of chaotic, but also in the regime of stable system behavior.

**3. Delay-Coordinate Control**

This control method can be particularly simple in experimental applications. Starting from  $m$ -dimensional vectors

$$\mathbf{x}(t) = (u(t), u(t - t_D), u(t - 2t_D), \dots),$$

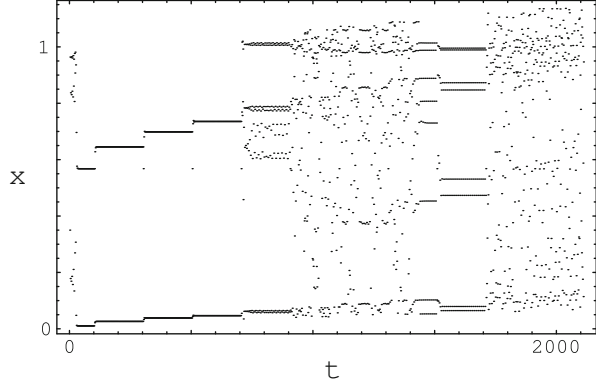
and the dynamical map of the form

$$\mathbf{x}_{i+1} = \mathbf{G}(\mathbf{x}_i, a_i, a_{i-1}, \dots, a_{i-\mu}),$$

we use again the ansatz

$$(\mathbf{x}_{i+1} - \mathbf{x}(i)(a_0)) = (\mathbf{D}_x \mathbf{G}(\mathbf{x}, a)|_{\mathbf{x}(i)(a_0), a_0} - \mathbf{D}_a \mathbf{G}(\mathbf{x}, a)|_{\mathbf{x}(i)(a_0), a_0} \mathbf{K}^T)(\mathbf{x}_i - \mathbf{x}(i)(a_0))$$

**Fig. 15.4** Delay-coordinate control (system: neuronal interaction). A portion of the signal with a fixed delay (varying in 11 steps) was added to the signal



that leads to

$$(\mathbf{x}_{i+1} - \mathbf{x}(i)(a_0)) = \mathbf{A}(\mathbf{x}_i - \mathbf{x}(i)(a_0)) + \mathbf{B}_a(a(i) - a_0) + \mathbf{B}_b(a_{i-1} - a_0)$$

with partial derivatives at  $\mathbf{x}_i(a_0)$  and  $\mu_0$ , respectively. The linear control

$$a_i - a_0 = -\mathbf{K}^T(\mathbf{x}_i - \mathbf{x}(i)(a_0)) - k(a_{i-1} - a_0),$$

with  $k$  as the control parameter, can, using

$$\mathbf{y}_{i+1} = (\mathbf{x}_{i+1}, a_i),$$

be written in a simpler way as

$$\mathbf{y}_{i+1} - \mathbf{y}(i)(a_0) = (\mathcal{A} - \mathcal{B}\mathbf{K}^T)(\mathbf{y}_i - \mathbf{y}(i)(a_0)),$$

where  $\mathcal{A} = (\{\mathbf{A}, \mathbf{B}_b\}, \{0, 0\})$ ,  $\mathcal{B} = (\mathbf{B}_a, 1)$ , and  $\mathcal{K} = (\mathbf{K}, k)$  are the quantities in the generated product space. Again, this equation can be stabilised using the method of pole placement; matrix  $\mathcal{A}$  can again be found by a method of numerical linear approximation. For obtaining the experimental vectors  $\mathbf{B}_a$  and  $\mathbf{B}_b$ , one has to rely on the system parameter  $a$ . In Fig. 15.4 we demonstrate that control on an unstable periodic orbit can be achieved with varying time delay.

#### 4. Feedback Control

This method can be seen as a special case of the delay-coordinate control, where we add to the dynamical system the by a factor  $c$  down-tuned system output of time  $t - \tau$ . The combined system (again for simplicity we constrain our presentation to one-dimensional systems) can then be written as

$$f(x, c) : x_{i+1} = \tilde{f}(x_i) + cx_{i-\tau}.$$

The method depends on the two parameters  $c$  and  $\tau$ . The variational equation has the form

$$\frac{dv}{dt} = D_x f(x(t), 0) v(t) + c D_c f(x(t), 0) Dg(x(t)) (v(t) - v(t - \tau)),$$

where  $g(t)$  is the (generally scalar) measurement at time  $t$ . The boundary of stabilisation can be explored by using Floquet methods.

Feedback control program outline:

```

perio = 22; xanf = 0.3682632865868;
nanz = 100; x = Nest[f, xanf, nanz];
Tabelle = NestList[f, x, perio];
eps = 0.004; eps = epsanf = 0.000005; del = 0.02; nanz = 1000;
JJ = NestList[f, 0.35, 100];
Do[ eps = eps + del;
    perio = 3; x = Nest[f, x, nanz];
    Tabelle = NestList[f, x, perio];
    J[i] = NestList[fff, x, 200], {i, 1, 10}];
Do[JJ = Join[JJ, J[i]], {i, 1, 10}];
ListPlot[JJ, Frame -> True, PlotRange -> All];
fff[x_] := Module[{xn}, xn = f[x];
    Do[Tabelle[[i]] = Tabelle[[i + 1]], {i, 1, perio - 1}];
    Tabelle[[perio]] = xn;
    xn = xn + eps Abs[xn - Tabelle[[2]]];
Return[xn]];

```

As will have emerged from our presentation so far, a general problem with the described control mechanisms is that they require considerable knowledge of the system to be controlled and that the system needs to be carefully led towards the desired solution. For many systems, this may not be easily available, and the control process may be rather slow. In the next section, we will present the limiter control method that avoids these complications and will be seen to be pretty close to the control mechanisms that are applied in macroeconomics. With this, for economics most relevant, control method we can easily achieve control on orbits of the original system, as well as, additionally, on desired orbits of the system plus controller.

## 15.3 Controlling Economics by Thresholds

In economics, controls are applied according to economics goals that the controller (state, federal banks, governments) wants to achieve. This is generally done by defining limits or bandwidths, after whenever crossing them, control actions take place. We will present in the following a chaos control method that is more realistic seen from the point of view of economics, using the quadratic map as the fundamental example of complex nonlinear dynamics. Later, we will motivate why the example of the logistic map is very appropriate and essential for describing the

evolution of macroeconomic processes. Our derivation will provide conditions for optimal stabilisation of economic dynamics and then we will explain why exactly the desire to control the fluctuations will even enhance periodic cycles, if not even the control itself is at their origin.

Let us thus describe how simple control mechanisms in economics may affect the evolution of the dynamics. Let us describe the threshold of the control threshold by  $x_{th}$ , above which the economy no longer develops according to its intrinsic dynamics. For a quadratic parabola, threshold control can be described by the equation

$$x_{n+1} = \begin{cases} \mu x_n(1 - x_n) & \text{if } \mu x_n(1 - x_n) \leq x_{th} \\ (1 - \alpha)\mu x_n(1 - x_n) + \alpha x_{th} & \text{if } \mu x_n(1 - x_n) > x_{th}. \end{cases} \quad (15.2)$$

Here,  $x_n$  and  $x_{n+1}$  denote the state variable at time  $n$  and  $n + 1$ , respectively.  $-\alpha$  is the proportionality factor of the perturbation by the applied control, whereas  $x_{th}$  defines the threshold for the state variable above which the correction is applied control, see Fig. 15.5a.

For general maps  $f$ , period- $k$  unstable periodic orbits ('UPO') are determined by the fixed points of the  $k$ -fold iterated map  $f^k$  (cf. Fig. 15.5b), with their stability being given by the derivative of this map at the fixed points. If the absolute value of the derivative of the control map is less than unity, the system can be stabilised on the UPO. We will show that based on this condition, the control mechanism can be optimised. Figure 15.5 shows the map when modified by the control, for different values of  $\alpha$ . Without loss of generality, we have set the system parameter

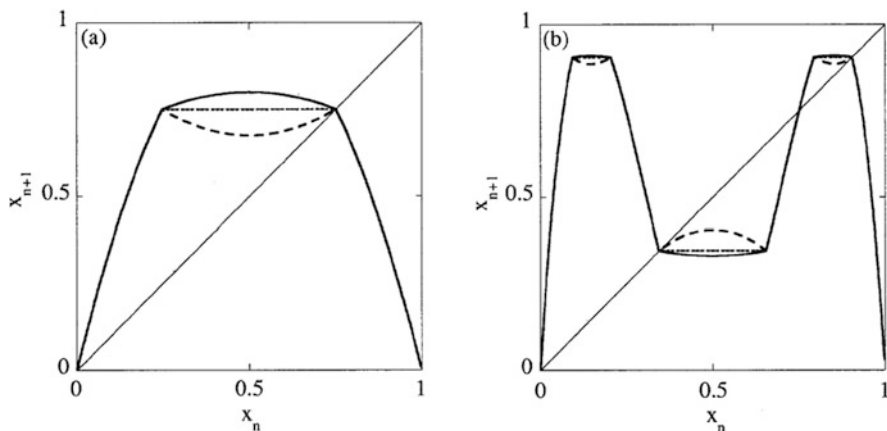


**Fig. 15.5** Modified maps used for limiter control of the period-1 orbit (a) and the period-2 orbit (b) of the logistic map, see (15.2). (a) Full line  $\alpha_{min} = 0.75$  and dashed line  $\alpha_{max} = 1.5$  indicate two intervention thresholds that can be seen as a chosen intervention bandwidth. Superstable orbits are obtained for  $\alpha = 1$  (dotted line). (b) Full line:  $\alpha_{min} = 0.93750$ ; dashed line:  $\alpha_{max} = 1.24999$ ; fine dashes:  $\alpha = 1$ . Note that the present use of  $\alpha$  differs from the later use of the symbol for describing the ‘scaling constant’

to  $\mu = 4$ , the *fully developed* chaos case (maximal chaos). There are two limiting values within which the map can be controlled: a maximal value  $\alpha_{max} > 1$  (dashed line) and a minimal value  $\alpha_{min} < 1$  (full line). The special case  $\alpha = 1$  provides superstable UPOs; this case already has been analysed by L. Glass et al. [12]. As the simplest example for our theoretical analysis, we focus on the unstable period-1 orbit. The derivative of the unperturbed system is  $\mu(1 - 2x^*) = -2$ , where  $x^* = 0.75$  denotes the fixed point; the absolute slope larger than 1 refers to an unstable orbit. First we consider the case where  $\alpha < 1$ , cf. Fig. 15.5. Driving the system slightly out of the fixed point  $x^*$ , the trajectory alternates between the two branches of the map that meet at the fixed point. In order to make the fixed point attractive, the absolute value of the product of the derivatives of the two branches at the fixed point must be smaller than 1. This leads to a condition for the minimal value of  $\alpha$ ,

$$|(1 - \alpha)(\mu(1 - 2x^*))^2| < 1.$$

Thus, the lower threshold becomes  $\alpha_{min} = 0.75$ . In the case of  $\alpha > 1$ , (long dashes), the trajectory propagates only along the perturbed branch after pushing the system out of the fixed point. Therefore, the corresponding condition is

$$|(1 - \alpha)(\mu(1 - 2x^*))| < 1,$$

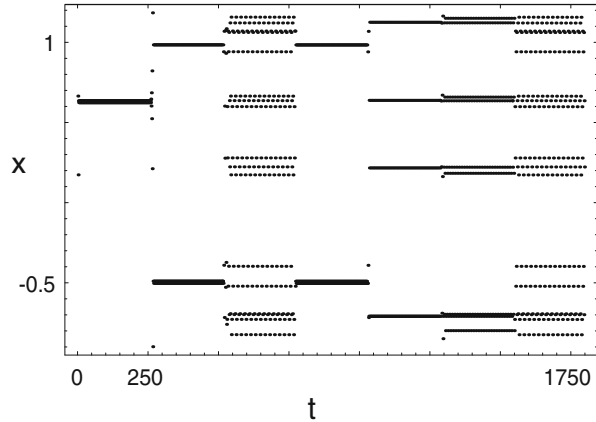
which yields the upper limit  $\alpha_{max} = 1.5$ . These results can readily be generalised to stabilise orbits of higher periodicity.

Note that this procedure can also be applied to the control of natural systems (cf. Ref. [8], first experiment) and for higher-dimensional maps. For  $\alpha = 1$ , the derivative becomes zero at the fixed point and the periodic orbits are superstable (Fig. 15.5, short dashes). Experimentally, this corresponds to a limiter  $x_{th}$  that is rigid, i.e., cannot be modified at all. At this point, the periodic orbits become optimally stable and therefore almost insensitive to noise (as a matter of fact, the diode used as limiter in the second experiment of Ref. [8] approximates this case). Because of these properties, this method is called ‘hard limiter’ control (HLC) [43–45].

This procedure of stabilising UPOs can be adapted for two-dimensional maps, as is shown by the example of the Hénon map, see Fig. 15.6. For the controlled Hénon map  $x_{n+1} = \tilde{x}_{n+1} := a + by_n - x^2$ , if  $\tilde{x}_{n+1} \leq x_{th}$  and  $x_{n+1} = (1 - \alpha)\tilde{x}_{n+1} + \alpha x_{th}$ , if  $\tilde{x}_{n+1} > x_{th}$ , with  $y_{n+1} = x_n$  for both cases, the effectivity-range of the stability parameter  $\alpha$  can be determined analogously. For the standard parameters  $a = 1.4$  and  $b = 0.3$  we obtain for the period-1 and the period-2 orbit  $\alpha = 0.79011 < \alpha < 1.68129$  and  $0.80090 < \alpha < 1.20408$ , respectively. Since the cutoff algorithm requires no computational effort in experiments, optimised control is provided in a the most simple way. A minor drawback of the presented control method is that the perturbations can be quite large, if not assisted by targeting procedures.

Whereas a substantial effort in the earlier presented control methods is that they require the identification of the orbits one might want to control on, here the effort is to identify the bifurcation points of the combined dynamical-and-controller system: Only for these values of the controller, true orbits of the original system

**Fig. 15.6** Fast switching of the dissipative Hénon map between periodicities  $p = 1, 2, 4, 8, 16$  using HLC.  $x$ -coordinates are shown over  $t = 250$  iteration steps each, where a slightly thickened line marks the position of the limiter. Control of high periodicities is at least as fast as the control of low periodicities



are obtained. This happens on a set of measure zero, but a similar characterisation applies to the periodic orbits seen in a space of all potential orbits. The simplicity of the threshold control drastically reduces the latency of the controller. As has been shown above, the limiter control can be optimised by using ‘hard limiters’, leading in the 1-d case to a description by the class of flat-topped maps. Earlier, Glass and Zeng had suggested these maps for regularising cardiac rhythms [12], in a more general context a chain of flat-topped map was used by Sinha and Biswas to investigate adaptive dynamics [39]. Moreover, Sinha and Ditto presented a simple network of flat-topped logistic maps which encodes numbers and performs arithmetic computations [40].

One may ask oneself whether flat-topped maps could, similarly to their relatives with of quadratic nonlinearities, also display a kind of universal behaviour. In contrast to the latter family, it is to be noted first that flat-topped unimodal maps—due to their flat tops—cannot show chaotic motion. As an ergodic chaotic trajectory would explore the entire attractor of the system, it eventually will land on the flat segment, from which it will continue on a periodic orbit. If we consider (non-ergodic) maps having separated attractors, the periodic motion can only be observed if the orbit visits the attractor which is associated with the flat segment of the map. Flat-topped maps can, however, undergo a period doubling cascade, as a function of the height of the top, as we show in Fig. 15.7 for three variants of the implementation of this concept.

It comes as little surprise that these processes can be treated in full parallel to the Feigenbaum treatment. In the first step, we therefore determine the properties of the bifurcation cascade and then will compare it with the Feigenbaum case. We will show that, generically, in flat-topped maps the single scaling for the opening of the forks of the Feigenbaum case is replaced by two different scaling factors. One of them is a trivial scaling by  $\alpha = 1$ , which is associated with the scaling of the top. The other scaling by  $\tilde{\alpha}$  depends on the derivatives of the map and can therefore not be universal, which is why for this splitted scaling, we propose the term “partial”

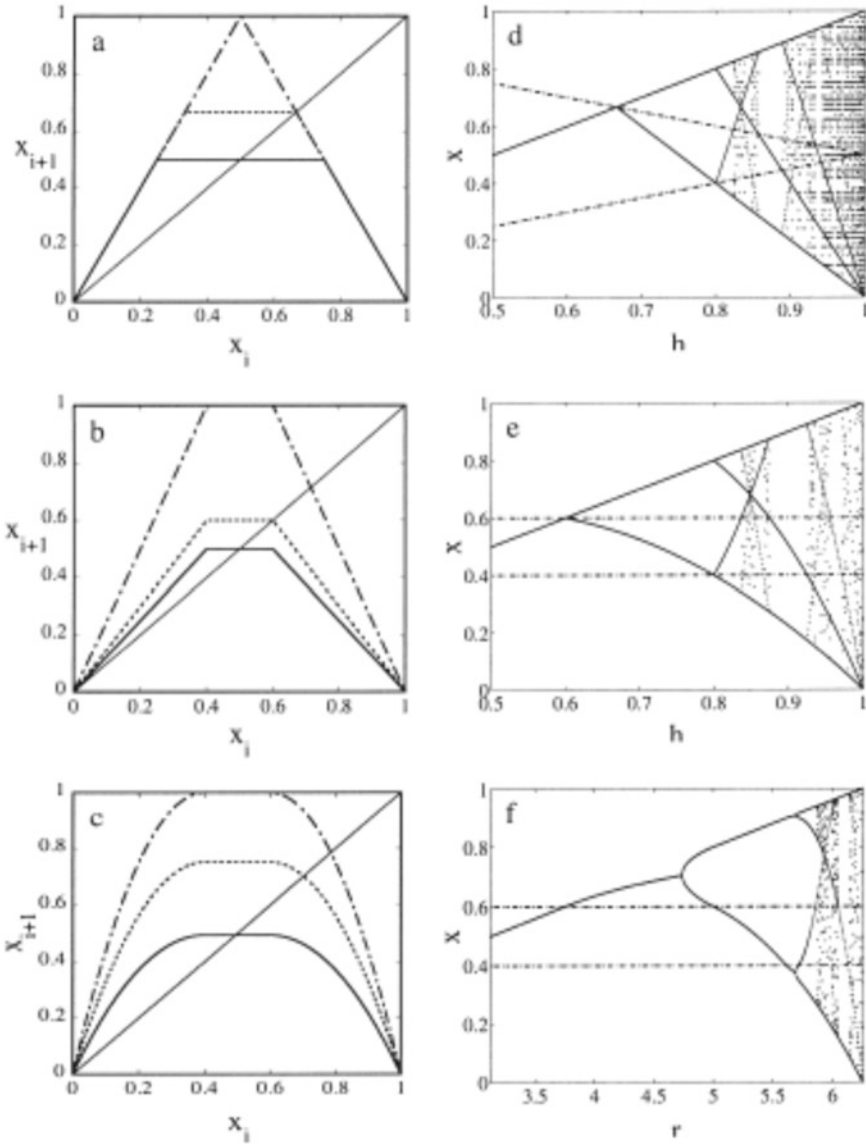


**Fig. 15.7** (a) Flat-topped tent, (b) spread tent, (c) spread logistic map, with corresponding generated bifurcation diagrams (d)–(f)

universality. In the course of period doubling, flat-topped maps show an exponential convergence towards the period doubling accumulation point. As a consequence, the value of the scaling exponent  $d$  diverges. Of practical interest is the observation that the convergence onto the asymptotic periodic orbit is exponential and usually reached within a few iterations when starting from arbitrary initial conditions.

To render life as easy as possible, we shall first switch to the flat-topped symmetric tent map. As the curvature of the side branches that the flap-topped parabola would introduce is of limited variation, this has no further influence on the generic behaviour. The flat-topped symmetric tent map is given by

$$x_{i+1} = \begin{cases} 1 - |2(x_i - 0.5)| & \text{for } 1 - |2(x_i - 0.5)| < h \\ h & \text{otherwise.} \end{cases} \quad (15.3)$$

Threshold  $h$  denotes our limiter, which is the natural choice of the bifurcation parameter. Figure 15.7a, d shows the HLC-controlled tent map along with its bifurcation diagram, where the threshold  $h$  is increased from  $h = 0.5$  to  $h = 1$ . For the diagram, the last 100 of a trajectory of 500 points were plotted, showing that the associated orbits are periodic, except for  $h = 1$ . Upon this increase of  $h$ , the length of the flat interval shrinks from  $I_{h=0.5} = 0.5$  to  $I_{h=1.0} = 0$ . In Fig. 15.7d, for each  $h$  the interval end points are shown as thin lines. In the bifurcation diagram, a period doubling bifurcation occurs whenever an end point collides with a  $2^n$ -periodic fixed point. Therefore, a new controlled orbit is born whenever the diagonal  $x_{n+1} = x_n$  first hits a flat interval of the  $2^n$ -fold iterated map. When  $h$  is increased further, the intersection point moves along the flat interval to the other end point, where the next period doubling bifurcation is generated. Because of the constant absolute slope of the map, all branches in the bifurcation diagram are straight lines. For an orbit of length  $2^n$ , the slope of the bifurcation branch that contains  $x = 0.5$  can be written as  $s_n = 2^{2^{n-1}}$ ,  $n > 0$ . The sequence of period doubling bifurcation can now be calculated as the intersections of this branch with the lines corresponding to the end points of the flat top. For  $n > 1$  this leads to

$$h_n = 1 - \frac{\prod_{k=0}^{n-2} (2^{2^k} - 1)}{2^{2^{n-1}} + 1},$$

where  $2^n$  denotes the periodicity of the cycle. The location of the threshold at which the periodicity becomes infinite can numerically be determined to be at  $h_\infty \simeq 0.82490806728021$ .

The scaling behaviour of 1-d unimodal maps is characterised by two constants  $\alpha$  and  $\delta$ . The constant  $\alpha$  describes asymptotically the scaling of the fork opening by subsequent period doubling, whereas  $\delta$  represents the scaling of the intervals of period  $2^n$  to that of period  $2^{n-1}$  near the period doubling accumulation point, i.e., at the transition to chaos. Both values depend on the leading order of the maximum of the map (the second order is of course the generic case). The usual Feigenbaum constants correspond to the prominent class of maps with non-vanishing curvature at the hump. Therefore, it is not a surprise that for flat-topped maps, Feigenbaum scaling results are changed. The value of  $\alpha$  can be determined from the fixed point



of the period doubling operator  $T$  (e.g., [36])

$$g(x) = Tg(x) = -\alpha g\left(g\left(-\frac{x}{\alpha}\right)\right), \tag{15.4}$$

where  $g(x)$  denotes the fixed point function. Following the Feigenbaum ansatz, we study the renormalised function

$$g_{n,1}(x) = (-\alpha)^n f_{h_{n+1}}^{2^n}\left(\frac{x}{(-\alpha)^n}\right),$$

at  $h_n$ , where  $2^n$  denotes the periodicity of the orbit. The scaling function  $g(x)$  then is obtained as  $g(x) = \lim_{i \rightarrow \infty} \lim_{n \rightarrow \infty} g_{n,i}(x)$ . The form of the rescaled functions  $g_{n,1}(x)$  for  $n = 0, 1, 2, 3$  motivates that  $g(x)$  will be a square wave. Therefore, we make the ansatz

$$g(x) = 1 + b(1 + \Theta(x - 1) - \Theta(x + 1)), \tag{15.5}$$

where  $\Theta(x)$  represents the Heaviside function. Insertion of 15.5 into 15.4 leads to

$$1 + b(1 + \Theta(x - 1) - \Theta(x + 1)) = -\alpha \left( 1 + b \left( 1 + \Theta\left(g\left(\frac{x}{-\alpha}\right) - 1\right) - \Theta\left(g\left(\frac{x}{-\alpha}\right) + 1\right) \right) \right).$$

This equation allows for  $\alpha = 1$  and  $b = -2$  as solutions.<sup>1</sup> The value of  $\alpha = 1$  implies that in the vicinity of the accumulation point  $h_\infty$ , the opening of the bifurcation fork does not change under subsequent period doubling bifurcations. However, as the map has everywhere a nonzero slope of absolute value 2, the ratio of the fork openings within a  $2^n$  periodic orbit is  $\tilde{\alpha} = 2$ .<sup>2</sup> This is illustrated in Fig. 15.8 which shows the location of the forks in the bifurcation diagram versus the periodicity of the orbit. Each circle represents a bifurcation fork, the openings of which can be calculated by multiplying all factors along the path, starting at the period 2 orbit. For example, in order to calculate the opening size of the from top fourth fork of period 16, we follow the bold path in Fig. 15.8 and obtain

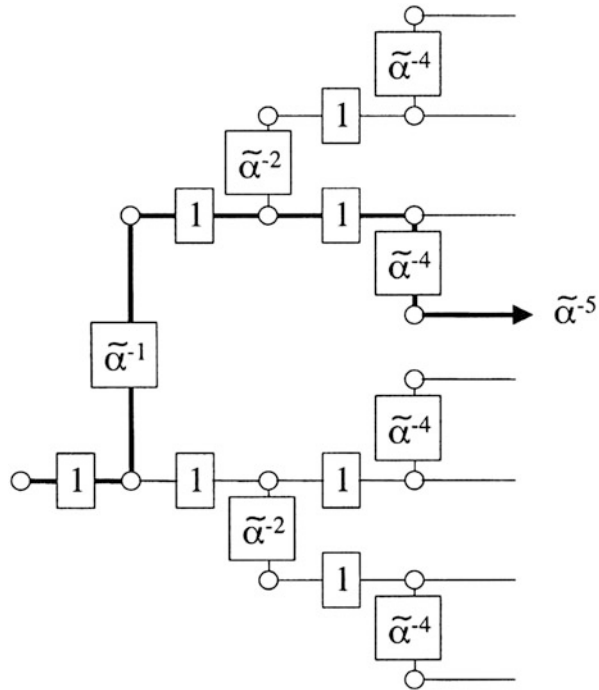
$$1 \circ \tilde{\alpha}^{-1} \circ 1 \circ 1 \circ \tilde{\alpha}^{-4} = \tilde{\alpha}^{-5}.$$

---

<sup>1</sup>For  $g(0) = 1$  one also could use the ansatz  $gn(x) = 1 + bx^{2^n}$  and take the limit for  $n \rightarrow \infty$ . Again, the solution is a square wave with  $b = -2$ . Using  $g(1) = -\alpha$  yields  $\alpha = 1$  and  $\delta^{-1} = 0$ .

<sup>2</sup>Scaling laws for ‘stars’ and ‘windows’ observed in the bifurcation diagram for  $h > h_\infty$  of the logistic map were already described by Sinha [38]. They both depend on the derivative of the map at the origin and are therefore not universal. The scaling factor for ‘stars’ and ‘windows’ of the tent map is 2.

**Fig. 15.8** Split scaling of forks: The horizontal scaling ( $\alpha = 1$ ) is universal. The vertical scaling ( $\tilde{\alpha}$ ) depends on the derivatives of the map



Note, that the value of  $\alpha = 1$  is only exact close to the accumulation point, whereas the value of  $\tilde{\alpha} = 2$  is always exact. Instead of considering the bifurcation points  $h_n$  at which periods of order  $2^n$  are born, the value of  $\delta$  can be determined by using the values  $H_n$  where the periodic orbits contain the point  $x = 0.5$ , as both sequences converge with the same behaviour to the accumulation point  $h_\infty$ . The value of the bifurcation parameter  $H_n$  is given by

$$H_n = 1 - \frac{\prod_{k=0}^{n-1} (2^{2^k} - 1)}{2^{2^n}}. \tag{15.6}$$

Equation 15.6 can be written recursively as

$$H_n = 1 - (1 - H_{n+1}) \frac{1}{1 - 2^{-2^n}},$$

which leads to

$$H_n = 1 - (1 - h_\infty) \prod_{k=0}^{\infty} \frac{1}{1 - 2^{-2^k}}. \tag{15.7}$$

Using

$$\prod_{k=0}^{\infty} (1 - 2^{-2^k})^{-1} \approx \left( 1 - \sum_{k=n}^{\infty} 2^{-2^k} \right)^{-1} \approx 1 + 2^{-2^n},$$

Eq. 15.7 reduces to

$$H_n = h_{\infty} - c 2^{-2^n}, \quad (15.8)$$

where  $c = 1 - h_{\infty}$ . Equation 15.8 reveals an exponential convergence towards the fixed point. Therefore, the ratio between two subsequent intervals  $H_n - h_{\infty}$  and  $H_{n+1} - h_{\infty}$ , which asymptotically determines the value of  $\delta$ , depends on  $n$  as

$$\delta(n)^{-1} = 2^{-2^n}.$$

This result means that in the case of the flat-topped tent map, the occurrence of period doubling does not follow a power law as in the Feigenbaum case. Rather, it is of exponential nature.

Unstable periodic orbits can only be controlled when the system is already in the vicinity of the orbit. As the initial transients can become very large, targeting algorithms have been designed [21, 37] that efficiently push the system onto the selected orbit. The flat-topped tent map and the corresponding tent map share the same orbit if the threshold of the flat-topped tent map coincides with the largest fixed point of the tent map. Due to the flat top, this orbit becomes stable. Initial conditions that lead to the flat top are on the selected orbit within one iteration. Iterating backwards, we can determine the intervals that lead to the orbit in two iterations, and so on. This approach is similar to the strange repeller escape problem. The relationship suggests that in our case, the convergence onto the selected orbit is exponential, which makes a targeting algorithm idle. The exact convergence onto the selected orbit depends on the size of the flat top. The larger the horizontal segment is, the faster is the convergence. As the size of the flat top is determined by the threshold, the time constant of convergence varies with the latter. We calculated the time constant for  $h_{\infty}$  by propagating back the interval associated with the flat top. For each back-iteration,  $2k$  new intervals of half the size of the intervals obtained by the previous step join the already recruited intervals (Fig. 15.9).

This property is due to the slope of the map, which in the present case equals 2. Figure 15.9 gives the number of back-iterations versus half of the number of the added intervals  $k$ . Let the differences between two subsequent values of  $k$  be denoted by  $\Delta(i)$ , where  $i$  denotes the order of the backward iteration. From their values, it is seen that  $k$  can be calculated iteratively as

$$k(i) = k(i - 1) + \Delta(i - 1),$$

where  $i \geq 2$ ,  $k(1) = 1$ ,  $\Delta(1) = 1$ ,  $\Delta(2i) = k(i)$  and  $\Delta(2i - 1) = k(i)$ .

Number of Back-Iterated Intervals

back iteration $i$	1	2	3	4	5	6	7	8	9	10	11	12
$k$	1	2	3	5	7	10	13	18	23	30	37	47
$D$	1	1	2	2	3	3	5	5	7	7	10	10

**Fig. 15.9** Split scaling of forks: The horizontal scaling ( $\alpha = 1$ ) is universal. The vertical scaling ( $\tilde{\alpha}$ ) depends on the derivatives of the map

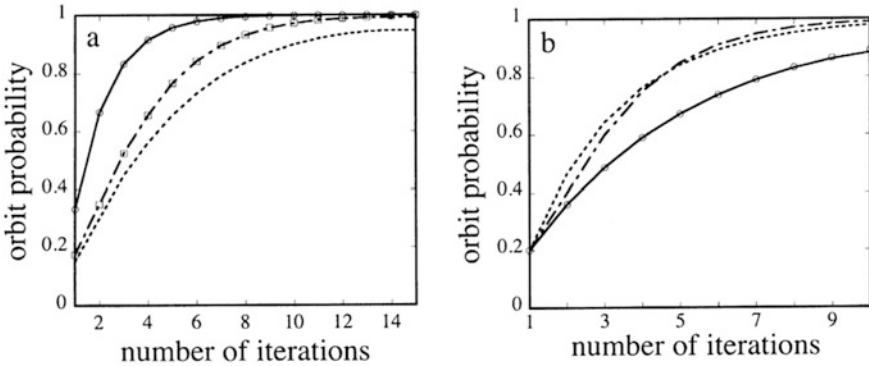


**Fig. 15.10** Convergence onto orbits versus steps. (a) Flat-topped tent map ( $h = 0.85$ ,  $h = h_\infty$ ,  $h = 2/3$ ). Circles and squares from back-iteration [Eq. 15.9] and from zeta function (Eq. 15.11), respectively. (b) Spread tent map ( $h = 1$ ,  $h = 0.8$ ,  $h = 0.6$ ); circles: results from  $\zeta$ -function (Eq. 15.11)

If  $L$  denotes the measure of naturally, i.e., equally distributed, initial conditions that do not lead to the selected orbit, the reduction of  $L$  due to  $i$ -fold back-iteration can be written recursively as

$$L(i + 1) = L(i) - 2k(i) \frac{l_0}{2^i}, \tag{15.9}$$

where  $l_0$  denotes the initial size of the flat top. If properly scaled,  $1 - L(i)$  is the probability measure for initial conditions to be controlled onto the selected orbits in  $i$  steps. Figure 15.10a shows the convergence onto the orbit for  $h = 2/3$ ,  $h = h_\infty$ . and  $h = 0.85$  (full line, dashed line, and broken line, respectively). The squares represent calculations using Eq. 15.9. For the system to be controlled, it needs to visit the flat segment of the graph. The determination of the measure of orbits that reach the horizontal fragment after  $n$  iterations is equivalent to the escape problem of a (hyperbolic) strange repeller. Indeed, the average rates either for landing on the controlled orbit or for the escape are given by the decreasing number of chaotic orbits as a function of iterations. For the numerical treatment of hyperbolic repellers, one standard method is cycle expansion [2, 3]. We used this approach to check our brute-force results for  $h = 2/3$ , cf. Fig. 15.10. The cycle expansion of the dynamical

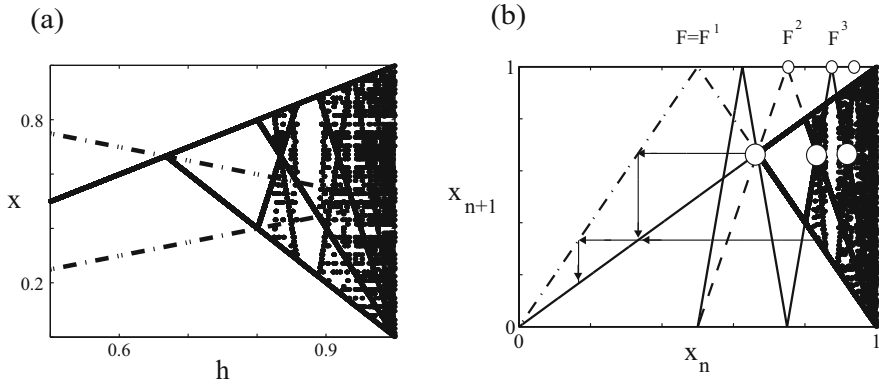


**Fig. 15.11** (a) Generic bifurcation diagram of flat-topped maps. The (for display reasons: tent) map is drawn over the vertical axis  $x$  (broken lines). To obtain the controlled map at control parameter  $h$ , replace the (rightwards pointing) peak of the map by a vertical segment positioned at  $h$ . The asymptotic controlled orbit points are also displayed with abscissa  $h$ , giving rise to a bifurcation diagram. (b) Relation between the  $n$ -fold iterates of  $F$  (graphs  $F^n$ ,  $n = 1, 2, 3$ , shown by dashed-dotted, dashed, and full lines) and the scaling of the ‘stars’ (large circles): Back-iterations (arrows) of the period-one fixed point  $x = 2/3$  yield successive star locations. Their scaling is therefore determined by the derivative  $F'(0)$ . A similar argument applies for the size of the ‘windows’ (whose  $x$ -values are located around the small circles)

$\zeta$ -function is then governed by the cycle that corresponds to the fixed point at  $x = 0$  and reads

$$1/\zeta = 1 - z\frac{1}{2}.$$

The escape rate  $\gamma$  is determined by the zero of the dynamical  $\zeta$ -function using  $z = \exp(\gamma)$ . For our case, this yields  $\gamma = \ln(2)$ , implying that for arbitrary initial conditions the probability of landing on the period 1-orbit within 5 iterations is  $p = 0.95$ .

The scalings induced by HLC also explain the large-scale repetitive star-like bifurcation structures and the adjacent repetitive empty bands (positions indicated in Fig. 15.11b by the large and the small circles, respectively). It is easy to see that the asymptotic scaling of these repetitive structures stars are both given by the derivative of the leftmost fixed point of the map. As a consequence, both scalings are again non-universal.

This ends our excursion on the statistical properties of the hard limiter controlled tent map. By generalising the fully analysed tent map example of HLC, we can, however, obtain insight into the behaviour and properties of more general systems. We demonstrate this by choosing a family of what we shall call ‘spread maps’: unimodal, and symmetric hard limiter controlled maps that are additionally characterised by a segment of fixed size  $2d$ . Why this is convenient will be apparent in a moment. We start for simplicity with family of maps that are close to the

previous tent map example, in which case we deal with the equation

$$x_{n+1} = \begin{cases} x_n \frac{h}{(0.5-d)} & \text{for } x_n \leq 0.5 - d \\ (1 - x_n) \frac{h}{(0.5-d)} & \text{for } x_n \geq 0.5 + d \\ h & \text{elsewhere.} \end{cases} \quad (15.10)$$

Choosing the height  $h$  at which we place the controller now entrains a change in the slope of the piecewise linear sides of the maps, yielding further insight into the properties of hard limiter control. As has already been promised at the beginning our explorations, the influence of the slope at the two sides is rather small and leaves the scaling properties and essentially also the bifurcation diagrams unchanged (cf. Fig. 15.7b, e). Since the flat top is symmetric about the line  $x = 0.5$  and of constant size, the corresponding envelopes are obtained as two parallel horizontal lines at  $0.5 + d$  and  $0.5 - d$ . Bifurcation can only occur at these two lines. The effect of the changed slopes of the map is reflected in the curved bifurcation branches shown in Fig. 15.7e, in comparison with the straight lines of the flat-topped tent map (Fig. 15.7d).

Due to the salient role of the horizontal segment for occurrence of bifurcations, the scaling by  $\alpha$  remains unchanged. In contrast, the scaling by  $\tilde{\alpha}$  changes from one period doubling to the next. Upon a decrease of  $h$ , we observe two effects that emerge related to orbit convergence. On the one hand, some of the orbits are lost, which reduces the number of intervals added by back-iteration. On the other hand, due to the decreased slope of the map, individual intervals become larger (except for the central one). The trade-off between these effects leads to an optimal convergence case at  $h \approx 0.8$ . Figure 15.10b shows the time constants obtained for decreasing heights ( $h = 1$  (full line),  $h = 0.8$  (dashed line), and  $h = 0.6$  (broken line)), using  $d = 0.1$ . For  $h = 1$ , the exponential decay constant can again be calculated using the cycle expansion. The dynamical  $\zeta$ -function then is

$$1/\zeta = 1 - \frac{1}{1-2d}z, \quad (15.11)$$

which leads to the escape rate  $\gamma = \ln(1/(1-2d))$ . In Fig. 15.10b, the calculated values are shown as circles.

To emphasise the origin of this phenomenon, we finally consider a last family of spread maps on the interval  $[0, 1]$ , characterised by horizontal flat top of a fixed length  $2d$ . We choose

$$x_{i+1} = \begin{cases} \mu x_i (1 - x_i - 2d) & \text{for } x_i \leq (0.5 - d) \\ \mu (x_i - 2d)(1 - x_i) & \text{for } x_i \geq (0.5 + d) \\ \mu (0.5 - d)^2 & \text{elsewhere} \end{cases} \quad (15.12)$$

where  $d$  again denotes half of the flat segment size, and  $\mu$  controls the opening of the underlying parabola (cf. Fig. 15.7c). This example, in distinction of the previous cases, is now differentiable on the interval  $[0, 1]$ . In this way, the height of the graph becomes a function of  $\mu$  (and the fixed chosen  $d$ ), as  $h = \mu(0.5 - d)^2$ . Given  $d$ , this restricts the range of  $\mu$  to  $0 < \mu \leq 1/(0.5 - d)^2$ . Upon increasing  $\mu$ , also this family exhibits a nontrivial bifurcation diagram (shown in Fig. 15.7f for  $d = 0.1$ ). The shape of this diagram differs greatly from those of the previous two families and is closer to the ordinary period doubling bifurcation diagram of the logistic map. This property is due to the smooth connections between the horizontal segment and the two branches of the map. Figure 15.12a and b illustrate the differing mechanisms at the first period doubling bifurcation for the flat-topped tent and the spread logistic maps. In the former case, the bifurcation abruptly emerges from the single flat segment of the second iteration. In contrast, the second iteration of the spread logistic map already has two different flat segments, and the bifurcation occurs along the smooth inter-segment connection. At the period doubling accumulation point these smooth transitions turn into step like transitions, conserving the scaling of  $\alpha = 1$ .

Wrapping these results up, for flat-topped maps, the scaling function  $g(x)$  is a square wave with a scaling factor  $\alpha = 1$  for subsequent period doubling bifurcation. The ratio of bifurcation fork openings within orbits of order  $2^n$  depends on the derivative of the map and therefore does not follow a universal behaviour. The scaling factor  $\delta$  diverges. Close to the transition point, this kills the power law behaviour for the occurrence of bifurcation, and an exponential law appears, which renders the observation of orbits of higher periodicity increasingly difficult.

We have shown that the limiter based control algorithm also works with the Hénon map, cf. Ref. [43]. This ends our excursion into natural control of nonlinear dynamical systems. In conclusion, we have demonstrated that control by threshold induces a number of naively unexpected phenomena that may be well worth

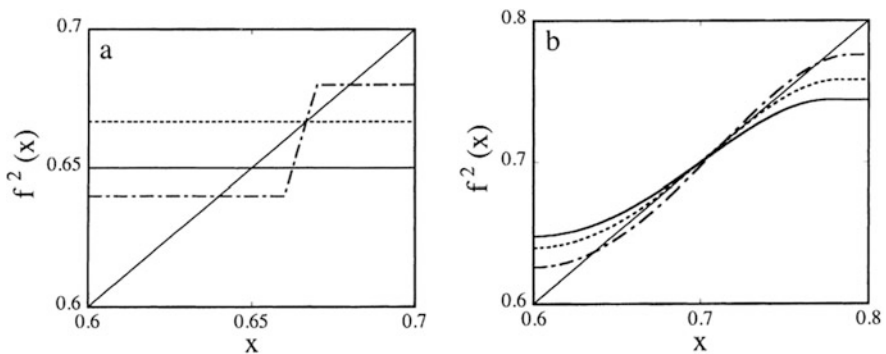


**Fig. 15.12** Bifurcation mechanisms of flat-topped spread tent (left panel) and logistic maps (right panel). Second iteration maps before, at, and after bifurcations. Parameters: tent:  $h = 0.65$ ,  $h = 2/3$ ,  $h = 0.68$ , logistic:  $\mu = 4.65$ ,  $\mu = 4.74$ ,  $\mu = 4.85$

to be taken into account when monitoring macroeconomic systems by the most fundamental control measures applied in economics dynamics.

## 15.4 Application to a Simple Model of Macroeconomics

### *'Greed and Control Rule Macroeconomics'*

We first motivate the principles that advocate more specifically to use the quadratic iterated map as a simple, but generic, model of macroeconomic development. In this model, a primary source of cycles can be identified. We then demonstrate a detailed mechanism of how cycles are additionally introduced when applying even the simplest control strategies. The principles of applying the simplest and most natural control method are explained, and the laws underlying the generation of (super)stable cycles by means of the control, are outlined. Finally, we propose an optimal control mechanism, work out its main properties and highlight the difficulties of its application in economics. The obtained insights add a new facet to the control advice by Kydland and Prescott [23]: The optimal system behaviour is not obtained by controlling on the natural cycle, but is achieved by a controlled period-one orbit. This not only requires a control policy that is kept fixed through time. To acquire the period-one state, a strong initial control effort is generally required, and control must permanently be maintained. In order to control the system on a period-one orbit, it may be advantageous if the system is in the chaotic regime. Finally we show how the regime of the dynamics can be identified by the system's response to control.

Chaos is composed of an infinite number of unstable periodic cycles of increasing periodicities. In order to exploit this reservoir of characteristic system behaviours, elaborate methods have been developed to stabilise (or 'control') intrinsically unstable orbits, using only small control signals [11, 25, 30, 34]. By the more detailed study of the potential of these control methods in economics [4, 14, 15, 17, 20], several limiting factors were identified. As a first shortcoming, the inherent latency of most of the above control approaches emerged. In the context of quickly changing economics, control, however, is required to be fast. As a second problem, some economic data cannot be collected in a continuous fashion. This renders the application of the standard control methods, that are based on the explicit knowledge of the geometry of the economic dynamics, tedious, and targeting methods, designed to improve the speed of convergence towards the desired solutions, inefficient. Moreover, the large amount of strong noise that is characteristic for economics tends to veil these structures. As a third requirement, the control should permit to be formulated in terms of a simple economics policy. For control strategies that are based on past observations (e.g., statistical data from the preceding year), this is not easily achievable. Moreover, these control strategies lead to policy functions involving time delays [24], which often entrain chaotic behaviour, as in the above-mentioned pioneering examples [6, 7, 28]. These observations apply in particular to time-delayed feedback control methods [14, 32] that for some time were proposed as



a means of controlling financial markets. Due to these problems, the interest in the application of dynamical systems methods for the control of economic dynamics, has decreased thereupon.

Economies naturally tend towards the recruitment of all available resources. In the following let us explain how human greed drives their economics towards the boundaries and fosters a natural tendency of the system to evolve towards maximally developed nonlinearities. While occasionally also animals are said to be greedy, human greed takes things further than just acquiring resources for one's self. The basis for this is in human society, in its ability to store and trade virtually unlimited amounts of goods. This has been triggered by the human's change from hunters to agriculture (manifested in the bible's and other tales' expel of humans from the paradise) and is fostered by the development of the necessary technological basis (wheel, communication, building). For humans, the distinction between constant, constant and exponential improvement of a state is, from the perceptual point; difficult (the focus is just on different observables that are constant (state, additive gain, gain factor)). Moreover, if the changes are small and slow enough, the three cases can hardly be distinguished. Only when the limits of economic systems are approached, the distinction between the last two models becomes important. In this case, nonlinearities matter, as they are required to keep the system within its boundaries.

For our modelling of the dynamics of such systems, we choose the iterative picture. The evolution of a simple model of economics takes place on three time scales: At the lowest level, perturbations affect a deterministically changing variable  $x$  that will be considered to represent a momentary degree of system exploitation (second level). This setting is completed (third level) by a greed-driven parameter  $\mu$ , expressing to what extent the corresponding system conformation covers the full theoretically available system size. For states far from the maximal exploitation of the resources allowed by parameter  $\mu$ , we allow the dynamics to grow almost linearly. Close to maximal exploitation, the next value consumption is required to be small, implementing in this way a kind of system recovery.

A corresponding simple and generic model of such dynamics is again provided by the iterated logistic map on a space that we may rescale to be the unit interval

$$f : [0, 1] \rightarrow [0, 1] : x_{n+1} = \mu x_n (1 - x_n).$$

On a time scale much slower than the one responsible for the iterative dynamics, the principle of economic greed will gradually drive the system, via the increase of the order parameter  $\mu$ , towards the 'critical' value  $\mu = 4$ , allowing for an ever-growing exploitation of the phase-space  $[0, 1]$ . As can easily be seen at 'criticality'  $\mu = 4$ , it is the nonlinearity that keeps the system states  $x$  away from the boundary: Starting with a small value  $x_0$ , upon iteration the value of  $x$  first increases in an almost linear fashion (the approximate proportionality factor being  $\mu$ ), but soon as  $x_n$  approaches the upper phase-space boundary (at  $x_n = a/4 = 1$ ), this behaviour is annihilated by the factor  $1 - x_n$  that sends the dynamics back to small values.

On the human greed-driven pathway towards the globalisation of resources ( $\mu \rightarrow 4$ ), the asymptotic system state (obtained for  $n \rightarrow \infty$ ) converges initially to a fixed state increasing in its value with  $\mu$ , then suddenly changes into a period-2 behaviour (two alternating values of  $x$ ), and then undergoes a continued period doubling bifurcation route, where a cascade of stable periodic orbits of increasing orders  $2^n$  (where  $n = 2, 3, 4 \dots$ ) characterises the asymptotic solutions [10]. Using renormalisation theory, it can be shown that in order to reach the next bifurcation,  $\mu$  progresses geometrically, with factor  $q \approx 1/4.67$ . This implies that the transition point to period infinity is reached within a finite interval of  $\mu$  (cf. Fig. 15.13). Beyond this period doubling accumulation point, chaos is possible and abundant, but while the value of parameter  $\mu$  can still be increased, we observe a succession of windows of periodic behaviour and chaotic behaviours [42], rendering a statement how much weight the parameters  $\mu$  leading to chaotic behaviour have, a highly nontrivial one [5]. The properties exhibited by the logistic map have been found to be characteristic for a large universality class of nonlinear processes (of which the logistic map is the simplest representative, see, e.g., [36]). Our model thus characterises a whole class of systems subject to such a process of self-organisation. The quadratic parabola has therefore been used in economics in a number of approaches. In particular, in an early example by Benhabib and Day [6], under suitable conditions, economics were found to follow the behaviour of the logistic map, providing an early indication for why economics could eventually become

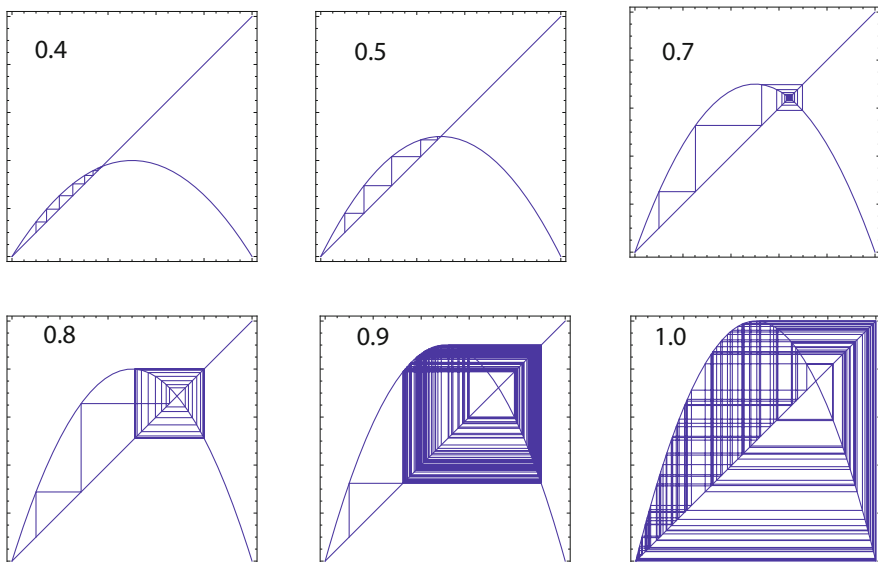


**Fig. 15.13** State sequences are obtained, upon increasing parameter  $\mu$ , from a logistic map as a model of economics. For small values of  $\mu$ , stable regular behavior emerges. As  $\mu$  is increased, the behavior becomes increasingly complicated, until chaotic behavior emerges. The figure insets represent the fractions of the maximally available environments that are accessible to the process

chaotic. In their model, there is a competition between the demand for two goods. The preference for one good is a function of past experience (this is taken account of by an iterative implementation) and of a constraint formulated in terms of a fixed budget. The nonlinearity parameter  $\mu$  is as a decreasing function of the prices.

One might ask what happens if  $\mu$  is driven beyond the critical value of  $\mu = 4$ . In this case, large-scale erratic behavior may be expected, as the process is no longer confined to the previously invariant interval (cf. Fig. 15.14). Seen from the model side, the process that now can leave the confinement of the unit interval, will leave behind a Cantor structure of initial conditions that have not yet managed to explore new lands outside the interval. After a potentially chaotic transient, the system settles in a new area of stability, where the same scenario takes place anew, starting at rescaled small  $\mu$ . We believe that in particular the effects by technical shocks may adequately be described in this framework. A simple thought experiment, taking place in a sub-domain of economy, provides us with an illustrative practical model. Consider, e.g., fishing in Norway, starting in a fjord with a single boat, focusing, say, on salmon. The annual catch  $x_n$  will be small in this case and will only mildly affect the fish population (captured by a parameter  $\mu \ll 1$ ). Twice as large or a doubled number of boats will roughly double the catch  $\bar{x}$ , but will still have a

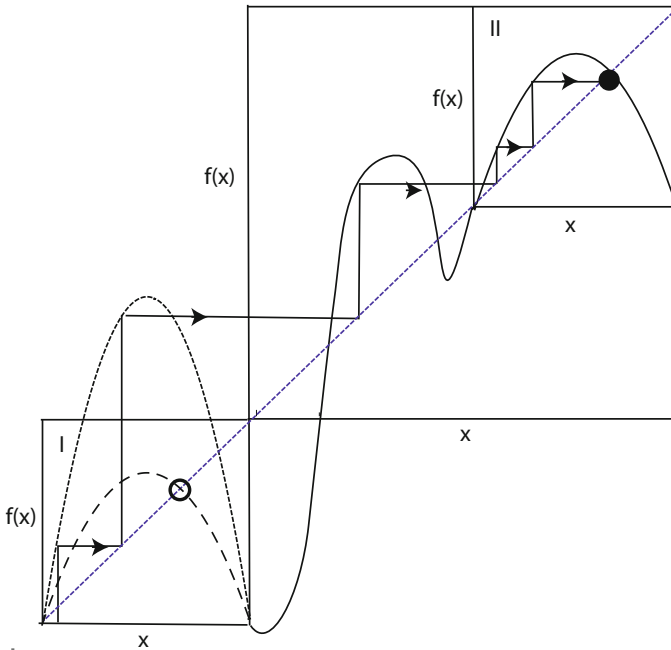


**Fig. 15.14** Mechanism of a crisis: Upon the increase of  $\mu$ , the previously stable fixed point (open circle) loses its stability. Later, the map leaves the unit-square confinement, and trajectories finally settle in another regime (box II) offering stable dynamics (full circle). The same mechanism will lead the process to yet another regime of stability, and so on

small effect on the fish population. This situation that can be captured by a roughly doubled parameter  $\mu$ . Guided by greed, this process holds on. The initially observed fixed point behaviour will finally lose its stability and a period doubling process is initiated, captured by  $\mu \rightarrow 4$  (such processes have indeed been observed in different ecological systems, like fish farms or sheep breeding). This is, because after a too large capture ( $x_n \approx a/4$ ), the system needs to recover. Finally, the fjord gets overfished, fishing enters a state of crisis (term ‘crisis’ is used in nonlinear dynamics in a closely corresponding context [13]), that holds on until a small number of larger ships equipped with novel technologies permit to exploit the whole of the Atlantic Ocean, fishing larger prey. The same pathway is then followed on this scaled-up environment, until fishing on this scale starts to have a profound environmental effect, this time on the ecological system of the Atlantic. After break down of fishing at this scale, swimming fish factories permit to do world-wide fishing, and the same process restarts on the world-wide scale. Finally, all oceans are overfished, where some of the fish species are endangered to the point of extinction. Traditional fishing then breaks down, forcing economics to develop novel technologies such as fish farms and leaving behind residuals of Cantor-set type of the traditional fishing (for an illustration see the sketch in Fig. 15.14).

## 15.5 Effects of Threshold (Limiter) Control

In real economics, the system state  $x$  (representing, e.g., demand or GDP) exhibits strong short-term fluctuations, often of local or external origin. Whereas in the case of small  $\mu$  such perturbations are stabilised by the system itself, for larger  $\mu$  they may lead to ever more long-lived erratic excursions. To incorporate these fluctuations into our model, we perturb  $x$  by multiplicative noise, for simplicity chosen uniformly distributed over a finite interval. The size  $str$  of the interval from which we sample the noise, is a measure for the amount of noise. To improve the predictability of economics under these circumstances, it is natural to apply control mechanisms to  $x$ ; to study the fundamental effects such a control has on the system behaviour, we have to choose the simplest control tool available that does not additionally complicate the behaviour of the system and the properties of which are well understood. The most natural control candidate with these properties is hard limiter control HLC [8, 9, 29, 43, 45]. This control mechanism simply acts by simply asking the value of  $x$  to not exceed a certain limit, a control mechanism that is simple and in reality often is imposed. In Fig. 15.15, three time series were generated by this model at fixed parameter  $\mu$  leading, in absence of noise, to superstable period-four orbit (for the definition of (super)stability of orbits see, e.g., [36]). Whereas the first time series represents the uncontrolled case, for the second series, a limiter at the highest cycle point was inserted, which is compared to a third series where the control was on the unstable period-one orbit. Even by the eye and quite against intuition, it is seen that the period-one orbit yields the highest average value  $\bar{x}$ .

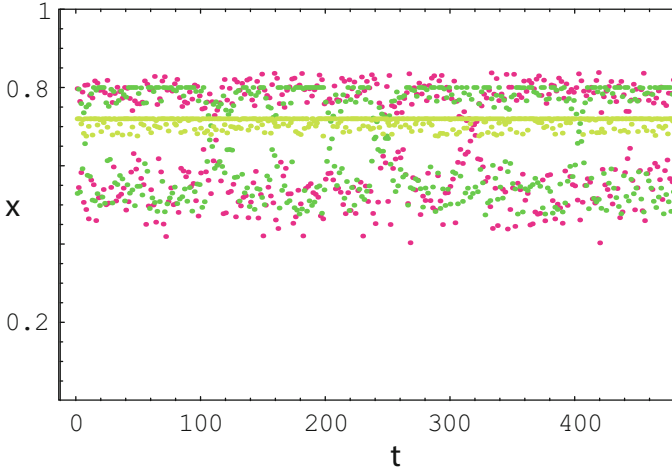


**Fig. 15.15** Noisy ( $str = 0.02$ ) time series  $x$  of a superstable period-four orbit. Red: uncontrolled; dark green: controlled in the maximal cycle point; light green: controlled in the unstable period-one orbit. Period-one orbit control yields the highest average  $\bar{x}$

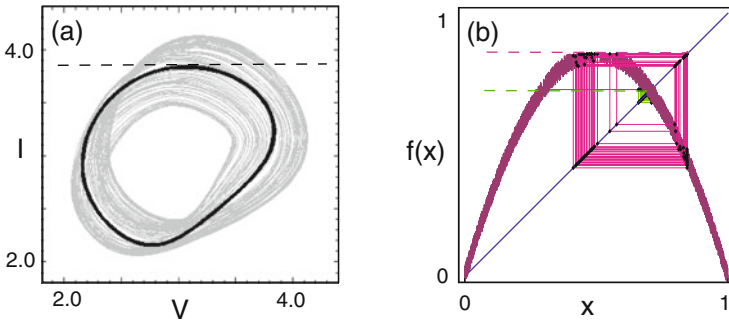


**Fig. 15.16** HLC for time-continuous and discrete dynamical systems with noise. Limiter positions are indicated by dashed lines. **(a)** HLC changes chaotic into period-one behaviour (modified from Corron et al. [9]). **(b)** HLC for the noisy logistic map. Placement of the limiter around the maximum of the map preserves the natural noisy period-two orbit (red). For lower placement, a modified period-one behaviour is obtained (green). Continuous dynamical systems can be mapped into discrete dynamical systems by using the method of Poincaré sections [31]

Exact results for the hard limiter control (HLC) have already been presented in this chapter. For reasons of convenience, we will once more exhibit the nontrivial features of this control: By introducing a limiter, orbits that sojourn into the forbidden area are eliminated (see Fig. 15.16). Modified in this way, the system tends to replace previously chaotic with periodic behaviour. By gradually restricting the phase-space, it is possible to transfer initially chaotic into ever

simpler periodic motion. When the modified system is tuned in such a way that the control mechanism is only marginally effective, the controlled orbit runs in the close neighbourhood of an orbit of the uncontrolled system. In a series of papers [8, 9, 29, 43, 45], this control approach was successfully applied in different experimental settings, and its properties were fully analysed.

The model demonstrates two interesting aspects of the control of dynamical systems. First, to some extent surprisingly from a naive physics point of view (d'Alembert's principle, for example), the natural system behaviour does not need to provide the economically most efficient working mode. Additional constraints can improve efficiency. Secondly, more surprisingly from an economics point of view, giving away—at absolutely no request in return, even without effects of feedback—can improve the efficiency of an economic system.

As has been already mentioned the time required to arrive in a close neighbourhood of the target orbit is an important characteristic of the control method. With the classical methods, unstable periodic orbits can only be controlled when the system is already in the vicinity of the target orbit. As the initial transients can become very long, algorithms have been designed to speed up this process [21, 37]. HLC renders targeting algorithms obsolete, as the control-time problem is equivalent to a strange repeller escape (control is achieved, as soon as the orbit lands on the flat top). As a consequence, the convergence onto the selected orbit is exponential [45].

It is also worthwhile emphasising that any control must be expected to have, beyond the effect of the control, a potentially strong effect on the system behaviour. The effects by HLC are fully described by one-dimensional systems. Due to the control, naturally and exclusively, only periodic behaviour is possible. Period doubling cascades emerge that have a super-exponential scaling  $\delta^{-1}(n) \sim 2^{-2^n}$  [45] and therefore are not of the Feigenbaum type. The convergence onto controlled orbits is exponential which renders targeting algorithms obsolete. Controlled orbits are unmodified original orbits only at bifurcation points of the controlled map. For generic one-parameter families of maps, all bifurcation points are regular, and isolated in a compact space. As a consequence, their Lebesgue measure is zero. These properties substantially modify the uncontrolled system behaviour.

## 15.6 Natural vs. Control-Induced Cycles

It is a natural general misunderstanding to believe that control methods only apply to inherently unstable systems. Unchanged control methods can similarly be used to control on unstable orbits of inherently stable systems. In either case, the control effort should be minimal. In the noise-free case, we have achieved optimal control if after an initial phase the controller does no longer exercise any noticeable strain. For HLC, this is naturally the case at the bifurcation points of the controlled map. Questions that remain are whether a corresponding statement also holds true for noisy systems, and on which of the orbits we should control.

Economic systems start their evolution in a noisy but stable period-one state, rendering economic predictions as simple as can be. To reduce noise, a limiter can be placed close to, or on top of the periodic point. As the system changes into a period-two, the question is whether to maintain control on the unstable period-one cycle, or whether to move on to the stable period-two. While intuition seems to favour the control of period-two (following a least effort principle, the natural tendency would suggest to follow the ‘natural’ system state), in fact, maintaining the period-one control is preferable, from most economic aspects. Not only that predictions of systems controlled in the latter way are simpler and therefore offer, as a consequence, simpler economic policies. Also most economic indicators (taxes, budgets, etc.) are evaluated over a period of 1 year. Finally, and even most importantly, the period-one  $x$ -average will be generally higher than that of the controlled period-two, as well as of any other higher-order cycle. This is a simple consequence of the convexity of the nonlinear map and can easily be proved. To abruptly change a natural higher-order periodic behaviour into a period-one state requires, however, generally a relatively strong initial control action. That this is beneficial nonetheless may appear as counter-intuitive to the public, and needs to be communicated in a well-formulated accompanying economic policy statement.

When the time-scale over which the external parameter  $\mu$  varies becomes comparable to the cycles wavelength, the optimality of the afore described control may break down, as continued adjustments need to be made in order to follow the changing location of the period-one. In this case, it may be preferential to control on the natural cycle. The most obvious control goal would be in this case to control the system as closely as possible along the underlying noise-free system. In the numerical control results presented below, we have dealt with both mentioned control strategies.

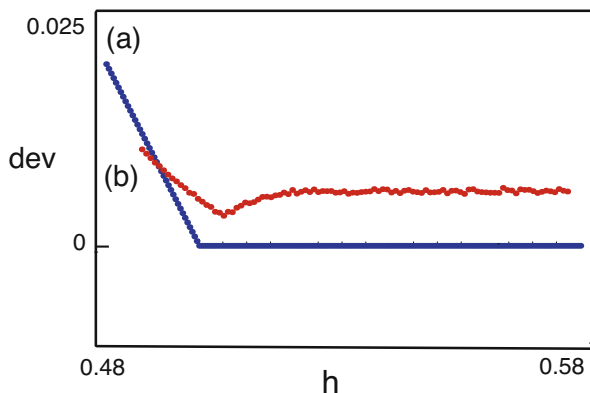
## 15.7 Detailed Control Results

The absolute difference between the ‘natural’ underlying solution and the controlled solution, per step, provides a suitable measure to assess the efficacy of a control.

### Control in the Regime of Stable Systems

If the underlying system is of periodicity larger than one and the control is on a period-one fixed point, then the control distance becomes particularly large and therefore this measure cannot be used for this case. For our numerical investigations, we restrict ourselves therefore to the control on superstable orbits (by choosing  $\mu = 2$  and  $\mu = 1 + 5^{1/2}$ , for the periods one and two, respectively), and apply the control at the cycle maximum. As a measure of efficacy, we calculate the average deviation of the noisy controlled relative to the noise-free system, denoted by  $dev$ , as a function of the noise and of the limiter position  $h$ . This seems to reflect best the natural tendency of the system to return into the vicinity of the uncontrolled noise-free system once the control is relaxed.

**Fig. 15.17** Dependence of  $dev$  on the control point  $h$  (summation over 500 orbit points, period-one orbit). **(a)** For zero noise, a piecewise linear function with a minimum (= optimal noise-free control point) emerges. **(b)** In the presence of noise ( $str = 0.02$ ), the function becomes nonlinear, with a nonzero minimum at the optimal noise-free control point



We find that for zero noise,  $dev(h)$  is a piecewise first order function (shown in Fig. 15.17 for the period-one orbit), where the nonzero slope, associated with  $h$  below the maximum of the function, depends on the periodicity and on the amount of nonlinearity expressed by  $\mu$ .

In the presence of noise, the formerly piecewise linear function becomes nonlinear, with the minimum being situated at the optimal control point of the noise-free system. For noise strengths  $str < 0.1$  considered to cover the realistic cases, the deviation is a function of first order in  $str$  (see Fig. 15.17b). The stronger the required corrections, the more the orbit histograms focus around the control point. The controlled orbit, however, deviates ever more from the original system orbit, which leads to a fast increase of  $dev$ .

The control on the superstable period-two orbit yields a similar picture. One important difference, though, is that the amount of noise under which control can still be maintained, decreases considerably. Yet, for stable orbits, control can beneficially be applied up to relatively large noise levels ( $str \sim 0.08$ ).

Control is lost when due to the effect of noise, interchange of orbit points occurs. This is the reason why in the presence of a substantial amount of noise, only low-order cycles can be controlled. For a period-four orbit, already a noise level of  $str > 0.01$  leads to the loss of control. Interestingly, the function  $dev(h, str)$  scales linearly with  $str$  (identical curves emerge, if  $h$  and  $dev$  are replaced by  $h/str$  and  $dev/str$ , respectively). As a rule of thumb, by means of optimal control, the deviation can be reduced by a factor of  $\sim 0.5$ .

### Control in the Regime of Chaotic Systems

If the underlying system is in the chaotic regime, all cycles are unstable, and the control on any of them is, from the point of view represented by the control distance, a-priori equally well justified and natural. Particularly favourable for economics is the fact that control can be established on a period-one orbit with zero control distance in the limit of vanishing noise.

For further investigations we again focus on the fully developed logistic map ( $\mu = 4$ ). To have control on true system orbits, the bifurcation points (cf.



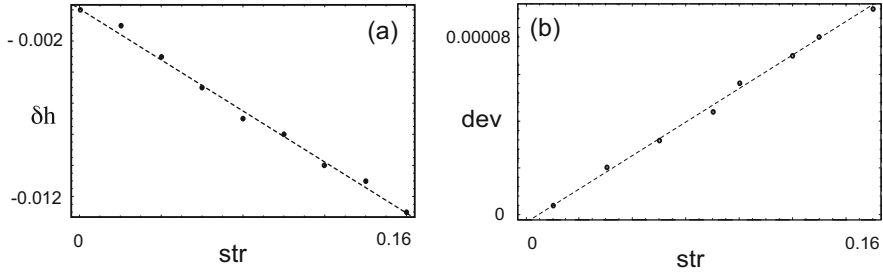


**Fig. 15.18** Results for the chaotic regime, where an unstable period-two orbit is controlled. **(a)** First order dependence of the optimal control point displacement  $\delta h$  on the noise strength  $str$ . **(b)** First order dependence of  $dev$  at the optimal control point, on the noise strength  $str$

Fig. 15.11a) must be chosen as the control points, the location of which can be determined analytically [45]. Without control, chaos prevents the system from staying on a given cycle. Accordingly, the efficacy of the control is measured as the difference between controlled noise-free and controlled noisy systems. In order to obtain a period-one orbit in the noise-free case, the limiter has to be adjusted to  $h = 0.75$ . Experiments show that in the presence of noise, the optimal control point moves away from the noise-free optimal control point. This is in contrast to the behaviour in the stable regime, and may be exploited to distinguish between the two cases.

The displacement is a linear function of the noise strength, as is the deviation  $dev$  measured at the optimal shifted control point. To provide an unstable noise-free period-two orbit, the controller was adjusted at  $h = 0.904$ . Again, the optimal control point's displacement and the minimal deviation are a function of first order in the noise strength (see Fig. 15.18a, b). The shift of the control point extends over an interval of more than  $\delta h = 0.1$ , and therefore is of a size comparable to the added noise.

Controlling period-four orbits yields an even stronger shift from the optimal noise-free controller position at  $h = 0.925$ . The amount of sustainable noise, however, is further reduced if compared to period-two (by a factor of  $\sim 0.5$ ). Beyond a noise strength of  $str = 0.04$ , the orbit escapes control.

## 15.8 Conclusions

Control mechanisms of limiter type are common in economics. Quite contrary to the expected and desired effect, it is inherent to this control method that superstable system behaviour is generated, irrespective whether the underlying behaviour periodic or chaotic. A first guess remedy would be the frequent change of the position of the limiter, to compensate for the amplified or newly created cyclic behaviour. This strategy, however, will generate even ever more erratic system

behaviour. Our analysis shows that it is more advantageous to keep the limiter fixed, adjusting it only over time scales where the system parameter  $\mu$  changes noticeably. In this way, reliable cycles of smaller periodicity will emerge. Among these cycles, period-one is generally the optimal one, also seen from most economic perspectives. To recruit this state, a strong initial intervention may be necessary, and the control must be permanent. Otherwise, a strong relaxation onto the suboptimal natural behaviour sets in. In the context of economics, these properties will be used as natural arguments against our proposed control. On the plus side, a very simple control policy can be formulated, which is of primary interest for western democracies.

To maximise system output  $\bar{x}$ , the minimal distance to the noise-free dynamics could be chosen as the control target. We demonstrated that when  $\mu$  varies slowly, this control generally does not lead to the optimum. If superstable orbits are controlled at the highest orbit point of the noise-free behaviour, the location of the optimal control point is independent from the noise strength. In the chaotic regime, in contrast, the optimal control point is displaced, by a function of first order in the noise strength. Controlling at this point reduces the *dev*-error roughly by one fourth, if compared to the control at the noise-free optimal point.

Detailed investigations show that the observed shift of the optimal control point also depends on the nature of the noise. If purely positive noise is added, the shift vanishes. From the perspective of economics, HLC-induced noise reduction can be regarded as a substantial improvement. Since the period-one orbit has substantial advantages, the control on the latter state is preferential.

Our framework could be of relevance for better understanding and monitoring economic behaviours. It has been found [1] that for either very underdeveloped or developed economies, stable fixed point behaviour is predominant. At an intermediate level, however, complex economics emerge that can induce chaotic dynamics of the entrepreneur's wealth,  $W_n$  [27]. In order to control this case, HLC in the form of a tax on assets with a sufficiently fast progression could be applied, forcing  $W_n$  to remain below a maximal value,  $W_{max}$ . With sufficient care, HLC on a period-one could be achieved, and excessive economic variations due to chaotic dynamics could be prevented. Political realisability will often require the use of 'softer' limiters (in the sense that  $W_n > W_{max}$  is not strictly prohibited), but the main features of HLC will be valid even in these cases (see our introductory part).

We emphasise that short-term cycles emerge on all levels of economics. It has become, e.g., a common observation, that the demands for certain professionals (in central Europe in particular for teachers) undergo large fluctuations, from 1 year to the next. In 1 year, severe problems are encountered in recruiting a sufficient number, so that the professional requirements have to be lowered, whereas in the next year, there is an excess supply. We propose to interpret this as the signature of an economy that has moved out of period-one behaviour. From the teaching quality as well as from the individual's biographies point of view, the occurrence of this effect should be prevented or smoothened. Our approach offers a perspective for understanding, studying and, potentially also engineering, such phenomena.

Our final remark refers to a possible interpretation of hard limiter control in economics and its connection with ethics and—potentially— even into the direction

of religion. We have found that controlling on a period-one orbit is often the optimal control strategy. Focusing on period-one in terms of GDP entrains to think about what should be done with ‘what is above’ this desired state. The most consistent interpretation probably is, that this is what can be given away, without suffering any loss in the longer term. In real world, such a control would be connected to annihilating or dispose a part of the economic power above the period-one state. Economic power that otherwise could be used, at a higher price to be paid for this later. Put in a nutshell, our investigations can be seen as pointing into the direction that sharing or giving away can be—contradicting principles of human individual selfishness—very beneficial for all. Religions emphasising this point as a religious policy have probably understood this point at an intuitive level; they might even have become successful not least because this attitude leads to more successful economies.

## References

1. Aghion, P., Bacchetta, P., Banerjee, A.: Financial development and the instability of open economies. *J. Monetary Econ.* **51**(6), 1077–1106 (2004)
2. Artuso, R., Aurell, E., Cvitanovic, P.: Recycling of strange sets: I. cycle expansions. *Nonlinearity* **3**(2), 325 (1990)
3. Artuso, R., Aurell, E., Cvitanovic, P.: Recycling of strange sets: II. Applications. *Nonlinearity* **3**(2), 361 (1990)
4. Bala, V., Majumdar, M., Mitra, T.: A note on controlling a chaotic tatonnement. *J. Econ. Behav. Organ.* **33**(3–4), 411–420 (1998)
5. Benedicks, M., Carleson, L.: On iterations of  $1 - ax^2$  on  $(-1, 1)$ . *Ann. Math.* **122**(1), 1–25 (1985)
6. Benhabib, J., Day, R.H.: Rational choice and erratic behaviour. *Rev. Econ. Stud.* **48**(3), 459–471 (1981)
7. Boldrin, M., Montrucchio, L.: On the indeterminacy of capital accumulation paths. *J. Econ. Theory* **40**(1), 26–39 (1986)
8. Corron, N.J., Pethel, S.D., Hopper, B.A.: Controlling chaos with simple limiters. *Phys. Rev. Lett.* **84**(17), 3835 (2000)
9. Corron, N.J., Pethel, S.D., Hopper, B.A.: A simple electronic system for demonstrating chaos control. *Am. J. Phys.* **72**(2), 272–276 (2004)
10. Feigenbaum, M.J.: The universal metric properties of nonlinear transformations. *J. Stat. Phys.* **21**(6), 669–706 (1979)
11. Garfinkel, A., Weiss, J.N., Ditto, W.L., Spano, M.L.: Chaos control of cardiac arrhythmias. *Trends Cardiovasc. Med.* **5**(2), 76–80 (1995)
12. Glass, L., Zeng, W.: Bifurcations in flat-topped maps and the control of cardiac chaos. *Int. J. Bifurcation Chaos* **4**(4), 1061–1067 (1994)
13. Grebogi, C., Ott, E., Yorke, J.A.: Crises, sudden changes in chaotic attractors, and transient chaos. *Phys. D: Nonlinear Phenom.* **7**(1–3), 181–200 (1983)
14. Hołyst, J., Żebrowska, M., Urbanowicz, K.: Observations of deterministic chaos in financial time series by recurrence plots, can one control chaotic economy? *Eur. Phys. J. B Condens. Matter Complex Syst.* **20**(4), 531–535 (2001)
15. Holyst, J.A., Hagel, T., Haag, G., Weidlich, W.: How to control a chaotic economy? *J. Evol. Econ.* **6**(1), 31–42 (1996)
16. Juglar, C.: Des crises commerciales et de leur retour périodique. ENS éditions (2014)

17. Kaas, L.: Stabilizing chaos in a dynamic macroeconomic model. *J. Econ. Behav. Organ.* **33**(3–4), 313–332 (1998)
18. Keynes, J.M.: *The General Theory of Employment, Interest and Money*. Macmillan Cambridge University Press (1936)
19. Kitchin, J.: Cycles and trends in economic factors. *Rev. Econ. Stat.* **5**, 10–16 (1923)
20. Kopel, M.: Improving the performance of an economic system: controlling chaos. *J. Evol. Econ.* **7**(3), 269–289 (1997)
21. Kostelich, E.J., Grebogi, C., Ott, E., Yorke, J.A.: Higher-dimensional targeting. *Phys. Rev. E* **47**(1), 305 (1993)
22. Kuznets, S.S.: *Secular Movement in Production and Prices: Their Nature and Their Bearing Upon Cyclical Fluctuations*. Houghton Mifflin, Boston (1930)
23. Kydland, F.E., Prescott, E.C.: Time to build and aggregate fluctuations. *Econometrica* **50**, 1345–1370 (1982)
24. Lorenz, H.W.: *Nonlinear Dynamical Economics and Chaotic Motion*, 2nd edn. edn. Springer, Berlin (1993)
25. Mariño, I.P., Rosa Jr, E., Grebogi, C.: Exploiting the natural redundancy of chaotic signals in communication systems. *Phys. Rev. Lett.* **85**(12), 2629 (2000)
26. Marx, K.: *Das Kapital*. Otto Meissner (1867)
27. Michetti, E., Caballé, J., Jarque, X.: Financial development and complex dynamics in emerging markets. In: *Proceedings of the New Economic Windows Conference, Salerno* (2004)
28. Montrucchio, L.: The occurrence of erratic fluctuations in models of optimization over infinite horizon. In: *Growth Cycles and Multisectoral Economics: The Goodwin Tradition*, pp. 83–92. Springer, Berlin (1988)
29. Myneni, K., Barr, T.A., Corron, N.J., Pethel, S.D.: New method for the control of fast chaotic oscillations. *Phys. Rev. Lett.* **83**(11), 2175 (1999)
30. Ott, E., Grebogi, C., Yorke, J.A.: Controlling chaos. *Phys. Rev. Lett.* **64**(11), 1196 (1990)
31. Peinke, J., Parisi, J., Rössler, O.E., Stoop, R.: *Encounter with Chaos: Self-Organized Hierarchical Complexity in Semiconductor Experiments*. Springer, Berlin (2012)
32. Pyragas, K.: Continuous control of chaos by self-controlling feedback. *Phys. Lett. A* **170**(6), 421–428 (1992)
33. Romeiras, F.J., Grebogi, C., Ott, E., Dayawansa, W.: Controlling chaotic dynamical systems. *Phys. D: Nonlinear Phenom.* **58**(1–4), 165–192 (1992)
34. Schuster, H.: *Deterministic Chaos: An Introduction*. Vch Verlagsgesellschaft mbH (1988)
35. Schuster, H.: *Handbook of Chaos Control*. Wiley, London (1999)
36. Schuster, H.G., Just, W.: *Deterministic Chaos: An Introduction*. Wiley, London (2006)
37. Shinbrot, T., Ditto, W., Grebogi, C., Ott, E., Spano, M., Yorke, J.A.: Using the sensitive dependence of chaos (the “butterfly effect”) to direct trajectories in an experimental chaotic system. *Phys. Rev. Lett.* **68**(19), 2863 (1992)
38. Sinha, S.: Unidirectional adaptive dynamics. *Phys. Rev. E* **49**(6), 4832 (1994). [https://scholar.google.com/scholar\\_lookup?title=Unidirectional%20adaptive%20dynamics&journal=Phys%20Rev%20E&volume=49&pages=4832-4842&publication\\_year=1994&author=Sinha%2CS](https://scholar.google.com/scholar_lookup?title=Unidirectional%20adaptive%20dynamics&journal=Phys%20Rev%20E&volume=49&pages=4832-4842&publication_year=1994&author=Sinha%2CS)
39. Sinha, S., Biswas, D.: Adaptive dynamics on a chaotic lattice. *Phys. Rev. Lett.* **71**(13), 2010 (1993)
40. Sinha, S., Ditto, W.L.: Dynamics based computation. *Phys. Rev. Lett.* **81**(10), 2156 (1998)
41. Stoop, R., Schindler, K., Bunimovich, L.: When pyramidal neurons lock, when they respond chaotically, and when they like to synchronize. *Neurosci. Res.* **36**(1), 81–91 (2000)
42. Stoop, R., Steeb, W.H.: Chaotic family with smooth Lyapunov dependence. *Phys. Rev. E* **55**(6), 7763 (1997)
43. Stoop, R., Wagner, C.: Scaling properties of simple limiter control. *Phys. Rev. Lett.* **90**(15), 154101 (2003)
44. Wagner, C., Stoop, R.: Optimized chaos control with simple limiters. *Phys. Rev. E* **63**(1), 017201 (2000)
45. Wagner, C., Stoop, R.: Renormalization approach to optimal limiter control in 1-d chaotic systems. *J. Stat. Phys.* **106**(1–2), 97–107 (2002)

**Part IV**  
**New Horizons for Understanding**  
**Economics**

# Chapter 16

## Kaldor–Kalecki New Model on Business Cycles



Giuseppe Orlando

### 16.1 The Model

Among the economic models, one of the most fruitful applications in the field of chaotic phenomena is that worked out by Kaldor in 1940 on the business cycle [18]. The author's intention, contrary to the traditional Keynesian multiplier–accelerator concept, was to explain from a macroeconomic viewpoint the fundamental reasons for cyclical phenomena.

However, the idea that the capitalist system could suffer from distinct and, in some ways, additional instabilities—such as the one worked out by Kaldor—prompted many authors to find out under which conditions abnormal behaviour could be produced, or under which conditions bifurcations or even chaos could be generated.

In Chap. 12 we presented the continuous time Kaldor model. Here we discuss the corresponding discrete time version

$$\begin{cases} Y_{t+1} - Y_t = \alpha(I_t - S_t) = \alpha[I_t - (Y_t - C_t)], \\ K_{t+1} - K_t = I_t - \delta K_t, \end{cases} \quad (16.1)$$

where  $Y$ ,  $I$ ,  $S$ ,  $K$  define income, investment, saving and capital, respectively. In Eq. (16.1)  $\alpha$  is the rate by which the output responds to excess investment and  $\delta$

---

Part of this chapter has appeared in [27, 28].

---

G. Orlando (✉)

University of Bari, Department of Economics and Finance, Bari, Italy

University of Camerino, School of Sciences and Technology, Camerino, Italy

e-mail: [giuseppe.orlando@uniba.it](mailto:giuseppe.orlando@uniba.it); [giuseppe.orlando@unicam.it](mailto:giuseppe.orlando@unicam.it)

represents the depreciation rate of capital. As seen in Chap. 12, Kaldor suggested that investment  $I = I(Y, K)$  and saving  $S = S(Y, K)$  are nonlinear s-shaped functions of income ( $Y$ ) and capital ( $K$ ).

Our proposed modifications are based on the following considerations. First of all, it should be noted that the difference in timing between consumption and investments reflects the process of observation, decision (including financing) and actual investment. Therefore, we can suppose that investment  $I_t$  at time  $t$  is proportional to a certain level of capital  $K_{t-1}$  at time  $t - 1$  according to a factor which is a function of the difference ( $K_{t-1}^d - K_{t-1}$ ) between desired capital  $K^d$  and owned capital  $K$ , i.e.

$$I_t = K_{t-1} \cdot f_1(K_{t-1}^d - K_{t-1}). \quad (16.2)$$

Similarly, consumptions  $C_t$  at time  $t$  can be taken proportional to income  $Y_t$  at the same time through a factor which is a function of the difference  $Y_t^d - Y_t$  between the desired  $Y^d$  and current income  $Y$ , i.e.

$$C_t = Y_t \cdot f_2(Y_t^d - Y_t). \quad (16.3)$$

Concerning the form of the function  $f_1(K^d - K)$ , it should be noted that the desired stock of capital depends on factors such as expected profit rate, expected level of output, etc. which can be linked to  $Y$ . In fact, for example, the simple accelerator model assumes that  $K$  is proportional to the level of production  $Y$  as follows:  $I = kY$  (where  $k$  is a parameter called “capital–output ratio”). The flexible accelerator model, instead, assumes that investments are modelled as  $I = s(K_{t-1}^d - K_{t-1})$ , where  $s \in (0, 1]$  is a coefficient representing the speed of adjustment. In the context of our model we assume that  $0 < f_1 < r$  for some  $r < 1$  (where  $r$  is a fraction of  $K_{t-1}$ ).

Function  $f_2(Y^d - Y)$  represents the fraction of income  $Y$  that is consumed; hence it is reasonable to assume that there exists a constant  $c > 0$  such that  $c < f_2 < 1$  everywhere. Notice that  $f_1$  and  $f_2$  are clearly increasing (the higher the difference between what is desired and what is owned is, and the higher is  $f$ ). According to Kaldor’s specifications  $I = I(Y, K)$  and  $C = C(Y, K)$  are sigmoidal [30]. In order to do so, most of papers on the Kaldor model have used the *arctg* function (see Fig. 16.1).

However, it is well known that the *arctg* function has some downsides from a numerical point of view (see Bradford and Davenport [6], Collicott [9], Walter [39], Gonnet and Scholl [10]) and it is not commonly used for modelling growth processes. Moreover, it prevents a connection to some important economical theories such as the classic Solow–Swan growth model.<sup>1</sup> For the abovementioned reasons, we suggest to use two variants of the *hyperbolic tangent* function, namely:

$$f_1(z_1) = \rho \frac{\exp(2z_1/\tau_1)}{\exp(2z_1/\tau_1) + 1} \quad \text{and} \quad f_2(z_2) = \frac{\exp(2z_2/\tau_2) + c}{\exp(2z_2/\tau_2) + 1}, \quad (16.4)$$

<sup>1</sup>For further considerations regarding this topic see Sect. A.2.

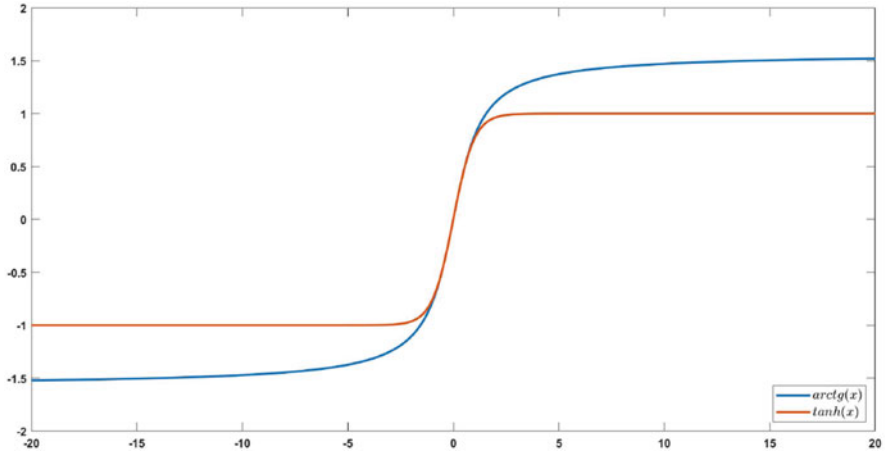


Fig. 16.1 Graph of  $arctg$  (blue) versus  $tanh$  (red)

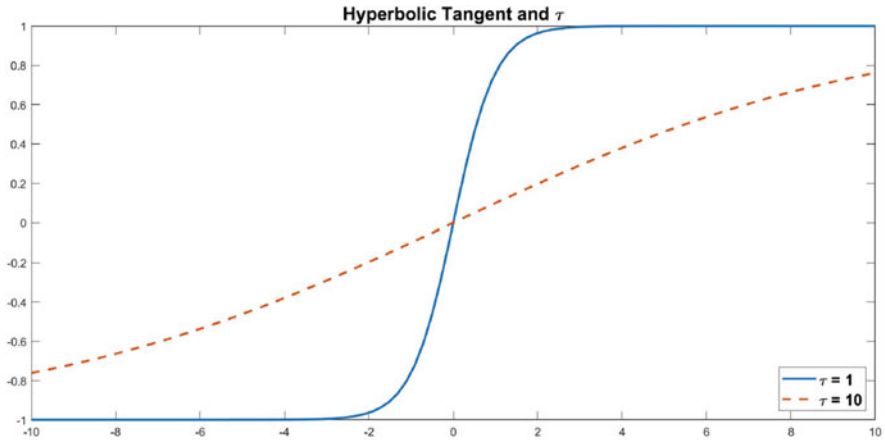


Fig. 16.2 Graph of the hyperbolic tangent showing how the parameter  $\tau$  determines the knee

so that  $f_1(z_1)$  goes to 0 as  $z_1 \rightarrow -\infty$  and tends to  $\rho$  as  $z_1 \rightarrow \infty$  whereas  $f_2(z_2)$  goes to  $c$  as  $z_2 \rightarrow -\infty$  and tends to 1 as  $z_2 \rightarrow \infty$ .  $\tau$  is the parameter controlling the slope of the function (see Fig. 16.2).

So far, we have specified the functions, but we still need to identify their arguments. We said that what counts for investment decisions is  $K^d$  and  $Y^d$ . As it is impossible to exactly know the desired values  $K^d$  and  $Y^d$ , we can infer them from the actual behaviour of economic agents as follows:

- As mentioned above, the desired stock of capital is associated with  $Y$  and  $K$ , hence it is legitimate to describe the difference  $K^d - K$  as a function of the difference between the relative income variation (defined as  $\Delta Y/Y$ ) and the



relative capital variation (defined as  $\Delta K/K$ ), i.e.

$$K_t^d - K_t = g_1 \left( \frac{Y_t - Y_{t-1}}{Y_{t-1}} - \frac{K_t - K_{t-1}}{K_{t-1}} \right). \quad (16.5)$$

If, for instance, the income variation (at time  $t - 1$ ) has been at 3%, a smaller capital growth (still at time  $t - 1$ ) could be interpreted by entrepreneurs as a need to adapt the stock of capital to economic growth (similarly to the Kalecki assumption (1935)[19] that the saved part of profit is invested and the capital growth is due to past investment decisions).

- Analogously, we can describe  $Y^d - Y$  as a function of the difference between the relative income variation and the relative consumption variation, i.e.

$$Y_t^d - Y_t = g_2 \left( \frac{Y_t - Y_{t-1}}{Y_{t-1}} - \frac{C_t - C_{t-1}}{C_{t-1}} \right). \quad (16.6)$$

Hence, we are assuming that the change in consumption is a kind of barometer of the state of health of the economy, so that, for example, in presence of high inflation, families revise and reduce their consumption. In other words, we want to give an account here of the variation in purchasing power due to inflation, or to those depressive effects of the business cycle (reduction of workers' contractual power, downsizing followed by dismissals, etc.) or the expansive effect (rise of real wages due to increased workers contract power because entrepreneurs need to expand production, easier access to credit, and so on).

Concerning the form of the functions  $g_1$  and  $g_2$ , we note that:

1. It is reasonable to assume that the difference  $x = \Delta Y/Y - \Delta K/K$  has an upper bound  $k > 0$ ,
2. For  $x = \Delta Y/Y - \Delta K/K > 0$  the difference  $K^d - K = g_1(x)$  increases with  $x$  and tends to  $+\infty$  (respectively  $-\infty$ ) as  $x \rightarrow k$  (respectively as  $x \rightarrow 0^+$ ),
3. For  $x = \Delta Y/Y - \Delta K/K \leq 0$  we can assume that  $K^d - K = g_1(x)$  has a constant negative value,
4. The same remarks can be made for the difference  $y = \Delta Y/Y - \Delta C/C$  and  $Y^d - Y = g_2(y)$

Hence, we shall assume that  $g_1 = g_2 = g$  has the form (see Fig. 16.3)

$$g(x) = \begin{cases} h & \text{for all } x \leq 0, \\ -\log((k/x)^s - 1) & \text{for all } x \in (0, k], \end{cases} \quad (16.7)$$

with  $h < 0$  such that  $f_1$  is close to zero. It should be noted that the shape of  $g$  is an approximation of the value function of Kahneman and Tversky [17] where on the left the function is assumed to be flat.

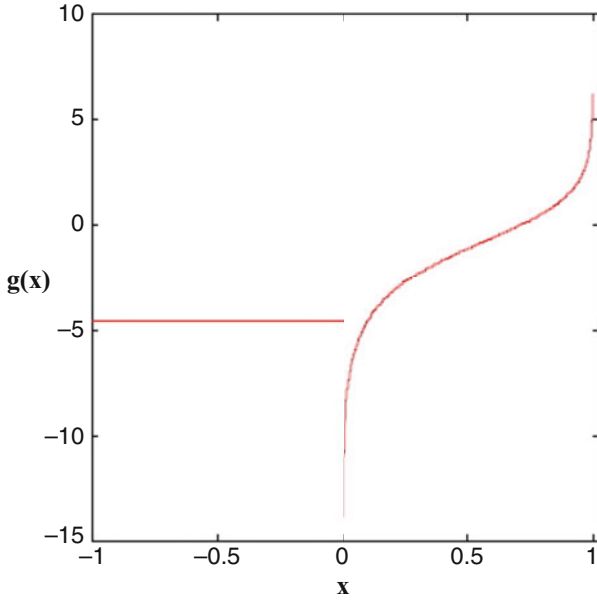


Fig. 16.3 Graph of  $g(x)$

To sum up, the proposed Kaldor model is

$$\left\{ \begin{array}{l} Y_{t+1} - Y_t = \alpha \left[ f_1 \left( g \left( \frac{Y_{t-1} - Y_{t-2}}{Y_{t-2}} - \frac{K_{t-1} - K_{t-2}}{K_{t-2}} \right) \right) + \right. \\ \qquad \qquad \qquad \left. f_2 \left( g \left( \frac{Y_t - Y_{t-1}}{Y_{t-1}} - \frac{C_t - C_{t-1}}{C_{t-1}} \right) \right) - Y_t \right], \\ K_{t+1} - K_t = f_1 \left( g \left( \frac{Y_{t-1} - Y_{t-2}}{Y_{t-2}} - \frac{K_{t-1} - K_{t-2}}{K_{t-2}} \right) \right) - \delta K_t. \end{array} \right. \quad (16.8)$$

These equations, together with (16.4) contain the parameters  $\alpha, \delta, \tau_1, \tau_2, \rho, \rho, k$  that have the following meaning:

1.  $\alpha$  is the coefficient denoting the speed adjustment of savings to investment. In the field of physics, its reciprocal is called delay and measures the time necessary for the adjustment. In other terms, if we assume that the time of reference 1 is equal to a year, then the savings will adjust themselves to the investment over this period. Therefore if  $\alpha = 1/2$ , this means to assert that 6 months are sufficient for achieving of the aforesaid adjustment. In general terms, we would assume  $\alpha$  to lay in the interval  $[1/4, 2)$ .

2.  $\delta$  is a percentage that determines the fixed capital which is lost during the productive process (due to obsolescence or actual consumption). In the model, when running simulations, we have chosen values between 3 and 6%.
3.  $\tau$  determines the “knee” of  $f$  function. It is, therefore, a measure of the reactivity of the function to the variation in its argument: as  $\tau$  grows the function is less steep. We have constricted ourselves to values between 1 and 20.
4.  $\rho$  measures the maximum possible level of investment in terms of capital. This value changes according to the economic system (pre-industrial, industrial, post-industrial) and the type of investment (i.e. high or low capital intensity). A reasonable choice is from the interval  $(0,0.2]$  where values around  $\rho = 0.16$  are optimal to describe our economy.
5.  $c = 1 - \hat{c}$  represents the average level of consumption. Its complement to 1, multiplied by actual income, determines the minimum level of consumption, therefore it is also called the “base” level. Similarly to  $\rho$ ,  $\hat{c}$ , is very sensitive to the type of economy in question, but in our context economically admissible values are assumed to be between 40 and 80%.
6. Parameter  $k$  changes according to the economic development. For instance, it could be that the percentage variation of  $Y - K$  (respectively— $C$ ) is low (for developed/less volatile economies) or high (for developing/more volatile economies). Experimentally we allowed maximum differences of around  $\pm 0.20\%$  for developed economies and  $\pm 1.20\%$  for developing economies.

In each of the abovementioned cases—for a quite broad range of parameters—we found that the model shows chaotic dynamics. In addition, the system can also be used for modelling lagged perturbations or shocks (see Sect. 16.1.1). Figures 16.4 and 16.5 illustrate two examples of the system’s dynamics that differ only because of their distinct initial conditions.

### 16.1.1 *Simulating Shocks in the Economy*

It is worth noting that using the proposed model it is possible to produce a shift that reflects the real situation mentioned by Kaldor, i.e., at a certain stage of the economy some factors exist that take place cumulatively and have the effect of shifting the saving and investment functions in one direction or another. In the model, this was achieved by operating a shift on  $f$  by adding or subtracting a value (i.e. the shock) to the argument. The shift operator gets into action when the capital or the income changes negatively; it has the effect of helping the system to recover from a crisis.

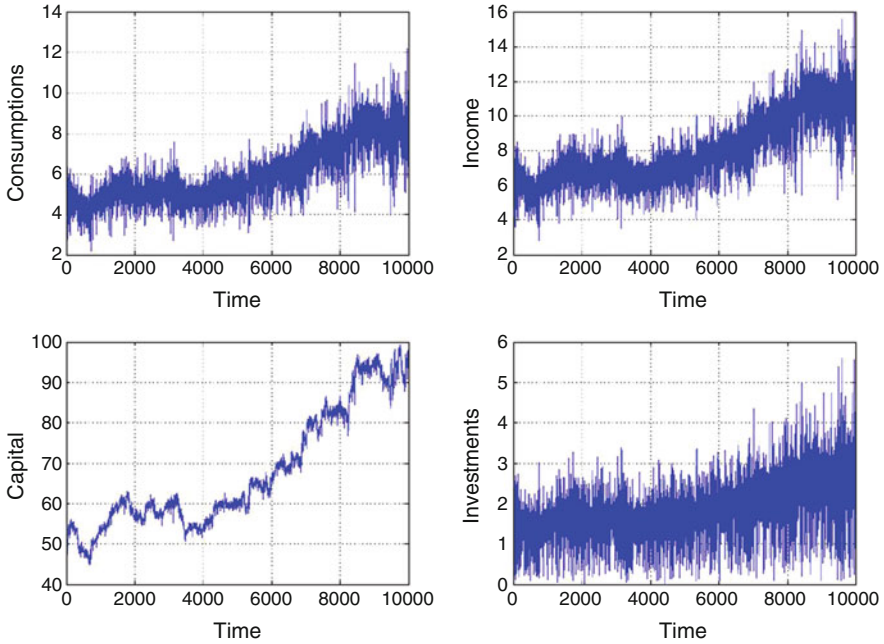


**Fig. 16.4** A simulation displaying a steady growth of the economy

### 16.1.2 *Consumptions, Savings and Economic Recessions*

The idea that an increase in the disposable income (possibly through fiscal stimulus such as tax rebates) automatically translates into an increase in the aggregate demand can be erroneous as it neglects the state of health of the economy (and therefore the confidence in it). In fact, if confidence in the economy is low, it could be that people may reduce their consumption during the recession years: consumers will continue the process of deleveraging (they use the money to pay off debt and save more) because of uncertainty in the future. For the abovementioned reason, in the suggested model we link the change in consumption to the change in income as follows (see (16.6)):

$$w = \frac{\Delta Y}{Y} - \frac{\Delta C}{C}, \quad (16.9)$$

which we believe describes correctly the behaviour of consumption.

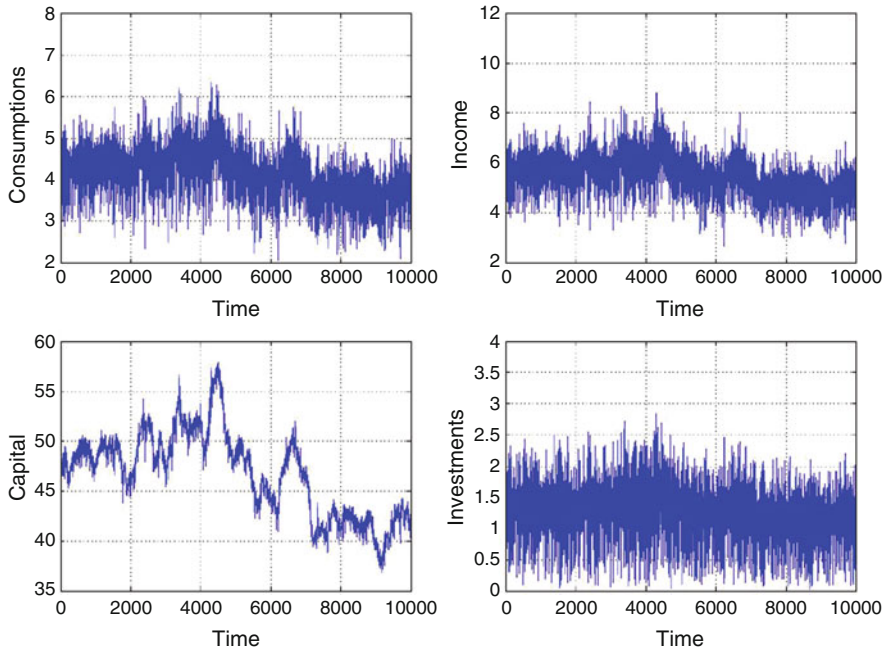


Fig. 16.5 A simulation displaying a steady economic decline

## 16.2 Numerical Proof of Chaotic Behaviour of the Model

Up to now the radical change dependence on initial conditions and the irregular trend of variables over time has only been showed graphically. This kind of evidence is not sufficient to prove the chaoticity of a system. Therefore we must use some numerical techniques in order to have a better insight of the possible chaotic nature of the system in Eq. (16.8). Specifically, we will report the results obtained by spectral analysis as well as the calculation of the correlation integral, the Lyapunov exponents, the Kolmogorov entropy and the embedding dimension discussed in earlier chapters.

### 16.2.1 Tools

Results shown in this Section were obtained using RRChaos [33] or MATLAB ver. 8.5.0.197613 (R2015a).

### 16.2.2 Spectral Analysis

As already mentioned, spectral analysis extracts the spectral content from a time series by decomposing it into different harmonics with different frequencies and, by doing that, it identifies the contribution of each harmonic to the overall signal (see for example Stoica and Moses [34]).

Spectral analysis may help identify chaos for a given time series to discover hidden periodicities in data. Yet, spectral analysis cannot distinguish if a signal is chaotic or stochastic, therefore this technique does not deliver a conclusive answer as observed by Moon [26] and (McBurnett [24]). However, as the proposed model is by construction deterministic, the spectral analysis can definitively help in understanding whether the system shows chaotic dynamics.

As an example the Figs. 16.6, 16.7 and 16.8 show the cobweb diagram, the orbit and the periodograms for different values of the parameters of the Logistic Maps.

For our Kaldorian system, we ran a simulation in order to show that for the generated time series there is no peak that clearly dominates all other peaks. Figure 16.9 and 16.10 show the behaviour of the power spectrum for the macroeconomic variables  $C, K, I, Y$  with rectangular and Hamming windows, respectively. The presence of several frequency peaks suggests that irregular orbits (chaos) can be identified in the proposed model.

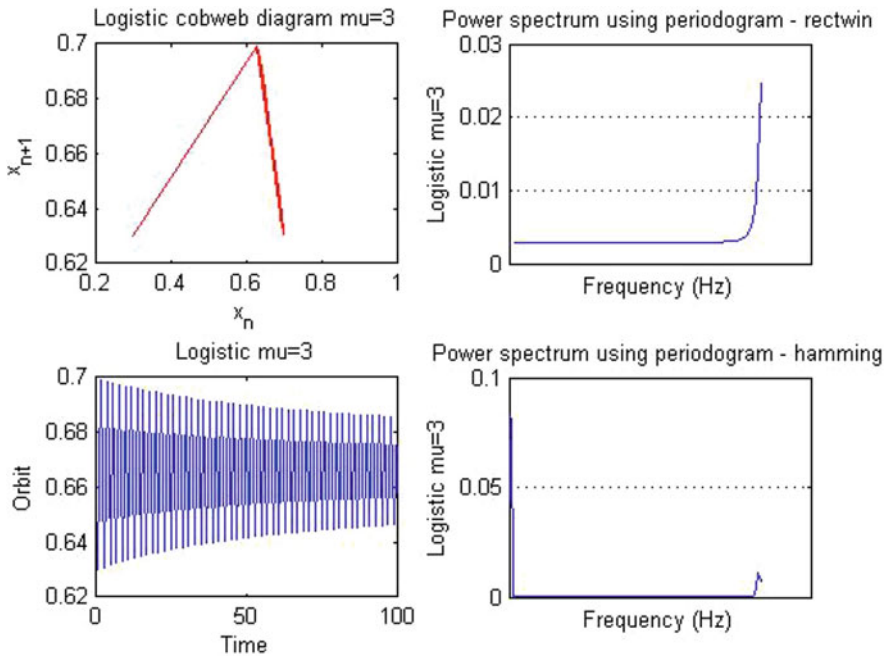


Fig. 16.6 Cobweb diagram and periodograms for the Logistic Map,  $\mu = 3$

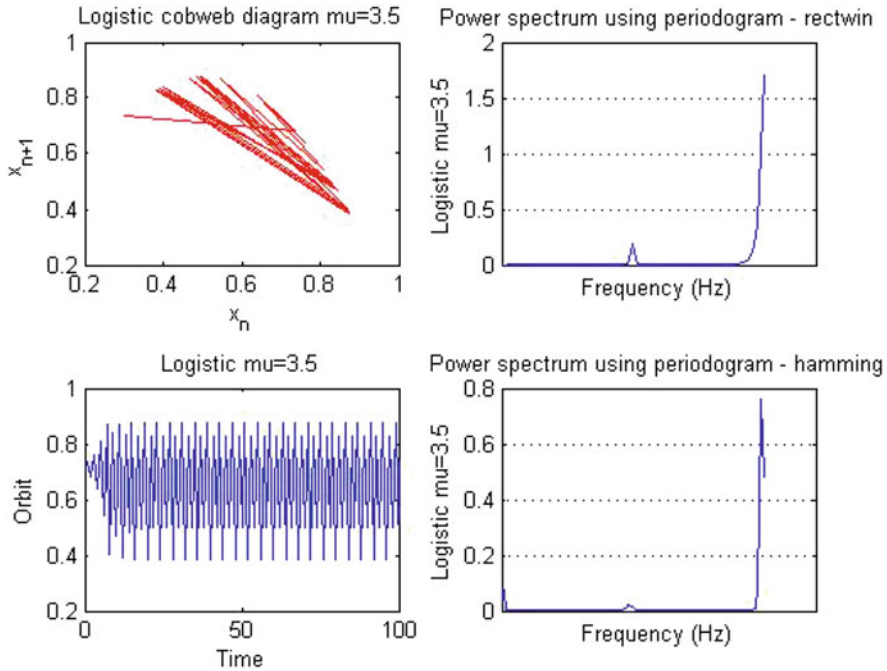


Fig. 16.7 Cobweb diagram and periodograms for the Logistic Map,  $\mu = 3.5$

### 16.2.3 Embedding Dimension

As discussed in Sect. 7.2, the embedding dimension is a statistical measure which indicates the smallest dimension required to embed an object (as for instance a chaotic attractor).

#### 16.2.3.1 Cao Embedding Dimension's Estimation

In order to compute this quantity, Cao [7] has suggested an algorithm based on the work of Kennel et al. [20] for estimating the embedding dimension (see [1, 37, 40]) through  $E1(d)$  and  $E2(d)$  functions, where  $d$  denotes the dimension. The function  $E1(d)$  stops changing when  $d$  is greater than or equal to the embedding dimension staying close to 1. The function  $E2(d)$ , instead, is used to distinguish deterministic from stochastic signals. If the signal is deterministic, there exist some  $d$  such that  $E2(d) \approx 1$  whilst if the signal is stochastic  $E2(d)$  is approximately 1 for all the values (see also [3, 4]).

Figure 16.11 illustrates the behaviour of  $E1$  and  $E2$  function for consumption, investment, capital and income of the proposed model. As observed in Cao [8], when the quantity  $E2$  has values close to 1, with some oscillations for small dimension,

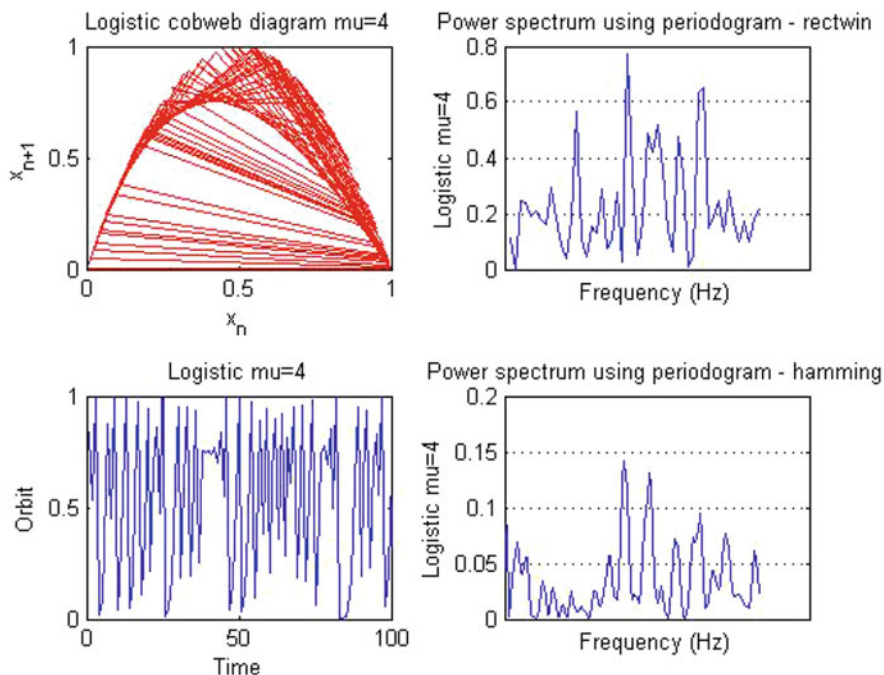


**Fig. 16.8** Cobweb diagram and periodograms for the Logistic Map,  $\mu = 4$ ; fully developed chaos, cf. Sect. 2.1)

the related time series is likely a random series. On the other hand, the presence of oscillatory behaviour away from 1 when embedding dimension is small implies some weak determinism in the considered time series. As it can be observed from Fig. 16.11 related to the proposed model, the quantity  $E2$  is not 1 but approaches this value for  $d \geq 10$ .

### 16.2.3.2 Symplectic Geometry Method

In addition to the Cao’s estimation, the symplectic geometry method (see M. Lei et al. [22], H. Xie et al. [43], M. Lei and G. Meng [21]) is used as a consistency check to verify the appropriate embedding dimension from a scalar time series. The symplectic similarity transformation is nonlinear and has measure-preserving properties i.e. time series remain unchanged when performing symplectic similarity transformation. For this reason symplectic geometry spectra (SGS) are preferred to singular value decomposition (SVD) (which is by nature a linear method that can bring distorted and misleading results e.g. see M. Palus and I. Dvorak [29]).



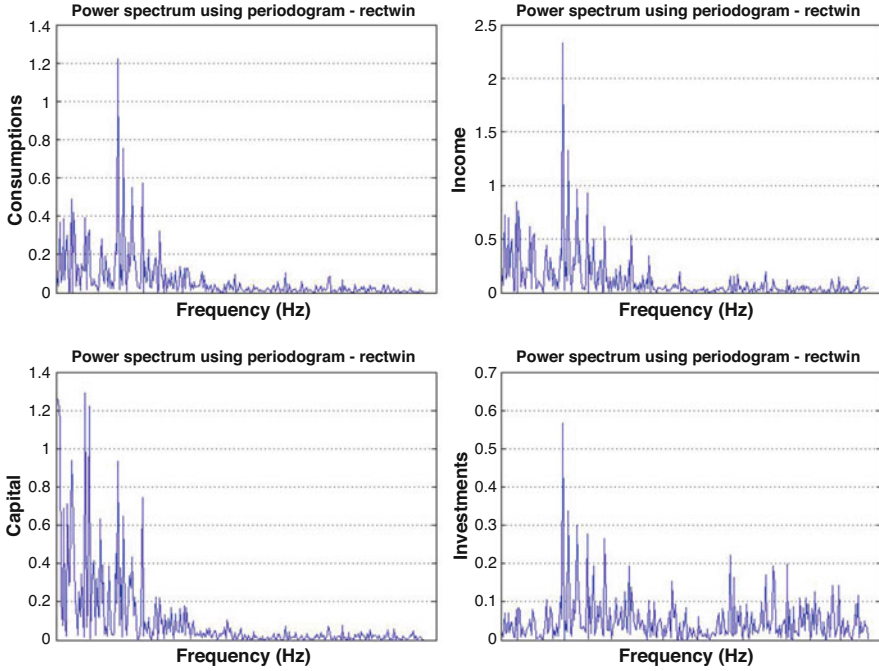


**Fig. 16.9** Power spectrum with rectangular window for  $K, I, C, Y$ . The irregularity of the spectrum hints at the possibility that the series are chaotic

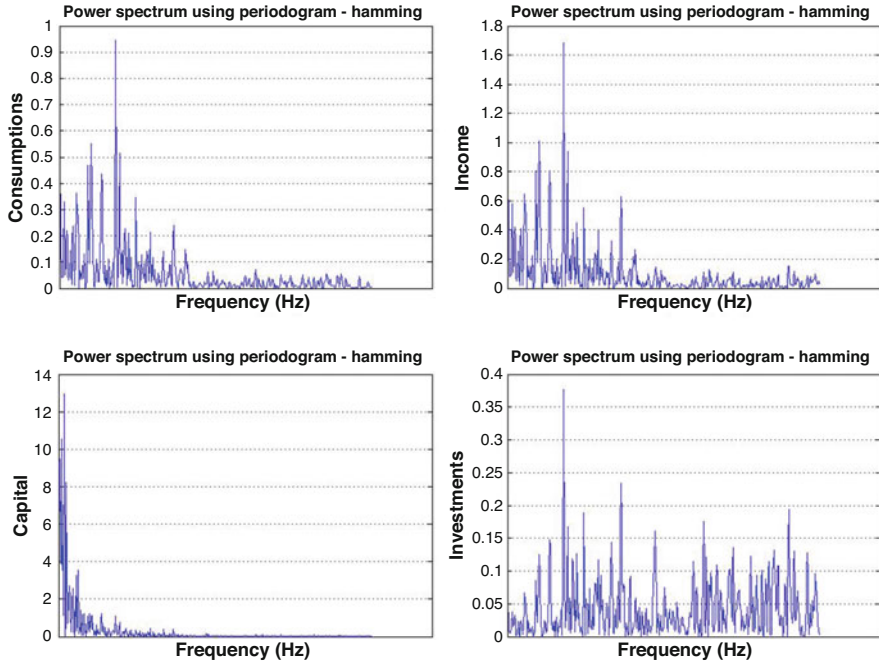
In Fig. 16.12a, b we show two examples of embedding dimension for a Gaussian white noise and the Logistic Map respectively, as obtained with the symplectic geometry method.

Figure 16.13 depicts the behaviour of the embedding dimension for consumption, investment, capital and income obtained using Symplectic Geometry Spectrum with Lei method. The behaviour of these curves is in accordance with that provided by other well-known chaotic systems in literature. This is another confirmation of the chaotic behaviour of the proposed model.

### 16.2.4 Correlation Integral

As mentioned in Sect. 6.3.2.1, the correlation integral  $C(r)$  of Eq. (6.12), measures the “degree of kinship” between two different points on the (strange) attractor and it “represents a direct arithmetic average of the pointwise mass function” Theiler [38].

In Fig. 16.14 we plot the value of the correlation integral versus  $r$ , and versus its logarithm in Fig. 16.15. It can be noted that when  $\ln(C(r))$  is plotted against  $\ln(r)$  the slope of the linear section can be interpreted as the dimensionality  $m$  of



**Fig. 16.10** Power spectrum with Hamming window for  $K, I, C, Y$ . The irregularity of the spectrum indicates that the series are chaotic

the phase-space orbit within that range of  $r$ . Finally the fact that  $\ln(C(r))$  increases regularly confirms that the system is deterministic.

### 16.2.5 Correlation Dimension

Another useful notion is the correlation dimension as defined in Definition 6.18 of Sect. 6.3.2.1. The correlation dimension is intended to measure the information content “where the limit of small size is taken to ensure invariance over smooth coordinate changes. This small-size limit also implies that dimension is a local quantity and that any global definition of fractal dimension will require some kind of averaging” [38].

In Fig. 16.16 it can be seen that the dimension of correlation is noninteger. As  $D_C$  is a “more relevant measure of the attractor than  $D^H$  because it is sensitive to the dynamical process of the coverage of the attractor” (Grassberger and Procaccia [13]), we can say that the system is fractal [11, 12].

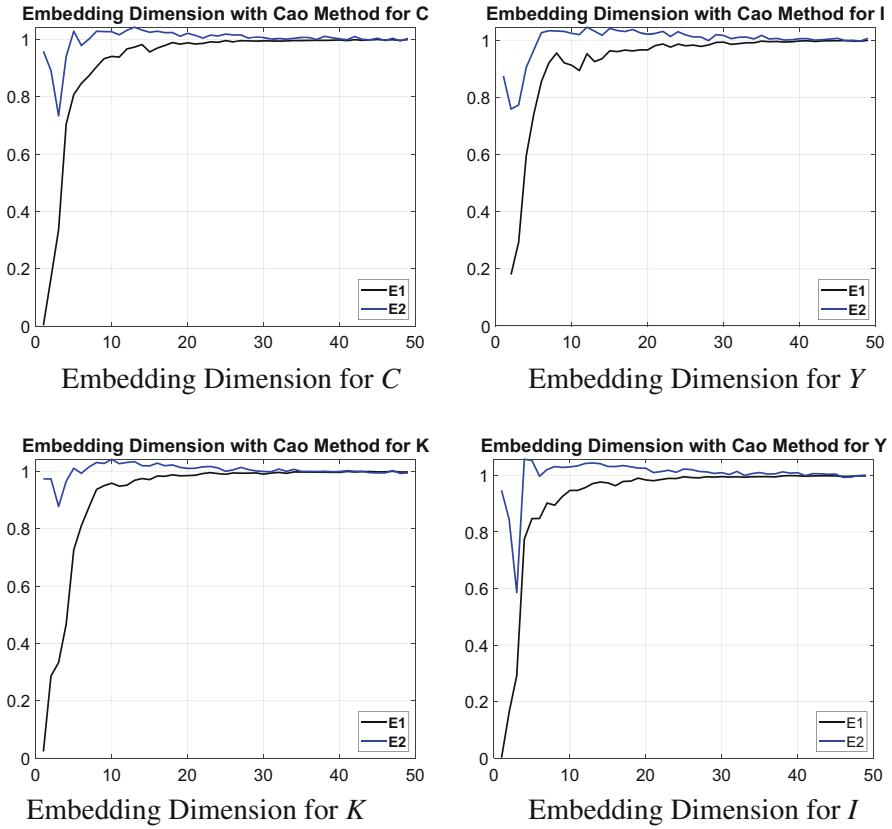
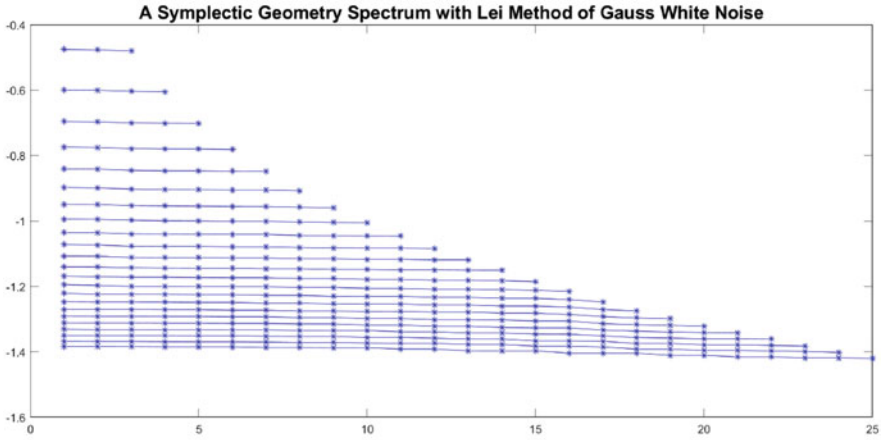


Fig. 16.11 Embedding Cao dimension ( $\tau = 1$ , data points = 10,000)

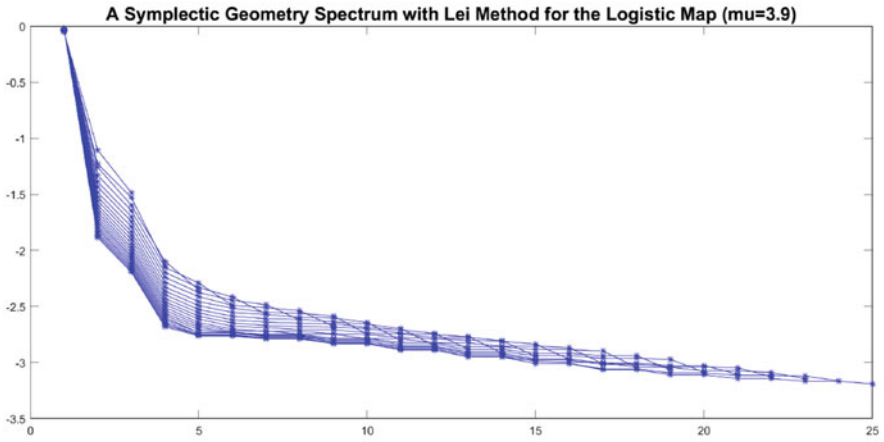
### 16.2.6 Lyapunov Exponents

Lyapunov exponents are used to measure the rate at which nearby trajectories of a dynamical system diverge (see Definition 6.6).

As a dynamic dissipative system is chaotic if its biggest Lyapunov's exponent is a positive number [23], we have adopted the Wolf algorithm [41, 42] to calculate the biggest Lyapunov exponent. Other methods can be found in Stoop [35, 36]. In our simulations, the calculated value has always been positive (see Table 16.1) with the calculated Lyapunov's exponents for 10,000 points simulated time series.



(a)



(b)

**Fig. 16.12** Embedding dimension symplectic geometry method. Ordinate is  $\log \frac{\sigma_i}{lr(\sigma_i)}$ , abscissa is  $i$ . The kink in the figure corresponds to the embedding dimension. **(a)** Embedding Dimension for a Gaussian white noise. **(b)** Embedding Dimension for the Logistic Map ( $\mu = 3.9$ )

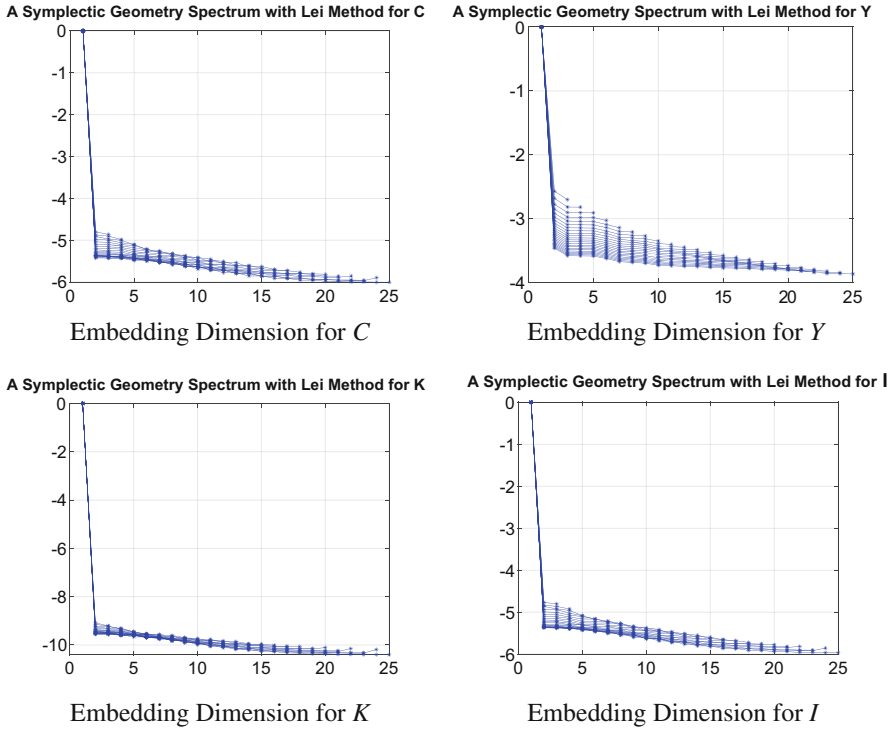


**Fig. 16.13** Embedding dimension symplectic geometry method (data points = 10,000). Ordinate is  $\log \frac{\sigma_i}{tr(\sigma_i)}$ , abscissa is  $i$ . The kink in the figure corresponds to the embedding dimension

### 16.2.7 Entropy

The Kolmogorov–Sinai  $KS$  entropy presented in Sect. 6.3.2.2 has been added to supplement the abovementioned analysis because  $KS$  converges to a positive value when time series are chaotic.

In order to measure  $KS$  we used the methodology suggested by J.C. Schouten et al. [31, 32] and we found that it was positive (e.g. Kolmogorov entropy = 21.34561, Kolmogorov entropy KML = 3.67711, relative standard error of KML[%] = 0.81194, total number of distances checked = 1,376,660, number of distances found = 15,280).

**Fig. 16.14** Correlation integral trend versus  $r$

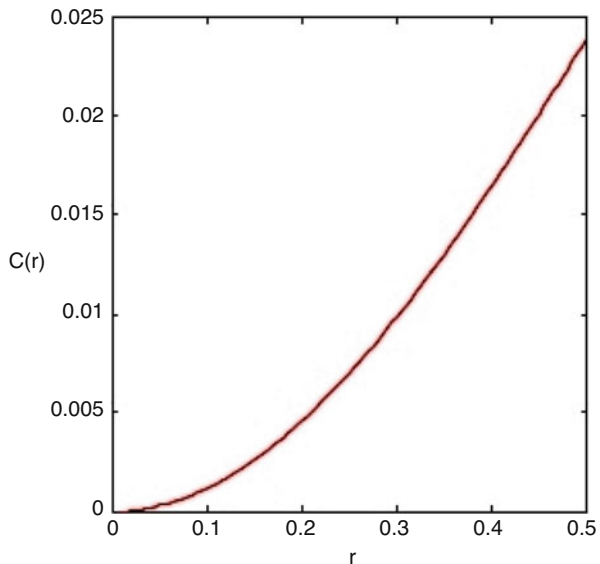


**Fig. 16.15** Log–log plot where the slope approximates the correlation integral

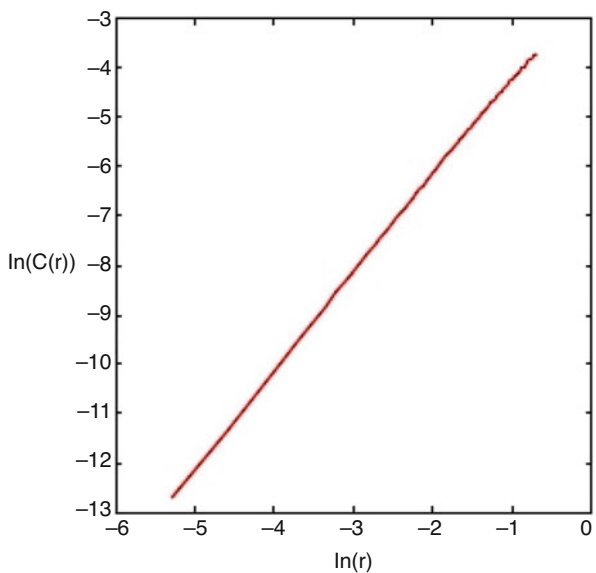


**Fig. 16.16** Correlation dimension when  $r \rightarrow 0$

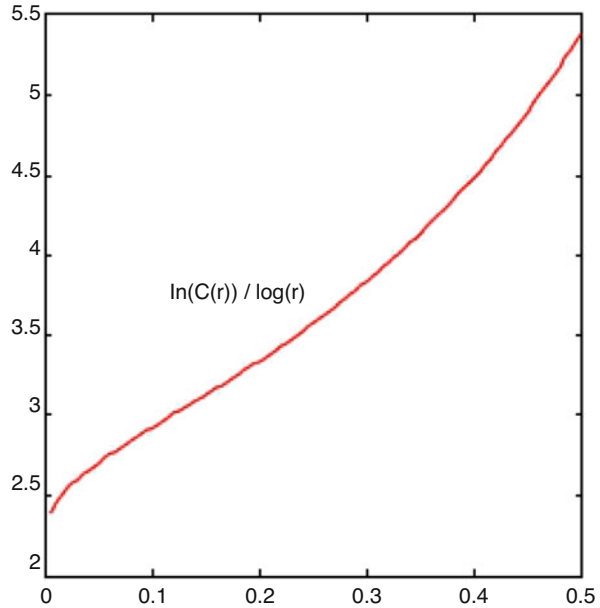


**Table 16.1** Lyapunov exponents

	Min	Max	Mean
Consumptions	6.22	11.399	10.885
Income	12.8338	19.6440	13.3534
Capital	7.3165	14.594	12.999
Investments	5.511	11.969	11.049

Notice that the iterated information corresponds to the embedding dimension

### 16.2.8 Chaotic Attractor

As we have repeatedly shown, the system behaves stochastically although we know that it is fully deterministic. In Table 16.2 we list the correlation integral versus the embedding dimension for 10,000 points time series of  $C$ ,  $Y$ ,  $K$  and  $I$ . Indeed, it can be observed that the correlation integral does not grow with the embedding dimension confirming that the system is deterministic [23].

Finally in Fig. 16.17 we present the strange attractor for the system obtained with software package RRChaos [33].

**Table 16.2** Correlation integral versus embedding dimension

Correlation integral for	Embedding dimension							
	2	3	4	5	6	7	8	
Consumptions	Min	0.053543	0.021604	0.0092081	0.0043155	0.0022121	0.0012546	0.00079854
	Max	0.71333	0.70895	0.70449	0.69998	0.69658	0.69372	0.69127
	Mean	0.30254	0.2599	0.23142	0.21153	0.19686	0.1859	0.17797
Income	Min	0.053543	0.021604	0.0092081	0.0043155	0.0022121	0.0012546	0.00079854
	Max	0.71333	0.70895	0.70449	0.69998	0.69658	0.69372	0.69127
	Mean	0.30254	0.2599	0.23142	0.21153	0.19686	0.1859	0.17797
Capital	Min	0.053543	0.021604	0.0092081	0.0043155	0.0022121	0.0012546	0.00079854
	Max	0.71333	0.70895	0.70449	0.69998	0.69658	0.69372	0.69127
	Mean	0.30254	0.2599	0.23142	0.21153	0.19686	0.1859	0.17797
Investments	Min	0.053543	0.021604	0.0092081	0.0043155	0.0022121	0.0012546	0.00079854
	Max	0.71333	0.70895	0.70449	0.69998	0.69658	0.69372	0.69127
	Mean	0.30254	0.2599	0.23142	0.21153	0.19686	0.1859	0.17797



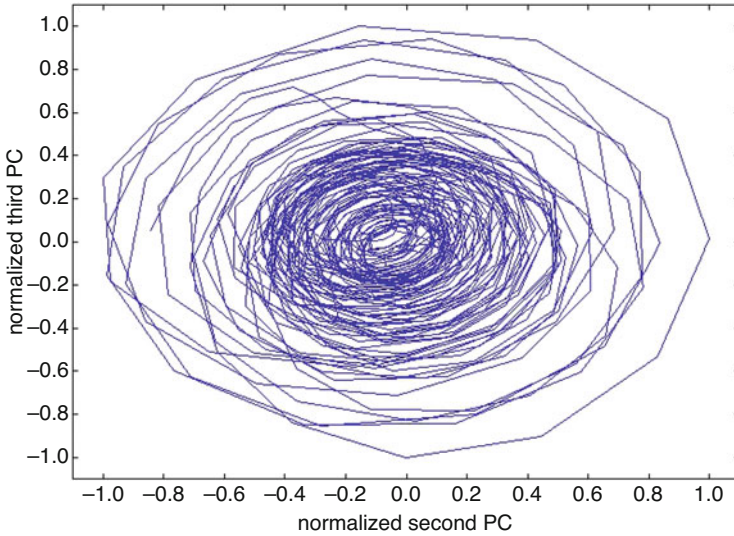


**Fig. 16.17** Strange attractor. Two-dimensional projection of the system in Eq. (16.8)

### 16.3 Conclusions

In literature, the usual set-up of the Kaldor's model use the trigonometric investment function  $\arctg$  [2, 5, 14–16, 25], etc. We have decided, instead, to try a variant of the hyperbolic tangent.

We wish to remark that an additional original contribution in our proposed model is the specification of consumption and investment as a function of the difference, respectively, between the growth rates of income and capital, and the growth rates of income and consumption. This has been achieved by considering, *à la* Kalecki, that the investment process has different timing than does consumption, hence the difference in the considered time lags (see Eq. (16.2) vs. Eq. (16.3)). Last but not least the model can accommodate external perturbations such as shocks by a translation of the argument of the function  $f$  (see Sect. 16.1.1).

### References

1. Adachi, M.: Embeddings and Immersions. American Mathematical Society, Providence (1993)
2. Agliari, A., Dieci, R., Gardin, L.: Homoclinic tangles in a Kaldor-like business cycle model. *J. Econ. Behav. Organ.* **62**, 324–347 (2007)
3. Arya, S., Mount, D.M.: Approximate nearest neighbor searching. In: Proceedings of the Fourth Annual ACM-SIAM Symposium on Discrete Algorithms (SODA'93), pp. 271–280 (1993)
4. Arya, S., Mount, D.M., Netanyahu, N.S., Silverman, R., Wu, A.Y.: An optimal algorithm for approximate nearest neighbor searching. *J. ACM* **45**(6), 891–923 (1998)

5. Bischi, G.I., Dieci, R., Rodano, G., Saltari, E.: Multiple attractors and global bifurcations in a Kaldor-type business cycle model. *J. Evol. Econ.* **11**, 527–554 (2001)
6. Bradford, R., Davenport, J.H.: Towards Better Simplification of Elementary Functions. In: ISSAC '02 Proceedings of the 2002 International Symposium on Symbolic and Algebraic Computation, pp. 16–22. ACM, New York (2002)
7. Cao, L.: Practical method for determining the minimum embedding dimension of a scalar time series. *Phys. D* **110**, 43–50 (1997)
8. Cao, L.: Determining minimum embedding dimension from scalar time series. In: Soofi, A., Cao, L. (eds.) *Modelling and Forecasting Financial Data. Studies in Computational Finance*, vol. 2, pp. 43–60. Springer, New York (2002). [https://doi.org/10.1007/978-1-4615-0931-8\\_3](https://doi.org/10.1007/978-1-4615-0931-8_3)
9. Collicott, S.H.: Never trust an arctangent (2012). [https://engineering.purdue.edu/~collicot/NTAA\\_files/Chapter1.pdf](https://engineering.purdue.edu/~collicot/NTAA_files/Chapter1.pdf)
10. Gonnet, G.H., Scholl, R.: *Scientific Computation*. Cambridge University Press, Cambridge (2009)
11. Grassberger, P.: Estimating the fractal dimension and entropies of strange attractors. In: Holden, A.V. (ed.) *Chaos*, pp. 291–311. Manchester University Press, Manchester (1986)
12. Grassberger, P., Procaccia, I.: Characterization of strange attractors. *Phys. Rev. Lett.* **50**, 346–349 (1983)
13. Grassberger, P., Procaccia, I.: Measuring the strangeness of strange attractors. *Phys. D* **9**, 189–208 (1983)
14. Januariao, C., Graaciob, C., Duarte, J.: Measuring complexity in a business cycle model of the Kaldor type. *Chaos Solitons Fractals* **42**(5), 2890–2903 (2009)
15. Janeiro, C., Gracio, C., Ramos, J.S.: Chaotic behaviour in a two-dimensional business cycle model. In: Elaydi, S., Cushing, J., Lasser, R., Ruffing, A., Papageorgiou, V., Assche, W.V. (eds.) *Proceedings of the International Conference, Difference Equations, Special Functions and Orthogonal Polynomials*, pp. 294–304. Munich (2005)
16. Kaddar, A., Alaoui, H.T.: Global existence of periodic solutions in a delayed Kaldor–Kalecki model. *Nonlinear Anal. Model. Control* **14**(4), 463–472 (2009)
17. Kahneman, D., Tversky, A.: Prospect theory: an analysis of decision under risk. *Econometrica* **47**(2), 263–292 (1979)
18. Kaldor, N.: A model of trade cycle. *Econ. J.* **50**(197), 78–92 (1940)
19. Kalecki, M.: A macrodynamic theory of business cycles. *Econometrica* **3**(3), 327–344 (1935)
20. Kennel, M.B., Brown, R., Abarbanel, H.D.I.: Determining embedding dimension for phase-space reconstruction using a geometrical construction. *Phys. Rev. A* **45**(6), 3403–3411 (1992)
21. Lei, M., Meng, G.: Symplectic principal component analysis: a new method for time series analysis. *Math. Probl. Eng.* **2011** (2011)
22. Lei, M., Wang, Z., Feng, Z.: A method of embedding dimension estimation based on symplectic geometry. *Phys. Lett. A* **303**(2–3), 179–189 (2002)
23. Lorenz, H.W.: *Nonlinear Dynamical Economics and Chaotic Motion*, 2nd edn. edn. Springer, Berlin (1993)
24. McBurnett, M.: Probing the underlying structure in dynamical systems: an introduction to spectral analysis, chap. 2, pp. 31–51. The University of Michigan Press (1996)
25. Mircea, G., Neamt, M., Opris, D.: The Kaldor and Kalecki stochastic model of business cycle, nonlinear analysis: modelling and control. *J. Atmos. Sci.* **16**(2), 191–205 (1963)
26. Moon, F.C.: *Chaotic Vibrations: An Introduction for Applied Scientists and Engineers*. Wiley, New York (1987)
27. Orlando, G.: Chaotic business cycles within a Kaldor–Kalecki Framework. In: *Nonlinear Dynamical Systems with Self-Excited and Hidden Attractors* (2018). [https://doi.org/10.1007/978-3-319-71243-7\\_6](https://doi.org/10.1007/978-3-319-71243-7_6)
28. Orlando, G.: A discrete mathematical model for chaotic dynamics in economics: Kaldor's model on business cycle. *Math. Comput. Simul.* **125**, 83–98 (2016). <https://doi.org/10.1016/j.matcom.2016.01.001>
29. Palus, M., Dvorak, I.: Singular-value decomposition in attractor reconstruction: Pitfalls and precautions. *Phys. D* **55**(1–2), 221–234 (1992)

30. Rosin, P.L.: Measuring sigmoidality. *Pattern Recogn.* **37**(8), 1735–1744 (2004)
31. Schouten, J., Takens, F., van den Bleek, C.: Estimation of the dimension of a noisy attractor. *Phys. Rev. E* **50**(3), 1851–1861 (1994)
32. Schouten, J., Takens, F., van den Bleek, C.: Maximum-likelihood estimation of the entropy of an attractor. *Phys. Rev. E* **49**(1), 126–129 (1994)
33. Schouten, J.C., den Bleek, C.M.V.: RRChaos, software package for analysis of (experimental) chaotic time series (1993). <http://reactorresearch.nl/handleidingen/rrchaos/rchaos.php>
34. Stoica, P., Moses, R.: *Spectral Analysis of Signals*. Prentice Hall, Englewood Cliffs (2005)
35. Stoop, R., Meier, P.: Evaluation of Lyapunov exponents and scaling functions from time series. *J. Opt. Soc. Am. B* **5**(5), 1037–1045 (1988)
36. Stoop, R., Parisi, J.: Calculation of Lyapunov exponents avoiding spurious elements. *Phys. D: Nonlinear Phenom.* **50**(1), 89–94 (1991)
37. Takens, F.: Dynamical systems and turbulence. In: *Lecture Notes in Mathematics*, vol. 898, chap. Detecting Strange Attractors in Turbulence, pp. 366–381. Springer, Berlin (1981)
38. Theiler, J.: Estimating fractal dimension. *J. Opt. Soc. Am. A* **7**(6), 1055–1073 (1990)
39. Walter, F.S.: *Waves and Oscillations: A Prelude to Quantum Mechanics*. Oxford University Press, Oxford (2010)
40. Whitney, H.: Hassler whitney collected papers. In: Eells, J., Toledo, D. (eds.) *Hassler Whitney Collected Papers. Contemporary Mathematicians*, vols. I, II. Birkhäuser, Basel-Boston-Stuttgart (1992)
41. Wolf, A.: Quantifying chaos with Lyapunov exponents. In: Holden, A.V. (ed.) *Chaos*, pp. 273–290. Manchester University Press, Manchester (1986)
42. Wolf, A., Swift, J.B., Swinney, H.L., Vastano, J.A.: Determining Lyapunov Exponents From a Time Series. *Phys. D.* **16**, 285–317 (1985)
43. Xie, H., Wang, Z., Huang, H.: Identification determinism in time series based on symplectic geometry spectra. *Phys. Lett. A* **342**(1–2), 156–161 (2005)

# Chapter 17

## Recurrence Quantification Analysis of Business Cycles



Giuseppe Orlando and Giovanna Zimatore

### 17.1 Introduction

There is a debate in the literature whether the dynamics of an economy is chaotic or stochastic, and whether shocks are endogenous or exogenous (e.g. RBC theory, Austrian School, Neo-Keynesian economics, etc.). Most studies concentrated on financial time series (e.g. stock indices) because of accessibility of data, frequency and length. For example, Mastroeni et al. [20, 21] found co-existence of stochastic and chaotic behaviour in copper time series and energy prices. In finance where data is abundant, both in terms of frequency and asset, results are mixed from no evidence, to weak evidence to evidence type [12]. Instead, in this book, with an extensive analysis on macroeconomic data (i.e. consumption, investment, capital and income), we focus on economic time series with the aim to investigate two issues. The first is the applications of recurrence plots, and their quantitative description provided by RQA, to dynamical regimes of business time series. The second issue we investigate is whether RQA can give some indications on the nature of business cycles as well, as on the nature of macroeconomic variables and the economy [30].

---

Part of this chapter has appeared in [30].

---

G. Orlando (✉)

University of Bari, Department of Economics and Finance, Bari, Italy

University of Camerino, School of Sciences and Technology, Camerino, Italy

e-mail: [giuseppe.orlando@uniba.it](mailto:giuseppe.orlando@uniba.it); [giuseppe.orlando@unicam.it](mailto:giuseppe.orlando@unicam.it)

G. Zimatore

eCampus University, Department of Theoretical and Applied Sciences, Rome, Italy

e-mail: [giovanna.zimatore@unicampus.it](mailto:giovanna.zimatore@unicampus.it)

RQA applications to economics and finance are not widespread, and started later than in other fields [5, 8, 14, 22, 38]. The interest in RQA by economists stemmed from the world financial crisis of 2007–2010, an event not anticipated by the mainstream of economic literature [16]. In fact, the majority of economists, basing their models on standard equilibrium, implicitly assumed that “economies are inherently stable and that they only temporarily get off track”, Colander et al. [7]. Moreover, the paradigm of the rational representative agent, “largely ignored” [7] the risk of new financial products and interconnections of markets. Therefore, RQA applied to economics was seen as a potential “tool for the revealing, monitoring, analysing and precursoring of financial bubbles, crises and crashes” Piskun and Piskun [34]. Fabretti and Ausloos [11] found examples in financial markets where RQA could detect a difference in state and recognize the critical regime, such that a warning before a crash (in their case 3 months in advance) would be given. Along this line, Addo et al. [1], looking for signals anticipating financial crises, highlighted “the usefulness of recurrence plots in identifying, dating and explaining financial bubbles and crisis”. In addition they claimed that the findings from the data analysis with recurrence plots “shows that these plots are robust to extreme values, non stationarity and to the sample; are replicable and transparent; are adaptive to different time series and finally, can provide better chronology of financial cycles since it avoids revision of crisis dates through time”. Strozzi et al. [35] studying the Nordic Spot Electricity Market Data confirm that determinism and laminarity detect “changes more clearly than standard deviation and then they provide an alternative measure of volatility”. Moloney et al. [22] investigating arbitrage-free parity theory for the Credit Default Swaps (CDS) and bond markets questioned the assumption of a stable equilibrium “which is central to the arbitrage-free parity theory”. In addition they found evidence of deterministic structures in the data and that “market is being trapped at certain levels” where “equivalence being trapped for a period of time is a characteristic of a nonlinear system (not a periodic or a random system)”.

## 17.2 Databases and Time Series

The variables on which we focus in the following study are: Capital (K), Consumption (C), investment (I) and Income (Y) (see Appendix A.1). Cyclical swings of economy are typically analysed in terms of the duration or the amplitude between a peak and the succeeding trough [4]. The cycle Peak-Trough-Peak (PTP) can be caused by various factors such as negative shocks in demand, in supply, in price and in credit (i.e. when “financial distress produces sharp discontinuities in flows of funds and spending and when the financial strains include tight monetary policy, much lessened availability of money and credit, sharp rises of interest rates, and deteriorating balance sheets for households, businesses, and financial institutions”) [10] as discussed by us in Chap. 11.

In order to study business cycles and recessions we will apply the RQA on time series extracted from different sources. This is because we want to have an extensive

set of data, with the highest number of points possible, covering the following dimensions: countries with different development paths (Sects. A.1.5 and A.1.3), differences in methods for computing the capital (M1, M2 Sect. A.1.5), gross versus net (Levy and Chen [17] Sect. A.1.4), etc. A further requirement was that, whenever possible, the number of time series should be balanced across variable or dimension.

For the variables  $K$  (capital),  $C$  (consumption),  $I$  (investment) and  $Y$  (income) modelled as described in Chap. 16, we collected 55 time series belonging to the following countries: Germany (DEU), Italy (ITA), Korea (KOR), United Kingdom (GBR), Turkey (TUR), Japan (JNP), Spain (ESP) and United States of America (USA). This in order not only to consider the evolution in time, but also to cover different types of economies (developed vs. developing, stagnating vs. expanding, etc.). Moreover, it is worth noticing that the aforementioned four variables differ in their units of measurement. In fact, the “stock” variable  $K$  represents the quantity existing at a certain point in time, whereas “flow” variables such  $C$ ,  $I$  and  $Y$  are measured over an interval of time. For this reason we balanced our dataset by gathering 41 flow and 14 stock variables.

### 17.2.1 Capital

As was mentioned in Sect. 17.1, while financial data are abundant and have many data points, economic time series are not many and data points are very few. This is especially true for capital stock (see Appendix A.1.4). In fact aggregate capital stock data is only collected on an annual basis. To analyse quarterly data, we considered the time series made available by Levy and Chen [17] who based their calculations on time series by: (a) Musgrave [23] for annual capital stock, (b) Citicorp [6] for investments and their price deflator series and (c) U.S. Bureau of Economic Analysis (BEA) for annual depreciation and discard figures.

Levy and Chen calculated quarterly data which is useful for “analysing the dynamic relationship between aggregate factors of production and output”; in fact “it is preferable to look at the data using quarterly observations because some dynamic phenomena that perhaps take place within the period of a year will not be captured if annual data is used. In addition, from an econometric point of view, the use of quarterly data instead of annual data quadruples the sample size which makes empirical statistical inference more reliable” [17].

Adopting the same basic notation, we: (1) distinguish between time series in nominal terms from time series in real terms (measured in 1987 dollars) by using the suffix 87; (2) denote Segmented Linear Interpolation as M1 and Numerical Iteration as M2; (3) adopt the following acronyms for the time series under scrutiny—Consumer Durable Goods (CDG), Producer Durable Goods and Equipment (PDG), Non-residential Business Structures (BS).

As was explained by Levy and Chen [17], the quarterly capital stock series are constructed using different procedures: “The first is a segmented linear year-to-year interpolation technique. The second technique exploits the dynamic relationship

between the capital stock and the corresponding capital investment series and uses annual beginning-of-the year and end-of-the-year capital stock data to estimate the implied quarterly depreciation rates for all three categories of the aggregate capital stock by numerical iteration over the depreciation rates until a convergence is achieved. These depreciation rates are then used along with the quarterly investment and the annual capital stock series to construct quarterly capital stock series" [17].

In our analysis, we focus on series built with Method 1 and 2 because, as shown by Dezhbakhsh and Levy[9] "linear interpolation of a trend stationary series superimposes a 'periodic' structure on the moments of the series" while, according to Jaeger's [13] "segmented linear interpolation reduces the size of shock persistence in a difference stationary series".

### ***17.2.2 Income, Investment and Saving***

Regarding the scope of our analysis we included countries that had very different development paths (see Appendix A.1.5) from the Organisation for Economic Co-operation and Development (OECD). OECD data are respectively

- Quarterly GDP Total, Percentage change, Quarterly National Accounts. This indicator is seasonally adjusted and it is measured in percentage change from previous quarter and from same quarter previous year [25].
- Investment (GFCF) Total, Annual growth rate (%). Aggregate National Accounts, SNA 2008 (or SNA 1993): Gross domestic product. Gross fixed capital formation (GFCF) is in million USD at current prices and PPPs, and in annual growth rates [24].
- Saving rate Total. % of GDP. National Accounts at a Glance [26].

### **17.3 Tools**

The basis of Recurrence Plots, RQA and RQE theory were discussed in Chap. 10. RQE computes recurrence quantifications on an epoch-by-epoch basis. The RPs shown in the following Figures were obtained with the CRP Matlab Toolbox ver. 5.22 rel. 32 [18]. RQA and RQE were obtained with the package RQA ver. 14.1 [37]. Statistical analysis was carried out by using Systat ver. 10.2 or MATLAB ver. 8.5.0.197613 (R2015a).

### **17.4 Results and Interpretation**

In this Section we show that, in some cases, early warning signals of dramatic changes (downturns/expansions) can be seen by computing recurrence variables within a moving window (epoch) shifted by a given number of points (delay)

throughout the whole sample (which is the RQE). Finally we demonstrate that RQA is a valid technique of investigation as it is able to distinguish between real and nominal data, as well as between net and gross time series.

### 17.4.1 Recurrence Quantification Analysis (RQA)

#### 17.4.1.1 Recurrence Plot (RP) on US GDP

Figure 17.1 shows the recurrence plot of US GDP% depicted right below its time series. From the RP, it is possible to observe the anticipating transitions to turbulent phases. The remarkable result consists of a correspondence between vertical lines in RP (i.e. chaos to chaos transitions) and the downturn/upturn periods.

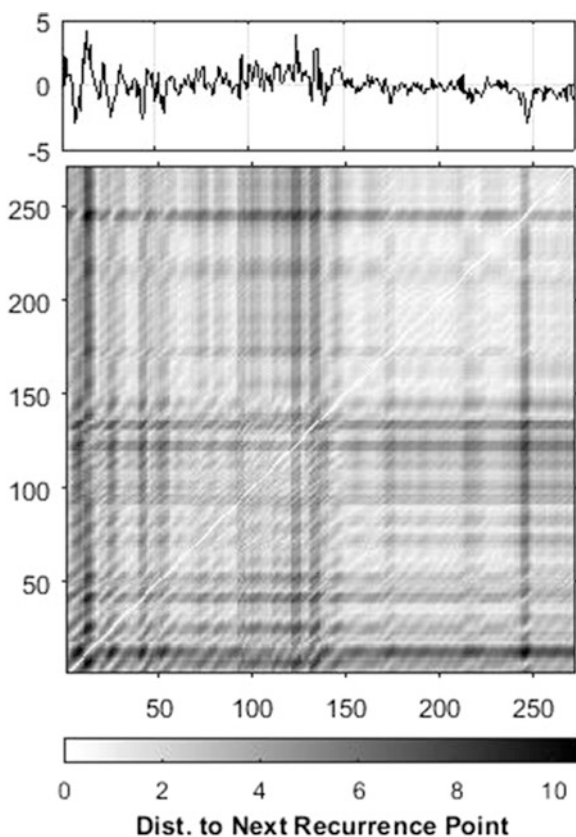


**Fig. 17.1** Changes in US GDP (above) and its Recurrence Plot (below). Data range: 01-01-1947 to 2016-01-01. ID: A191RP1Q027SBE. Gross Domestic Product, Percent Change from Preceding Period, Quarterly, Seasonally Adjusted Annual Rate. Source: St. Louis Fed, FRED database. Note the alignment between shocks and vertical lines in RP



### 17.4.1.2 RQA Applied to Business Cycle Data

RQA defines the overall complexity of the signal in terms of quantitative indices deriving from RP. Here, RQA was carried out on 55 time series from the dataset mentioned above (see Appendices A.1.3–A.1.5) with the following input parameters [37]: time lag (or delay: the spacing between selected input points) = 1; embedding = 10 (embedding dimension: estimated number of dominant operating variables); radius (largest normed distance at and below which recurrent points are defined and displayed) = 80; line (minimum number of sequential recurrent points required to define diagonal and vertical lines) = 5. Time lag = 1 has been chosen because, differently from financial time series, economic time series have few data. Moreover, as specified in Sect. 7.1.1, quarterly data are independent (they do not suffer from autocorrelation). The method chosen for normalizing vectors in higher dimensional space uses the Euclidean norm and *meandist* is the method for rescaling the recurrence matrix (i.e. the mean of rescaled distances) [19]. It is worth mentioning that the radius has been set with the objective of maximizing the difference among the time series of the whole dataset. This happens because when the radius is too large, the determinism can saturate, while when the radius is too small, few recurrences points in RP could not describe the differences among the time series.

While more details will be provided in Sect. 17.4.3, here we can tell in advance that with regard to US quarterly capital data, as reconstructed by Levy and Chen (see Table A.4), no significant differences have been observed between interpolation methods M1 and M2, while differences have been found to exist between real and nominal as well as between net and gross time series (see Table 17.1, row 1, where  $p > 0.1$  for all the RQA measures, PC1 and PC2).

**Table 17.1** Mann–Whitney *U* Test (*p*-values)

Row	#	Groups <sup>a</sup>	REC	DET	MAXLINE	ENT	TREND	LAM	TT	PC1	PC2
1	14 <sup>b</sup>	Method	0.796	1	0.301	0.439	0.796	0.439	0.439	0.897	0.197
2	55 <sup>c</sup>	Variable	0.001	<0.001	<0.001	0.028	0.002	<0.001	<0.001	<0.001	0.026
3	35 <sup>d</sup>	Country	0.071	0.253	0.436	0.162	0.157	0.126	0.469	0.253	0.146
4	55 <sup>e</sup>	Measure	<0.001	<0.001	<0.001	0.209	0.772	<0.001	0.967	<0.001	0.772

PC1 and PC2 calculated on REC, DET, MAXLINE and ENT

<sup>a</sup> **Method:** M1, M2; **Variables:** C, I, K, Y; **Country:** Germany (DEU), Italy (ITA), Korea (KOR), United Kingdom (GBR), Turkey (TUR), Japan (JNP), Spain (ESP), United States (USA); (Unit **Measure:** Flow, Stock; (Time Series')

<sup>b</sup> Number of time series considered by method: 8 M1, 6 M2

<sup>c</sup> Number of time series considered by variable: 10 C, 11 I, 14 K, 20 Y

<sup>d</sup> 4 DEU, 4 ITA, 4 KOR, 4 GBR, 3 TUR, 4 JNP, 4 ESP, 8 USA

<sup>e</sup> Number of time series considered by measure: 41 flow, 14 stock

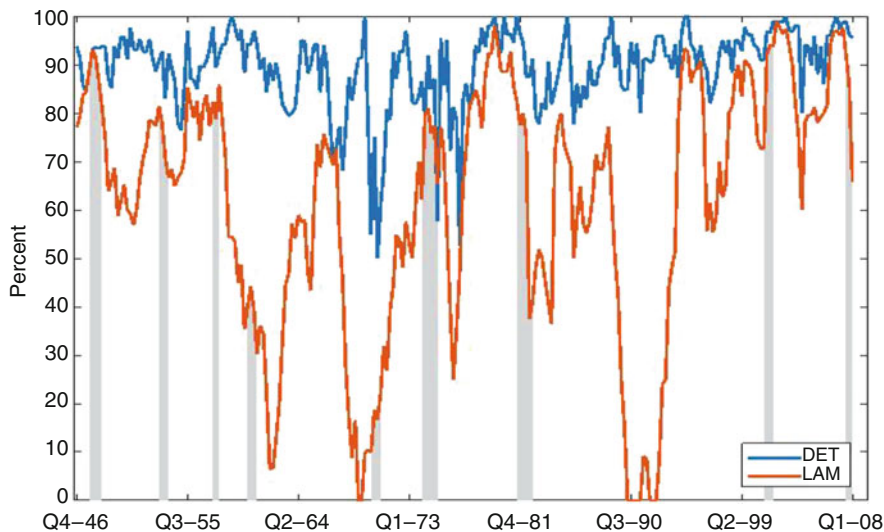


**Fig. 17.2** Dynamical analysis in the sliding window mode (RQE) where percent of laminarity (LAM) and percent of determinism (DET) refer to the same time series as in Fig. 17.1. Overlapping sliding windows of 50 data points shifted by 1 point (49 data point overlaps) were taken. Variables are plotted in central position in standardized units (su), i.e., after subtracting the average value from absolute values and dividing by standard deviation in each window

### 17.4.1.3 Recurrence Quantification Epoch (RQE) on Business Cycle Data

To better understand the time evolution of these economic data, RQE analysis was carried out on business cycle time series with the following parameters: Window size = 50 points; shift = 1 point; lag = 1; embedding = 10; radius = 80; line = 5. Even in this case, as well as in RP, the drop of DET corresponds to the grey vertical line indicated by FRED DATA (see Fig 17.2).

These results are in line with what was reported by Bastos and Caiados [3], who, comparing 23 stock market indices of both developed and developing countries, found a reduction in DET and LAM during the sub-prime mortgage crisis and even dramatic fall, during the burst of the technology bubble. The latter was also documented in the analysis of the dot-com bubble by Fabretti and Ausloos [11] and Kousik et al. [15], where DET and LAM reached the highest values during the bullish period and declined before the bubble burst. Moreover, according to Piskun et al. [34], laminarity (LAM) “is the most suitable measure, sensitive to critical events on markets”, whereas the inverse of laminarity reflects the market volatility (Strozzi et al. [36]).

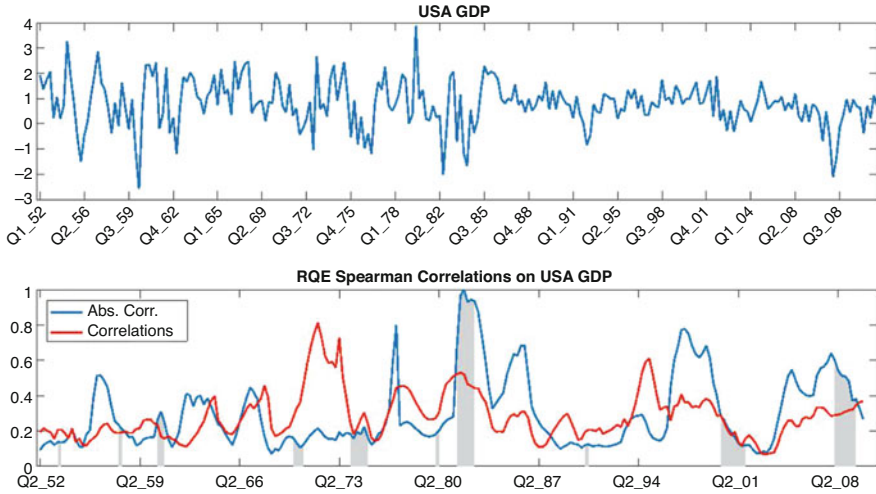


**Fig. 17.3** Maximum correlations (in blue) between RQE measures versus recession periods (in grey) on the US GDP [25]. As shown in the figure a change in the index is often linked to a recession. Spearman correlations (below) versus the final test signal (above). RQE absolute correlation (in blue) is displayed next to correlation (red). See how the RQE correlation calculated as in Eq. (10.6) is more reactive than the other and it is able to detect more finely changes in the original times series. Difference in the  $x$ -axis numbering between the picture above and below, is due to the windowing mechanism. Source Orlando and Zimatore [29]

### 17.4.1.4 RQE Correlation Index

In order to understand the limitations of the proposed method and to provide further detail regarding the power of RQA in anticipating transitions from laminar to turbulent phases, we resort to the *RQE (absolute) correlation index* described in Orlando and Zimatore [29] and here already discussed in Sect. 10.3.2.

As was shown in [29], while the RQE correlation index (10.6) is able to detect 9 of the 10 intervals in which a random signal was perturbed, the results displayed on Fig. 17.3 are less conclusive.

## 17.4.2 Principal Component Analysis (PCA) on RQA

PCA is a multivariate statistical analytical tool successfully applied to time series. The aim of this method is to minimize redundant information[2], [39]. In this book, we apply PCA to recurrence measures estimated from the aforementioned economic data, by taking advantage of the combined use of the two techniques. Therefore, PCA has been carried out on the main four RQA measures: REC, DET, MAXLINE and ENT. The percentage of total variance explained is respectively: PC1 = 81%; PC2 = 11%; PC3 = 5%; PC4 = 3%.

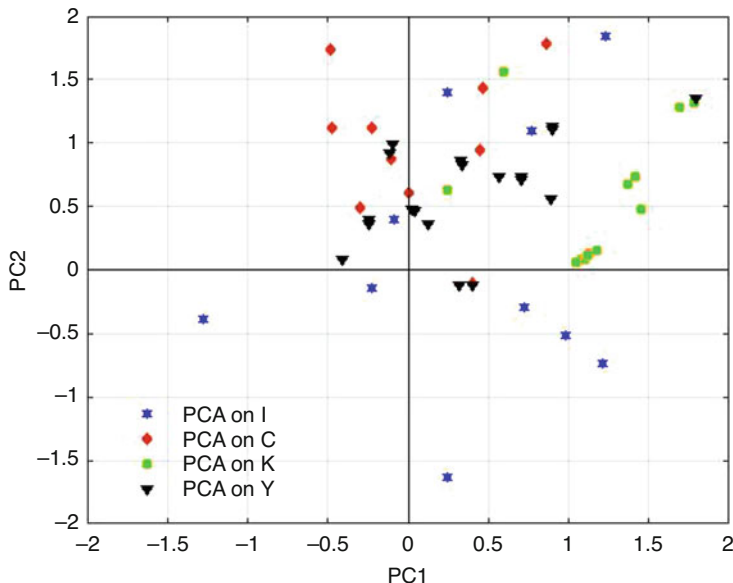


**Fig. 17.4** Dynamical features of business time series in a principal component space as reported in Appendix A.9. Different symbols (letters) indicate the four macroeconomic variables: I-Investment, C-Consumption, Y-Income, K-Capital. Note how K-capital is clustered

In Fig. 17.4 PC1 vs PC2 is shown for every data series in Table A.9. As those are obtained from RQA data, it is possible to observe that RQA preserves some structural differences between income, consumption, investment (flow variables) and capital (stock variable).

In order to check whether there are differences among the four macroeconomic variables, we applied the Mann–Whitney  $U$  test. This test belongs to the class of nonparametric tests and it checks the null hypothesis that a randomly selected value from one sample is less than or greater than a randomly selected value from another sample. In our case we found (see Table 17.1) that all measures are distinct at  $p < 0.001$ .

### 17.4.3 Statistical Analysis on RQA

An additional statistical analysis was performed on the obtained RQA measures. Spearman's correlations among these parameters were estimated. A multivariate analysis of variance (MANOVA) test was conducted for I, C, Y and K variables, for different countries, measures, investment goods, terms and interpolation methods. Data is expressed as means  $\pm$  standard deviations.

We anticipate that, in following Sects. 17.4.3.1 and 17.4.3.2, the results of our tests show that RQA is able to capture the difference between stock and flow (**measures**) as well as the dissimilarities between the four macroeconomic variables (**variables**). In addition, the fact that different countries (**countries**) with very different evolutions are not distinguishable, might be an indication of the chaotic nature of economics, as in chaos different paths originate from the same underlying deterministic dynamic. Furthermore, the analysis on different interpolation methods provides equivalent results.

### 17.4.3.1 Mann–Whitney Test

The nonparametric Mann–Whitney test was carried out on the RQA measures from the whole dataset (see Table A.9).

In summary, we observe that (between groups) results in row 1 Table 17.1:

- Fail to reject the null hypothesis that Methods 1 or 2 are equal (i.e. RQA is able to discriminate between methods).
- The distributions of the four variables C, I, Y, K are not the same (see row 2, Table 17.1) imply that RQA can identify differences in the macroeconomic variables.
- The distributions of data belonging to different countries (Germany (DEU), Italy (ITA), Korea (KOR), United Kingdom (GBR), Turkey (TUR), Japan (JNP), Spain (ESP) and USA) do not reject the null hypothesis that they are equal (see row 3, Table 17.1), i.e. RQA cannot find substantial differences between countries. In other terms, even though the economic development between countries was different, from the structural point of view a given time series is just an instance of the same hidden process. This is a general property of deterministic models where the same model can generate any sort of path depending on perturbations. The distributions of flow and stock variables are different (see row 4, Table 17.1) to confirm that RQA can detect differences in the nature of those macroeconomic variables.

### 17.4.3.2 Kruskal–Wallis Test

To further confirm the ability of RQA in capturing the differences between macroeconomic variables, the following Table 17.2 reports the  $p$ -values on RQA of the Kruskal–Wallis Test performed on the time series displayed in Table A.9.

**Table 17.2** *p*-Values on RQA from 55 (#C=10, #I=11, #K=14, #Y=20) business time series

Mean	SDev	Mean/SDev	REC	DET	MAXLINE	ENT	TREND	LAM	TT	PC1	PC2
0.012080589	0.000137346	3.33E-07	0.001264944	3.14E-05	2.26E-05	0.027594729	0.002148292	8.61E-08	7.08E-06	8.05E-05	0.00054498

## 17.5 Conclusions

So far, in the literature, there are no clear indications whether economic data are chaotic or not. This chapter applied RPs and their quantitative description provided by RQA to detect structural changes in the dynamical regime of business time series. RQA assesses the amount of deterministic structure of time series. Here it was shown that RQA is an efficient and relatively simple tool in nonlinear analysis of a wide class of signals. Therefore, RQA may be suitable to study business cycles and could be used for early detection of recessions (even though some limitations are apparent Sect. 17.4.1.4).

The results reported so far have revealed the applicability of this methodology to economic time series; especially where other methods may fail because of randomness, nonlinearity and non-stationarity of data, and have given new insights into underlying dynamics. In fact both PCA and statistical analysis on RQA seem to validate the technique as macroeconomic variables are clearly distinguishable. In addition RQA seems to confirm that different paths in economic development may originate from the same underlying deterministic dynamic (which is an indication of chaos).

More research, along this line, has been done. For example, we tested whether RQA, applied to both real data and simulations obtained from a nonlinear economic model on the business cycle [27], may present analogies and/or similarities. This could be helpful in understanding the nature of economic dynamics, i.e., analogies of real data with a time series produced by a deterministic chaotic model would indicate the presence of chaos in economy. Specifically, in [31] we analysed, through the RQE correlation index, the time series of the US GDP versus the income as generated from a Kaldor–Kalecki model [28]. In [33] we complemented the abovementioned analysis by adding Poincaré Plot and related quantifiers in order to detect spatio-temporal recurrent patterns in dynamical systems. The performed analysis brings evidences on fractal dimension and entropy measures for both real data and model's simulations. The final goal was, not only to discover whether real and simulated business cycle dynamics have similar characteristics, but also to validate the model as a suitable tool to simulate reality. In [32] we challenged the wisdom that only stochastic models are able to simulate reality. Thus, we compared an Ornstein–Uhlenbeck stochastic process with a Kaldor–Kalecki deterministic chaotic model and we showed that the proposed chaotic model is able to represent reality as well and, furthermore, it may reproduce an extreme event (e.g. a black swan).

We believe that this long lasting research, even that is not yet concluded, has provided a contribution to the quest of the nature of economy and, in essence, of human behaviour. Apart from philosophical considerations, the implication of chaos is very practical: tools to interpret and manage economy should be rethought and recast. Luckily, in other fields such as physics, meteorology, engineering, etc. there is a wide array of readily available results. We believe that an interdisciplinary approach to economics could bring significant benefits to the discipline.

## References

1. Addo, P.M., Billio, M., Guegan, D.: Nonlinear dynamics and recurrence plots for detecting financial crisis. *N. Am. J. Econ. Finance* **26**, 416–435 (2013)
2. Bartholomew, D.J.: The foundations of factor analysis. *Biometrika* **71**(2), 221–232 (1984)
3. Bastos, J.A.: Recurrence Quantification Analysis of Financial Markets. In: *Chaos and Complexity Theory for Management: Nonlinear Dynamics*, vol. 7, pp. 50–61 (2012)
4. Bry, G., Boschan, C.: Standard business cycle analysis of economic time series. In: *Cyclical Analysis of Time Series: Selected Procedures and Computer Programs*, pp. 64–150. NBER (1971)
5. Chen, W.S.: Use of recurrence plot and recurrence quantification analysis in Taiwan unemployment rate time series. *Phys. A: Stat. Mech. Appl.* **390**(7), 1332–1342 (2011)
6. Citicorp: Database Services, CITIBASE: Macroeconomic Database (1993)
7. Colander, D., Goldberg, M., Haas, A., Juselius, K., Kirman, A., Lux, T., Sloth, B.: The financial crisis and the systemic failure of the economics profession. *Crit. Rev.* **21**(2-3), 249–267 (2009). <https://doi.org/10.1080/08913810902934109>
8. Crowley, P.M., Schultz, A.: A new approach to analyzing convergence and synchronicity in growth and business cycles: cross recurrence plots and quantification analysis. *Bank of Finland Research Discussion Paper* (16) (2010)
9. Dezhbakhsh, H., Levy, D.: Periodic properties of interpolated time series. *Econ. Lett.* **44**(3), 221–228 (1994)
10. Eckstein, O., Sinai, A.: The mechanisms of the business cycle in the postwar era. In: *The American Business Cycle: Continuity and Change*, pp. 39–122. University of Chicago Press, Chicago (1986)
11. Fabretti, A., Ausloos, M.: Recurrence plot and recurrence quantification analysis techniques for detecting a critical regime. Examples from financial market indices. *Int. J. Mod. Phys. C* **16**(5), 671–706 (2005)
12. Faggini, M., Bruno, B., Parziale, A.: Does chaos matter in financial time series analysis? *Int. J. Eco. Fin. Iss.* **9**(4), 18 (2019)
13. Jaeger, A.: Shock persistence and the measurement of prewar output series. *Econ. Lett.* **34**(4), 333–337 (1990)
14. Karagianni, S., Kyrtsov, C.: Analysing the dynamics between US inflation and Dow Jones index using non-linear methods. *Stud. Nonlinear Dyn. Econom.* **15**(2) (2011)
15. Kousik, G., Basabi, B., Chowdhury, A.R.: Using recurrence plot analysis to distinguish between endogenous and exogenous stock market crashes. *Phys. A: Stat. Mech. Appl.* **389**(9), 1874–1882 (2010)
16. Krugman, P.: How Did Economists Get It So Wrong? *New York Times* (2009)
17. Levy, D., Chen, H.: Estimates of the aggregate quarterly capital stock for the post-war us economy. *Rev. Income Wealth* **40**(3), 317–349 (1994)
18. Marwan, N.: Cross recurrence plot toolbox 5.21 (R31c) (2016). <http://tocsy.pik-potsdam.de/CRPtoolbox/>
19. Marwan, N., Romano, M.C., Thiel, M., Kurths, J.: Recurrence plots for the analysis of complex systems. *Phys. Rep.* **438**(5–6), 237–329 (2007)
20. Mastroeni, L., Vellucci, P., Naldi, M.: Co-existence of stochastic and chaotic behaviour in the copper price time series. *Resour. Policy* **58**, 295 – 302 (2018). <https://doi.org/10.1016/j.resourpol.2018.05.019>. Special Issue on Mining Value Chains, Innovation and Learning
21. Mastroeni, L., Vellucci, P., Naldi, M.: A reappraisal of the chaotic paradigm for energy commodity prices. In: *Energy Economics* (2018)
22. Moloney, K., Raghavendra, S.: A linear and nonlinear review of the arbitrage-free parity theory for the CDS and bond markets. In: *Topics in Numerical Methods for Finance*, pp. 177–200. Springer, Berlin (2012)
23. Musgrave, J.C.: Fixed reproducible tangible wealth in the United States, revised estimates. *Surv. Curr. Bus.* **72**(1), 106–137 (1992)



24. OECD: Investment GFCF (indicator) (2016). <https://doi.org/10.1787/b86d1fc8-en>
25. OECD: Quarterly GDP (indicator) (2016). <https://doi.org/10.1787/b86d1fc8-en>
26. OECD: Saving rate GFCF (indicator) (2016). <https://doi.org/10.1787/ff2e64d4-en>
27. Orlando, G.: A discrete mathematical model for chaotic dynamics in economics: Kaldor's model on business cycle. *Math. Comput. Simul.* **125**, 83–98 (2016). <https://doi.org/10.1016/j.matcom.2016.01.001>
28. Orlando, G.: Chaotic business cycles within a Kaldor–Kalecki Framework. In: *Nonlinear Dynamical Systems with Self-Excited and Hidden Attractors* (2018). [https://doi.org/10.1007/978-3-319-71243-7\\_6](https://doi.org/10.1007/978-3-319-71243-7_6)
29. Orlando, G., Zimatore, G.: RQA correlations on real business cycles time series. In: *Indian Academy of Sciences Conference Series—Proceedings of the Conference on Perspectives in Nonlinear Dynamics—2016*, vol. 1, pp. 35–41. Springer, Berlin (2017). <https://doi.org/10.29195/iascs.01.01.0009>
30. Orlando, G., Zimatore, G.: Recurrence quantification analysis of business cycles. *Chaos Solitons Fractals* **110**, 82–94 (2018). <https://doi.org/10.1016/j.chaos.2018.02.032>
31. Orlando, G., Zimatore, G.: RQA correlations on business cycles: a comparison between real and simulated data. *Adv. Nonlinear Dyn. Electron. Syst.* **17**, 62–68 (2019). [https://doi.org/10.1142/9789811201523\\_0012](https://doi.org/10.1142/9789811201523_0012)
32. Orlando, G., Zimatore, G.: Business cycle modeling between financial crises and black swans: Ornstein–Uhlenbeck stochastic process vs Kaldor deterministic chaotic model. *Chaos* **30**(8), 083129 (2020)
33. Orlando, G., Zimatore, G.: Recurrence quantification analysis on a Kaldorian business cycle model. *Nonlinear Dyn.* (2020). <https://doi.org/10.1007/s11071-020-05511-y>
34. Piskun, O., Piskun, S.: Recurrence quantification analysis of financial market crashes and crises (2011). arXiv preprint arXiv:1107.5420
35. Strozzi, F., Gutierrez, E., Noè, C., Rossi, T., Serati, M., Zaldivar, J.: Application of Non-Linear Time Series Analysis Techniques to the Nordic Spot Electricity Market Data. *Libero istituto universitario Carlo Cattaneo* (2007)
36. Strozzi, F., Zaldivar, J.M., Zbilut, J.P.: Recurrence quantification analysis and state space divergence reconstruction for financial time series analysis. *Phys. A: Stat. Mech. Appl.* **376**, 487–499 (2007)
37. Webber, C.L.: RQA software ver. 14.1. RQC.exe and RQE.exe files are included in RQA software ver. 14.1 (2014). <http://homepages.luc.edu/~cwebber/>
38. Zbilut, J.P.: Use of recurrence quantification analysis in economic time series. In: *Economics: Complex Windows*, pp. 91–104. Springer, Berlin (2005)
39. Zimatore, G., Hatzopoulos, S., Giuliani, A., Martini, A., Colosimo, A.: Comparison of transient otoacoustic emission responses from neonatal and adult ears. *J. Appl. Physiol.* **92**(6), 2521–2528 (2002)

# Chapter 18

## An Empirical Test of Harrod's Model



Giuseppe Orlando and Fabio Della Rossa

While Kaldor's theory strongly influenced the academic debate on business cycles, Harrod's theory inspired Solow's seminal paper "A Contribution to the Theory of Economic Growth" (1956) [36], that set the basis for modern growth theory. However, a recent re-evaluation of Harrod's theory [4, 14] challenges Solow's interpretation "which ultimately dominated the profession's view of Harrod" [14]. According to Solow, the Harrod model "implied a tendency toward progressive collapse of the economy". However this has "little to do with the problem of long-run growth as Solow understood it, but instead addressed medium-run fluctuations, the inherent instability" of economies" [14].

There are several reasons why in this chapter we focus on the Harrod's model. First of all, it is because of the abovementioned influence on the foundation of modern growth theory. Secondly, the Harrod model provides a dynamic framework and some guidelines to policy-makers, in terms of supply-side policies. In fact, they should consider the combination of investment, technological change, population

---

Part of this chapter has appeared in [27].

---

G. Orlando (✉)

University of Bari, Department of Economics and Finance, Bari, Italy

University of Bari, Department Mathematics, Bari, Italy

University of Camerino, School of Sciences and Technology, Camerino, Italy

e-mail: [giuseppe.orlando@uniba.it](mailto:giuseppe.orlando@uniba.it); [giuseppe.orlando@unicam.it](mailto:giuseppe.orlando@unicam.it)

F. Della Rossa

University of Naples "Federico II", Department of Electrical Engineering and Information Technology, Naples, Italy

Department of Electronics, Information and Bioengineering, Politecnico di Milano, Milan, Italy

e-mail: [fabio.dellarossa@unina.it](mailto:fabio.dellarossa@unina.it); [fabio.dellarossa@polimi.it](mailto:fabio.dellarossa@polimi.it)

© The Author(s), under exclusive license to Springer Nature Switzerland AG 2021

283

G. Orlando et al. (eds.), *Non-Linearities in Economics*, Dynamic Modeling

and Econometrics in Economics and Finance 29,

[https://doi.org/10.1007/978-3-030-70982-2\\_18](https://doi.org/10.1007/978-3-030-70982-2_18)

growth, unemployment and aggregate demand. Another reason is that, in his framework, the warranted rate of growth is not a single (moving) equilibrium, but a “highly unstable” one. This takes the name of Harrod’s knife-edge instability or the *instability principle*.

Similarly, but from a different starting point (i.e. static analysis and microeconomic foundations of macroeconomic dynamics), Leijonhufvud defines the notion of a stability corridor as a time-path in which economic activities “are reasonably well coordinated” [22]. Moreover the system is likely to behave differently for large than for moderate displacements from the “full coordination” time-path. Within some range from the path (referred to as “the corridor” for brevity), the system’s homeostatic mechanisms work well, and deviation-counteracting tendencies increase in strength. Outside that range, these tendencies become weaker as the system becomes increasingly subject to “effective demand failures”. If the system is displaced sufficiently “far out”, the forces tending to bring it back may be so weak and sluggish that for all practical purposes the Keynesian “unemployment equilibrium” model is a sensible representation of its state. Inside the corridor, multiplier-repercussions are weak and dominated by neoclassical market adjustments. Outside the corridor, they should be strong enough for effects of shocks to the prevailing state to be endogenously amplified. Up to a point, multiplier-coefficients are expected to increase with distance from the ideal path. Within the corridor, the presumption is in favour of “monetarist” policy prescriptions, outside of it in favour of “fiscalist”. Finally, although within the corridor market forces will be acting in the direction of clearing markets, institutional obstacles of the type familiar from the conventional Keynesian literature may, of course, intervene to make them ineffective at some point. Thus, a combination of monopolistic wage-setting in unionized occupations and legal minimum-wage restrictions could obviously cut the automatic adjustment process short before “equilibrium employment” is reached [22].

Both views, macroeconomic and dynamic (by Harrod) and static and micro-founded (by Leijonhufvud) converge to the “existence of thresholds at the start of the mechanisms that are at work” [21]. Therefore, the idea of dynamically unstable multiple equilibria or the alternative Harrod’s suggestion of a Leijonhufvud’s “corridor stability” is worth exploration in our opinion. In particular, whereas in the 1970s and the 1980s unemployment and stagflation discarded those theories, in the twentieth century “in the leading Western economies there have been prolonged periods when more saving would have been beneficial, and others with every appearance of inadequate effective demand” [12]. As the Harrod’s model is one of the few able to predict that, “it still deserves serious attention” [12].

## 18.1 Background and Literature

The renewed interest in Harrod’s also due to an epistemological work that has Besomi among its main contributors: “plunging into the original texts soon made it obvious that the subject of Harrod’s dynamics was more intricate than the portrait

given in textbook rendition" [4] and that many interpretations were erroneous. Baumol [2], for instance, asserts that "the main achievement of his [Harrod's] model lies in the ideas it inspired in those who did not fully understand it". In fact Harrod himself "claimed that his dynamics was essentially different from, and indeed more fundamental than, the mainstream interpretation of it (an interpretation which, of course, reflected the notion of dynamics which gained almost universal acceptance after the war)" [4].

The so-called Harrod's Dynamics is the result of a number of works resumed in "The Making of Harrod's Dynamics" by Besomi [4] and the most significant of which are "Towards a Dynamic Economics" (1948) [16] and "Economic Essays" (1972) [17]. This happened because Harrod "returned several times on the topic of his essays in correspondence with Keynes, who sometimes managed to force him to re-formulate his propositions" [4].

Harrod identified two stages in explaining economic dynamics: the first was the determination of the rate of growth at the equilibrium (given a certain ratio of saving over income and investment per unit increase of output), the second was related to the changes of those ratios (changes that would lead to different equilibria and would be responsible for cycles).

Because of the different formulations, Harrod's theory led to several distinct interpretations. For example, according to Tinbergen [39], the model was a combination of multiplier and accelerator that could not give rise to cyclical behaviour, but could only lead to an explosive growth or to an equilibrium. Samuelson [31, 32], in a different formulation with lagged variables, found that for a range of the multiplier and accelerator coefficients, there would be a cyclical behaviour.

Apart from that, the so-called Harrod-Domar model was extensively used to explain growth as the result of the optimal combination of saving and investment. This led to a debate on other factors determining the growth as well as around the multiplicity of equilibria and their instability. For example, according to Solow [36], relaxing Harrod's assumption of a constant capital/output ratio, the system would have drifted towards full employment. Moreover, while Harrod stressed the mentioned "principle of instability" to describe the adjustments between effective accumulation of capital and warranted accumulation, Solow's interpretation solved the puzzle by assuming that the warranted rate of growth ( $G_w$ ) was constant and that technology was flexible (even though Harrod insisted on the fact that the  $G_w$  depended on time and cycle). Therefore, when Axel Leijonhufvud [22] sketched the idea of a corridor, in *Economic Dynamics* [15] Harrod confessed that it was an appropriate approach to what he was thinking about failures of effective demand.

Robinson [30] summarized a long debate on the post-Keynesian front and showed how multiple equilibria could be attained if different propensities to save across social classes were considered. Last but not least Kalecki (1933-1939) [20] and Kaldor [19] focused on the technical progress, on the non-linearities of the investment and savings functions and on the determinants of investment decisions. This inspired a number of works: from multiple attractors and global bifurcations [6] to homoclinic tangles [1], from the global existence of periodic solutions [18] to the existence of chaotic behaviour, not for a single specific value, but within a

reasonable interval for each parameter [25, 26]. Shaikh [34] explains key differences between Harrodian and Keynesian theories and policies, proves the stability of the Harrodian warranted path and shows that the Keynesian paradox of thrift is transient. Moudud [23] shows how to combine taxation with public investments in order to raise the warranted growth rate (which, according to Harrod, is otherwise reduced by an increase in the budgeted deficit/GDP ratio). Serrano et al. [33] claim that Harrod's instability is an instance of what Hicks calls "static instability" and they show that the Sraffian Supermultiplier [24] model overcomes the Harrodian instability. Skott [35] contends that there is no need to introduce autonomous demand as the "driver of long-run economic growth and as a stabilizing force", but it would suffice to model "the supply side (the labour market) and/or economic policy" to obtain those results.

Finally Yoshida [41] and Sportelli [37, 38] offered, from the 1990s Harrod's Dynamics, a theoretical framework to explain jointly economic growth and business cycles through the Harrod's "instability principle". However for Yoshida the instability derives from a putty-clay technology in conjunction with flexibility of prices, while for Sportelli the instability derives from the gaps between Harrod's rates of growth: actual, warranted and natural. Further, in that framework [37], it has been shown that opening to foreign trade can lead to reducing cyclical instability of the economy as was suggested by Harrod.

## 18.2 Material and Methods

### 18.2.1 Cycles

Cyclical fluctuations in economy, Fig. 18.1, correspond to the duration or the amplitude between a high/peak and the succeeding low/trough [8]. The so-called peak–trough–peak (PTP) cycle affects the whole economy (e.g., wages, demand, prices, credit, etc.). Seasonal swings are typically short-term, but cyclical fluctuations could last for years. A depression is a prolonged and deep recession. As mentioned by Eckstein [11] "financial distress produces sharp discontinuities in flows of funds and spending and when the financial strains include tight monetary policy, much lessened availability of money and credit, sharp rises of interest rates, and deteriorating balance sheets for households, businesses, and financial institutions".

### 18.2.2 US Recessions

In the following Fig. 18.2 we display the path of US investments alongside recessions as reckoned by FRED (Table 18.1).

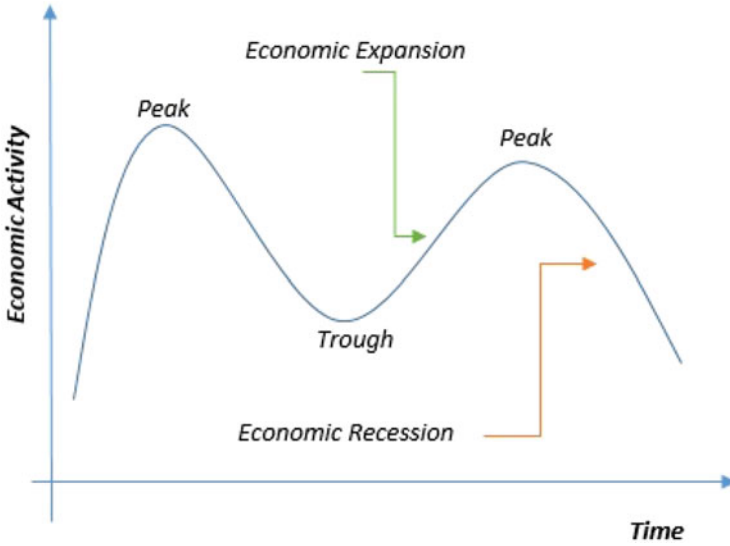


**Fig. 18.1** The business cycle can be classified into four stages: (1) expansion when economic activity grows steadily; (2) boom when the aggregate demand grows more than the aggregate output which overheats the economy; (3) recession phase when the aggregate output cools down after a peak; (4) recovery after a *trough*. The so-called specific cycle amplitude corresponds to the vertical distance between the peak and the trough

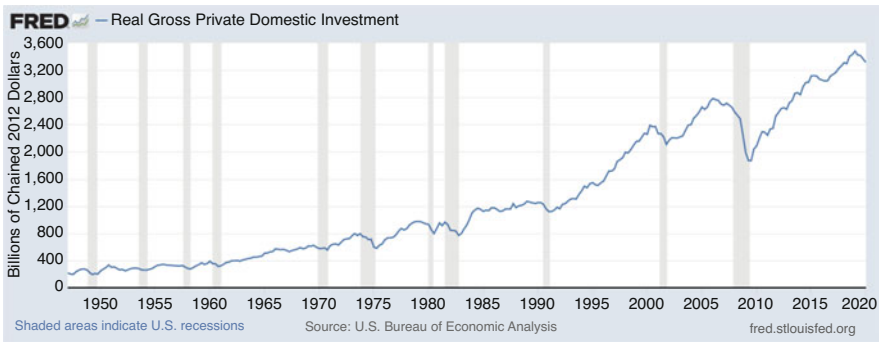


**Fig. 18.2** US real gross private domestic investment (GPDIC1), billions of chained 2012 dollars, seasonally adjusted annual rate. Source: FRED, Federal Reserve Bank of St. Louis; <https://fred.stlouisfed.org/series/GPDIC1>, 25 May 2020. Greyed areas correspond to periods of economic recessions (Table 18.1)

**Table 18.1** US recessions

Recessions			
From		To	
Quarter	Year	Quarter	Year
Q4	1948	Q4	1949
Q3	1953	Q1	1954
Q4	1957	Q1	1958
Q3	1960	Q1	1961
Q1	1970	Q4	1970
Q1	1974	Q2	1975
Q1	1980	Q2	1980
Q3	1981	Q4	1982
Q3	1990	Q1	1991
Q2	2001	Q4	2001
Q1	2008	Q3	2009

US. Bureau of Economic Analysis [3]

### 18.2.3 Empirical Data

In order to perform our test, we have retrieved data from several sources such as the Maddison Project, the World Bank, *IMF* and *BEA*. Annual world GDP estimate has been retrieved from the Maddison–Penn world table [7, 13], (from 1946 to 1961). This has been linked up with *World Bank*<sup>1</sup> and *IMF*<sup>2</sup> data (available from 1961 to 2018). Annual data has been changed into quarterly via the compounding law. Time series are retrieved from their original dataset or from FRED as detailed in the Appendix A Sect. A.1.

## 18.3 Calibration of Harrod's Model

To test empirically the Harrod model we evaluated the average distance between the historical data series reported in Appendix A.1 and the orbit produced by Eq. (13.23) starting at time 0. Mathematically, we want to compute the quantity:

$$D = \frac{1}{286} \sum_{t=0}^{286} \left( d(t) - \frac{1}{\hat{\tau}} \int_t^{t+1} \hat{\phi}(\hat{\tau}\tilde{t}, P) d\tilde{t} \right)^2, \quad (18.1)$$

<sup>1</sup><https://data.worldbank.org/indicator/NY.GDP.MKTP.KD.ZG>.

<sup>2</sup>[https://www.imf.org/external/datamapper/NGDP\\_RPCH@WEO/OEMDC/ADVEC/WEO\\_WORLD](https://www.imf.org/external/datamapper/NGDP_RPCH@WEO/OEMDC/ADVEC/WEO_WORLD).

**Table 18.2** Harrod model parameters

#	Given model		Calibration		
			Cal. #1	Cal. #2	Cal. #3
	Parameter	Given value/range	Calibrated value		
1	$\alpha$	0.5	0.28	0.29	1.09
2	$\epsilon$	[0.2, 1.31]	0.13	0.58	0.52
3	$\sigma$	[2, 4)	1.42	1.67	2.45
4	$G_f$	0.03	0.03	0.00	0.54
5	$C^*$	4	4.00	4.00	3.18
6	$\beta$	2.5	2.50	2.50	2.20
7	$m$	0.07	0.04	0.04	1.23
8	$\varphi$	15	15.00	15.00	14.89
9	$\xi$	0.18	0.18	0.18	0.20
10	$\mu$	1.4	0.78	0.90	2.06
11	$\gamma$	1	0.56	0.57	0.36
12	$\delta$	6.2	6.20	6.20	5.94
13	$\zeta$	1.9	1.06	1.09	2.25
Value of $D$			0.38	0.71	0.55

Original data as provided in [37] with related calibrations.  $\bar{G} = \max G_n$

where  $d(t)$  is the vector that stacks the data of the rate of growth of domestic income, the expected rate of growth of aggregate demand, the share of income saved and the net export rate for the quarter  $t$  ( $t = 0$  is the first quarter of 1947,  $t = 286$  is the second quarter of 2018). Similarly,  $P$  is the vector of the 13 parameters of the model (reported in Table 18.2), and  $\hat{\phi}$  stacks the four variables that solve the differential equation (13.23) with parameters set in  $P$  starting at  $\hat{\phi}(0, P) = d(0)$ : the integral between  $t$  and  $t + 1$  allows us to compute the average value of the (continuous) signal over the quarter of interest, to be compared with the data. Note that an additional dummy parameter  $\hat{\tau}$  has been added. This parameter permits us to rescale the time of the signal produced by the model, in order to best fit with the time-scale of the data. The optimization variables are the 13 + 1 parameters of Eq. (13.23), since they have physical meaning only when positive, this adds a set of constraints to be satisfied. Formally speaking, in order to find the best fitting solution, we solve the following constrained optimization problem:

$$\begin{aligned}
 \min_{P, \hat{\tau}} \frac{1}{286} \sum_{t=0}^{286} \left( d(t) - \frac{1}{\hat{\tau}} \int_t^{t+1} \hat{\phi}(\hat{\tau} \tilde{t}, P) d\tilde{t} \right)^2 \\
 \text{s.t. } \hat{\phi}(\hat{\tau} t, P) \text{ is a solution of Eq. (13.23) with parameters set as } P \\
 \hat{\phi}(0, P) = d(0) \\
 P \geq 0, \hat{\tau} > 0.
 \end{aligned} \tag{18.2}$$



This problem is solved using the interior point method [5, 9] implemented in the Matlab `fmincon` routine. Since the problem is not convex, the optimization algorithm may converge to a local optimal solution. To better explore the space of the optimal solutions, we introduce a multi-start algorithm: the optimization is then run several times starting from a randomly perturbed sample drawn from a distribution centred in the parameter setting provided in Sportelli and Celi [37].

To evaluate the abovementioned version the Harrod model, Table 18.2 reports the parameters for both the original model and three calibrations we have obtained that present qualitatively different behaviours (together with the value of their distance  $D$  for calibration #2,  $D$  is computed with  $t \leq 6$ ). The model, calibrated with real data, may display convergence to a long-run equilibrium (calibration #1, Fig. 18.3), divergence (calibration #2, Fig. 18.4) as well as a lightly damped oscillatory behaviour (calibration #3, Fig. 18.5). It is worth saying that the global optimum is obtained with calibration #1. However, with calibrations #2 and #3, we displayed sub-optimal results to provide a context for our results. In fact, qualitatively, we obtain similar values to the ones in [37]. Moreover we agree with this conclusion “when the value of  $\epsilon$  is large enough, the long period dynamics of the saving rate is such that it can generate an irregular cycle in the system only if the net export rate is very low. On the contrary, starting from positive and meaningful values of the net export rate, the system may simply generate a limit cycle (or at most a double cycle) if a higher  $\epsilon$  works together with adequate competitiveness on the foreign markets. This is the only formal result consistent with Harrod’s intuition that a more moderate cyclical instability can emerge in an open economy compared to a closed one” [37].

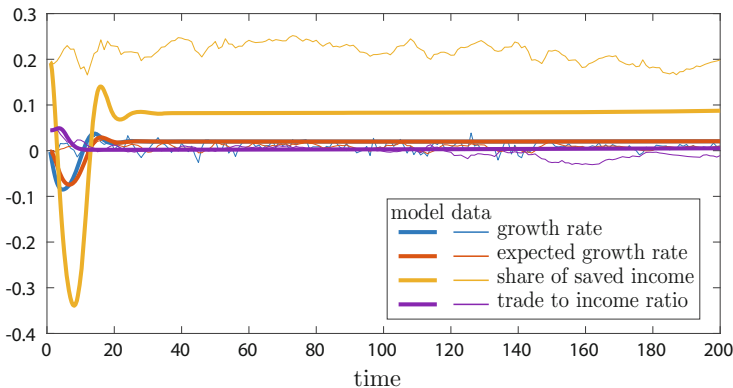


**Fig. 18.3** Time series obtained with parameters of calibration #1 that displays convergence to the long-run equilibrium

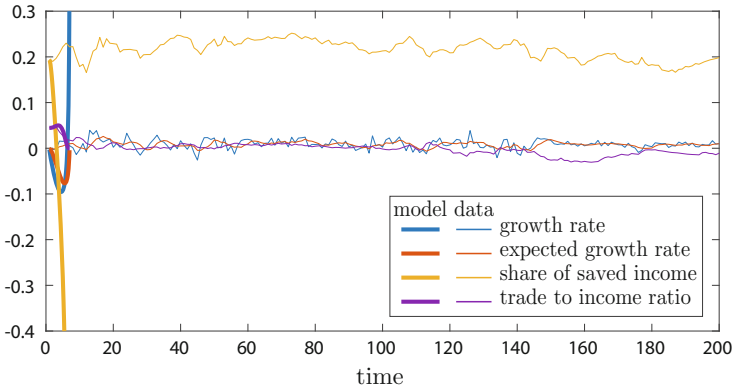


**Fig. 18.4** Time series obtained with parameters of calibration #2 that displays divergence from the long-run equilibrium

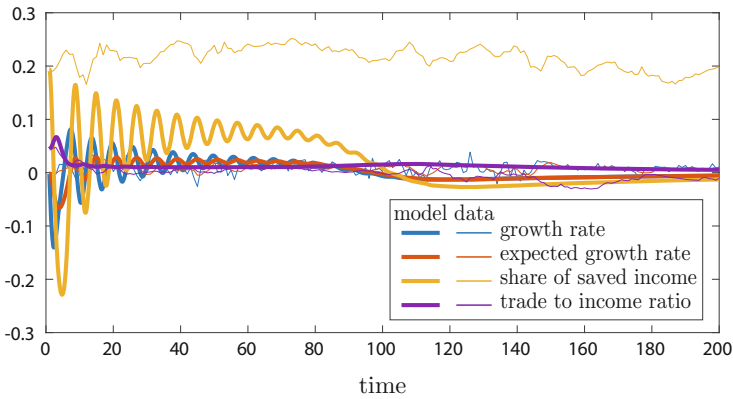


**Fig. 18.5** Time series obtained with parameters of calibration #3 that displays lightly damped oscillatory behaviour around the long-run equilibrium

### 18.4 Conclusions

The Harrod's model [16] has the merit of rearranging Keynes's ideas into a dynamic framework with some additional specification on the supply side. In fact "where the warranted growth rate represents an economy's growth path on which aggregate demand and supply remain in balance, the model's natural growth rate reflects the supply of productive resources and the level of technology, the long-run limit to real output growth. The interaction between the warranted and natural growth rates provides a useful perspective for policymaking in today's environmentally constrained global economy. Also, since the growth of the labour force is built into the natural growth path, the model also helps to clarify policy choices in an

economy impacted by immigration” [40]. Therefore “supply-side policies must be developed along with the standard Keynesian demand side policies, and the interactions between the two require disaggregated policies to address specific types of investment, technological change, and demand. That is, it is not generally possible to solve the unemployment problem by simply expanding aggregate demand” [40]. Harrod’s theory, and thereof modelization built on that [36, 37, 40, 41], may thus be seen as the link between classical economy (that stressed the importance of investment for growth) and the Keynesian approach “primarily concerned with the demand and income generating effect of investment” [10]. In real life, this theory was put into practice in India. In fact, the Indian fifth five year plan for the years 1974–1979 was based on a mix of a Harrod macroeconomic model and a Leontief inter-industry model, and it was aimed at achieving both self-reliance and growth. Main priorities on the industrial sectors were the development of: (1) core industry, (2) industry for export and diversification, (3) mass consumption production, (4) small industry and ancillary industry feeders of large industries. The target growth rate was 4.4% and, as a result, the actual growth rate was 4.8% [10].

Having said that, to recall the importance of the model, this test shows (for a specific set of parameters) that it is possible to find a match between Harrod’s suggestions and reality. This is relevant because in the long-standing debate about chaos and non-linear dynamics in economy, even the general usefulness of those concepts was questioned. “Stochastic modelling has proven to be able to simulate reality fairly well. However, a stochastic behaviour implies that reality is about exogenous randomness, while a chaotic behaviour means that reality is deterministic and non-linearities are endogenous” [28]. The ability of chaotic deterministic models to replicate reality is the common thread throughout this book [29].

## References

1. Agliari, A., Dieci, R., Gardin, L.: Homoclinic tangles in a Kaldor-like business cycle model. *J. Econo. Behav. Organ.* **62**, 324–347 (2007)
2. Baumol, W.J.: Review: Daniele Besomi, *The Making of Harrod’s Dynamics*. *Hist. Polit. Econ.* **32**(4), 1037–1039 (2000)
3. BEA: USA Recessions, Gross Domestic Product [A191RP1Q027SBEA] - US. Bureau of Economic Analysis (2016). <https://fred.stlouisfed.org/series/A191RP1Q027SBEA>. Retrieved from FRED, Federal Reserve Bank of St. Louis; November 10, 2016
4. Besomi, D.: *The Making of Harrod’s Dynamics*. Springer, Berlin (1999)
5. Biggs, M.: Constrained minimization using recursive quadratic programming. In: Dixon, L., Szergo, G. (eds.) *Towards Global Optimization*. North-Holland, Amsterdam (1975)
6. Bischi, G.I., Dieci, R., Rodano, G., Saltari, E.: Multiple attractors and global bifurcations in a Kaldor-type business cycle model. *J. Evol. Econ.* **11**, 527–554 (2001)
7. Bolt, J., van Zanden, J.L.: The Maddison Project: collaborative research on historical national accounts. *Econ. Hist. Rev.* **67**(3), 627–651 (2014)
8. Bry, G., Boschan, C.: Standard business cycle analysis of economic time series. In: *Cyclical Analysis of Time Series: Selected Procedures and Computer Programs*, pp. 64–150. NBER (1971)

9. Byrd, R.H., Hribar, M.E., Nocedal, J.: An interior point algorithm for large-scale nonlinear programming. *SIAM J. Optim.* **9**(4), 877–900 (1999)
10. Dash, L.N.: *World Bank and Economic Development of India*. APH Publishing, Totnes (2000)
11. Eckstein, O., Sinai, A.: The mechanisms of the business cycle in the postwar era. In: *The American Business Cycle: Continuity and Change*, pp. 39–122. University of Chicago Press, Chicago (1986)
12. Eltis, W.: *Harrod–Domar Growth Model*, pp. 1–5. Palgrave Macmillan, London (2016). [https://doi.org/10.1057/978-1-349-95121-5\\_1267-1](https://doi.org/10.1057/978-1-349-95121-5_1267-1)
13. Feenstra Robert C., R.I., Timmer, M.P.: The Next Generation of the Penn World Table. *Am. Econ. Rev.* **105**(10), 3150–3182 (2015). <https://doi.org/10.15141/S5J01T>
14. Halsmayer, V., Hoover, K.D.: Solow's Harrod: transforming macroeconomic dynamics into a model of long-run growth. *Eur. J. Hist. Econ. Thought* **23**(4), 561–596 (2016). <https://doi.org/10.1080/09672567.2014.1001763>
15. Harrod, R.: *Economic Dynamics*. Palgrave Macmillan, London (1973)
16. Harrod, R.F.: *Towards a Dynamic Economics: Some Recent Developments of Economic Theory and Their Application to Policy*. MacMillan and Company, London (1948)
17. Harrod, R.F.S.: *Economic Essays*, 2nd edn. Macmillan, London (1972)
18. Kaddar, A., Alaoui, H.T.: Global existence of periodic solutions in a delayed Kaldor–Kalecki model. *Nonlinear Anal. Model. Control* **14**(4), 463–472 (2009)
19. Kaldor, N.: *Essays on Economic Stability And Growth*, vol. 1. Duckworth, London (1960)
20. Kalecki, M.: *Studies in the Theory of Business Cycles, 1933–1939*. A.M. Kelley, New York (1966)
21. Le Page, J.: Growth-employment relationship and Leijonhufvud's corridor. *Recherches Economiques de Louvain* **80**(2), 111–124 (2014)
22. Leijonhufvud, A.: Effective demand failures. *Swedish J. Econ.* **75**(1), 27–48 (1973)
23. Moudud, J.K.: The role of the state and Harrod's economic dynamics: toward a new policy agenda? *Int. J. Polit. Econ.* **38**(1), 35–57 (2009)
24. Nikiforos, M.: *Some Comments on the Sraffian Supermultiplier Approach to Growth and Distribution*. Levy Economics Institut (2018). <https://doi.org/10.2139/ssrn.3180146>
25. Orlando, G.: A discrete mathematical model for chaotic dynamics in economics: Kaldor's model on business cycle. *Math. Comput. Simul.* **125**, 83–98 (2016). <https://doi.org/10.1016/j.matcom.2016.01.001>
26. Orlando, G.: Chaotic business cycles within a Kaldor–Kalecki Framework. In: *Nonlinear Dynamical Systems with Self-Excited and Hidden Attractors* (2018). [https://doi.org/10.1007/978-3-319-71243-7\\_6](https://doi.org/10.1007/978-3-319-71243-7_6)
27. Orlando, G., Della Rossa, F.: An empirical test on Harrod's open economy dynamics. *Math.* **7**(6), 524 (2019). <https://doi.org/10.3390/math7060524>
28. Orlando, G., Zimatore, G.: Business cycle modeling between financial crises and black swans: Ornstein–Uhlenbeck stochastic process vs Kaldor deterministic chaotic model. *Chaos* **30**(8), 083129 (2020)
29. Orlando, G., Zimatore, G.: Recurrence quantification analysis on a Kaldorian business cycle model. *Nonlinear Dyn.* (2020). <https://doi.org/10.1007/s11071-020-05511-y>
30. Robinson, J.: Harrod after twenty-one years. *Econ. J.* **80**, 731–737 (1970)
31. Samuelson, P.A.: A synthesis of the principle of acceleration and the multiplier. *J. Polit. Econ.* **47**(6), 786–797 (1939)
32. Samuelson, P.A.: Dynamics, statics, and the stationary state. *Rev. Econ. Stat.* **25**, 58–68 (1943)
33. Serrano, F., Freitas, F., Bhering, G.: The Trouble with Harrod: the fundamental instability of the warranted rate in the light of the Sraffian Supermultiplier. *Metroeconomica* **70**(2), 263–287 (2019). <https://doi.org/10.1111/meca.12230>
34. Shaikh, A.: Economic policy in a growth context: a classical synthesis of Keynes and Harrod. *Metroeconomica* **60**(3), 455–494 (2009). <https://doi.org/10.1111/j.1467-999X.2008.00347.x>
35. Skott, P.: Autonomous demand, harrodian instability and the supply side. *Metroeconomica* **70**(2), 233–246 (2019). <https://doi.org/10.1111/meca.12181>
36. Solow, R.M.: A contribution to the theory of economic growth. *Q. J. Econ.* **70**(1), 65–94 (1956)

37. Sportelli, M., Celi, G.: A mathematical approach to Harrod's open economy dynamics. *Metroeconomica* **62**(3), 459–493 (2011)
38. Sportelli, M.C.: Dynamic complexity in a Keynesian growth-cycle model involving Harrod's instability. *J. Econ.* **71**(2), 167–198 (2000)
39. Tinbergen, J.: Harrod, R. F., The Trade Cycle. An Essay *Weltwirtschaftliches Archiv*(XLV), 89–91 (1937)
40. Vandenberg, H., Rosete, A.R.M.: Extending the Harrod–Domar model: warranted growth with immigration, natural environmental constraints, and technological change. *Am. Rev. Polit. Econ.* **3**(1), (2019)
41. Yoshida, H.: Harrod's 'knife-edge' reconsidered: An application of the Hopf bifurcation theorem and numerical simulations. *J. Macroecon.* **21**(3), 537–562 (1999)

# Chapter 19

## Testing a Goodwin's Model with Capacity Utilization to the US Economy



Ricardo Azevedo Araujo and Helmar Nunes Moreira

### 19.1 Introduction

The effort to understand business cycles within a growth framework is widespread in today's Economics. Theories such as the real business cycles (RBC) (see Kydland and Prescott [18]) and the dynamic stochastic general equilibrium (DSGE) (Blanchard e Kiyotaki [6]) have become a benchmark of mainstream macroeconomics. In these frameworks, a representative agent chooses not only the consumption, but also the amount of labour to be supplied to maximize the lifetime utility. Fluctuations then arise as the optimal response of the agent to exogenous shocks, which may be either productivity or demand shocks. But in fact, the idea that growth and fluctuations are intertwined phenomena can be traced back to the seminal work of Richard Goodwin [12] who developed a growth-cycle model. His class struggle model blends aspects of the Harrod–Domar growth model with the Phillips curve, highlighting that trend and cycle are indissolubly fused, which yields endogenous cycles (see Harcourt [14]).

In this vein, Goodwin presents a theory of economic fluctuations, whereby the economic variables interact with each other in an endogenous way. Hence, the cycle emerges from the interaction of deterministic variables, and not as the outcome of the exogenous aleatory shocks. Formally, the growth-cycle framework consists of two simultaneous non-linear dynamic equations, one for the employment rate and the other for the wage share. We can interpret it as a Lotka–Volterra's predator–prey

---

R. A. Araujo (✉)

University of Brasilia, Department of Economics, Brasilia, Brazil  
e-mail: [rsaaraujo@unb.br](mailto:rsaaraujo@unb.br)

H. N. Moreira

University of Brasilia, Department of Mathematics, Brasilia, Brazil  
e-mail: [helmar@mat.unb.br](mailto:helmar@mat.unb.br)

model in a Marxian framework, in which the wage share is the predator and the employment rate is the prey.

Although providing a compelling explanation for economic cycles, for some authors such as Tavani and Zamparelli [24] and Harvie [15], the Goodwin model seems to be too simplified to explain the long-run shifts in the growth cycle. Zipperer and Skott [26, p. 56], for instance, challenge the model on the grounds that “the large fluctuations in utilization rates, for instance, must raise questions for the adequacy of the Goodwin model, which takes utilization as constant”.

To furnish the model with more realism, some authors extended it to consider under-capacity utilization. By introducing this possibility, it is obtained that the model assigns a more inclusive role to demand. As pointed out by Hein [16, p. 248], “the rate of capacity utilization is the important indicator for the development of demand concerning the capital stock in existence and thus becomes one of the major factors influencing investment decisions.” Sasaki [20], for instance, blended Kaleckian and Marxian macro-dynamic features into the model. The author then presents an extension to Goodwin’s formulation in which an autonomous investment function is introduced in the lines of the post-Keynesian growth model. Then he shows that the obtained system has an asymptotically stable equilibrium that can be destabilized into a limit cycle.

Araujo et al. [1] also focused on capacity utilization as a new variable. Here we also aim at testing an extended Goodwin’s model with capacity utilization as an additional variable, however, with a crucial difference. While their model considers an autonomous investment function that relies on the accelerator principle (see e.g. Skott [22]), we preserve the Goodwin formulation in which there is no autonomous investment. And, unlike Sasaki, we introduce capacity utilization through Skott’s [21] formulation of an output expansion function. This avoids the criticisms against the Kaleckian investment functions raised by Blecker [7] and Skott [22].

Our paper has some similarities with Flaschel [10] who also advanced an extension of the Goodwin growth-cycle model considering under-capacity utilization growth in the presence of Skott’s output expansion function. But there are also some important differences. The first one refers to the way the extensions are made. While we built our extension following Goodwin, and considering less than full capacity growth according to Skott, Flaschel departed from Skott’s formulation by adding a Phillips curve in his 2D model. Using this route, he ends up using the capital-output ratio as a proxy for capacity utilization. Besides, Flaschel writes the model in terms of the rate of profit, while we focused on the profit share which provides a more precise picture of the income distribution.

Although the obtained model departs from [10] and [1], we also have found that the system admits a family of periodic solutions if the output expansion function registers as a function of the income distribution only. The model does not display periodic solutions if we introduce the employment rate into “Skott’s rule”. In this last case the qualitative properties of the model change and it becomes locally stable. To illustrate these results, we carry out the analysis both in terms of general functions as well as particular examples. The main contribution of this chapter lies in providing a simple baseline model to study distributive dynamics that deals

with the interactions amongst income distribution, labour, and goods markets while presenting empirical support.

Finally, we test the model for the US economy. As pointed out by Zipperer and Skott [26, pp. 52–53], the choice of the US economy is convenient insofar as “it is as close as one gets to a closed economy, the size of the public sector is relatively modest, and unlike Japan and many European economies, the USA did not have large amounts of hidden unemployment in backward sectors for a good part of the postwar period. With respect to data, moreover, quarterly series are available for some of the key variables in heterodox models.”

To test the extended model for the US economy by using quarterly data from 1970 to 2019, we have adopted a VAR methodology. The main results of the generalized impulse-response functions provided by the VAR model confirms the profit-squeeze mechanism: a positive profit share innovation positively affects both the employment rate but the rate of capacity utilization, suggesting a profit-led pattern. We also performed the traditional Granger causality test, which yields significant results. We organize the chapter as follows. After this introductory Section, Sect. 19.2 presents an extension to the Goodwin model by including the rate of capacity utilization as a new variable. Section 19.3 studies the stability and presents simulations. Section 19.4 offers the econometric estimations of the model for the US economy, and Sect. 19.5 presents our conclusions.

## 19.2 Adding Capital Utilization to Goodwin's Model

In the original Goodwin model [12], the endogenous variables are the wage share,  $\omega$ , and the employment rate,  $v$ . Here following Skott [21], we write the system in terms of the profit share,  $h$ , instead of the wage share. As in the original model, let us consider a closed economy without government activity that uses capital,  $k$ , and labour,  $L$ , to produce output,  $q$ , by using a fixed coefficient technology. The model is built under the concept of full capacity utilization, namely  $\mu = 1$ . Then, by introducing the possibility of under-capacity utilization, namely  $\mu < 1$  it yields a version of the model that considers a more inclusive role for demand. In the real world, the stock of capital is often underutilized and we can use the rate of capacity utilization as a measure of demand thus providing a less stylized explanation to the growth cycle.

$$q = \min \left[ \frac{k\mu}{\sigma}, \frac{l}{a} \right]. \quad (19.1)$$

Following Goodwin, the capital-full capacity output ratio is constant but departing from his formulation, we assume that the labour-output ratio is also constant. The efficiency condition of the Leontief function requires that  $\frac{k\mu}{\sigma} = \frac{l}{a}$ . As we assume that  $\sigma$  and  $a$  are assumed to be constants, and considering that the hat



over the variables denotes the growth rate, the dynamic efficiency condition may be written as

$$\hat{k} + \hat{\mu} = \hat{l}. \quad (19.2)$$

Let us assume that workers do not save and that the propensity save of capitalists is denoted by  $s$ . Assuming, for the sake of simplicity only, that there is no depreciation of the stock of capital, the change in the stock of capital is given by  $\dot{k} = s(q - wl)$ , where  $w$  is the wage. Considering that  $h = 1 - w/a$  denotes the profit share<sup>1</sup> since  $w/a$  is the wage share, it allows us to write, after some algebraic manipulation, the variation of the stock of capital as

$$\hat{k} = sh\mu/\sigma. \quad (19.3)$$

To determine the dynamic path of  $\mu$ , let us recall that by definition  $\mu = q/q^f$ , where  $q^f$  stands for the full capacity output. Then, by introducing the possibility of under-capacity utilization, we obtain a version of the model that considers a more inclusive role for demand. This allows a less stylized (simplified) explanation of growth cycles that actually take into account the fact that, in the real world, the stock of capital is often underutilized. Hence, after some algebraic manipulation, we conclude that

$$\hat{\mu} = \hat{q} - \hat{k}. \quad (19.4)$$

To derive the dynamical path for  $q$ , let us follow Skott [22] through his formulation of an output expansion function. According to this specification, higher profitability stimulates the rate of expansion of production per unit of capital. The rationale here is that a positive demand shock increases the profit share, with the firms increasing the growth rate of output as a response:

$$\hat{q} = \phi(h), \quad (19.5)$$

with  $\phi'(h) > 0$ . But Skott [21] presented an alternative specification in which he writes the price function in terms of the employment level too. The rationale rests on the fact that there are adjustment costs concerning output expansion and employment expansion. Skott and Ryo [23, p. 837] for instance, consider that “[h]igh rates of employment increase the costs of recruitment, and since the quit rate tends to rise when labour markets are tight, the gross recruitment needs associated with any given rate of expansion increase when low unemployment makes it difficult

---

<sup>1</sup>Our choice of writing the system in terms of the profit share instead of the wage share is related to the fact that the extension presented here is made by using the expansion output function due to Skott [22], which registers as a function of the profit share.

to attract new workers.” In this case, expression (19.5) may be rewritten as

$$\hat{q} = \phi(h, v), \quad (19.6)$$

with  $\phi_h(h, v) > 0$  and  $\phi_v(h, v) < 0$ . In what follows we will generally refer to the output expansion function as

$$\hat{q} = \phi(\cdot). \quad (19.7)$$

And we will make explicit if we are referring to either (19.5) or (19.6). As we show below, the dynamics of the model changes substantially if we consider one of these two options. Hence, by substituting expressions (19.3) and (19.7) into expression (19.4), we obtain the differential equation for the rate of capacity utilization, namely:

$$\dot{\mu} = \mu[\phi(\cdot) - sh\mu/\sigma]. \quad (19.8)$$

Expression (19.8) shows, on the one hand, that if the capital accumulation grows at a lower rate than the output, then the rate of capacity utilization will increase since there will be a pressure on the use of the existing stock of capital. On the other hand, if the capital accumulation grows at a higher pace than the output expansion, the rate of capacity utilization will be on the wane, meaning that the under-utilization of the stock of capital will increase. Let us define the function  $F(\mu, h) = \phi(\cdot) - sh\mu/\sigma$ . This allows us to rewrite expression (19.8) as

$$\hat{\mu} = F(\mu, h). \quad (19.9)$$

By substituting expression (19.4) into expression (19.3), we obtain after some algebraic manipulation:

$$\hat{l} = \phi(\cdot). \quad (19.10)$$

The employment level is defined as  $v = l/n$ . Then it is possible to show that in the presence of under-capacity utilization the differential equation for the employment level may be written as

$$\dot{v} = v[\phi(\cdot) - \eta], \quad (19.11)$$

where  $\eta$  is the growth rate of population. To model the labour market, Goodwin [12] has assumed a Marxian reserve army mechanism translated in terms of a Phillips Curve, in which the growth rate of real wages increases with the employment rate. Here let us adopt the following linear specification:

$$\hat{w} = \theta(v - v^o), \quad (19.12)$$

where  $v^o$  denotes the natural rate of employment. Such specification is a simplified version of the expectations-augmented wage Phillips curve adopted by Chiarella et al. [8]. By following Goodwin [12], we do not focus on the dynamics of prices. Hence, we assume that the expectations of inflation do not enter the expression (19.12), thus generating this version of the wage Phillips curve. Since  $h = 1 - w/a$ , by taking the derivative with respect to time yields  $\dot{h} = -\dot{w}/a$ . Then, by substituting  $\dot{h}$  into expression (19.12), after some algebraic manipulation we obtain

$$\dot{h} = \theta(1 - h)(v^o - v). \quad (19.13)$$

We already mentioned that some authors, such as Sasaki [20] and Araujo et al. [1], have already extended the Goodwin model to consider the possibility of under-capacity utilization. The advantage of the approach presented here is in its parsimony. After introducing a new equation for the dynamic path of capacity utilization, the only behavioural relation that we add to the model is the output expansion function by Skott [22]. In the next section, we study under what circumstances such extension preserves the main conclusions of the original model while offering some additional insights.

### 19.3 The Existence and Stability of Equilibria

Let us now consider the dynamical model of three autonomous non-linear differential equations formed by expressions (19.8), (19.11), and (19.13). In steady state the relevant solution  $P^* = (v^*, h^*, \mu^*)$  (with economic meaning) can be obtained by considering  $\dot{v} = \dot{h} = \dot{\mu} = 0$ .

But now we distinguish between the two versions of the output expansion function. If we consider  $\hat{q} = \phi(h)$ , then the interior solution is obtained as follows. From expression (19.13),  $v^* = v^o$ , since  $h < 1$ . Then, from expression (19.11), the value of  $h^*$  is given implicitly by  $h^* = \phi^{-1}(\eta)$ . The value of  $\mu^*$  is then given by expression (19.8) according to:  $\mu^* = \sigma\eta/s\phi^{-1}(\eta)$ . By using the Hopf theorem, we can prove the following:

**Proposition 19.1** *If  $\hat{q} = \phi(h)$ , the internal equilibrium point  $P^* = (v^*, h^*, \mu^*)$  of the dynamic system formed by expressions (19.8), (19.11), and (19.13) always has a negative real root and a pair of pure imaginary roots, thus admitting a family of periodic solutions.*

**Proof** To prove this fact let us consider the Jacobian matrix calculated in  $P^* = (v^*, h^*, \mu^*)$ , which is given by

$$\begin{bmatrix} 0 & v^o\phi'(h^*) & 0 \\ -\theta(1 - h^*) & 0 & 0 \\ 0 & \mu^*[\phi'(h^*) - (s\mu^*)/\sigma] & -\eta \end{bmatrix}.$$

By setting  $S_1(P^*)$ ,  $S_2(P^*)$ , and  $S_3(P^*)$  as the coefficients of the characteristic polynomial of matrix  $J$  evaluated at  $P^*$ , i.e.:

$$\lambda^3 + S_1\lambda^2 + S_2\lambda + S_3 = 0,$$

where

$$S_1(P^*) = -\text{tr } J(P^*) = \eta.$$

The value of  $S_2(P^*)$  is given by the sum of the principal minors of  $J$ , namely  $S_2(P^*) = \det(J_1)(P^*) + \det(J_2)(P^*) + \det(J_3)(P^*)$ , which yields

$$S_2(P^*) = v^o \phi'(h^*) \theta (1 - h^*).$$

The third coefficient of the characteristic polynomial, namely  $S_3(P^*)$ , is given by  $S_3(P^*) = -\det J(P^*)$ . Hence

$$S_3(P^*) = \eta \theta (1 - h^*) v^o \phi'(h^*).$$

Then we conclude  $S_1(P^*) > 0$ ,  $S_2(P^*) > 0$ , and  $S_3(P^*) > 0$  as  $0 < h^* < 1$  and  $\phi'(h^*) > 0$ . Besides, we compute the value of  $E$  as  $E(P^*) = S_1(P^*)S_2(P^*) - S_3(P^*)$ . After some algebraic manipulation, one obtains

$$E(P^*) = 0.$$

Then  $S_2 > 0$  and  $E(P^*) = 0$ . Under such conditions, Asada and Semmler [2] show that the characteristic polynomial has a pair of pure imaginary roots.<sup>2</sup> According to Guckenheimer and Holmes [13], if the characteristic polynomial at  $P^*$  has a pair of pure imaginary eigenvalues and no other eigenvalues with zero real parts, there exist some non-constant periodic solutions of the system.

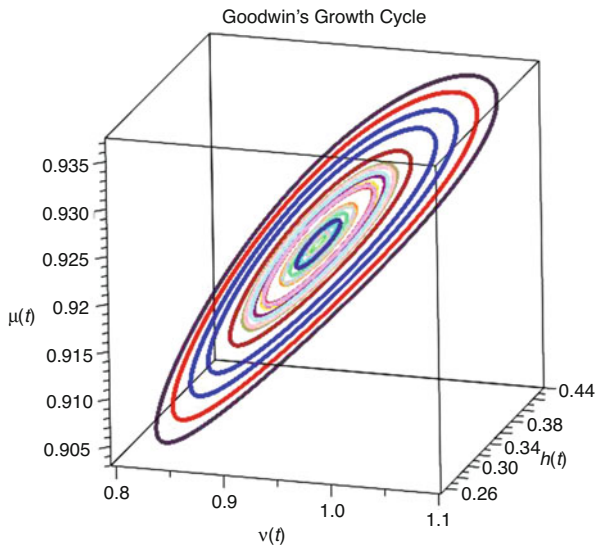
To illustrate the periodic orbits, let us assume a particular functional form for the expansion function. Let us consider that  $\hat{q} = \phi(h) = 0.91h - 0.041$ . Such specification is different from the usual choices by Skott, in which a highly non-linear function is adopted. We have chosen a linear specification because we want to emphasize that the cyclical solution of the model does not depend on the ad-hoc choice of a non-linear output expansion function.<sup>3</sup>

---

<sup>2</sup>For Asada and Semmler [2, p. 634], the characteristic polynomial has a pair of pure imaginary roots if and only if  $S_2 > 0$  and  $E = 0$ .

<sup>3</sup>Flaschel [10] also considered a linear expansion function and justified that choice claiming that "behaviour around the steady state should at first be assumed to be as linear as possible in order to investigate the dynamics first on the basis of intrinsic or unavoidable non-linearities solely, that is, as linear growth rate dynamics".

**Fig. 19.1** Periodic solutions in the space  $(v, h^o, \mu)$  when the expansion function depends on income distribution only



In addition, we assume that  $v^o = 0.96$ ,  $\eta = 0.2775$ ,  $\theta = 0.5$ , and  $(s/\sigma) = 0.86$ . Then, the steady state values are  $v^* = 0.94$ ,  $h^* = 0.35$ , and  $\mu^* = 0.9219269103$ . The characteristic polynomial of the Jacobian matrix is given by  $\lambda^3 + 0.2775\lambda^2 + 0.2780050\lambda + 0.2275 = 0$ . It has a pair of pure imaginary roots  $\lambda_{1,2} = \pm 0.527261794557504i$  and a negative real root  $\lambda_3 = -0.2775$ . According to the Proposition 19.1, all solutions are periodic. A family of periodic solutions of  $v(t)$ ,  $h(t)$ , and  $\mu(t)$ , is illustrated in Fig. 19.1.

If we consider the alternative specification for the output expansion function, namely  $\hat{q} = \phi(h, v)$ , we obtain another solution. From expression (19.11), the value of  $h^*$  is given implicitly by  $\phi(v^o, h^*) = \eta$  after determining the value of  $v^* = v^o$  from (19.13). Then, the value of  $\mu^*$  is then given by expression (19.8) according to:  $\mu^* = \sigma \eta / (sh^*)$ . By using the Routh–Hurwitz criterion, we can prove the following:

**Proposition 19.2** *If the output expansion function depends both on the profit share and the employment level, the singular point  $P^* = (v^*, h^*, \mu^*)$  of the system formed by expressions (19.8), (19.11), and (19.13) is locally stable.*

**Proof** Now the Jacobian calculated in  $P^* = (v^*, h^*, \mu^*)$  is given by

$$\begin{bmatrix} v^o \phi_v(v^o, h^*) & v^o \phi_h(v^o, h^*) & 0 \\ -\theta(1 - h^*) & 0 & 0 \\ \mu^* \phi_v(v^o, h^*) & \mu^* [\phi_h(v^o, h^*) - (s\mu^*)/\sigma] - \eta \end{bmatrix}.$$

The necessary and sufficient condition for the local stability is that all roots of the characteristic equation have negative real parts, which from the Routh–Hurwitz criterion requires that  $S_1(P^*) > 0$ ,  $S_2(P^*) > 0$ ,  $S_3(P^*) > 0$ , and

$E(P^*) = S_1(P^*)S_2(P^*) - S_3(P^*) > 0$ , where  $S_1(P^*)$ ,  $S_2(P^*)$ , and  $S_3(P^*)$  are the coefficients of the characteristic polynomial of matrix  $J$  evaluated at  $P^*$ , which is given by

$$\lambda^3 + S_1\lambda^2 + S_2\lambda + S_3 = 0,$$

where

$$S_1(P^*) = -\text{tr } J(P^*) = -v^o\phi_v(v^o, h^*) + \eta,$$

which is positive since all the parameters are positive,  $0 < h^* < 1$  and  $\phi_v(v^o, h^*) < 0$ . The value of  $S_2(P^*)$  is given by  $S_2(P^*) = \det(J_1)(P^*) + \det(J_2)(P^*) + \det(J_3)(P^*)$ , which yields

$$S_2(P^*) = v^o\phi_h(v^o, h^*)\theta(1 - h^*) - \eta\phi_v(v^o, h^*)v^o$$

which is positive since all the parameters are positive,  $0 < h < 1$ , and  $\phi_h(v^o, h^*) > 0$  and  $\phi_v(v^o, h^*) < 0$ . Hence, we conclude that  $S_2(P^*) > 0$ . The third coefficient of the characteristic polynomial, namely  $S_3(P^*)$ , is given by  $S_3(P^*) = -\det J(P^*)$ . Hence

$$S_3(P^*) = \eta\theta(1 - h^*)v^o\phi_h(v^o, h^*).$$

As  $0 < h^* < 1$  and  $\phi_h(v^o, h^*) > 0$ , we conclude that the sign of  $S_3(P^*) > 0$ . Besides, since  $E(P^*) = S_1(P^*)S_2(P^*) - S_3(P^*)$ , we obtain

$$E(P^*) = \phi_v(v^o, h^*)v^o[-\eta^2 + v^o\eta\phi_v(v^o, h^*) - \phi_h(v^o, h^*)\theta(1 - h^*)].$$

From the hypothesis made, it is easy to see that  $E(P^*) > 0$ . Then we conclude that the interior equilibrium  $P^* = (v^*, h^*, \mu^*)$  given by  $v^* = v^o$ ,  $\phi(v^o, h^*) = \eta$  and  $\mu^* = \sigma\eta/s h^*$  is asymptotically stable (Fig. 19.2).

To illustrate the stable equilibrium, let us assume that the expansion function is given by  $\hat{q} = \phi(h) = 0.91h - 0.2v - 0.041$ . With this specification, and using the above parameters, we obtain the following equilibrium point  $v^* = 0.94$ ,  $h^* = 0.3197802198$ , and  $\mu^* = 0.9017821466$ . The characteristic polynomial is given by  $\lambda^3 + 0.25\lambda^2 + 0.302586\lambda + 0.01803766 = 0$ . It has a negative real root  $\lambda_1 = -0.062$  and a pair of complex roots  $\lambda_{2,3} = -0.094 \pm 0.531125220632141i$ . According to the Proposition 19.2, the singular point  $P^* = (0.94, 0.3197802198, 0.9017821466)$  is asymptotically stable, which can be illustrated as follows (Figs. 19.3 and 19.4).

These results show that the introduction of the rate of capacity utilization as a new variable in the Goodwin framework through the output expansion function changes the dynamical property of the system. If the output expansion function depends only on the income distribution, the model displays a family of periodic solutions.

**Fig. 19.2** Vector field in the space  $(v, h, \mu)$  when the expansion function depends on income distribution only

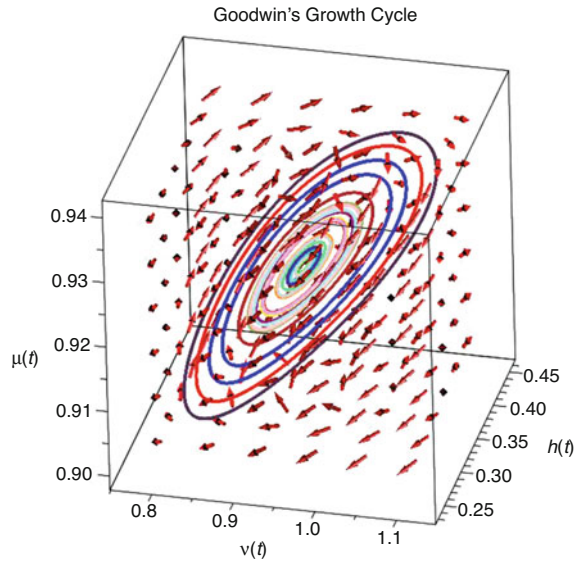
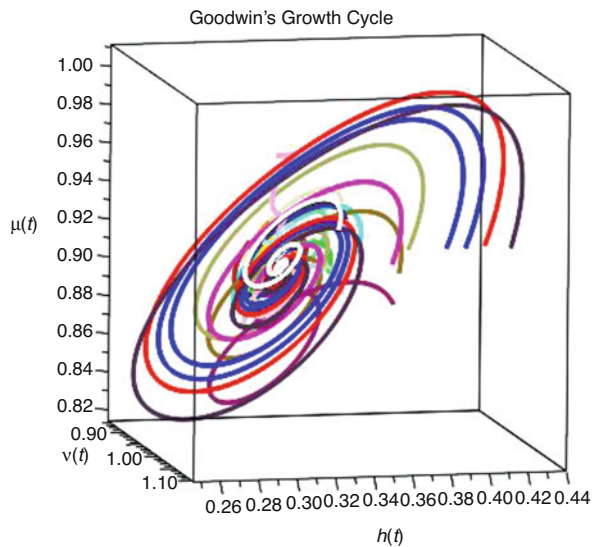


**Fig. 19.3** Local stable equilibrium for  $(v, h, \mu)$  when the expansion function depends on income distribution and employment level



If it also depends on the employment level, the dynamical property of the system changes from a centre to a stable equilibrium. Within the Goodwin literature in which the profit squeeze is the outcome, the profit-led is the most probable regime. But in the end, the prevalence of wage-led or profit-led regimes depends on the combination of parameters, which is the content of the next.

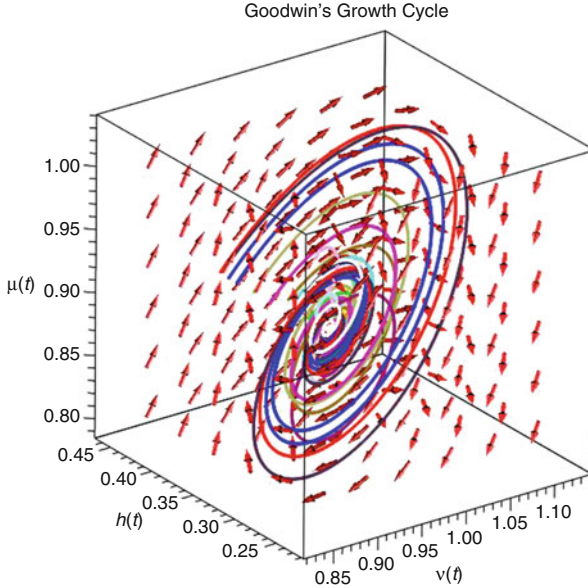


**Fig. 19.4** Vector field for  $(v, h, \mu)$  when the expansion function depends on income distribution and employment level

**Proposition 19.3** *The interior equilibrium is either profit-led or wage-led depending on the sign of  $\phi_h(v^*, h^*) - s\mu^*$ . If  $\phi_h(v^*, h^*) > s\mu^*$  we have a profit-led demand regime, and if  $\phi_h(v^*, h^*) < s\mu^*$  we have a wage-led demand regime.*

**Proof** From expression (19.8) evaluated in steady state, we can write

$$F(\mu^*, h^*) = \phi_h(v^*, h^*) - s\mu^*/\sigma = 0. \tag{19.14}$$

By the implicit function theorem, we know that

$$\frac{\partial \mu}{\partial h} = -\frac{F_h}{F_\mu} = \frac{\phi_h(v^*, h^*) - s\mu^*}{sh^*}.$$

Then the sign of  $\frac{\partial \mu}{\partial h}$  depends on the sign of the numerator. If  $\phi_h(v^*, h^*) > s\mu^*$ , then  $\frac{\partial \mu}{\partial h} > 0$  and we have a profit-led demand regime, and if  $\phi_h(v^*, h^*) < s\mu^*$ , then  $\frac{\partial \mu}{\partial h} < 0$  and we have a wage-led demand regime.

To study the existence of limit cycles, let us adopt the Hopf bifurcation theorem for the system formed by expressions (19.8), (19.11), and (19.13) when the output function also depends on the employment level using  $\eta > 0$  as the bifurcation parameter. Note that for  $\eta = \eta^*$ , the Jacobian matrix  $J = J(P^*)$  has a pair of complex eigenvalues with zero real part if and only if:  $S_2 > 0$  and  $E(P^*) = S_1(P^*)S_2(P^*) - S_3(P^*) = 0$ . Then we can prove the following proposition.



**Proposition 19.4** *If the output expansion function depends both on the income distribution and the employment level, the system (19.8), (19.11), and (19.13) does not admit a limit cycle.*

**Proof** To study the existence of a limit cycle, let us adopt the Hopf bifurcation theorem (see Gandolfo [11]). We have to check firstly if there exists a parameter, known as the parameter of bifurcation, which makes  $E(v^o, \eta) = 0$ . From expression (19.15) one obtains

$$\phi_v(v^o, h^*)v^o[-\eta^2 + v^o\eta\phi_v(v^o, h^*) - \phi_h(v^o, h^*)\theta(1 - h^*)] = 0. \quad (19.15)$$

From expression (19.15), two parameters are candidates to the bifurcation parameter,  $\eta > 0$  and  $\theta$ . As  $\phi_v(v^o, h^*)v^o > 0$  we obtain a quadratic equation in  $\eta$ , namely:

$$\eta^2 - v^o\phi_v(v^o, h^*)\eta + \phi_h(v^o, h^*)\theta(1 - h^*) = 0. \quad (19.16)$$

It is easy to see that  $\theta$  cannot be the bifurcation parameter since

$$\theta = \frac{-\eta^2 + v^o\phi_v(v^o, h^*)\eta}{\phi_h(v^o, h^*)\theta(1 - h^*)} < 0. \quad (19.17)$$

Now let us try  $\eta$  as the bifurcation parameter. The discriminant of the quadratic expression (19.16) is given by

$$\Delta = [v^o\phi_v(v^o, h^*)]^2 - 4\phi_h(v^o, h^*)\theta(1 - h^*). \quad (19.18)$$

To yield a relevant solution,  $\Delta$  has to be larger than zero, which requires that  $[v^o\phi_v(v^o, h^*)]^2 > 4\phi_h(v^o, h^*)\theta(1 - h^*)$ . If this condition holds, then the only possible solution is

$$\eta^* = \frac{v^o\phi_v(v^o, h^*)}{2} + \frac{\sqrt{\Delta}}{2} \quad (19.19)$$

since the conjugate root is negative. But even in the case of expression (19.19), we obtain after some algebraic manipulation that  $\eta < 0$ . Then, one concludes that  $E(P^*) > 0$ . Therefore, the polynomial characteristic has no two purely imaginary, simple conjugate eigenvalues at  $\eta = \eta^*$ . Thus, the system (19.8), (19.11), and (19.13) has no periodic orbits.

Then we demonstrated in this section that the extended Goodwin model using the Skott formulation of an output expansion function admits a family of periodic

solutions<sup>4</sup> if such function relies only on the profit share as in Skott [22]. If it also registers as a function of the employment level as in Skott [21], then the system displays no periodic orbits. Such a result is in strike contrast with the empirical literature testing extended versions of the Goodwin model even we consider the possibility of under-capacity utilization (See e.g. [26]). Then we are prone to conclude that the most parsimonious specification in which the product expansion functions depends only on the income distribution makes the model fit better the data. In the next section, we present one of these exercises.

## 19.4 Testing the Extended Goodwin Model on the US Economy

The theory of endogenous distributive cycles has been examined empirically in a significant number of studies. Qualitative support can be found in Desai [9], Harvie [15], Veneziani and Mohun [25], and Zipperer and Skott [26], amongst others. Barbosa-Filho and Taylor [4], Basu et al. [5], Kiefer and Rada [17], and Barbosa-Filho [3] provide parametric quantitative evidence.

The present paper adopts a country-specific time series approach to the problem. We followed the Vector Auto-Regressive (VAR) methodology used by Barbosa-Filho [3]. He has focused on the impulse-response function for establishing the pattern for the US economy has concluded that the “rate of employment goes down after an exogenous increase in the wage share, as well as that the wage share goes up after an exogenous increase in the rate of employment. These results are characteristic of a Marxian profit-led economy (...).” However, the conclusion that the economy is a Marxian profit-led economy does not confirm the existence of distributive cycles unambiguously for the US economy. To establish this result other econometric tests, such as causality should have been adopted.

Our dataset is quarterly and comprehends the period between 1970 and 2019. All series are from the Federal Reserve Bank of St. Louis. Employment rate series were obtained as the opposite of the unemployment rates. We compute the profit share as the opposite of the compensation of employees as a percentage of the net domestic income at production prices. For the VAR estimations, we converted the series to logarithmic form. From an empirical point of view, distributive cycles can be interpreted as the short-run dynamics that generate the long-run trend as a result of non-linear interactions. Then, as a preliminary step, we detrended our time series using the traditional Hodrick–Prescott filter with a smoothing parameter of 1600, as depicted in Figs. 19.5, 19.6, and 19.7. Values of cyclical deviations of the trend are shown on the left axis, while values of the trend itself are on the right. We focus on the relationship between the variable trends.

---

<sup>4</sup>Araujo et al. [1] have already shown a similar result. But those authors have assumed an independent investment function that departs from the Goodwin formation.

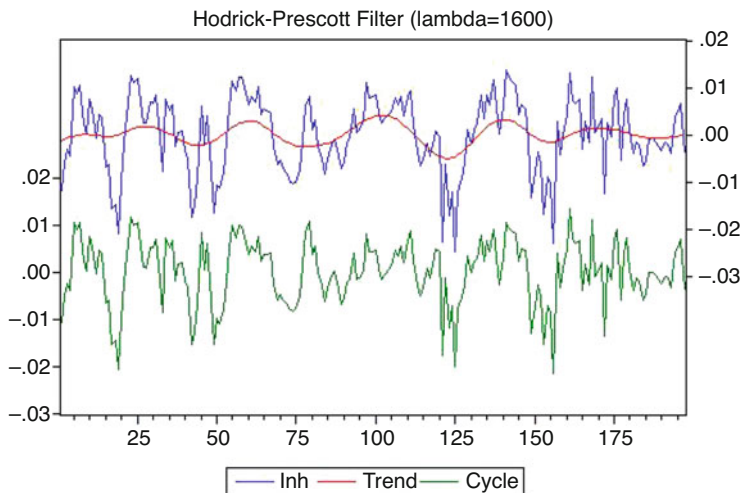


**Fig. 19.5** Profit share series: quarterly data from 1970q1 to 2019q3

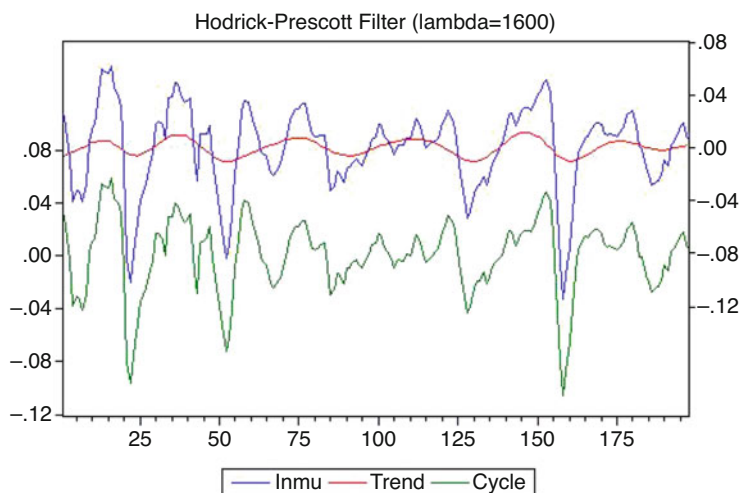


**Fig. 19.6** Capacity utilization series: quarterly data from 1970q1 to 2019q3

The traditional VAR approach assumes that all series in the model are stationary. In this sense, the first step in the econometric analysis is to check whether the detrended series contains a unit root. To this end, the Kwiatkowski–Phillips–Schmidt–Shin (KPSS), and the Augmented Dickey–Fuller (ADF) tests are performed. The null hypothesis of the KPSS test is that the series is stationary, and the null hypothesis of the ADF test is that the series is non-stationary. The outcome of these tests (see Appendix A.3) indicated that the three detrended time series are  $I(0)$ .

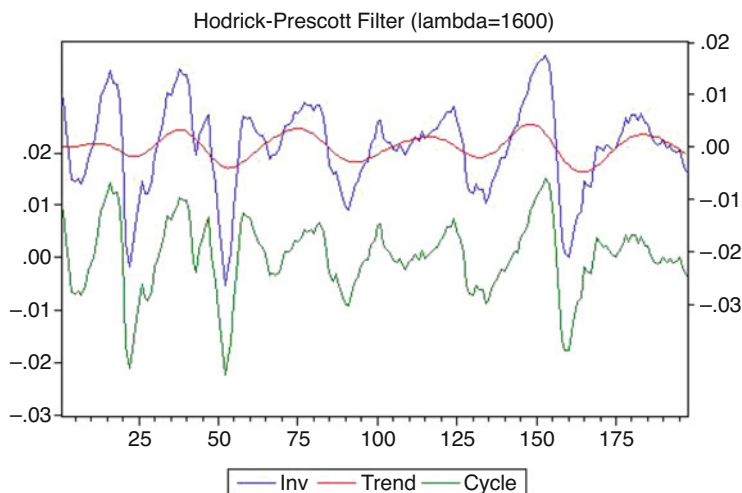


**Fig. 19.7** Employment level series: quarterly data from 1970q1 to 2019q3

The next step is to determine the appropriate lag length employing the Akaike (AIC), Schwartz (SC), and Hannan–Quinn (HQ) information criteria. All these criteria suggest that VAR(2) is the best model (see Table A.13 in Appendix A.3). In this sense, our benchmark specification with three variables, one constant, and two lags, provides a parsimonious model. The parameters of the VAR model are estimated by the OLS method, and four diagnostic tests are performed (see the Appendix A.3). The first one indicates that the VAR model with two lags is stable insofar as the inverse roots of the AR characteristic polynomial have a modulus less than one and lie inside the unit circle (see Fig. A.1).

The second one is performed to check the autocorrelation hypothesis. Since the  $p$ -value of the Lagrange Multiplier test is about 0.53 in the first lag (see Table A.15), there is no evidence of autocorrelation in the benchmark model specification. The third one, the White heteroscedasticity test with cross terms, has a  $p$ -value close to zero. This suggests that there is no homoscedasticity in the residuals of the model. The last one, the Jarque–Bera test with Cholesky's covariance (Lutkepohl [19]), suggests that the model residuals have a normal distribution, but this result is sensible to the orthogonalization method.

The parameters estimated by VAR models are hard to be interpreted (the  $t$ -tests on individual coefficients are not valid because the regressors, in general, are highly collinear). Considering this, we follow the standard literature of time series econometrics and focus only on the generalized impulse-response functions. Figure 19.8 presents the impulse-response functions to study how the series react to shocks from other variables. The most relevant column is the first one, as it focuses on the response of the employment level and capacity utilization to an exogenous shock in the profit share.

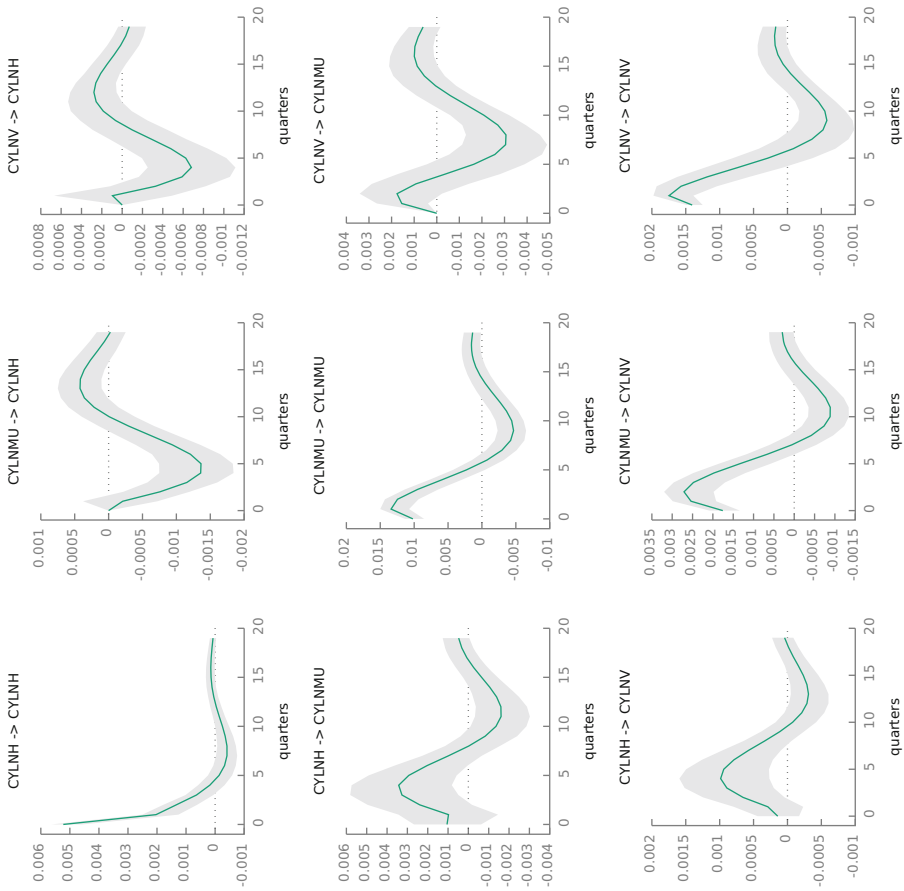


Fig. 19.8 Impulse response—HP filter

In line with the theoretical model presented, we expect, for a profit-led regime, that a positive shock in the profit share increases both the employment rate and the capacity utilization. Results indicate that a positive disturbance in the profit share increases both the capacity utilization and the employment level. The positive impact on the employment rate is expected insofar as higher profitability increases accumulation, which leads to higher levels of employment. That corresponds to the traditional distributive cycle mechanism. With higher levels of employment, we could expect a further increase in capacity utilization due to the higher consumption of the working class. Then we have a profit-led regime.

In Table A.14 in the Appendix, we report the Granger causality test. Results support the hypothesis that profit share causes the employment level and capacity utilization. But causality also runs in the opposite direction, with the employment level and capacity utilization causing the profit share. That underpins the idea that those variables are intrinsically related to the business cycle, and it is not possible to refer to any of them as exogenous. The aforementioned Table A.14 in the Appendix reports the estimate  $p$ -values.

As discussed at the beginning of this section, from an empirical point of view, we can interpret distributive cycles as the short-run cycles that generate the long-run trend as a result of non-linear interactions. Using quarterly data for the US economy, we did find some empirical support to conclude that both growth and demand regime have been profit-led in the considered period. The standard VAR model specification provided some evidence that a positive profit share shock affects, in the same direction, both economic growth and the rate of capacity utilization.

## 19.5 Conclusions

In this chapter, we extended Goodwin's model by considering the rate of capacity utilization as a new variable in the system. The introduction of this variable allows us to better understand the connections amongst the employment level, profit share, and rate of capacity utilization. When using the output expansion as a function of the profit share only, the model exhibits periodic orbits, implying that original insight of the Goodwin model is preserved. But supposing that the output expansion also as a function of the employment level, the model has an asymptotically stable equilibrium that displays no periodic orbits amongst the variables (which departs from Goodwin's prediction of endogenous distributive cycles).

Finally, we empirically addressed the relationship between employment, income distribution, and capacity utilization to the US economy using quarterly data from 1970 to 2019. By using generalized impulse-response functions provided by the VAR model, we have concluded that a positive profit share innovation affects the employment rate and the rate of capacity utilization positively, suggesting a profit-squeeze mechanism. Granger causality also gives support to the idea that all variables are intrinsically related and determined by each other. Even though these results correspond to an indirect assessment of our theoretical model, they show that

our theoretical framework can reproduce the main dynamics found in data, adding some robustness to the analysis made by us.

## References

1. Araujo, R.A., Dávila-Fernández, M.J., Moreira, H.N.: Some new insights on the empirics of Goodwin's growth-cycle model. *Struct. Change Econ. Dyn.* **51**, 42–54 (2019)
2. Asada, T., Semmler, W.: Growth and finance: an intertemporal model. *J. Macroecon.* **17**(4), 623–649 (1995)
3. Barbosa-Filho, N.H.: Elasticity of substitution and social conflict: a structuralist note on Piketty's Capital in the Twenty-first century. *Camb. J. Econ.* **40**(4), 1167–1183 (2015)
4. Barbosa-Filho, N.H., Taylor, L.: Distributive and demand cycles in the US economy—a structuralist Goodwin model. *Metroeconomica* **57**(3), 389–411 (2006)
5. Basu, D., Chen, Y., Oh, J.S.: Class struggle and economic fluctuations: VAR analysis of the post-war US economy. *Int. Rev. Appl. Econ.* **27**(5), 575–596 (2013)
6. Blanchard, O.J., Kiyotaki, N.: Monopolistic competition and the effects of aggregate demand. *Am. Econ. Rev.* **77**, 647–666 (1987)
7. Blecker, R.: Wage-led versus profit-led demand regimes: the long and the short of it. *Rev. Keynes. Econ.* **4**(4), 373–390 (2016)
8. Chiarella, C., Flaschel, P., Franke, R.: Foundations for a Disequilibrium Theory of the Business Cycle: Qualitative Analysis and Quantitative Assessment. Cambridge University Press, Cambridge (2005)
9. Desai, M.: Growth cycles and inflation in a model of the class struggle. *J. Econ. Theory* **6**(6), 527–545 (1973)
10. Flaschel, P.: Viability and corridor stability in Keynesian supply-driven growth. *Metroeconomica* **52**(1), 26–48 (2001)
11. Gandolfo, G.: Economic Dynamics: Study Edition. Springer, Berlin (1997)
12. Goodwin, R.M.: Socialism, Capitalism & Economic Growth. Cambridge University Press, Cambridge (1967)
13. Guckenheimer, J., Holmes, P.J.: Nonlinear oscillations, dynamical systems, and bifurcations of vector fields. In: Applied Mathematical Sciences, vol. 42. Springer, New York (2013). <https://doi.org/10.1007/978-1-4612-1140-2>
14. Harcourt, G.: Fusing indissolubly the cycle and the trend: Richard Goodwin's profound insight. *Camb. J. Econ.* **39**(6), 1569–1578 (2015)
15. Harvie, D.: Testing Goodwin: Growth Cycles in Ten OECD Countries. *Camb. J. Econ.* **24**(3), 349–376 (2000)
16. Hein, E.: Distribution and Growth After Keynes: A Post-Keynesian Guide. Edward Elgar (2014)
17. Kiefer, D., Rada, C.: Profit maximising goes global: the race to the bottom. *Camb. J. Econ.* **39**(5), 1333–1350 (2015)
18. Kydland, F.E., Prescott, E.C.: Time to build and aggregate fluctuations. *Econometrica* **50**, 1345–1370 (1982)
19. Lütkepohl, H.: Introduction to Multiple Time Series Analysis. Springer, Berlin (2013)
20. Sasaki, H.: Cyclical growth in a Goodwin–Kalecki–Marx model. *J. Econ.* **108**(2), 145–171 (2013)
21. Skott, P.: Conflict and Effective Demand in Economic Growth. Cambridge University Press, Cambridge (1989)
22. Skott, P.: Growth, instability and cycles: Harrodian and Kaleckian models of accumulation and income distribution. In: Setterfield, M. (ed.) Handbook of Alternative Theories of Economic Growth, Chapters, chap. 5. Edward Elgar Publishing (2010)

23. Skott, P., Ryoo, S.: Macroeconomic implications of financialisation. *Camb. J. Econ.* **32**(6), 827–862 (2008)
24. Tavani, D., Zamparelli, L.: Endogenous technical change, employment and distribution in the goodwin model of the growth cycle. *Stud. Nonlinear Dyn. Econom.* **19**(2), 209–216 (2015)
25. Veneziani, R., Mohun, S.: Structural stability and Goodwin's growth cycle. *Struct. Change Econ. Dyn.* **17**(4), 437–451 (2006)
26. Zipperer, B., Skott, P.: Cyclical patterns of employment, utilization, and profitability. *J. Post Keynesian Econ.* **34**(1), 25–58 (2011)



# Chapter 20

## Financial Stress, Regime Switching and Macrodynamics



Pu Chen and Willi Semmler

### 20.1 Introduction

Since the seminal papers on cointegration by Engle and Granger [7] and Johansen [16] vector error correction model (VECM) has been widely used to model macroeconomic time series. The virtue of VECM is that it permits to test both the economic concepts of equilibrium and the adjustment process towards the equilibrium. Then, the long-run equilibrium relations as well the adjustment to the equilibrium can be empirically testable. However, the phenomena of business cycles point to differences in the adjustment process during different phases of the business cycle. Hence, regime switching vector autoregressive models have been used by many researchers, such as Hamilton [11], Mittnik et al. [18] and Chen et al. [5], to take into account the impact of the different phases in the business cycle. Balke et al. [3] combine these two classes of models and present the regime switching vector error correction models. Since then, regime switching VECM has been applied in numerous empirical analysis.

Balke et al. [3] applied threshold VECM to reflect discrete adjustment responses to a cointegrating relationship when it is “too far from the equilibrium”. The cointegration relation is obtained through a regression relying on the super consistency of the least square (LS) estimator. The model specification is verified through tests of

---

P. Chen

Melbourne Institute of Technology, Melbourne, VIC, Australia

e-mail: [pchen@academic.mit.edu.au](mailto:pchen@academic.mit.edu.au)

W. Semmler (✉)

New School for Social Research, Department of Economics, New York, NY, USA

University of Bielefeld, Department of Economics, Bielefeld, Germany

e-mail: [semmlerw@newschool.edu](mailto:semmlerw@newschool.edu)

the existence of the threshold nonlinearity. Hansen et al. [12] propose a maximum likelihood estimation for a two regime threshold VECM, where the switching variable is also the endogenous cointegrating relationship. A grid search algorithm is proposed to estimate both the cointegration vector and the threshold value for the regime classification simultaneously. An R package is available for this class of threshold VECMs.<sup>1</sup>

Most empirical research works of threshold VECMs follow the approach proposed in Hansen et al. [12], Bec et al. [4], Saikkonen [20, 21]. They present a more general class of regime switching error correction models, where the number of regimes can be more than two and the switching can be a discontinuous adjustment or a continuous smooth transition. Saikkonen [21] points out a difficulty in this class of models is “to determine theoretically the exact number of  $I(1)$  components in the models”. Hence, it is inconclusive how to test the cointegration rank in this class of models. Common to the mentioned regime switching error correction models is that the cointegrating relations are linear, and the adjustments are nonlinear or switching. The thresholds are determined endogenously.

Gonzalo et al. [9] take a different approach to regime switching error correction models. In their models, the cointegrating relations are switching whereas the adjustment is linear. The switching variable is an exogenously stationary variable. This approach is less attractive as the switching long-run equilibrium relations are hard to justify. In addition, leaving an influencing variable not included in the VECM is also hard to justify. In this chapter, we will present a specific regime switching VECM where the cointegrating relation is linear, while the switching is determined by a stationary variable in the system.

## 20.2 Self-exciting Threshold Cointegrated Autoregressive Model

We consider a regime switching autoregressive model of order  $p$  that consists of two regimes:

$$\begin{aligned} \Delta X_t = & \left( \alpha^{(1)} \beta X_{t-1} + \sum_{j=1}^{L-1} \phi_j^{(1)} \Delta X_{t-j} + u_t^{(1)} \right) \mathbf{1}_{[f_{t-d} \leq \tau]} + \\ & \left( \alpha^{(2)} \beta X_{t-1} + \sum_{j=1}^{L-1} \phi_j^{(2)} \Delta X_{t-j} + u_t^{(2)} \right) \mathbf{1}_{[f_{t-d} > \tau]}, \end{aligned} \quad (20.1)$$

$$u_t^{(i)} \sim N(0, \Sigma^{(i)}), \text{ for } i = 1, 2,$$

---

<sup>1</sup>See Stigler et al. [22] for more details.

where  $X_t$  is a  $p$  dimensional vector,  $\beta$  is a  $p \times r$  matrix with  $p > r$ ,  $\beta$  is called cointegration vectors,  $r$  is called cointegration rank,  $f_{t-d}$  is the threshold variable observed at time  $t - d$ , and the regimes are defined by the prespecified threshold values  $-\infty = \tau_0 < \tau < \infty$ . For  $f_{t-d} = g(\Delta X_{j,t-1}, \Delta X_{j,t-2}, \dots, \Delta X_{j,t-d})$ , i.e., the threshold variable is a function of the lagged endogenous variables

$$f_{t-d} = g(\Delta X_{j,t-1}, \Delta X_{j,t-2}, \dots, \Delta X_{j,t-d}) = X_{j,t-1},$$

i.e., the threshold variable is simply a component of  $X_t$  with one lag.  $\tau$  is the threshold value. The model is called *self-exciting threshold cointegrated autoregressive model* of order  $L$  with two regimes, and it is denoted as SETCIAR( $L, d, 2$ ).

Our model differs from many threshold VECMs mentioned in the previous section in that the switching variable is an  $I(0)$  (integrated of order 0) variable which does not involve any estimation. In addition, the threshold value  $\tau$  is such that the sample can be separated into two different regimes by a suitable setting.

This setting simplifies many technical issues in parameter estimation and specification tests. In principle, the data analysis could be conducted in the two separate subsamples, each of which is a conventional VECM. The only issue of concern is how to take into account the restriction of the same cointegration relations across the two regimes to increase the efficiency of estimation.

### 20.2.1 Test of Cointegration Rank

As described in the last section, the test of the cointegration rank could be done in principle in two separate subsamples. This approach might, however, lead to conflicting results with respect to the cointegration rank in the two subsamples. We use the fact that the cointegration space is identical in the two regimes and test the cointegration rank in the whole sample. The procedure can be described as follows:

- Run the auxiliary regression:

$$\Delta X_t = \hat{\pi}_0 + \sum_{i=1}^{L-1} \hat{\pi}_i^{(1)} \Delta X_{t-i} \mathbf{1}_{[X_{j,t-1} \leq \tau]} + \sum_{i=1}^{L-1} \hat{\pi}_i^{(2)} \Delta X_{t-i} \mathbf{1}_{[X_{j,t-1} > \tau]} + \hat{u}_t, \quad (20.2)$$

$$X_{t-1} = \hat{\theta}_0 + \sum_{i=1}^{L-1} \hat{\theta}_i^{(1)} \Delta X_{t-i} \mathbf{1}_{[X_{j,t-1} \leq \tau]} + \sum_{i=1}^{L-1} \hat{\theta}_i^{(2)} \Delta X_{t-i} \mathbf{1}_{[X_{j,t-1} > \tau]} + \hat{v}_t, \quad (20.3)$$

- let

$$\hat{\Sigma}_{vv} = \frac{1}{T} \sum_{t=1}^T \hat{v}_t \hat{v}_t'$$

$$\hat{\Sigma}_{uu} = \frac{1}{T} \sum_{t=1}^T \hat{u}_t \hat{u}_t'$$

$$\hat{\Sigma}_{vu} = \frac{1}{T} \sum_{t=1}^T \hat{v}_t \hat{u}_t'$$

$$\hat{\Sigma}_{uv} = \frac{1}{T} \sum_{t=1}^T \hat{u}_t \hat{v}_t'$$

- Calculate the eigenvalues of

$$\hat{\Sigma}_{vv}^{-1} \hat{\Sigma}_{vu} \hat{\Sigma}_{uu}^{-1} \hat{\Sigma}_{uv}, \tag{20.4}$$

with ordered eigenvalues  $\hat{\lambda}_1 > \hat{\lambda}_2 > \dots > \hat{\lambda}_p$ . These eigenvalues can be used to calculate the Johansen test statistics. Following [15], we have the trace test:

$$\mathcal{L}_A - \mathcal{L}_0 = -T \sum_{i=r+1}^p \log(1 - \lambda_i). \tag{20.5}$$

The critical value for the tests can be found in [17].

### 20.2.2 Parameter Estimation

Following Lemma 13.1 in [17], after a proper normalization, the eigenvectors of (20.4) that correspond the  $r$  largest eigenvalues span the cointegration space and hence are consistent estimator of  $\beta$ . After obtaining a consistent estimator of  $\hat{\beta}$ , the other regime-dependent parameters can be estimated through the following regression:

$$\begin{aligned} \Delta X_t = & \left( \hat{\alpha}^{(1)} \hat{\beta} X_{t-1} + \sum_{i=1}^{L-1} \hat{\phi}_i^{(1)} \Delta X_{t-i} \right) \mathbf{1}_{[X_{j,t-1} \leq \tau]} + \\ & \left( \hat{\alpha}^{(2)} \hat{\beta} X_{t-1} + \sum_{i=1}^{L-1} \hat{\phi}_i^{(2)} \Delta X_{t-i} \right) \mathbf{1}_{[X_{j,t-1} > \tau]} + \hat{u}_t. \end{aligned} \tag{20.6}$$

In the above regression we plug in the estimated  $\hat{\beta}X_{t-1}$  as a regressor. Because  $\hat{\beta}$  is consistent, then the estimator  $\hat{\alpha}^{(i)}$ ,  $\hat{\phi}_l^{(i)}$  are consistent for  $i = 1, 2$  and  $l = 1, 2, \dots, L - 1$ .

### 20.2.3 Test of Switching

A key hypothesis of the regime switching VECM in (20.1) is the existence of two regimes. This should, however, be tested against the data. To test the null of no switching against the alternative of switching, a likelihood ratio test can be applied, given that the cointegrating relations have consistently been estimated. This boils down to testing the following parameter restrictions in the linear regression of (20.6):

$$H_O : (\alpha^{(1)}, \phi_1^{(1)}, \dots, \phi_{L-1}^{(1)}) = (\alpha^{(2)}, \phi_1^{(2)}, \dots, \phi_{L-1}^{(2)}) \quad ,$$

$$H_A : (\alpha^{(1)}, \phi_1^{(1)}, \dots, \phi_{L-1}^{(1)}) \neq (\alpha^{(2)}, \phi_1^{(2)}, \dots, \phi_{L-1}^{(2)}) .$$

## 20.3 Test of the Model on Economic Data

The dynamic interaction between financial stress and real output has drawn renewed attention of many researchers after the global financial crisis. Mittnik et al. [18, 19] develop a decision theoretical model that results in asymmetric interaction in different regimes. Mittnik et al. [18] and Chen et al. [5] apply regime switching VAR models to take into account the nonlinearity in the data. Following this approach, we apply a regime switching vector error correction model to investigate asymmetric adjustments to the equilibrium in different regimes.

We consider three variables in our study: the IMF financial stress index, the industrial output index, and the short-term interest rate. These three variables are chosen to be a measure of the real output, a measure of the financial stress, and a measure of the policy responses, respectively. The data are from IMF and OECD statistics.

The IMF Financial Soundness Indicators (FSI) is available for a large number of EU countries [1].<sup>2</sup> The IMF's (2011) FSI<sup>3</sup> refers to three major sources and measures of instability, namely: (1) a bank related index—a 12-month rolling beta of bank stock index and a Ted or interbank spread, (2) a security related index—a corporate bond yield spread, an inverted term spread, and a monthly stock returns (measured as declines), 6-month rolling monthly squared stock returns and finally, (3) an exchange rate index—a 6-month rolling monthly squared change in real exchange rates. All three sets of variables are detrended and scaled with their standard deviations in order to normalize the measures. Both the Industrial Production Indices and the short run interest rates are taken from the OECD Statistics.

### ***20.3.1 Discrimination of Regimes***

Identification of regimes is critical in modelling a Multi-Regime VAR (MRVAR) model [8, 19]. While many researches identify the regimes based on the sign and the size of the error correction term, which represent deviations from the long-run equilibrium, we identify the regime by the periods of the interest rate cuts or the periods of interest rate hikes. Typically during recession periods of a business cycle, we observe consecutive interest rates cuts, while during expansion periods, we observe rate hikes. Interest rate cuts and interest rate hikes reflect different policy responses to different economic circumstances, which aim at adjusting the economy to the long-run equilibrium state. This way of identification of the regimes simplifies the model specification and inference. In principle, we could divide the cointegration analysis in two separate subsamples of the respective regimes. However, a joint

---

<sup>2</sup>The Federal Reserve Bank of Kansas City and the Fed St. Louis have also developed a general financial stress index, called KCFSI and STLFSI, respectively. The KCFSI and the STLFSI take into account the various factors generating financial stress. The KC index is a monthly index, the STL index a weekly index, to capture more short run movements, see also Hatzius et al. [13]. Those factors can be taken as substitutes for the leverage ratios as measuring financial stress. See also the Bank of Canada index for Canada, i.e., Illing and Lui [14]. Both the KCFSI and STLFSI include a number of variables and financial stress is related to an: (1) increase in the uncertainty of the fundamental value of the assets, often resulting in higher volatility of the asset prices, (2) increase in uncertainty about the behaviour of the other investors, (3) increase in the asymmetry of information, (4) increase in the flight to quality, (5) decrease in the willingness to hold risky assets, and (6) decrease in the willingness to hold illiquid assets. The principle component analysis is then used to obtain the FSI. Linear OLS coefficients are normalized through their standard deviations and their relative weights computed to explain an FSI index. A similar procedure is used by Adrian and Shin [2] to compute a macro economic risk premium. We want to note that most of the variables used are highly correlated with credit spreads. The latter have usually the highest weight in the index, for details see Hakkio and Keeton [10, Tables 2–3].

<sup>3</sup>This is published for advanced as well for developing countries, see IMF (2008) and IMF FSI (2011).

analysis will increase the efficiency of the inference and also avoid the problem that we might obtain two different sets of cointegration relations.

### 20.3.2 Model Specification

The specification of the model consists of the following three steps:

- Test of unit roots in the time series

Country	USA	DEU	FRA	ITA	ESP
log(IP)					
ADF	0.0100	0.02396	0.2013	0.1491	0.4520
PP	0.5449	0.1041	0.4711	0.4966	0.7575
CFSI					
ADF	0.7328	0.6946	0.3821	0.2185	0.2185
PP	0.9481	0.8363	0.8438	0.841	0.8410
R					
ADF	0.4813	0.0907	0.1197	0.0427	0.0972
PP	0.8503	0.5502	0.5597	0.4685	0.4166

- Selection of the lag length in a two regime VAR in level  $L$ , for a system consisting of three variables  $y_t = (\log(IP_t), CFSI_t, R_t)'$ .

The results of the lag selection using the BIC criteria are summarized in the following table:

Country	USA	DEU	FRA	ITA	ESP
Lag length regime 1	2	2	2	2	2
Lag length regime 2	2	2	2	2	2

- Testing the cointegration rank in a two regime VECM for the selected lag length  $L - 1$ . The following tables show the results of Johansen trace test for the five countries respectively:

USA	teststatistic	critical_value
r <= 0	24.5834318	21.49
r <= 1	9.4880552	15.02
r <= 2	0.7729179	8.19
DEU	teststatistic	critical_value
r <= 0	31.709765	21.49
r <= 1	11.640522	15.02
r <= 2	1.955265	8.19
FRA	teststatistic	critical_value

r <= 0		41.628683	21.49
r <= 1		15.789192	15.02
r <= 2		1.084153	8.19
ITA			
		teststatistic	critical_value
r <= 0		32.67530	21.49
r <= 1		10.07149	15.02
r <= 2		1.95474	8.19
ESP			
		teststatistic	critical_value
r <= 0		26.58546122	21.49
r <= 1		13.46680497	15.02
r <= 2		0.02376718	8.19

The test results show that only in the system of FRA there are two cointegration relations, while in all other four countries there is only one cointegration relation in the system respectively.

- Model selection based on information criteria to discriminate between one regime VECM and two regime VECM. We estimate a standard one regime VECM and a two regime VECM for a system consisting of three variables  $y_t = (FSI_t, IP_t, R_t)'$ . We use AIC to discriminate between a VECM or an MRVECM. The AIC is given by

$$AIC(M, p_1, p_2) = \sum_{j=1}^M \left[ T_j \log |\hat{\Sigma}_j| + 2n \left( np_j + \frac{n+3}{2} \right) \right], \quad (20.7)$$

where  $M = 2$  is the number of regimes;  $p_j$  is the autoregressive order of regime  $j$ ;  $T_j$  is the number of observations associated with regime  $j$ ;  $\hat{\Sigma}_j$  is the estimated covariance matrix of the residuals of regime  $j$ ; and  $n$  denotes the number of variables in the vector  $y_t$ .<sup>4</sup>

Country	USA	DEU	FRA	ITA	ESP
AIC OR	198.6	358.8	100.3	299.2	212.5
AIC MR	34.6	327.6	73.7	238.6	180.7

The values of the AIC criteria of the one regime models are all larger than those of the AIC criteria of the two regime models. Hence the AIC information criteria favour the two regime VECMs.

---

<sup>4</sup>The AIC takes into account for possible heterogeneity in the constant terms,  $c_j$ , and residual covariance,  $\Sigma_j$ , across regimes. This AIC criterion is also applied in Mittnick and Semmler [18].



- Test of regime switching

Since a one regime VACM can be seen as a multi-regime with identical parameters in the different regimes, we can test the existence of multi-regimes through testing the null of equal parameters across different regimes against the alternative of unequal parameters in different regimes.

$$H_0 : (\alpha^{(1)}, \phi_l^{(1)}, \dots, \phi_{L-1}^{(1)}) = (\alpha^{(2)}, \phi_l^{(2)}, \dots, \phi_{L-1}^{(2)})$$

$$H_A : (\alpha^{(1)}, \phi_l^{(1)}, \dots, \phi_{L-1}^{(1)}) \neq (\alpha^{(2)}, \phi_l^{(2)}, \dots, \phi_{L-1}^{(2)})$$

Country	USA	DEU	FRA	ITA	ESP
<i>p</i> -value	1.005E-13	0.00010	6.47E-08	6.84E-10	9.98E-06

The test results show clearly that the null of one regime is rejected in all five countries, i.e., the data support the specification of regime switching VECMs. This is consistent with the results of model selection based on the AIC criteria.

### 20.3.3 Impulse and Response

The following impulse response functions (see Fig. 20.1) are the within-regime impulse response function (see Ehrmann [6] for more details). They can be used to trace out short run dynamics of the system. The impulses are all a one unit impulses, the responses are the responses of the system in (20.1), i.e., they are the industrial output, the financial stress index and the short run interest rate denoted by  $(IP_t, FSI_t, R_t)$ , respectively.

The three graphs on the first row are responses of  $(IP_t, FSI_t, R_t)$  to a one unit positive impulse of  $IP$ . The graphs on the second row are responses to the shock of a one unit increase in  $FSI$ . The graphs in the third row are responses to the shock of a one unit increase in  $R$ . The first three rows are impulse responses in the rate-cut regime. The second three rows are impulse responses in the non-rate-cut regime. We observe:

- A one unit output shock will have a long lasting positive effect on the output over 20 periods. The effects are stronger in the non-rate-cut regime than in the rate-cut regime. In the rate-cut regime the effects of the output shock on  $FSI$  and  $R$  are statistically insignificant, in the non-rate-cut regime the output shock will decrease the financial stress and decrease the short-term interest rate.
- A one unit financial stress shock has lasting effects on the financial stress in both regimes over 20 quarters. Its effects are more persistent in the non-rate-cut regime than in the rate-cut regime. The shock has negative effects on the output in both regimes. Interestingly, the shock has opposite effects on the short-term interest

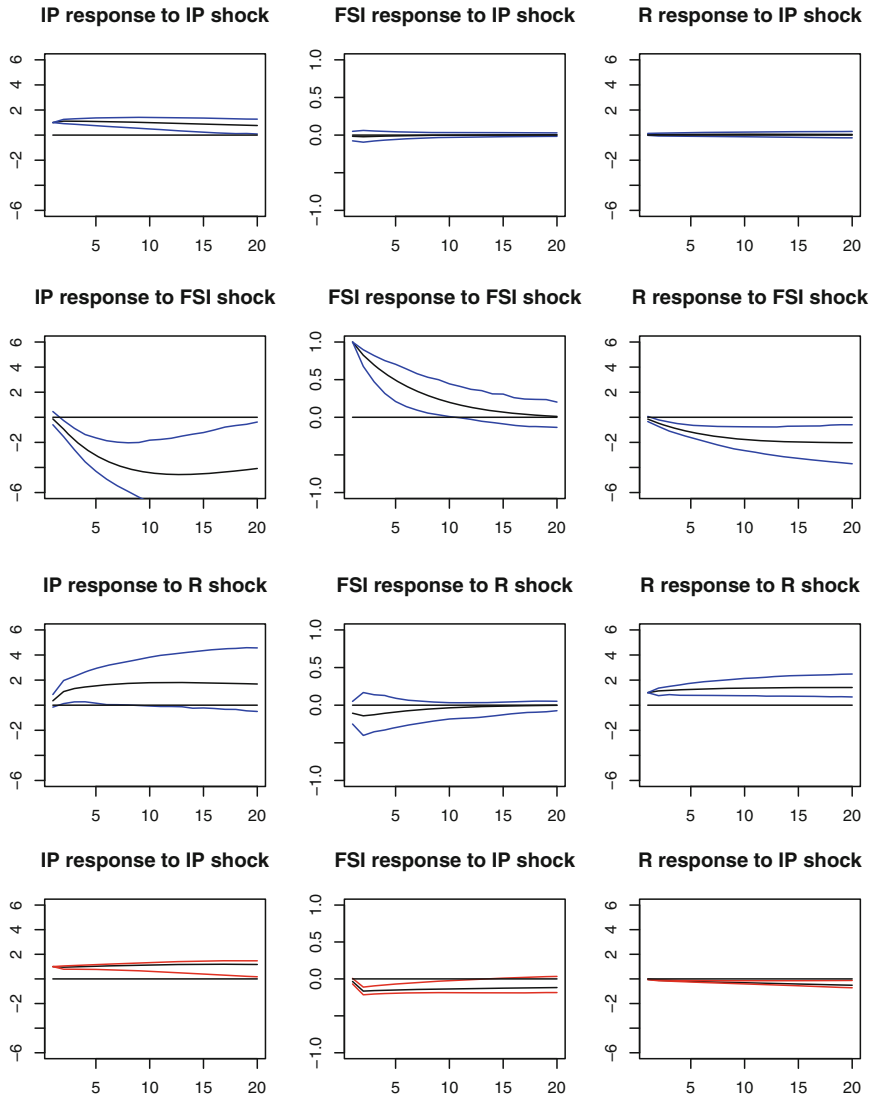


**Fig. 20.1** Impulse response function of the rate-cutting and the non-rate-cutting regimes USA showing that: (1) a positive output shock may have positive effect on the output, almost no effect on *FSI* and *R* in the rate-cut regime, and a negative effect in the non-rate-cut regime on financial stress short-term interest rate; (2) a positive financial stress shock has positive effects on the financial stress in non-rate-cut and rate-cut regimes, negative effects on the output in both regimes, opposite effects on the short-term interest rate; (3) a positive interest rate shock has positive effects on the short-term interest rate, a negative impact on the output in the non-rate-cut regime, a positive impact in the rate-cut regime, a positive effect on the financial stress in the non-rate-cut regime, and negligible in the rate-cut regime

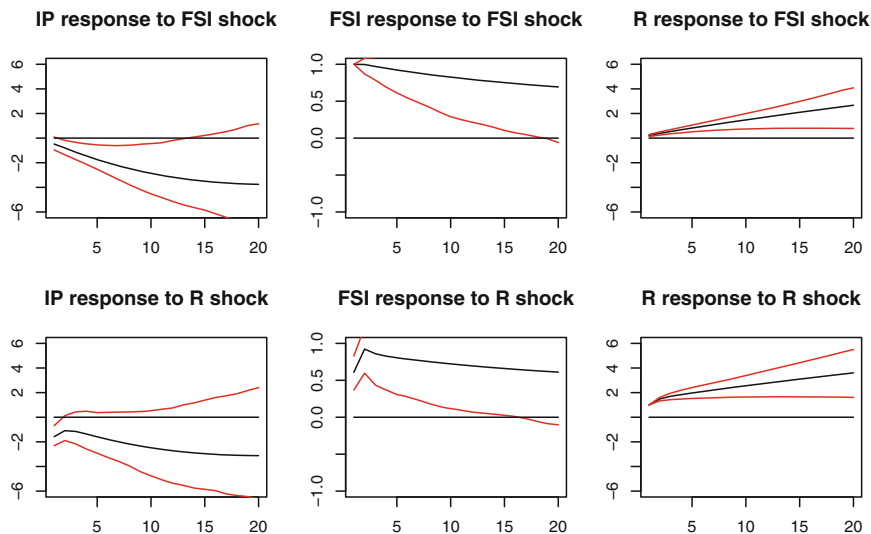


Fig. 20.1 (continued)

rate. While in the rate-cut regime the financial stress shock will decrease the short-term rate, in the non-rate-cut regime it will increase the short-term interest rate.

- The one unit interest rate shock has lasting effects on the short-term interest rate. Its effects are significantly larger in the non-rate-cut regime than in the rate-cut regime. The interest rate shock has different effects in the two regimes. While in the non-rate-cut regime an interest hike shock has a negative impact on the output, it has a positive impact on the output in the rate-cut regime, though the effects are not statistically significant. In the non-rate-cut regime, the interest rate shock will increase the financial stress; its effect in the rate-cut regime is insignificant.

The following graphs (see Fig. 20.2) are the impulse response functions of Germany. The three graphs on the first row are responses of (*IP*, *FSI*, *R*) to a one unit impulse of *IP*. The three graphs in the second row are responses to *FSI*. The first three rows contain the responses in the rate-cut regime and the second three rows contain the responses in the non-rate-cut regime.

- A one unit output shock will have a long lasting positive effect on the output over 20 periods. The effects are similar and statistically significant in both the non-rate-cut regime and the rate-cut regime. The one unit output shock has no statistically significant effect on the financial stress and the short-term interest rate in both regimes.
- The shock of a one unit increase in financial stress index has lasting effects on the financial stress in both regimes. While in the rate-cut regime the effects die

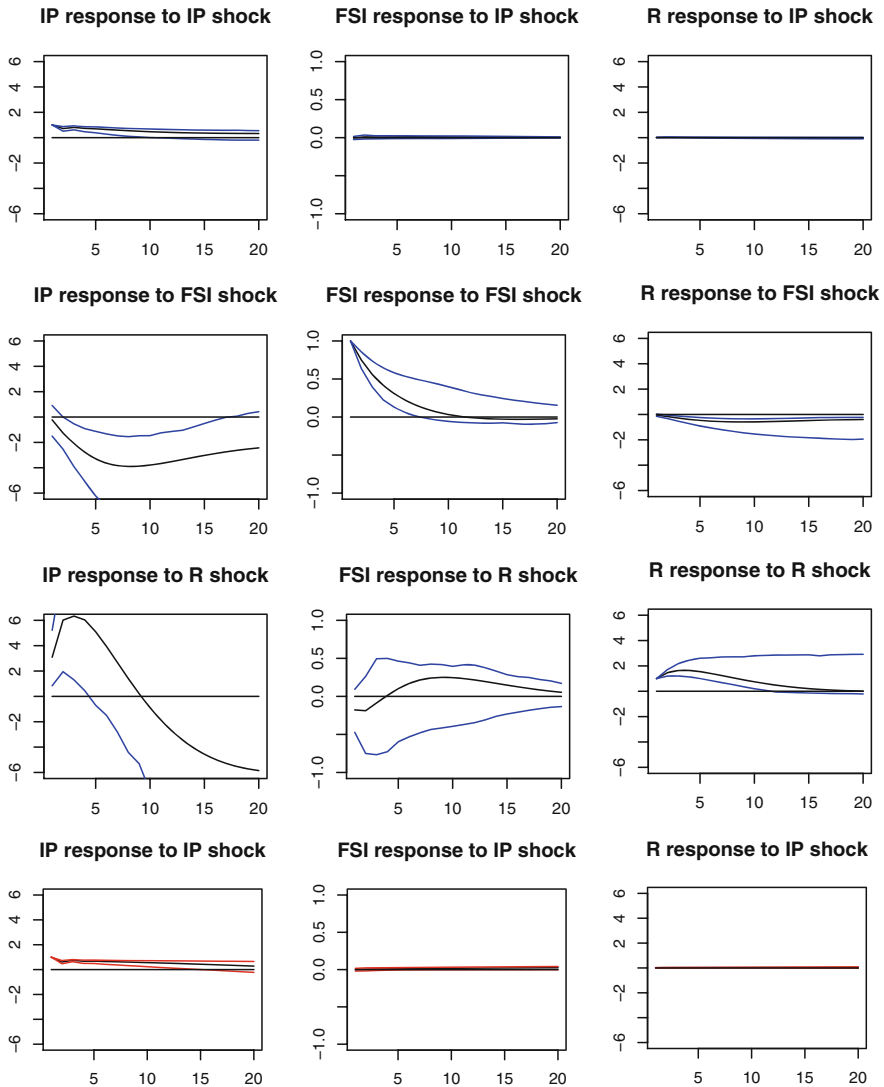


**Fig. 20.2** Impulse response function of the rate-cutting and non-rate-cut regimes in DEU showing that: (1) A positive output shock may have positive effect on the output, almost no effect on *FSI* and *R* in the rate-cut regime, and a negative effect in the non-rate-cut regime on financial stress short-term interest rate; (2) A positive financial stress shock has positive effects on the financial stress in non-rate-cut and rate-cut regimes, negative effects on the output in both regimes, opposite effects on the short-term interest rate; (3) A positive interest rate shock has positive effects on the short-term interest rate, a negative impact on the output in both regimes, a positive (but statistically insignificant) effect on the financial stress in the non-rate-cut regime and rate-cut regime

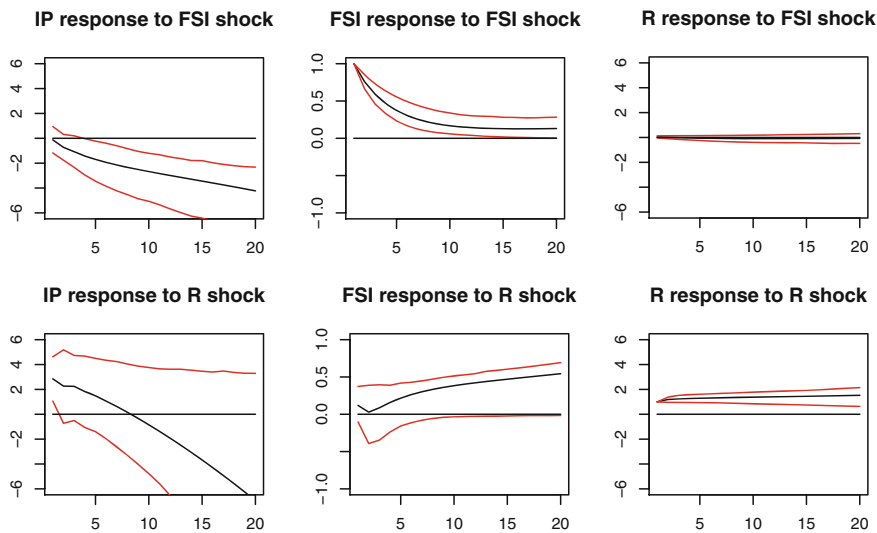


Fig. 20.2 (continued)

out after 20 periods, the effects remain significant in the non-rate-cut regime. The shock has negative effects on the output in both regimes. However, the effects in the non-rate-cut regime are stronger than in the rate-cut regime. The shock has a negative effect on the short-term interest rate in the rate-cut regime, while its effects in the non-rate-cut regime are statistically insignificant.

- A one unit interest rate shock has lasting effects on the short-term interest rate in the non-rate-cut regime. Its effects in the rate-cut regime vanish after 10 periods. The unitary shock (one unit positive impulse) in interest rate has a negative effect on the output in both regimes, though the effects are not statistically significant. In both regimes, the shock of one unit increase in the short-term interest rate will increase the financial stress, although these effects are not statistically significant.

The next diagrams are the impulse response functions for Italy (see Fig. 20.3). The orders of the IRFs are organized in the same way as in the previous graphs. In the Italian case we observe:

- A one unit output shock will have a lasting effect on the output in both regimes. The effect is slightly stronger in the non-rate-cut regime. Its effects on the financial stress and the short-term interest rate are statistically insignificant in both regimes.
- A one unit financial stress shock has a significant negative impact on output in both regimes. The effects are stronger in the non-rate-cut regime. The effects of the financial stress shock on financial stress die out in the rate-cut regime after 15 periods, while the effects remain persistent in the non-rate-cut regime. Notably, the responses of the short-term interest rate are negative in the rate-cut regime,

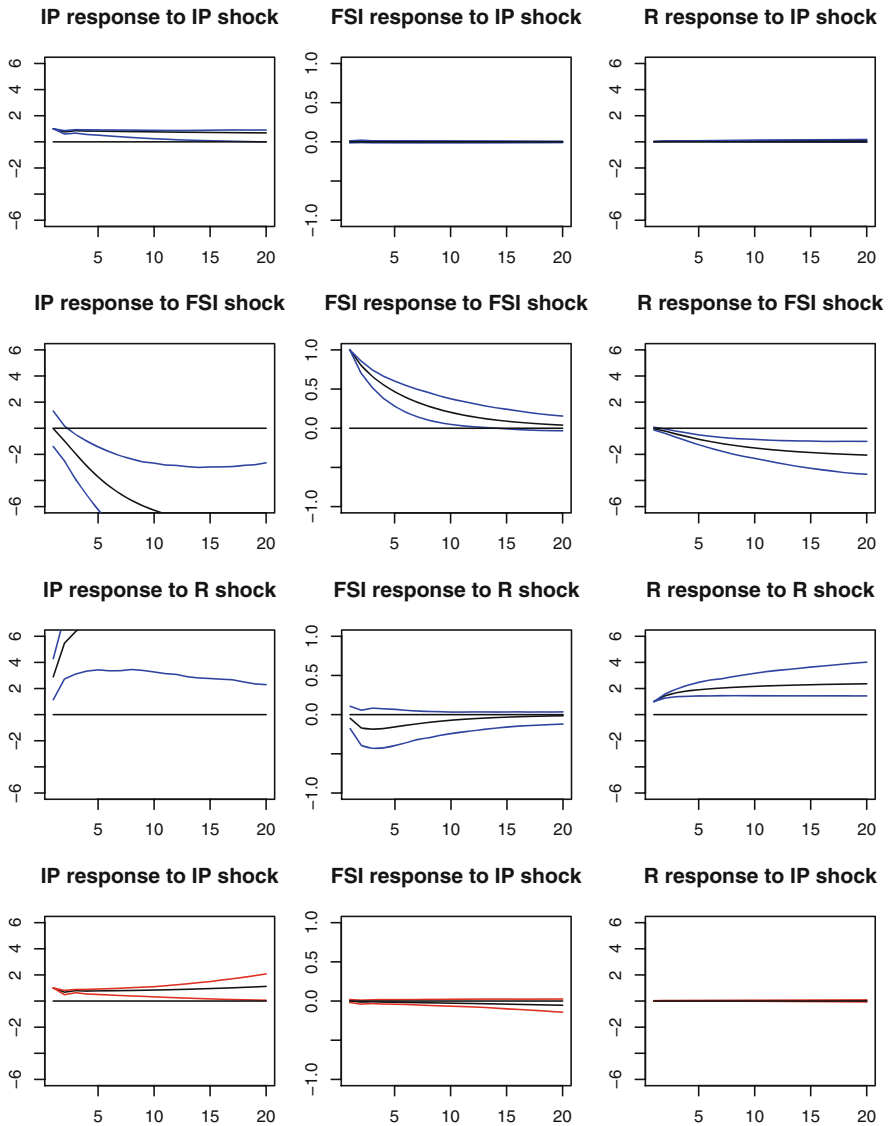


**Fig. 20.3** Impulse response function of the rate-cutting and the non-rate-cutting regimes ITA showing that: (1) A positive output shock may have positive effect on the output and no statistically significant effect on *FSI* and *R*; (2) A positive financial stress shock has positive effects on the financial stress in non-rate-cut and rate-cut regimes, negative effects on the output in both regimes, opposite effects (but statistically not significant) on the short-term interest rate; (3) A positive interest rate shock has positive effects on the short-term interest rate, a positive impact on the output in both regimes and no effect on the financial stress

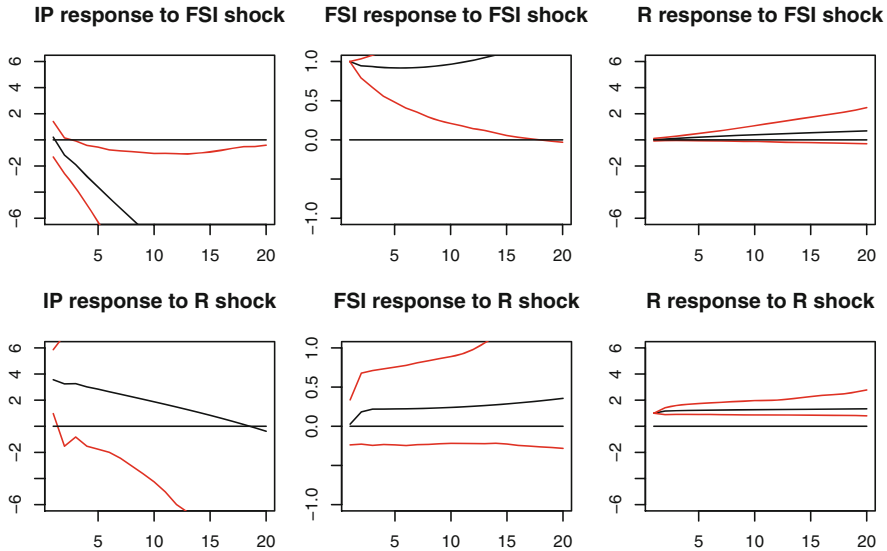


Fig. 20.3 (continued)

but positive in the non-rate-cut regime, though the effects are not statistically significant.

- While a one unit interest rate shock has no significant effects on the financial stress in both regimes, it has positive impact on output in both regimes. The shock has positive and persistent effects on the short-term interest rate in both regimes. The effects are stronger in the rate-cut regime.

Because the impulse response functions of the four European countries are by and large very similar (see Figs. 20.2, 20.3, 20.4 and 20.5), we summarize the features of the IRFs in the following Table 20.1.

- While the responses of *IP* to *FSI* are negative and significant in both regimes, the responses of *IP* to *R* are in most cases statistically insignificant in both regimes. The responses of *IP* to an output shock are statistically significant and long lasting in both regimes.
- The responses of *FSI* to financial stress shocks are decreasingly lasting in both regimes. However, while the responses will die out in the rate-cut regime, the responses remain positive in the non-rate-cut regime permanently. The responses of *FSI* to interest rate shocks and to output shocks are statistically insignificant in both regimes.
- The responses of *R* to output shocks are statistically insignificant in both regimes. Notably, the responses of *R* to a financial stress shock are negative and significant in the rate-cut regime, while the responses are positive and significant in the non-rate-cut regime. The responses of *R* to short-term interest rate shocks are in most cases persistently lasting in both regimes.

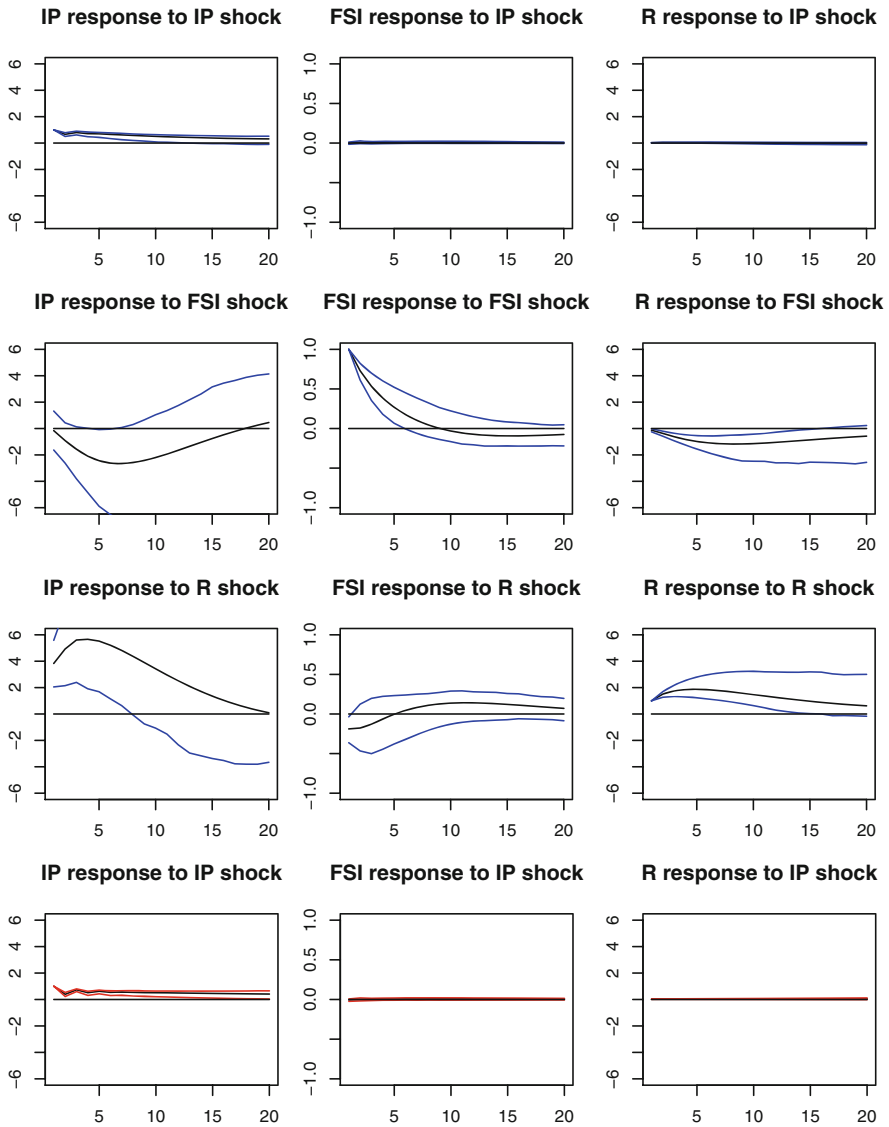


**Fig. 20.4** Impulse response function of the rate-cutting and the non-rate-cutting regimes FRA displaying similar results of Fig. 20.3



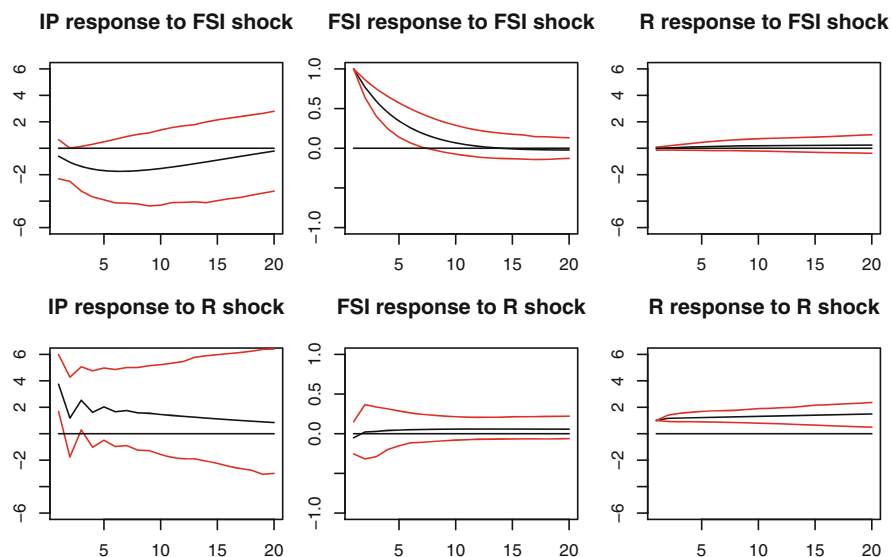


Fig. 20.4 (continued)

## 20.4 Concluding Remarks

Using the IMF financial stress index and OECD industrial production index and short-term interest rate data, for the USA, the EU countries, our regime switching vector error correction model enables us to conduct a parallel analysis in different regimes. By using the regime switching VECM, we could show that the responses are asymmetric in the two different regimes, namely the rate-cut regime and the non-rate-cut regime.

Generally, the financial stress shocks have a large and persistent negative impact on the real side of the economy, and the impact is stronger in the non-rate-cut regime than in the rate-cut regime. This asymmetric impact of financial stress on the real side of the economy is because rate cuts as an instrument of the monetary policy are often aimed at reducing the financial stress and hence offset the impact of the latter on the real activity, while in the rate hikes regime increase in interest rate will worsen the financial stress, enforcing the adverse effect of the latter on the real activities.

Looking at the impact of real activities on the financial stress: they are statistically insignificant in both regimes. Empirically, we find that financial stress shocks have asymmetric effects on the short-term interest rate, depending on the regime the economy is in. Overall, in the rate-cut regime a financial stress shock will decrease the short-term rate while in the non-rate-cut regime the shock will increase the short-term rate though in some cases the effects are not statistically significant.

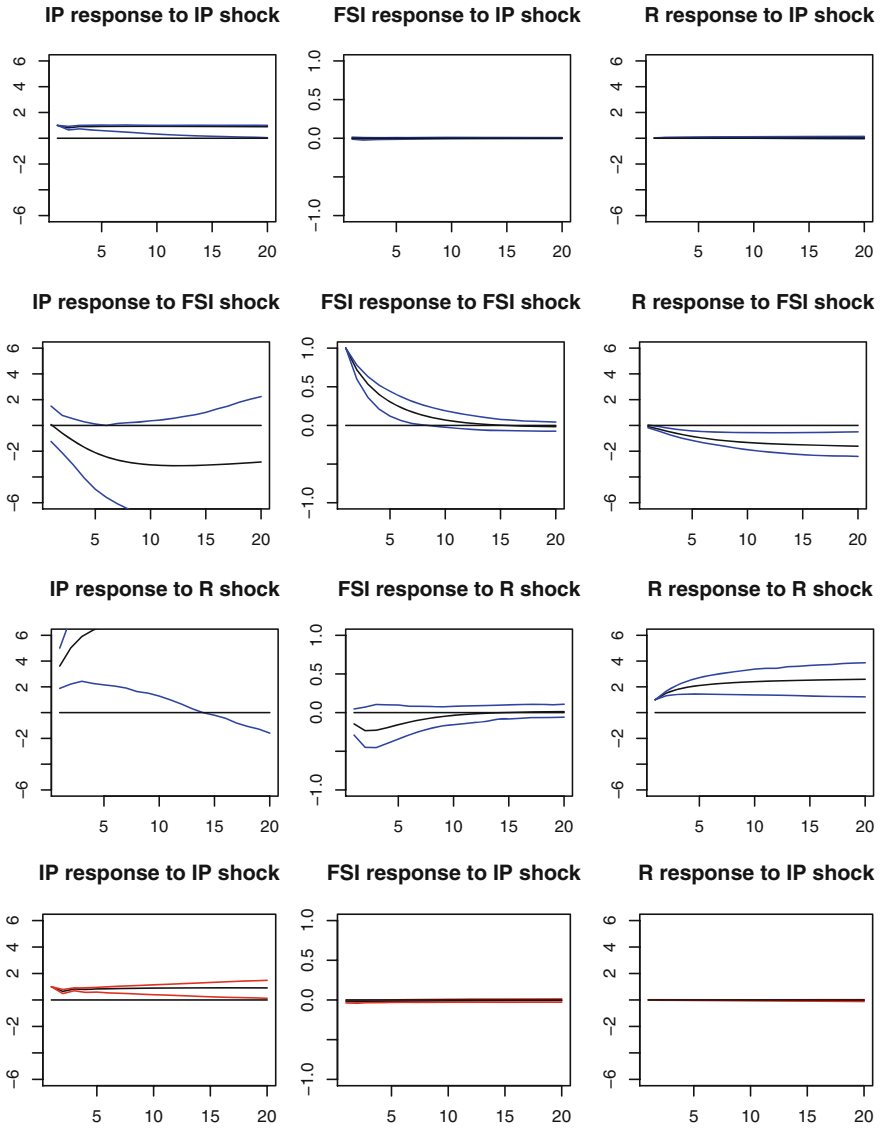


**Fig. 20.5** Impulse response function of the rate-cutting and the non-rate-cutting regimes ESP displaying similar results of Fig. 20.3

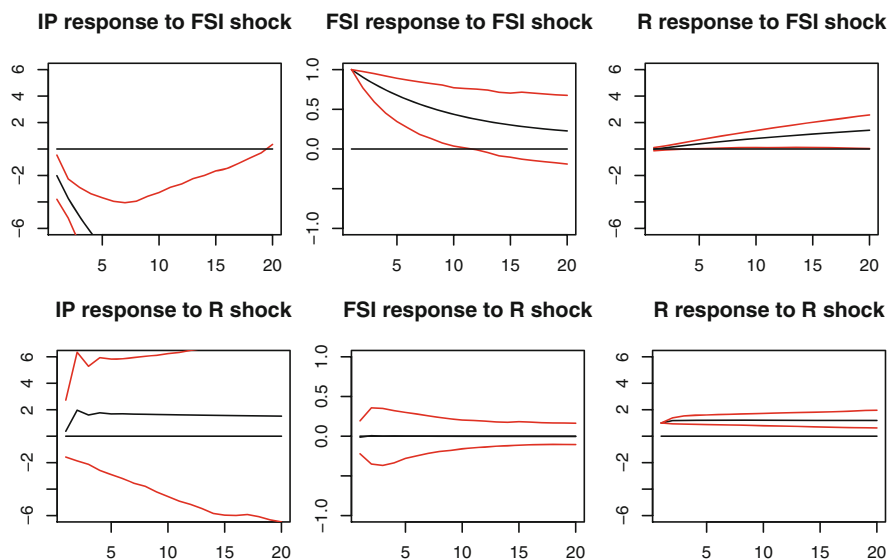


**Fig. 20.5** (continued)

While there is heterogeneity across countries with smaller countries showing weaker channels in the financial-real interaction, there is more similarity in larger economies. Across countries, there are common features in the sense that the European countries show very similar response patterns in the two regimes, respectively.

**Table 20.1** Summary of the results of the impulse response functions for Germany, France, Italy and Spain

	Response of IP	Response of FSI	Response of R
DEU (RC)			
IP shock	Temporally decreasing	Insignificant	Insignificant
FSI shock	Negative and significant	Temporal decreasing	Negative and significant
R shock	Insignificant	Insignificant	Temporally decreasing
(NRC)			
IP shock	Temporally decreasing	Insignificant	Insignificant
FSI shock	Negative and significant	Temporal decreasing	Insignificant
R shock	Insignificant	Insignificant	Temporally increasing
FRA (RC)			
IP shock	Positive lasting	Insignificant	Insignificant
FSI shock	Insignificant	Temporal decreasing	Negative and significant
R shock	Insignificant	Insignificant	Positive and lasting
(NRC)			
IP shock	Positive lasting	Insignificant	Insignificant
FSI shock	Insignificant	Temporal decreasing	Positive and significant
R shock	Insignificant	Insignificant	Positive and lasting
ITA (RC)			
IP shock	Persistently lasing	Insignificant	Insignificant
FSI shock	Negative and significant	Temporally decreasing	Negative and significant
R shock	Positive and significant	Insignificant	Temporally increasing
(NRC)			
IP shock	Temporal increasing	Insignificant	Insignificant
FSI shock	Negative and significant	Persistently lasting	Positive but insignificant
R shock	Insignificant	Insignificant	Positive lasing
ESP(RC)			
IP shock	Constantly lasting	Insignificant	Insignificant
FSI shock	Insignificant	Temporal decreasing	Negative and significant
R shock	Temporally positive	Insignificant	Temporally increasing
(NRC)			
IP shock	Temporal increasing	Insignificant	Insignificant
FSI shock	Negative and significant	Temporal decreasing	Positive and significant
R shock	Insignificant	Insignificant	Persistently lasting

## References

1. The IMF 2019 Financial Soundness Indicators Compilation Guide (2019 FSI Guide) (2020). <https://www.imf.org/en/Data/Statistics/fsi-guide>. Accessed 20 Oct 2020
2. Adrian, T., Shin, H.S.: Liquidity and leverage. *J. Finan. Intermed.* **19**(3), 418–437 (2010)
3. Balke, N.S., Fomby, T.B.: Threshold cointegration. *Int. Econ. Rev.* **3**, 627–645 (1997)
4. Bec, F., Rahbek, A.: Vector equilibrium correction models with non-linear discontinuous adjustments. *Econ. J.* **7**(2), 628–651 (2004)

5. Chen, P., Semmler, W.: Financial stress, regime switching and spillover effects: evidence from a multi-regime global VAR model. *J. Econ. Dyn. Control* **91**, 318–348 (2018)
6. Ehrmann, M., Ellison, M., Valla, N.: Regime-dependent impulse response functions in a markov-switching vector autoregression model. *Econ. Lett.* **78**(3), 295–299 (2003)
7. Engle, R.F., Granger, C.W.: Co-integration and error correction: representation, estimation, and testing. *Econometrica* **55**, 251–276 (1987)
8. Ernst, E., Semmler, W., Haider, A.: Debt-deflation, financial market stress and regime change—evidence from Europe using MRVAR. *J. Econ. Dyn. Control* **81**, 115–139 (2017)
9. Gonzalo, J., Pitarakis, J.Y.: Threshold effects in cointegrating relationships. *Oxf. Bull. Econ. Stat.* **68**, 813–833 (2006)
10. Hakkio, C.S., Keeton, W.R. et al.: Financial stress: what is it, how can it be measured, and why does it matter? *Econ. Rev.* **94**(2), 5–50 (2009)
11. Hamilton, J.D.: *Time Series Analysis*. Princeton University Press, Princeton (2020)
12. Hansen, B.E., Seo, B.: Testing for two-regime threshold cointegration in vector error-correction models. *J. Econ.* **110**(2), 293–318 (2002)
13. Hatzius, J., Hooper, P., Mishkin, F.S., Schoenholtz, K.L., Watson, M.W.: Financial conditions indexes: A fresh look after the financial crisis. Tech. rep., National Bureau of Economic Research (2010)
14. Illing, M., Liu, Y.: Measuring financial stress in a developed country: an application to Canada. *J. Financ. Stab.* **2**(3), 243–265 (2006)
15. Johansen, S.: Statistical analysis of cointegration vectors. *J. Econ. Dyn. Control* **12**(2–3), 231–254 (1988)
16. Johansen, S.: Estimation and hypothesis testing of cointegration vectors in Gaussian vector autoregressive models. *Econometrica* **59**, 1551–1580 (1991)
17. Johansen, S.: *Likelihood-Based Inference in Cointegrated Vector Autoregressive Models*. Oxford University Press, Oxford (1995)
18. Mittnik, S., Semmler, W.: Regime dependence of the fiscal multiplier. *J. Econ. Behav. Organ.* **83**, 502–522 (2013)
19. Mittnik, S., Semmler, W.: Estimating a banking-macro model using a multi-regime VAR. In: *Advances in Non-linear Economic Modeling*, pp. 3–40. Springer, Berlin (2014)
20. Saikkonen, P.: Stability results for nonlinear error correction models. *J. Econ.* **127**(1), 69–81 (2005)
21. Saikkonen, P.: Stability of regime switching error correction models under linear cointegration. In: *Econometric Theory*, pp. 294–318 (2008)
22. Stigler, M.: Threshold cointegration: overview and implementation in R (2010). <http://stat.ethz.ch/CRAN/web/packages/tsDyn/vignettes/ThCointOverview.pdf>. Accessed 19 Jul 2020

# Appendix A

## A.1 The Dataset

Time series are taken from a range of sources such as the US Bureau of Economic Analysis (BEA), IMF, the World Bank, Penn World Table by Feenstra et al. [7], Levy and Chen [13] and the OECD as retrieved from their original dataset or from FRED and explained in detail below.

### A.1.1 US Recessions

Table A.1 shows USA Recessions, as retrieved from FRED (Federal Reserve Bank of St. Louis).

### A.1.2 World GDP Data

For testing Harrod's model, annual world GDP estimate has been retrieved from the Maddison–Penn world table [4, 8], (from 1946 to 1961). This has been linked up with the World Bank (<https://data.worldbank.org/indicator/NY.GDP.MKTP.KD.ZG>) and IMF ([https://www.imf.org/external/datamapper/NGDP\\_RPCH@WEO/OEMDC/ADVEC/WEOWORLD](https://www.imf.org/external/datamapper/NGDP_RPCH@WEO/OEMDC/ADVEC/WEOWORLD)) data (available from 1961 to 2018). Annual data has been changed into quarterly via the compounding law.

**Table A.1** US recessions

Recessions			
From		To	
Quarter	Year	Quarter	Year
Q4	1948	Q4	1949
Q3	1953	Q1	1954
Q4	1957	Q1	1958
Q3	1960	Q1	1961
Q1	1970	Q4	1970
Q1	1974	Q2	1975
Q1	1980	Q2	1980
Q3	1981	Q4	1982
Q3	1990	Q1	1991
Q2	2001	Q4	2001
Q1	2008	Q3	2009

US Bureau of Economic Analysis[2]

### A.1.3 BEA Data

In Table A.2 we list the time series considered for our analysis on business cycle as retrieved from FRED. Units were transformed in percent change from preceding period (apart from time series n. 3 for which percent change was already taken).

In Table A.3 we list the time series considered for testing Harrod's model as retrieved from FRED.

### A.1.4 Levy and Chen Data—USA

In Table A.4 we list the time series on capital reconstructed as described by Levy and Chen [13].

**Table A.2** Time series on consumption, income and investment

No.	Time series	Data points	Frequency	Data range (from to)	Type	Account code/ID
1	USA PCEC	274	Quarterly	nnnnnnn-01 to 2015-07-01	C	DPCERC1tnote:BEA-1
2	USA DPCER	275	Quarterly	nnn-01 to nn-01	C	DPCERL1tnote:BEA-2
3	USA GDP	274	Quarterly	1947-01-01 to 2015-07-01	Y	A191RC1tnote:BEA-3
4	USA RGDPDI FI	274	Quarterly	1947-04-01 to 2015-07-01	I	A007RL1tnote:BEA-4

(continued)

**Table A.2** (continued)

No.	Time series	Data points	Frequency	Data range (from to)	Type	Account code/ID
5	USA GPDI	274	Quarterly	1947-01-01 to 2015-07-01	I	A006RC1note:BEA-5
6	USA RGPDI	275	Quarterly	1947-04-01 to 2015-10-01	I	A006RL1note:BEA-6

US Bureau of Economic Analysis, Personal Consumption Expenditures (PCEC), Seasonally Adjusted Annual Rate, Percent Change, retrieved from FRED, Federal Reserve Bank of St. Louis; <https://research.stlouisfed.org/fred2/series/PCEC/>, January 2, 2016

US Bureau of Economic Analysis, Real Personal Consumption Expenditures (DPCERL1Q225SBEA), Seasonally Adjusted Annual Rate, Percent Change, retrieved from FRED, Federal Reserve Bank of St. Louis; <https://fred.stlouisfed.org/series/DPCERL1Q225SBEA>, June 21, 2016

US Bureau of Economic Analysis, Gross Domestic Product (GDP), Seasonally Adjusted Annual Rate, Percent Change, retrieved from FRED, Federal Reserve Bank of St. Louis; <https://research.stlouisfed.org/fred2/series/GDP/>, January 3, 2016

US Bureau of Economic Analysis, Real Gross Private Domestic Investment: Fixed Investment (A007RL1Q225SBEA), Seasonally Adjusted Annual Rate, Percent Change, retrieved from FRED, Federal Reserve Bank of St. Louis; <https://research.stlouisfed.org/fred2/series/A007RL1Q225SBEA/>, January 3, 2016

US Bureau of Economic Analysis, Gross Private Domestic Investment (GPDI), Seasonally Adjusted Annual Rate, Percent Change, retrieved from FRED, Federal Reserve Bank of St. Louis; <https://research.stlouisfed.org/fred2/series/GPDI/>, January 2, 2016

US Bureau of Economic Analysis, Real Gross Private Domestic Investment (A006RL1Q225SBEA), Seasonally Adjusted Annual Rate, Percent Change, retrieved from FRED, Federal Reserve Bank of St. Louis; (A006RL1Q225SBEA), <https://research.stlouisfed.org/fred2/series/A006RL1Q225SBEA/>, June 27, 2016

### A.1.5 OECD Data

Regarding the scope of our analysis, we included countries that had very different development paths. OECD data are, respectively, quarterly GDP (percent change),<sup>1</sup> investment (GFCF) (annual growth rate %)<sup>2</sup> and saving rates (% of GDP).<sup>3</sup>

In the following we start, first, by listing the data directly taken from the OECD database (Tables A.5 and A.8) and then the time series as retrieved from FRED (Tables A.6 and A.7); units were transformed in percent change from preceding period (Table A.8).

<sup>1</sup>Quarterly GDP total, percent change, previous period, Q2 1947–Q1 2016. Source: Quarterly National Accounts. This indicator is seasonally adjusted, and it is measured in percent change from previous quarter and from the same quarter previous year [16].

<sup>2</sup>Investment (GFCF) total, annual growth rate (%), 1951–2014. Source: Aggregate National Accounts, SNA 2008 (or SNA 1993); gross domestic product. Gross fixed capital formation (GFCF) is in million USD at current prices and PPPs, and in annual growth rates [15].

<sup>3</sup>Saving rate total, % of GDP, 1970–2014. Source: National Accounts at a Glance [17].



**Table A.3** BEA time series

No.	Time series	Data points	Frequency	Data range (from to)	BEA account code
1	USA SAVE	287	Quarterly	1947-01-01 to 2018-07-01	A929RC1note:BEA-1
2	USA GPDIC1	287	Quarterly	1947-04-01 to 2018-07-01	A006RXtnote:BEA-2
3	USA NETEXP	287	Quarterly	1947-01-01 to 2018-07-01	A019RCtnote:BEA-3
4	USA GDPDEF	287	Quarterly	1947-04-01 to 2018-07-01	A191RDtnote:BEA-4
5	USA GPD	287	Quarterly	1947-01-01 to 2018-07-01	A191RCtnote:BEA-5

US Bureau of Economic Analysis, Gross Saving (GSAVE), retrieved from FRED, Federal Reserve Bank of St. Louis; <https://fred.stlouisfed.org/series/GSAVE>, 20 February 2019

US Bureau of Economic Analysis, Real Gross Private Domestic Investment (GPDIC1), retrieved from FRED, Federal Reserve Bank of St. Louis; <https://fred.stlouisfed.org/series/GPDIC1>, 20 February 2019. US Bureau of Economic Analysis

Net Exports of Goods and Services (NETEXP), retrieved from FRED, Federal Reserve Bank of St. Louis; <https://fred.stlouisfed.org/series/NETEXP>, 20 February 2019

US Bureau of Economic Analysis, Gross Domestic Product: Implicit Price Deflator (GDPDEF), retrieved from FRED, Federal Reserve Bank of St. Louis; <https://fred.stlouisfed.org/series/GDPDEF>, 20 February 2019

US Bureau of Economic Analysis, Gross Domestic Product (GDP), retrieved from FRED, Federal Reserve Bank of St. Louis; <https://fred.stlouisfed.org/series/GDP>, 20 February 2019

**Table A.4** Time series on Capital—USA

No.	Code	Terms	Gross/net	Goods	Method	Type
1	M1BS87G	Real	Gross	BS	1	K
2	M1CDGG	Nominal	Gross	CDG	1	K
3	M1CDG87G	Real	Gross	CDG	1	K
4	M2BS87G	Real	Gross	BS	2	K
5	M2CDGG	Nominal	Gross	CGD	2	K
6	M2CDG87G	Real	Gross	CGD	2	K
7	M1BSG	Nominal	Gross	BS	1	K
8	M1PDGG	Nominal	Gross	PDG	1	K
9	M2PDG87G	Real	Gross	PDG	2	K
10	M1BS87N	Real	Net	BS	1	K
11	M1CDG87N	Real	Net	CGD	1	K
12	M1PDG87N	Real	Net	PDG	1	K
13	M2BS87N	Real	Net	BS	2	K
14	M2PDG87N	Real	Net	PDG	2	K

Data points = 175, data range = 1948–1991

**Table A.5** Time series on income

No.	Time series	Data points	Data range (from to)	Type	Country	Code/ID
1	Tot Q GDP perc. c. KOR	183	1970 (Q2)–2015 (Q4)	Y	Korea	TQGDP PC_CHGPP KOR
2	Tot Q GDP perc. c. GBR	243	1955 (Q2)–2015 (Q4)	Y	UK	TQGDP PC_CHGPP GBR
3	Tot Q GDP perc. c. ESP	223	1960 (Q2)–2015 (Q4)	Y	Spain	TQGDP PC_CHGPP ESP
4	Tot Q GDP perc. c. JPN	222	1960 (Q2)–2015 (Q3)	Y	Japan	TQGDP PC_CHGPP JPN
5	Tot Q GDP perc. c. TUR	222	1960 (Q2)–2015 (Q3)	Y	Turkey	TQGDP PC_CHGPP TUR
6	Tot Q GDP perc. c. DEU	223	1960 (Q2)–2015 (Q4)	Y	Germany	TQGDP PC_CHGPP DEU
7	Tot Q GDP perc. c. ITA	223	1960 (Q2)–2015 (Q4)	Y	Italy	TQGDP PC_CHGPP ITA
8	Tot Q GDP perc. c. USA	275	1947 (Q2)–2015 (Q4)	Y	USA	TQGDP PC_CHGPP USA

Organization for Economic Co-operation and Development

Quarterly GDP total, percent change, previous period, Q2 1947–Q4 2015. Source: Quarterly National Accounts, OECD [16]

### A.1.6 RQA Tables

Table A.9 reports the RQA calculated on 55 real-world time series and the related PCA.

## A.2 Considerations on *tanh* versus *arctan*

To our knowledge, many papers (see Mircea et al. [14], Kaddar and Alaoui [12], Januário et al. [10] Agliari et al. [1], Januario et al. [11], Bischi et al. [3], etc.) on the Kaldor's model have adopted the *arctan* function. However, this function has some well-known issues (see Bradford and Davenport [5], Collicott [6], Walter [18], Gonnet and Scholl [9]):

- *arctan* has a branch cut at infinity
- *arctan* poses an issue to calculators with vector addition when the components of the resultant vector are found as it is hard to distinguish the quadrant of the angle.

Table A.6 Time series on consumption

No.	Time series	Data points	Frequency	Data range (from to)	Type	Account code/ID
1	Private Final Cons. in Korea	179	Quarterly	1970-01-01 to 2014-07-01	C	KORPFCEQDSMEItnote:OECD-C-1
2	Private Final Cons. in USA	143	Quarterly	1947-01-01 to 2013-01-01	C	USAPFCEQDSNAQtnote:OECD-C-2
3	Private Final Cons. in Italy	94	Quarterly	1991-01-01 to 2014-04-01	C	ITAPFCEQDSNAQtnote:OECD-C-3
4	Private Final Cons. in the UK	172	Quarterly	1970-01-01 to 2012-10-01	C	GBRPFCEQDSNAQtnote:OECD-C-4
5	Private Final Cons. in Turkey	111	Quarterly	1987-01-01 to 2014-07-01	C	TURPFCEQDSMEItnote:OECD-C-5
6	Private Final Cons. in Germany	179	Quarterly	1970-01-01 to 2014-07-01	C	DEUPFCEQDSMEItnote:OECD-C-6
7	Private Final Cons. in Spain	78	Quarterly	1995-04-01 to 2014-07-01	C	ESPPFCEQDSMEItnote:OECD-C-7
8	Private Final Cons. in Japan	82	Quarterly	1994-04-01 to 2014-07-01	C	JPNPFCEQDSMEItnote:OECD-C-8

Organization for Economic Co-operation and Development, Private Final Consumption Expenditure in Korea© (KORPFCEQDSMEI), retrieved from FRED, Federal Reserve Bank of St. Louis; <https://research.stlouisfed.org/fred2/series/KORPFCEQDSMEI>, June 10, 2016

Organization for Economic Co-operation and Development, Private Final Consumption Expenditure in United States© (USAPFCEQDSNAQ), retrieved from FRED, Federal Reserve Bank of St. Louis; <https://research.stlouisfed.org/fred2/series/USAPFCEQDSNAQ>, June 10, 2016

Organization for Economic Co-operation and Development, Private Final Consumption Expenditure in Italy© (ITAPFCEQDSNAQ), retrieved from FRED, Federal Reserve Bank of St. Louis; <https://fred.stlouisfed.org/series/ITAPFCEQDSNAQ>, June 21, 2016

Organization for Economic Co-operation and Development, Private Final Consumption Expenditure in the United Kingdom© (GBRPFCEQDSNAQ), retrieved from FRED, Federal Reserve Bank of St. Louis; <https://fred.stlouisfed.org/series/GBRPFCEQDSNAQ>, June 21, 2016

Organization for Economic Co-operation and Development, Private Final Consumption Expenditure in Turkey© (TURPFCEQDSMEI), retrieved from FRED, Federal Reserve Bank of St. Louis; <https://fred.stlouisfed.org/series/TURPFCEQDSMEI>, June 21, 2016

Organization for Economic Co-operation and Development, Private Final Consumption Expenditure in Germany© (DEUPFCEQDSMEI), retrieved from FRED, Federal Reserve Bank of St. Louis; <https://fred.stlouisfed.org/series/DEUPFCEQDSMEI>, June 21, 2016

Organization for Economic Co-operation and Development, Private Final Consumption Expenditure in Spain© (ESPPFCEQDSMEI), retrieved from FRED, Federal Reserve Bank of St. Louis; <https://fred.stlouisfed.org/series/ESPPFCEQDSMEI>, June 21, 2016

Organization for Economic Co-operation and Development, Private Final Consumption Expenditure in Japan© (JPNPFCEQDSMEI), retrieved from FRED, Federal Reserve Bank of St. Louis; <https://fred.stlouisfed.org/series/JPNPFCEQDSMEI>, June 21, 2016

**Table A.7** Time series on investment

No.	Time series	Data points	Frequency	Data range (from to)	Type	Account code/ID
1	Tot. Prod. of Inv. Goods for Germany	240	Quarterly	1955-01-01 to 2014-10-01	I	PRMNVG01 IXOB DEUtnote:OECD-I-1
2	Tot. Prod. of Inv. Goods for Italy	176	Quarterly	1971-01-01 to 2014-10-01	I	PRMNVG01 IXOB ITAtnote:OECD-I-2
3	Tot. Prod. of Inv. Goods for Spain	200	Quarterly	1965-01-01 to 2014-10-01	I	PRMNVG01 IXOB ESPnote:OECD-I-3
4	Tot. Prod. of Inv. Goods for Korea	140	Quarterly	1980-01-01 to 2014-10-01	I	PRMNVG01 IXOB KORtnote:OECD-I-4
5	Tot. Prod. of Inv. Goods for Japan	240	Quarterly	1955-01-01 to 2014-10-01	I	PRMNVG01 IXOB JPNtnote:OECD-I-5
6	Tot. Prod. of Inv. Goods for the UK	188	Quarterly	1968-01-01 to 2014-10-01	I	PRMNVG01 IXOB GBRtnote:OECD-I-6
7	Tot. Prod. of Inv. Goods for the Euro Area	115	Quarterly	1985-01-01 to 2013-07-01	I	PRMNVG01 IXOB EA17tnote:OECD-I-7
8	Tot. Prod. of Inv. Goods for Brazil	96	Quarterly	1991-01-01 to 2014-10-01	I	PRMNVG01 IXOB BRAtnote:OECD-I-8

Organization for Economic Co-operation and Development, Total Production of Investment Goods for Manufacturing for Germany© (PRMNVG01DEQ661N), retrieved from FRED, Federal Reserve Bank of St. Louis; <https://fred.stlouisfed.org/series/PRMNVG01DEQ661N>, June 22, 2016

Organization for Economic Co-operation and Development, Total Production of Investment Goods for Manufacturing for Italy© (PRMNVG01ITQ661N), retrieved from FRED, Federal Reserve Bank of St. Louis; <https://fred.stlouisfed.org/series/PRMNVG01ITQ661N>, June 22, 2016

Organization for Economic Co-operation and Development, Total Production of Investment Goods for Manufacturing for Spain© (PRMNVG01ESQ661N), retrieved from FRED, Federal Reserve Bank of St. Louis; <https://fred.stlouisfed.org/series/PRMNVG01ESQ661N>, June 21, 2016

Organization for Economic Co-operation and Development, Total Production of Investment Goods for Manufacturing for the Republic of Korea© (PRMNVG01KRQ661N), retrieved from FRED, Federal Reserve Bank of St. Louis; <https://fred.stlouisfed.org/series/PRMNVG01KRQ661N>, June 22, 2016

Organization for Economic Co-operation and Development, Total Production of Investment Goods for Manufacturing for Japan© (PRMNVG01JPQ661S), retrieved from FRED, Federal Reserve Bank of St. Louis; <https://fred.stlouisfed.org/series/PRMNVG01JPQ661S>, June 22, 2016

Organization for Economic Co-operation and Development, Total Production of Investment Goods for Manufacturing for the United Kingdom© (PRMNVG01GBQ661N), retrieved from FRED, Federal Reserve Bank of St. Louis; <https://fred.stlouisfed.org/series/PRMNVG01GBQ661N>, June 22, 2016

Organization for Economic Co-operation and Development, Total Production of Investment Goods for Manufacturing for the Euro Area© (PRMNVG01IEZQ661N), retrieved from FRED, Federal Reserve Bank of St. Louis; <https://fred.stlouisfed.org/series/PRMNVG01IEZQ661N>, June 22, 2016

Organization for Economic Co-operation and Development, Total Production of Investment Goods for Manufacturing for Brazil© (PRMNVG01BRQ661N), retrieved from FRED, Federal Reserve Bank of St. Louis; <https://fred.stlouisfed.org/series/PRMNVG01BRQ661N>, June 22, 2016

**Table A.8** Time series on income

No.	Code/ID	Data points	Data range (from to)	Type	Country
1	B1_GE GPSA KOR Y	184	1970 (Q2)–2016 (Q1)	Y	Korea
2	B1_GE GPSA GBR Y	244	1955 (Q2)–2016 (Q1)	Y	United Kingdom
3	B1_GE GPSA ESP Y	224	1960 (Q2)–2016 (Q1)	Y	Spain
4	B1_GE GPSA JPN Y	224	1960 (Q2)–2016 (Q1)	Y	Japan
5	B1_GE GPSA TUR Y	224	1960 (Q2)–2016 (Q1)	Y	Turkey
6	B1_GE GPSA DEU Y	224	1960 (Q2)–2016 (Q1)	Y	Germany
7	B1_GE GPSA ITA Y	224	1960 (Q2)–2016 (Q1)	Y	Italy
8	B1_GE GPSA USA Y	276	1947 (Q2)–2016 (Q1)	Y	USA
9	B1_GE GPSA ICE Y	224	1960 (Q2)–2016 (Q1)	Y	Iceland
10	B1_GE GPSA GRE Y	224	1960 (Q2)–2016 (Q1)	Y	Greece
11	B1_GE GPSA FRA Y	224	1960 (Q2)–2016 (Q1)	Y	France

B1\_GE: Gross domestic product—expenditure approach, GPSA: growth rate compared to previous quarter, seasonally adjusted, quarterly data[17]

For example,  $\arctan(0) = 0$  only some of the time. Other times,  $\arctan(0) = \pi$ . For this reason, the correct evaluation of  $\arctan$  requires the so-called quadrant analysis.

- The analytical relation  $\arctan(-x) = -\arctan(x)$  can be dangerous as it can destroy quadrant information if poorly applied.
- For a real number  $x$  such that  $x \neq 0$

$$f(x) = \arctan(x) + \arctan\left(\frac{1}{x}\right) = \begin{cases} \frac{\pi}{2} & \text{for } x > 0 \\ -\frac{\pi}{2} & \text{for } x < 0 \end{cases}$$

is constant. In other terms the expression

$$f'(x) = \frac{1}{1+x^2} + \frac{1}{1+\frac{1}{x^2}}\left(-\frac{1}{x^2}\right) \tag{A.1}$$

is zero. In fact, by simplifying Eq. (A.1), we get

$$\frac{1}{1+x^2} - \frac{1}{1+x^2} = 0. \tag{A.2}$$

**Table A.9** RQA tables on 55 (10 C, 11 I, 14 K, 20 Y) real time series

No.	Table	Row	VARTYPE	Mean	SDev	Mean/SDev	REC	DET	MAXLINE	ENT	TREND	LAM	TT	PC1	PC2
1	1	1	C	1.777	0.81	2.194	29.378	85.402	61	4.294	136.25	61.948	11.65	-0.324	0.482
2	4	1	C	0.036	0.027	1.333	43.097	94.998	79	4.842	-478.416	94.018	19.367	0.834	1.778
3	4	2	C	0.008	0.007	1.143	33.81	87.074	78	4.352	-297.973	72.693	12.338	-0.013	0.606
4	4	3	C	0.002	0.007	0.286	33.161	90.138	51	3.386	-830.171	76.903	11.397	-0.507	1.764
5	4	4	C	0.007	0.011	0.636	35.871	87.623	119	4.602	-269.715	77.533	17.028	0.377	-0.110
6	4	5	C	0.104	0.07	1.486	37.327	93.103	70	4.641	-1033.278	83.873	15.057	0.437	1.432
7	4	6	C	0.012	0.011	1.091	35.559	91.303	77	4.803	-375.587	79.913	16.398	0.421	0.933
8	1	2	C	3.628	3.705	0.979	36.367	83.902	61	4.351	-37.051	66.174	12.537	-0.128	0.871
9	4	7	C	0.012	0.012	1.000	31.714	87.231	46	4.295	-1085.41	62.903	11.415	-0.244	1.118
10	4	8	C	0.003	0.009	0.333	33.79	81.644	32	4.206	-665.148	67.68	18.212	-0.497	1.116
11	1	5	I	1.861	4.474	0.416	31.876	85.859	75	4.4	-28.101	69.081	13.577	-0.112	0.391
12	1	4	I	4.754	9.352	0.508	29.896	83.641	86	4.332	62.648	68.847	12.848	-0.246	-0.143
13	5	8	I	0.014	0.084	0.167	21.259	78.507	62	3.377	-31.291	1.544	6	-1.293	-0.371
14	5	3	I	0.017	0.166	0.102	36.92	92.653	158	4.983	62.794	0.558	9.25	0.962	-0.535
15	5	7	I	0.01	0.106	0.094	46.648	97.998	101	4.926	22.772	-1.000	-1.000	1.202	1.836
16	5	2	I	0.013	0.148	0.088	33.509	95.903	162	5.375	85.122	-1.000	-1.000	1.186	-0.766
17	5	5	I	0.019	0.04	0.475	36.548	91.517	147	4.654	-346.672	82.689	12.85	0.697	-0.303
18	5	4	I	0.031	0.101	0.307	36.625	95.962	92	4.884	-30.778	-1.000	-1.000	0.740	1.082
19	5	6	I	0.004	0.055	0.073	29.899	85.265	166	4.454	-171.536	11.062	8.27	0.229	-1.648
20	1	6	I	6.652	23.279	0.286	36.854	90.155	59	4.554	-16.148	73.575	14.389	0.218	1.399
21	5	1	I	0.014	0.106	0.132	45.291	96.838	196	5.862	6.948	0.71	8	1.989	-0.656

(continued)

Table A.9 (continued)

No.	Table	Row	VARTYPE	Mean	SDev	Mean/SDev	REC	DET	MAXLINE	ENT	TREND	LAM	TT	PC1	PC2
22	2	1	K	0.795	0.213	3.732	40.636	96.762	164	4.646	-177.904	95.871	13.835	1.102	0.128
23	2	2	K	2.063	1.578	1.307	49.091	97.757	126	5.504	-550.28	97.38	32.02	1.664	1.263
24	2	3	K	1.326	0.709	1.870	46.6	97.335	155	4.868	-91.22	97.034	16.142	1.385	0.725
25	2	4	K	0.795	0.218	3.647	40.31	96.296	164	4.614	-187.832	93.601	13.948	1.058	0.077
26	2	5	K	2.065	1.63	1.267	50.133	97.803	126	5.626	-563.075	97.464	34.254	1.759	1.296
27	2	6	K	1.351	0.709	1.906	46.031	96.965	154	4.859	-79.771	95.36	15.629	1.344	0.673
28	2	7	K	1.982	1.262	1.571	32.326	91.168	85	4.536	30.812	81.613	15.054	0.217	0.625
29	2	8	K	-2.227	1.332	-1.672	39.81	92.865	70	4.766	-64.058	85.803	17.326	0.569	1.551
30	2	10	K	0.8	0.208	3.846	41.086	96.852	164	4.703	-199.62	96.006	13.791	1.148	0.147
31	2	11	K	1.351	0.669	2.019	46.282	97.062	164	4.92	-84.862	95.369	16.497	1.429	0.476
32	2	12	K	1.087	0.508	2.140	41.227	95.608	164	4.64	-26.505	95.948	13.481	1.074	0.078
33	2	13	K	0.8	0.214	3.738	40.916	96.152	164	4.645	-197.501	95.159	13.303	1.087	0.098
34	2	14	K	1.102	0.495	2.226	41.636	95.808	165	4.637	-45.891	94.458	13.881	1.123	0.112
35	2	15	K	1.085	0.517	2.099	40.65	95.509	164	4.569	-6.188	94.382	12.881	1.017	0.055
36	1	3	Y	1.718	1.023	1.679	30.557	89.043	81	4.619	-43.274	78.851	16.586	0.101	0.350
37	3	1	Y	1.797	1.794	1.002	30.968	87.728	52	4.468	-374.438	78.095	15.104	-0.138	0.910
38	3	2	Y	0.668	1.037	0.644	34.246	86.134	81	4.403	-79.834	83.786	23.891	0.003	0.477
39	3	3	Y	0.948	1.067	0.888	38.779	92.614	74	5.444	-215.569	90.229	25.694	0.875	1.084
40	3	4	Y	1.043	1.342	0.777	33.352	90.282	68	4.896	-353.221	76.736	15.068	0.316	0.814
41	3	5	Y	1.106	1.975	0.560	41.844	88.807	100	4.905	-12.32	86.814	20.025	0.679	0.705
42	3	6	Y	0.631	1.146	0.551	31.472	79.052	59	4.457	-144.772	63.676	14.243	-0.429	0.071
43	3	7	Y	0.688	1.049	0.656	35.618	84.17	94	5.118	-345.894	78.936	18.107	0.378	-0.146

44	3	8	Y	0.87	1.043	0.834	28.543	85.44	61	4.468	-58.462	72.342	15.107	-0.264	0.347
45	6	1	Y	1.779	1.787	0.996	31.074	88.582	53	4.422	-376.179	78.704	15.211	-0.120	0.991
46	6	6	Y	0.631	1.146	0.551	31.472	79.052	59	4.457	-144.772	63.676	14.243	-0.429	0.071
47	6	11	Y	0.733	1.211	0.605	61.613	93.222	163	4.908	-388.96	92.733	24.88	1.767	1.359
48	6	7	Y	0.685	1.05	0.652	35.392	83.743	93	5.015	-343.31	77.453	17.654	0.299	-0.136
49	6	4	Y	1.042	1.342	0.776	33.322	90.439	68	4.854	-352.012	77.334	14.95	0.301	0.843
50	6	3	Y	0.951	1.068	0.890	38.794	92.772	74	5.434	-215.298	89.832	25.877	0.876	1.103
51	6	2	Y	0.67	1.036	0.647	34.181	86.195	81	4.429	-76.604	83.343	23.523	0.016	0.467
52	6	5	Y	1.104	1.974	0.559	41.879	88.925	100	4.897	-11.964	86.957	19.855	0.681	0.721
53	6	8	Y	0.874	1.048	0.834	28.492	85.82	61	4.436	-59.29	71.393	14.937	-0.267	0.389
54	6	9	Y	0.938	1.872	0.501	36.055	94.132	102	5.23	-361.949	94.077	21.774	0.864	0.536
55	6	10	Y	0.916	2.599	0.352	31.693	92.659	69	5.28	191.97	86.792	35.778	0.546	0.708

Table and row, respectively, indicate relevant time series considered

PC1 and PC2 are calculated on REC, DET, MAXLINE and ENT, parameters: LAG=1, EMB=10, EUCLIDEAN DIST=3, MEANDIST=2, RADIUS=40, LINE=5

REC (percent recurrence) = # recurrent points within the set threshold (i.e., RADIUS)/# total points

LAM (percent laminarity) = # recurrent points forming vertical lines / # REC. Reported as -1.000 if # REC=0

(trapping time) = mean vertical line length. Reported as -1.000 if # LINE vertical = 0



- For  $x, y \in \mathbb{R}$  such that  $x \neq 0$

$$\arctan(x) + \arctan(y) = \begin{cases} \arctan\left(\frac{x+y}{1-xy}\right) & \text{for } xy < 1 \\ \arctan\left(\frac{x+y}{1-xy}\right) + \pi & \text{for } xy > 1, x, y > 0 \\ \arctan\left(\frac{x+y}{1-xy}\right) - \pi & \text{for } xy > 1, x, y < 0. \end{cases}$$

So the issue with the  $\arctan$  is that for  $\frac{x+y}{1-xy}$  it is possible to pass through  $\infty$  even when both  $x$  and  $y$  are finite (namely when  $xy = 1$ ). In addition  $\frac{x+y}{1-xy}$  goes from large positive to large negative (and vice versa).

Hence, the reason why we decided to choose the hyperbolic tangent is that we did not want to run into the above-mentioned issues, as the function  $\tanh(z)$  is an analytical function of  $z$  that is defined over the whole complex  $z$ -plane and does not have branch cuts and branch points. In addition hyperbolic functions can be defined as simple rational functions of the exponential function of  $z$ ; for real values of argument, they are real-valued functions and, last but not least, hyperbolic functions are periodic with a real period  $2\pi i$  or  $\pi i$  (versus the half-period of  $[-\frac{\pi}{2}, \frac{\pi}{2}]$  for the  $\arctan$ ).

### A.3 Test Results of the Goodwin Model on US Economy

#### A.3.1 Unit Root Tests

From the ADF and DF-GLS tests presented in Tables A.10, A.11 and A.12, we conclude that detrended time series do not have unitary roots.

**Table A.10** ADF and DF-GLS tests for the detrended profit share series

Method	Intercept ( $t$ -statistic)	Trend/intercept ( $t$ -statistic)	Prob.
ADF	-6.303916	-6.287742	0.01
DF-GLS	-2.850337	-3.991788	0.01

**Table A.11** ADF and DF-GLS tests for the detrended capacity utilization

Method	Intercept ( $t$ -statistic)	Trend/intercept ( $t$ -statistic)	Prob.
ADF	-6.443794	-6.4273	0.01
DF-GLS	-5.358919	-6.155664	0.01

**Table A.12** ADF and DF-GLS tests for the detrended employment level

Method	Intercept ( <i>t</i> -statistic)	Trend/intercept ( <i>t</i> -statistic)	Prob.
ADF	-5.724463	-5.707365	0.01
DF-GLS	-4.234430	-5.282049	0.01

### A.3.2 Lag Length Criteria

In table A.13, we show that all the tests employed, namely AIC, SC and HQ, confirm that a VAR with 2 lags is the better specification to the model.

### A.3.3 Granger Non-causality Test

In table A.14, the Granger non-causality test allows us reject the null that there is no causality between the variables in all cases.

**Table A.13** Lag length criteria

Lag	AIC	SC	HQ
0	-19.05770	-19.000624	-19.03685
1	-23.48974	-23.28392	-23.40636
2	-23.90029 <sup>a</sup>	-23.54009 <sup>a</sup>	-23.74436 <sup>a</sup>
3	-23.85545	-23.34088	-23.64698
4	-23.84410	-23.17517	-23.57310
5	-23.79447	-22.97117	-23.46093
6	-23.73363	-22.75596	-23.33756
7	-23.75110	-22.61907	-23.29249
8	-23.74217	-22.45576	-23.22102

<sup>a</sup>Indicates lag order selected by the criterion  
 AIC, akaike information criterion  
 SC, Schwarz information criterion  
 HQ, Hannan–Quinn information criterion

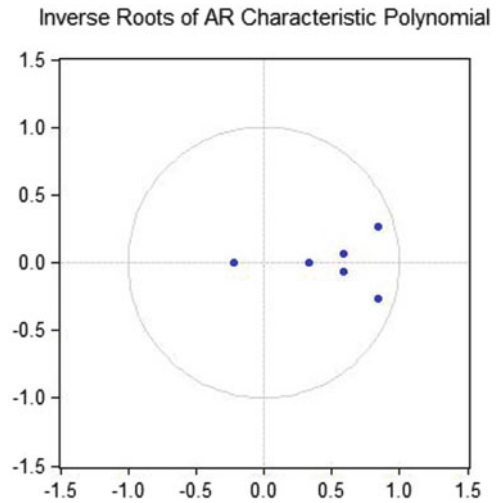
**Table A.14** Pairwise Granger causality tests

Null hypothesis	F-statistic	Prob.
$\mu$ does not cause $h$	11.2425	2.E-05
$\mu$ does not cause $v$	-5.358919	-6.155664
$h$ does not cause $\mu$	5.91624	0.0032
$h$ does not cause $v$	4.22609	0.0160
$v$ does not cause $h$	13.7628	3.E-06
$v$ does not cause $\mu$	5.85223	0.0034

**Table A.15** Autocorrelation LM test

Lags	LM-stat	Prob.
1	8.033584	0.5308
2	10.60378	0.3038
3	11.70280	0.2306

**Fig. A.1** Inverse roots of AR characteristic polynomial



### A.3.4 Autocorrelation Test

In Table A.15, the  $p$ -value of the LM test in the first lag points to no autocorrelation in the model specification.

### A.3.5 Stability of VAR

Figure A.1 shows that the inverse roots of the characteristic polynomial lie inside the unit circle, thus proving the stability of VAR.

## A.4 Financial Stress, Regime Switching and Macrodynamics

The data in the following are related to the estimation of model reported in Chapter 20.

### A.4.1 Estimation Results

UAS

Response Y1 :

Call:

lm(formula = Y1 ~ 0 + CI1 + CI2 + Z2)

Residuals:

	Min	1Q	Median	3Q	Max
	-4.3042	-0.3200	-0.0346	0.3350	1.6155

Coefficients:

	Estimate	Std. Error	t value	Pr(> t )	
CI1	-0.021528	0.005803	-3.710	0.000256	***
CI2	-0.019034	0.006877	-2.768	0.006071	**
Z2	0.085960	0.089910	0.956	0.339963	
Z2	-0.720779	0.121243	-5.945	9.3e-09	***
Z2	0.619314	0.206680	2.996	0.003007	**
Z2	-0.017067	0.087487	-0.195	0.845491	
Z2	-0.500733	0.205907	-2.432	0.015728	*
Z2	0.716359	0.370439	1.934	0.054270	.
Z2St	9.799366	2.618460	3.742	0.000226	***
Z2NSt	8.763251	3.122889	2.806	0.005410	**

---

Signif. codes: 0 '\*\*\*' 0.001 '\*\*' 0.01 '\*' 0.05 '.' 0.1 ' ' 1

Residual standard error: 0.5746 on 249 degrees of freedom  
 Multiple R-squared: 0.3077, Adjusted R-squared: 0.2799  
 F-statistic: 11.07 on 10 and 249 DF, p-value: 1.366e-15

Response Y2 :

Call:

lm(formula = Y2 ~ 0 + CI1 + CI2 + Z2)

Residuals:

	Min	1Q	Median	3Q	Max
	-0.50888	-0.10160	0.00029	0.09216	0.67331

Coefficients:

	Estimate	Std. Error	t value	Pr(> t )	
CI1	0.0007286	0.0017491	0.417	0.677	
CI2	-0.0029499	0.0020730	-1.423	0.156	
Z2	-0.0064500	0.0271012	-0.238	0.812	
Z2	0.8170348	0.0365457	22.357	< 2e-16	***
Z2	-0.0515848	0.0622988	-0.828	0.408	
Z2	-0.1239410	0.0263709	-4.700	4.31e-06	***

Z2	0.8964068	0.0620658	14.443	< 2e-16	***
Z2	0.1741562	0.1116599	1.560	0.120	
Z2St	-0.3555005	0.7892716	-0.450	0.653	
Z2NSt	1.3726344	0.9413196	1.458	0.146	

---

Signif. codes: 0 '\*\*\*' 0.001 '\*\*' 0.01 '\*' 0.05 '.' 0.1 ' ' 1

Residual standard error: 0.1732 on 249 degrees of freedom  
Multiple R-squared: 0.8055, Adjusted R-squared: 0.7977  
F-statistic: 103.2 on 10 and 249 DF, p-value: < 2.2e-16

Response Y3 :

Call:

lm(formula = Y3 ~ 0 + CI1 + CI2 + Z2)

Residuals:

	Min	1Q	Median	3Q	Max
	-1.24842	-0.04737	0.01539	0.06202	0.62568

Coefficients:

	Estimate	Std. Error	t value	Pr(> t )
CI1	-0.001147	0.001647	-0.696	0.486793
CI2	-0.001677	0.001952	-0.859	0.391017
Z2	-0.019040	0.025519	-0.746	0.456316
Z2	-0.317148	0.034413	-9.216	< 2e-16 ***
Z2	0.110889	0.058662	1.890	0.059880 .
Z2	-0.056034	0.024832	-2.257	0.024903 *
Z2	0.068606	0.058443	1.174	0.241559
Z2	0.354798	0.105142	3.374	0.000858 ***
Z2St	0.413961	0.743202	0.557	0.578030
Z2NSt	0.861273	0.886375	0.972	0.332153

---

Signif. codes: 0 '\*\*\*' 0.001 '\*\*' 0.01 '\*' 0.05 '.' 0.1 ' ' 1

Residual standard error: 0.1631 on 249 degrees of freedom  
Multiple R-squared: 0.4983, Adjusted R-squared: 0.4782  
F-statistic: 24.74 on 10 and 249 DF, p-value: < 2.2e-16

DEU

Response Y1 :

Call:

lm(formula = Y1 ~ 0 + CI1 + CI2 + Z2)

Residuals:

	Min	1Q	Median	3Q	Max
	-4.6104	-0.9759	0.1005	0.8901	4.2094

Coefficients:

	Estimate	Std. Error	t value	Pr(> t )	
CI1	-0.030082	0.008529	-3.527	0.000500	***
CI2	-0.016754	0.010384	-1.614	0.107894	
Z2	-0.312315	0.070909	-4.404	1.58e-05	***
Z2	-0.846365	0.414972	-2.040	0.042449	*
Z2	4.356535	0.898185	4.850	2.17e-06	***
Z2	-0.383271	0.107941	-3.551	0.000459	***
Z2	-0.637484	0.616605	-1.034	0.302205	
Z2	0.937635	1.355205	0.692	0.489659	
Z2St	14.903988	4.087707	3.646	0.000324	***
Z2NSt	8.386001	5.008474	1.674	0.095315	.

---

Signif. codes: 0 '\*\*\*' 0.001 '\*\*' 0.01 '\*' 0.05 '.' 0.1 ' ' 1

Residual standard error: 1.402 on 249 degrees of freedom  
 Multiple R-squared: 0.2639, Adjusted R-squared: 0.2344  
 F-statistic: 8.929 on 10 and 249 DF, p-value: 1.552e-12

Response Y2 :

Call:

lm(formula = Y2 ~ 0 + CI1 + CI2 + Z2)

Residuals:

Min	1Q	Median	3Q	Max
-0.48358	-0.11645	-0.00612	0.09462	0.84283

Coefficients:

	Estimate	Std. Error	t value	Pr(> t )	
CI1	0.002840	0.001089	2.607	0.00967	**
CI2	0.004020	0.001326	3.031	0.00269	**
Z2	0.011172	0.009057	1.234	0.21850	
Z2	0.739553	0.053000	13.954	< 2e-16	***
Z2	-0.149310	0.114717	-1.302	0.19427	
Z2	0.003049	0.013786	0.221	0.82512	
Z2	0.753068	0.078753	9.562	< 2e-16	***
Z2	-0.153896	0.173087	-0.889	0.37480	
Z2St	-1.341432	0.522084	-2.569	0.01077	*
Z2NSt	-1.929305	0.639685	-3.016	0.00283	**

---

Signif. codes: 0 '\*\*\*' 0.001 '\*\*' 0.01 '\*' 0.05 '.' 0.1 ' ' 1

Residual standard error: 0.179 on 249 degrees of freedom  
 Multiple R-squared: 0.7211, Adjusted R-squared: 0.7099  
 F-statistic: 64.37 on 10 and 249 DF, p-value: < 2.2e-16

Response Y3 :

Call:

lm(formula = Y3 ~ 0 + CI1 + CI2 + Z2)

Residuals:

	Min	1Q	Median	3Q	Max
	-0.62563	-0.04667	-0.00572	0.05050	0.57775

Coefficients:

	Estimate	Std. Error	t value	Pr(> t )	
CI1	-0.0026283	0.0005873	-4.475	1.16e-05	***
CI2	0.0009444	0.0007150	1.321	0.18777	
Z2	0.0069302	0.0048826	1.419	0.15704	
Z2	-0.0816146	0.0285737	-2.856	0.00465	**
Z2	0.4802570	0.0618463	7.765	2.12e-13	***
Z2	0.0023727	0.0074325	0.319	0.74982	
Z2	-0.0380330	0.0424576	-0.896	0.37123	
Z2	0.1669123	0.0933153	1.789	0.07488	.
Z2St	1.2244665	0.2814672	4.350	1.98e-05	***
Z2Nst	-0.3817482	0.3448685	-1.107	0.26939	

---

Signif. codes: 0 '\*\*\*' 0.001 '\*\*' 0.01 '\*' 0.05 '.' 0.1 ' ' 1

Residual standard error: 0.09653 on 249 degrees of freedom  
 Multiple R-squared: 0.6035, Adjusted R-squared: 0.5876  
 F-statistic: 37.91 on 10 and 249 DF, p-value: < 2.2e-16

FRA

Response Y1 :

Call:

lm(formula = Y1 ~ 0 + CI1 + CI2 + Z2)

Residuals:

	Min	1Q	Median	3Q	Max
	-5.2160	-0.8313	-0.0256	0.8534	2.9165

Coefficients:

	Estimate	Std. Error	t value	Pr(> t )	
CI11	-0.022609	0.010656	-2.122	0.03485	*
CI12	-0.013747	0.006840	-2.010	0.04553	*
CI21	-0.009797	0.011265	-0.870	0.38533	
CI22	-0.015175	0.006136	-2.473	0.01407	*
Z2	-0.359760	0.073769	-4.877	1.93e-06	***
Z2	-0.518231	0.578740	-0.895	0.37142	
Z2	2.622130	0.784568	3.342	0.00096	***
Z2	-0.580714	0.087013	-6.674	1.63e-10	***
Z2	-0.882209	0.678616	-1.300	0.19481	

```
Z2      -0.304945    1.271613   -0.240   0.81068
Z2St    17.506928     8.369754    2.092   0.03749 *
Z2NSt   12.732507     8.149832    1.562   0.11950
```

---

Signif. codes: 0 '\*\*\*' 0.001 '\*\*' 0.01 '\*' 0.05 '.' 0.1 ' ' 1

Residual standard error: 1.266 on 247 degrees of freedom  
 Multiple R-squared: 0.2769, Adjusted R-squared: 0.2418  
 F-statistic: 7.884 on 12 and 247 DF, p-value: 1.985e-12

Response Y2 :

Call:  
 lm(formula = Y2 ~ 0 + CI1 + CI2 + Z2)

Residuals:

	Min	1Q	Median	3Q	Max
	-0.32420	-0.07719	-0.00816	0.07479	0.36201

Coefficients:

	Estimate	Std. Error	t value	Pr(> t )	
CI11	0.0027942	0.0010420	2.682	0.00782	**
CI12	0.0017387	0.0006688	2.600	0.00989	**
CI21	0.0016161	0.0011016	1.467	0.14364	
CI22	0.0011026	0.0006000	1.838	0.06733	.
Z2	0.0089416	0.0072136	1.240	0.21632	
Z2	0.7226645	0.0565928	12.770	< 2e-16	***
Z2	-0.1061146	0.0767199	-1.383	0.16787	
Z2	0.0022721	0.0085086	0.267	0.78967	
Z2	0.7763191	0.0663592	11.699	< 2e-16	***
Z2	0.0355327	0.1243460	0.286	0.77530	
Z2St	-2.2199693	0.8184455	-2.712	0.00715	**
Z2NSt	-1.3640623	0.7969402	-1.712	0.08822	.

---

Signif. codes: 0 '\*\*\*' 0.001 '\*\*' 0.01 '\*' 0.05 '.' 0.1 ' ' 1

Residual standard error: 0.1238 on 247 degrees of freedom  
 Multiple R-squared: 0.78, Adjusted R-squared: 0.7693  
 F-statistic: 72.97 on 12 and 247 DF, p-value: < 2.2e-16

Response Y3 :

Call:  
 lm(formula = Y3 ~ 0 + CI1 + CI2 + Z2)

Residuals:

	Min	1Q	Median	3Q	Max
	-0.66976	-0.03917	-0.00326	0.04256	0.55536



## Coefficients:

	Estimate	Std. Error	t value	Pr(> t )	
CI11	-0.0023404	0.0007933	-2.950	0.00348	**
CI12	-0.0010796	0.0005092	-2.120	0.03499	*
CI21	0.0014095	0.0008387	1.681	0.09412	.
CI22	0.0004279	0.0004568	0.937	0.34984	
Z2	0.0113364	0.0054922	2.064	0.04005	*
Z2	-0.1886088	0.0430880	-4.377	1.77e-05	***
Z2	0.4536679	0.0584122	7.767	2.15e-13	***
Z2	0.0035198	0.0064782	0.543	0.58739	
Z2	0.0500872	0.0505239	0.991	0.32248	
Z2	0.1366102	0.0946733	1.443	0.15030	
Z2St	1.5332117	0.6231398	2.460	0.01456	*
Z2NSt	-0.7771781	0.6067663	-1.281	0.20145	

---

Signif. codes: 0 '\*\*\*' 0.001 '\*\*' 0.01 '\*' 0.05 '.' 0.1 ' ' 1

Residual standard error: 0.09423 on 247 degrees of freedom  
 Multiple R-squared: 0.6165, Adjusted R-squared: 0.5978  
 F-statistic: 33.08 on 12 and 247 DF, p-value: < 2.2e-16

## ITA

Response Y1 :

Call:

lm(formula = Y1 ~ 0 + CI1 + CI2 + Z2)

## Residuals:

Min	1Q	Median	3Q	Max
-4.1314	-0.9066	0.0853	0.8361	3.3934

## Coefficients:

	Estimate	Std. Error	t value	Pr(> t )	
CI1	-0.05140	0.01967	-2.613	0.009520	**
CI2	-0.01458	0.02360	-0.618	0.537087	
Z2	-0.25974	0.07453	-3.485	0.000581	***
Z2	-0.84642	0.40186	-2.106	0.036182	*
Z2	3.24466	0.73791	4.397	1.63e-05	***
Z2	-0.31816	0.10541	-3.018	0.002805	**
Z2	-1.31439	0.57341	-2.292	0.022728	*
Z2	0.85086	1.17999	0.721	0.471537	
Z2St	24.02949	9.19996	2.612	0.009551	**
Z2NSt	6.85465	11.07099	0.619	0.536381	

---

Signif. codes: 0 '\*\*\*' 0.001 '\*\*' 0.01 '\*' 0.05 '.' 0.1 ' ' 1

Residual standard error: 1.372 on 249 degrees of freedom  
 Multiple R-squared: 0.1793, Adjusted R-squared: 0.1463

F-statistic: 5.439 on 10 and 249 DF, p-value: 2.703e-07

Response Y2 :

Call:

lm(formula = Y2 ~ 0 + CI1 + CI2 + Z2)

Residuals:

	Min	1Q	Median	3Q	Max
	-0.43339	-0.08835	-0.00486	0.07351	0.48315

Coefficients:

	Estimate	Std. Error	t value	Pr(> t )
CI1	0.001147	0.002027	0.566	0.5721
CI2	-0.004455	0.002432	-1.832	0.0681 .
Z2	0.007418	0.007680	0.966	0.3350
Z2	0.798872	0.041411	19.291	<2e-16 ***
Z2	-0.154101	0.076041	-2.027	0.0438 *
Z2	-0.015995	0.010862	-1.473	0.1421
Z2	0.945586	0.059090	16.002	<2e-16 ***
Z2	0.214504	0.121597	1.764	0.0789 .
Z2St	-0.575723	0.948051	-0.607	0.5442
Z2NSt	2.101402	1.140860	1.842	0.0667 .

---

Signif. codes: 0 '\*\*\*' 0.001 '\*\*' 0.01 '\*' 0.05 '.' 0.1 ' ' 1

Residual standard error: 0.1414 on 249 degrees of freedom

Multiple R-squared: 0.7741, Adjusted R-squared: 0.7651

F-statistic: 85.34 on 10 and 249 DF, p-value: < 2.2e-16

Response Y3 :

Call:

lm(formula = Y3 ~ 0 + CI1 + CI2 + Z2)

Residuals:

	Min	1Q	Median	3Q	Max
	-0.61162	-0.04247	0.00116	0.05225	0.57112

Coefficients:

	Estimate	Std. Error	t value	Pr(> t )
CI1	0.003987	0.001558	2.559	0.01110 *
CI2	0.001613	0.001869	0.863	0.38892
Z2	0.008605	0.005904	1.458	0.14622
Z2	-0.164785	0.031836	-5.176	4.67e-07 ***
Z2	0.412723	0.058458	7.060	1.65e-11 ***
Z2	0.001994	0.008351	0.239	0.81149
Z2	0.050449	0.045426	1.111	0.26783
Z2	0.157956	0.093480	1.690	0.09233 .
Z2St	-1.939109	0.728831	-2.661	0.00831 **

Z2NSt -0.678377 0.877055 -0.773 0.43998

---

Signif. codes: 0 '\*\*\*' 0.001 '\*\*' 0.01 '\*' 0.05 '.' 0.1 ' ' 1

Residual standard error: 0.1087 on 249 degrees of freedom

Multiple R-squared: 0.6013, Adjusted R-squared: 0.5853

F-statistic: 37.56 on 10 and 249 DF, p-value: < 2.2e-16

ESP

Response Y1 :

Call:

lm(formula = Y1 ~ 0 + CI1 + CI2 + Z2)

Residuals:

	Min	1Q	Median	3Q	Max
	-6.8188	-0.7661	0.0857	0.8912	3.7255

Coefficients:

	Estimate	Std. Error	t value	Pr(> t )
CI1	-0.005423	0.003076	-1.763	0.079120 .
CI2	-0.009271	0.005372	-1.726	0.085645 .
Z2	-0.232775	0.072704	-3.202	0.001544 **
Z2	-0.468354	0.496402	-0.943	0.346340
Z2	2.209631	0.774192	2.854	0.004679 **
Z2	-0.396459	0.115467	-3.434	0.000698 ***
Z2	-2.556434	0.933940	-2.737	0.006642 **
Z2	1.714808	1.323997	1.295	0.196459
Z2St	3.055453	1.678804	1.820	0.069957 .
Z2NSt	4.424431	2.901769	1.525	0.128594

---

Signif. codes: 0 '\*\*\*' 0.001 '\*\*' 0.01 '\*' 0.05 '.' 0.1 ' ' 1

Residual standard error: 1.359 on 249 degrees of freedom

Multiple R-squared: 0.1295, Adjusted R-squared: 0.09456

F-statistic: 3.705 on 10 and 249 DF, p-value: 0.0001208

Response Y2 :

Call:

lm(formula = Y2 ~ 0 + CI1 + CI2 + Z2)

Residuals:

	Min	1Q	Median	3Q	Max
	-0.43382	-0.07172	-0.00660	0.06308	0.52136

Coefficients:

	Estimate	Std. Error	t value	Pr(> t )
CI1	0.0004013	0.0003029	1.325	0.187
CI2	-0.0002469	0.0005291	-0.467	0.641
Z2	-0.0072140	0.0071606	-1.007	0.315
Z2	0.7115438	0.0488907	14.554	<2e-16 ***
Z2	-0.1052133	0.0762504	-1.380	0.169
Z2	-0.0050644	0.0113724	-0.445	0.656
Z2	0.8923137	0.0919841	9.701	<2e-16 ***
Z2	0.0193351	0.1304008	0.148	0.882
Z2St	-0.2589694	0.1653459	-1.566	0.119
Z2NSt	0.1326148	0.2857960	0.464	0.643

---

Signif. codes: 0 '\*\*\*' 0.001 '\*\*' 0.01 '\*' 0.05 '.' 0.1 ' ' 1

Residual standard error: 0.1338 on 249 degrees of freedom  
Multiple R-squared: 0.6985, Adjusted R-squared: 0.6864  
F-statistic: 57.7 on 10 and 249 DF, p-value: < 2.2e-16

Response Y3 :

Call:

lm(formula = Y3 ~ 0 + CI1 + CI2 + Z2)

Residuals:

Min	1Q	Median	3Q	Max
-0.70281	-0.04322	0.00555	0.04430	0.56517

Coefficients:

	Estimate	Std. Error	t value	Pr(> t )
CI1	0.0006248	0.0002331	2.680	0.00785 **
CI2	-0.0004809	0.0004072	-1.181	0.23868
Z2	0.0134097	0.0055104	2.434	0.01566 *
Z2	-0.1555518	0.0376234	-4.134	4.87e-05 ***
Z2	0.4417635	0.0586778	7.529	9.40e-13 ***
Z2	-0.0040956	0.0087515	-0.468	0.64020
Z2	0.0839661	0.0707855	1.186	0.23667
Z2	0.1818118	0.1003487	1.812	0.07122 .
Z2St	-0.4027356	0.1272404	-3.165	0.00174 **
Z2NSt	0.3452909	0.2199317	1.570	0.11769

---

Signif. codes: 0 '\*\*\*' 0.001 '\*\*' 0.01 '\*' 0.05 '.' 0.1 ' ' 1

Residual standard error: 0.103 on 249 degrees of freedom  
Multiple R-squared: 0.5869, Adjusted R-squared: 0.5703  
F-statistic: 35.37 on 10 and 249 DF, p-value: < 2.2e-16

## References

1. Agliari, A., Dieci, R., Gardin, L.: Homoclinic tangles in a Kaldor-like business cycle model. *J. Econ. Behav. Organ.* **62**, 324–347 (2007)
2. BEA: USA Recessions, Gross Domestic Product [A191RP1Q027SBEA] - US. Bureau of Economic Analysis (2016). <https://fred.stlouisfed.org/series/A191RP1Q027SBEA>. Retrieved from FRED, Federal Reserve Bank of St. Louis; November 10, 2016
3. Bischi, G.I., Dieci, R., Rodano, G., Saltari, E.: Multiple attractors and global bifurcations in a Kaldor-type business cycle model. *J. Evol. Econ.* **11**, 527–554 (2001)
4. Bolt, J., van Zanden, J.L.: The Maddison Project: collaborative research on historical national accounts. *Econ. Hist. Rev.* **67**(3), 627–651 (2014)
5. Bradford, R., Davenport, J.H.: Towards Better Simplification of Elementary Functions. In: ISSAC '02 Proceedings of the 2002 International Symposium on Symbolic and Algebraic Computation, pp. 16–22. ACM, New York (2002)
6. Collicott, S.H.: Never trust an arctangent (2012). [https://engineering.purdue.edu/~collicot/NTAA\\_files/Chapter1.pdf](https://engineering.purdue.edu/~collicot/NTAA_files/Chapter1.pdf)
7. Feenstra, R.C., Inklaar, R., Timmer, M.: The next generation of the Penn World Table. Tech. rep., National Bureau of Economic Research (2013)
8. Feenstra Robert C., R.I., Timmer, M.P.: The Next Generation of the Penn World Table. *Am. Econ. Rev.* **105**(10), 3150–3182 (2015). <https://doi.org/10.15141/S5J01T>
9. Gonnet, G.H., Scholl, R.: *Scientific Computation*. Cambridge University Press, Cambridge (2009)
10. Januaria, C., Graaciob, C., Duartea, J.: Measuring complexity in a business cycle model of the Kaldor type. *Chaos Solitons Fractals* **42**(5), 2890–2903 (2009)
11. Januario, C., Gracio, C., Ramos, J.S.: Chaotic behaviour in a two-dimensional business cycle model. In: Elaydi, S., Cushing, J., Lasser, R., Ruffing, A., Papageorgiou, V., Assche, W.V. (eds.) *Proceedings of the International Conference, Difference Equations, Special Functions and Orthogonal Polynomials*, pp. 294–304. Munich (2005)
12. Kaddar, A., Alaoui, H.T.: Global existence of periodic solutions in a delayed Kaldor–Kalecki model. *Nonlinear Anal. Model. Control* **14**(4), 463–472 (2009)
13. Levy, D., Chen, H.: Estimates of the aggregate quarterly capital stock for the post-war us economy. *Rev. Income Wealth* **40**(3), 317–349 (1994)
14. Mircea, G., Neamt, M., Opris, D.: The Kaldor and Kalecki stochastic model of business cycle, nonlinear analysis: modelling and control. *J. Atmos. Sci.* **16**(2), 191–205 (1963)
15. OECD: Investment GFCF (indicator) (2016). <https://doi.org/10.1787/b86d1fc8-en>
16. OECD: Quarterly GDP (indicator) (2016). <https://doi.org/10.1787/b86d1fc8-en>
17. OECD: Saving rate GFCF (indicator) (2016). <https://doi.org/10.1787/ff2e64d4-en>
18. Walter, F.S.: *Waves and Oscillations: A Prelude to Quantum Mechanics*. Oxford University Press, Oxford (2010)

## Back Cover

The last decades have seen important and fundamental contributions demonstrating to us that economic systems evolve like complex systems. Economists were, however, not alone in such an experience, as similar advances were achieved in other fields of research, such as non-linear dynamics, physics, biology, computer science, etc., at the same time. Although this book has a focus on economic problems, it is in an interdisciplinary perspective, capable of providing readers and researchers from a larger circle of readers with new insights and new ideas in the field of non-linear dynamics and, in general, of complexity theory.